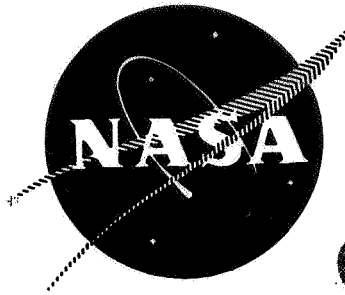NASA CR 72559

R-7879

CASE FILE
COPY

SPACE STORABLE ENGINE CHARACTERIZATION

FINAL REPORT

by

R. V. Burry

prepared for

NATIONAL AERONAUTICS AND SPACE ADMINISTRATION

Contract NAs3-12024

Rocketdyne
North American Rockwell

FINAL REPORT

SPACE STORABLE ENGINE CHARACTERIZATION

by

R. V. Burry

Prepared for

NATIONAL AERONAUTICS AND SPACE ADMINISTRATION

CONTRACT NAS3-12024

March 1970

Approved by

E. B. Monteath
Program Manager
Advanced Technology Programs

Technical Management
John W. Gregory
NASA Lewis Research Center
Cleveland, Ohio
Liquid Rocket Technology Branch

ROCKETDYNE
A Division of North American Rockwell Corporation
6633 Canoga Avenue
Canoga Park, California 91304

FOREWORD

This report was prepared by the Rocketdyne Division of the North
American Rockwell Corporation under Contract NAS3-12024. This is
the final report and summarizes the results of studies conducted
from September 1968 through March 1969. The contract was adminis-
tered by the Lewis Research Center of the National Aeronautics and
Astronautics Administration, Cleveland, Ohio. The NASA Project
Manager for the contract was Mr. John W. Gregory.

The purpose of the contract was to analyze, evaluate, select and
design a pump-fed FLOX/methane engine system. This engine has a
thrust level of 5000-pounds (22200 N) and is completely regeneratively-
cooled with a channel construction thrust chamber.

The investigation was divided into two tasks: (1) Engine Turbopump
Drive Cycle Investigation, and (II) Engine Preliminary Design Evalu-
ation. In Task I, candidate drive cycles were evaluated and the best
system was selected. In Task II, a preliminary design investigation
of a flight-weight engine using the selected pump drive cycle was con-
ducted.

ABSTRACT

A 5000-pound (22200 N) thrust FLOX/methane engine system for space applications was investigated. The engine is pump-fed with a milled channel, regeneratively cooled thrust chamber. A series of engine design candidates and design points were evaluated in terms of performance, complexity, operational flexibility and development ease. A description of these components is provided. An expander drive cycle using heated methane to provide power to two turbines operating in parallel was selected as the best engine configuration. A chamber pressure of 500 psia (3450 kN/m^2) and a mixture ratio of 5.25 were selected as the best design point.

A preliminary design investigation of the selected engine system, major components, and operational capability was conducted. Results of this investigation are described. The engine system has a weight of 89 pounds (40.4 kg) and is capable of delivering a specific impulse value over 400 seconds (3920 N-sec/kg) within an envelope of 21.4 by 40.9 inches (53.4 by 104 cm). Tank head start, throttling, idle mode, self-pressurization, and engine thrust uprating capability are provided by the engine.

ACKNOWLEDGMENT

CONTENTS

L I S T   O F   F I G U R E S
(Continued)

L I S T   O F   F I G U R E S

(Continued)

LIST OF TABLES

INTRODUCTION

Many space missions require propulsion systems that not only provide high performance but whose propellants can be maintained for extended periods of time in space. The propellant combination using 82.6-percent fluorine/17.5-percent oxygen (FLOX) as the oxidizer and methane as the fuel is admirably suited to this purpose. This propellant combination has high specific impulse with good bulk density and is characterized by relatively mild cryogenic temperatures. In addition, there is little difference between the usable temperature range of the oxidizer and the fuel.

These features have lead to considerable interest in these propellants, and considerable work has been accomplished in developing component technology. Contracts such as NAS3-11191 (Ref. 1) and NAS3-12011 (Ref. 2) have developed injector and thrust chamber cooling technology. Nozzle performance has been described under Contract NASw-1229 (Ref. 3). Fluorine pump technology is being developed in Contract NAS3-12022 (Ref. 4).

In the current contract, engine system design and operational characteristics have been investigated using component technology information developed in contracts such as those described above. Basic requirements of this engine system are listed below.

TABLE 1
ENGINE DESCRIPTION

Thrust, pound (vacuum) (N)	5000 (22200)
Feed System	Pump
Nozzle	Bell Contour
Cooling	Full Regenerative
Thrust Chamber Construction	Nontubular, Channel Construction
Environment	Space: Earth, Mars, Moon, Jupiter, Saturn
Number of Starts	4 or more
Duration, sec (full thrust)	500
Throttling	10:1 (tentative requirement)

With these requirements thrust chamber designs, turbopump drive cycles and pump-turbine arrangements were investigated. Candidate configurations were evaluated considering performance, ease of development, complexity and operational capability. Tradeoffs between the evaluation criteria were made to arrive at the configuration most suited to the requirements. The selected engine system configuration was then investigated to provide a preliminary design description of the components and system operation.

The investigation was divided into two tasks: Task I - Engine Turbopump Drive Cycle Evaluation and Task II - Engine Preliminary Design Evaluation. In Task I, candidate thrust chamber designs, turbopump drive cycles, and pump-turbine arrangements will be defined and evaluated. The best engine configuration was selected and a nominal design point specified. In Task II the component and system features of this engine were investigated to provide a preliminary design and operational description of a flight weight engine system.

SUMMARY

Investigation of a turbopump-fed FLOX/methane engine was conducted to
determine the characteristics of the complete engine system. Thrust
chamber design, turbopump drive cycles, and pump-turbine arrangements
were evaluated to define the best engine configuration. A preliminary
design of the selected system was then provided.

TASK I – ENGINE TURBOPUMP DRIVE CYCLE EVALUATION

Candidate engine configurations were evaluated to determine the system best
suited to the engine requirements. Emphasis was placed upon attaining high
performance within the framework of technology currently available or being
developed. Regeneratively-cooled designs were first investigated for
channel construction thrust chambers. Design points were selected and
cooling channel configurations were established. Candidate drive cycles
and turbomachinery arrangements were then evaluated at these design points.
Two configurations were selected for further investigation. Based upon
these investigations, the expander drive cycle with dual turbines was selected.
This engine would provide high performance and operational versatility with
a reasonable development program.

THRUST CHAMBER ANALYSIS

The first step was the investigation of regeneratively-cooled channel con-
struction thrust chambers for a range of operating conditions. From the
results of this analysis two design points were selected for further thrust
chamber and drive cycle investigation.

THRUST CHAMBER DESIGN POINTS

Chamber Pressure, psia (kN/m^2)	Expansion Ratio	Thrust Chamber Mixture Ratio, (O/F)
500 (3450)	60:1	5.25
800 (5520)	100:1	5.25

The chamber pressures were selected on the basis of cooling analyses and fabrication considerations. A pressure of 800 psia (5520 kN/m^2) appeared to be a maximum chamber pressure value for the nickel, channel construction thrust chamber design. At chamber pressures higher than this, cooling jacket pressure drops are high and variations in assumptions regarding nominal heat flux level or method of fabrication can significantly increase pressure drop and fabrication difficulty. The chamber pressure value of 500 psia (3450 kN/m^2) was selected as a point where design feasibility is relatively unaffected by perturbations in the ground rules.

A thrust chamber mixture ratio of 5.25 was selected. This mixture ratio was selected at a point less than stoichiometric to provide maximum delivered specific impulse and low methane temperatures at the cooling jacket exit. An expansion ratio of 100:1 was selected for 800 psia (5520 kN/m^2) chamber pressure, and a value of 60:1 was selected for the 500 psia (3450 kN/m^2) chamber pressure to maintain equivalent thrust chamber envelopes.

For the two design points, a thrust chamber description was derived for each engine drive cycle. These descriptions included coolant channel design, and in the case of the auxiliary heat exchanger cycle, the design of a thrust chamber nozzle heat exchanger for turbine power. A channel design involving two step variations in channel width was selected as the best compromise be-tween weight, pressure drop, and ease of fabrication. All channel designs were feasible for both nominal thrust and throttled operation. The 500 psia

4

(3450 kN/m^2) designs had relatively large channels and were less sensitive to heat flux level than the 800 psia (5520 kN/m^2) designs. The lower chamber pressure designs represent easier development than the higher pressure (5520 kN/m^2) designs.

TURBOPUMP DRIVE CYCLE SELECTION

To provide turbopump power, five major drive cycle candidates were investigated at the selected design points:

1. Gas Generator (A) - Low flow turbine
2. Gas Generator (B) - High flow turbine, topping arrangement
3. Thrust chamber tapoff
4. Auxiliary heat exchanger
5. Expander

Engine systems and flow schematics were described for each of these drive cycles. Using the previously described thrust chamber designs, power balances were performed to define turbopump requirements. Based on these requirements, pump and turbine designs were established for single shaft, gear driven, and dual shaft turbomachinery arrangements. Performance was calculated assuming 94-percent specific impulse efficiency; operational limits, and potential development problems were identified. Based on these characteristics a turbomachinery arrangement and drive cycle were selected.

Turbomachinery Arrangement Selection

Performance, design and development characteristics were compared and the dual turbine arrangement was selected for all drive cycles. This arrangement provides an efficient, simple engine system with turbine flexibility during transient operation.

The single shaft turbopump arrangement was unattractive for all drive cycles. This turbopump penalized the methane pump and turbine efficiencies by forcing them to run at the slower, FLOX pump, speed. This led to a small impeller discharge widths for the methane pump, which increases fabrication difficulty. The large shaft makes the methane pump inducer have rather small blades which, with reasonable tip clearance values, may compromise suction performance. The gear driven and dual turbine arrangements were more attractive, in that each pump operatives at its own speed and high

efficiency can be attained. Methane inducer designs for these arrangements are unrestricted by the drive shaft and have better suction performance potential.

The dual turbine arrangements have fewer development subcomponents than the gear-driven arrangement. In parallel flow, dual turbine arrangements, the turbine designs can, in most cases, be made identical. Therefore, in the sub-component area the dual turbine arrangement has an additional FLOX bearing while in contrast the gear driven arrangement has an additional FLOX valve, gears, additional methane bearings, and the associated lubrication system.

Associated with the gear-driven arrangement is the start sequence limitation in which long thermal conditioning times are anticipated, because power application to the methane pump must be delayed until FLOX pump power is also desired. The dual turbine arrangements, particularly the parallel-flow arrangement, are independent in operation and, therefore, are more flexible for development tests, engine system start and throttling. In the early phases of start, for example, the methane turbine can be powered while the FLOX turbopump is inoperative. The power input to the methane pump materially assists in reducing the methane side priming time. From this consideration, the dual turbine arrangements were more attractive.

Drive Cycle Comparison

From an initial comparison of the drive cycles, the expander and auxiliary heat exchanger cycles were selected for further study. The expander cycle has the highest performance. Development ease was very reasonable. The auxiliary heat exchanger cycle is the easiest to develop but has low performance. No other cycles offered any significant advantages.

Engine specific impulse for the candidate drive cycles is illustrated in Fig. 1. For both design points the expander and gas generator (B) cycles have the highest specific impulse. Gas generator (B) performance is somewhat reduced by a high engine weight. The remaining drive cycles have specific impulse values nominally 1 percent lower. Since engine specific impulse of the low turbine flow cycles is significantly affected by the drive system character

6
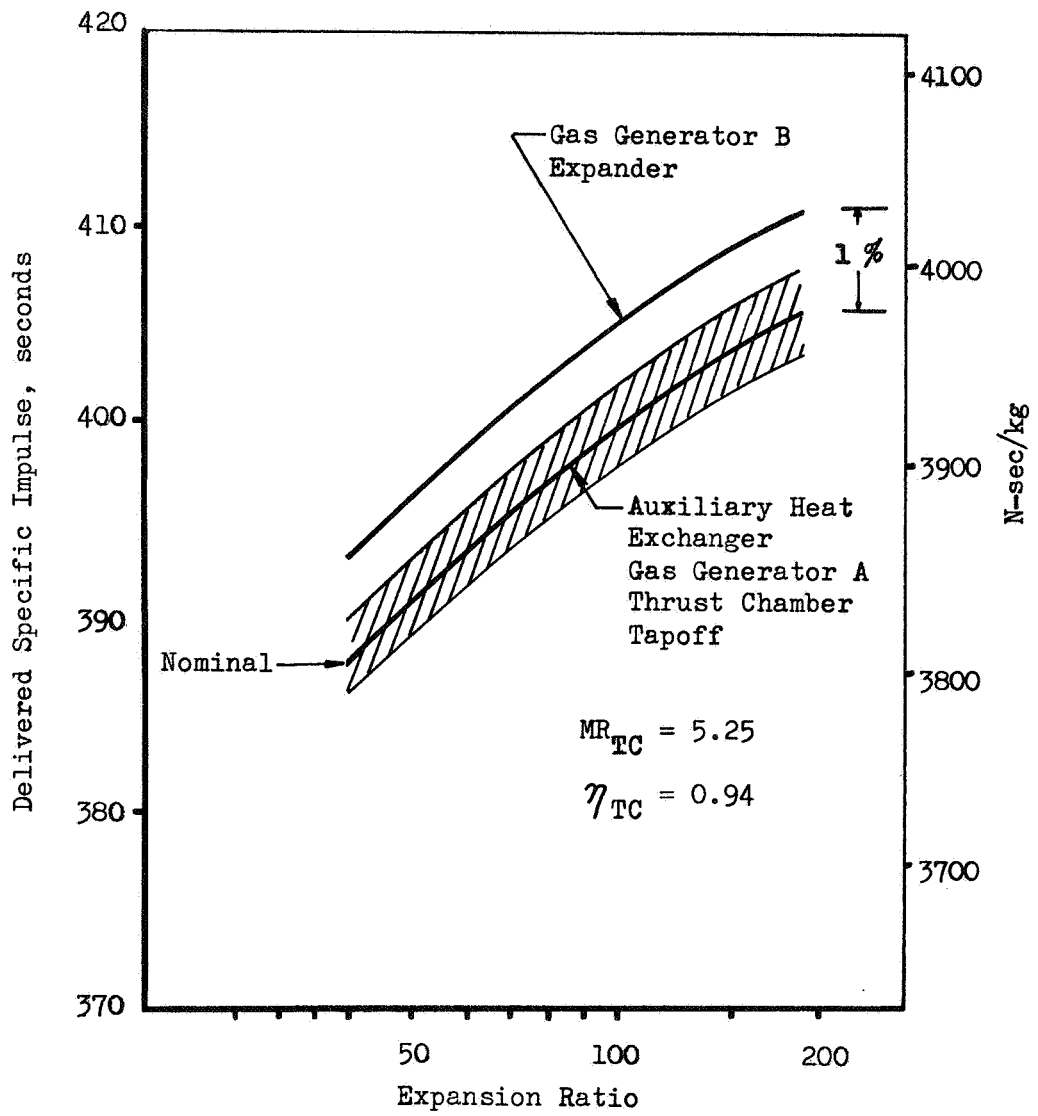
Figure 1 . Drive Cycle Performance.

(turbine efficiency, pressure drop, inlet temperature), the specific impulse is shown as a band.

Drive cycle development problems are summarized in Table 2. The single most significant potential problem is that of turbine nozzle coking in the cycles using FLOX/methane combustion products to power the turbines: gas generator (A), gas generator (B), and thrust chamber tapoff. In the small turbine flow passages, coking could severely reduce turbine performance and represents a significant potential development problem. The next most significant item is the control of the small amounts of hot, corrosive gas in the FLOX/methane-powered turbine cycles.

Of all the drive cycles, the auxiliary heat exchanger appears to have the fewest development problems, with the expander cycle being slightly more difficult. In the expander and gas generator (B) cycles, the pump, turbine and thrust chamber are closely connected and a variation in one component can significantly affect the operation of the other components. At the higher chamber pressure the engine balances for these cycles are sensitive to this interdependence and in the course of development a component design variation could easily make it incompatible with the remainder of the feed system. Expander cycle sensitivity to this interdependence is greatly diminished at the 500 psia (3450 kN/m^2) design point.

Drive Cycle Selection

Further investigation of the expander and auxiliary heat exchanger cycles resulted in recommendation of the expander cycle operating at 500 psia (3450 kN/m^2) and reasonable development program.

Detailed energy balances were established for the auxiliary heat exchanger and expander cycles. Throttling and engine system perturbation analyses were performed. The results of these investigations reaffirm the conclusions of the general investigation. The 800 psia (5520 kN/m^2) expander cycle is the

TABLE 2

ENGINE DRIVE CYCLE DEVELOPMENT FEATURES

THRUST CHAMBER TAPOFF, GAS GENERATOR A, GAS GENERATOR B

- CORROSIVE, HIGH TEMPERATURE TURBINE WORKING FLUID
- TURBINE NOZZLE COKING PROBABLE
- DEVELOPMENT OF TAPOFF SYSTEM OR GAS GENERATOR
- CONTROL OF SMALL FLOW, HOT CORROSIVE FLUID
- GAS GENERATOR B COMPONENT INTERDEPENDENCE

AUXILIARY HEAT EXCHANGER

- CONTROL OF SMALL GAS FLOWS
- HEAT EXCHANGER DEVELOPMENT

EXPANDER

- COMPONENT INTERDEPENDENCE

highest performing engine, but because of its sensitivity and potential problems it would be the most difficult to develop. The 500 psia (3450 kN/m^2) chamber pressure auxiliary heat exchanger cycle is the easiest to develop but has low performance. The 800 psia (5520 kN/m^2) auxiliary heat exchanger cycle and 500 psia (3450 kN/m^2) expander cycle engines are comparable in performance and development ease. Engine start and throttling ease are similar, engine uprating in performance and thrust is more attractive with the 500 psia (3450 kN/m^2) expander, and at equal design points the expander cycle will always out-perform the auxiliary heat exchanger cycle (Fig. 1). The expander cycle at 500 psia (3450 kN/m^2) chamber pressure was, therefore, recommended for further investigation.

TASK II – ENGINE PRELIMINARY DESIGN EVALUATION

A preliminary design was prepared for a flight-weight FLOX/methane engine using an expander turbine drive cycle. The engine was designed to reliably provide high performance for a variety of potential space missions. Capability for multiple restarts, long duration, and prolonged storage in the space environment were provided. Versatility of operation was emphasized. The nominal engine design represents a reasonable balance between these features and engine system cost.

The engine system has a nominal thrust of 5000-pound thrust (22200 N). Sufficient power and design margin are included to allow for development program contingencies. Should these margins not be required, engine uprating capability to 7000-8000 pound thrust (31100-35600 N) at 700 psia (4820 kN/m^2) is available with no performance loss. A 60:1 expansion ratio nozzle has been used. Engine performance improvement capability is provided by designing for possible nozzle extensions and mixture ratio changes.

ENGINE SYSTEM DESCRIPTION

The engine system design is illustrated in Fig. 2 and system operation described in Table 3. In the engine system, separate methane and FLOX turbopumps are driven in parallel by gaseous methane which has been heated in the thrust chamber coolant circuit. The thrust chamber is completely regeneratively cooled and has an expansion area ratio of 60:1. The coaxial element injector has an integral gimbal block and is welded to the thrust chamber. All ducting is of rigid lines with welded interconnects to provide economical, reliable connections for the long duration space mission requirement. Two engine mounted inlet valves and two hot gas valves are used to control the engine. The turbine bypass line and bypass control valve regulate the level of

Figure 2

FLOX METHANE
ENGINE CHARACTERISTICS

Nominal Thrust, pounds (N)	5000	(22,200)
Specific Impulse, sec ($\frac{N-sec}{kg}$)	399.2	(3910)
Expansion Area Ratio	60:1	
Engine Weight, pounds (kg)	89	(40.4)
Length, inches (cm)	41	(104)
Diameter, inches (cm)	21	(53.4)
Pump-Fed,		
Regeneratively Cooled		

12
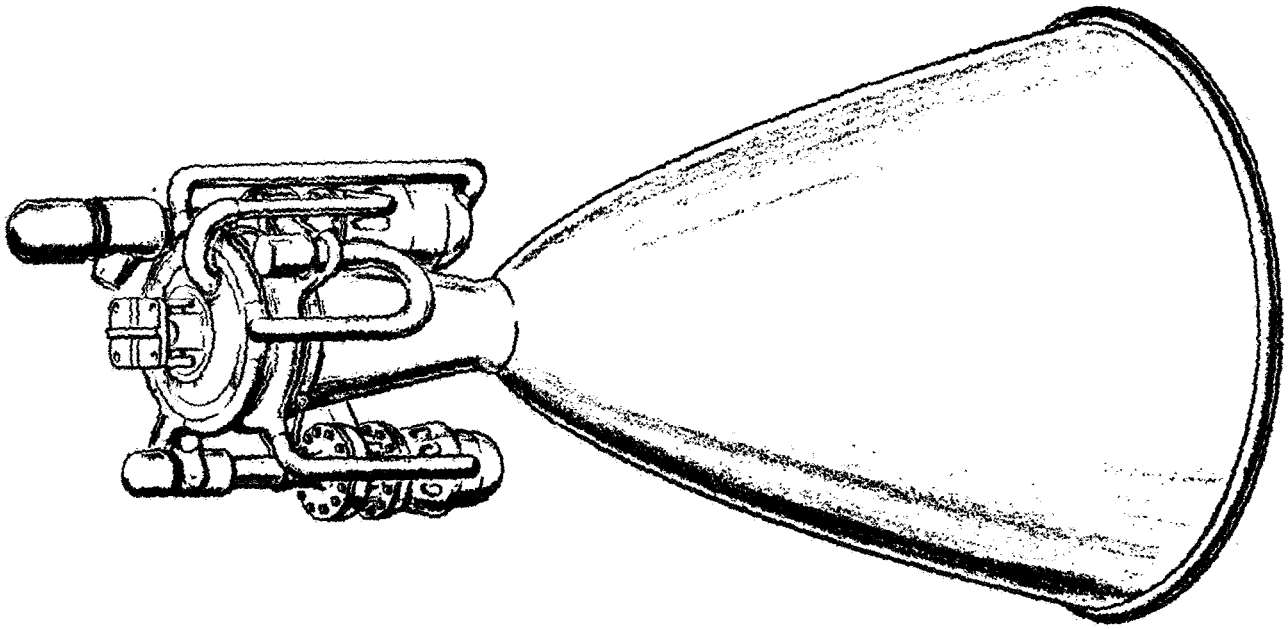
TABLE 3

ENGINE SYSTEM CHARACTERISTICS

Thrust, lb (N)	5000 (22200)	500 (2220)
Engine Specific Impulse, sec $\left(\dfrac{\text{N-sec}}{\text{kg}}\right)$	399.2 (3910)	366 (3590)
Engine Mixture Ratio, O/F	5.25	5.25
Thrust Chamber		
Chamber Pressure, psia (kN/m^2)	500 (3450)	53 (350)
Mixture Ratio, O/F	5.25	5.25
Weight Flow, lb/sec (Kg/sec)	12.52 (5.68)	1.37 (.62)
Specific Impulse, sec (N-sec/kg)	399.2 (3910)	366 (3590)
Expansion Ratio	60	60
Pumps, O/F		
Flow, lb/sec (Kg/sec)	10.52/2.00(4.77/.91)	1.15/.22 (.52/.10)
Discharge Pressure, psia (kN/m^2)	669/1269 (4610/8750)	79/125 (540/860)
Number of Stages	1/2	1/2
Speed, 1000 rpm (1000 rad/sec)	39.1/67.2(4.09/7.02)	8.1/12.2(.846/1.27)
Horsepower (KW)	27.9/42.0(20.8/31.3)	.18/.20 (.13/.15)
Turbine, O/F		
Methane Flow, lb/sec (Kg/sec)	0.74/0.85 (.34/.39)	0.033/0.034 (.015/.015)
Inlet Temperature, °R (K)	1300 (722)	1750 (972)
Number of Stages	1/1	1/1
Bypass, lb/sec (Kg/sec)	.42 (.19)	.15 (.068)

total turbine power. A turbine control valve is used on the hot gas inlet line to the FLOX turbine to proportion power between the methane and FLOX pumps. Engine thrust and mixture ratio are controlled by the hot gas valves. The design of these engine components utilizes technology that is current or is currently being developed.

At the nominal thrust level a specific impulse value of 399.2 seconds (3910 N-sec/kg) can readily be attained. Based on results of NASA sponsored test programs, specific impulse values over 400 seconds (3920 N-sec/kg) are projected. The engine weight is 89 pounds (40.4 kg).

ENGINE COMPONENT DESCRIPTION

Designs for major engine components are illustrated in Fig. 3.

Turbomachinery

Two separate turbopumps are used to provide control ease in transient operation and flexibility of component arrangement. Each pump operates at its optimum speed. The FLOX pump has a single stage with a shrouded centrifugal impeller. The methane pump is a two-stage pump with centrifugal impellers. Pump bearings are cooled by the individual propellants. Bearing DN and seal speeds are less than values to be demonstrated in NAS3-12022 (Ref. 4).

Inducers are used on both pumps to meet low NPSP requirements. To assure uniform flow to the inducers, a short section of ducting is provided between the main valves and the pump inlets. Analyses of pump suction requirements indicate potential for pumping saturated and two-phase propellants at low pump speeds.

14

Oxidizer Pump

Fuel Pump

Coaxial Injector

Milled Channel
Thrust Chamber

Figure 3 . FLOX/CH$_4$ ENGINE COMPONENTS
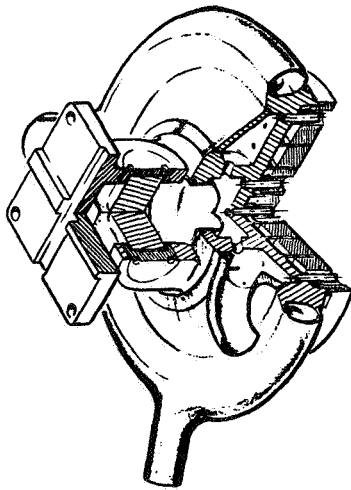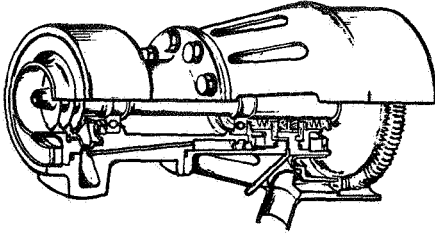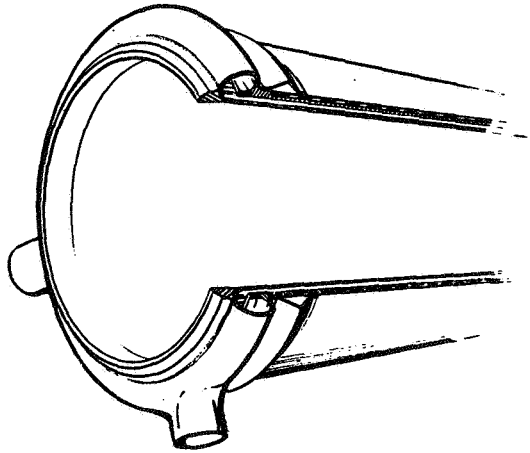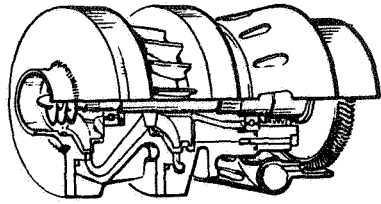
Single-row velocity compounded turbines with partial admission are used to power both pumps. These turbines use methane as the working fluid in a parallel flow arrangement.

Thrust Chamber

The regeneratively-cooled thrust chamber is made using advanced fabrication channel construction techniques. The thrust chamber is of electroformed nickel with channels mechanically milled. A two-step variation in channel width is used as a compromise between pressure drop, weight and fabrication ease. An 80-percent bell nozzle is used with the nozzle contour designed to optimize performance within a fixed envelope. An up-pass cooling arrangement is used to provide good coolant properties in the high heat flux region of the nozzle. The heat flux profile was based upon data from Contract NAS3-11191. Thrust chamber construction was based upon regeneratively-cooled thrust chambers fabricated under NAS3-11191 (Ref. 1).

Injector

Hot methane from the turbine exhaust is collected in the injector fuel manifold and distributed to the injector elements. FLOX enters the oxidizer dome directly from the pump exit. The injector is a coaxial type with a methane-cooled copper face. Pressure drops during throttling are maintained by the recessed element design. Performance is maintained by the high methane velocity which increases during throttling due to its bulk temperature increase.

The injector is welded to the thrust chamber to save weight and to increase reliability. The gimbal bearing is an integral part of the injector and is a simple Hooke type with Fabroid bearing surfaces. The injector oxidizer dome has a single inlet and a tapoff port for tank pressurization. The annular

16

fuel inlet manifold has three inlets, one from each of the turbines and one from the bypass valve. A fuel tapoff port is also provided for tank pressurization.

ENGINE OPERATIONAL FEATURES

Engine characteristics were described for transient conditions and alternate operational modes, as listed in Table 4. Engine transient operations were investigated using a dynamic simulation model which provides a step-by-step description of engine operation during the transient. Engine start transients were investigated for a range of initial engine temperatures. Control sequences and valve requirements were defined. Start times of 3 to 6 seconds, including thermal conditioning and priming, were achieved. With the flexibility allowed by the dual turbines, no indication of pump stall, turbine overspeed, or thrust chamber overheating was observed. Capability for reducing the start time is indicated. Engine cutoff transients were investigated and a sequence defined.

Pressure-fed idle-mode was investigated for several control systems and engine inlet pressures. Transients were described for initial engine temperatures of 250 R (139 K). A region of allowable chamber pressure and mixture ratio operation was determined based upon chamber wall temperatures. Depending on inlet pressures, thrust levels of 200-300 pounds (890-1340 N) can be achieved.

Engine thrust variation both in throttling and in uprating was investigated. Engine control requirements were identified. Throttling conditions were defined over a 10:1 range. Effects of tank conditions on the 10:1 throttled balance were evaluated. Pump speeds in the low thrust range are such that pumping of saturated or two-phase propellants may be possible, allowing operation without tank pressurization. By designing the nominal engine

17

TABLE 4

ENGINE FEATURES

- TANK HEAD START

- NO START RESTRICTIONS

    1) NO PRECONDITIONING

    2) NO VEHICLE ORIENTATION RESTRICTION

    3) QUICK RESTART CAPABILITY

- 10:1 THROTTLING

    1) LANDING

    2) LOW THRUST MANEUVERS

- ENGINE THRUST UPRATING

    1) NO PERFORMANCE LOSS

    2) SMALL HARDWARE MODIFICATION

- SELF-PRESSURIZING (NO VEHICLE PRESSURIZATION SYSTEM)

- PRESSURE-FED IDLE MODE

    1) PROPELLANT SETTLING

    2) LOW THRUST MANEUVERS

    3) RESIDUAL CONSUMPTION

for 20-percent bypass, there is sufficient power margin to allow engine uprating to the 7000-8000-pound (31100-35600 N) thrust level. The design points of the turbomachinery are such that this uprating can be accomplished with little or no modification.

Provisions were made for the engine to provide pressurants for the propellant tanks. At thrust levels greater than 500-1000 pounds (2220-4450 N) sufficient FLOX and methane manifold pressure is available to provide regulated tank pressures of 60-80 psia (410-550 kN/m^2). Turbopump speed and suction requirements are very low in this region.

CONCLUSIONS AND RECOMMENDATIONS

The following conclusions and recommendations were made as a result of these engine characterization investigations.

1. Design and development of pump-fed, regeneratively-cooled engines are feasible at the 5000 pound (22200 N) thrust level. Several engine configurations can supply thrust chamber cooling, flexible operation and reasonable development.

2. On the basis of channel construction thrust chamber development a chamber pressure of 500 psia (3450 kN/m^2) represents significantly more development ease than chamber pressures in the 800 psia (5520 kN/m^2) range.

3. The potential of turbine nozzle coking exists with drive cycles powered by FLOX/methane combustion products: gas generator (A), gas generator (B) and thrust chamber tapoff cycles. This represents a potentially severe development problem for these drive cycles. Drive cycles using heated methane for turbine power (expander and auxiliary heat exchanger) represent the greatest ease of development because of the clean working fluid and system simplicity.

4. An expander cycle engine system operating at 500 psia (3450 kN/m^2) chamber pressure represents the best compromise between performance and development ease for the current application.

5. On the basis of ease of development and flexibility of operation particularly in engine start, individual turbines for each pump arranged for parallel flow are the most attractive pump-turbine configuration.

6. An expander cycle engine designed for a nominal thrust of 5000 pounds (22200 N) weighs 89 pounds (40.4 kg), can provide over 400 seconds (3910 N-sec/kg) of specific impulse, and has an envelope of 21 by 41 inches (53.4 by 104 cm).

7. The engine can start on tank-head under a variety of conditions, throttle, provide pressurization, and operate in idle-mode.

8. Although it must be experimentally verified, analytical predictions of pump suction performance indicate the capability to pump saturated and, potentially, two-phase propellants at low pump speeds.

9. Substantial engine power margin exists providing the potential for thrust uprating to the 7000-8000-pound (31200-35600 N) thrust level. Performance increases are also available through use of nozzle extension and light-weight nozzle concepts.

TASK I - ENGINE TURBOPUMP DRIVE CYCLE EVALUATION

Thrust chamber designs, turbopump drive cycles and pump-turbine arrangements were evaluated on the basis of engine performance, weight, complexity, development ease, and ease of throttling. Considering these tradeoffs between various evaluation criteria the most promising engine configuration was selected. This engine configuration was carried into Task II where a preliminary design evaluation was made.

The Task I effort was divided into four areas. In the first, Regenerative Cooling Analysis, thrust chamber cooling characteristics were evaluated parametrically to guide selection of design points for further engine evaluation. The second area, Regenerative Thrust Chamber Design, includes thrust chamber configuration evaluations for different drive cycles at the two design points and establishment of recommended designs. In the third area, Turbopump Drive Cycle Analysis, a series of turbopump drive cycles and turbine-pump arrangements were evaluated and the two most promising configurations selected. These two configurations were further evaluated in the Cycle Energy Balance Area, and a final engine configuration and design point selected. The studies conducted in these areas are summarized in the following section.

REGENERATIVE COOLING ANALYSIS

To provide an initial assessment of thrust chamber cooling and a guide
to the selection of engine design points, the methane coolant temperature
rise and pressure drop were determined for a 5000-pound (22200 N)-thrust
regeneratively-cooled chamber as a function of the parameters listed
below.

Chamber Pressure, psia (kN/M^2)	250 - 1000 (1720-6900)
Nozzle Area Ratio	40 - 100
Mixture Ratio (O/F)	4.0 - 5.7
Carbon Layer Effectiveness, Q_m/Q_p	0.76 - 1.0
Coolant Inlet Temperature, R (K)	173 - 260 (96-144)
Coolant Outlet Pressure/Chamber Pressure, P_o/P_c	1.25 - 3.0

DISCUSSION OF ASSUMPTIONS

The results of a parametric study can be greatly influenced by the
selection of the underlying assumptions. Pertinent assumptions are dis-
cussed in the following pages. In the absence of test data, certain
assumptions were made in the parametric investigation concerning the
methane and combustion product film coefficients. Test data were
acquired in mid-contract and incorporated in the final design of the
thrust chamber.

Thrust Chamber Geometry

A conventional thrust chamber geometry with an 80 percent length bell
nozzle was utilized. The nozzle contour produced maximum performance

within a given length. A combustion chamber characteristic length of 30 inches (76cm) was selected from performance considerations. The selected chamber contraction ratio of 4 was based on Ref. 5, which indicated higher contraction ratios resulted in reduced heat load to the regenerative coolant. A convergence half-angle of 15-degrees (0.26rad) was selected and is representative of current production thrust chambers.

Coolant Passage Parameters

The regeneratively-cooled thrust chambers were of channel (nontubular) construction throughout (including the high area ratio nozzle portion). A channel is characterized by four dimensions. For a given thrust chamber, specification of these dimensions and the number of channels as a function of axial length is necessary to define a channel design:
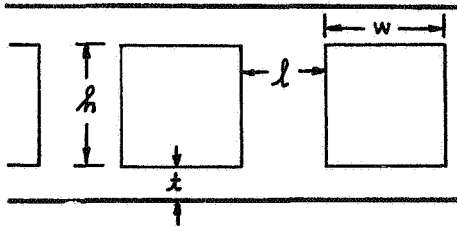
$w = w(X)$ = channel width

$\ell = \ell(X)$ = land width

$t = t(X)$ = wall thickness

$h = h(X)$ = channel height

$n = n(X)$ = number of channels

where $X = 0$ is the throat position.

For this parametric investigation, a simplified description of the channels in which the land width and wall thickness were held constant:

$$\ell(X) = \ell(0)$$
$$t(X) = t(0)$$

was used to permit rapid evaluation.

26

The number of channels was allowed to vary through the use of branches or splices. The branch points were selected from stress considerations. This approach represents the minimum pressure drop design as it allows high design wall temperatures throughout the chamber.

At the peak heat flux position, channel height was made equal to channel width, and both this dimension and the land width were selected based on the maximum allowable wall temperature. If a minimum width limit were encountered, the width was set equal to the limiting value and the height adjusted to give the maximum allowable wall temperature. With the land width constant, channel width variation with length is determined by thrust chamber geometry. Channel height is adjusted to give the desired gas-side wall temperature profile.

A cooling evaluation of nickel, stainless steel, and Hastelloy X over a range of chamber pressure in Reference 5, indicated that nickel was superior at high heat flux levels (high pressure) due to high thermal conductivity. At lower chamber pressure, the choice of material was not critical from a cooling standpoint. Nickel was, therefore, used for the thrust chamber.

Restrictions were placed on the channel dimensions based upon consideration of fabrication ease. Based on standard machining procedures, a minimum hot-gas wall thickness is 0.020-0.025 inches (0.051-0.063 cm). The 0.025-inch (0.063 cm) wall (constant along the chamber length) was used as nominal and the thinner wall was investigated in the perturbation studies. These wall thicknesses are most beneficial in reducing coolant pressure drops or wall temperature in the combustor and in the throat region. In the nozzle thicker walls may be preferred.

The minimum dimensions for channel width (0.040-inch - 0.102cm), height (0.025-inch -0.063cm) and land width (0.030-inch -0.076cm) also represent nominal machining limits based upon standard tolerance considerations.

Based on the wall thicknesses used in this analysis, a maximum allowable surface temperature, 1700 F (1200K), was specified for nickel. By maintaining the wall temperature constant at this maximum value throughout the thrust chamber, pressure drop would be minimized. However, in the low heat flux regions of the nozzle, the channel height necessary to maintain this temperature would be high. To make the nozzle designs reasonable from a weight standpoint and the resulting pressure drop information more realistic, the design wall temperature in the nozzle was reduced to 1000 F (810K). Channel height at nozzle exit was typically reduced by a factor of two with thrust chamber weight decreased by 30 - 40 percent.

Combustion-Gas Flow Field

The estimation of the convective heat input is very strongly dependent on local combustion-gas mass velocity (ρV) at the edge of the boundary layer. The mass velocity at the edge of the boundary layer is determined from the combustion-gas potential flow field in the vicinity of the wall. In the combustion zone, the combustion-gas flow is taken to be uniform and parallel with local wall mass velocities obtained from one-dimensional flow considerations. In the region of the throat a modified Sauer transonic flow field solution is utilized to determine the wall sonic point. This usually occurs only a few degrees upstream of the geometric throat. Use of a one-dimensional flow field in the nozzle can result in

28

considerable error. Therefore, an axially symmetric flow field analysis (method of characteristics) was used to supply the correct gas mass velocity at the wall.

Combustion-Gas Convective Heat Input

An integral boundary layer approach was used to predict gas-side film coefficients. This approach, as described in Ref. 5, requires definition of the point of boundary layer initiation and an initial energy thickness. In the absence of FLOX/methane test data in the desired region, specification of these initial conditions was made from results of previous investigations.

Peak heat flux values are about 20 Btu/in^2-sec ($3270j/cm^2$-sec) at 1000 psia (68.9 kN/M^2) with the peak heat flux occurring slightly upstream of the geometric throat. Heat flux levels in the nozzle are lower than predicted by simplified Bartz equation. The accuracy of the boundary layer equations in the nozzle has generally been substantiated by data taken under NASA Contracts NASw-1229 and NAS3-11191 (Ref. 3 and 1).

Coolant Side Assumptions

The cooling analysis used methane only as the coolant. An upper limit of 1500 F (1090K) was placed on the methane temperature to prevent decomposition. An up-pass cooling circuit was selected based on Ref. 5. A standard semiempirical relationship for forced convection turbulent flow of the Dittus-Boelter form was selected. The coolant properties were based on a film temperature as recommended by McAdams (Ref. 6). The film temperature utilized was the arithmetic mean of wall and bulk temperature.

The basic relationship is given below.

$$N_{Nu} = 0.023 \ N_{Re}^{0.8} N_{Pr}^{0.4} \emptyset_c \emptyset_R \emptyset_{entrance}$$

The factors, $\bar{\emptyset}_c$ and $\bar{\emptyset}_R$, represent curvature and wall roughness enhancement on the basic cooling capability. The factor, $\bar{\emptyset}_{entrance}$, is an entrance region enhancement factor which is very small for this up-pass cooling method. Based on considerable heated curved tube experimental data with hydrogen and nitrogen tetroxide (Ref. 7 and 8), the nozzle downstream curvature was designed to achieve peak curvature enhancements of 1.5.

The enhancement effect of surface roughness was not considered in the parametric investigation ($\bar{\emptyset}_R$ = 1.0) due to the uncertainty of correlating the roughness parameter with film temperature properties. In general, roughness enhancement values could amount to about a 10- to 20-percent increase in methane cooling capability based upon experimental results for hydrogen. A nominal surface roughness of 100×10^{-6} inches (254×10^{-6} cm) was used in the pressure drop calculations. The total jacket pressure losses include the momentum loss and exit manifold loss (one head).

COOLANT TEMPERATURE RISE

The exit bulk temperature of the methane regenerative coolant was determined as a function of various parameters. It was found in Ref. 5 that propellant mixture ratio had a negligible effect on the integrated heat input to the thrust chamber, and the heat load was described as a function of chamber geometry, chamber pressure, and wall temperature profile.

The coolant enthalpy rise was determined from the total heat load (with corrections for carbon layer) and coolant flowrate. The latter parameter is directly related to mixture ratio and specific impulse, such that the

$$\Delta H = \frac{\Sigma Q}{\dot{W}_c} = Q \cdot \frac{Q_m}{Q_p} \cdot \frac{I_{sp} \ (1 + MR)}{F}$$

The resulting methane coolant exit temperatures as a function of the previously noted parameters are presented in Fig. 4 for an inlet temperature of 173 R (96K). Higher inlet temperatures are reflected almost exactly in equivalent higher exit temperatures for the nominal high exit values of interest. The highest exit temperature noted (Fig. 4) is about 1260 R (700K) for the case of Q_m/Q_p = 1.0, 1000 psia (6890 kN/M^2) pressure, 100:1 nozzle area ratio, and a 5.7:1 mixture ratio. This would be about 80 R (44K) higher for the maximum inlet temperature of 260 R (144K) being studied. Temperatures are about 125 and 275 R (70 and 153K) lower for Q_m/Q_p = 0.9 and 0.76, respectively. The exit temperature was estimated for throttled conditions. Exit temperature values are shown in Fig. 5. Temperatures for the 10:1 throttled condition were 250 - 300 R (139-166K) higher than the full thrust values.

COOLANT PRESSURE LOSS

Parametric regenerative cooling pressure losses were determined based on detailed cooling channel designs for the parameters of interest. A parametric study of two-dimensional heat flow effects in channels was conducted. The results of the 2-D analysis were used in conjunction with the peak heat flux levels to determine the channel spacing. The minimum land width encountered in this study is about 0.045 inches (0.114 cm) based upon the peak heat flux value of 20 Btu/in.^{2}-sec (3270 j/cm^2-sec). Since the parametric study is with constant land width designs, the throat represents the most severe region.
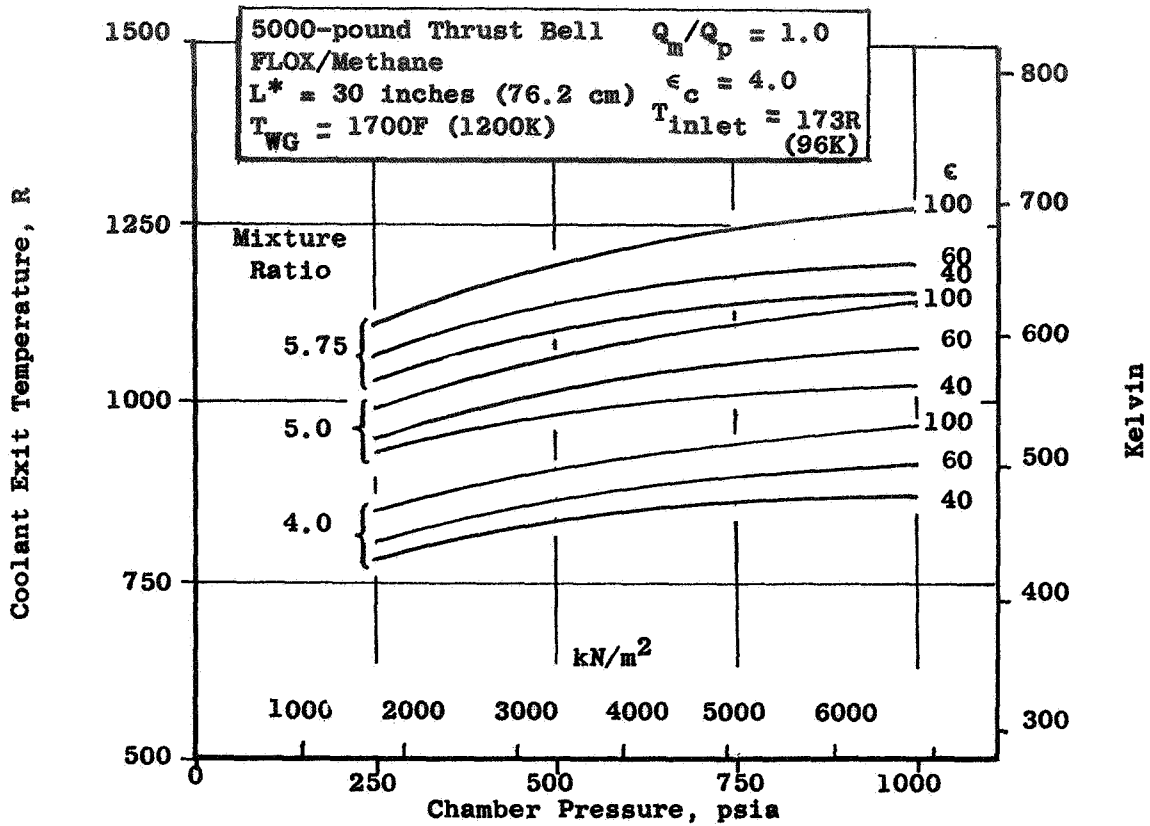
Figure 4.   Coolant Exit Temperature vs Chamber Pressure
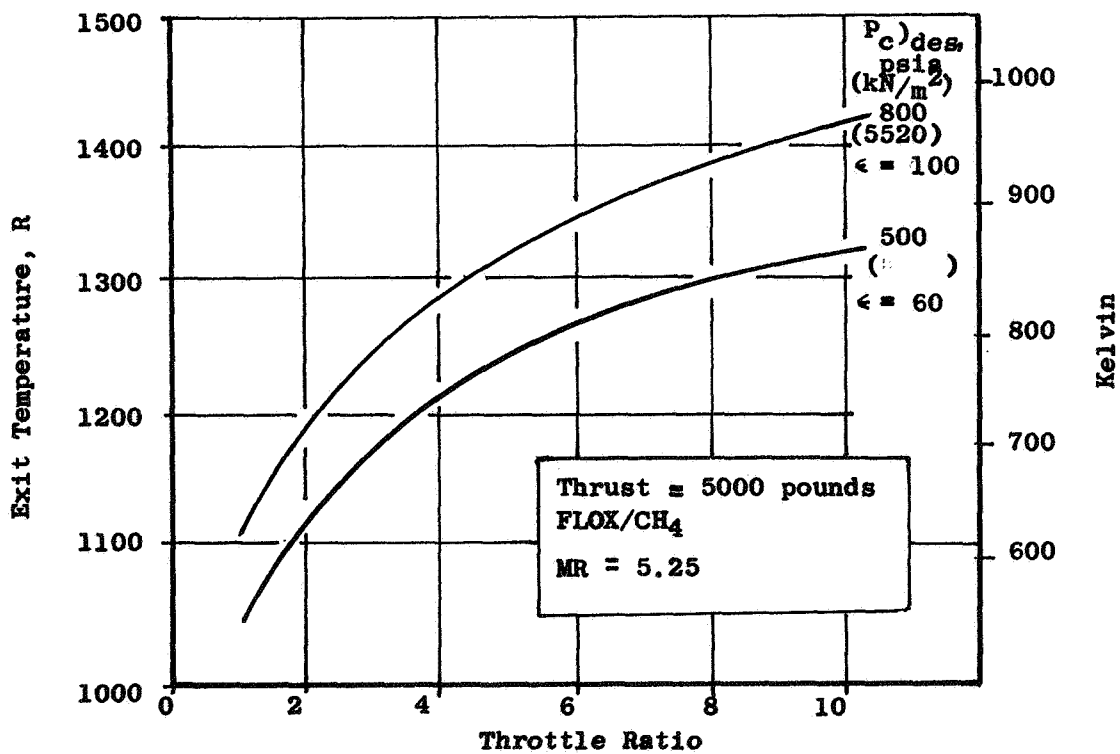
Figure 5.   Fuel Exit Temperature vs Throttle Ratio, Nozzle Area Ratio and Mixture Ratio ($Q_m/Q_p = 1$).

32

The results of the parametric pressure drop evaluation are presented in Fig. 6 through 9, Figure 6 shows the effect of chamber pressure and required jacket outlet pressure on coolant pressure drop for Q_m/Q_p = 1.0. The lower pressure drop at higher coolant pressures results from the increased methane density. It is apparent that high outlet pressures as would be associated with an expander cycle can reduce the coolant pressure drop by a factor of two. The coolant pressure drop increases markedly with chamber pressure (due to increased heat flux level) but is still quite reasonable ($\sim$50%) even at 1000 psia (6890 kN/M^2) chamber pressure.

The effect of Q_m/Q_p is shown in Fig. 7. This factor is the most significant parameter in terms of affecting pressure drop. The pressure drop is reduced by a factor of four at high pressure if the lowest value (Q_m/Q_p = 0.76) is assumed. A 10-percent increase in heat load at 1000 psia (6890 kN/M^2) raises the pressure drop from 40 to 60 percent. A 25-percent increase in head load was found to result in a coolant pressure loss in excess of 100 percent of chamber pressure.

Coolant mixture ratio effects are described by Fig. 8. At the indicated inlet temperature, the effect of mixture ratio variation is not particularly significant, amounting to less than 50 psi (3.44 kN/M^2) difference in coolant pressure loss over the range considered (4.0 $\leq$ MR $\leq$ 5.7). Increasing the inlet temperature to 260R (144K) results in a more substantial effect ($\sim$140 psi (970 kN/M^2) difference between extremes) of mixture ratio on pressure drop.

The effects of nozzle area ratio variation are shown in Fig. 9. Area ratio effects are even less significant than mixture ratio. At a chamber pressure of 1000 psia (6890 kN/M^2) and a low inlet temperature (Fig. 9), less than 8 percent pressure drop variation separates ϵ = 40 and ϵ = 100 designs. At 260 R (144K) inlet temperature the pressure loss difference increases to about 16 percent.
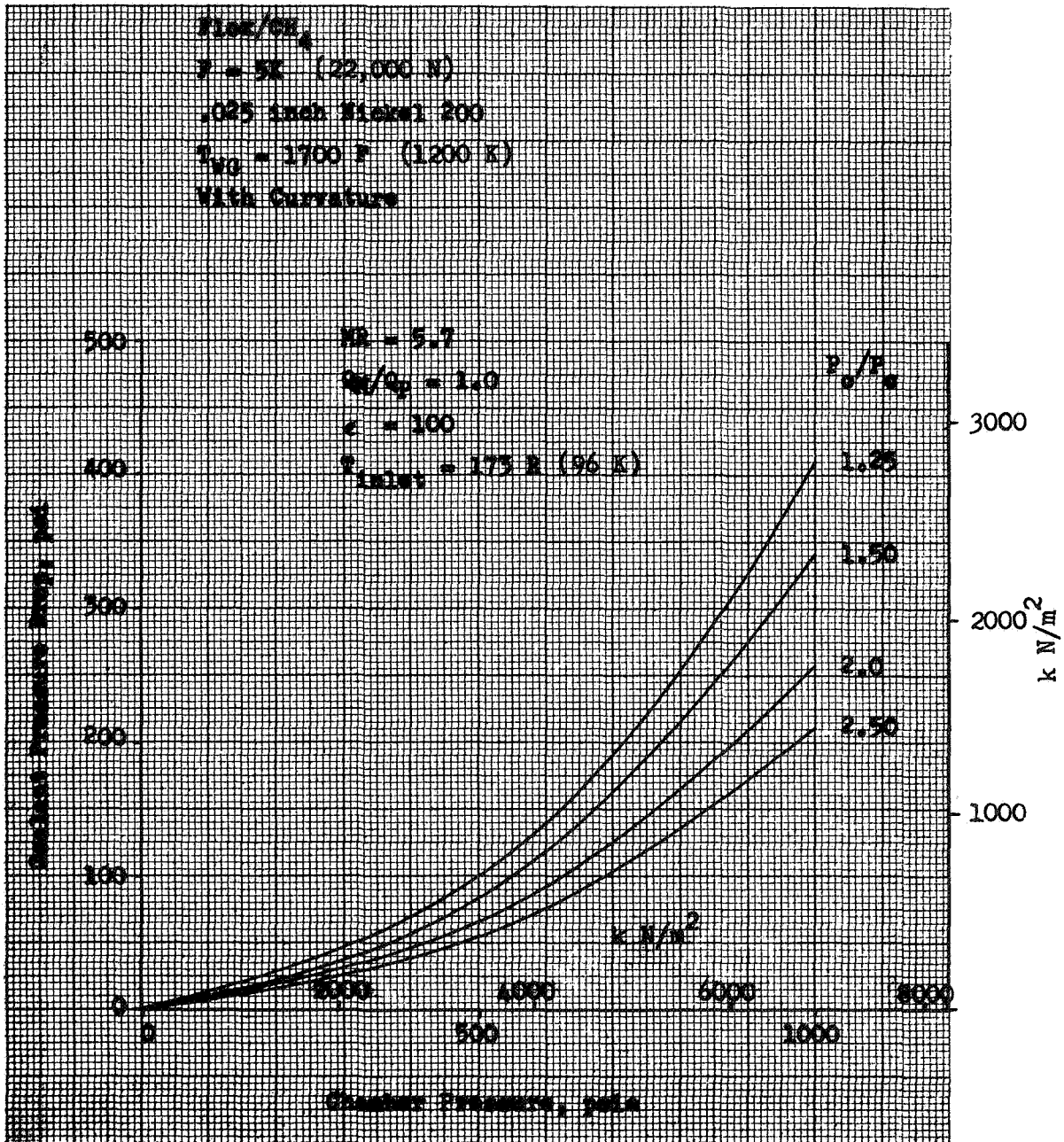
Figure 6. Coolant Pressure Drop vs Chamber Pressure and Relative Coolant Outlet Pressure.
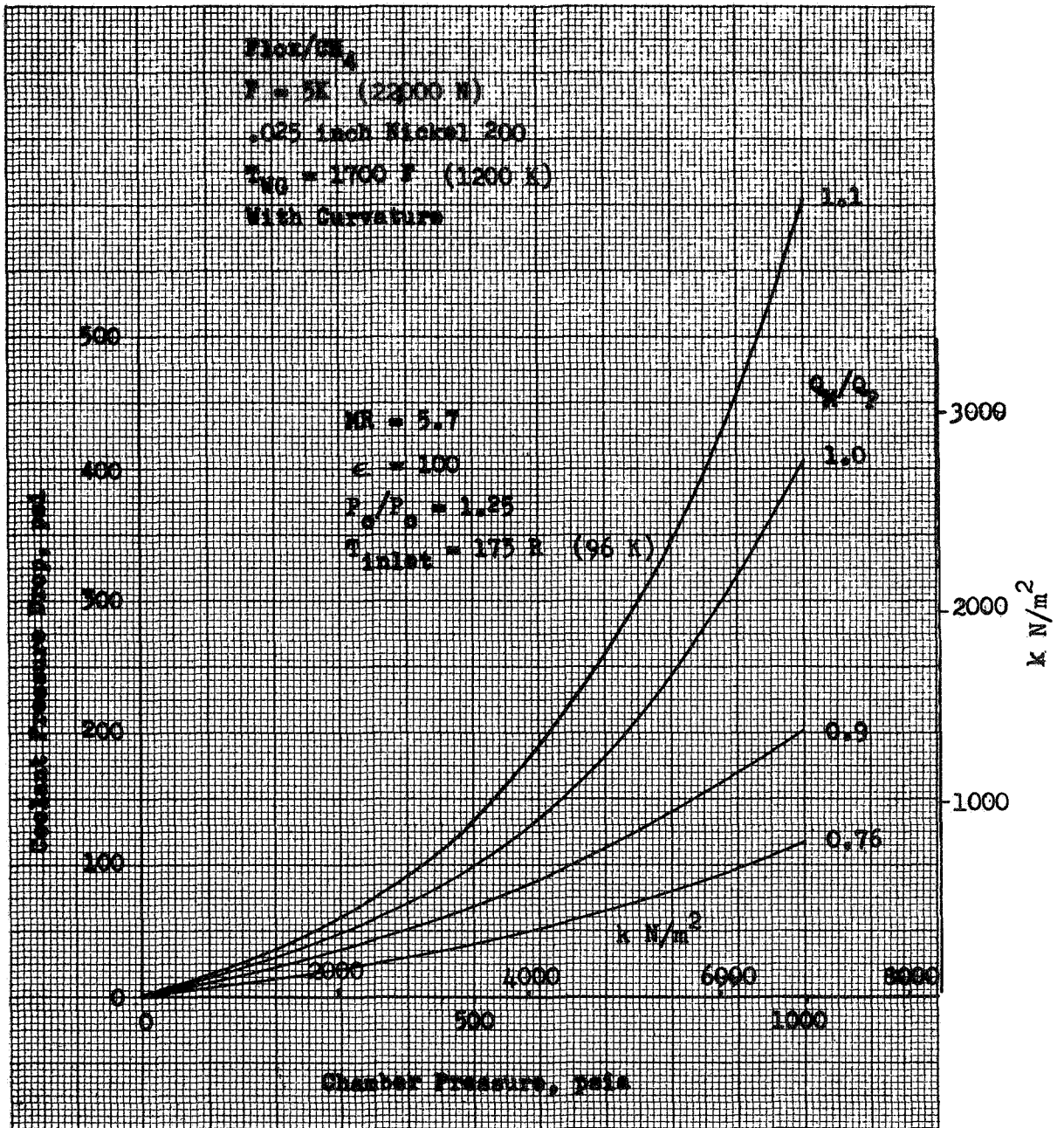
Figure 7. Coolant Pressure Drop vs Chamber Pressure and Relative HeatFlux Level.

35
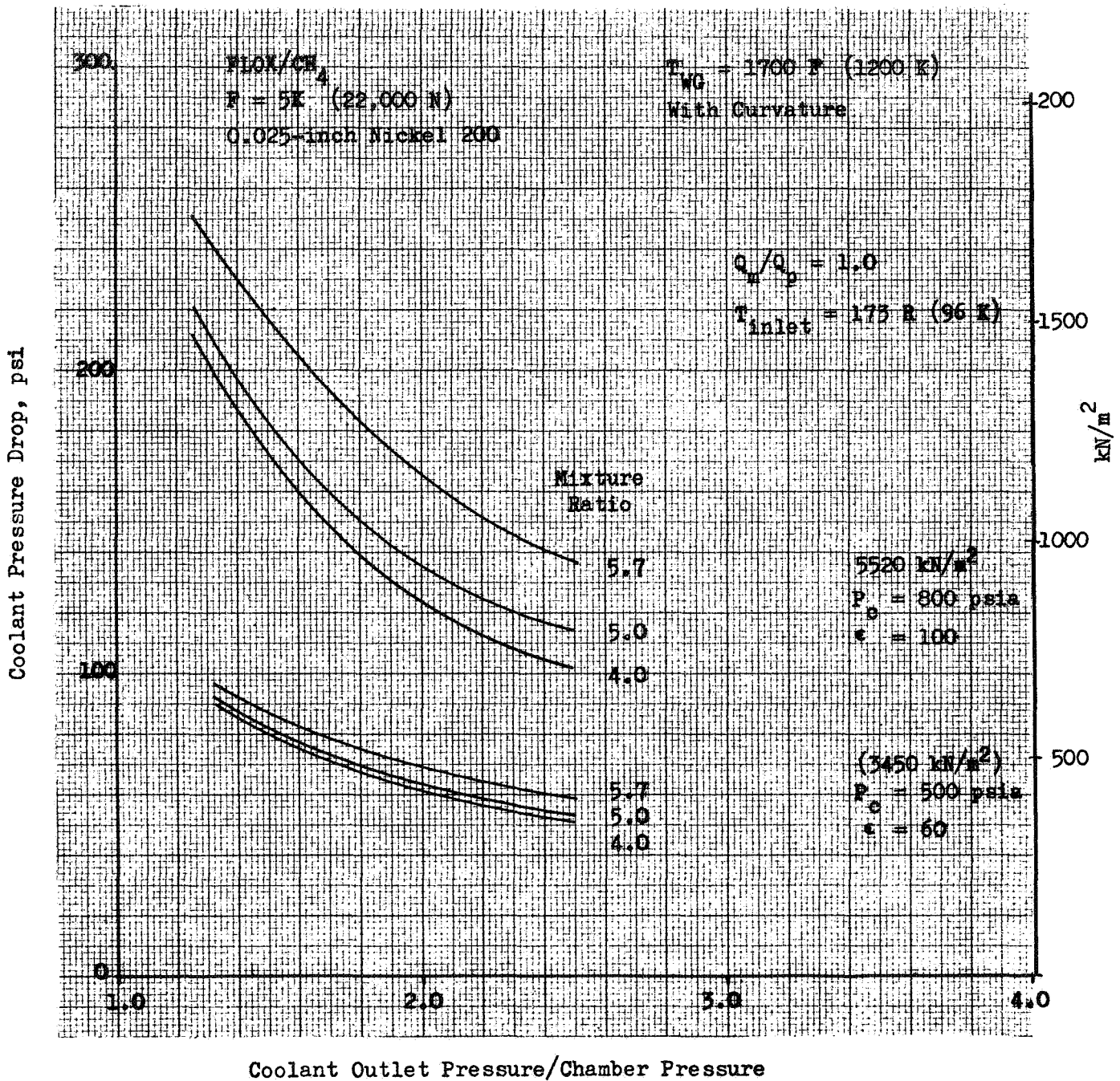
Figure 8. Coolant Pressure Drop vs Ratio of Coolant Outlet Pressure/
Chamber Pressure, Chamber Pressure, and Mixture Ratio,
FLOX/CH$_4$, F = 5K
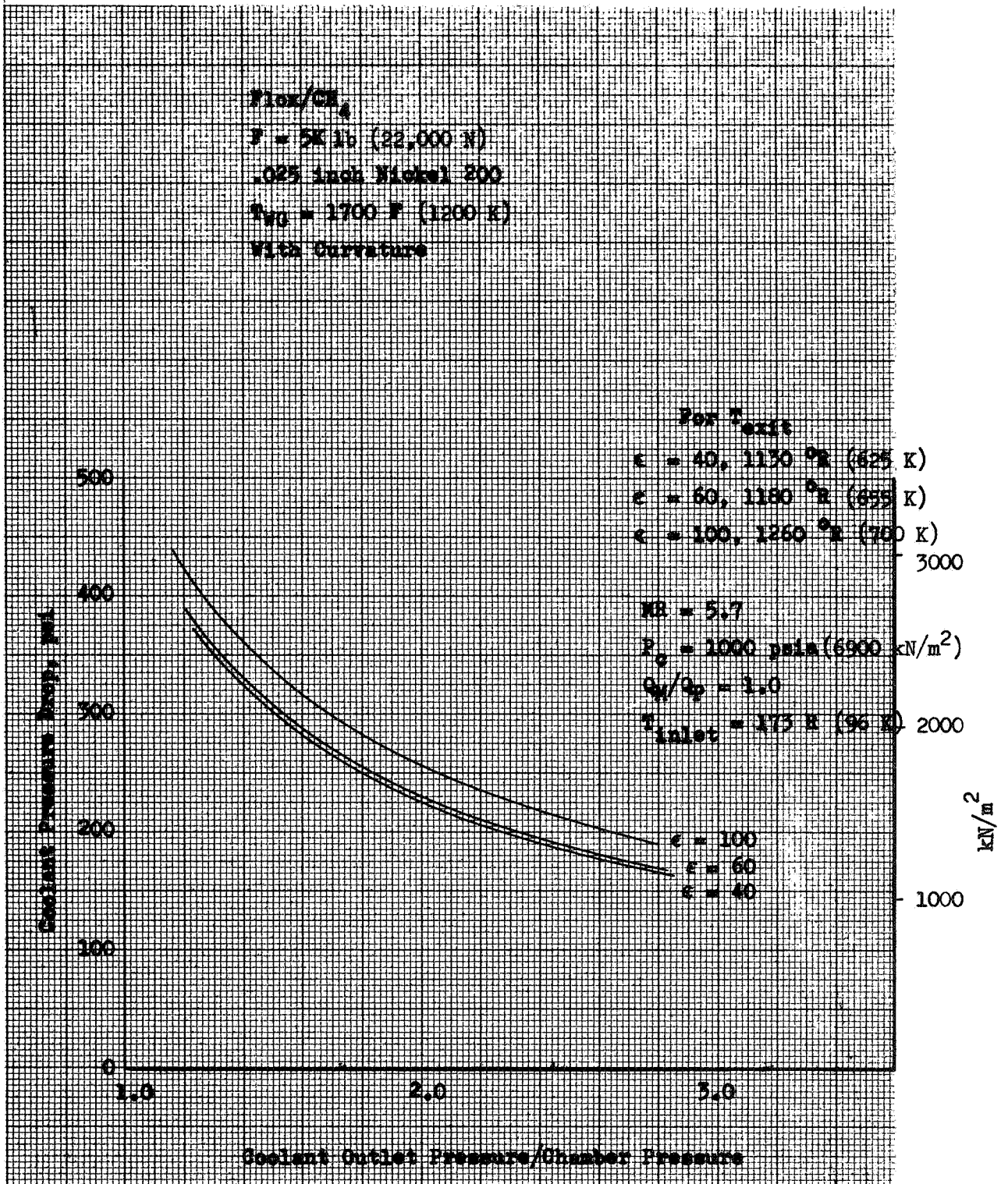
Figure 9. Coolant Pressure Drop vs Ratio of Coolant Pressure/Chamber
Pressure and Area Ratio FLOX/CH$_4$, F = 5K.

CHANNEL DIMENSIONS

Channel and land width dimensions at the throat for the nominal heat
transfer ground rules are described in Fig. 10. All the dimensions
are within the acceptable region as defined earlier.

GROUND RULE PERTURBATION

The basic parametric study was extended to examine the effect of four
basic ground rules: (1) curvature enhancement, (2) hot gas wall
thickness, (3) gas-side film coefficient, and (4) channel taper.

The basic parametric study was extended to consider the effect of no
coolant curvature enhancement ($\emptyset_c = 1.0$) in the throat region. Under
such conditions, the required coolant mass flux must be increased to
compensate for loss of the curvature factor resulting in increased
coolant pressure drop. The basic trends are the same as previously
noted, except that the coolant pressure losses have increased as
expected. A direct comparison of the curvature effect is presented
in Fig. 11 for the case of $Q_m/Q_p = 1.0$. At the maximum chamber pressure,
deletion of curvature enhancement increases coolant pressure drop from
40 to almost 60 percent of chamber pressure.

The effect of the curvature enhancement factor on channel dimensions
is illustrated in Fig. 12. The case of a non-curvature enhancement
results in a square channel dimension less than 0.040 inches (0.102cm)
at 1000 psia (6890 kN/M^2) chamber pressure. At 800 psia (5530 kN/M^2)
the channel dimensions are above this value.
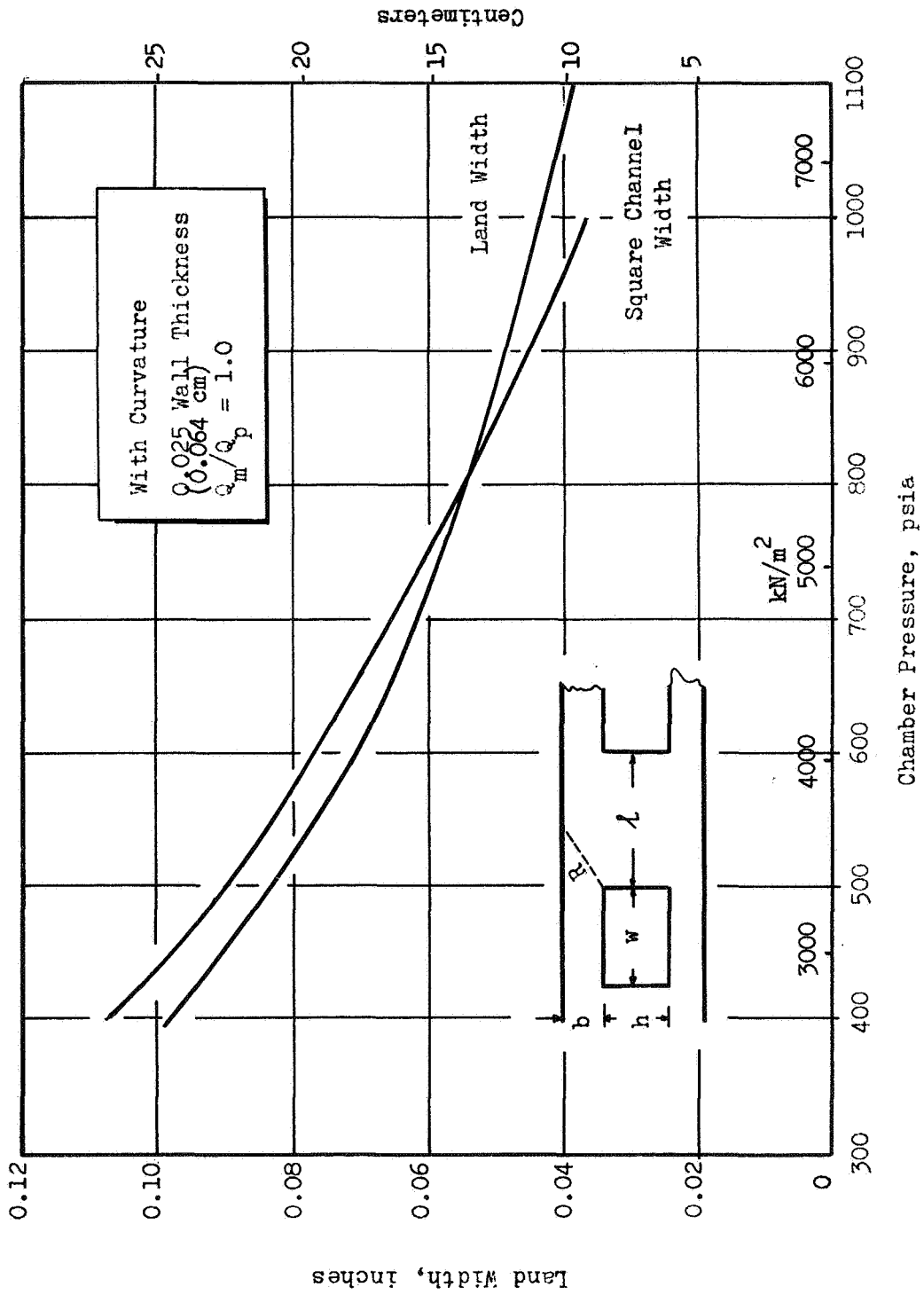
Figure 10. Land Width and Channel Dimensions.

39
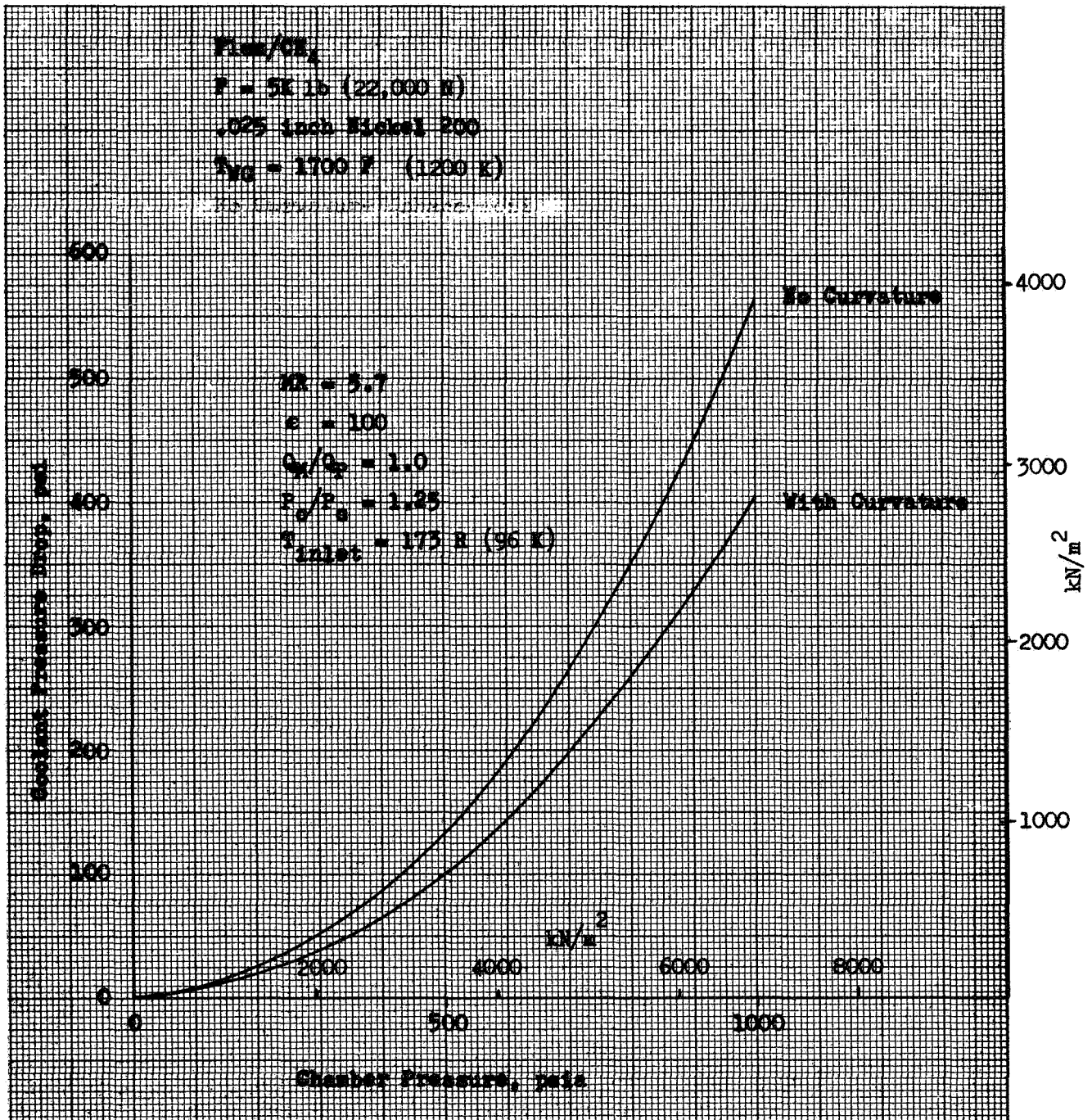
Figure 11. Coolant Pressure Drop vs Chamber Pressure and Curvature Enhancement.

The pressure drop without curvature enhancement can be reduced by thining the combustion-side wall thickness. The effect of reducing the thickness to 0.020 inch (0.051cm)was investigated at the maximum chamber pressure level, and the results are presented in Fig. 13. At a nominal $P_o/P_c = 1.25$, pressure drop is 430 psi, (2960 kN/M^2) which compares favorably with the basic curvature case and thicker wall. It should be pointed out that the pressure drop in all cases is reduced by thinning the wall. This also affects the channel dimensions and land width requirements (Fig. 14).

An alternate method of calculating gas-side convective film coefficients which is commonly used is the Bartz simplified equation. In general, this method predicts heat fluxes higher than the boundary layer approach. The resulting Bartz throat heat flux values are approximately 30-percent higher at the throat than comparable boundary layer equation values. These higher heat flux levels will reflect in higher coolant pressure losses at comparable chamber pressures. Parametric results using the Bartz relation are presented in Fig. 15 and 16.

In general, use of the Bartz simplified approach appears to limit the application of FLOX/methane propellants to chamber pressures of 800 psia (5520 kN/M^2) (for $\Delta P/P_c \leq 0.5$). The boundary layer approach would tend to indicate that chamber pressures of 1000 psia (6890 kN/M^2) are generally achievable. Resolution of these basic differences will not be possible until hot-firing data becomes available.
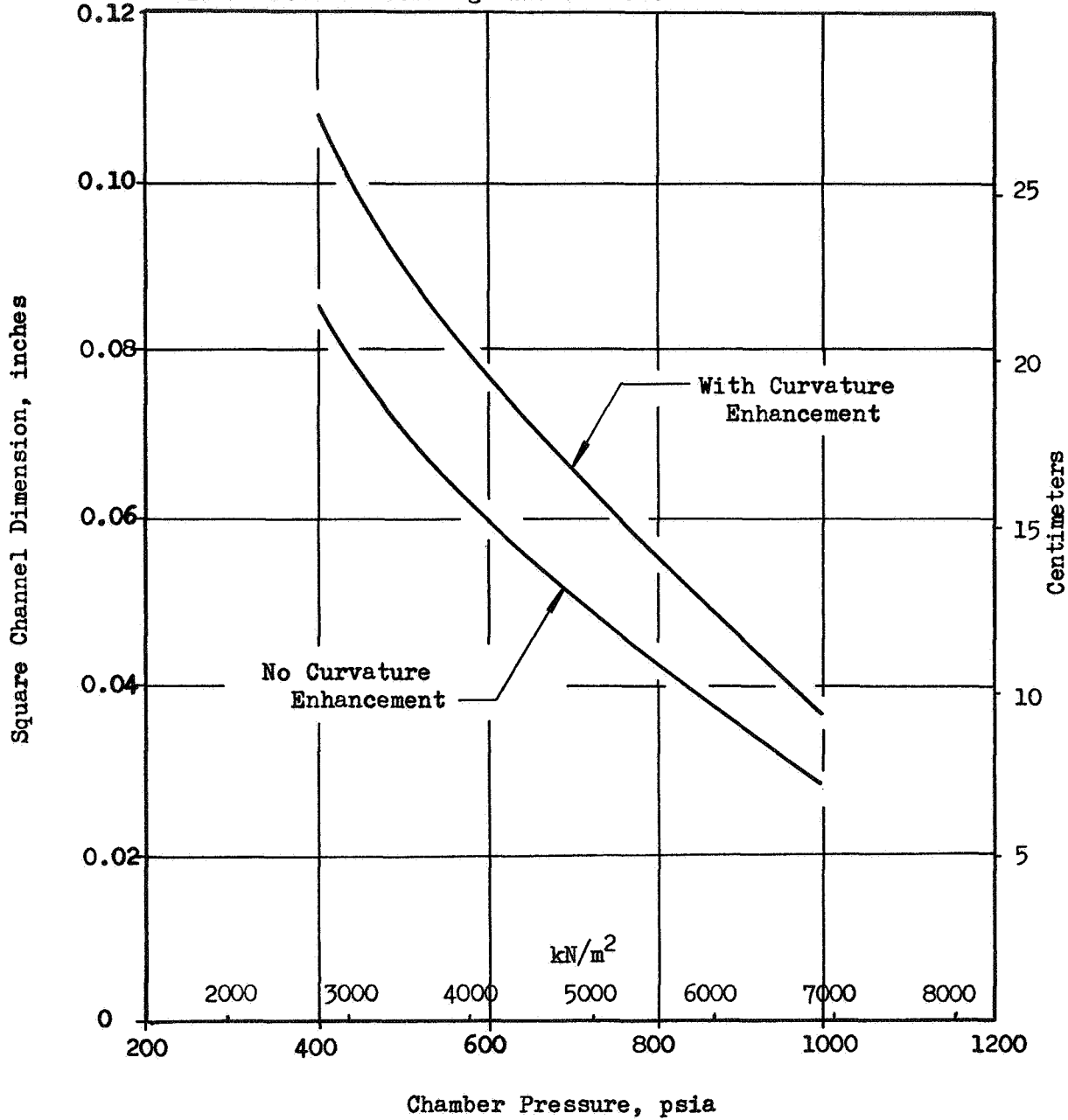
Figure 12. Minimum Square Channel Dimension Requirements.
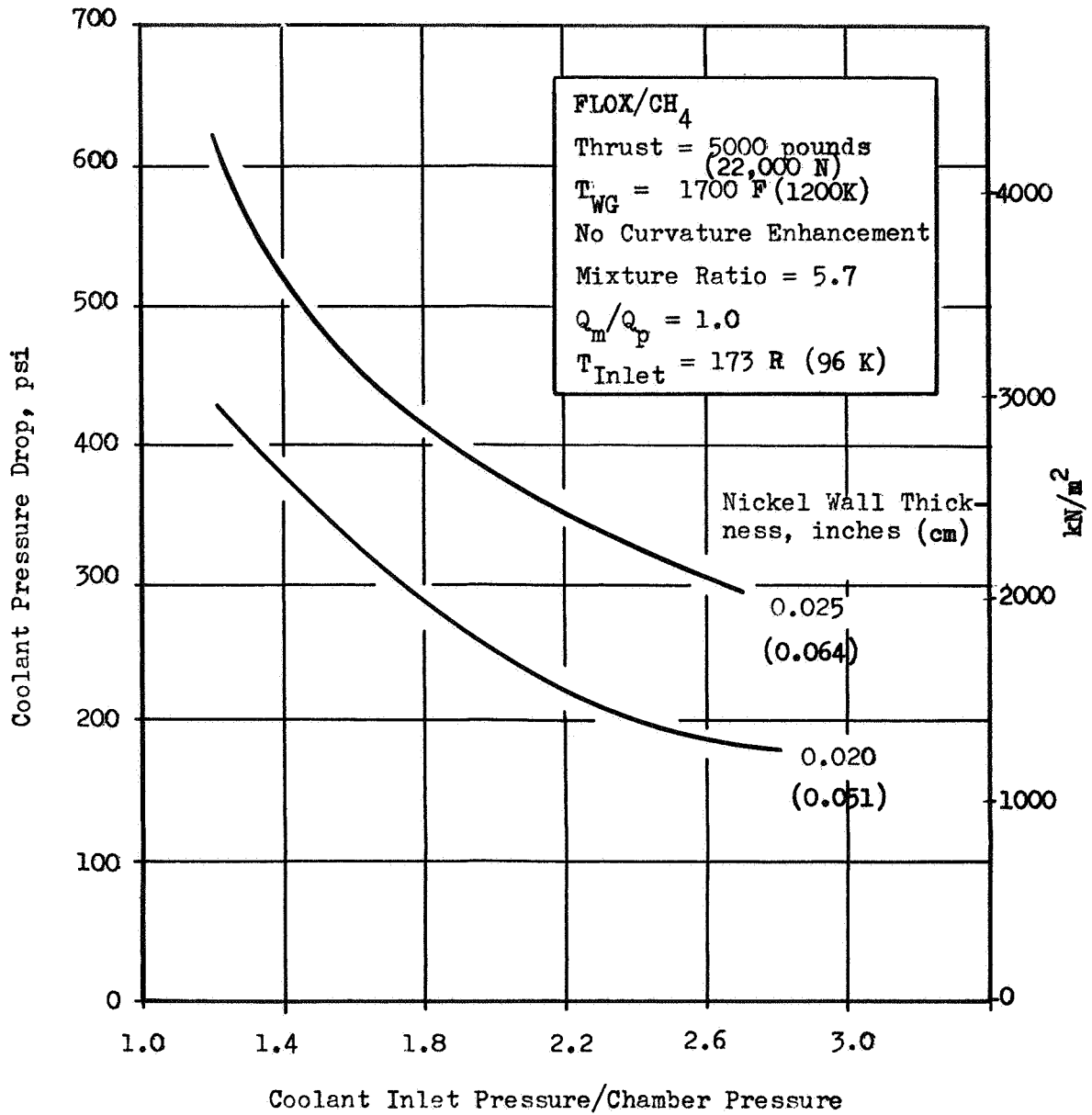
Figure 13. The Effect of Wall Thickness on Coolant Pressure Drop.

43
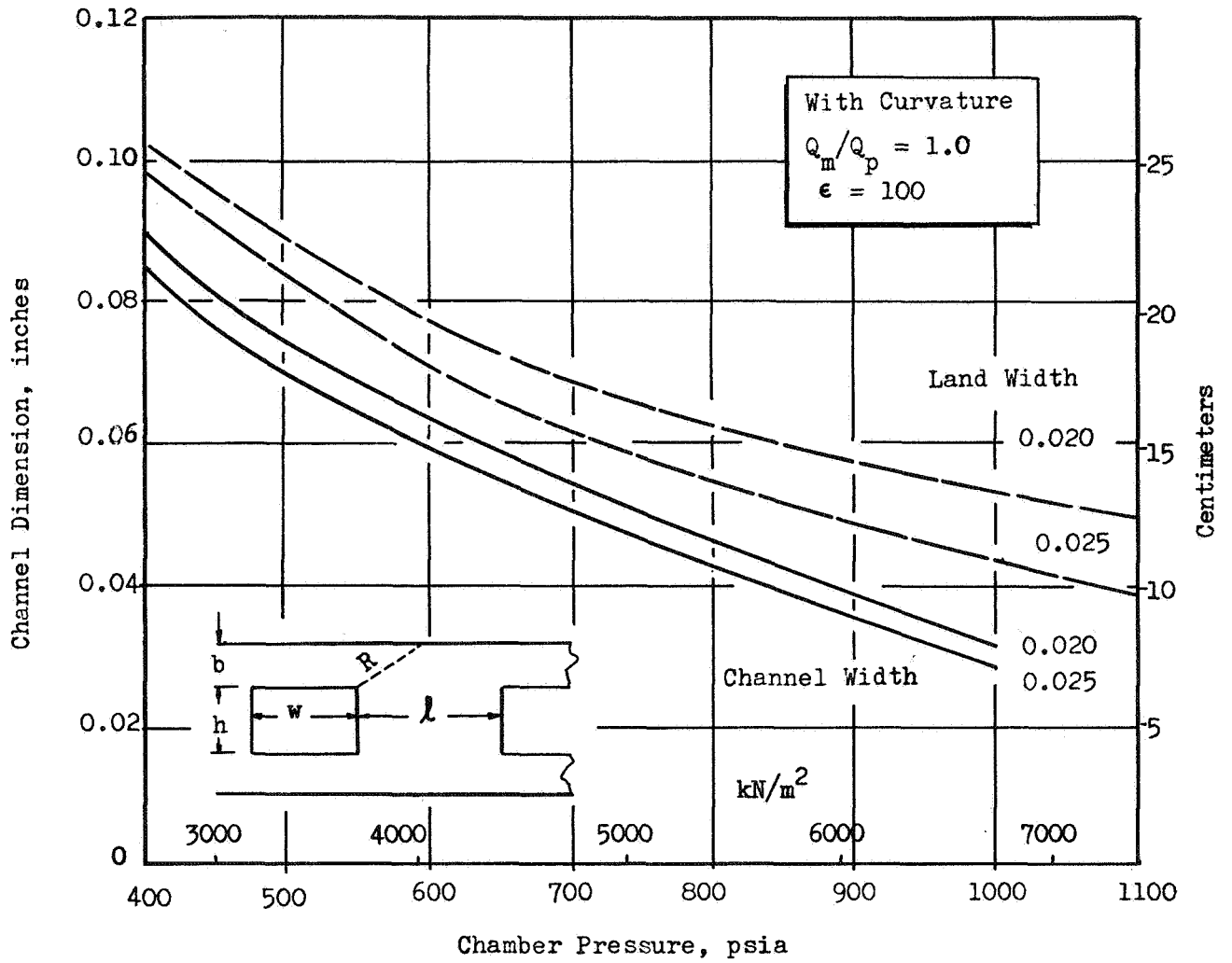
Figure 14 . Effect of Wall Thickness on Channel Dimensions

44
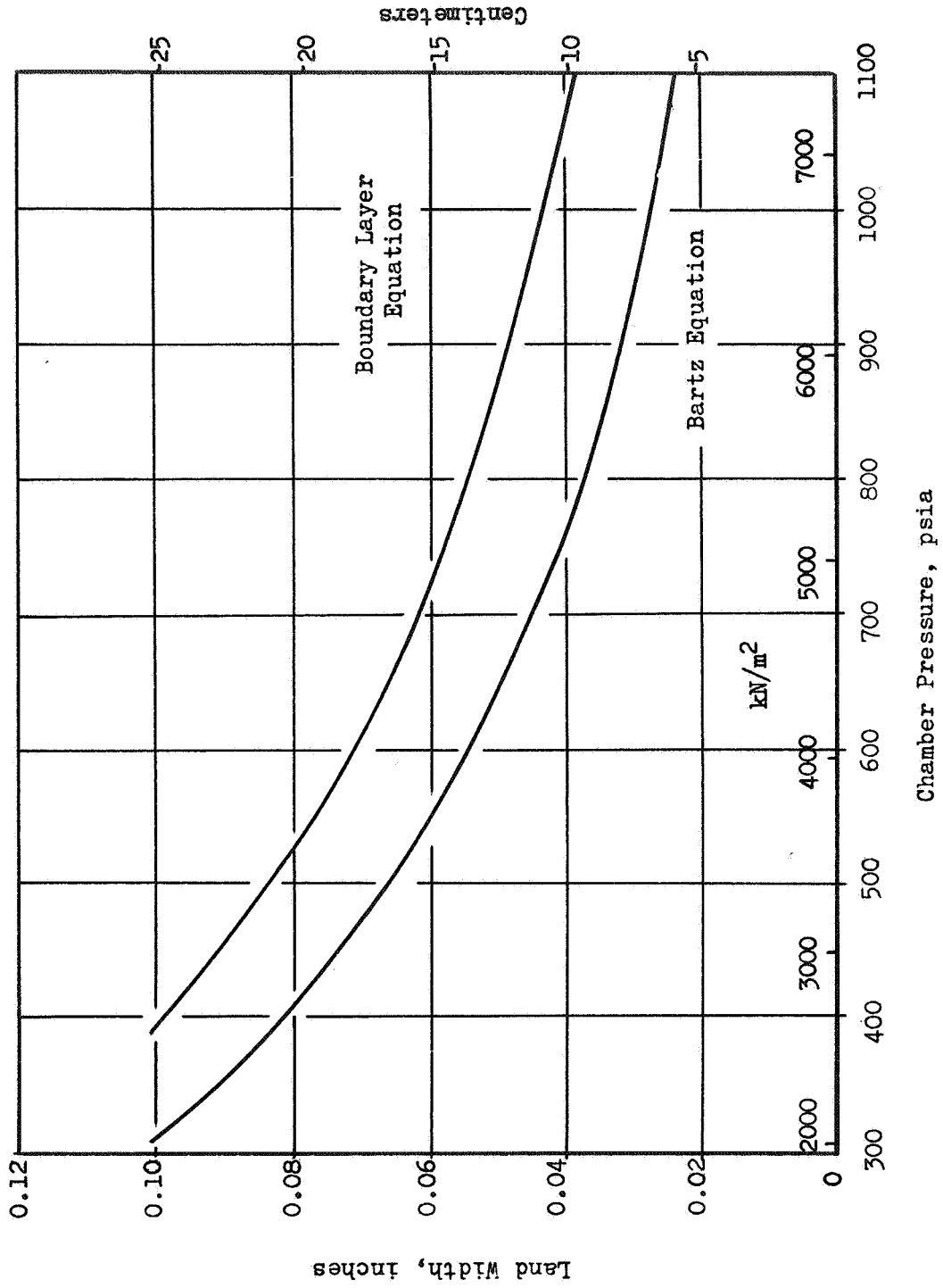
Figure 15. Effect of Heat Flux on Chamber Dimensions

45
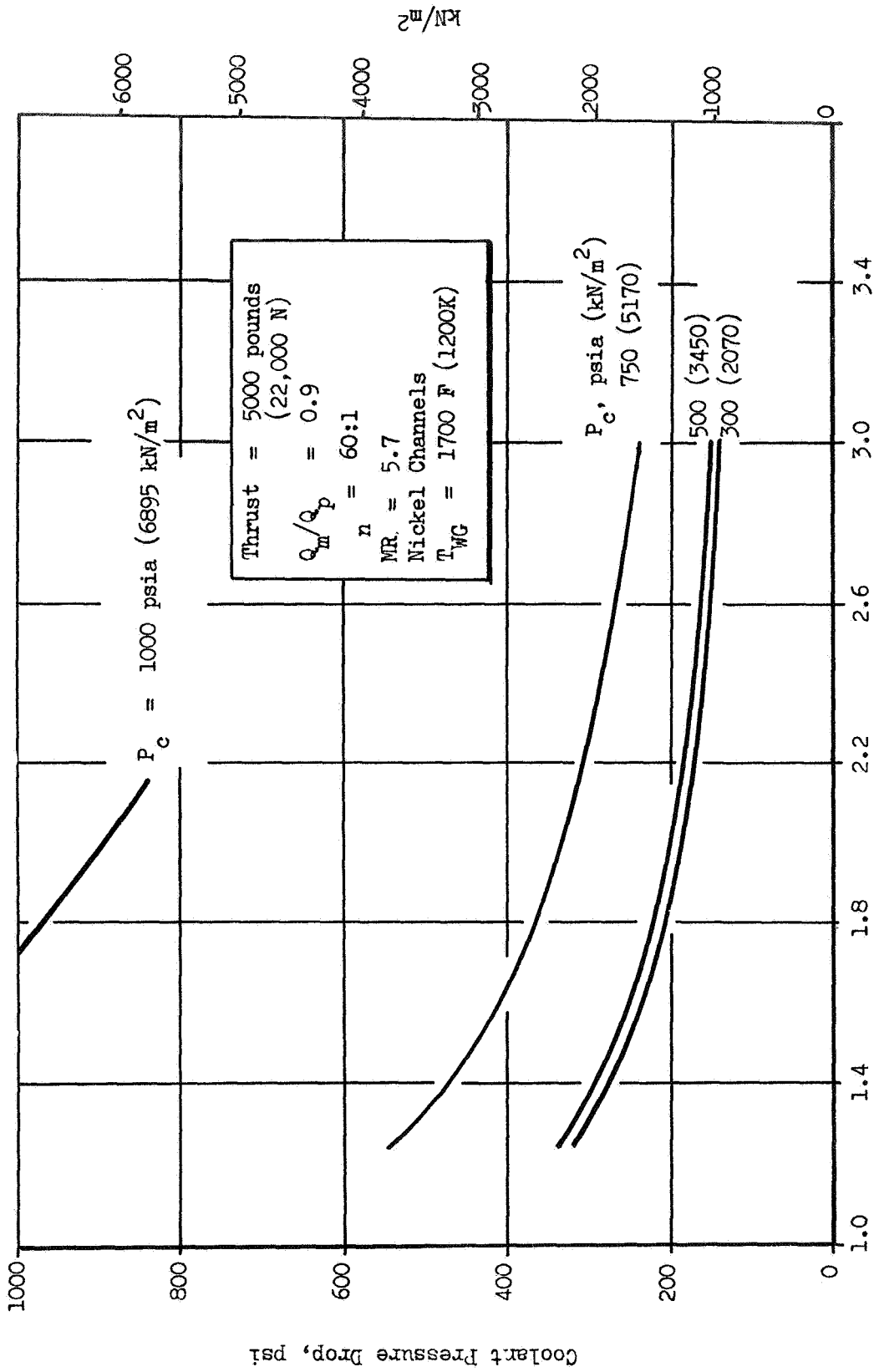
Figure 16. Coolant Pressure Loss for Regeneratively Cooled
Chambers Based Upon Bartz Equation

kN/m²

Coolant Outlet Pressure/Chamber Pressure

Coolant Pressure Drop, psi

Thrust = 5000 pounds
(22,000 N)
$\dot{Q}_m/\dot{Q}_p$ = 0.9
n = 60:1
MR. = 5.7
Nickel Channels
T_{WG} = 1700 F (1200K)

P_c = 1000 psia (6895 kN/m²)

P_c, psia (kN/m²)
750 (5170)
500 (3450)
300 (2070)

The effect of five basic channel design concepts on the coolant pressure drop and chamber weight was investigated. The results of the study are presented in Table 5 for the nominal chamber design parameters noted.

Concept 1 results in the minimum pressure loss and weight of the concepts considered. This is the design approach used in the previous parametric regenerative cooling studies. The tapered channel without splices (Concept 2) results in 55 psi (380 kN/m^2) and 1.5 pound (0.68 kg) increases in pressure drop and weight, respectively, over Concept 1. In this particular case, the maximum height in the nozzle was limited to minimize weight. This height limit results in a lower wall temperature in the nozzle. (See Table 5.)

Two approaches to Concept 3 were considered: 1) unlimited height, and 2) limited height. With no limit on nozzle channel height (other than that imposed by a maximum wall temperature) the pressure drop was comparable to that of Concept 2; the weight, however, was almost double. Limiting height to 0.050-inch (0.127 cm) resulted in comparable weight but increased pressure loss. Concept 4 is seen to result in both relatively high pressure drop and weight. Concept 5 appears to be superior to Concept 4 but inferior to concepts 1, 2, and 3, insofar as pressure loss and weight are concerned.

The primary benefit of the tapered channel concept is that the increased channel width decreases both the land width and the channel height. The constant width design can closely approach the tapered designs as the number of steps is increased.

47

TABLE 5

CHANNEL TAPER DESIGN CONCEPTS

MR = 5.0   Curvature Enhancement

P_c = 1000 psia(6890 kN/m^2)   Wall Thickness = 0.025-inch(.064 cm) (ϵ < 4)

ϵ = 60:1   = 0.040-inch(0.102 cm) (ϵ > 4)

Concept No.	Description	Pressure Drop, psi(kN/m^2)	Weight,* pounds (Kg)	Wall Temperature at Nozzle Exit, F (K)
1	Tapered channels with branching (branch points dictated by stress).	365 (2520)	18.5 (8.4)	1000 (811)
2	Tapered channels, no branching (maximum width limited by stress.	420 (2900)	20.0 (9.1)	-94 (203)
3a	Stepped width, no branching (no height limit).	422 (2910)	38.9 (17.6)	1000 (811)
3b	Stepped width no branching (height limited).	462 (3190)	23.4 (10.6)	-147 (174)
4	Constant width, no branching (height limited).	450 (3100)	42.0 (19.1)	-119 (189)
5	Constant width with branching (height limited).	513 (3540)	23.9 (10.8)	-165 (164)

*Weight includes 0.025-inch (0.064 cm) thick back-up panel

DESIGN POINT SELECTION

From consideration of the results of the parametric regenerative cooling analysis and FLOX/methane test information, two design points were selected (Table 6).

TABLE 6
THRUST CHAMBER DESIGN POINTS

Chamber Pressure, (kN/M^2) psia	Expansion Ratio	Thrust Chamber Mixture Ratio, (O/F)
500(3450)	60:1	5.25
800(5520)	100:1	5.25

From a review of the parametric cooling analysis chamber pressure values of 800 and 500 psia (5520 and 3450 kN/M^2) were selected as design points for further evaluation. With the nominal ground rules the pressure drop is over 400 psi (2760 kN/M^2) at a chamber pressure of 1000 psia (6890 kN/M^2) and channel width is near the region of fabrication difficulty. The perturbation analysis indicated that a change in any one of the ground rules concerning curvature, heat flux level or fabrication would significantly increase the pressure drop and fabrication difficulty at 1000 psia (6890 kN/M^2) chamber pressure. A chamber pressure of 800 psia (5520 kN/M^2) is the most reasonable maximum chamber pressure value for this engine. The chamber pressure of 500 psia (3450 kN/M^2) was selected as a design point where design feasibility is relatively unaffected by perturbations in the ground rules.

Mixture ratio has a relatively small effect on thrust chamber pressure drop, but significantly affects the methane exit temperature. For lower

mixture ratios the exit temperatures, particularly in throttling, are significantly lower than at a mixture ratio of 5.7. In addition, with FLOX/methane, injector mixing requirements are less strenuous at mixture ratio values below 5.7, the stoichiometric point, and high combustion efficiency should be easier to attain. This is indicated in FLOX/methane test results. A thrust chamber mixture ratio of 5.25 was, therefore, selected for both chamber pressures.

Thrust chamber expansion ratio makes little difference on pressure drop and ideally would be optimized for each chamber pressure. As an estimate of a near optimum value, equivalent thrust chamber envelopes were maintained. An expansion ratio of 100:1 was selected for 800 psia (5520 kN/m^2) chamber pressure and a value of 60:1 was selected for the 500 psia (3450 kN/m^2) chamber pressure.

REGENERATIVE THRUST CHAMBER DESIGN

Regeneratively-cooled thrust chamber design information was provided
for bell nozzle chambers operating at the two design points. Channel
dimensions and taper were optimized considering fabrication ease,
pressure drop and weight. For the resulting fixed thrust chamber and
channel geometry, certain operating conditions and ground rules were
perturbed and their effect on wall temperatures, pressure drop, and
coolant condition determined.

GROUND RULES AND ASSUMPTIONS

Most of the assumptions used were the same as for the parametric regenera-
tive cooling investigation. Nominal film coefficients were defined for
Q_m/Q_p = 1.0. A methane inlet temperature of 245R (136K) reflecting
potential end of flight conditions was used. Additional limitations
included a minimum 0.050-inch (0.127 cm) channel height in the nozzle
to reduce the possibility of plugging, and maximum gas side wall temp-
eratures of 1700F (1200K) in the throat and 1600F (1120K) in the
combustor. Stress limits were based upon a minimum safety factor of
2.0 with a wall pressure differential equal to the local coolant
static pressure. For determining the coolant side heat transfer coeffi-
cient the Dittus-Boelter equation was used, with no curvature or
roughness enhancement.

CHANNEL CONFIGURATION SELECTION

The principal factors considered in optimizing the channel design were
coolant pressure drop, channel weight, and fabrication costs. Channel
configuration alternatives are listed in Table 5. Throat dimensions
for these alternatives are selected based on the maximum allowable
wall temperature and the peak heat flux as described in Table 7.

TABLE 7

CHANNEL DIMENSIONS AT PEAK HEAT FLUX POSITION

Chamber Pressure, psia (kN/m^2)	Peak Heat Flux, $Btu/sec/in^2$ (J/cm^2-sec)	t(o) inches (cm)	w(o)=H(o) inches (cm)	ℓ(o) inches (cm)	n(o)
500 (3450)	11.0 (1797)	0.025 (0.064)	0.072 (0.183)	0.079 (0.201)	55
800 (5520)	16.6 (2712)	0.020 (0.051)	0.050 (0.127)	0.054 (0.137)	65

Channels with these dimensions can be fabricated with relative ease, since values less than 0.04-inches (0.102 cm) have been achieved with no difficulty in test samples. The 0.025-inch (0.063 cm) wall thickness can also be fabricated with relative ease and is sufficient for the 500 psia (3450 kN/M^2) chamber. The lower wall thickness of 0.020 (0.051 cm) inches is attractive for the 800 psia (5520 kN/M^2) chamber in terms of lower pressure drop and slightly larger chamber dimensions. This wall thickness can be fabricated but fabrication may be somewhat more time consuming than for the larger wall thickness.

Channel dimension variations upstream and downstream of the throat were investigated to select the best channel contour. As shown in Table 5, configurations ranging from a constant channel width design (Case 4), which minimize machining requirements, to designs with large variations in channel width (Cases 1,3) and more complex machining are considered. Channel height in the combustor was based on meeting allowable wall temperatures. In the nozzle lower wall temperatures were acceptable, and limits on channel height were imposed and the tradeoff between reduced nozzle weight and increased pressure drop was assessed.

An increased wall thickness in the nozzle was considered to reduce nozzle machining cost. Wall thickness values of 0.040 inches (0.102 cm) can reduce cost and in the low heat flux region the effect on pressure drop is slight. Channel width is limited by stress to some multiple of the wall thickness. The increased wall thickness in the nozzle will, therefore, allower wider channels.

Nozzle Optimization

Curves of nozzle weight as a function of nozzle pressure drop were generated for the different channel concepts to aid in selecting the optimum configuration. These are shown in Fig. 17 for the 500 psia (3450 kN/M^2) chamber pressure nozzle. A trade-off evaluation between thrust chamber weight and the effect of increased pressure drop or specific impulse indicated that teduction of weight should receive the most emphasis. The branched and tapered design is lightest, while the constant width, constant number design is heaviest. Second lightest design is the two-step design with a maximum 0.050-inch (0.127 cm) channel height in the nozzle. Since this is also second from a fabrication cost standpoint, it was chosen for the final design. The same result trends occur for the 800 psia (3520 kN/M^2) chamber pressure design. Again, the two-step design is only slightly heavier than the tapered design with no branches. Because of the cost, the two-step design was also chosen for the 800 psia (5520 kN/M^2) chamber (see following section).

Combustor Optimization

Most of the thrust chamber weight is in the nozzle, while most of the pressure drop is in the combustor and there is little trade-off between weight and pressure drop. In designing the combustor, a maximum throat wall temperature of 1700F (1200K) and a temperature in the combustion zone of 1600F (1140K) was used. Reducing the cylindrical combustor wall temperature to achieve additional margin results in additional pressure drop (see Fig. 18). Reducing the throat temperature produces an even greater pressure drop, although a 100F (56K) reduction is feasible. Higher pressure drops would occur with the 800 psia (5520 kN/M^2) chamber pressure design, and for the purpose of comparison it was decided to use the same wall temperatures for both cases.
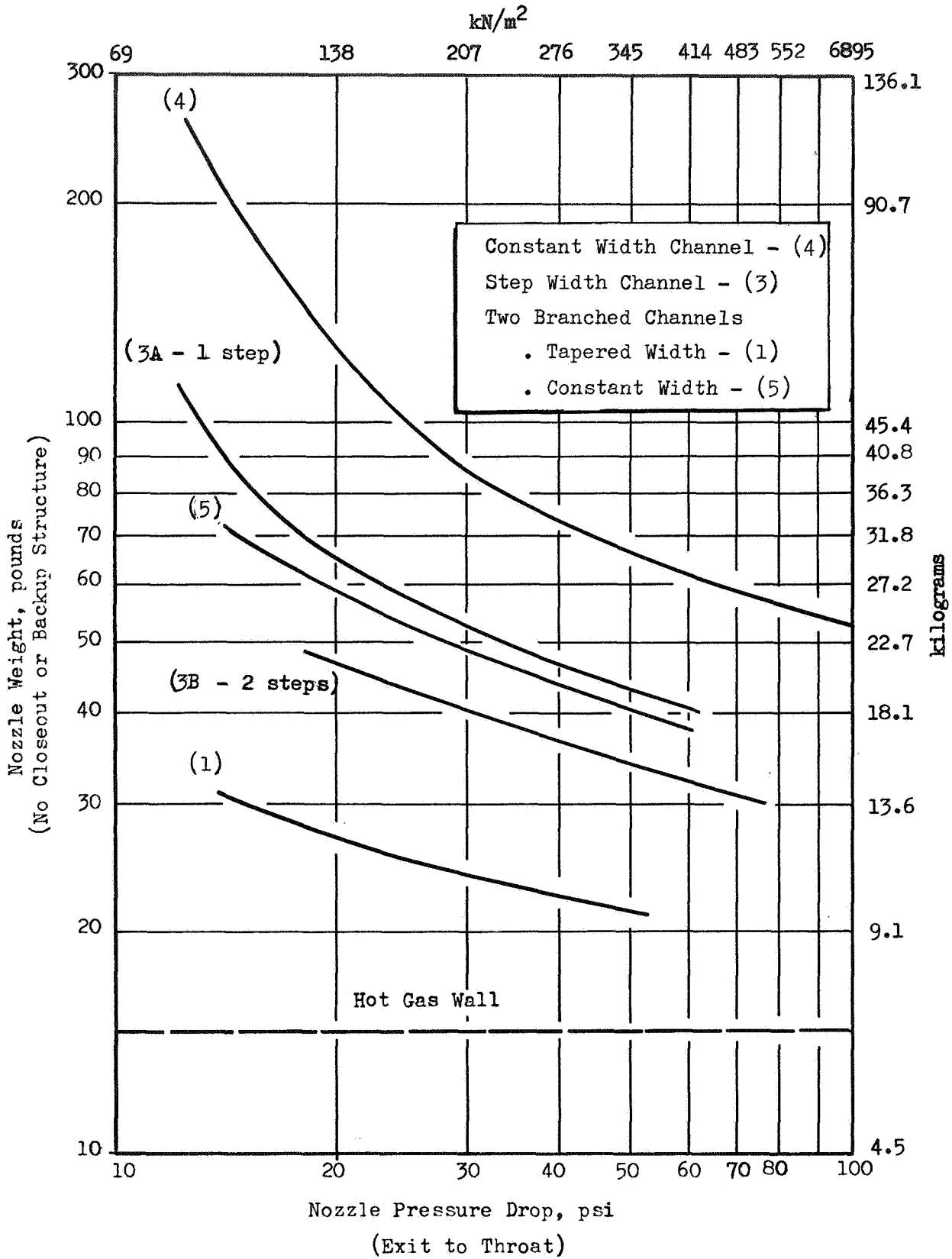
Figure 17. Channel Configuration Comparison
Chamber Pressure = 500 psia
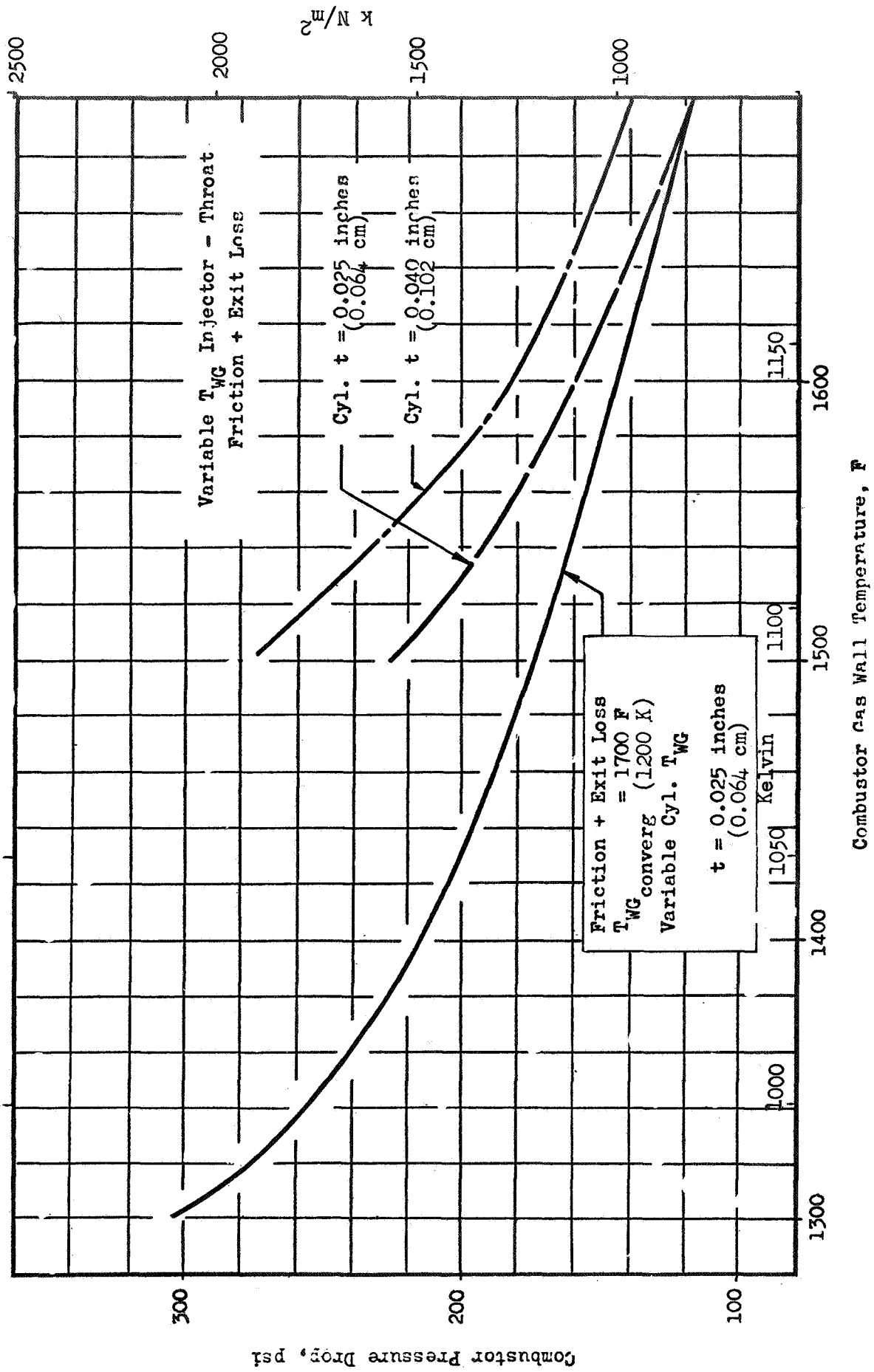
Figure 18. Effect of Wall Temperature on Combustor Pressure Drop.

55

Fabrication Evaluation

A brief study was conducted to determine the relative expense of manufacturing the different channel concepts. Table 8 describes the fabrication process used as a basis for the evaluation. Processes directly affected by the channel designs were evaluated in terms of required man hours and included in the relative cost comparison.

TABLE 8

GROUND RULES FOR FABRICATION EVALUATION

- Nickel 200 Thrust Chamber Blank
- Contour Machining to Inner/Outer Contours
- Machinery Set-Up
- Conventional Milling to Produce Coolant Channels
- Fill Channels with Wax
- Prepare Surface for Electroform
- Electroform Nickel to Close Out Channels
- Remove Wax Filler
- Final Machining and Clean Up

A relative comparison of the costs of the various concepts may be found in Table 9. The constant width, constant number of channels is cheapest but also heaviest. The most expensive is fully tapered channels with branching. Branching is expensive because of the additional number of channels required. Consequently, the most attractive designs from a fabrication standpoint are the constant width and the step width designs. The step designs will have a short taper transition section at the step to avoid additional pressure drop and also to provide a predictable flow field in this region.

TABLE 9

RELATIVE FABRICATION COSTS

(Excluding Setup Time)

Concept	Description	Machining Cost	Electroform Cost
4	Constant Width Channels	50%	100%
3A	One Step Variation in Channel Width	100%	100%
3B	Two Step Variation in Channel Width	135%	100%
1	Two Branched Channels, Tapered Width	500%	280%
5	Two Branched Channels, Constant Width	320%	280%

HEAT EXCHANGER DESIGN

The auxiliary heat exchanger cycle uses a nozzle heat exchanger to provide energy for the turbine working fluid (methane). Heat exchanger designs were provided based on heating a methane flow sufficient for nominal thrust turbine power.

Heat exchanger designs for this engine are described in Fig. 19 and 20. To obtain 1960R (1090K) temperature, the heat exchanger occupies the nozzle from an expansion ratio of 30 to the exit. Because of the small flows involved, this heat exchanger has 0.040 inch (0.102 cm) channels. The main coolant

57

FIGURE 19. HEAT EXCHANGER DESIGN
CHAMBER PRESSURE = 800 PSIA
[5520 kN/m²]
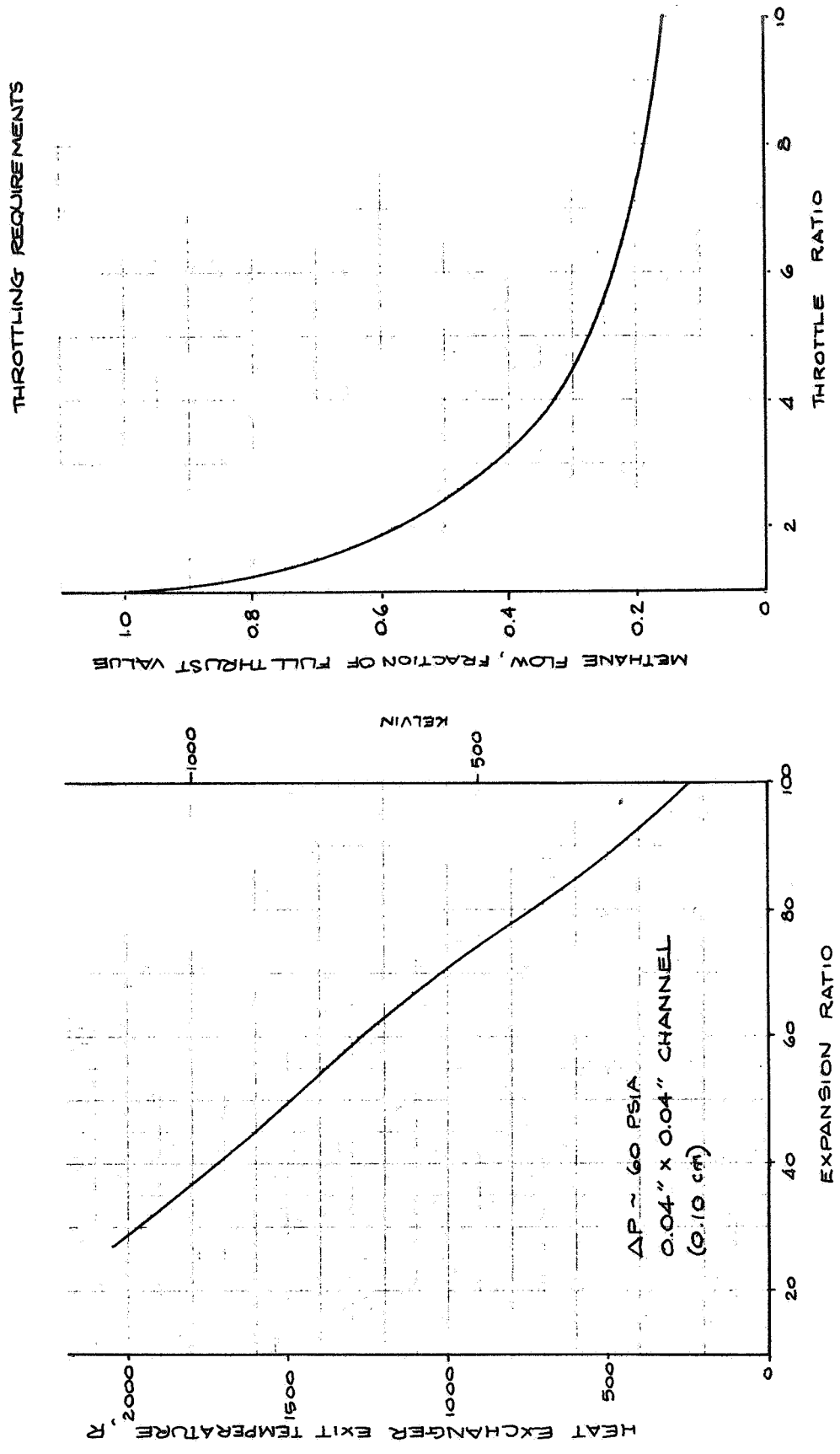
FIGURE 20. HEAT EXCHANGER DESIGN

CHAMBER PRESSURE = 500 PSIA
(3450 k N/m²)

THROTTLING REQUIREMENTS

METHANE FLOW, FRACTION OF FULL THRUST VALUE

THROTTLE RATIO

KELVIN

ΔP ≈ 30 PSI
0.04" x 0.04" CHANNEL
(0.10 cm)

HEAT EXCHANGER EXIT TEMPERATURE, °R
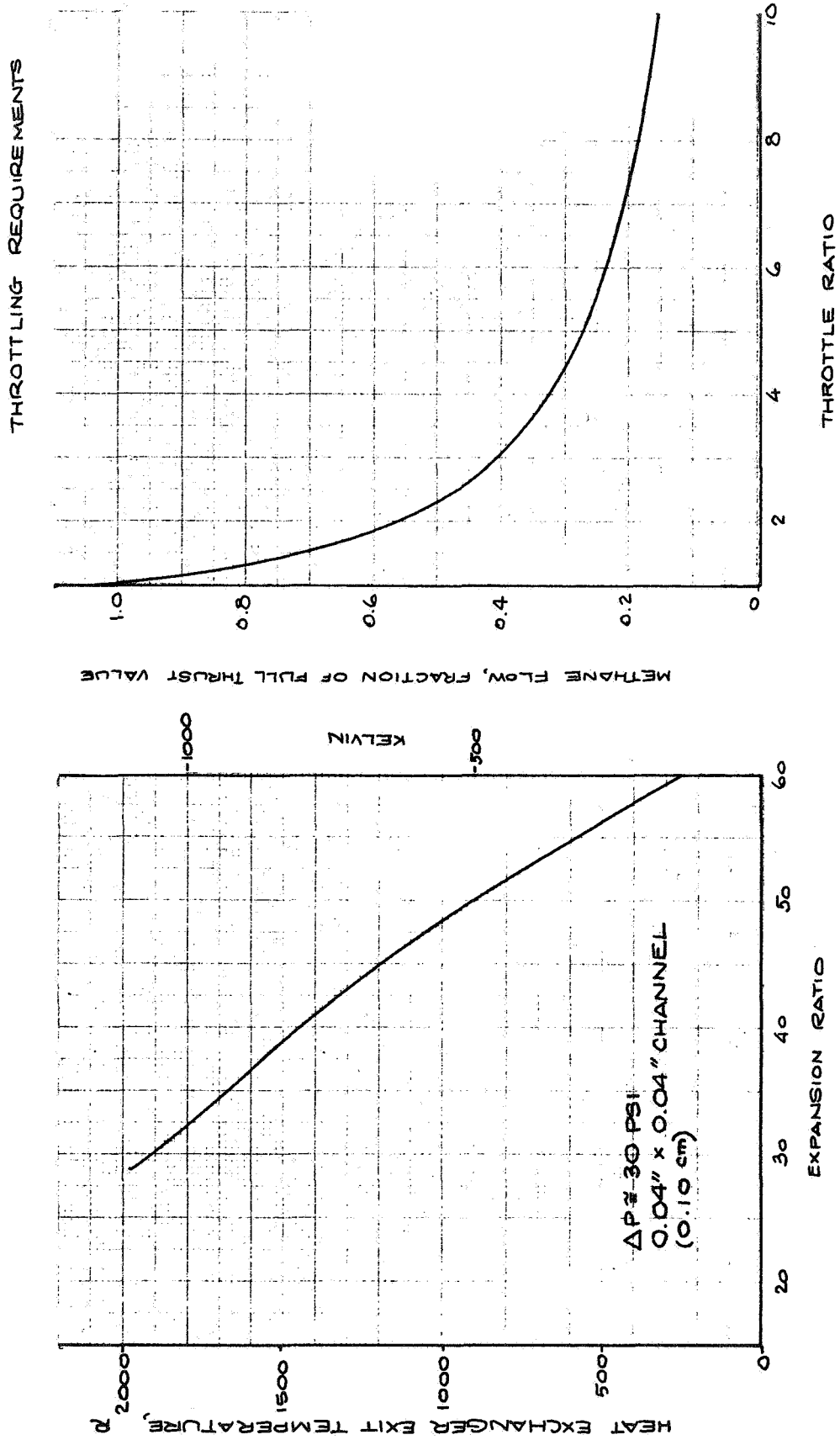
EXPANSION RATIO

would enter the nozzle at an expansion ratio of 30, significantly nearer the throat than on the expander cycle. This results in a lower methane temperature rise than in the Expander cycle and in different pressure drops.

As the engine is throttled the heat exchanger cooling requirements rather than turbine power define the heat exchanger flow required. This is illustrated in Fig. 19 and 20, where the methane flow necessary to cool the heat exchanger decreases at somewhat lesser rate than the engine throttle ratio. The flow required to power the turbines decreases faster than the throttle ratio. Excess flow bypasses the turbine and is ducted into the injector to improve throttled performance.

THRUST CHAMBER DESIGNS

Thrust chamber cooling channels were designed using the two-step width variation configuration and assuming $Q_m/Q_p = 1.0$. Primary emphasis was placed on designs for the auxiliary heat exchanger and expander cycles since they were appearing to be the most attractive. Cooling jacket pressure drops and exit temperatures were calculated for the other drive cycles and, except for the differences due to lower engine mixture ratio and jacket pressure, were similar to the expander cycle thrust chamber characteristics.

Channel characteristics for the auxiliary heat exchanger chamber are in Table 10. The smallest channel width occurs in the heat exchanger section with the throat width significantly larger at 500 psia (3450 kN/M^2) pressure and slightly larger at 800 psia (5520 kN/M^2) wall temperature in the throat and combustor are slightly lower than the maximum values in anticipation of engine throttling (discussed in a following section).

60

TABLE 10

NOMINAL CHANNEL DESIGNS

Nominal Channel Designs

Chamber Pressure, psia (kN/M²)	500 (3450)		800 (5520)	
Drive Cycle	Auxiliary Heat Exchanger	Expander	Auxiliary Heat Exchanger	Expander
Inlet Manifold ∈	30	60	32	100
Exit Conditions				
Width, in (cm)	0.040 (0.102)	0.234 (0.594)	0.040 (0.102)	0.172 (0.437)
Height, in (cm)	0.040 (0.102)	0.05 (0.127)	0.040 (0.102)	0.050 (0.127)
Wall Thickness, in (cm)	0.040 (0.102)	0.040 (0.102)	0.040 (0.102)	0.040 (0.102)
Throat Conditions				
Width, in (cm)	0.072 (0.183)	0.072 (0.183)	0.047 (0.119)	0.042 (0.107)
Height, in (cm)	0.068 (0.173)	0.065 (0.165)	0.054 (0.137)	0.048 (0.122)
Wall Thickness, in (cm)	0.025 (0.064)	0.025 (0.064)	0.020 (0.051)	0.020 (0.051)
Wall Temperature, F (K)	1670 (1185)	1700 (1200)	1700 (1200)	1719 (1210)
Combustor Conditions				
Width, in. (cm)	0.072 (0.183)	0.072 (0.183)	0.0468 (0.119)	0.042 (0.107)
Height, in. (cm)	0.1-0.2 (0.25-0.5)	0.09-0.2 (0.23-0.5)	0.104 (0.264)	0.070 (0.178)
Wall Thickness, in. (cm)	0.025 (0.064)	0.025 (0.064)	0.020 (0.051)	0.025 (0.635)
Wall Temperature, F (K)	1520 (1100)	1540 (1111)	1600 (1144)	1632 (907)
Exit Temperature, R (K)	1070 (594.4)	1240 (688.8)	1094 (607.7)	1372 (762.1)
Pressure Drop, psi (kN/M²)	172 (1190)	188 (1300)	324 (2230)	312 (2150)

Thrust chamber designs for the expander cycle are described in Table 10.
Minimum channel widths are 0.072 inches (0.183 cm) at 500 psia (3450 kN/M^2)
and 0.042 inches (0.107 cm) at 800 psia (5520 kN/M^2). The methane enters
at the nozzle exit and flows toward the injector. Since there is less
methane cooling the thrust chamber than for the auxiliary heat exchanger
cycle, the methane exit temperature rise is greater.

Perturbations of Operating Conditions

For the nominal thrust chamber designs the effects of throttle ratio, heat
flux level, inlet temperature, and thrust chamber mixture ratio were in-
vestigated. In the investigation pressure drop, exit temperature, and
critical wall temperature variations were described for each of the cycles
and design points.

Auxiliary Heat Exchanger Cycle. Thrust chamber perturbations for the 800
psia (3520 kN/M^2) design were evaluated. The effect of throttle ratio is
shown in Fig. 21. Thrust chamber wall temperatures do not exceed 1700 F
(1200 K) over the 10:1 thrust range. The methane exit temperature increases
some 400 F (222K) at the 10:1 throttled condition. Phase change will
occur in the cooling jacket at throttle ratios greater than about 1.5.
This phase change, however, occurs in regions of relatively low heat
flux and is not anticipated to be a heat transfer problem.

The overall heat flux level has a significant effect on thrust chamber
wall temperatures. The nominal heat flux profile ($Q_m/Q_p = 1.0$) is
based on the boundary layer equation. Increasing the heat flux level
20-percent above this model results in wall temperatures which are
above the allowable value. This effect is mitigated somewhat by several
factors.
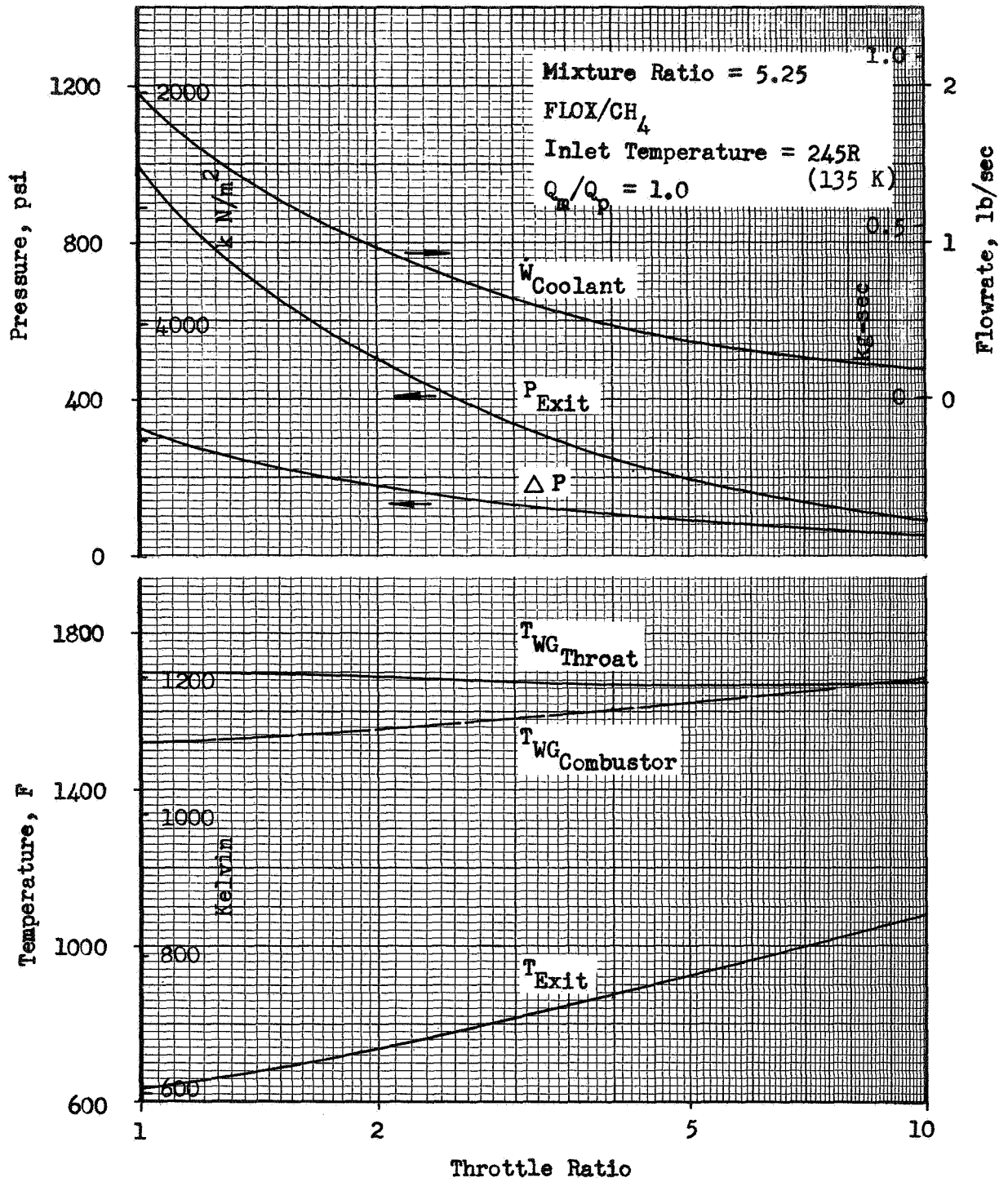
Figure 21.   Heat Exchanger Cycle, 800 P_c, Effects of Throttling
(5520 k N/m^2)

First, as a safety margin, curvature enhancement has been ignored. Recent square channel data have indicated throat cooling enhancements similar to that in tubes. Thus, wall temperature margins of 100-200 F (55-110 K) are available in the throat region. Second, the channels can be artificially roughened to provide additional thermal margin. A third factor would be the flexibility associated with the channel design, in which channel height could be reduced to increase cooling capability.

Some characteristics of the thrust chamber at higher heat flux values are listed in Table 11. Both perturbations to the nominal design and cooling channel redesign effects are shown. In addition to a $Q_m/Q_p = 1.2$ case, the effect of a heat flux profile based on data taken under Contract NAS3-11191 was evaluated. It can be seen that for the higher heat flux values, the 800 psia (5520 kN/m^2) design involves either excessive wall temperatures or, with redesign, very high pressure drops.

Inlet temperature and mixture ratio effects were evaluated. Mixture ratio increase to 5.7 raised the throat wall temperature to 1790 F (1240 K) while decreasing pressure drop slightly. Inlet temperature reduction reduced the exit temperature correspondingly and gave a slight decrease in pressure drop.

Perturbation effects are similar for the 500 psia (3450 kN/m^2) thrust chamber design (Fig. 22). Phase-change occurs in the channels with about 10-percent throttling. The lower heat flux levels associated with 500 psia (3450 kN/m^2) chamber pressure slightly diminish the magnitude of the perturbation effects.

Expander Cycle. Thrust chamber perturbations for the 500 psia (3450 kN/m^2) are shown in Fig. 23. Throttling (Figure 23) poses no heat transfer

64

TABLE 11

GAS-SIDE HEAT FLUX PERTURBATIONS

Chamber Pressure = 800 psia (5520 kN/M²)

Auxiliary Heat Exchanger

CASE	DESIGN	EXIT TEMPERATURE, R (K)	WALL COMBUSTOR, F (K)	TEMPERATURE THROAT, F (K)	ΔP, PSI (kN/m²)	CHANNEL HEIGHT IN (cm)
$Q_m/Q_p = 0.9$	Nominal	1020 (567)	1485 (1081)	1560 (1122)	195 (1340)	0.054 (0.137)
$Q_m/Q_p = 0.76$	Nominal	1910 (506)	1330 (994)	1380 (1022)	173 (1190)	0.054 (0.137)
$Q_m/Q_p = 1$	Nominal	1094 (608)	1600 (1144)	1700 (1200)	214 (1480)	0.054 (0.137)
$Q_m/Q_p = 1.2$	Nominal	1212 (673)	1804 (1258)	1980 (1356)	249 (1720)	0.054 (0.137)
	Redesign	1234 (686)	1600 (1144)	1700 (1200)	491 (3390)	0.040 (0.102)
Triplet Injector (NAS3-11191)	Nominal	1241 (689)	2343 (1557)	1973 (1352)	242 (1670)	0.054 (0.137)
	Redesign	1279 (711)	1600 (1144)	1700 (1200)	602 (4150)	0.045 (0.114)
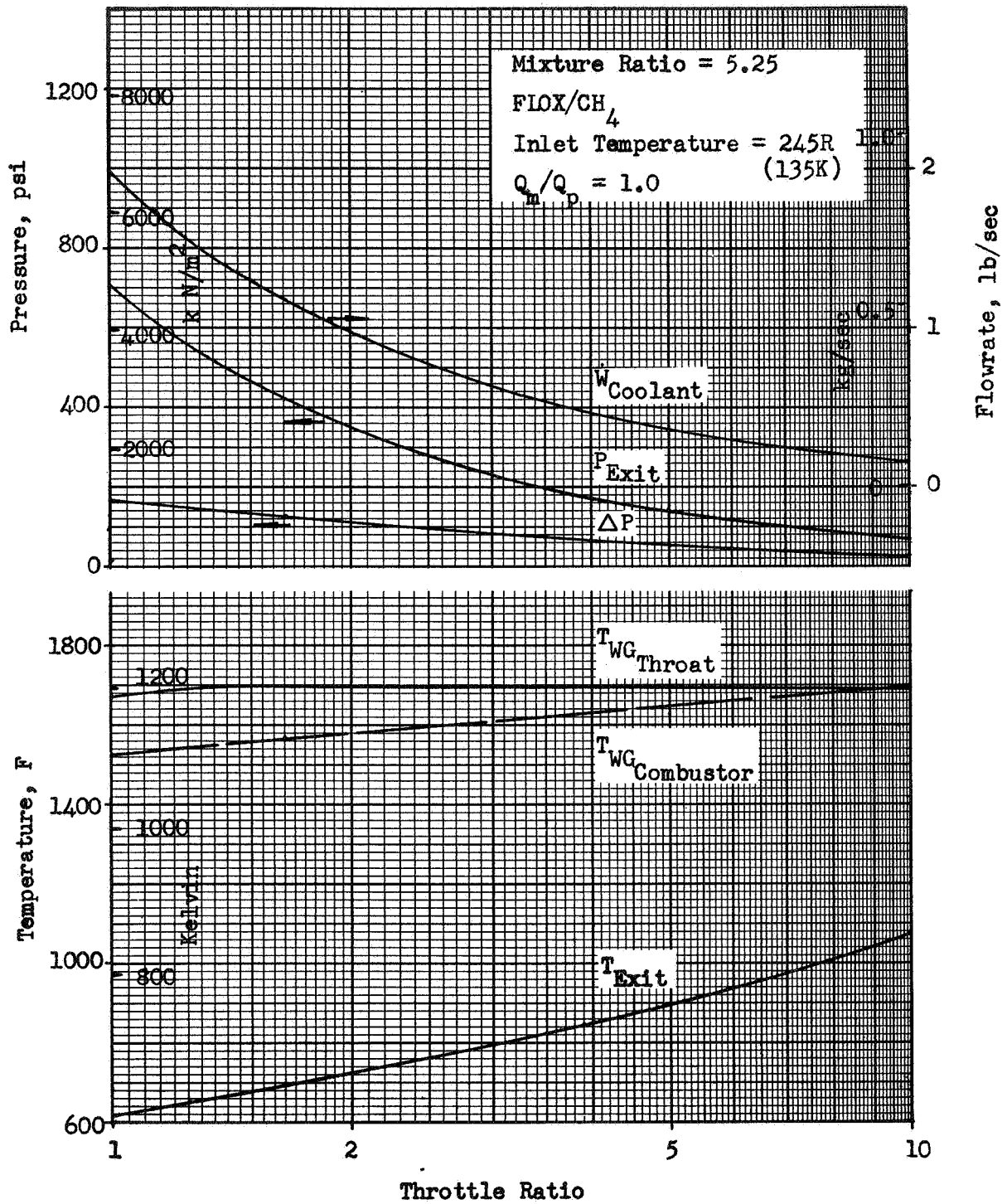
Figure 22 . Heat Exchanger Cycle, 500 P_c, Effects of Throttling
(3450 k N/m^2)
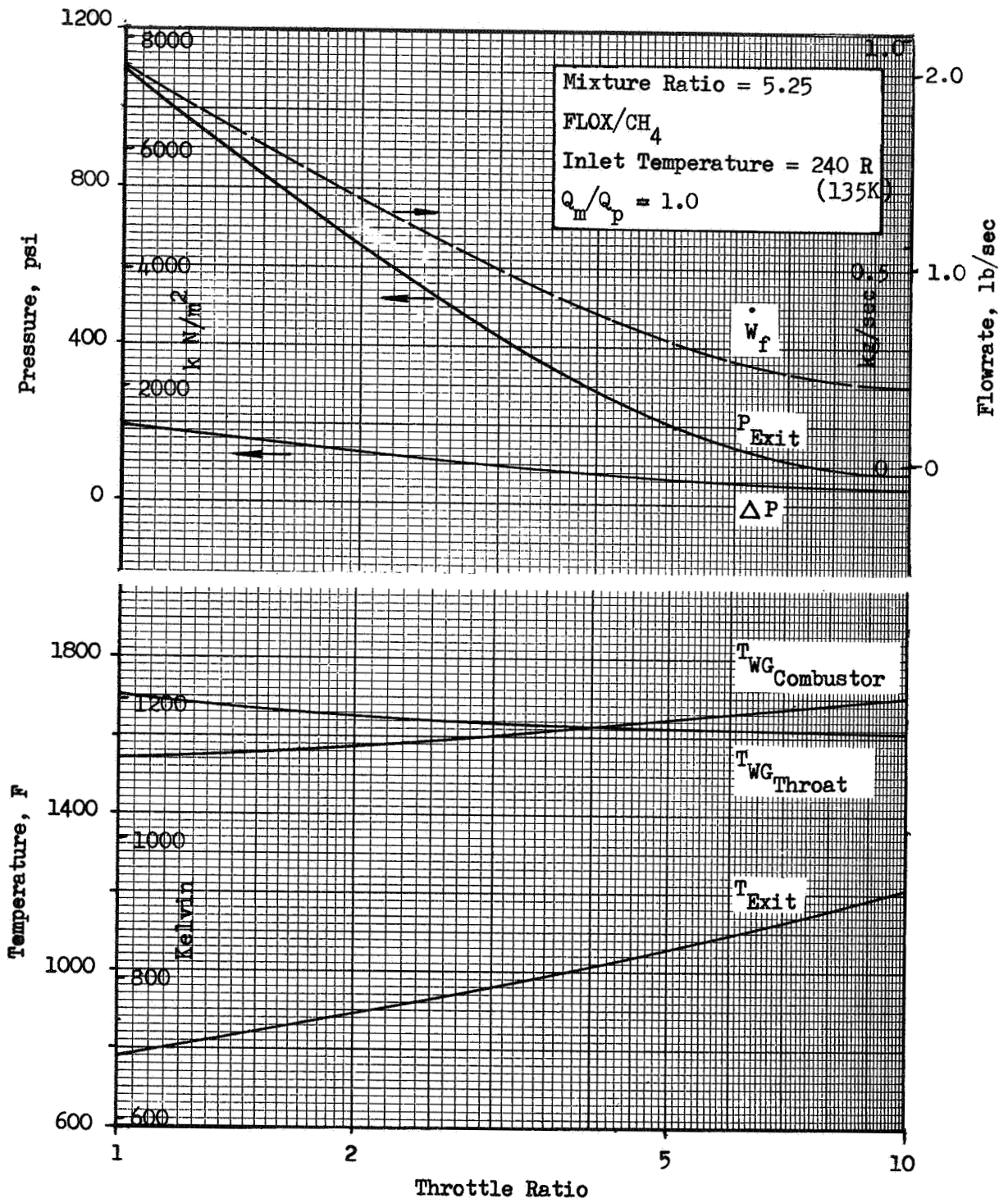
Figure 23 . Expander Cycle, 500 P_c , Effects of Throttling
(3450 k N/m^2)

problem for this cycle since wall temperatures are below 1700 F (1200K).
Phase change will occur at throttle ratios greater than 2, with the
heat flux levels even less than in the auxiliary heat exchanger cycles,
since the phase change region is nearer the nozzle exit. An increase
in heat flux level results in increased wall temperatures. These
increases however, are slightly less than at 800 psia (5520 kN/M^2).
Chamber characteristics at higher heat fluxes are listed in Table 12.
As for the 800 psia (5520 kN/M^2) auxiliary heat exchanger, thrust chamber
high wall temperatures result; channel redesigns, however, are more
reasonable.

In the 800 psia (5520 kN/M^2) expander cycle (Fig. 24), phase change
occurs at throttle ratios greater than 3. Reasonable wall temperatures
can be maintained over the 10:1 range with the throttling range of 2 to 3
being the most severe. Other effects are similar to those discussed for
the 500 psia (3450 kN/M^2) thrust chamber.

TABLE 12

GAS-SIDE HEAT FLUX PERTURBATIONS

Chamber Pressure = 500 psia (3450 kN/m²)
Expander Cycle

CASE	DESIGN	EXIT TEMPERATURE, R (K)	WALL COMBUSTOR, F (K)	TEMPERATURE THROAT, F (K)	ΔP, PSI (kN/m²)	CHANNEL HEIGHT IN (CM)
$Q_m/Q_p = 0.9$	NOMINAL	1170 (650)	1430 (1050)	1580 (1133)	173 (1190)	0.065 (0.165)
$Q_m/Q_p = 0.76$	NOMINAL	1055 (586)	1250 (950)	1390 (1028)	152 (1050)	0.065 (0.165)
$Q_m/Q_p = 1$	NOMINAL	1250 (694)	1540 (1111)	1700 (1200)	188 (1300)	0.065 (0.165)
		1240 (689)	1600 (1144)	1700 (1200)	137 (940)	0.065 (0.165)
$Q_m/Q_p = 1.2$	NOMINAL	1400 (778)	1740 (1222)	1910 (1317)	217 (1500)	0.065 (0.165)
	REDESIGN	1415 (786)	1600 (1144)	1700 (1200)	330 (2280)	0.047 (0.119)
TRIPLET INJECTOR	NOMINAL	1340 (744)	2100 (1422)	1800 (1256)	193 (1330)	0.065 (0.165)
(NAS3-11191)	REDESIGN	1355 (753)	1600 (1144)	1700 (1200)	272 (1880)	0.056 (0.142)
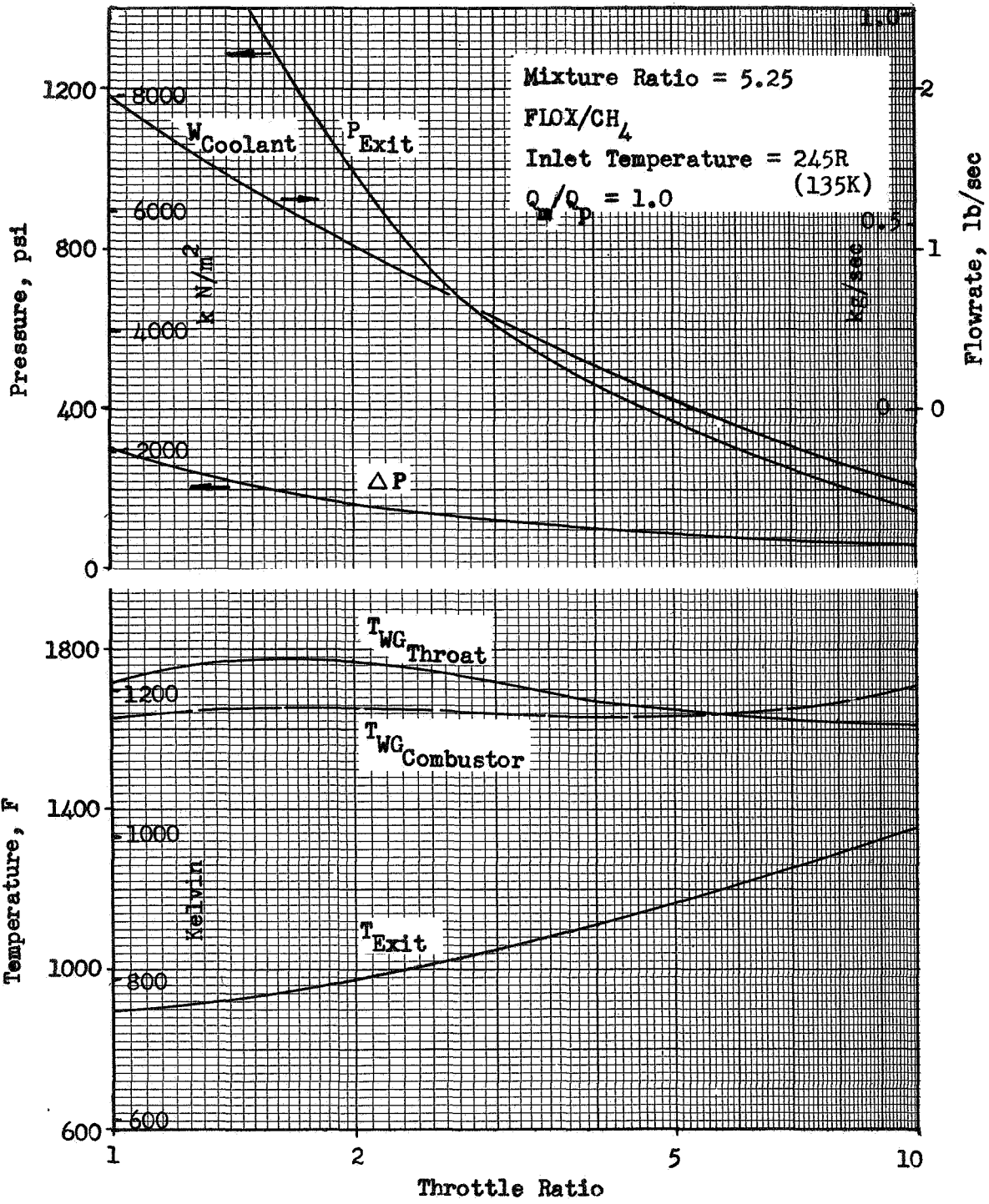
Figure 24 . Expander Cycle, 800 P_c, Effects of Throttling
(5520 k N/m^2)

70

TURBOPUMP DRIVE CYCLE ANALYSIS

Turbopump drive cycle candidates were defined and evaluated at the two selected design points. Engine components capable of meeting the system requirements were described for each drive cycle. Engine start and throttling were evaluated and any operating restrictions imposed by the components or systems were identified. A comparison of the drive cycle capability was made on the basis of performance, development ease, system complexity and production ease. Both qualitative and numerical rating comparisons were made. Two drive-cycle configurations were selected at each design point for further investigation.

ENGINE REQUIREMENTS AND GROUND RULES

The engine system operating requirements are listed below.

ENGINE OPERATING REQUIREMENTS

Nominal Thrust, lb (N)	5000 (22200)
Environment	Space
Mission Duration	Long
Number of Starts	4-10
Operating Duration, sec	~500
Throttling	10/1

Engine systems were designed to meet these requirements.

The two previously selected design points were used for engine evaluation

Chamber Pressure, psia (kN/m^2)	Expansion Area Ratio	Thrust Chamber Mixture Ratio O/F
500 (3450)	60	5.25
800 (5520)	100	5.25

71

The thrust chamber mixture ratio is that of the hot combustion products flowing through the chamber and nozzle. For topping cycles the thrust chamber and engine mixture ratios are identical. In other drive cycles, the engine mixture ratio will be lower than the thrust chamber mixture ratio.

Delivered thrust chamber performance was determined using a 94 percent efficiency on the theoretical one-dimensional shifting equilibrium performance at normal boiling temperatures. This efficiency can readily be attained with the 80 percent length bell nozzles used on the engines. For topping cycles the delivered engine performance is the same as the thrust chamber values. For the other cycles, in which turbine exhaust is ducted overboard, the engine specific impulse is lower. The low turbine flow cycles (i.e., gas generator (A), thrust chamber tapoff, and auxiliary heat exchanger) had an assumed secondary thrust coefficient of 1.5. This assumed value represents a mean between the nozzle injection and auxiliary nozzle techniques for turbine exhaust utilization. It was found that the system specific impulse variation for the two methods was small.

CANDIDATE PUMP-TURBINE DRIVE CYCLES

The pump-turbine drive cycles which were investigated are shown in Table 13. As can be seen, these cycles differ in the source of the turbine drive fluid and also in the utilization of the turbine exhaust gases. Some of the cycle characteristics are discussed in the following sections.

Gas Generator Cycle (A)

The gas generator cycle (A) utilizes small amounts of propellants tapped from the main propellant feed system and combusted in a gas generator for turbine drive fluid. The turbine drive gases expand through the turbine and are either injected into the main nozzle or an auxiliary nozzle.

The gas generator cycle (A) has been used to power numerous existing engine systems with a variety of propellant combinations. Among these are the J-2 (O_2/H_2), H-1 $(O_2/Kerosene)$, and Titan II $(N_2O_4/50-50)$.

72

ENGINE TURBOPUMP DRIVE CYCLES

GAS GENERATOR CYCLE

CHAMBER TAPOFF CYCLE

EXPANDER CYCLE

AUXILIARY HEAT EXCHANGER CYCLE
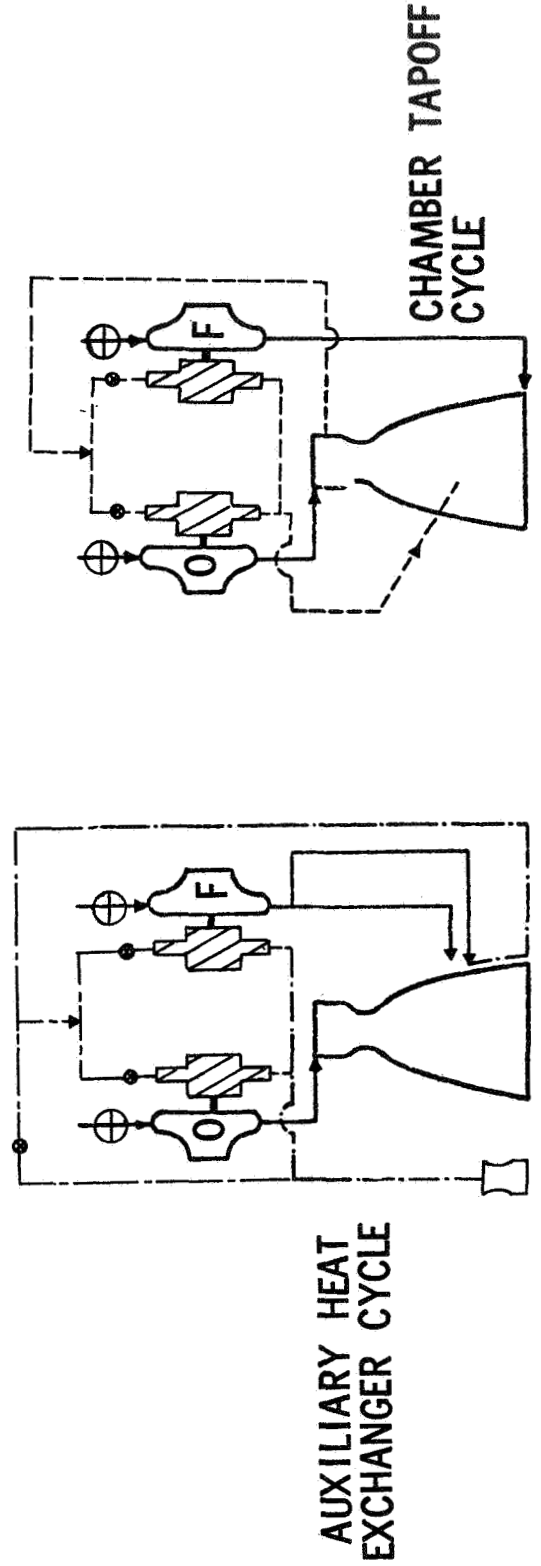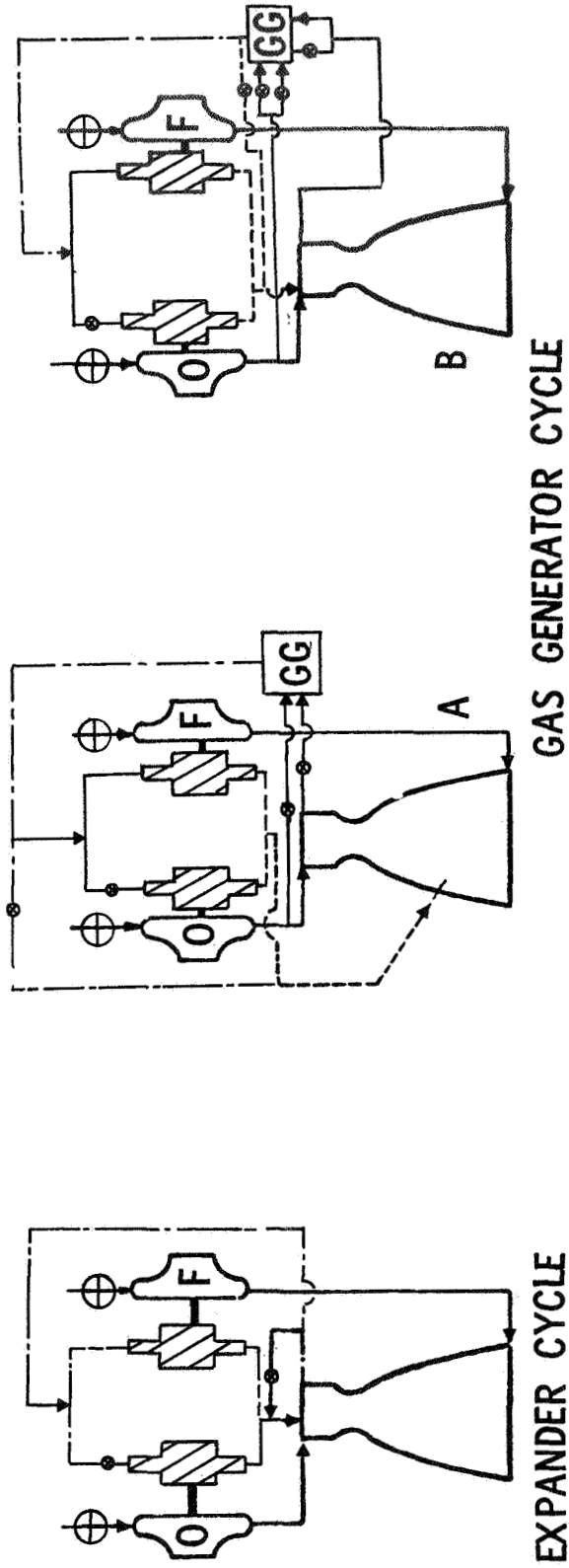
A preliminary engine balance for the gas generator (A) cycle is presented in Table 14. The gas generator operates at a low mixture ratio (fuel rich) to provide a turbine gas temperature which allows reasonable turbine materials and speeds. The low performing turbine exhaust results in 0.5 percent decrease in engine specific impulse. The turbine working fluid contains both solid carbon which may lead to turbine coking and hydrogen fluoride which may cause material compatibility problems.

The turbine exhaust utilization techniques which appear attractive for the gas generator cycle (A) are the nozzle injection technique and the use of an auxiliary nozzle. The nozzle injection technique utilizes the turbine exhaust gases by choking them into the main nozzle at a point where the pressure of the main nozzle and turbine exhaust gases are approximately equal. The injected gases produce performance by expanding to the nozzle exit pressure. This technique provides a well integrated propulsion system package with no thrust misalignment. When used in conjunction with a system which throttles, the nozzle injection technique may encounter pressure matching problems between the mainstream and turbine exhaust gases. This occurs because the turbine exhaust pressure decreases more rapidly than the nozzle wall pressure as the system is throttled.

The auxiliary nozzle technique utilizes a separate nozzle to expand the turbine exhaust gases. It would be theoretically possible to expand the gases to the same area ratio as the primary nozzle. This would be impractical, however, due to the large size and weight of the auxiliary nozzle and would still give a specific impulse loss due to the turbine gas temperature being lower than that of the main chamber.

The basic candidate gas generator cycle (A) uses gaseous methane obtained from the cooling jacket exit for the gas generator. It is also possible to supply the gas generator with liquid methane tapped from the main fuel duct. Comparison of engine balance results indicate that the performance and operating parameters of the two systems are nearly identical.

74

TABLE 14

GAS GENERATOR CYCLE (A), THRUST CHAMBER TAPOFF CYCLE ENGINE BALANCE

Chamber Pressure/Area Ratio, psia (kN/m^2)	500/60 (3450)	800/100 (5520)
Engine Mixture Ratio, O/F	5.073	4.941
Engine Specific Impulse, sec (N-sec/kg)	397.4 (3894)	402.6 (3945)
Total Propellant Flowrate, lb/sec (Kg/sec)	12.58 (5.71)	12.42 (5.63)
Secondary Mixture Ratio, O/F	0.3677	0.3224
Turbine Flowrate, lb/sec (Kg/sec)	0.1029 (.0467)	0.1733 (.0786)
Oxidizer Pump Discharge Pressure, psia (kN/m^2)	631.5 (4350)	980.4 (6760)
Fuel Pump Discharge Pressure, psia (kN/m^2)	730.5 (5040)	1212.4 (8360)

TABLE 15

OXIDIZER RICH (GAS GENERATOR A)

	Fuel Rich		Oxidizer Rich	
Chamber Pressure, psia (kN/m^2)	500	(3450)	500	(3450)
Gas Generator Mixture Ratio, O/F	0.3		100	
Temperature, R (K)	1960	(1089)	1960	(1089)
C* Ideal, fps (m/sec)	4220	(1286)	2540	(774)
Gas Composition (gm moles/100 gms)				
C (Solid)	2.15		–	
H_2	3.85		–	
F_2	–		–	
HF	1.0		0.25	
Turbine Flow (PR = 16), lb/sec (Kg/sec)	0.12	(.054)	0.37	(.168)
Engine Specific Impulse, sec (N-sec/kg)	397	(3890)	390	(3820)

The gaseous fuel GG supply system was retained for further analysis
and the liquid fuel GG supply system eliminated for the following reasons:
(1) the gaseous fuel GG supply system has a slightly higher fuel flowrate
available for regenerative cooling; (2) the gaseous fuel GG supply system
presents a less difficult gas generator injector design problem; and
(3) for throttleable systems the gas generator fuel supply flow control
would be simplified if the propellant were a gas.

Gas generator cycle systems have traditionally operated with fuel-rich
combustion in the gas generator thus eliminating the materials corrosion
problems which occur with oxidizer-rich gas generators. Use of an
oxidizer-rich gas generator would, however, eliminate solid carbon from
the exhaust products, as shown in Table 15. To obtain temperatures
comparable to the fuel-rich gas generators, the oxidizer-rich gas genera-
tor must have a mixture ratio of 100. Because of the small fuel flowrate,
control of the flow and efficient combustion would be difficult. Although
no solid carbon is produced, a considerable amount of fluorine is available
and at this temperature would be extremely reactive. In addition, the
energy content of the fluid is lower than for a fuel-rich gas generator
and engine system performance would be degraded, as illustrated for the
gas generator (A) cycle in Table 15. A fuel-rich gas generator, therefore,
is used.

Thrust Chamber Tapoff Cycle

With the exception of a different turbine drive fluid source, the thrust
chamber tapoff cycle is similar to the gas generator cycle (A). In
the thrust chamber tapoff cycle, combustion products are tapped from
the primary combustion chamber for use as turbine drive gases (Fig. 24).
This cycle, therefore, has a primary injector mixture ratio which is

76

the same as the engine mixture ratio. A preliminary balance is shown
in Table 14.

Performance, turbine working fluid, and low turbine flow characteristics are identical to the gas generator (A). The proper turbine
working fluid temperatures are obtained through an experimental investigation of tapoff port location. The cycle is simpler than the gas
generator cycle since the auxiliary combustor with its attendant lines
and valves is eliminated.

Auxiliary Heat Exchanger Cycle

The auxiliary heat exchanger cycle differs from the gas generator
cycle (A) in that the turbines are driven by heated methane instead of
combustion gases. Since only a single combustion process is involved
the system is less complex and more easily controlled. The methane is
a clean non-corrosive working fluid. Engine performance estimates for
$\epsilon = 100, 800$ psia (5520 kN/m^2) are shown in Table 16. Specific impulse
values at 500 psia (3450 kN/m^2), $\epsilon = 60$ are about one percent lower.

TABLE 16

AUXILIARY HEAT EXCHANGER ENGINE BALANCE

TURBINE TEMPERATURE, R (K)	1160 (644)	1360 (756)	1560 (867)	1760 (978)
MIXTURE RATIO, O/F	4.426	4.543	4.637	4.708
SPECIFIC IMPULSE, SEC (N-sec/kg)	397.6(3890)	399.3(3910)	400.5(3925)	401.4 (3935)
PROPELLANT FLOW, LB/SEC(Kg/sec)	12.57(5.70)	12.52(5.68)	12.48(5.66)	12.46(5.65)
TURBINE FLOWRATE, LB/SEC(Kg/sec)	.364(.165)	.304(.138)	.258(.117)	225 (.102)
FLOX PUMP PRESSURE,	980 psia (6760 kN/m^2)			
METHANE PUMP PRESSURE,	214 psia (8370 kN/m^2)			

Several system arrangements are possible for the auxiliary heat exchanger cycle depending on the exact source of the hot methane: (1) methane tapped for the thrust chamber cooling jacket, (2) methane from the tank heated in a heat exchanger, and (3) methane tapped downstream of the pump heated in a heat exchanger. In the first case the methane temperature is about 1160 R (644 K) at the cooling jacket exit. In the next two cases, a portion of the thrust chamber nozzle is used as a heat exchanger to obtain high methane temperatures 1700 R (943 K) and increase engine performance. As can be seen from Table 16 the performance of these two cycles is as much as 1 percent higher than where the methane is taken from the cooling jacket. The nozzle heat exchanger cycle arrangement is, therefore, more attractive.
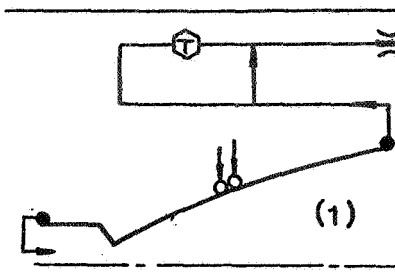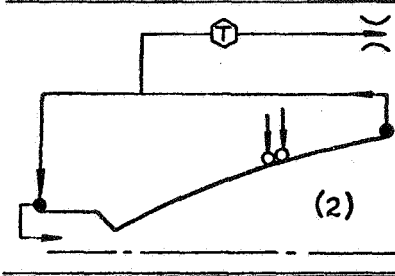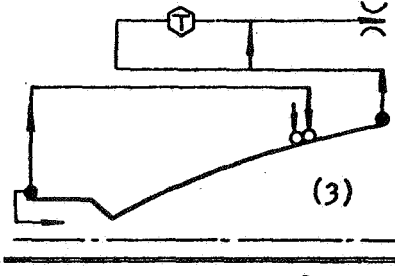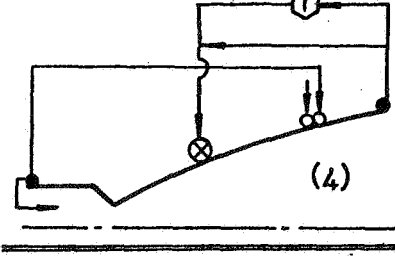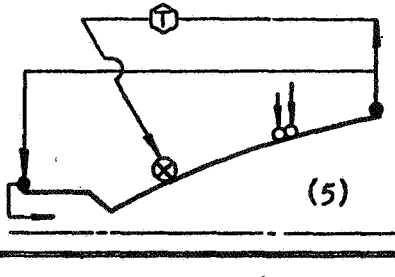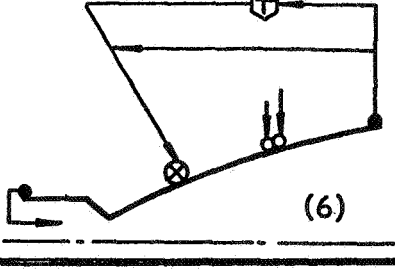
When fuel is obtained directly from the tank the turbine design is highly dependent upon the pressure available in the fuel tank. The low working fluid pressure will result in a turbine design which is relatively large and heavy. For turbine designs which have a low exit pressure, a diffuser would be required for testing at sea level. When turbine drive fluid is obtained from the pump exit, the turbine design is similar to that of the gas generator cycle (A) and this cycle arrangement was selected.

Additional flow alternatives for the auxiliary heat exchanger cycle are illustrated in Table 17. Their characteristics are described for full thrust and 10/1 throttling with a constant engine mixture ratio. Injection of the turbine exhaust into the main nozzle (No. 4-6) is attractive from a packaging standpoint, however there are three drawbacks:

1. Thrust chamber complexity is increased since the gas must be injected through slots in the lands.

2. For throttled engines, injection must occur at $\epsilon = 30$ resulting in slight performance loss compared to an auxiliary nozzle.

3. The turbine exhaust will cool the nozzle portion downstream of the injection point necessitating a larger heat exchanger.

TABLE 17

EFFECT OF SECONDARY FLOW UTILIZATION ON SYSTEM OPERATING CONDITIONS.

| | Throttle Ratio | Thrust Chamber | | | |
		MR	T_f Rankin (Kelvin)	$\dot{w}$ lb/sec (kg/sec)	I_s lb$_f$-sec/lb$_m$ (N-sec/kg)	Comment
(1)	1	5.25	1094 (607)	0.305 (0.138)	163 (1597)	Auxiliary start system required. Results for auxiliary nozzle area ratio = 3.0.
	10	5.7	1540 (855)	0.048 (0.022)	177 (1735)	
(2)	1	5.25	1094 (607)	0.305 (0.138)	163 (1597)	Auxiliary start system required. Results for auxiliary nozzle area ratio = 3.0.
	10	4.74	1593 (884)	0.0096 (0.0043)	172 (1686)	
(3)	1	5.25	973 (540)	0.305 (0.138)	163 (1597)	Tank-head start. Results for auxiliary nozzle area ratio = 3.0.
	10	6	1275 (708)	0.12 (0.05)	178 (1744)	
(4)	1	5.25	973 (540)	0.305 (0.138)	162 (1588)	Tank-head start. Larger heat exchanger due to secondary injection cooling. Must inject secondary flow at area ratio = 30 instead of 14 due to large decrease in turbine exit pressure when throttling.
	10	6	1275 (708)	0.12 (0.05)	177 (1735)	
(5)	1	5.25	1094 (607)	0.305 (0.138)	162 (1588)	Auxiliary start system required to eliminate slow start. Larger heat exchanger due to secondary injection cooling. Must inject secondary flow at area ratio = 30 instead of 14 due to large decrease in turbine exit pressure when throttling.
	10	4.74	1593 (884)	0.0096 (0.0043)	171 (1696)	
(6)	1	5.25	1094 (607)	0.305 (0.138)	162 (1588)	Auxiliary start system required to eliminate slow start. Larger heat exchanger due to secondary injection cooling. Must inject secondary flow at area ratio = 30 instead of 14 due to large decrease in turbine exit pressure when throttling.
	10	5.7	1540 (855)	0.048 (0.022)	176 (1725)	

Of the remaining alternatives, No. 2 is most attractive because of the low secondary flow at throttled conditions and was used in the evaluations.

Gas Generator Cycle (B)

The gas generator cycle (B) produces turbine drive fluid by combustion of all the system fuel flow with a suitable amount of oxidizer in a separate pre-combustor or gas generator. The combustion gases expand through a low pressure ratio turbine and flow into the main combustion chamber as shown in Figure 28. A small percentage (5 percent) of this flow is bypassed around the turbine to ensure system control. The principal advantage of this cycle is that all of the propellants are expanded in the primary nozzle and the system does not have the performance loss associated with the secondary flow system of the gas generator cycle (A). A further advantage is the fact that the engine and primary mixture ratios are identical. A preliminary engine balance is shown in Table 18.

TABLE 18

GAS GENERATOR CYCLE (B) ENGINE BALANCE

Chamber Pressure/Area Ratio (kN/m^2)	500/60 (3450/60)	800/100 (5520/100)
Engine Mixture Ration, O/F	5.25	5.25
Engine Specific Impulse, sec (N-sec/kg)	399.2 (3910)	405.9 (3980)
Total Propellant Flowrate, lb/sec (Kg/sec)	12.52 (5.68)	12.32 (5.59)
Precombustor Mixture Ratio, O/F	.3347	.2871
Turbine Flowrate, lb/sec (Kg/sec)	2.541 (1.153)	2.409 (1.093)
Oxidizer Pump Discharge Pressure, psia (kN/m^2)	876.2 (6040)	1486.9 (10250)
Fuel Pump Discharge Pressure, psia (kN/m^2)	989.6 (6820)	1694.9 (11690)

Turbine working fluid and temperatures are similar to the gas generator (A). Turbine coking and material compatibility may be problems. The precombustor requires valves adding complexity to the system. In addition in this topping-type cycle all feed system components are closely related and under some circumstance the engine may be very sensitive to the individual component designs.

Expander Cycle

In the expander cycle, fuel is heated in the regenerative cooling jacket, flows through the turbine, and is injected into the primary combustion chamber. A small percentage of the fuel (5%) bypasses the turbine to ensure system control. Since all of the propellants are expanded in the primary nozzle, this cycle has no secondary flow performance losses and no engine to primary mixture ratio shift. The cycle is basically simple and the methane provides a clean working fluid.

This fuel-powered cycle has previously been associated with the RL-10 hydrogen-fueled engine. Energy available for turbine power depends on the temperature of the fuel coming out of the cooling jacket and the specific heat of the fuel. Methane, like hydrogen, has sufficient energy to power the turbine. However, the heat capacity of methane is about one-third that of hydrogen and, at equal temperatures, the energy potential per pound of fuel will be substantially less than with hydrogen. The temperatures associated with this FLOX/methane engine are, as shown in the previous section, substantially higher than for oxygen/hydrogen engines and the energy is more than sufficient to provide turbine power.

Preliminary engine balances are shown in Table 19.

TABLE 19

EXPANDER CYCLE ENGINE BALANCE

Chamber Pressure/Area Ratio (kN/m^2)	500/60 (3450/60)		
Turbine Efficiency	.5	.6	.7
Engine Mixture Ratio, O/F	5.25	5.25	5.25
Engine Specific Impulse, sec (N-sec/kg)	399.2(3910)	399.2(3910)	399.2(3910)
Total Propellant Flowrate, lb/sec (Kg/sec)	12.52(5.68)	12.52(5.68)	12.52(5.68)
Turbine Flowrate, lb/sec (Kg/sec)	1.904(.864)	1.904(.864)	1.904(.864)
Turbine Pressure Ratio	1.500	1.381	1.308
Oxidizer Pump Discharge Pressure, psia (kN/m^2)	631.5(4350)	631.5(7350)	631.5(4350)
Fuel Pump Discharge Pressure, psia (kN/m^2)	1102.4(7600)	1032.1(6820)	989.6(7120)

As in the gas generator (B) cycle the feed system components are inter-related. A change in turbomachinery efficiency for example, while not affecting specific impulse, will change the entire cycle pressure balance. At some conditions the engine balance may be sensitive and the engine design should incorporate sufficient power margin to provide for potential component variations.

THROTTLING EVALUATION

The throttling capability of each of the pump-turbine power cycles was evaluated. Considerations were: (1) the use of throttling injectors in the main combustion chamber and in the gas generators, (2) the control systems required for thrust and mixture ratio control, (3) turbomachinery design, and (4) performance losses due to a throttling requirement. The evaluation is summarized in Table 20.

TABLE 20

THROTTLING EVALUATION

CYCLE / CRITERIA	GG (A)	THRUST CHAMBER TAPOFF	AUXILIARY HEAT EXCHANGER	GG (B)	EXPANDER
MAIN INJECTOR	HIGHER PRESSURE DROPS	HIGHER PRESSURE DROP; MUST PROVIDE TAPOFF REGION OVER 10:1 PRESSURE RANGE	HIGHER PRESSURE DROPS	HIGHER PRESSURE DROPS	HIGHER PRESSURE DROPS
POWER SOURCE	TURBINE BYPASS VALVE REQUIRED TO LIMIT G.G. THROTTLING		HEAT EXCHANGER FLOW CONTROL REQUIRES TURBINE BYPASS VALVE	DUAL MANIFOLD REQUIRED IN PRE-COMBUSTOR	NO MODIFICATION FOR THROTTLING
CONTROLS THRUST	SIMULTANEOUS CONTROL OF 4 VALVES REQUIRED	SIMULTANEOUS CONTROL OF 2 VALVES REQUIRED		SIMULTANEOUS CONTROL OF 5 VALVES REQUIRED	SIMULTANEOUS CONTROL OF 2 VALVES REQUIRED
MIXTURE RATIO	CONTROL OF ENGINE AND GG REQUIRED	MUST PROVIDE ACCEPTABLE TAPOFF GASES		CONTROL OF ENGINE AND PRECOMBUSTOR REQUIRED	
TURBOMACHINERY DESIGN	GOOD	HIGHER PUMP DISCHARGE PRESSURES REQUIRED			
STABILITY	GOOD	GOOD	GOOD	UNCHOKED TURBINES MAY BE SUSCEPTIBLE TO FEED SYSTEM COUPLING AND COMBUSTION INSTABILITIES	
PERFORMANCE FULL THRUST	-0.4 SEC @ $P_c = 500$ (3450 kN/m^2) -0.7 SEC @ $P_c = 800$ (5520 kN/m^2)	-0.4 SEC @ $P_c = 500$ -0.7 SEC @ $P_c = 800$	-0.7 SEC @ $P_c = 500$ -1.1 SEC @ $P_c = 800$	NO PERFORMANCE LOSS DUE TO THROTTLING REQUIREMENT	

83

Throttling Injectors - Main Combustion Chamber

The goal of main combustion chamber injector design is: (1) to provide high performance and stable operation and (2) to minimize injector pressure losses. It is usually necessary to accept higher than desired pressure losses in order to maintain performance and stability. The design pressure drops for throttling injectors vary considerably with the type of injector and the properties of the propellants prior to injection.

To provide a relatively simple injector while at the same time maintaining reasonable pressure drops, a variety of concepts are available: (1) dual manifold, (2) gas-gas injection, (3) recessed coaxial element, and (4) oxidizer heating. Each of these concepts has been experimentally investigated with propellants other than FLOX/methane and shown to function successfully. The net effect of these methods is to give throttled pressure drops which are high enough to provide stable operation while full thrust pressure drops are relatively low. The dual manifold approach is straight forward in application and is particularly attractive for high throttle ratios. It involves more complex manifold design and additional valves. Within the 10/1 throttling range the recessed coaxial element approach is a most attractive design but must be demonstrated for the FLOX/methane propellants.

The main injectors on all drive cycles appear capable of utilizing these concepts and no significant difference was found between the drive cycles. For the system evaluations nominal $\Delta P_i/P_c$ design values of 0.40 and 0.25 were assumed for the fuel and oxidizer injectors respectively. With the injector types discussed these values are sufficiently high to maintain high performance and stable operation over the 10/1 throttled range.

Turbine Throttling Requirements

As the engine is throttled, the turbine power requirements and, therefore, the flow required decreases more rapidly than the thrust of the main chamber. For 10:1 engine throttling, the required turbine flow decreases by 20-30:1 for both the low-flow turbine drive cycles and the high-flow turbine or topping cycles. The exact turbine flow variation depends upon system pressure drops and pump inlet pressure. In the expander and thrust chamber tapoff cycles, this large variation in turbine flow is controlled with the turbine valves and does not affect the design of other components. In the remaining cycles, the power source design can be materially affected.

Auxiliary Heat Exchanger. As the engine is throttled the primary design requirement becomes maintenance of acceptable heat exchanger wall temperatures rather than turbine power. An excess of heat exchanger flow exists and bypasses the turbine to be dumped overboard or back into the injector manifold (Table 17). The turbine valves must be designed to maintain proper heat exchanger temperature as well as control turbine power.

Gas Generator Cycle. The precombustor in the gas generator cycle (B) must also be provided with a throttleable injector. The throttling ratio of this injector is the same as the main combustion chamber injector (i.e., approximately 10 to 1). It would be possible to use the same injector concept in the precombustor as is used in the main combustion chamber. The problem with this concept is that the precombustor injector pressure losses are quite high since the precombustor operates at a much higher pressure than the main combustion chamber.

Precombustor injector pressure drops shown equivalent in percent to the main injector values result in pump discharge pressures which are unacceptably high. The most promising concept for reducing these pressure drops is the use of the dual manifold. Oxidizer and fuel injector pressure drops equal to 20 percent of the precombustor pressure were used for the dual manifold concept.

Gas Generator Cycle (A). The gas generator in the gas generator cycle (A) is unique in that it must be capable of throttling ratios of 20-30/1 which were felt to be beyond the capabilities of a fixed area injector. Two concepts for reducing the gas generator injector throttling ratio were considered. The first is the use of the dual manifold concept and the second is the use of a turbine bypass system. The dual manifold concept was discussed for the gas generator cycle (B). The only difference for the gas generator cycle (A) is that both the fuel and the oxidizer inlet lines will require two control valves. The turbine bypass concept uses fixed area injectors in the gas generator with a throttling capability of approximately 10 to 1. For gas generator throttling greater than 10 to 1, the flowrate remains constant and the excess turbine drive gas is bypassed around the turbine. This concept is attractive because it both reduces the gas generator throttling ratio and relieves the gas generator flow control problems. The turbine bypass concept has the disadvantage of producing higher than the required secondary flowrate at gas generator throttle ratios greater than 10 to 1. This gives a slight engine specific impulse loss in the 10/1 throttled condition.

The engine bypass concept was used for the gas generator cycle (A) because it requires fewer control valves than the dual manifold concept and because it does not complicate the design of the gas generator.

Thrust and Mixture Ratio Controls

Table 21 summarizes the control system considerations for a throttleable engine. It is necessary to control mixture ratio during throttling because the oxidizer and fuel feed systems do not behave in the same manner. On the gas generator cycles the mixture ratio of both the engine and the gas generator must be controlled. The following table lists the number of control valves which must be operated simultaneously for each cycle:

TABLE 21

NUMBER OF CONTROLS REQUIRED FOR THROTTLING

Gas Generator (A)	4
Thrust Chamber Tapoff	2
Auxiliary Heat Exchanger	3
Gas Generator (B)	5
Expander	2

In the thrust chamber tapoff cycle, an additional control valve may be required to provide acceptable tapoff gas properties during throttling since injector characteristics may vary and affect gas properties at the tapoff port.

In the auxiliary heat exchanger cycle, it was necessary to control the heat exchanger flowrate during throttling. It was found that the required heat exchanger flowrate for any given thrust level was always greater than or equal to the required turbine flowrate at that thrust level. For all conditions in which the required heat exchanger flowrate was greater than the required turbine flowrate, the excess flow was bypassed around the turbine.

Turbomachinery

All of the 500 psia (3450 kN/m^2) turbopump designs were capable of throttling with the engine balance at 10 percent thrust being dependent on pump inlet pressures. Differences were more significant at the 800 psia (5520 kN/m^2) design point. The design values of pump discharge pressure are higher due to increased injector pressure drops. The higher pump discharge pressures result in a reduction in pump efficiencies and also a reduction in pump impeller tip widths.

At 800 psia (5520 kN/m^2) the gas generator (B) and expander cycle fuel pump designs are very sensitive to the pressure drop required for throttling. With high injector pressure drops, the nominal design discharge pressures exceed 2500 psia (15500 kN/m^2) and the associated impeller designs may be difficult to fabricate because of the small tip width.

Performance

All pump-turbine power cycles will have a performance loss during throttling due to increased drag and kinetics losses in the nozzle. Combustion losses usually also increase during throttling.

In the gas generator (B) and expander cycles, a throttling requirement does not result in any performance losses other than those discussed above. A throttling requirement does, however, produce additional performance losses in the low turbine flow cycles. The increased injector pressure drop requirements result in higher pump discharge pressure and, therefore, higher turbine flow requirements. The resulting cycle losses produce a decrease in engine specific impulse. At a chamber pressure of

TABLE 22

THROTTLING EVALUATION – TURBOMACHINERY CONSIDERATIONS

CHAMBER PRESSURE – 800 psia (5520 kN/m^2)

CYCLE		GG (A) CYCLE	THRUST CHAMBER TAPOFF	AUXILIARY HEAT EXCHANGER	EXPANDER CYCLE	GG (B) CYCLE
PUMP DISCHARGE PRESSURE RISE DUE TO THROTTLING, psia (kN/m^2)	F	+170 (1170)	+170 (1170)	+170 (1170)	+600 (4130)	+602 (4140)
	O	+80 (550)	+80 (550)	+80 (550)	+80 (550)	+640 (4400)
PUMP EFFICIENCY CHANGE DUE TO THROTTLING	F	-2%	-2%	-2%	-8%	-8%
	O	-1%	-1%	-1%	-1%	-7%
POWER BALANCE		YES	YES	YES	YES	YES
IMPELLER TIP WIDTH, INCHES (cm)	F	0.052 (0.132)	0.052 (0.132)	0.053 (0.135)	0.035 (0.089)	0.036 (0.091)
	O	0.089 (0.216)	0.089 (0.216)	0.089 (0.216)	0.089 (0.216)	0.057 (0.145)
CRITICAL SPEED		ALL DESIGNS MUST CONSIDER POSSIBLE CRITICAL SPEED OPERATION				
STABILITY		GOOD	GOOD	GOOD	UNCHOKED TURBINES PROVIDE COUPLING FOR POSSIBLE FEED SYSTEM AND COMBUSTION INSTABILITY	
TURBINE THROTTLING RATIO FOR 10:1 ENGINE THROTTLING (P$_c$ = 800)		21	21	26	15	15

89

800 psia (55.2 kN/m^2) the full thrust engine specific impulse due to a throttling requirement is 0.2 percent for the gas generator (A) and thrust chamber tapoff cycles and 0.3 percent for the auxiliary heat exchanger cycle.

In the thrust chamber tapoff and auxiliary heat exchanger cycles, the cycle losses decrease as the engine is throttled. This occurs because the pump power requirements (and, therefore, the turbine flow requirements) decrease much more rapidly than the thrust level. In the gas generator cycle losses will increase as the engine is throttled. This occurs because of the turbine bypass system used to limit gas generator throttling.

CONTROL SYSTEM SELECTION

An engine control system selection study was conducted to establish the most
favorable control configuration for each of the candidate turbine arrange-
ments and turbine drive cycles. The results of this study provided the basic
control system configuration for each of the candidate cycles and provided a
relative comparison of the turbine arrangements and drive cycles, based upon
control system considerations.

Ground Rules

Ground rules that apply to the control system and start system are summarized
below.
1. Multiple start capability (4 or more)
2. Unspecified minimum time between restarts
3. Moderate start and cutoff time requirements
4. All configurations have engine mounted shutoff
   valves upstream of pumps.

Additional engine control system features were also established prior to select-
ing the control system for each candidate cycle. The oxidizer pump seal package
design requires that a helium purge be used between the shaft riding intermediate
seals during operation. This purge should be activated whenever propellants were
on either side of the seal to preclude any inter-seal leakage during start or
cutoff procedures. An oxidizer system purge during the fuel lead and lag por-
tions of the start and cutoff transients is used to eliminate the possibility
of contaminates in the oxidizer system and to prevent the fuel from flowing back
through the oxidizer side.

During engine start a fuel lead is assumed since the fuel side (including cool-
ing jacket) primes slower than the oxidizer side. This will assure adequate cool-
ing conditions in the jacket at ignition and will avoid large thrust chamber mixture
ratio excursions during the start transient. Since the pumps are to be cooled and
lubricated with the respective propellants, it was considered necessary that the
propellants be admitted to the pumps (main valves opened) before rotation of the

pumps. This will eliminate the possibility of scuffing the passivation film in the oxidizer pump and the possible damage to the face riding seals.

Engine throttling has also been included as a system feature to provide greater flexibility in mission applications. Engine mixture ratio control must also be provided in conjunction with the variable thrust control feature. As the engine throttles, relative changes in fuel and oxidizer pump power requirements must be compensated for with a mixture ratio control system to maintain a constant engine mixture ratio and assure simultaneous depletion of the on-board propellants. It is also desirable to be able to start the engine to any thrust level within the throttle range.

Start System

Engine start methods were reviewed. The tank head start method is the simplest and most attractive of the methods considered and was selected as a basis of engine comparison. Should more rapid priming and preconditioning be needed, a pneumatic power source could be used for the low flow turbine cycles.

Control System - Single Turbine

For the single turbine arrangement control systems are described in Fig. 25 . A variable area FLOX valve is used for mixture ratio control in start and throttling. Bypass and shutoff valves in the turbine line are used to control power. During start the turbine is isolated from the fuel lead to prevent FLOX pump rotation until the bearings and seals are wet and to allow FLOX line purge during the fuel lead. The turbine inlet valve is indicated to assure turbine isolation. The control characteristics of the single turbine are summarized in Table 23 . The methane side will thermally condition and prime using the tank pressure alone. Thermal conditioning times may be 5 to 20 seconds, depending upon initial engine temperatures and tank pressures.

Control System - Dual Turbines, Series and Parallel

Start and cutoff sequences of single and dual turbine are compared in Fig. 26. Since the single turbine must be isolated during portions of the start, the fuel

92

FIGURE 25. CONTROL SYSTEM - SINGLE TURBINE
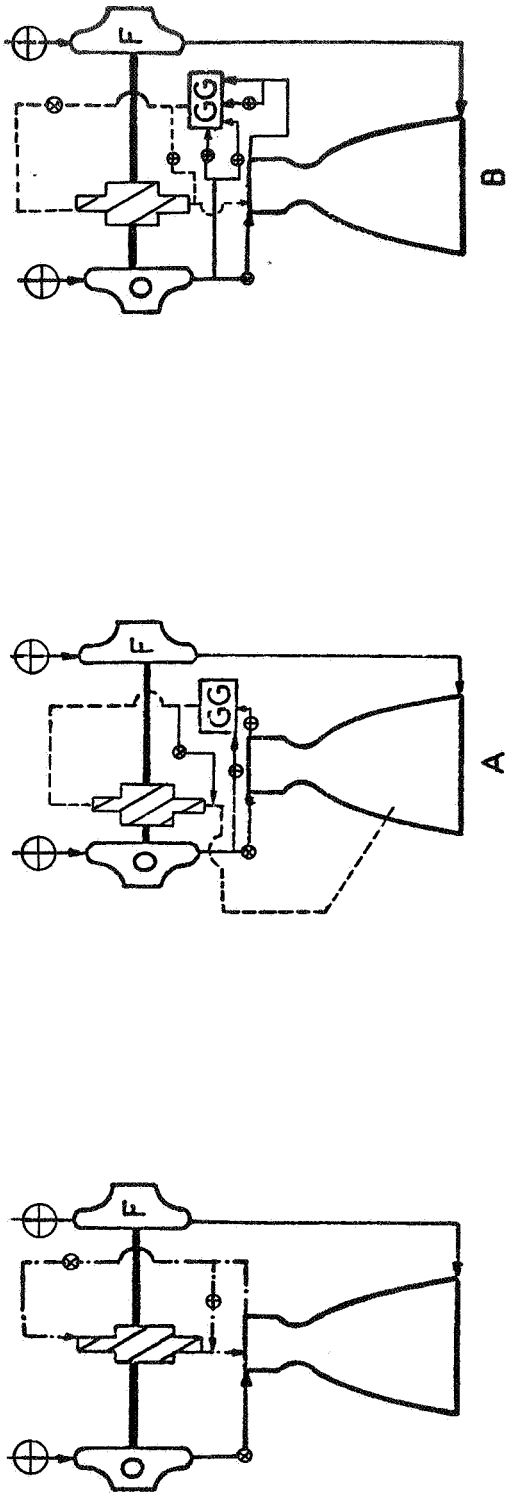
A

B

GAS GENERATOR CYCLE

EXPANDER CYCLE

CHAMBER TAPOFF CYCLE

AUXILIARY HEAT EXCHANGER CYCLE

93
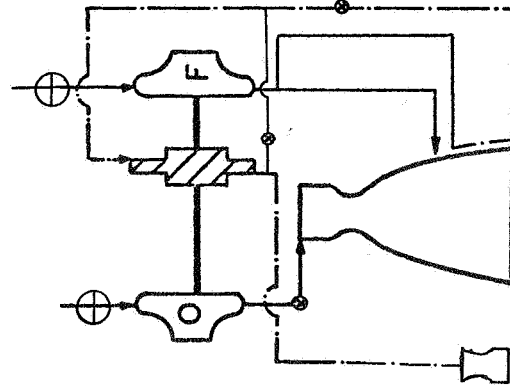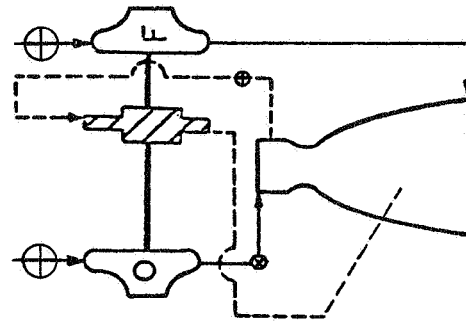
Table 23

CONTROL SYSTEM - SINGLE TURBINE

DRIVE CYCLE FEATURE	EXPANDER	AUXILIARY HEAT EXCHANGER	GAS GENERATOR A	THRUST CHAMBER TAPOFF	GAS GENERATOR B
START SYSTEM	TANK HEAD, IDLE MODE	TANK HEAD, IDLE MODE	TANK HEAD, IDLE MODE	TANK HEAD, IDLE MODE	TANK HEAD, IDLE MODE
START TIME*	LONG	MODERATE	MODERATE	LONG	MODERATE
MAIN VALUES (O/F)	1/1	1/1	1/1	1/1	1/1
THRUST CONTROL,					
HOT METHANE	2	2	—	—	—
HOT FLOX/METHANE	—	—	1	1	1
LIQUID (O/F)	—	—	1/1	—	2/1
MIXTURE RATIO CONTROL (FLOX)	1	1	1	1	1
PURGES	1	1	1	2	1

* SHUTDOWN MAY BE LONG SINCE TURBINE SHOULD BE STOPPED PRIOR TO CLOSING OXIDIZER MAIN VALVE.
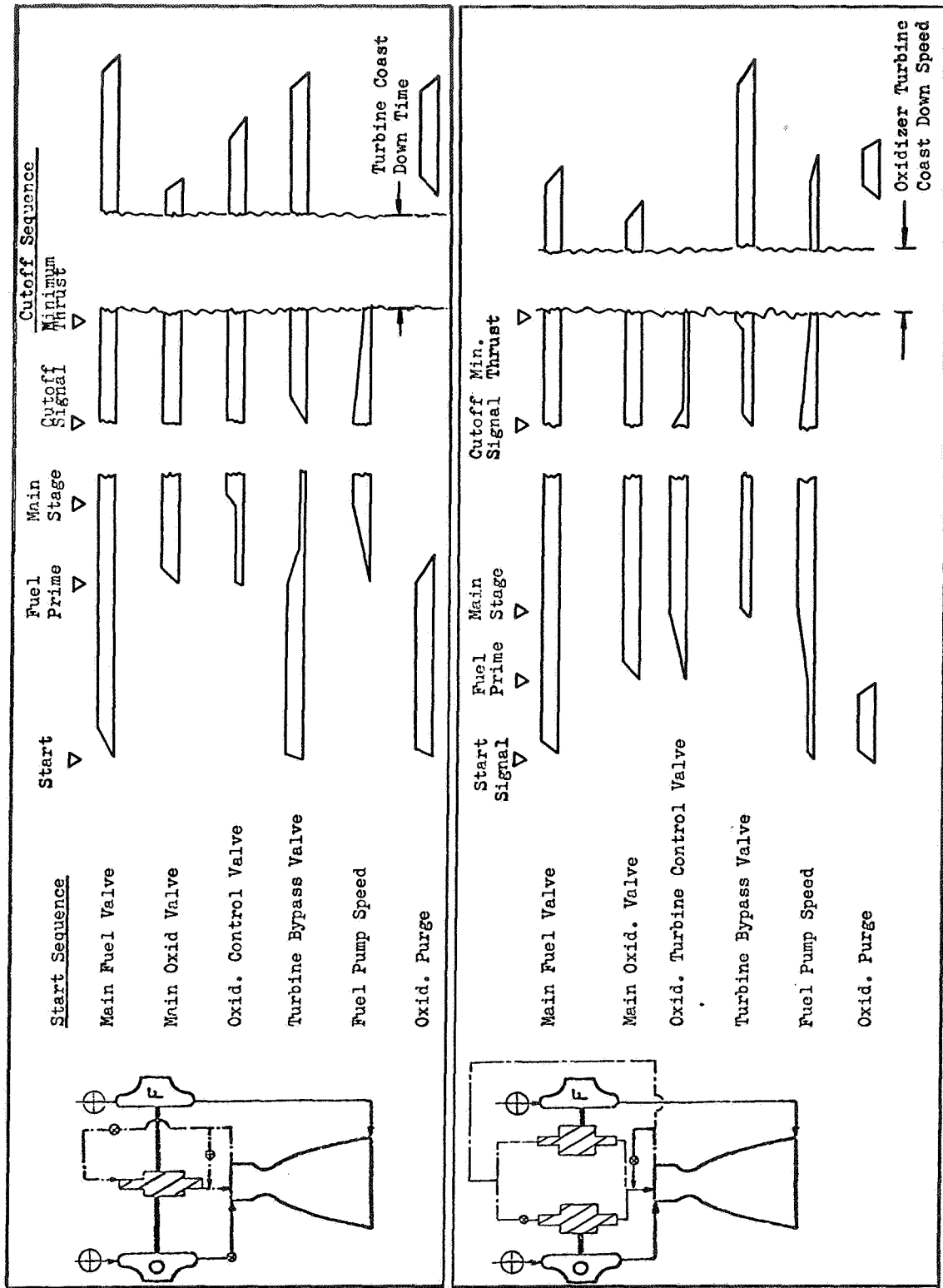
Figure 26. Comparison of Purge System Restrictions on Single and Parallel Turbines

95

system must prime using only tank head. In the dual shaft arrangement, the fuel turbine is not isolated and provides pump power to assist in priming. Thus, the priming and preconditioning times would be shorter with less propellant loss during start.

The resulting control systems for parallel and series turbines are shown in Fig. 27 and 28. Control components are summarized in Table 24.

PUMP CONFIGURATION EVALUATION

Pump configurations were evaluated for each drive cycle, turbomachinery arrangement and design point. An approach was used in which pump design limits were imposed upon a parametric description of pump characteristics. Individual pumps could then be specified for any engine configuration. Pump efficiencies were estimated for the small pump sizes.

For the specific speed range required for these engine cycles, shrouded centrifugal impeller pumps are most appropriate. This configuration will produce relatively high efficiency and be reasonable to manufacture.

Pump Design Criteria

A study was conducted to define and specify pump design parameter limits for the parametric analysis of FLOX/methane engine systems. Limits were established based upon present technology (1970) as represented by current 12 GPM fluorine pump design (NAS3-12022) and the projected technology obtainable with a five-year development program (1975). Table 25 summarizes the pump design limits which were established.

The pump design limits for methane were based upon present designs operating in RP-1 fuel. Problems and failures in RP-1 fuel are minimal and, therefore, these designs are conservative with significant growth potential.
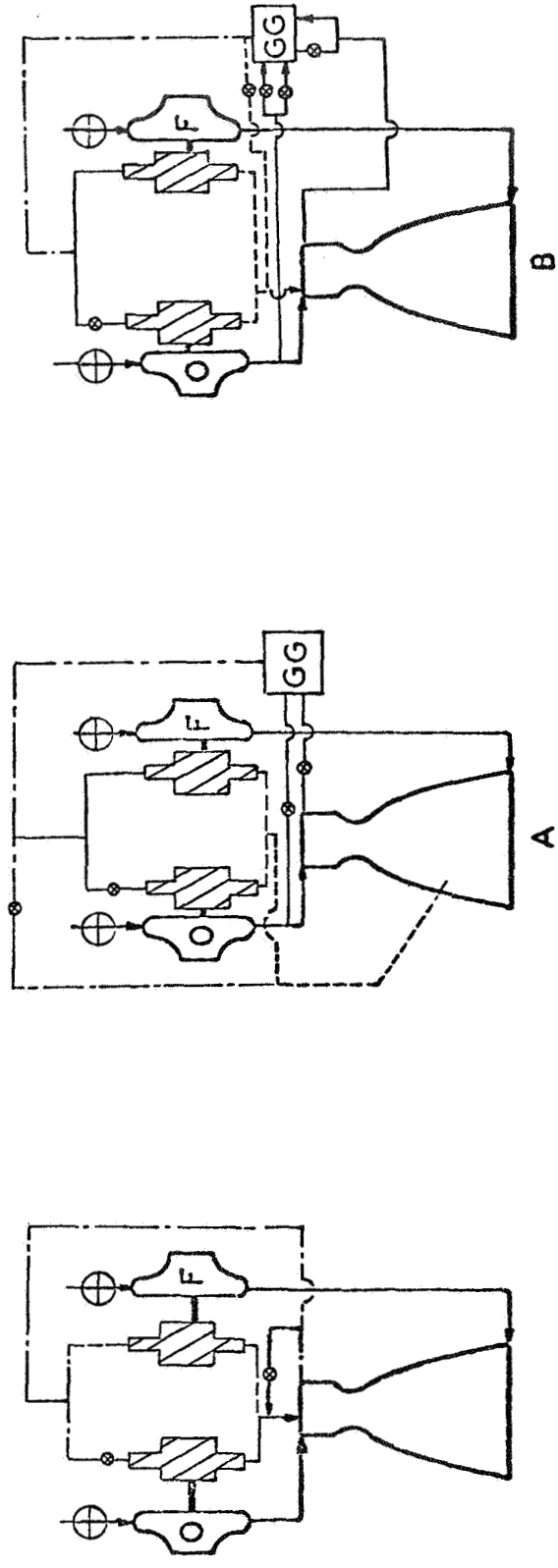
GAS GENERATOR CYCLE   A   B
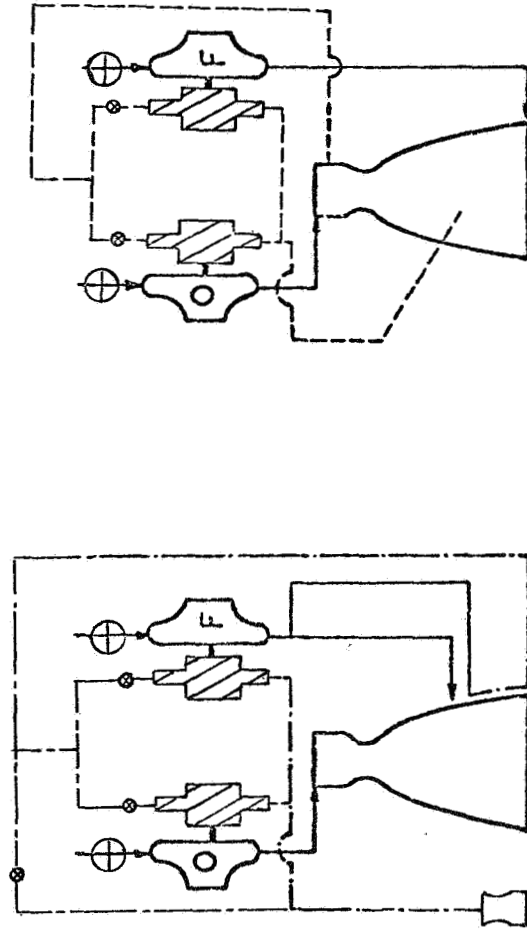
EXPANDER CYCLE

CHAMBER TAPOFF CYCLE

AUXILIARY HEAT EXCHANGER CYCLE

Figure 27. Parallel Turbine Control Systems

97

FIGURE 28 - CONTROL SYSTEM - SERIES TURBINE
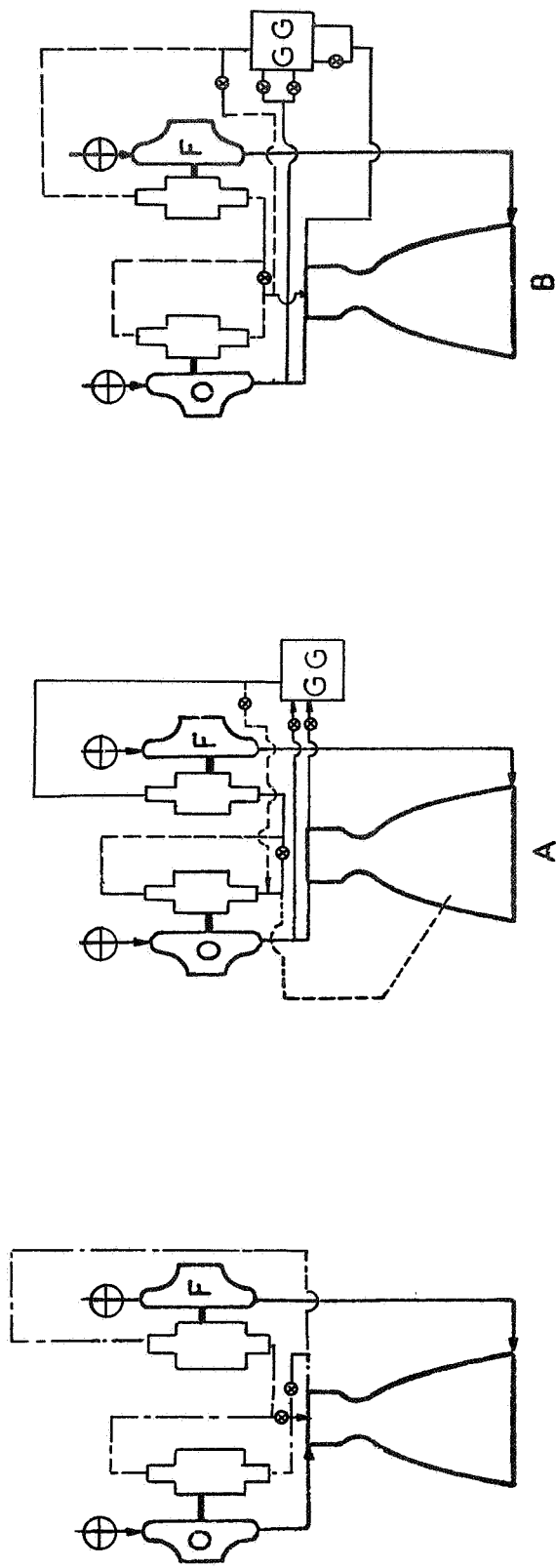
A

B

GAS GENERATOR CYCLE
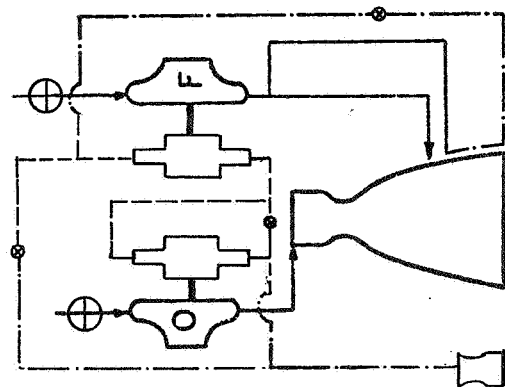
CHAMBER TAPOFF CYCLE

EXPANDER CYCLE
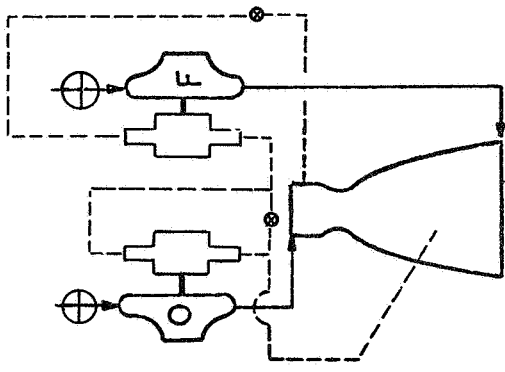
AUXILIARY HEAT EXCHANGER CYCLE

TABLE 24. CONTROL SYSTEM – DUAL TURBINES

DRIVE CYCLE FEATURE	EXPANDER	AUXILIARY HEAT EXCHANGER	GAS GENERATOR A	THRUST CHAMBER TAPOFF	GAS GENERATOR B
START SYSTEM	TANK HEAD	TANK HEAD*	TANK HEAD*	TANK HEAD*	TANK HEAD
START TIME	MODERATE	SHORT	SHORT	LONG	SHORT
MAIN VALVE (O/F)	1/1	1/1	1/1	1/1	1/1
THRUST/MIXTURE RATIO CONTROL					
HOT METHANE	2**	2**	--	--	--
FLOX/METHANE	--	--	2**	2**	2**
LIQUID (O/F)	--	--	1/1	--	2/1
PURGES	1	1	1	2	1

* RAPID START CAN BE ACHIEVED USING SIMPLE AUXILIARY SYSTEM.

** EXTRA VALVE MAY BE NECESSARY FOR SERIES TURBINES.

99

TABLE 25

PUMP DESIGN LIMITS

	FLOX		Methane	
	1970	1975	1970	1975
Bearing DN x 10^{-6}, mm-rpm (mm-rad/s)	0.75(0.078)	1.0(.105)	1.2(.126)	1.8(.188)
Seal Speed, fps (m/s)	180 (55)	250 (76)	250 (76)	400 (122)
Diameter Ratio	0.8 Max.			
Wear Ring Clearance, inches (cm)	0.003 Radial (.0076)			
Impeller Tip Width, inches (cm)	0.030 to 0.070 (.076 to .178)			
Suction Specific Speed, $\dfrac{rpm(gpm)^{0.5}}{ft^{0.75}} \left[\dfrac{rad(\ell/min)^{0.5}}{sec\ m^{0.75}} \right]$	30,000 (14868)			

Bearing DN - FLOX Pump. The fluorine pump of Ref. 4 is designed for a DN of 0.75 x 10^6 mm-rpm (0.078 mm-rad/sec). Values of DN in this range have recently been reported. Consequently, the value of 0.75 x 10^6 mm rpm (0.078 x 10^6 mm-rad/sec) is legitimate state-of-the-art. A value of 1.0 x 10^6 mm-rpm (0.105 x 10^6 mm-rad/sec) was selected as a limit for 1975 as a reasonable projection from current technology.

Seal Rubbing Speed - FLOX Pump. Seals utilizing aluminum oxide against titanium carbide cermet with a nickel binder running at speeds up to 183 fps (56 m/s) have been reported (Ref. 9). This value is currently being used in the fluorine pump design of Ref. 4. A 1970 FLOX pump seal speed limit of 180 fps (55 m/s) was selected for the parametric study. The 1975 FLOX pump seal speed limit was estimated as 250 fps (76 m/s). This value was based upon a reasonably expected advancement in technology.

Diameter Ratio. As in all centrifugal pump designs, the ratio of the impeller eye diameter to the impeller tip diameter should be below 0.8.

Minimum Wear Ring Clearance. Rocketdyne pumps have been designed with approximately 0.003 inches (0.0076 cm) radial wear ring clearance. This appears to be about the minimum that can be held, considering stackup tolerances and bearing looseness. Axial movement should not be a problem with only shrouded impellers being considered.

Impeller Tip Width. With the low flowrates and small sizes which will be encountered in this study, it is possible that the desired impeller configuration will be impossible to make, consequently the impeller tip width of the candidate designs will be checked against various manufacturing techniques to verify fabrication feasibility. It is estimated that minimum tip width is between 0.030 and 0.070-inch (0.076-0.178 cm).

Suction Specific Speed. Suction specific speeds of 23,000 in fluorine have been reported (Ref. 10). Due to the small size of these pumps, a limiting suction specific speed of 30,000 was estimated for use in the parametric study.

Pump Efficiency Prediction

The thrust level of the engine system requires propellant pumps which are small relative to most current pumps. Efficiency estimates for these small-size pumps for use in engine system evaluation studies require adjustment from the large pump efficiency data usually used.

The scaling of large pumps of known performance to a small size does not usually produce a pump of similar performance. Two of the major reasons for this are the impeller wear ring clearances and the relative roughness of the fluid passage walls, both of which increase in the small sizes. The wear ring clearance increases leakage losses while the relative roughness increases the fluid friction losses. This increase in losses requires a downward adjustment of the pump efficiency estimates. These adjustments were made assuming an impeller of about one-inch diameter.

The adjusted curve along with the conventional large pump curve is shown in Fig. 29 . It can be seen in this figure that the adjusted small pump curve agrees very well with efficiencies computed from an Airesearch curve from Ref. 11 and the information taken from Ref. 12. The Hydraulic Institute, Byron Jackson, and Moody adjustments are all based upon adjusting the ratio of the total relative losses by the ratio of the impeller diameter raised to some power. It can be seen that the small pump curve also agrees reasonably well with these scaling methods except possibly at very low specific speeds.
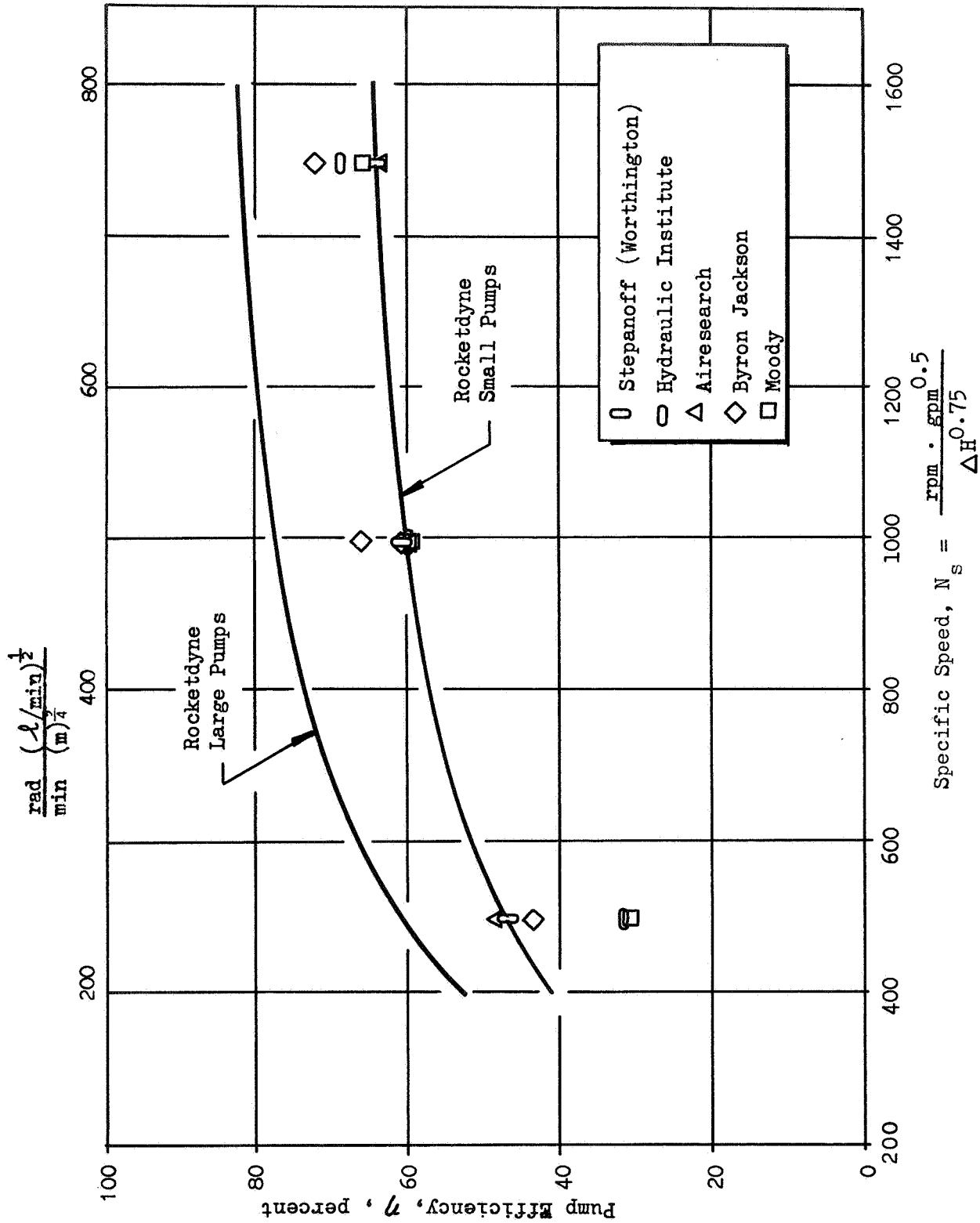
Figure 29 . Pump Efficiency as a Function of Specific Speed

The "small pump" curve of pump efficiency versus specific speed is used to estimate FLOX and methane pump efficiencies for the parametric studies.

Pump Operating Limit Curves

Pump efficiency versus pump speed was plotted for an engine mixture ratio of 5.25 and a series of pump discharge pressures. These are presented in Fig. 30 for one-stage FLOX pumps and for one- and two-stage methane pumps in Fig. 31 and 32 . Cross-plotted on these curves are the seal speed, bearing DN, and impeller diameter ratio limit regions identified in Table 25 . The limits are plotted as regions due to variations in the mechanical design of the turbopump.

These curves were used in selecting the operating speed of pumps being evaluated for the requirements of the various engine cycles and chamber pressures. For a given pump discharge pressure requirement, the pump speed and efficiency were selected to be near the left hand or most conservative boundary.

At high discharge pressures, single-stage pump efficiency decreases as can be seen in Fig. 31. Where the efficiency difference was significant, two-stage methane pumps were selected. One-stage FLOX pumps were used throughout because discharge pressures were relatively low and to avoid the increased potential rubbing surface of the two-stage pumps.

Methane-cooled bearings for the FLOX pump were briefly considered but, as can be seen in Fig. 30 , the FLOX seal speed is as limiting as the bearing DN. There would be no advantage in pump speed and the increased overhang required to incorporate the seal package between the FLOX pump, and a methane bearing presents a potential rubbing problem. FLOX cooling bearings were, therefore, selected for the FLOX pump.

Pump Design

Pumps were defined for each engine configuration using the parametric curves. The FLOX pumps were all single stage. Shaft size and thus bearing and seal diameter increased with higher discharge pressure. To maintain consistent DN and
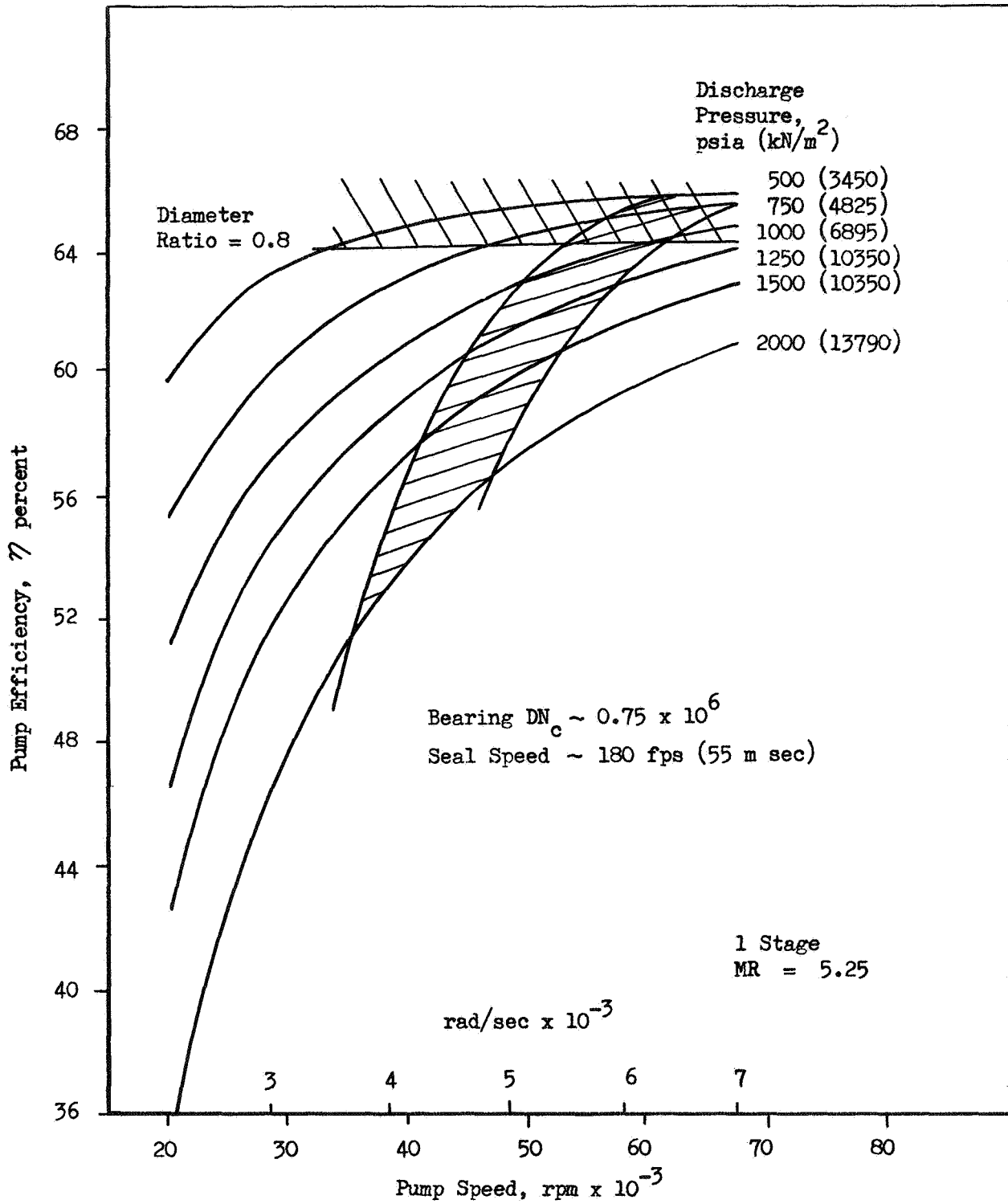
Figure 30. Flox Pump Efficiency and Operating Limits
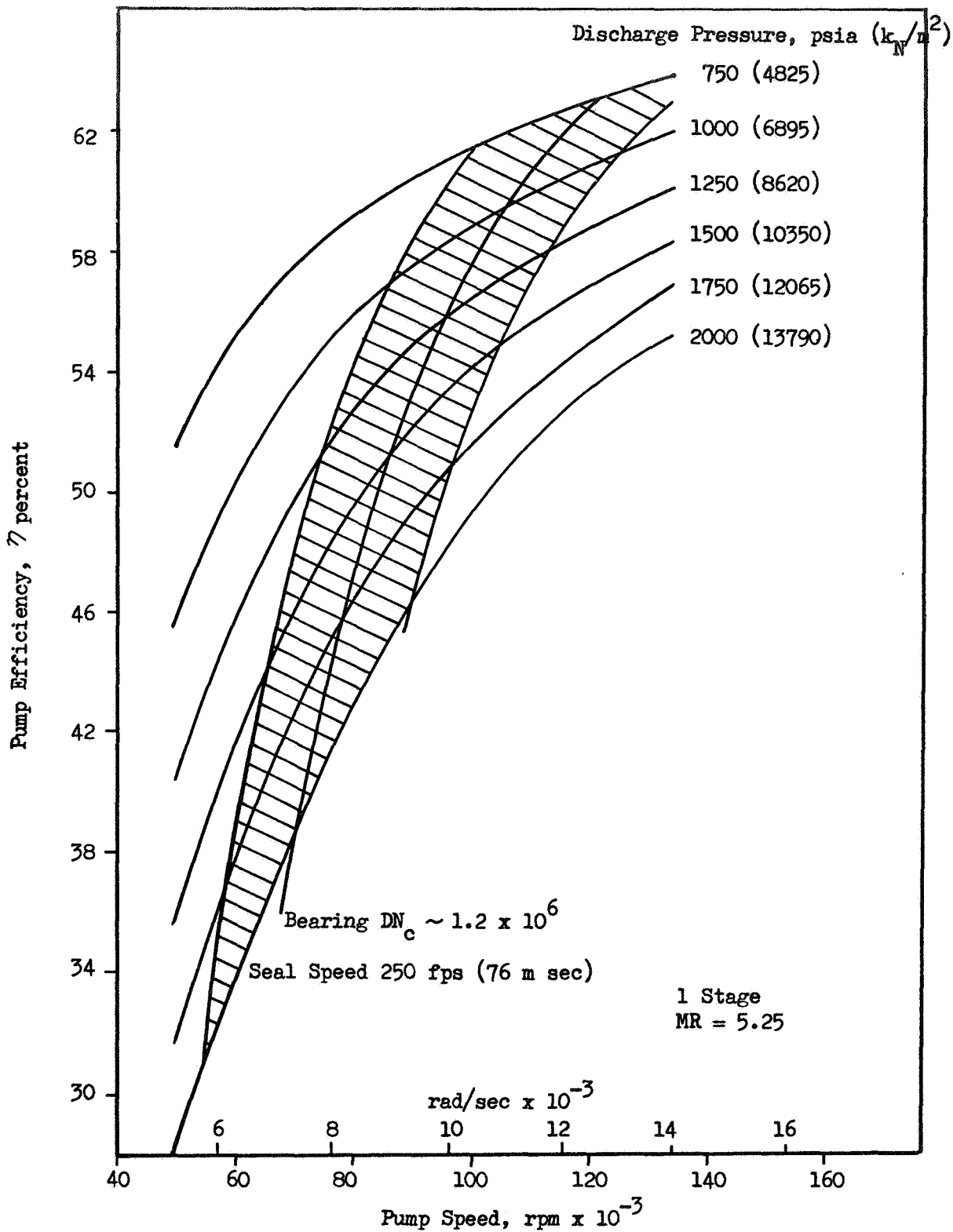
Figure 31. CH_4 Pump Efficiency and Operating Limits
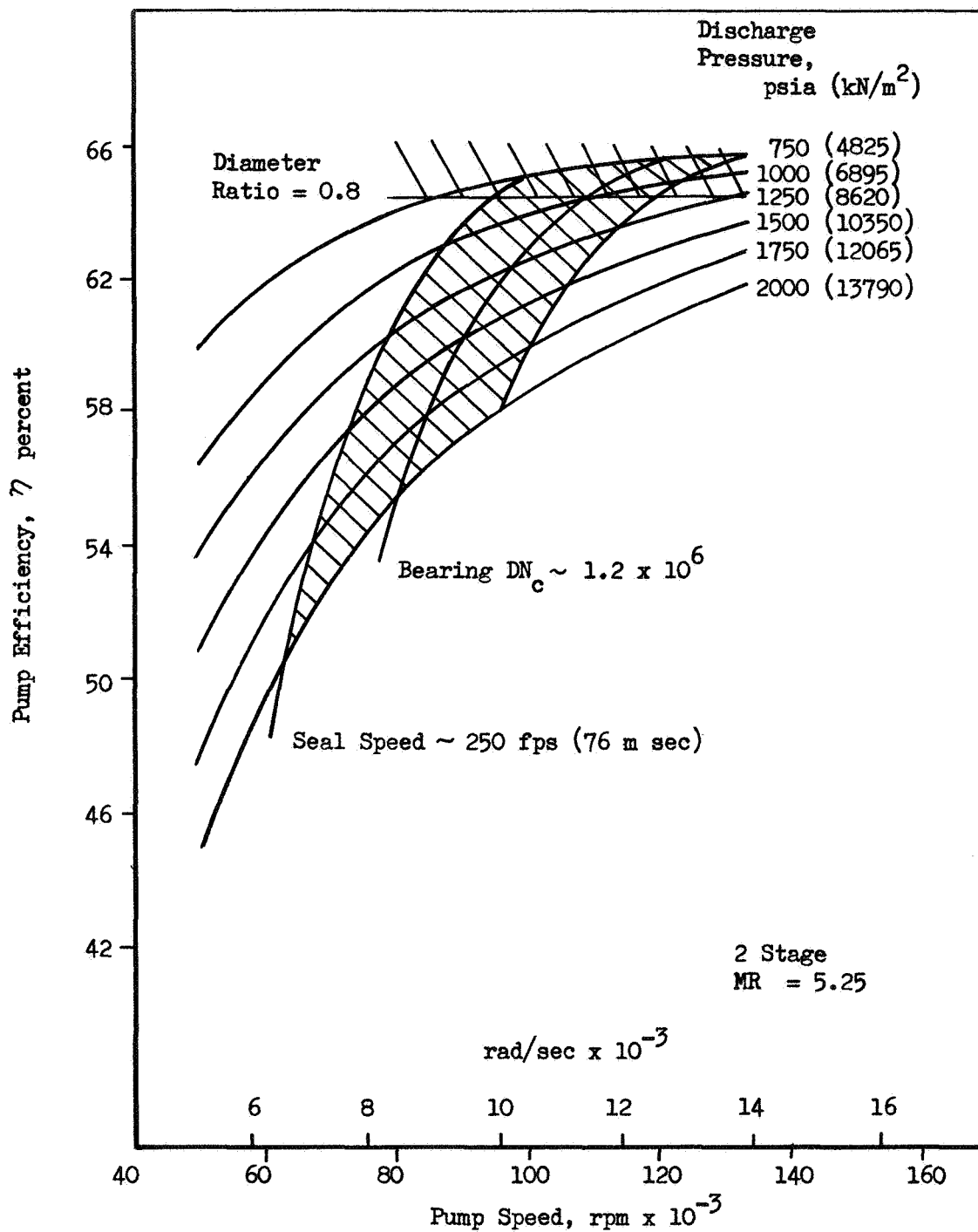
Figure 32. CH_4 Pump Efficiency and Operating Limits

seal speed values, rotating speed was decreased as discharge pressure increased. The FLOX pumps operated at 50,000 rpm (5230 rad/sec) for low discharge pressures and at 40,000 rpm (4190 rad/sec) for high discharge pressures. Bearing DN and seal speed values were the same for all FLOX pumps. The NPSP values required were 12 to 17 psia (0.83 to 1.17 kN/m^2).

Methane pumps were sized in a similar manner with the seal speed values of 250 fps (76 m/s) predominating and a bearing DN (slightly lower than the selected design limit value. The low turbine flow cycles at 500 psia (34.5 kN/m^2) used one-stage methane pumps. Two-stage methane pumps were used for the other configurations. In dual shaft and gear-driven configurations, the methane pumps operated at speeds of 70,000 to 80,000 rpm (7310 to 8360 rad/sec) with the higher discharge pressure pumps at the lower speed to maintain consistent seal speeds. In the single-shaft pump arrangement, the methane pump operated at the FLOX pump speed. NPSP values required were around 5 psia (0.35 kN/m^2).

Design Differences. The resulting pump designs all reflect the same bearing and seal technology. Differences appear, however, in the impeller and the inducer of the methane pumps. At high discharge pressures, the impeller tip width becomes quite small. Values of 0.035-inch (0.089 cm) (recirculation not included) and lower are required. These are encountered in the expander and gas generator (B) cycles, particularly in the single shaft arrangements. Some fabrication difficulty would be involved relative to lower pressure pumps with tip widths in the 0.060-inch (0.15 cm) range. In the methane pump on the single-shaft arrangement, the inducer is built around the drive shaft. Within this annulus the inducer blades become quite small and may cause fabrication difficulty or inlet performance degradation.

TURBINE ARRANGEMENTS

A series of turbine arrangements were investigated to establish the best configuration for each drive cycle. For each arrangement, turbines were analyzed and the design giving the best performance was selected. Preliminary design

sketches were made to assess design problems. Turbine operating temperatures were varied and a design value was selected based upon performance and development ease. Turbine coking, a potential problem with turbines using FLOX/methane combustion products, was investigated. Assessing performance, development ease, and the operational aspects described previously, turbomachinery arrangements are recommended.

Candidate Arrangements

Four turbine-pump arrangements were considered as shown in Fig. 23.

Single-Shaft Pumps Back-to-Back. This configuration offers advantages such as: a) the total horsepower of both pumps being developed in one turbine allows a more desirable turbine design; b) it is not overly complicated with either gearing or control problems. This configuration does penalize the methane pump efficiency, as the speed is limited by the FLOX seal and/or bearing.

Single Turbine Gear-Driven. The gear-driven configuration has the advantage of developing the total horsepower of both pumps in a single turbine. Both the pumps and the turbine can be operated at the most desirable speed and provide good suction characteristics. The additional bearings and gears result in increased turbomachinery complexity.

Dual Shaft with Turbines in Series or in Parallel. As in the single-geared pump this configuration minimizes suction performance problems and allows each pump to operate at its most desirable speed. Chances of catastrophic failure are minimized by isolating each propellant in its own machine.

Turbine Design Criteria

One of the major turbine design goals is high efficiency. The turbine efficiency which can be attained is closely related to the isentropic velocity ratio, which is the ratio of the pitch velocity (U) to the isentropic spouting

Dual Shafts

Turbines in Series

Turbines in Parallel

Direct Drive

Single Geared Pump
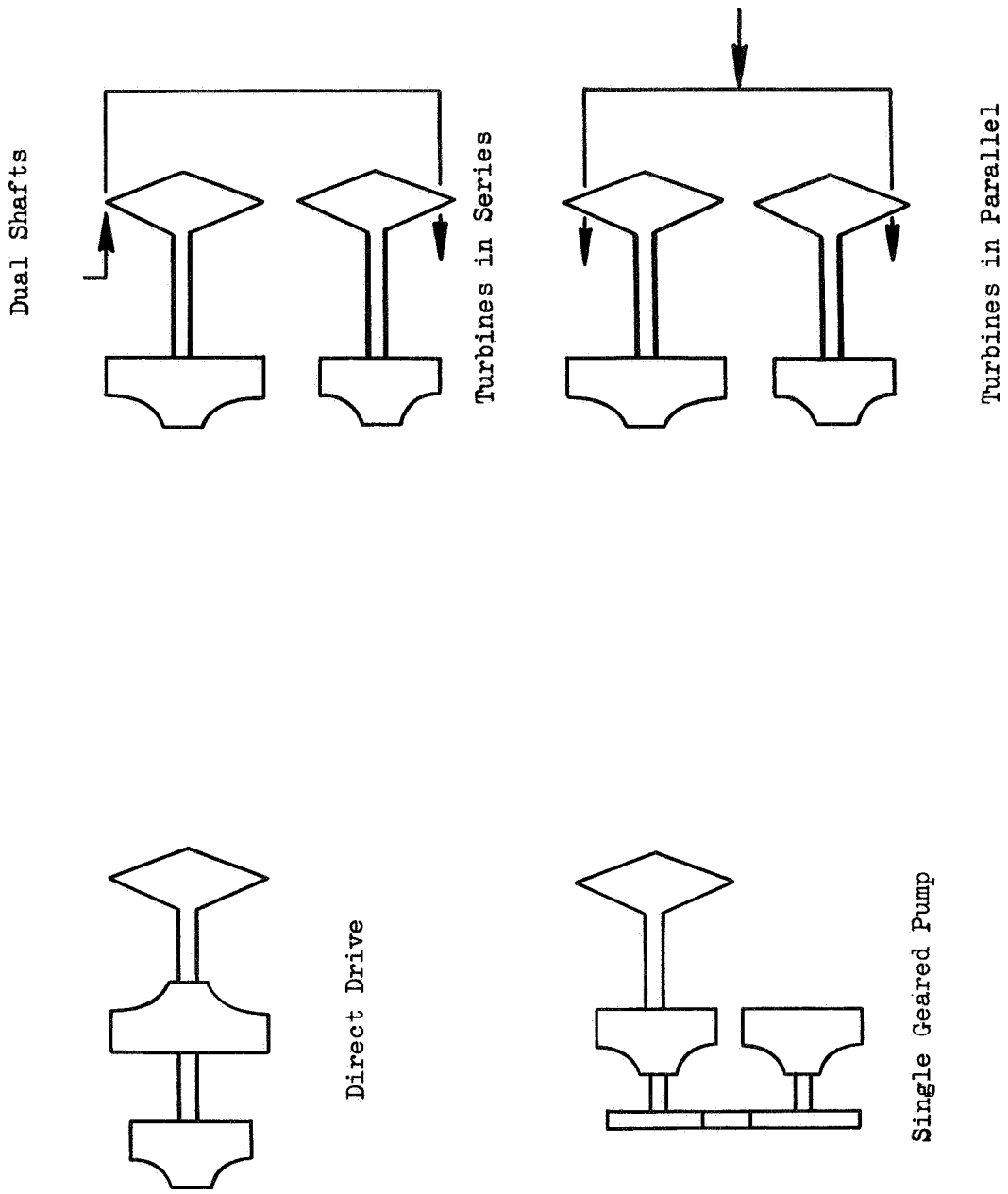
Figure 33 . Turbopump Configurations

109

velocity (C_o). For high pressure ratio stages such as used in the gas generator (A) cycle, the isentropic spouting velocity is supersonic. Correspondingly high pitch line velocity is required to operate at acceptable turbine efficiency. Low pressure ratio turbine designs used in the gas generator (B) and expander cycles generally operate below the critical pressure ratio and require lower pitch line velocities than the gas generator (A) type cycles to produce high efficiency.

From consideration of stress, fabrication, and testing certain limits were placed on the turbine design. Centrifugal stress provided an upper bound on pitch diameter, rotating speed and blade height. As a simplified bound on the turbine stress, a maximum tip speed of 1500 fps (457 m/s) was used for material temperatures below 1500 F (1090K). Preliminary layouts of turbomachinery configurations indicate that because of bearing and seal package size, turbine pitch diameters will have minimum size limits. A lower limit on pitch diameter of 2.0-inch (5.08 cm) was established. Turbine blade heights can become very small for this low thrust level. To promote ease of fabrication and to diminish the effect of gas leakage on efficiency, blade heights of 0.15-inch (0.38 cm) were judged to be a lower limit. On the low turbine flow drive cycles in which the gases are dumped overboard, turbine development can be facilitated by limiting the turbine discharge pressure to values greater than 14.7 psia (101 k N/m^2). Therefore, outlet pressure in the 20 psia (138 k N/m^2) range were used.

Turbines

Turbines were analyzed and defined to match the pump power and speed requirements. A variety of turbines were analyzed for each engine configuration. In this analysis single-row impulse and two-row velocity-compounded turbines were considered. For the low flow turbines, both pressure ratio and turbine type were considered. The turbine operating conditions were selected to minimize the weight flow necessary to provide the required pump power. In the high flow cycles [expander and gas generator (B)], both turbine types were considered and the pressure ratio was adjusted to give the required pump horsepower. Resulting turbine efficiencies are described below.

Chamber Pressure, psia (kN/m^2)	Representative Turbine Efficiency	
	Low Flow Turbines	Topping or High Flow Turbines
500 (3450)	0.4 – 0.5	0.45 – 0.65
800 (5520)	0.45 – 0.55	0.55 – 0.65

The low flow turbines [used in gas generator (A)], thrust chamber tapoff, and auxiliary heat exchanger cycles, generally had two-row turbines, while the topping cycle turbines for the most part used single-row turbines. For most of the engines, some amount of partial admission was used to give high turbine performance.

Turbine Inlet Temperature

The effect of turbine inlet temperature on engine performance was investigated. For the expander cycle, the turbine inlet temperature was the thrust chamber cooling jacket exit temperature. The temperatures (and the pressure drops associated with them) were based upon the thrust chamber heat transfer analyses described previously with Q_m/Q_p = 1.0. Increases in the heat flux levels could increase both temperature and pressure drop.

For the auxiliary heat exchanger, the effect of turbine inlet temperature on performance and the temperature available from a nozzle heat exchanger are shown in Fig. 34 . The methane temperature was restricted to below 1960R (1090K) to avoid coking. A turbine inlet temperature of 1860R (1030K) was selected.

In the remaining cycles which use $FLOX/CH_4$ combustion products, turbine inlet temperature is governed by the mixture ratio of the two propellants. For the gas generator (A) cycle, the effect of inlet temperature on performance and the gas generator mixture ratio are shown in Fig. 35 . The same curves are also representative of the thrust chamber tapoff cycle, where the mixture ratio would be that of the gases tapped from the main combustion chamber. A turbine inlet temperature of 1960R was selected.

111

Figure 34

EFFECT OF TURBINE INLET TEMPERATURE

AUXILIARY HEAT EXCHANGER CYCLE
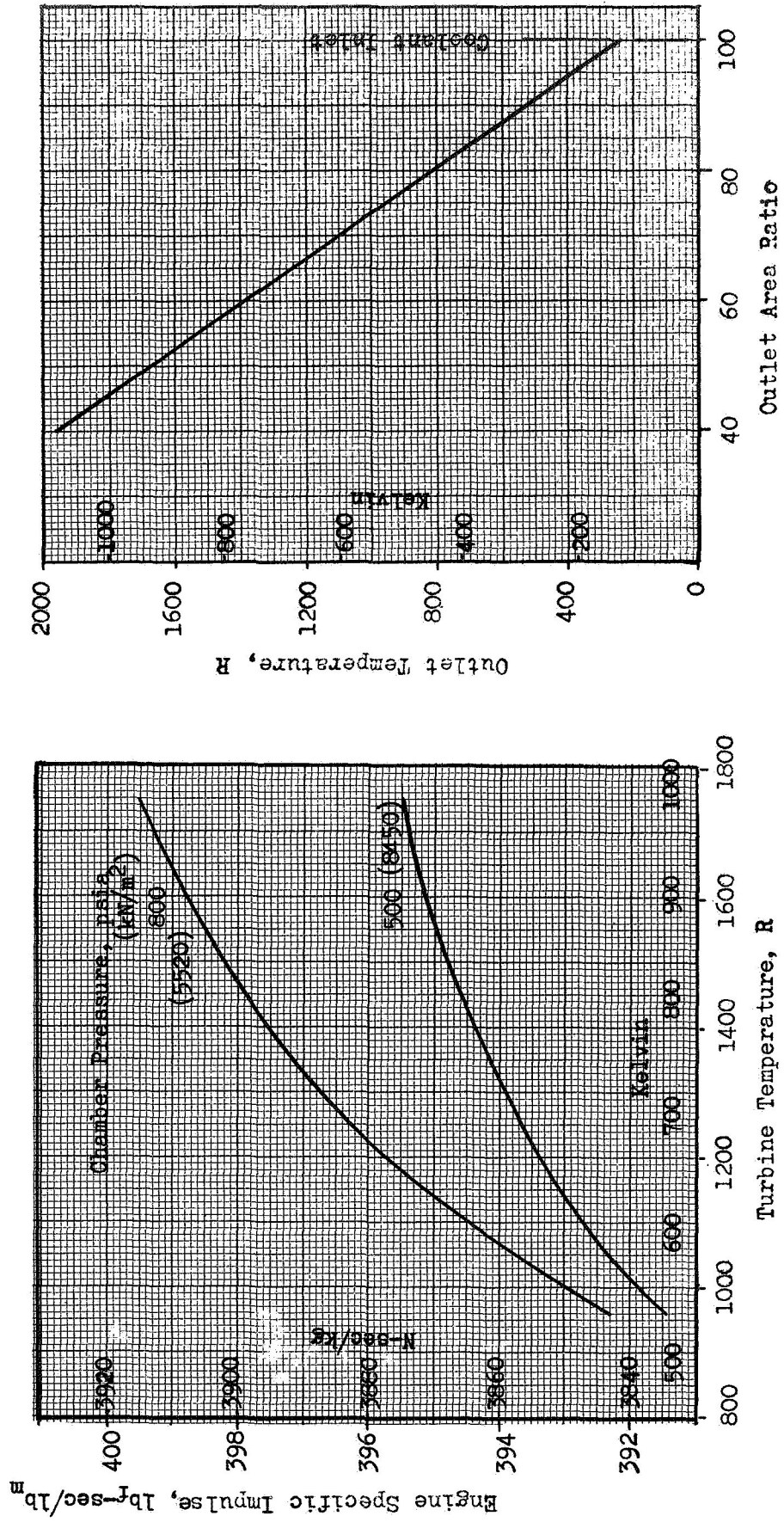
Figure 35

EFFECT OF TURBINE INLET TEMPERATURE GAS GENERATOR (A) CYCLE

113
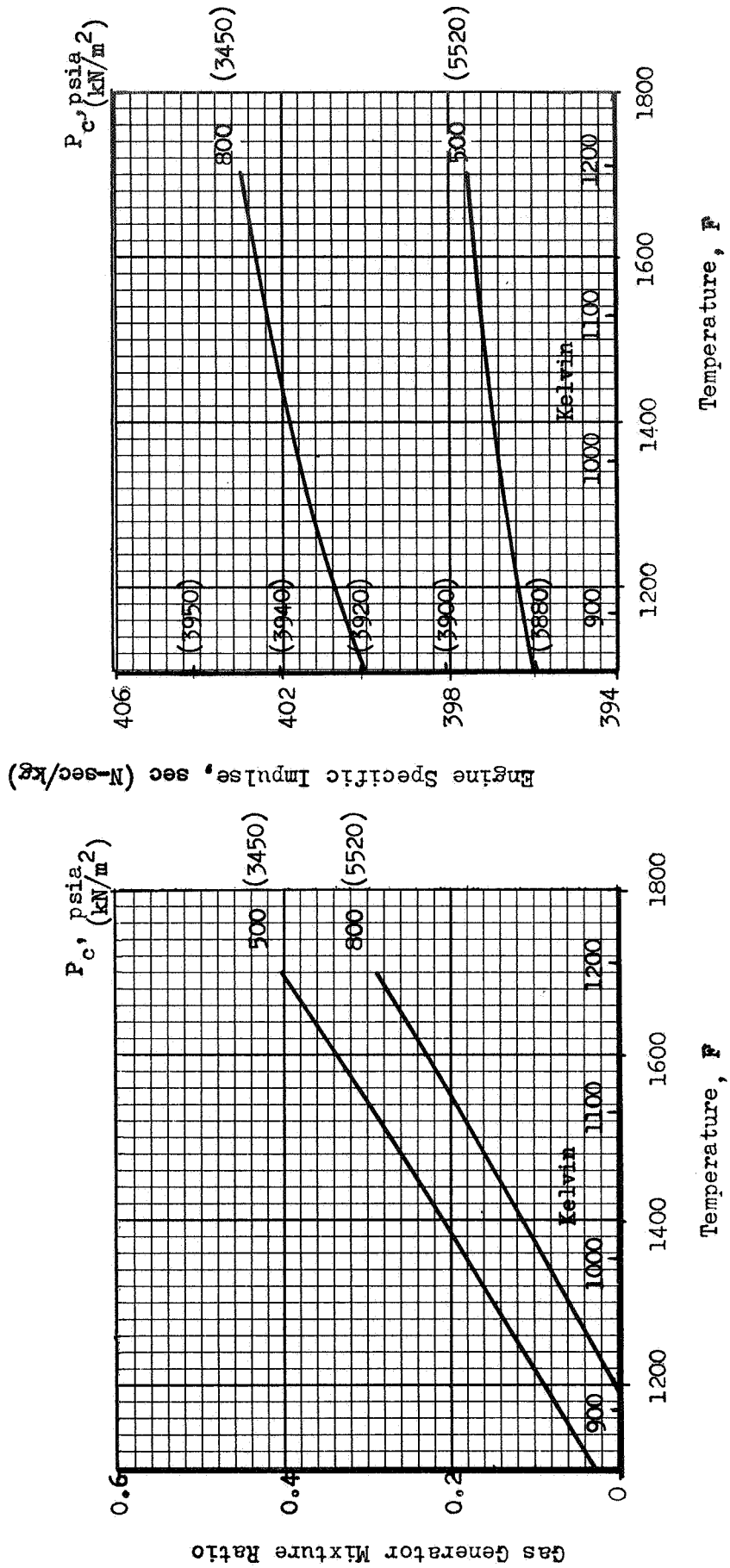
In the gas generator (B) cycle, engine performance is unaffected by the turbine temperature. However, turbine pressure ratio, and therefore pump discharge pressure, is affected. As gas generator mixture ratio is decreased, both turbine temperature and the available turbine flow are diminished. This requires higher turbine pressure ratios and, in turn, higher pump discharge pressures. A temperature of 1960 R (1090K) was selected.

Turbine Nozzle Coking

Based on experience with LOX/RP-1 engines, turbine coking appears to be a potential problem which could have a major effect upon a development program. Typical of the decrease in turbine nozzle area with LOX/RP is that which occurs with the F-1 engine turbine, as shown in Fig. 36. At 1500 F (1090K) the turbine nozzle area decreases by 9-percent over a 125-second firing. Since the FLOX/CH$_4$ turbines are considerably smaller and longer firing times ($\sim$ 500 sec) are anticipated, these carbon deposition rates would be totally unacceptable.

By comparing the solid carbon concentration in FLOX/CH$_4$ combustion products at a given temperature with the concentration in LOX/RP products, turbine data were scaled to give an estimate of carbon deposition that might be encountered. These are shown in Fig. 37. Comparing these with the turbine nozzle sizes expected for the FLOX/CH$_4$ engine indicates that the nozzle area reduction would be very severe, as shown in Fig. 38. The temperatures could be raised above 1800 F (1250K) and the deposition reduced at the expense of developing a high temperature turbine. Temperature could be lowered with the possibility of producing soft carbon; however, performance losses or pump discharge pressure increases are significant. A third alternative would be to reduce the F$_2$ concentration in the FLOX to reduce carbon concentration. This would result in significant performance losses, as shown in Table 26 and the carbon reduction is slight.

From these considerations, turbine inlet temperatures were selected. For the turbines using FLOX/CH$_4$ combustion products, the selected temperatures avoid the use of high temperature turbines, however turbine coking remains as a major development problem.

114

TURBINE COKING

- LOX-RP PRODUCTS
- DEGRADES POWER

COKING WITH LOX/RP-1 TURBINE WORKING FLUID
F-1 ENGINE S/N 034
TESTS 4 THRU 9 AT EDWARDS IBI IN 1967

TEST	4	5	6	7	8	9
	T_{ti}-1500° F	T_{ti}-1500° F	T_{ti}-1700° F	T_{ti}-1715° F	T_{ti}-1400° F	T_{ti}-1500° F

$\frac{A_e}{A_e \text{ REF}}$

1.00, 0.96, 0.92, 0.88, 0.84

TOTAL TEST TIME, SEC.

0, 100, 200, 300, 400, 500, 600, 700, 800, 900

A_e - TURBINE NOZZLE EFFECTIVE AREA
A_e REF - FIRST A_e OF TEST 4
T_{ti} - TURBINE INLET TEMPERATURE
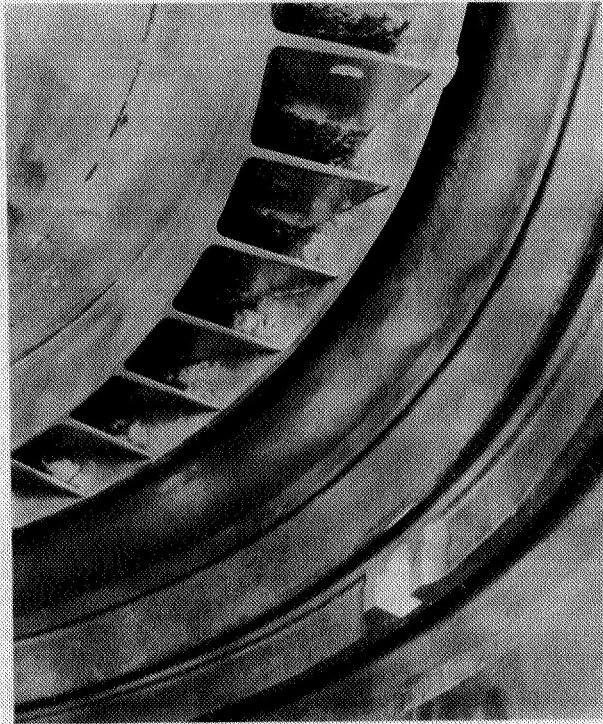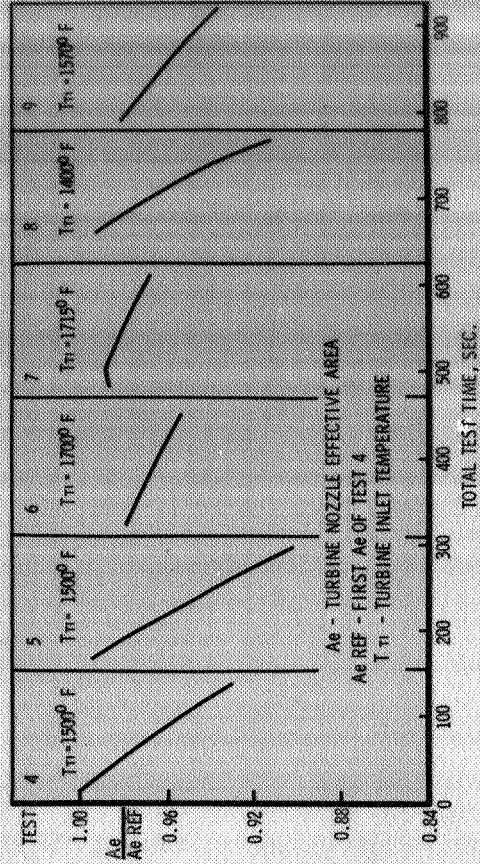
MARK 10 NOZZLES
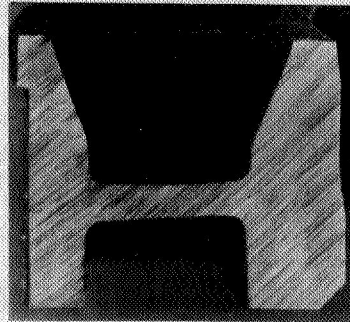
RADIAL SECTION

AXIAL SECTION

MARK 3 TURBINE FIRST STAGE NOZZLE

Figure 37

ESTIMATED CARBON DEPOSITION

DEPOSITION = f [TEMPERATURE, SOLID CARBON CONCENTRATION, TIME]
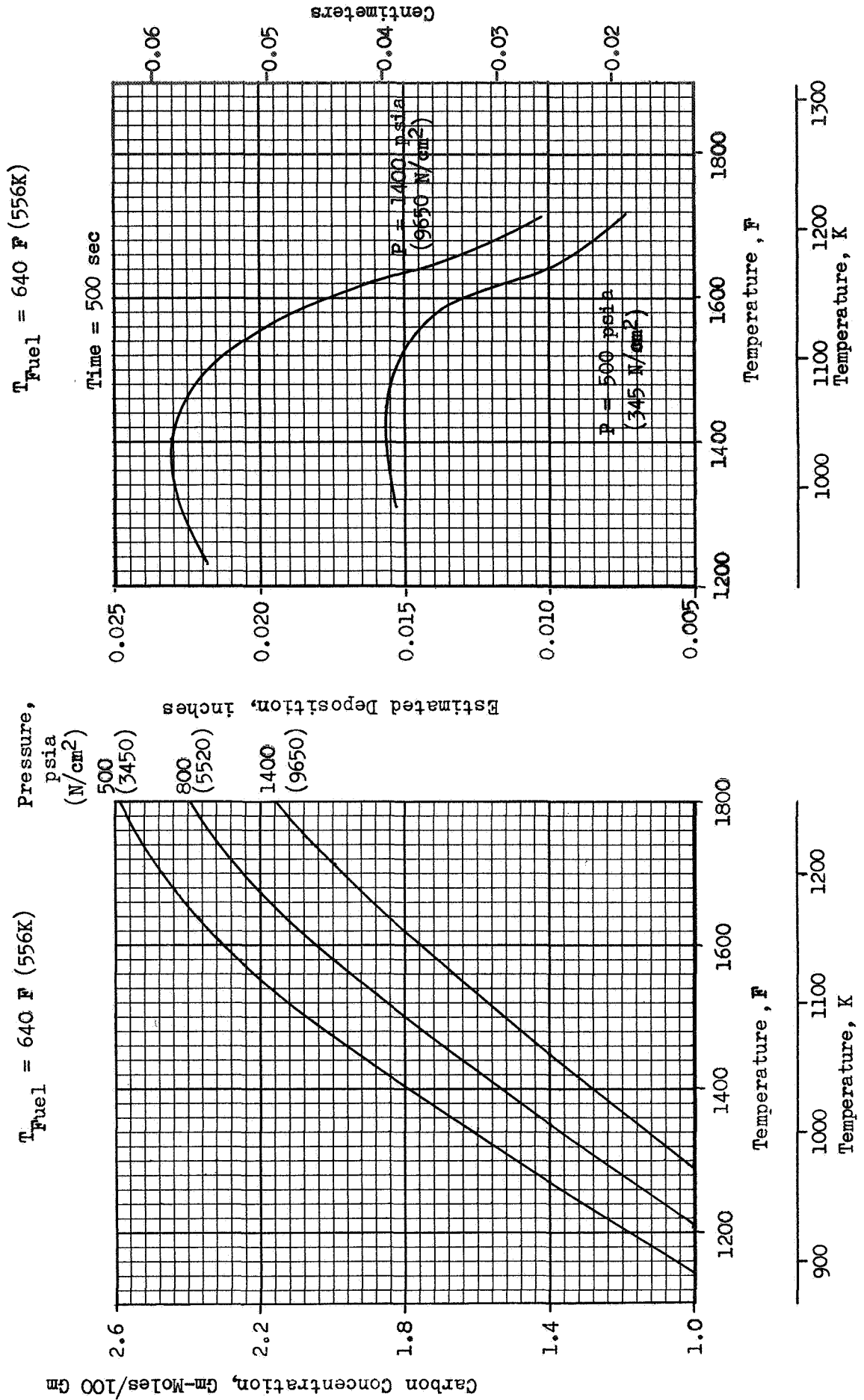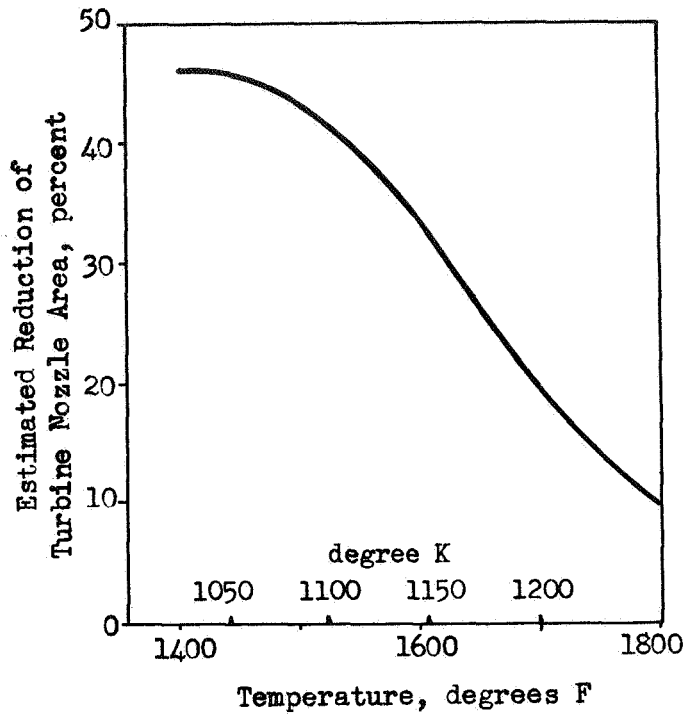
Figure 38. Effect of Temperature on
Turbine Area Reduction

TABLE 26

EFFECT OF FLOX CONCENTRATION

	0.3	0.3
Gas Generator Mixture Ratio	0.3	0.3
Gas Generator Temperature, R (K)	1880 (1044)	1887 (1048)
Percent F_2	70	82.5
Carbon Concentration (gm moles/100 gms)	1.59	1.63
Theoretical Thrust Chamber Specific Impulse (MR = 5.25), sec (N-sec/kg)	421 (4130)	428 (4200)

Turbomachinery Design Evaluation

Figures 39 through 42 present preliminary conceptual layouts of the three
different turbopump arrangements being considered. These layouts were made
to assess the physical and mechanical limitations and problems associated
with the various arrangements and are full size.

Dual shaft configurations are shown in Fig. 39 and 40 . Figure 39 presents
a FLOX pump with FLOX-lubricated bearings, and a seal package containing a
face riding seal, a purged intermediate shaft riding seal, and a face riding
hot gas seal. The cavities between the two face riders and the shaft seal
are drained. The face riding seals ride on the inner bearing race and on the
turbine wheel so that the turbine overhang could be reduced. Figure 40 pre-
sents a two-stage methane pump with methane-lubricated bearings. This pump runs
at about twice the speed of the FLOX pump.

Figure 41 presents a geared arrangement of pumps designed to meet the same
requirements as the previous designs. All bearings, gears and seals run in
methane with the exception of one FLOX-lubricated bearing and the primary FLOX
seal. The FLOX-lubricated bearing reduces the FLOX pump overhang without com-
promising the FLOX pump speed. A single-stage methane pump is shown for compari-
son with the two-stage version in Fig. 42 . The advantage of the geared arrange-
ment is that all the horsepower is produced in one turbine, thus improving the
turbine design. This improvement must be weighed against the disadvantage of
gears, gearcase, and additional bearings and side loads.

A single shaft arrangement running at the FLOX pump seal speed limit is shown
in Fig. 42 . The bearings are methane lubricated. The long axial stackup and
high torque transmission require a relatively large shaft which may introduce
critical speed problems. The methane inducer inlet and turbine design are com-
promised in this arrangement because of the large shaft and the low speed, re-
spectively.
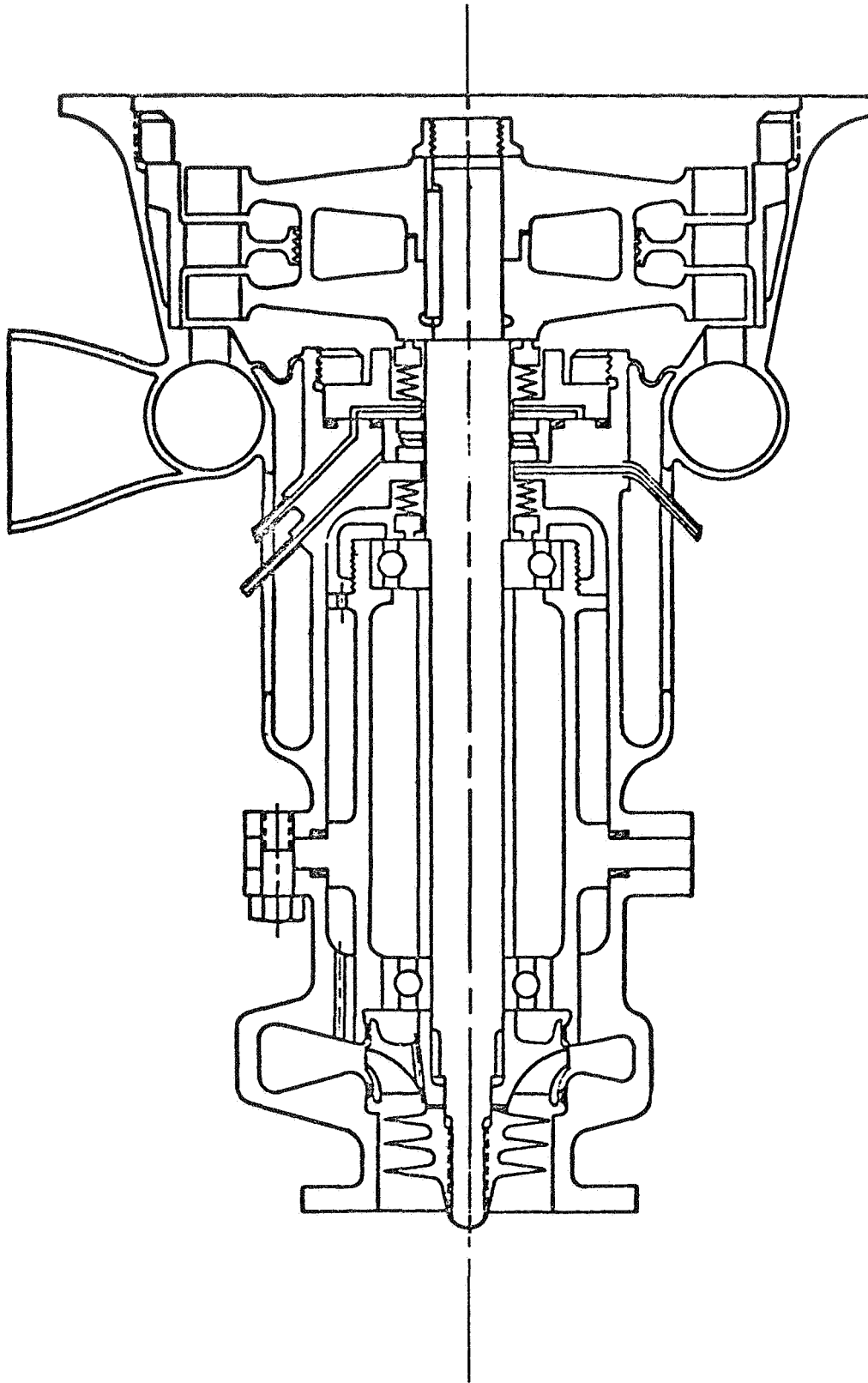
Figure 39 . 5000-pound Thrust FLOX Pump, Dual Shaft.
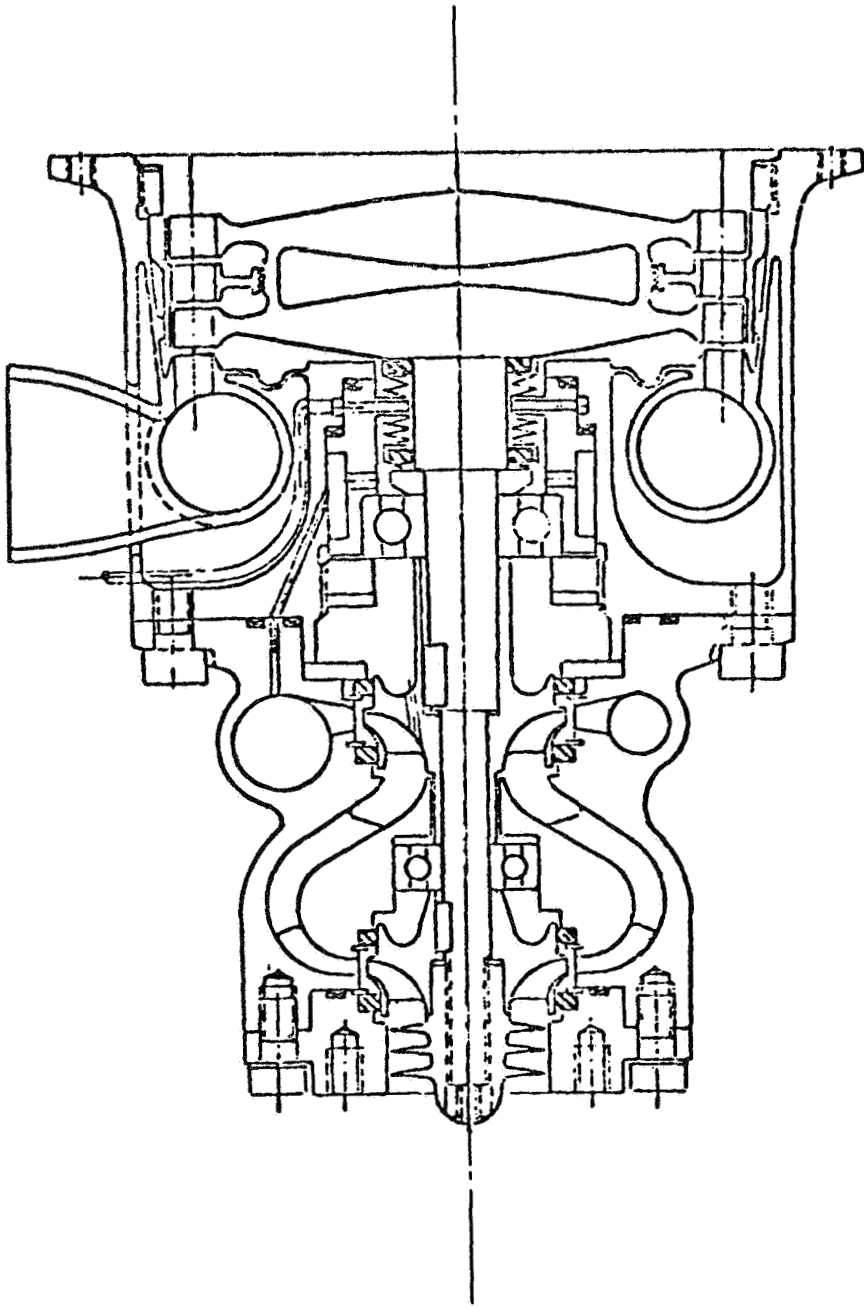
Figure 40. 5000-pound Thrust Methane Turbopump, Dual Shaft.
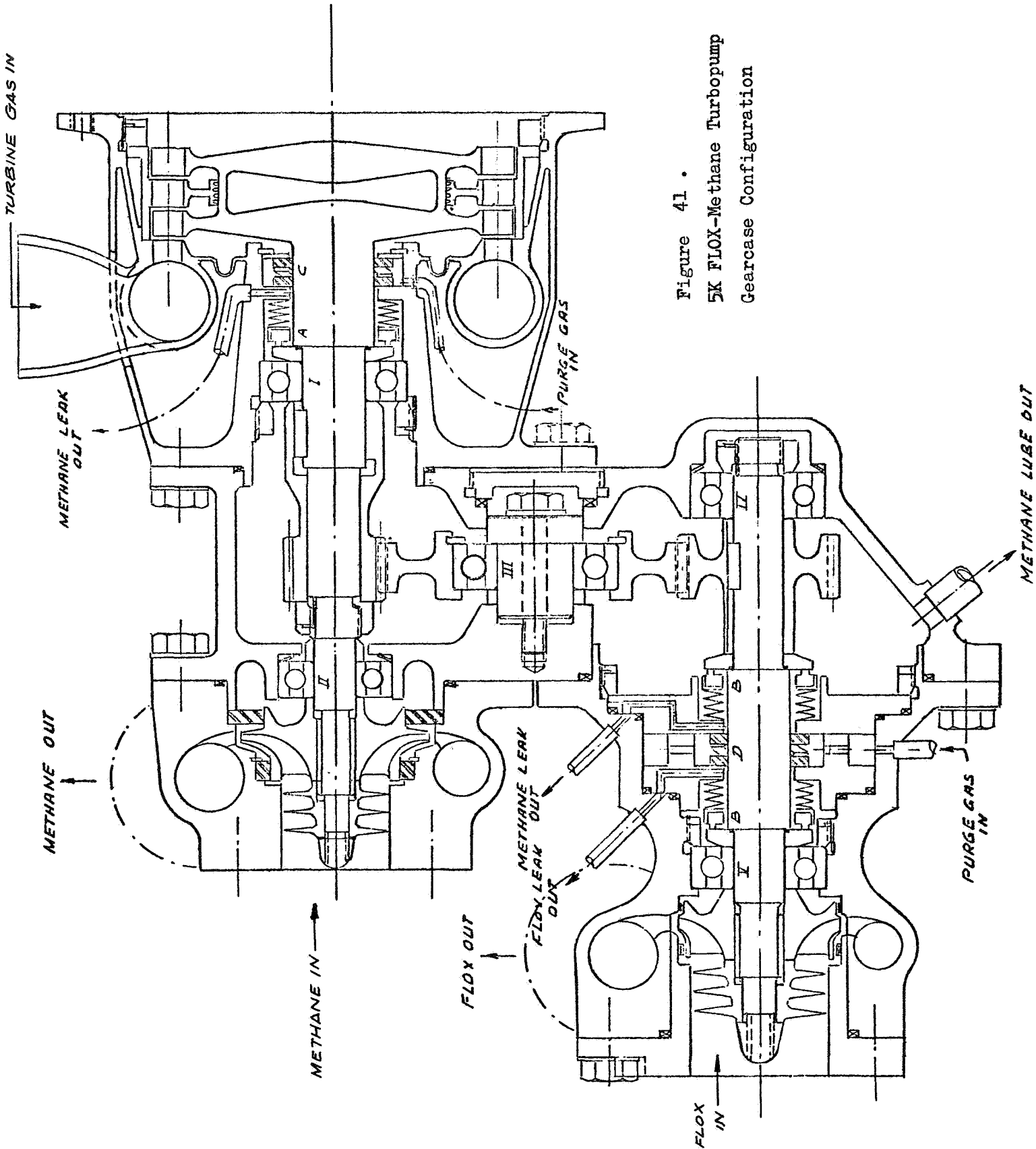
Figure 41.
5K FLOX-Methane Turbopump
Gearcase Configuration

121
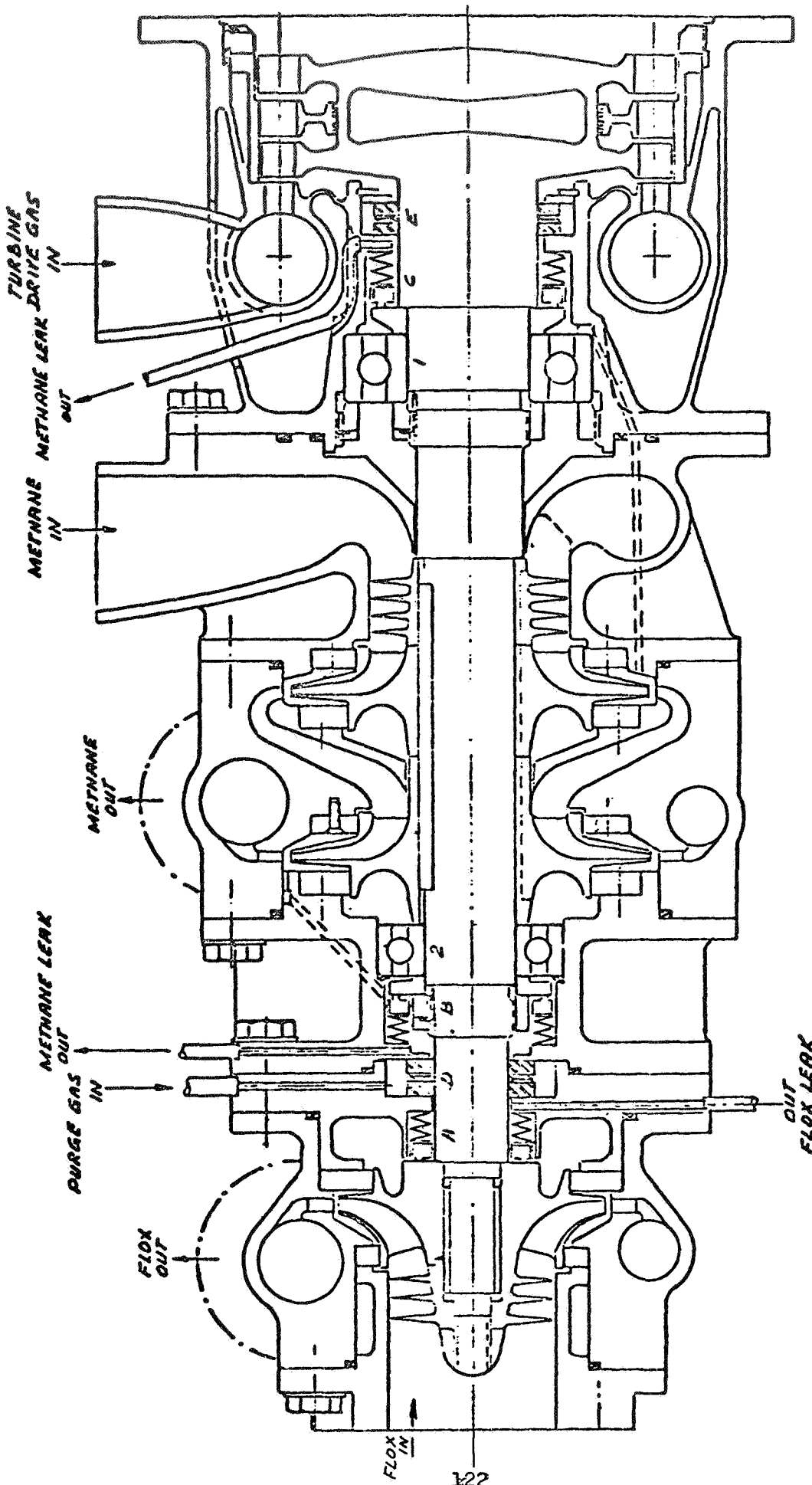
Figure 42 . 5K FLOX-Methane Turbopump Single Shaft Configuration.

Turbomachinery Arrangement Selection

Design features, performance, and potential development features of the turbomachinery arrangements for each drive cycle are described in Tables 27 to 34 . Selected arrangements are indicated with an asterisk. In general, the single shaft turbopump penalizes the methane pump and turbine efficiencies by forcing them to run at slower, FLOX pump, speed. This leads to small impeller discharge widths for the methane pump, which increases fabrication difficulty. This large shaft makes the methane pump inducer have rather small blades which, with reasonable clearance values, may compromise suction performance.

Associated with these is the start sequence limitation in which long thermal conditioning times are anticipated, because power application to the methane pump must be delayed until FLOX pump power is also desired. The single-shaft arrangement failed to appear attractive for any of the drive cycles.

The gear drive and dual turbine arrangements were attractive in that each pump can operate at its own speed and higher efficiency can be attained. Both the dual turbine series flow and the gear-driven arrangements use all the turbine flow and turbine nozzles are, therefore, slightly larger than for the parallel flow, dual-turbine arrangement. The gear-driven arrangements have an extra FLOX control valve, three gears, extra methane bearings and seals, and the associated lubrication system. This is offset in the dual turbine system by the extra FLOX bearing and turbine. The parallel flow turbines can in many cases be made identical.

The dual turbine arrangements, particularly the parallel flow arrangement, are independent in operation and are, therefore, more flexible for development tests, engine system start and throttling. In the early phases of start, for example, the methane turbine can be powered while the FLOX turbopump is inoperative. The power input to the methane pump materially assists in reducing the methane side priming time.

From these considerations the dual turbine arrangements were selected for all drive cycles.

TABLE 27.

TURBOMACHINERY COMPARISON

DRIVE CYCLE: EXPANDER

CHAMBER PRESSURE: 500 PSIA (3450 kN/m²)

FEATURE	SERIES	PARALLEL*	GEAR DRIVEN	SINGLE SHAFT
ENGINE SPECIFIC IMPULSE, SEC. (N-sec/kg)	399.2 (3912)	399.2 (3912)	399.2 (3912)	399.2 (3912)
EFFECTIVE SPECIFIC IMPULSE, SEC. (N-sec/kg)	398.9 (3909)	398.9 (3909)	398.1 (3901)	398.5 (3905)
PUMP STAGES	1/2	1/2	1/2	1/2
IMPELLER DIAMETER, IN. (cm)	1.5/1.73 (3.8)/(44)	1.5/1.39 (3.8)/(3.53)	1.5/1.39 (3.8)/(3.53)	1.5/2.32 (3.8)/(5.9)
TIP WIDTH, IN. (cm)	0.107/0.056 (0.273)/0.143	0.107/0.060 (0.273)/(0.153)	0.107/0.060 (0.273)/(0.153)	0.107/0.051 (0.273)/(0.13)
TURBINE STAGES	1/1	1/1	1	1
TURBINE DIAMETER, IN. (cm)	2.3/2 (5.85)/(5.08)	2/2 (5.08)/(5.08)	2 (5.08)	3.7 (9.4)
COMMENT:	1. Low turbine pressure ratio. 2. FLOX turbine bypass required. 3. Additional FLOX bearing.	1. 50-percent admission 2. Additional FLOX bearing.	1. Start sequence limited. 2. Additional seal, bearings, gears.	1. Start sequence limited. 2. Inducer suction performance poor.

*Recommended Configuration

TABLE 28.

TURBOMACHINERY COMPARISON

DRIVE CYCLE: GAS GENERATOR (B)

CHAMBER PRESSURE: 500 PSIA   (3450 kN/m^2)

FEATURE	SERIES	PARALLEL*	GEAR DRIVEN	SINGLE SHAFT
ENGINE SPECIFIC IMPULSE, SEC. (N-sec/kg)	399.2 (3912)	399.2 (3912)	399.2 (3912)	399.2 (3912)
EFFECTIVE SPECIFIC IMPULSE, SEC. (N-sec/kg)	398.9 (3909)	398.9 (3909)	398.1 (3901)	398.7 (3901)
PUMP STAGES	1/2	1/2	1/2	1/2
IMPELLER DIAMETER, IN. (cm)	1.42/1.88 (3.61)/(4.77)	1.42/1.39 (3.61)/(3.53)	1.42/1.39 (3.61)/(3.53)	1.42/1.88 (3.61)/(4.77)
TIP WIDTH, IN. (cm)	0.1/0.55 (0.255)/(0.14)	0.1/0.06 (0.255)/(0.153)	0.1/0.06 (0.255)/(0.153)	0.1/0.055 (0.255)/(0.14)
TURBINE STAGES	1/1	1/1	1	1
TURBINE DIAMETER, IN. (cm)	2.6/2.7 (6.6)/(6.85)	2.5/2.2 (6.35)/(5.59)	2.5 (6.35)	2.5 (6.35)
COMMENT:	1. Low turbine pressure ratio. 2. Additional FLOX bearing. 3. FLOX turbine by-pass required.	1. Low turbine pressure ratio. 2. Additional FLOX bearing.	1. Low turbine pressure ratio. 2. Start sequence limited. 3. Additional seals, bearings, gears.	1. Low turbine pressure ratio. 2. Start sequence limited. 3. Inducer suction performance poor.

125

TABLE 29.

TURBOMACHINERY COMPARISON

DRIVE CYCLE
THRUST CHAMBER TAPOFF:
GAS GENERATOR (A)
CHAMBER PRESSURE: 500 PSIA (3450 kN/cm^2)

FEATURE	SERIES	PARALLEL*	GEAR DRIVEN	SINGLE SHAFT
ENGINE SPECIFIC IMPULSE, SEC. (N-sec/kg)	397 (3890)	396 (3880)	397.0 (3891)	395.9 (3879)
EFFECTIVE SPECIFIC IMPULSE, SEC. (N-sec/kg)	396.5 (3885)	395.6 (3876)	396 (3880)	395 (3870)
PUMP STAGES	1/1	1/1	1/1	1/1
IMPELLER DIAMETER, IN. (cm)	1.50/1.37 (3.8)/3.48)	1.50/1.37 (3.8)/(3.48)	1.50/1.37 (3.8)/(3.48)	1.50/2.90 (3.8/(7.36)
TIP WIDTH, IN. (cm)	0.107/0.053 (0.273)/(0.135)	0.107/0.053 (0.273)/(0.135)	0.107/0.053 (0.273)/(0.135)	0.107/0.040 (0.273)/(0.102)
TURBINE STAGES	2/1	2/2	2	2
TURBINE DIAMETER, IN. (cm)	3.2/2 (8.13)/(5.08)	2.9/2 (7.36)/(5.08)	2 (5.08)	3.8 (9.66)
COMMENT:	1. 50-percent admission 2. Additional FLOX bearing.	1. 70-percent admission. 2. Additional FLOX bearing.	1. Start sequence limited. 2. Additional seals, gears, bearings.	1. Start sequence limited. 2. Small fuel pump tip width 3. Inducer suction performance poor.

TABLE 30.

TURBOMACHINERY COMPARISON

DRIVE CYCLE: AUXILIARY HEAT EXCHANGER

CHAMBER PRESSURE: 500 PSIA (3450 Kn/m^2)

FEATURE	SERIES	PARALLEL*	GEAR DRIVEN	SINGLE SHAFT
ENGINE SPECIFIC IMPULSE, SEC. (N-sec/kg)	395.6 (3876)	394 (3860)	395.9 (3879)	393.9 (3859)
EFFECTIVE SPECIFIC IMPULSE, SEC. (N-sec/kg)	395.1 (3871)	393.7 (3857)	394.8 (3868)	393.4 (3854)
PUMP STAGES	1/1	1/1	1/1	1/1
IMPELLER DIAMETER, IN. (cm)	1.50/1.37 (3.8)/(3.48)	1.50/1.37 (3.8)/(3.48)	1.50/1.37 (3.8)/(3.48)	1.50/2.90 (3.8)/(7.36)
TIP WIDTH, IN. (cm)	0.107/0.053 (0.273)/(0.135)	0.107/0.053 (0.273)/(0.135)	0.107/0.053 (0.273)/(0.135)	0.107/0.040 (0.273)/(0.102)
TURBINE STAGES	2/1	2/1	2	2
TURBINE DIAMETER, IN. (cm)	3.5/2 (3.9)/(5.08)	2.8/2 (7.11)/(5.08)	2.2 (5.59)	3.5 (8.9)
COMMENT:	1. 60-percent admission. 2. Addisional FLOX bearing.	1. 80-percent admission 2. Additional FLOX bearing.	1. Start sequence limited. 2. Additional seals, bearings, gears.	1. Fuel pump tip width small. 2. Inducer suction performance poor. 3. Start sequence limited.

TABLE 31.

TURBOMACHINERY COMPARISON
DRIVE CYCLE: EXPANDER
CHAMBER PRESSURE: 800 PSIA (5520 kN/m^2)

FEATURE	SERIES*	PARALLEL	GEAR DRIVEN	SINGLE SHAFT
ENGINE SPECIFIC IMPULSE, SEC. (N-sec/kg)	405.9 (3978)	405.9 (3978)	405.9 (3978)	405.9 (3978)
EFFECTIVE SPECIFIC IMPULSE, SEC. (N-sec/kg)	4.05.6 (3975)	4.05.6 (3975)	404.6 (3966)	4.05.6 (3975)
PUMP STAGES	1/2	1/2	1/2	1/2
IMPELLER DIAMETER, IN. (cm)	1.5/2 (3.8)/(5.08)	1.5/2.1 (3.8)/(5.34)	1.5/2 (3.8)/(5.08)	1.5/2.68 (3.8)/(6.8)
TIP WIDTH, IN. (cm)	0.092/0.043 (0.234)/(0.11)	0.092/0.04 (0.234)/(0.102)	0.092/0.042 (0.234)/(0.107)	0.092/0.035 (0.234)/(0.09)
TURBINE STAGES	1/1	2/1	1	2
TURBINE DIAMETER, IN. (cm)	2.5/2 (6.35)/(5.08)	2/2 (5.08)/(5.08)	2 (5.02)	2 (5.08)
COMMENT:	2. Low turbine pressure. 3. FLOX turbine by-pass required. 4. Additional FLOX bearing.	1. Small fuel pump tip width. 2. 30-percent admission. 3. Additional FLOX bearing. 4. Sensitive engine balance.	2. 70-percent admission. 3. Sensitive engine balance. 4. Additional seals, gears, bearings. 5. Start sequence limited.	2. 60-percent admission. 3. Sensitive engine balance. 4. Fuel inducer performance poor. 5. Start sequence limited.

TABLE 32.

TURBOMACHINERY COMPARISON

DRIVE CYCLE: AUXILIARY HEAT EXCHANGER

CHAMBER PRESSURE: 800 PSIA (5520 kN/m²)

FEATURE	SERIES	PARALLEL*	GEAR DRIVEN	SINGLE SHAFT
ENGINE SPECIFIC IMPULSE, SEC. (N-sec/kg)	399.1 (3911)	398.1 (3901)	400.4 (3924)	399.4 (3914)
EFFECTIVE SPECIFIC IMPULSE, SEC. (N-sec/kg)	398.2 (3902)	397.8 (3898)	399 (3910)	398.5 (3905)
PUMP STAGES	1/2	1/2	1/2	1/2
IMPELLER DIAMETER, IN. (cm)	1.5/1.5 (3.8)/(3.8)	1.5/1.5 (3.8)/(3.8)	1.5/1.5 (3.8)/(3.8)	1.5/2.4 (3.8)/(6.1)
TIP WIDTH, IN. (cm)	0.092/0.057 (0.234)/(0.146)	0.092/0.057 (0.234)/(0.146)	0.092/0.057 (0.234)/(0.146)	0.092/0.049 (0.234)/(0.124)
TURBINE STAGES	1/2	2/2	2	2
TURBINE DIAMETER, IN. (cm)	4.7/2 (11.9)/(5.08)	2.6/2.2 (6.6)/(5.59)	3.2 (8.12)	4 (10.2)
COMMENT:	1. 80-percent admission. 2. Additional FLOX bearing.	1. Additional FLOX bearing.	1. Start sequence limited. 2. Additional seals, gears, bearings.	1. Start sequence limited. 2. Fuel inducer performance poor.

TABLE 33.

TURBOMACHINERY COMPARISON

DRIVE CYCLE: THRUST CHAMBER TAPOFF; GAS GENERATOR (A)

CHAMBER PRESSURE: 800 PSIA (5520 kN/m²)

FEATURE	SERIES	PARALLEL*	GEAR DRIVEN	SINGLE SHAFT
ENGINE SPECIFIC IMPULSE, SEC. (N-sec/kg)	401.8 (3938)	401.3 (3933)	402.4 (3944)	401.9 (3939)
EFFECTIVE SPECIFIC IMPULSE, SEC. (N-sec/kg)	401 (3930)	401 (3930)	401.2 (3932)	401.3 (3933)
PUMP STAGES	1/2	1/2	1/2	1/2
IMPELLER DIAMETER, IN. (cm)	1.5/1.4 (3.8)/(3.56)	1.5/1.4 (3.8)/(3.56)	1.5/1.4 (3.8)/(3.56)	1.5/2.2 (3.8)/(5.59)
TIP WIDTH, IN. (cm)	0.092/0.055 (0.234)/(0.14)	0.092/0.055 (0.234)/(0.14)	0.092/0.055 (0.234)/(0.14)	0.092/0.049 (0.234)/(0.124)
TURBINE STAGES	1/1	2/2	2	2
TURBINE DIAMETER, IN. (cm)	4.5/2 (11.4)/(5.08)	3/2.1 (8.13)/(5.34)	2.9 (7.36)	3.6 (9.14)
COMMENT:	1. 70-percent admission. 2. Additional FLOX bearing.	1. Additional FLOX bearing.	1. Start sequence limited. 2. Additional seals, gears, bearings.	1. Start sequence limited. 2. Fuel inducer performance poor.

TABLE 34.

TURBOMACHINERY COMPARISON

DRIVE CYCLE: GAS GENERATOR (B)

CHAMBER PRESSURE: 800 PSIA (5520 kN/m²)

FEATURE	SERIES	PARALLEL*	GEAR DRIVEN	SINGLE SHAFT
ENGINE SPECIFIC IMPULSE, SEC. (N-sec/kg)	405.9 (3978)	405.9 (3978)	405.9 (3978)	405.9 (3978)
EFFECTIVE SPECIFIC IMPULSE, SEC. (N-sec/kg)	405.4 (3973)	405.6 (3975)	404.4 (3964)	405.6 (3975)
PUMP STAGES	1/2	1/2	1/2	1/2
IMPELLER DIAMETER, IN. (cm)	2.23/1.95 (5.66)/(4.95)	2.23/1.82 (5.66)/(4.62)	2.17/1.82 (5.52)/(4.62)	2.32/3.22 (5.66)/(8.18)
TIP WIDTH, IN. (cm)	0.07/0.044 (0.178)/(0.112)	0.07/0.045 (0.178)/(0.114)	0.072/0.045 (0.183)/(0.114)	0.067/0.032 (0.17)/(0.082)
TURBINE STAGES	1/1	2/1	1	1
TURBINE DIAMETER, IN. (cm)	3.2/2 (8.13)/(5.08)	2/2 (5.08)/(5.08)	2.8 (7.11)	2 (5.08)
COMMENT:	1. Low turbine pressure ratio. 2. Additional FLOX bearing. 3. FLOX turbine bypass required. 4. Small fuel pump tip width.	1. 80-percent admission. 2. Additional FLOX bearing. 3. Small fuel pump tip width.	1. Small fuel pump tip width. 2. Start sequence limited. 3. Additional seals, bearings, gears.	1. Small fuel pump tip width. 2. Start sequence limited. 3. Inducer suction performance poor. 4. Engine balance sensitive.

DRIVE CYCLE SELECTION

A comparison of candidate drive cycle features was first made on a qualitative basis. Then a numerical rating system was devised and used to make a selection of two drive cycles at each design point.

Engine descriptions for the candidate drive cycles are given in Tables 35 and 36. For both design points the expander and gas generator (B) cycles have the highest specific impulse. Gas generator (B) performance is somewhat reduced by the high engine weight. The remaining drive cycles have specific impulse values about 4 seconds lower. The pumps operate at the same design values of DN and seal speed except for the 500 psia (3450 kN/m^2) FLOX pumps which, except in the gas generator (B) cycle, operate at a lower speed to provide more acceptable impeller geometry. In the 800 psia (5520kN/m^2) topping cycles (expander and gas generator (B), impeller tip width is small and fabrication may be more difficult than for the other cycles.

In the turbine area, the topping cycles have the fewer turbine wheels. Blades heights are essentially the same, but the topping cycles have slightly larger turbine nozzles. The expander cycle has a lower turbine operating temperature at full thrust than the other cycles.

Drive cycle development problems are summarized in Table 37. Designations used in the table are:

NA — Not applicable.

A — Normal development item.

B — Minor development problem. Small technical risk due to fabrication or sensitivity with component modification possible.

C — Significant development problem; moderate technical risk with system redesign possible.

D — Potential major development problem; considerable technical risk with configuration change or program delay possible.

TABLE 35

ENGINE DRIVE CYCLE CHARACTERISTICS
CHAMBER PRESSURE – 500 PSIA

	EXPANDER	AUXILIARY HEAT EXCHANGER	GAS GENERATOR A	TCTO	GAS GENERATOR B
ENGINE SPECIFIC IMPULSE, SEC	398.9	395.2	395.7	395.7	398.1
ENGINE MIXTURE RATIO (O/F)	5.25	4.73	4.94	4.94	5.25
ENGINE SYSTEM WEIGHT, POUND	92.3	95.8	97.5	94.4	104.1
TURBOPUMP CONFIGURATION	Parallel	Parallel	Parallel	Parallel	Parallel
PUMP (O/F):					
DISCHARGE PRESSURE, PSIA	680/1270	680/942	680/942	680/942	1090/1270
NUMBER OF STAGES	1/2	1/1	1/1	1/1	1/2
NPSH REQUIRED, PSI	13/6	13/8	13/8	13/8	17/6
SPEED, RPM	40000/70000	40000/85000	40000/85000	40000/85000	45000/70000
BEARING DN (10^6)	0.57/0.93	0.57/1.05	0.57/1.05	0.57/1.05	0.71/0.93
IMPELLER EXIT, INCH	0.104/0.056	0.104/0.053	0.104/0.051	0.104/0.051	0.086/0.056
TURBINE (O/F):					
INLET TEMPERATURE, R	1245	1860	1960	1960	1960
PRESSURE RATIO	1.43/1.43	10/12	5/7	5/7	1.2/1.2
INLET PRESSURE, PSIA	845	200/240	100/140	100/140	710/710
NUMBER OF STAGES	1/1	2/1	2/2	2/2	1/1
BLADE HEIGHT, INCH	0.15/0.19	0.15/0.15	0.15/0.15	0.15/0.15	.33/.33
NOZZLE THROAT, INCH	0.14/0.18	0.06/0.06	0.07/0.09	0.07/0.06	0.25/0.25
PITCH DIAMETER, INCH	2/2	2.8/2	2.9/2	2.9/2	2.5/2.2

TABLE 35A

ENGINE DRIVE CYCLE CHARACTERISTICS

CHAMBER PRESSURE   3450 k N/m^2

	EXPANDER	AUXILIARY HEAT EXCHANGER	GAS GENERATOR A	TCTO	GAS GENERATOR B
ENGINE SPECIFIC IMPULSE, N-sec/kg	3909	3872	3877	3877	3901
ENGINE MIXTURE RATIO (O/F)	5.25	4.73	4.94	4.94	5.25
ENGINE SYSTEM WEIGHT, kg	41.9	43.4	44.2	42.8	47.3
TURBOPUMP CONFIGURATION	Parallel	Parallel	Parallel	Parallel	Parallel
PUMP (O/F):					
DISCHARGE PRESSURE, k N/m^2	4680/8750	4680/6490	4680/6490	4680/6490	7500/8750
NUMBER OF STAGES	1/2	1/1	1/1	1/1	1/2
NPSH REQUIRED, k N/m^2	90/41	90/55	90/55	90/55	117/41
SPEED, rad/sec	4180/7320	4180/85000	4180/85000	4180/8900	4700/7320
BEARING DN (10^6)					
IMPELLER EXIT, cm	0.264/0.142	0.264/0.153	0.264/0.13	0.264/0.13	0.218/0.142
TURBINE (O/F):					
INLET TEMPERATURE, K	692	1030	1090	1090	1090
PRESSURE RATIO	1.43/1.43	10/12	5/7	5/7	1.2/1.2
INLET PRESSURE, k N/m^2	5820	1380/1650	690/965	690/965	4900/4900
NUMBER OF STAGES	1/1	2/1	2/2	2/2	1/1
BLADE HEIGHT, cm	0.38/0.48	0.38/0.38	0.38/0.38	0.38/0.38	0.84/0.84
NOZZLE THROAT, cm	0.36/0.46	0.15/0.15	0.178/0.228	0.178/0.15	0.63/0.63
PITCH DIAMETER, cm	5.08/5.08	7.1/5.08	7.4/5.08	7.4/5.08	6.35/5.6

TABLE 36

ENGINE DRIVE CYCLE CHARACTERISTICS
CHAMBER PRESSURE – 800 PSIA

	EXPANDER	AUXILIARY HEAT EXCHANGER	GAS GENERATOR A	TCTO	GAS GENERATOR B
ENGINE SPECIFIC IMPULSE, SECOND	405.6	400.1	400.6	400.6	405.6
ENGINE MIXTURE RATIO (O/F)	5.25	4.56	4.76	4.76	5.25
ENGINE SYSTEM WEIGHT, POUND	93.7	94.4	97.1	92.5	108.9
TURBOPUMP CONFIGURATION	Series	Parallel	Parallel	Parallel	Parallel
PUMP (O/F):					
DISCHARGE PRESSURE, PSIA	1060/2400	1060/1560	1060/1560	1060/1560	2090/2400
NUMBER OF STAGES	1/2	1/2	1/2	1/2	1/2
NPSP REQUIRED, PSI	17/5	17/6	17/6	17/6	11/5
SPEED, RPM	50000/60000	50000/70000	50000/70000	50000/70000	35000/60000
BEARING DN (10^6)	0.75/1.05	0.75/1.05	0.75/1.05	0.75/1.05	0.75/1.05
IMPELLER EXIT, INCH	0.089/0.037	0.090/0.052	0.090/0.052	0.090/0.052	0.057/0.037
TURBINE (O/F):					
INLET TEMPERATURE, R	1326	1860	1960	1960	1960
PRESSURE RATIO	1.20/1.55	16/16	10/14	10/14	1.45/1.45
INLET PRESSURE, PSIA	1330/2060	320/320	140/240	140/240	1370
NUMBER OF STAGES	1/1	2/1	2/2	2/2	2/1
BLADE HEIGHT, INCH	0.18/0.15	0.15/0.15	0.15/0.15	0.15/0.15	0.15/0.15
NOZZLE THROAT, INCH	0.15/0.13	0.040/0.040	0.06/0.04	0.06/0.04	0.013/0.013
PITCH DIAMETER, INCH	2.5/2	2.6/2.2	3/2.1	3/2.1	2/2

TABLE 36A

ENGINE DRIVE CYCLE CHARACTERISTICS

CHAMBER PRESSURE 5520 k N/m^2

	EXPANDER	AUXILIARY HEAT EXCHANGER	GAS GENERATOR A	GAS TCTO	GAS GENERATOR B
ENGINE SPECIFIC IMPULSE, N-sec/kg	3975	3931	3926	3926	3975
ENGINE MIXTURE RATIO (O/F)	5.25	4.56	4.76	4.76	5.25
ENGINE SYSTEM WEIGHT, kg	42.5	42.8	44.1	42.	49.5
TURBOPUMP CONFIGURATION	Series	Parallel	Parallel	Parallel	Parallel
PUMP (O/F):					
DISCHARGE PRESSURE, k N/m^2	7300/16500	7300/10700	7300/10700	7300/10700	14400/16500
NUMBER OF STAGES	1/2	1/2	1/2	1/2	1/2
NPSP, k N/m^2	117/34	117/41	117/41	117/41	117/34
SPEED, rad/sec	5230/6280	5230/7320	5230/7320	5230/7320	3660/6230
BEARING DN (10^6)					
IMPELLER EXIT, cm	0.226/0.094	0.229/0.132	0.229/0.132	0.229/0.132	0.145/0.094
TURBINE (O/F):					
INLET TEMPERATURE, K	736	1030	1090	1090	1090
PRESSURE RATIO	1.20/1.55	16/16	10/14	10/14	1.45/1.45
INLET PRESSURE, k N/m^2	9160/14200	2200/12200	965/1650	965/1650	9450
NUMBER OF STAGES	1/1	2/1	2/2	2/2	2/1
BLADE HEIGHT, cm	0.46/0.38	0.38/0.38	0.38/0.38	0.38/0.38	0.38/0.38
NOZZLE THROAT, cm	0.38/0.33	0.1/0.1	0.15/0.1	0.15/0.1	0.033/0.033
PITCH DIAMETER, cm	6.35/5.08	6.6/5.59	7.62/5.34	7.62/5.34	5.08/5.08

TABLE 37 .   DRIVE CYCLE DEVELOPMENT PROBLEMS

DEVELOPMENT ITEM	EXPANDER	AUX. HEAT EXCHANGER	GGA	TCTO	GGB
1. THRUST CHAMBER					
JACKET DESIGN	B	B	B	B	B
PRESSURE DROP, TEMPERATURE	B	A	A	A	B
INJECTOR	A	A	A	B	B
2. PUMPS					
BEARING/SEALS	A	A	A	A	A
EFFICIENCY	B	A	A	A	B
IMPELLER TIP WIDTH	B	A	A	A	A
3. TURBINES					
CARBON DEPOSITION	NA	NA	D	D	D
EFFICIENCY	B	A	A	A	B
DYNAMIC SEALS	A	A	B	B	C
4. POWER SOURCE					
TAPOFF/MANIFOLD	NA	NA	NA	B	NA
GAS GENERATOR INJECTOR	NA	NA	B	NA	A
HEAT EXCHANGER	NA	A	NA	NA	NA
5. VALVES/CONTROLS/LINES					
HOT GAS VALVES	A	A	C	C	C
CONTROL/MEASUREMENT OF SMALL FLOWS	NA	A	B	B	NA
HOT GAS LEAKAGE	A	A	B	B	C
6. ENGINE START					
TIME	B	A	A	B	A
TEMPERATURE DEPENDENCE	B	A	A	A	A

The single most significant potential problem is that of turbine nozzle coking in the cycles using FLOX/methane combustion products to power the turbines: gas generator (A), gas generator (B), and thrust chamber tapoff. As indicated previously in the small turbine flow passages, coking could severely reduce turbine performance and represents a significant potential development problem. The next most significant item is the control of the small amounts of hot, corrosive gas in the FLOX/methane powered turbine cycles. Of all the drive cycles, the auxiliary heat exchanger appears to have the fewest development problems, with the expander cycle being slightly more difficult. The minor development problems indicated for the expander cycle are largely due to the engine balance sensitivity at the 800 psia (5520 kN/m^2) chamber pressure described in the following section. This sensitivity is greatly diminished at the 500 psia (3450 kN/m^2) design point.

The performance of the drive cycles is directly related to the characteristics of the engine components. Some cycles are more sensitive to these component variations than others. With these cycles potential development problems exist since a small variation in one component could significantly affect the entire engine. For the drive cycle candidates, a series of component characteristic variations were assumed. Using exchange factors, these variations were related to changes in pump discharge pressure or to specific impulse. These are described in Tables 38 and 39. At the high chamber pressure, it can be seen that both the gas generator (B) and the expander cycle pump discharge pressures are very sensitive, particularly to injector pressure drop increase and turbine efficiency decrease. The pump pressure for the remaining cycles is not as sensitive, however engine specific impulse is sensitive to component variations. At the low chamber pressure all systems are less sensitive.

The components, lines, valves and manifolds associated with the drive cycles are summarized in Table 40 to give an indication of system complexity. The expander cycle is the simplest of all the cycles, while the gas generator (B) engine is the most complex.

TABLE 38. ENGINE SYSTEM SENSITIVITY

Chamber Pressure = 500 psia (3450 kN/m²)

Drive Cycle	Parameter	Units	Characteristic Variation						Parameter Perturbation
			ΔP_{Inj} + 30 psi (+207 kN/m²)	ΔP_{Jacket} + 100 psi (+689 kN/m²)	ΔT_{Fuel} + 100 R (+56K)	$\Delta\eta$ Fuel Pump -0.05	$\Delta\eta$ Oxid Pump -0.05	$\Delta\eta$ Tur -0.15	
Expander	P_D (Oxid)	psi (kN/m²)	+30 (+207)	-	-	-	-	-	+30 (+207)
	P_D (Fuel)	psi (kN/m²)	+56 (+387)	+119 (+820)	-30 (-207)	+14 (+96)	+10 (+69)	+63 (+435)	+232 (+1600)
Gas Generator (B)	P_D (Oxid)	psi (kN/m²)	+46 (+318)	+6 (+41)	-	+7 (+48)	+7 (+48)	+39 (+269)	+105 (+725)
	P_D (Fuel)	psi (kN/m²)	+42 (+290)	+105 (+725)	-	+7 (+48)	+6 (+41)	+34 (+235)	+194 (+1340)
Gas Generator (A); Thrust Chamber Tapoff	P_D (Oxid)	psi (kN/m²)	+30 (+207)	-	-	-	-	-	+30 (+207)
	P_D (Fuel)	psi (kN/m²)	+30 (+207)	+100 (+690)	-	-	-	-	+130 (+897)
	I_s	sec (N-sec/kg)	-.094 (-92)	-.13 (-1.28)	-	-.11 (1.08)	-.1 (-.98)	-.51 (-5.0)	-0.94 (-.92)
Auxiliary Heat Exchanger	P_D (Oxid)	psi (kN/m²)	+30 (+207)	-	-	-	-	-	+30 (+207)
	P_D (Fuel)	psi (kN/m²)	+30 (+207)	+100 (+690)	-	-	-	-	+130 (+897)
	I_s	sec (N-sec/kg)	-.12 (-1.18)	-.16 (-1.57)	+.41 (+4.02)	-.15 ('-1.47)	-.12 (-1.18)	-.67 (-6.57)	-.81(-1.22) (-7.94)(-11.9

TABLE 39. ENGINE SYSTEM SENSITIVITY

Chamber Pressure = 800 psia (5520 kN/m²)

Drive Cycle	Parameter	Units	Characteristic Variation						Parametric Perturbation
			ΔP_{Inj} +50 psi (+345 kN/m²)	ΔP_{Jacket} +250 psi (+1725 kN/m²)	T_{CH_4} +200 R (+111 K)	$\Delta\eta$ Fuel Pump -0.05	$\Delta\eta$ Oxid Pump -0.05	$\Delta\eta$ Tur -0.15	
Expander	P_D (Oxid)	psi (kN/m²)	+50 (+345)	-	-	-	-	-	+50 (+345)
	P_D (Fuel)	psi (kN/m²)	+132 (+910)	+325 (+2240)	-160 (-1105)	+100 (+690)	+46 (+318)	+400 (+2760)	+843 (+5820)
Gas Generator (B)	P_D (Oxid)	psi (kN/m²)	+100 (+690)	+33 (+228)	-	+27 (+186)	+26 (+179)	+150 (+1035)	+336 (+2320)
	P_D (Fuel)	psi (kN/m²)	+90 (+621)	+277 (+1910)	-	+25 (+173)	+24 (+166)	+140 (+965)	+556 (+3840)
Gas Generator (A); Thrust Chamber Tapoff	P_D (Oxid)	psi (kN/m²)	+50 (+345)	-	-	-	-	-	+50 (+345)
	P_D (Fuel)	psi (kN/m²)	+50 (+345)	+250 (+1725)	-	-	-	-	+300 (+2070)
	I_s	sec (N-sec/kg)	-0.16 (-1.57)	-0.35 (-3.43)	-	-0.21 (-2.06)	-0.17 (-1.67)	-0.90 (-8.82)	-1.79 (-17.65)
Auxiliary Heat Exchanger	P_D (Oxid)	psi (kN/m²)	+50 (+345)	-	-	-	-	-	+50 (+345)
	P_D (Fuel)	psi (kN/m²)	+50 (+345)	+250 (+1725)	-	-	-	-	+300 (+2070)
	I_s	sec (N-sec/kg)	-0.20 (-1.96)	-0.44 (-4.31)	+1.5 (+14.7)	-0.28 (-2.74)	-0.23 (-2.27)	-1.20 (-11.75)	-.85(-2.35)(-8.33)(-23)

TABLE 40

DRIVE CYCLE COMPLEXITY

DRIVE CYCLE COMPONENT	EXPANDER	AUXILIARY HEAT EXCHANGER	GAS GENERATOR A	THRUST CHAMBER TAPOFF	GAS GENERATOR B
1. Main Valves	2	2	2	2	2
2. Control Valves	2	3	4	2	5
3. Thrust Chamber	1	1	1	1	1
4. Main Injector	1	1	1	1	1
5. Gas Generator Body	-	-	1	-	1
6. Gas Generator Injector	-	-	1	-	1
7. Heat Exchanger	-	1	-	-	-
8. Tapoff	-	-	-	1	-
9. High Pressure Ducts	9	9	8	6	13
10. Low Pressure Ducts	2	5	7	6	2
11. High Pressure Manifolds	4	5	5	4	8
12. Low Pressure Manifolds	-	1	1	1	-
13. Turbopump Body	2	2	2	2	2
14. Pump-Impellers	3	3	3	3	3
15. Pump Bearings/Seals	7	7	7	7	7
16. Purge Lines/Valves	3	3	3	3	3
17. Seal Drains	3	3	3	3	3
18. Turbine Wheels	2	3	4	4	2
19. Gimbal	1	1	1	1	1
20. Actuators	2	2	2	2	2
Total Subcomponents	44	52	56	49	57

Engine System Comparison Ratings

Based on the previous system and turbomachinery analyses, the candidate turbo-machinery arrangements and drive-cycles were compared to arrive at recommended engine system configurations. To assist in these comparisons a rating system was used. The ratings combined the multitude of engine design features into four comparison factors (with 100 being the best value): performance, development ease, reliability and production ease. These factors can then be weighed relative to each other and an overall comparison be determined.

Engine Performance. The primary factor in the performance rating was the engine specific impulse, which combined the thrust chamber performance at 94-percent efficiency with the cycle losses and turbomachinery leakage. System weights were evaluated including engine weight and tankage weights. Variation in the latter weights were due to differences in engine mixture ratio and NPSH requirements. Weight differences between cycles were converted into an equivalent specific impulse difference using an exchange factor of 15 pounds of hardware per second of specific impulse. This was added to the engine performance to give an effective specific impulse.

Rating of this effective specific impulse was made with the maximum value receiving 100 points and lesser values evaluated at one point per second of effective specific impulse. For a typical mission, the entire range of specific impulse represents a variation in payload of 170 pounds (77 kg) out of a total of 8000 (3630 kg). The ratings are presented in Table 41.

Engine Development Ease. From consideration of the design features of both the turbomachinery arrangements and the drive cycles, certain development problems were identified. Considering these problems, their significance, and the usual items in a development program, a rating describing the ease of development was determined. Using this approach, the relative ease of development of the various engine configurations is shown in Table 42. As shown, the auxiliary heat exchanger cycle is the easiest engine to develop. It is followed in ease of development by the expander cycle.

TABLE 41
DRIVE CYCLE PERFORMANCE RATING

DRIVE CYCLE CHAMBER PRESSURE	EXPANDER	AUXILIARY HEAT EXCHANGER	GAS GENERATOR A	THRUST CHAMBER TAPOFF	GAS GENERATOR B
500 PSIA $(3450k \ N/m^2)$	93	89	90	90	92
800 PSIA $(5520k \ N/m^2)$	100	94	95	95	99

TABLE 42
ENGINE SYSTEM DEVELOPMENT EASE RANKING

DRIVE CYCLE CHAMBER PRESSURE	EXPANDER	AUXILIARY HEAT EXCHANGER	GAS GENERATOR A	THRUST CHAMBER TAPOFF	GAS GENERATOR B
500 PSIA $(3450k \ N/m^2)$	74	87	64	62	42
800 PSIA $(5520k \ N/m^2)$	63	79	54	53	33

143

Engine System Reliability. Engine system reliability was evaluated on a relative basis by examination of the subcomponents associated with major engine components. For each subcomponent, the number, the operating environment (temperature, pressure, fluid), and the number of operations were used in assigning a rating. These subcomponent ratings were then summed to give an indication of the relative reliability of the engine systems. This is shown in Table 43. The auxiliary heat exchanger and expander cycles rate highest in reliability.

Engine System Production. A rating of engine production was made to give an evaluation of the relative ease of production once the engine system had been developed. Production ease ratings are given in Table 44. The expander cycle rates highest, due primarily to the small number of components to be fabricated.

Drive Cycle Selection

Ratings for all the drive cycles are summarized in Tables 45 and 46. Based upon these ratings, the methane-powered expander and the auxiliary heat exchanger cycles were selected for further investigation.

At 500 psia (3450 kN/m^2), the expander cycle has the highest performance and production ease ratings. Development ease and reliability potential are both reasonable in rating values. The auxiliary heat exchanger cycle is the easiest to develop but has the lowest performance rating. Although the other cycles were intermediate in performance, they were significantly lower in all other categories. Therefore, the expander and auxiliary heat exchanger cycles were selected.

At the 800 psia (5520 kN/m^2) design point, the expander cycle balance is sensitive and the development rating is lower; a more significant development advantage exists for the auxiliary heat exchanger cycle. However, the two methane-powered drive cycles are significantly higher rated than the other cycles and were selected for further investigation.

144

TABLE 43
ENGINE SYSTEM RELIABILITY RANKING

	500 PSIA (3450k N/m²)	800 PSIA (5520k N/m²)
CHAMBER PRESSURE / DRIVE CYCLE	500 PSIA $(3450k\ N/m^2)$	800 PSIA $(5520k\ N/m^2)$
AUXILIARY HEAT EXCHANGER	85	83
EXPANDER	84	83
THRUST CHAMBER TAPOFF	70	68
GAS GENERATOR (A)	64	62
GAS GENERATOR (B)	54	54

TABLE 44
RELATIVE ENGINE SYSTEM PRODUCTION COSTS FOR CANDIDATE DRIVE CYCLES

	EXPANDER	G.G. (A)	G.G. (B)	AUX. HEAT EXCHANGER	T.C. TAPOFF
COMPLEXITY (30)	30	15	18	20	25
FABRICATION EASE (30)	30	15	15	25	20
ENGINE SYSTEM ASSEMBLY (30)	30	20	15	25	30
ACCEPTANCE TEST (10)	8	4	2	6	10
TOTAL	98	54	50	76	85

TABLE 45

ENGINE DRIVE CYCLE RATING

Chamber Pressure = 500 psia(3450 kN/m^2)

Expansion Ratio = 60:1

DRIVE CYCLE RATING AREAS	EXPANDER	AUXILIARY HEAT EXCHANGER	GAS GENERATOR A	THRUST CHAMBER TAPOFF	GAS GENERATOR B
SPECIFIC IMPULSE sec(N-sec/kg)	398.9 (3909)	395.2 (3872)	395.7 (3877)	395.7 (3877)	398.9 (3909)
PERFORMANCE	93	89	90	90	92
RELIABILITY	84	85	64	70	54
DEVELOPMENT EASE	74	87	64	62	42
PRODUCTION EASE	98	76	54	85	50
COMMENT:		1. Single stage methane pump.	1. Coking problem. 2. Single-stage methane pump.	1. Coking problem. 2. Single-stage methane pump.	1. Coking problem.

146

TABLE 46

ENGINE DRIVE CYCLE RATING

Chamber Pressure = 800 psia (5520 kN/m^2)
Expansion Ratio = 100:1

RATING AREAS / DRIVE CYCLE	EXPANDER	AUXILIARY HEAT EXCHANGER	GAS GENERATOR A	THRUST CHAMBER TAPOFF	GAS GENERATOR B
SPECIFIC IMPULSE sec (N-sec/kg)	405.6 (3975)	400.1 (3921)	400.6 (3926)	400.6 (3926)	405.6 (3975)
PERFORMANCE	100	94	95	95	99
RELIABILITY	84	83	62	68	54
DEVELOPMENT EASE	63	79	54	53	33
PRODUCTION EASE	98	76	54	85	50
COMMENTS:	1. Engine system very sensitive to component design. 2. Throttling limited.		1. Coking problem.	1. Coking problem.	1. Engine system very sensitive to component design. 2. Coking problem.

147

CYCLE ENERGY BALANCES

The expander and auxiliary heat exchanger drive cycles selected in the
previous evaluation, were further evaluated at each of the two design
points. Detailed engine schematics and pressure budgets were defined.
Mass and energy balances were performed at both nominal and off-design
conditions. Based on this information, comparisons of performance,
ease of development, and operational potential were used to select an
engine configuration and design point for the Task II preliminary
design.

NOMINAL ENGINE SYSTEMS

Engine system schematics are shown in Figure 43 . The valves
shown are sufficient to control engine start, shutdown and throttling. The 800 psia
(5520 kN/M^2) Expander cycle schematic is a series turbine arrangement and
requires an oxidizer turbine bypass for control in throttling. During
chilldown and idle-mode operation the methane flows through the bypass
line; oxidizer turbine rotation is prevented by the control valve at
the turbine inlet.

In the schematics the shaded valves must have low or zero leakage
since they isolate fluid source while the engine is shut down. The
remaining valves do not have stringent leakage requirements. The
auxiliary heat exchanger systems have a pneumatic valve on the start
system. Other pneumatic valves common to all engines and not shown
are for (1) pump seal purges, (2) valve actuation power source, and
(3) FLOX line purge.
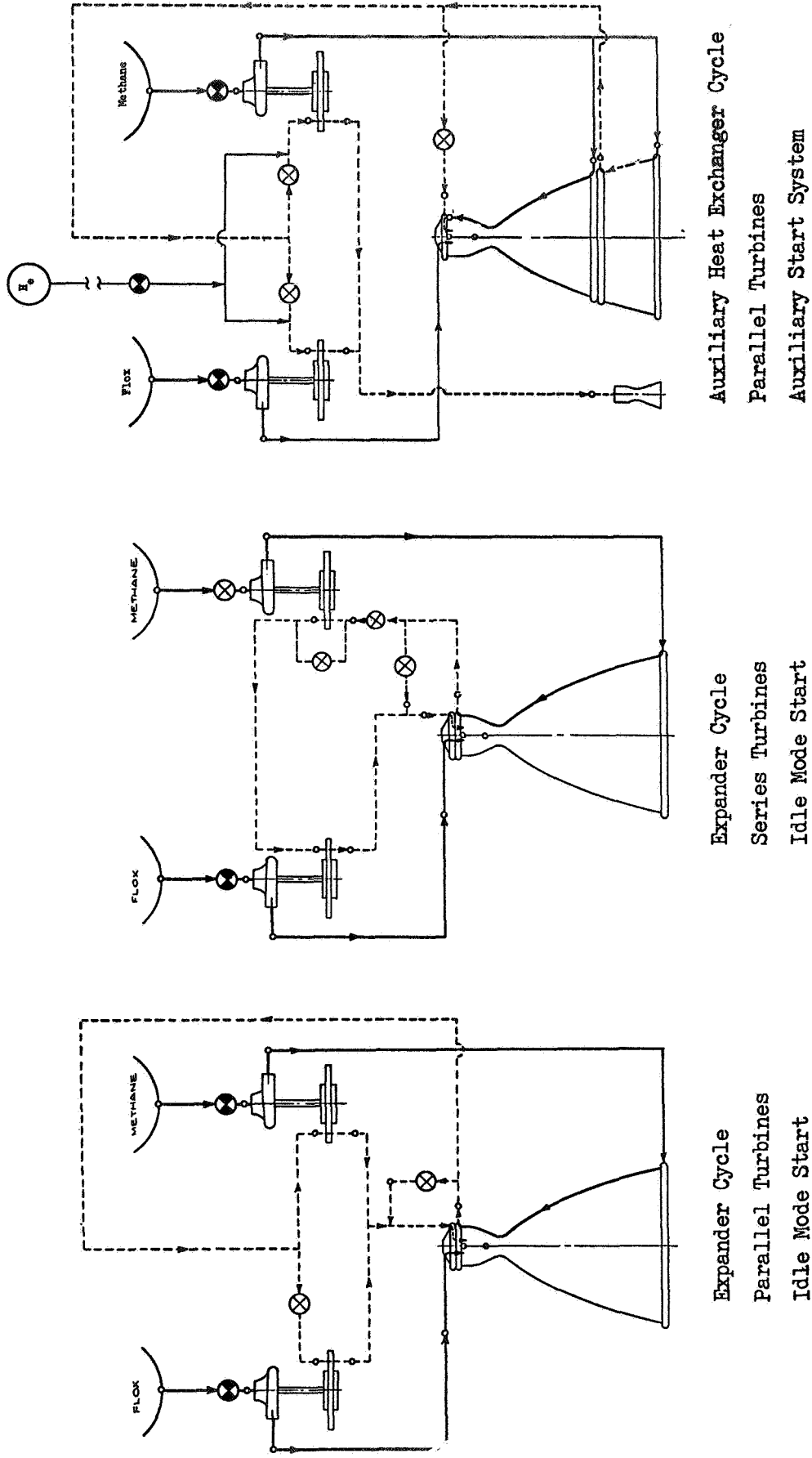
Auxiliary Heat Exchanger Cycle
Parallel Turbines
Auxiliary Start System

Expander Cycle
Series Turbines
Idle Mode Start

Expander Cycle
Parallel Turbines
Idle Mode Start

Figure 43 . Cycle Schematics

150

In the schematics, the shaded values must have low or zero leakage since they isolate fluid source while the engine is shut down. The remaining valves do not have stringent leakage requirements. The auxiliary heat exchanger systems have a pneumatic valve on the start system. Other pneumatic valves common to all engines and not shown are for (1) pump seal purges, (2) valve actuation power source, and (3) FLOX line purge.

Nominal engine balances are presented in Tables 47 and 48 for expander and auxiliary heat exchanger cycles, respectively. At equivalent design points the ex ander provides one percent advantage in specific impulse, and about seven pounds less engine weight. The weight difference is due to a lighter thrust chamber, fewer valves, and no auxiliary start system. For both drive cycles, the area ratio $=100$ design point gives ~ 1.5 percent specific impulse advantage with only a slight weight increase. Engine system design and development, however, are more difficult at the higher chamber pressure.

A brief system perfor ance comparison was made for a representative space mission. For the Mars Orbiter Mission (Ref. 9) payload estimates of about 8000 pounds (3630 kg) were made. The 500 psia (3450 kN/m^2) Expander and the 800 psia (5520 kN/m^2) auxiliary heat exchanger engine gave the same payloads, with the 500 psia (3450 kN/m^2) auxiliary heat exchanger engine about 70 pounds (31.8 kg) less and the 800 psia (5520 kN/m^2) Expander 100 pounds (45.4 kg) greater payload.

ENGINE SYSTEM DESIGN VARIATIONS

The nominal engine designs were critiqued and the effect of possible design changes on engine characteristics were assessed. In the expander cycles the design variations are reflected in the pump discharge pressure; the engine specific impulse remains the same. These effects are shown in

151

TABLE 47

EXPANDER ENGINE SYSTEM

	PARALLEL		SERIES	
THRUST, POUND (N)	5000	(22200)	5000	(22200)
ENGINE SPECIFIC IMPULSE, SEC(N-sec/kg)	398.9	(3910)	405.6	(3970)
ENGINE MIXTURE RATIO, O/F	5.25		5.25	
ENGINE WEIGHT, LB (Kg)	81.6	(37.0)	84.7	(38.4)
TURBOPUMP CONFIGURATION	PARALLEL		SERIES	
THRUST CHAMBER				
CHAMBER PRESSURE, PSIA (kN/m²)	500	(3450)	800	(5520)
MIXTURE RATIO, O/F	5.25		5.25	
WEIGHT FLOW, LB/SEC (Kg/sec)	12.52	(5.68)	12.32	(5.59)
SPECIFIC IMPULSE, SEC(N-sec/kg)	399.2	(3913)	405.9	(3973)
EXIT TEMPERATURE, R (K)	1250	(694)	1315	(731)
EXPANSION RATIO	60		100	
PUMPS, O/F				
FLOW, LB/SEC (Kg/sec)	10.52/2.00	(4.77/.907)	10.35/1.97	(4.69/.894)
DISCHARGE PRESSURE, PSIA (kN/m²)	680/1270	(4690/3760)	1060/2400	(7310/16550)
NPSP, PSIA (kN/m²)	12/6	(83/41)	17/5	(117/34)
NUMBER OF STAGES	1/2		1/2	
SPEED, 1000 RPM(1000 rad/sec)	40/70	(4.2/7.3)	50/60	(5.2/6.3)
HORSEPOWER (KW)	31.6/44.6	(23.6/32.3)	50.6/108.8	(37.7/81.1)
EFFICIENCY, PERCENT	64/59		63/46	
TURBINE, O/F				
FLOW, LB/SEC (Kg/sec)	.92/.96	(.42/.44)	1.87/1.84	(.85/.83)
INLET TEMPERATURE, R (K)	1245.	(692)	1326/1278	(737/710)
PRESSURE RATIO	1.43/1.43		1.20/1.55	
EXIT PRESSURE, PSIA (kN/m2)	756	(5210)	1110/1332	(7650/9180)
NUMBER OF STAGES	1/1		1/1	
EFFICIENCY, PERCENT	45/62		65/58	
BYPASS, LB/SEC (Kg/sec)	0.12	(.054)	0.10	(.045)

TABLE 48

AUXILIARY HEAT EXCHANGER ENGINE SYSTEM

THRUST, POUNDS (N)	5000 (22200)	5000 (22200)
ENGINE SPECIFIC IMPULSE, SEC(N-sec	395.2 (3870)	400.1 (3920)
ENGINE MIXTURE RATIO, O/F	4.73	4.56
ENGINE WEIGHT, LB (Kg)	88.2 (40.0)	92.2 (41.8)
TURBOPUMP CONFIGURATION	PARALLEL	PARALLEL
THRUST CHAMBER		
CHAMBER PRESSURE, PSIA (kN/m^2)	500 (3450)	800 (5520)
MIXTURE RATIO, O/F	5.25	5.25
WEIGHT FLOW, LB/SEC (Kg/sec)	12.43 (5.64)	12.2 (5.53)
SPECIFIC IMPULSE, SEC	399.3 (3913)	405.9 (8973)
EXIT TEMPERATURE, R (K)	1060 (589)	1094 (608)
EXPANSION RATIO	60	100
PUMPS, O/F		
FLOW, LB/SEC (Kg/sec)	10.44/2.21 (4.74/1.00)	10.25/2.25 (4.65/1.02)
DISCHARGE PRESSURE, PSIA(	681/942 (4700/6500)	1060/1560 (7310/10760)
NPSP, PSIA (kN /m^2)	13/8.0 (90/55)	16/6 (110/41)
NUMBER OF STAGES	1/1	1/2
SPEED, 1000 RPM (1000 rad/sec)	40/85	50/70
HORSEPOWER (KW)	32.2/35.5 (4.2/8.9)	51.3/62.9 (15.2/7.3)
EFFICIENCY, PERCENT	63.8/58.5 (24.0/26.5)	62.9/57.7 (38.3/46.3)
TURBINE, O/F		
FLOW, LB/SEC (Kg/sec)	0.12/0.099 (.054/.045)	0.14/0.15 (.064/.068)
INLET TEMPERATURE, R (K)	1860 (1033)	1860 (1033)
PRESSURE RATIO	10/12	16.0/16.0
EXIT PRESSURE, PSIA (kN/m^2)	20.0/20.0 (138/138)	20.0/20.0 (138/138)
NUMBER OF STAGES	2/1	2/1
EFFICIENCY, PERCENT	41.4/51	47.1/53
BYPASS, LB/SEC (Kg/sec)	0.0	0.0

Fig. 44. Turbine design changes reflect efficiency and pressure ratio effects resulting from common turbines, single turbines, or full admission turbines. The nominal design is based upon dual-shaft, partial admission turbines. Variations around the turbine inlet temperature of 1860 R are also illustrated. Similar information is shown in Fig. 45 and 46 for the auxiliary heat exchan er cycle in terms of specific impulse variation. Possible variations in system pressure drops and in the turbine exhaust performance are also illustrated. The additive effect of these factors is shown as maximum and minimum performance values.

ENGINE SYSTEM THROTTLING

Using engine energy balance techniques described in Appendix A, the candidate engine systems were throttled over a 10:1 thrust range. Thrust chamber characteristics were based upon the heat transfer analyses (such as Fig. 21). Turbomachinery characteristics were represented by head flow coefficient curves. Pump inlet pressures were: methane - 80 psia (550 kN/m^2) FLOX - 50 psia (345 kN/m^2). Lower values would affect the throttling balance.

Expander cycle energy balance at 10:1 throttling is presented in Table 49. Engine specific impulse values are some 1.5 percent higher than for the auxiliary heat exchanger cycle. Thrust chamber temperatures are significantly higher than at full thrust, and the resulting turbine flowrates are very small. The bypass flow is equivalent to the flow through the turbine. For the 500 psia (3450 kN/m^2) expander, engine characteristics are shown as a function of thrust in Fig. 47 to 49.

154

Figure 44.

EXPANDER CYCLE FUEL PUMP DISCHARGE PRESSURE EFFECT OF DESIGN VARIATIONS
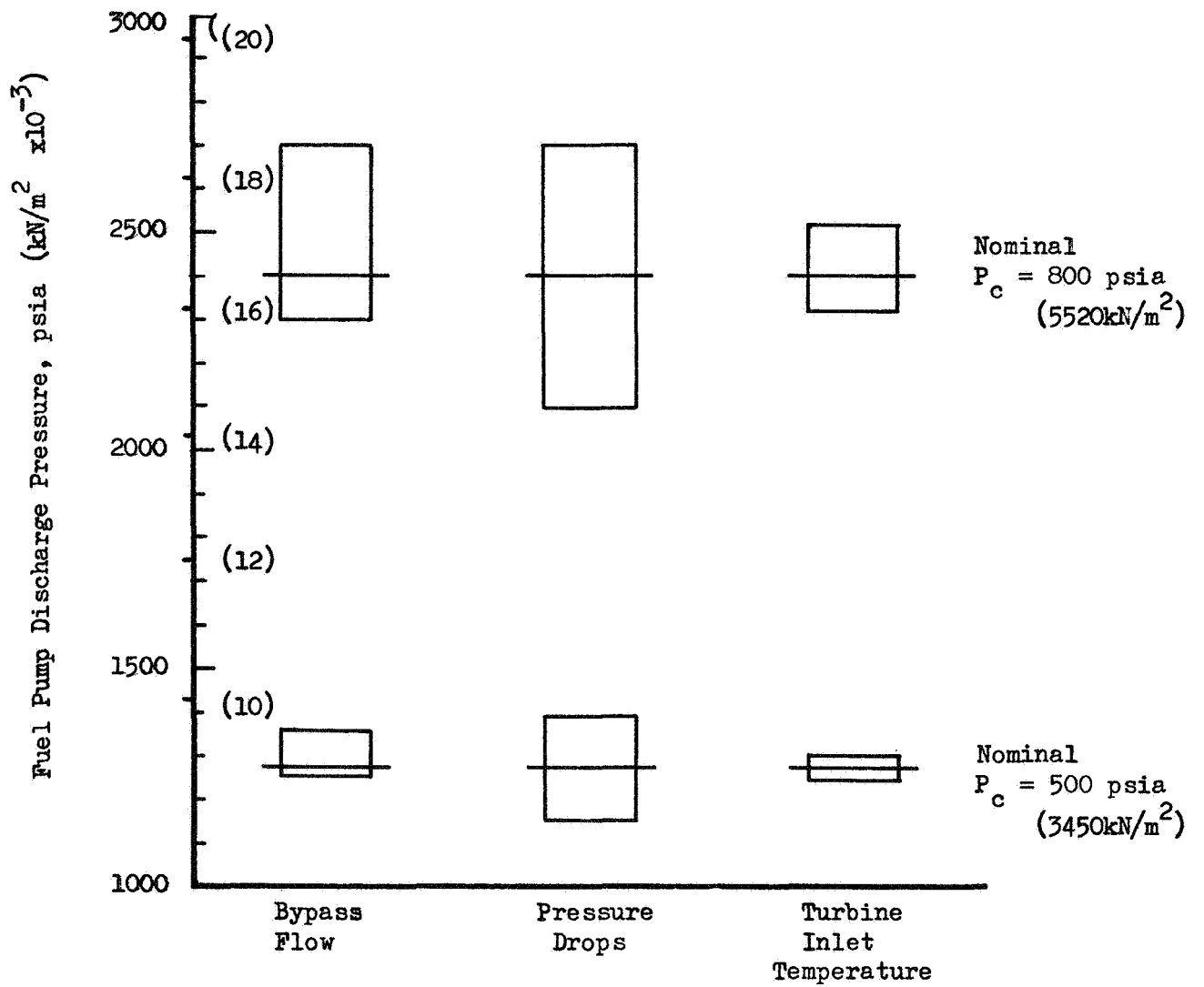
CHAMBER PRESSURE = 500 PSIA (3450 kN/m^2)

EXPANSION AREA RATIO = 60

THRUST CHAMBER MIXTURE RATIO = 5.25

N-sec/kg

3940 3920 3900 3880 3860

Maximum

Nominal

Minimum

Turbine   Inlet   System   Turbine
Design   Temperature   Pressure   Exhaust
                                  Drops   Performance

402 400 398 396 394 392

Delivered Specific Impulse, second
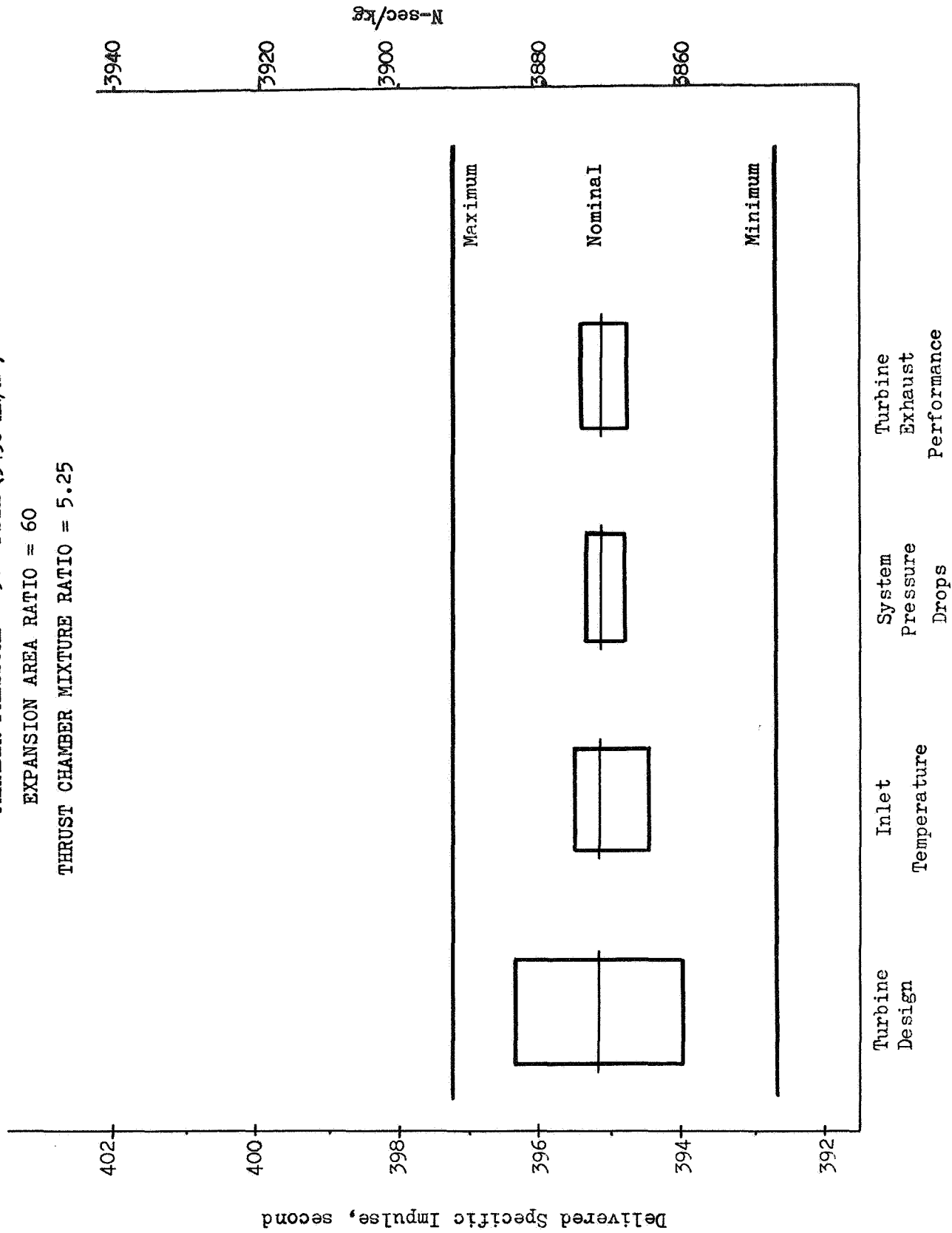
Figure 45. Auxiliary Heat Exchanger Specific Impulse
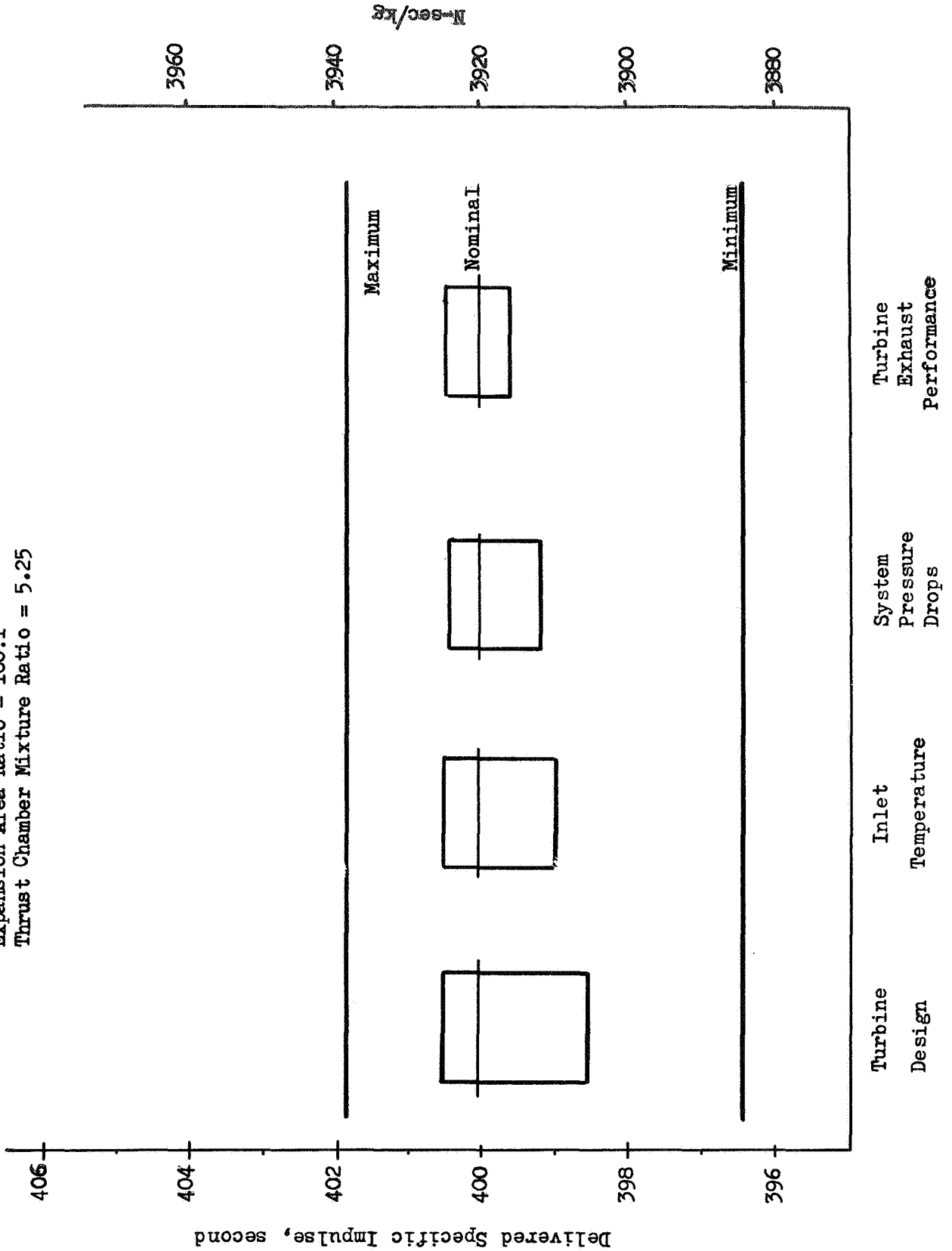
Figure 46. Auxiliary Heat Exchanger Specific Impulse

TABLE 49

EXPANDER ENGINE SYSTEM (THROTTLED)

	PARALLEL	SERIES
THRUST, LB (N)	500 (2220)	500 (2220)
ENGINE SPECIFIC IMPULSE, SEC(N-sec/kg)	366 (3585)	373 (3650)
ENGINE MIXTURE RATIO, O/F	5.25	5.25
DESIGN PRESSURE, PSIA (kN/M²)	500 (3450)	800 (5520)
TURBOPUMP CONFIGURATION (kN/M²)	PARALLEL	SERIES
THRUST CHAMBER		
CHAMBER PRESSURE, PSIA (kN/M²)	500 (3450)	80 (550)
MIXTURE RATIO, O/F	5.25	5.25
WEIGHT FLOW, LB/SEC (kg/sec)	1.33 (0.6)	1.31 (0.59)
SPECIFIC IMPULSE, SEC (N-sec/kg)	366 (3585)	373 (3650)
EXIT TEMPERATURE, R (K)	1670 (925)	1816 (1005)
PUMPS, O/F		
FLOW, LB/SEC (kg/sec)	1.12/.21 (.506/.095)	1.10/0.21 (.498/.095)
DISCHARGE PRESSURE, PSIA(kN/M²)	65/122 (450/840)	103/174 (710/1200)
SPEED, 1000 RPM (1000 rad/sec)	6/12 (0.6/0.13)	10/11.5 (1.0/1.2)
HORSEPOWER (kw)	0.08/0.19 (0.06/0.14)	0.38/0.56 (0.28/0.42)
EFFICIENCY, PERCENT	59/53	47/38
TURBINE, O/F		
FLOW, LB/SEC (kg/sec)	0.046/0.036 (0.021/0.016)	0.087/0.066 (0.039/0.03)
INLET TEMPERATURE, R (K)	1670 (920)	1816 (1005)
PRESSURE RATIO	1.11/1.06	1.05/1.09
EXIT PRESSURE, PSIA (kN/M²)	84 (580)	123/129 (840/890)
EFFICIENCY, PERCENT	6/31	29/31
BYPASS, LB/SEC (kg/sec)	0.13 (0.059)	0.12 (0.054)
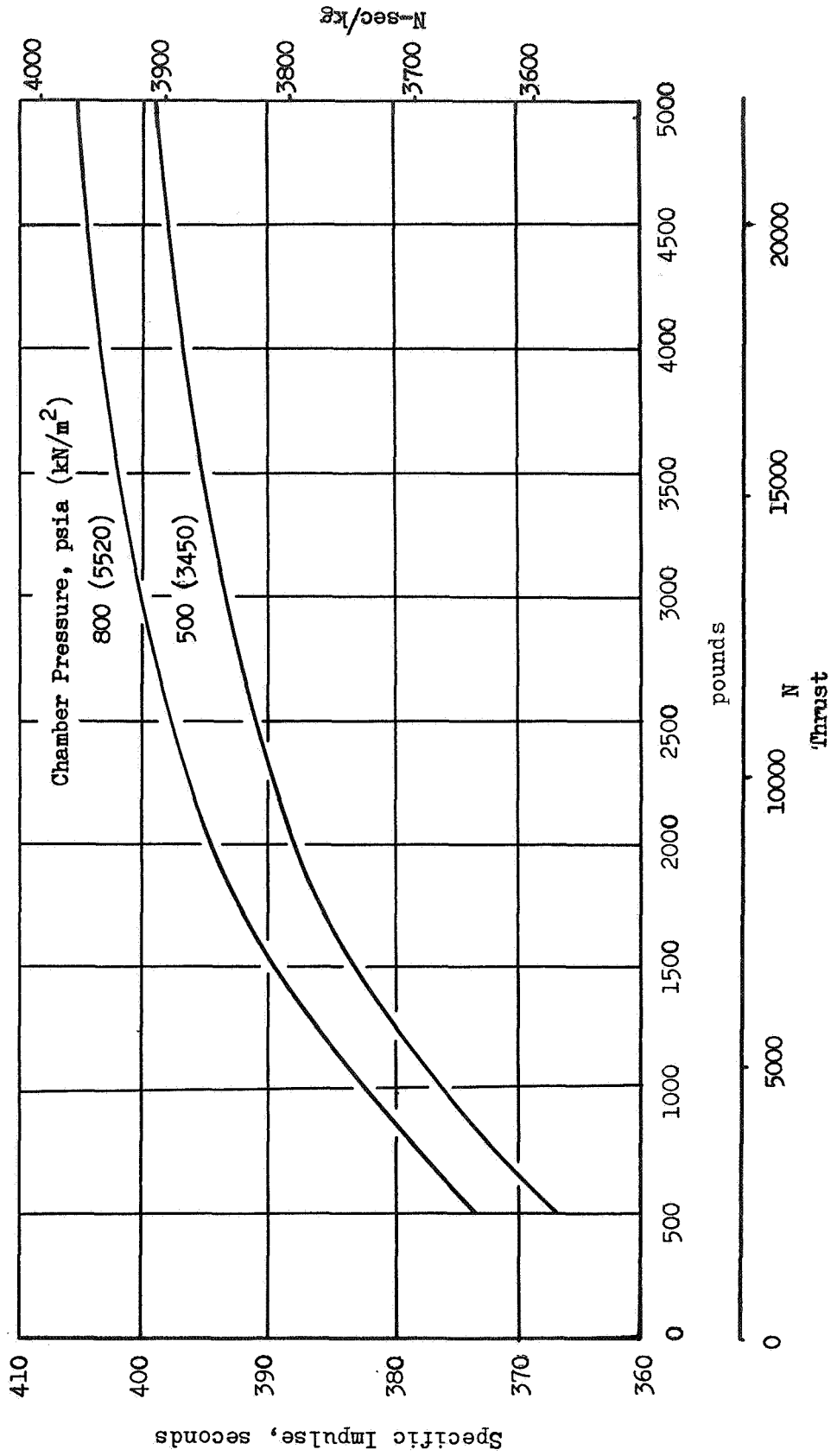
Figure 47. Expander Cycle Performance as a Function of Thrust
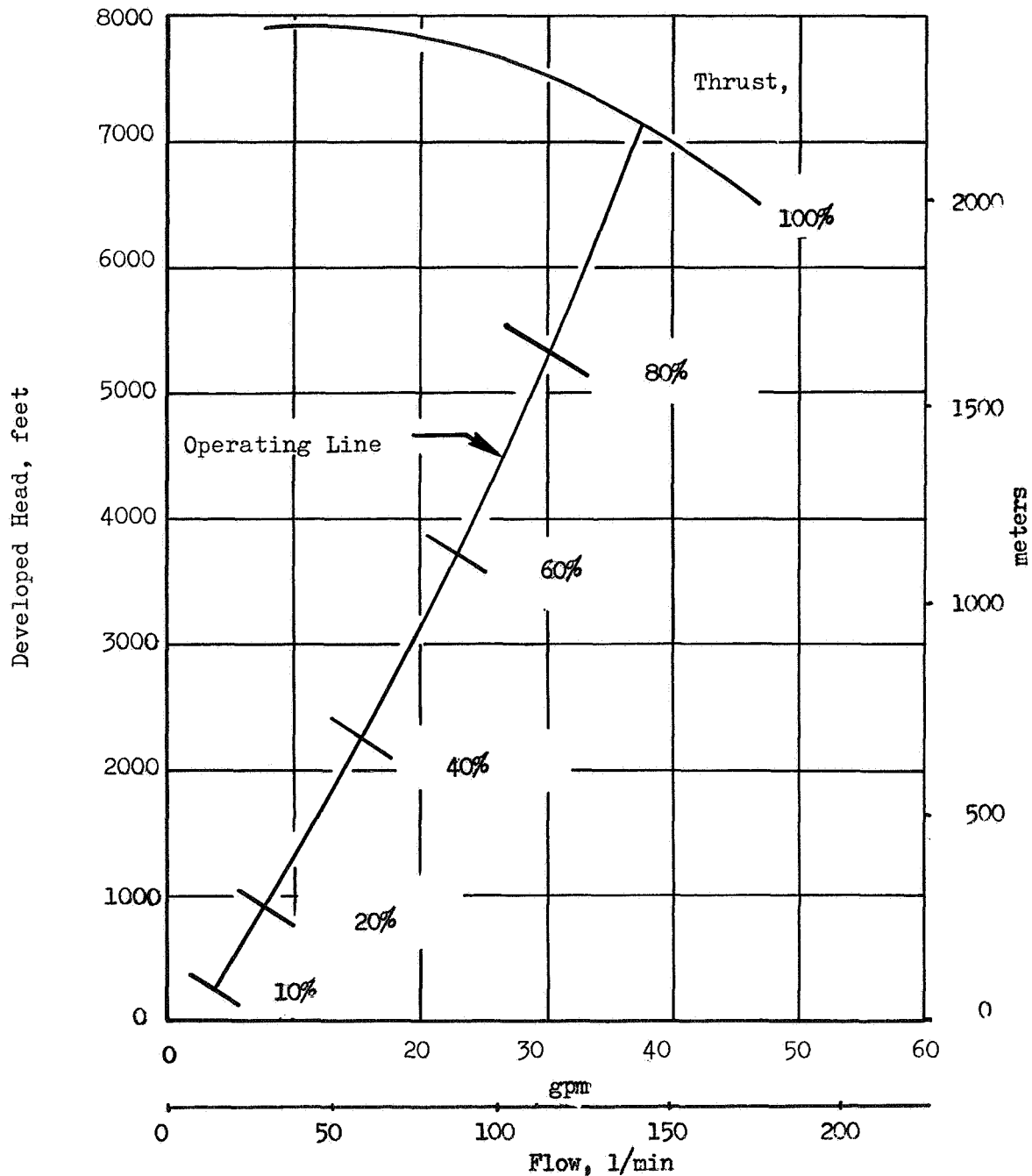
Figure 48   Methane Pump, Expander Cycle,
Chamber Pressure = 500 psia
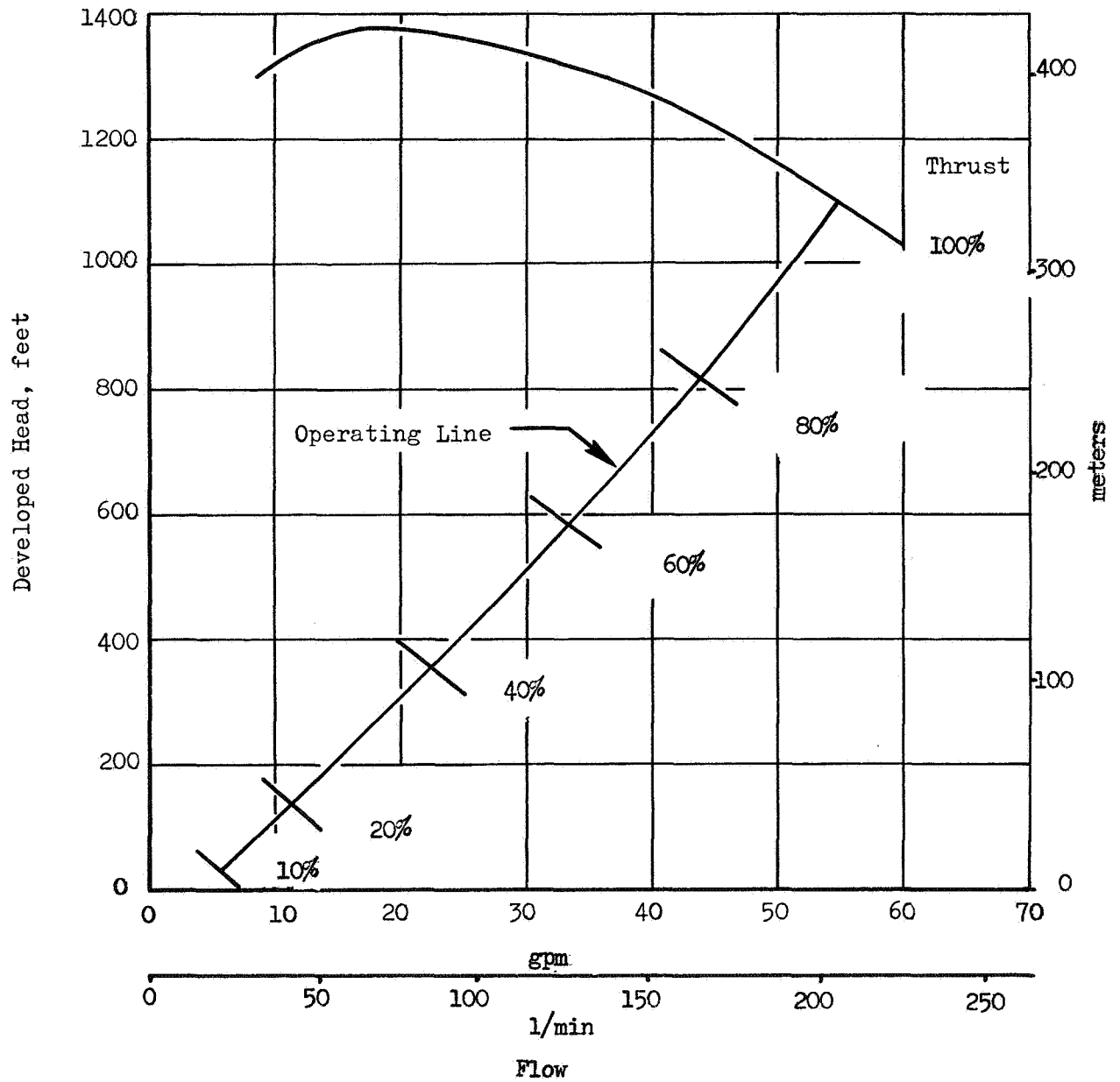
Figure 49 . FLOX Pump Expander Cycle, Chamber Pressure = 500 psia.

161

TABLE 50

AUXILIARY HEAT EXCHANGER ENGINE SYSTEM (THROTTLED)

THRUST, LB (N)	500 (2220)	500 (2220)
ENGINE SPECIFIC IMPULSE, SEC (N-sec/kg)	362.6	367.9
ENGINE MIXTURE RATIO, O/F	4.73	4.56
DESIGN PRESSURE, PSIA (kN/M^2)	500 (3450)	800 (5520)
TURBOPUMP CONFIGURATION	PARALLEL	PARALLEL
THRUST CHAMBER		
CHAMBER PRESSURE, PSIA (kN/M^2)	51.7 (356)	32.6 (570)
MIXTURE RATIO, O/F	4.81	4.75
WEIGHT FLOW, LB/SEC (kg/sec)	1.35 (0.61)	1.35 (0.61)
SPECIFIC IMPULSE, SEC (N-sec/kg)	363.1 (795)	369.3 (850)
EXIT TEMPERATURE, R (K)	1440	1540
PUMPS, O/F		
FLOW, LB/SEC (kg/sec)	1.14/0.24 (0.51/0.11)	1.11/0.24 (0.5/0.11)
DISCHARGE PRESSURE, PSIA (kN/M^2)	67/109 (460/750)	106/182 (730/1230)
SPEED, 1000 RPM (1000 rad/sec)	6/15 (0.6/1.6)	10.5/17.4 (1.1/1.8)
HORSEPOWER (kw)	0.1/0.15 (0.075/0.11)	0.42/0.65 (0.31/0.48)
EFFICIENCY, PERCENT	58.7/51.1	46.8/41.7
TURBINE, O/F		
FLOW, LB/SEC (kg/sec)	0.002/0.0021 (0.0009/0.0009)	0.0043/0.0056 (0.0019/0.0025)
INLET TEMPERATURE, R (K)	1860 (1030)	1860 (1030)
PRESSURE RATIO	8.2/12.9 (3.5/3.5)	13.4/16.3
EXIT PRESSURE, PSIA (kN/M^2)	0.45/0.45	0.79/0.79 (5.9/15.9)
EFFICIENCY, PERCENT	8.3/10	13.2/15.3
BYPASS, LB/SEC (kg/sec)	0.031 (0.014)	0.037 (0.017)

Engine energy balances at the 10:1 throttled condition are shown in Table 50. This throttling was conducted at constant engine mixture ratio. Therefore, the thrust chamber mixture ratio varied from the 5.25 value at full thrust. Because of the small amount of turbine flow, there is little difference between thrust chamber and engine specific impulse. Turbine temperature remains at the full thrust value, with most of the heat exchanger flow bypassing the turbines. For the 800 psia (5520 kN/M^2) auxiliary heat exchanger engine, engine operation as a function of thrust is shown in Fig. 50 to 52.

OFF DESIGN OPERATION

The heat flux level in the thrust chamber and the propellant inlet conditions were among the off-design conditions investigated for the candidate engine cycles. For the fixed designs, the parameters were perturbed and engine characteristics required to maintain the design thrust and mixture ratio determined. These effects are illustrated in Fig. 53 and 54.

In Fig. 53 the effect of variations in heat flux level on the auxiliary heat exchanger cycle balance at 800 psia (5520 kN/M^2) is snown. The higher heat flux results in treater jacket and injector pressure drops as well as increased thrust chamber wall temperatures. The increased pressure drops are provided by a slight increase in pump speed. Additional turbine flow would be necessary and engine specific impulse would decrease by 0.1 second (5N-sec/kg). Variations in pump speeds due to propellant inlet temperature variations were evaluated and found to be slight.

Perturbations in the operating conditions of a 500 psia (3450 kN/M^2) expander cycle engine are shown in Fig. 54. Increases in heat flux level affect this expander cycle discharge pressure somewhat less than the 800 psia (5520 kN/M^2) auxiliary heat exchanger cycle because of the lower heat flux involved and the compensating effect of the increased temperature. As shown, the turbine bypass flow is approximately double that of the

163
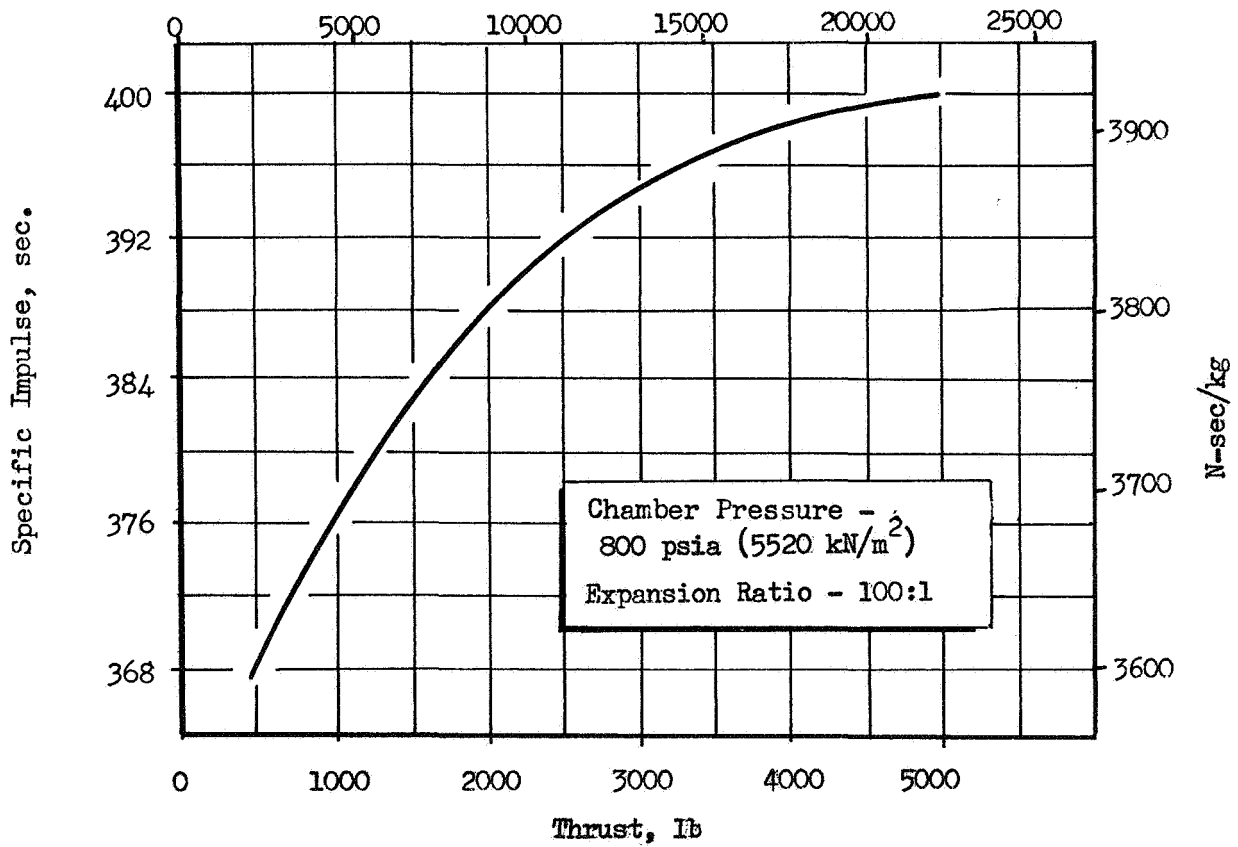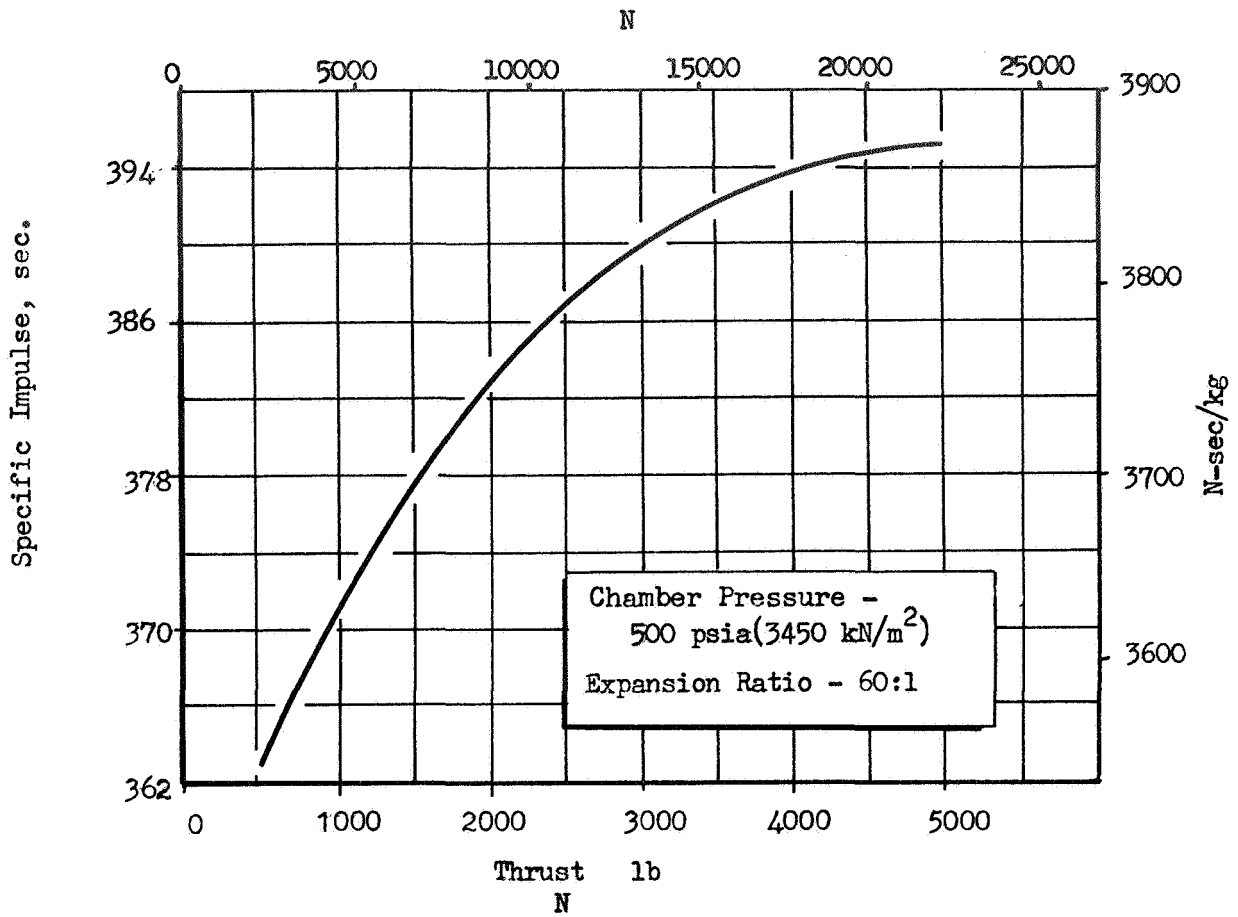
Figure 50 . Auxiliary Heat Exchanger Throttling Performance
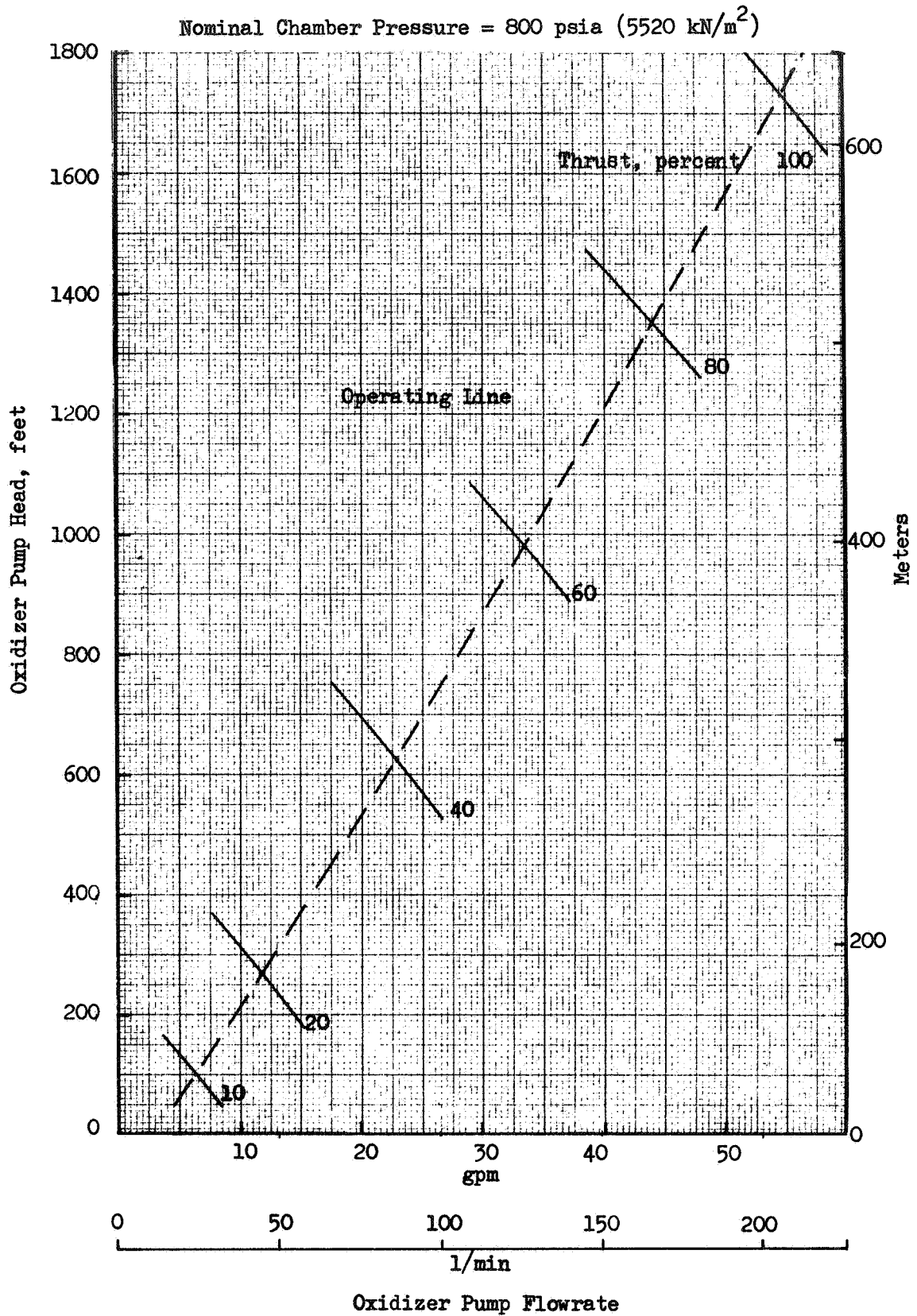
Figure 51. Oxidizer Pump Operating Line for Auxiliary Heat Exchanger Cycle

165

Nominal Chamber Pressure = 800 psia (5520 kN/m^2)
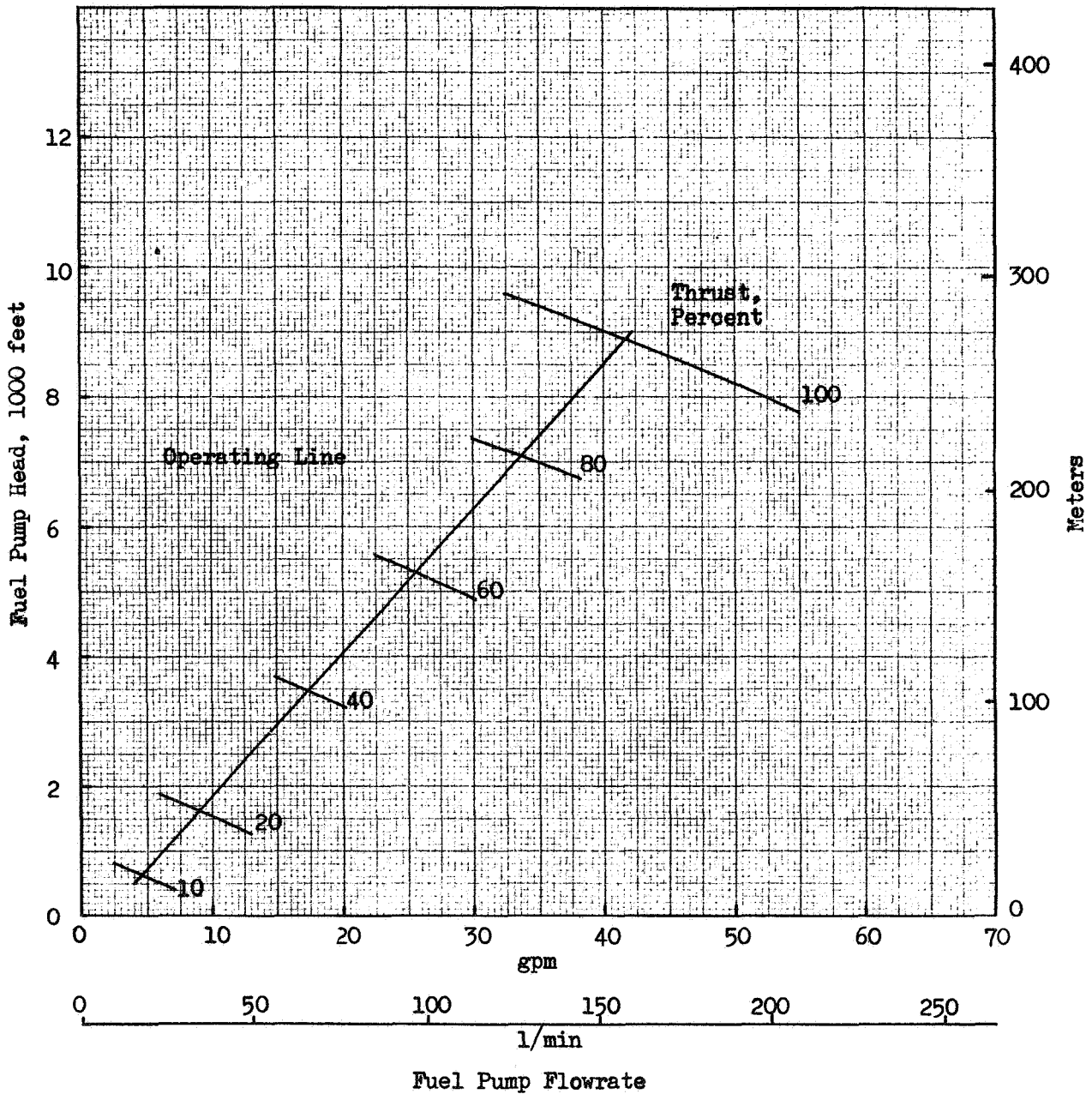
Figure 52. Fuel Pump Operating Line for Auxiliary Heat Exchanger Cycle

166
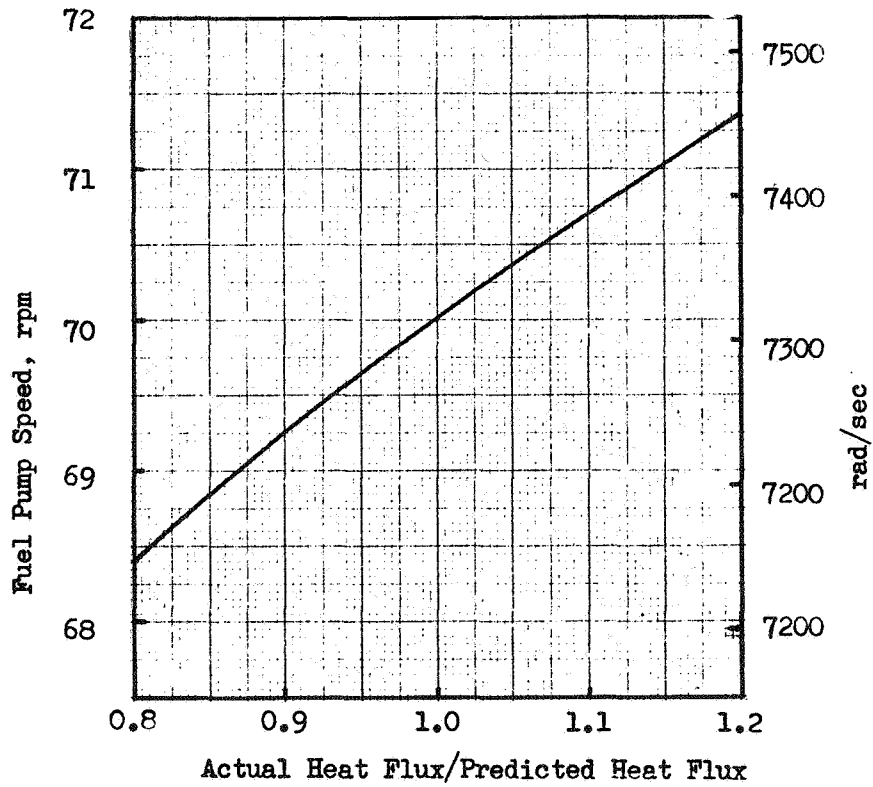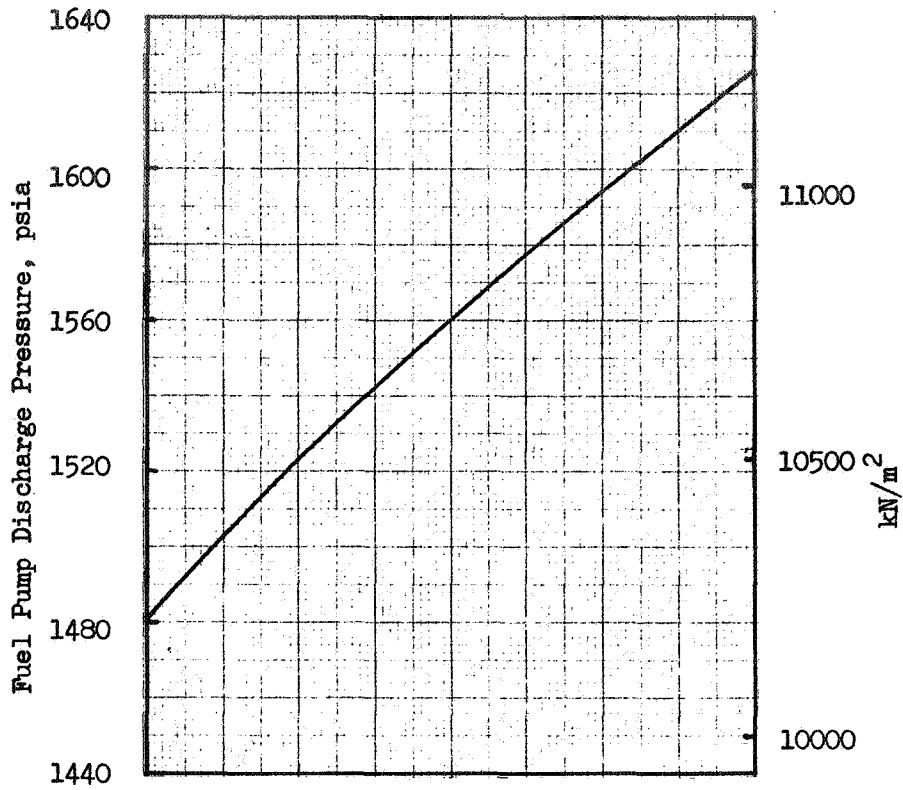
Figure 53   Effect of Cooling Jacket Heat Flux on
Auxiliary Heat Exchanger Cycle
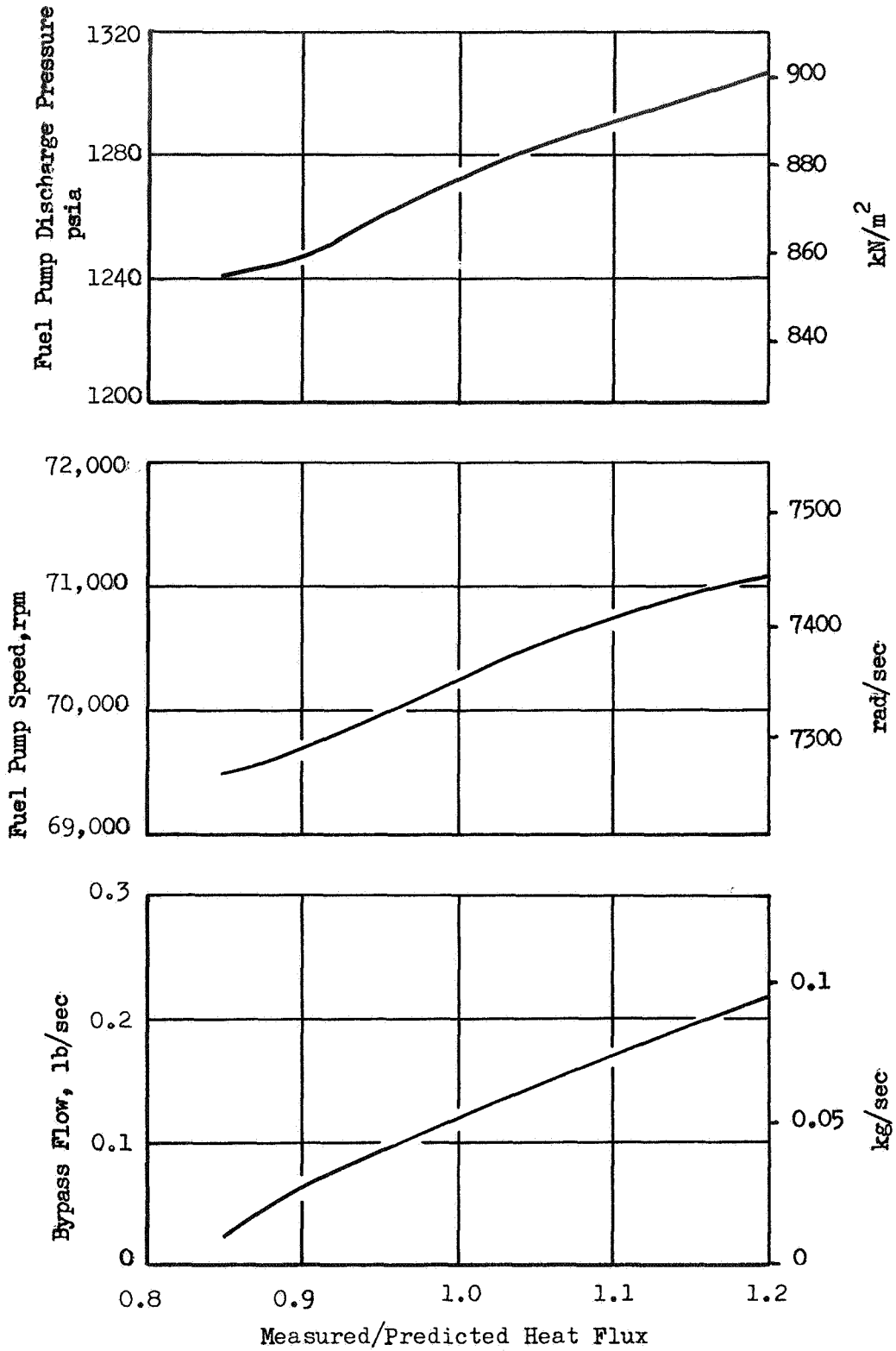
Figure 54   Effect of Heat Flux Level on Expander Cycle Balance,
Chamber Pressure = 500 psia

nominal design point. If lower heat flux values are encountered there
is some point at which there is insufficient turbine power to drive
the cycle. If these lower values were anticipated, additional bypass
flow should be designed into the nominal engine.

ENGINE SYSTEM UPRATING

A brief investigation of engine uprating was conducted. Two areas were
considered: increased specific impulse, and increased thrust.

Performance Increases

The most direct way of increasing performance is through increasing the
expansion ratio. This is illustrated in Fig. 55, where increasing the
expansion ratio from 60 to 100 raises the specific impulse 5 seconds
(49 N-sec/kg).

The nozzle extension could be regeneratively cooled, film-cooled, or
radiation cooled, with little difference between cycles and design points.
Regenerative cooling at these high area ratios would present little
problem. Additional heat input to the methane would occur, but the
pressure drop would be very small. Increased engine weight could
offset some of the performance gain. The turbine exhaust of the
auxiliary heat exchange cycle or fluid tapped from the expander engine
downstream of the turbine could be used to film-cool a high performance
extension.

169
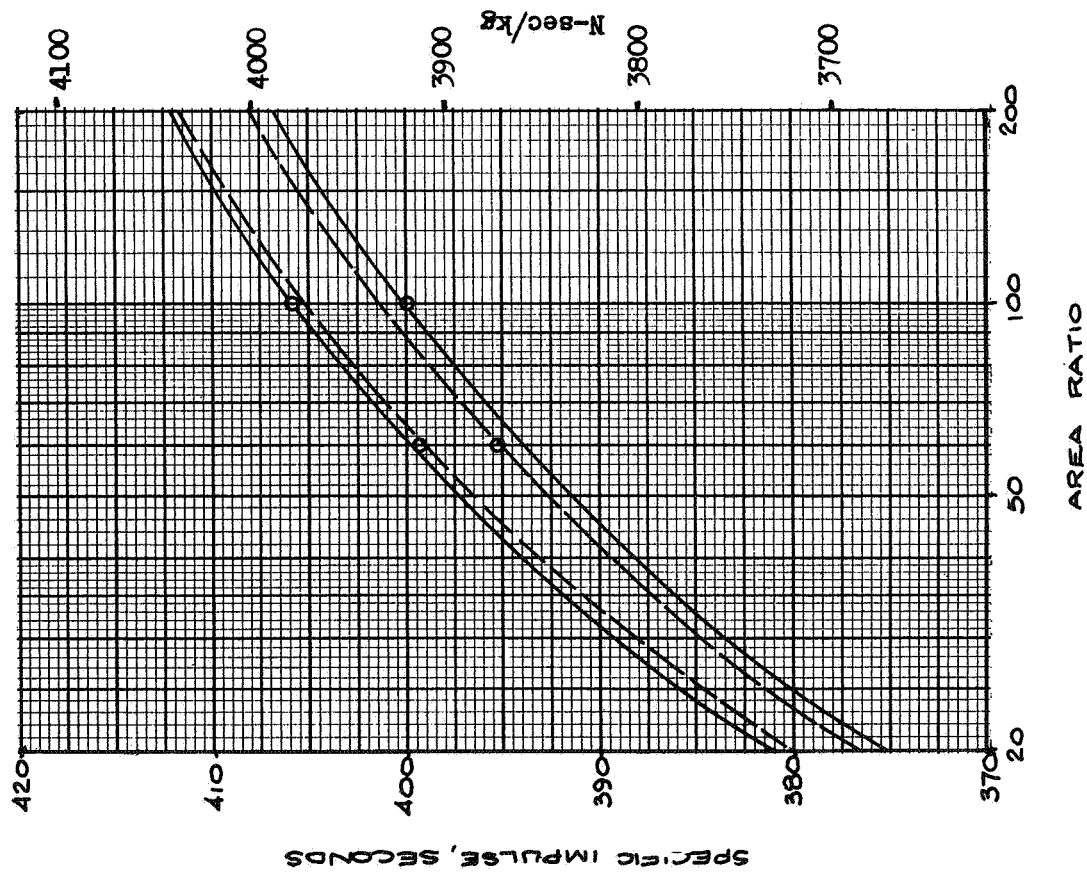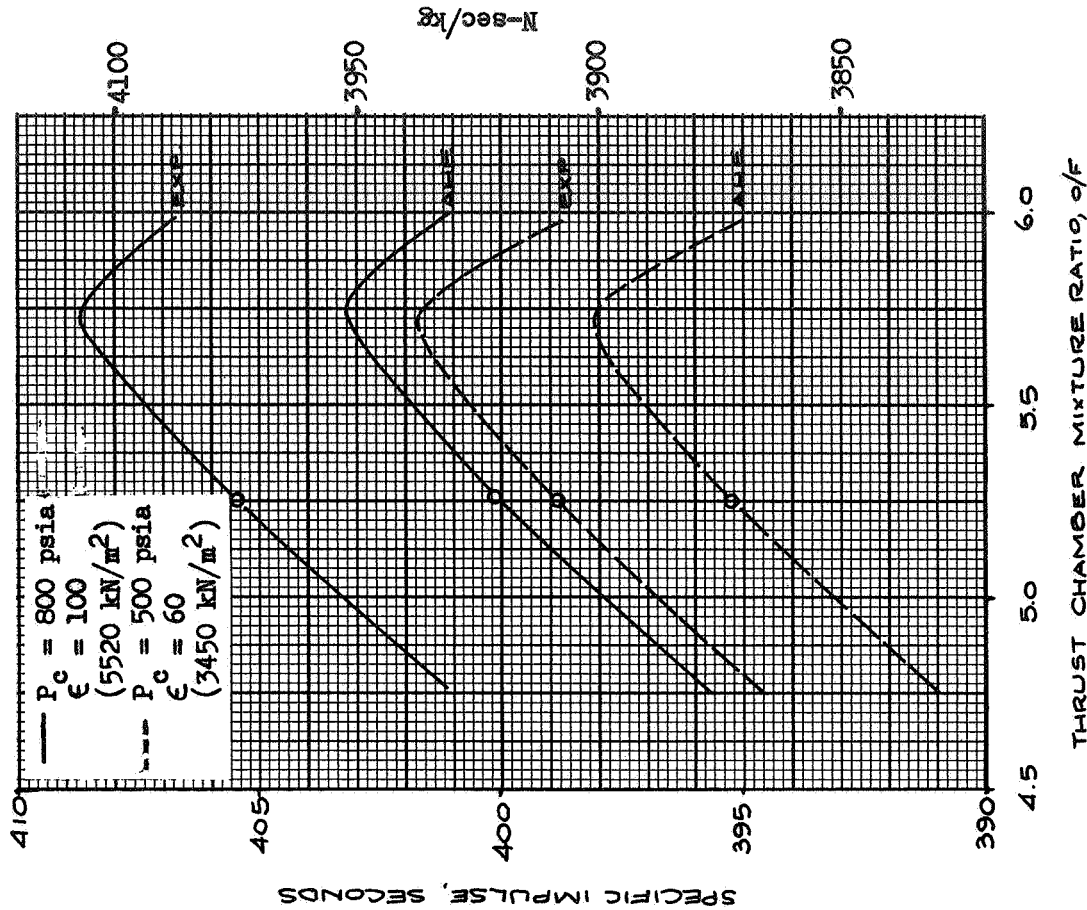
Figure 55. Performance Uprating

A radiation-cooled nozzle extension may also be possible. Investigation of material temperatures are slightly lower for the $\epsilon = 100$ attachment at 800 psia (5500 kN/m^2) than the $\epsilon = 60$ attachment at 500 psia (3450 kN/m^2) material compatibility with the products of combustion would be a significant consideration for both design points.

The effect of mixture ratio on theroetical specific impulse is also shown in Fig. 55. An increase of about 3 seconds is possible (30 N-sec/kg), however, this may be difficult to attain, since injector mixing requirements to obtain high combustion efficiency are quite severe at the higher mixture ratio values.

Thrust Increase

Thrust uprating can be accomplished in two ways: throat area increase or chamber pressure increase. Thus uprating to 8000 pounds (35600 N) completely by throat area increase would result in thrust chamber redesign. With the exit area held constant, the expansion ratio would be significantly reduced and specific impulse would decrease about 1.3 percent. To maintain the performance, engine length would be significantly increased. Pump flowrates would be increased 60 percent. This is applicable to both drive cycles, however, the available turbine energy would be reduced for the expander cycle and may create a problem.

Thrust uprating by chamber pressure increase can be effected while maintaining the basic thrust chamber geometry and performance. The designs would be different for the higher flow and heat flux. Turbomachinery must be designed for both increased flow and discharge pressure. Since the 800 psia (5520 kN/m^2) engines already have high pump discharge pressures and thrust chamber cooling is a significant development problem, the chamber pressure uprating is only applicable to the 500 psia (3450 kN/m^2) design point engine.

Fuel pump discharge pressures for expander cycle uprating to 8000 pound (35600N) thrust vary considerably with the injector pressure drop and turbine power avilable. As shown in Fig. 44, an 800 psia (5520 kN/M^2), 5000-pound (22200N) thrust engine with throttling injector pressure drops has fuel pump discharge pressure requirements of 2400 to 2800 psia (16500 to 19300 kN/M^2). A 5000-pound (22200N) thrust, 500 psia (3450 kN/M^2) throttling engine uprated directly to 8000-pound (35600N) thrust would have discharge pressures in excess of these because of reduced turbine inlet temperature and the pressure drop increase in the fixed flow passages. This would require turbomachinery overdesign factors of 3-4 and would be unreasonable. By redesign of the flow passages downstream of the turbine, particularly in the injector, fuel pump discharge pressures of the uprated engine could be in the 2000 psia (8900 kN/M^2) range, making engine uprating feasible.

In the auxiliary heat exchanger engine, the pump discharge pressures increase slightly more than 60-percent. The increased pump discharge pressure will require relatively more turbine flow and engine specific impulse will be reduced. For uprating to 8000-pound (35600N) thrust, the specific impulse decreases over 0.8 percent for direct uprating and slightly over 0.3 percent with some engine modification.

ENGINE SYSTEM DEVELOPMENT EASE

Based upon the engine characteristics defined in the previous sections, the ease of development of the candidates was evaluated. The evaluation is divided into three component areas (Tables 51, 52 and 53) each subdivided. into fabrication, development testing, and potential development problems.

In the thrust chamber/injector area (Table 51) the 500 psia (3450 kN/M^2) expander cycle is easiest to fabricate became of the larger channel dimensions. Development testing is slightly more involved for the expander cycles since feed

TABLE 51

THRUST CHAMBER/INJECTOR DEVELOPMENT COMPARISON

DRIVE CYCLE	AUXILIARY HEAT EXCHANGER		EXPANDER	
CHAMBER PRESSURE psia (kN/m^2)	500 (3450)	800 (5520)	500 (3450)	800 (5520)
FABRICATION				
MIN. CHANNEL WIDTH, in. (cm)	0.04 (0.102)	0.04 (0.102)	0.072 (0.183)	0.042 (0.107)
WALL THICKNESS (THROAT), in. (cm)	0.025 (0.064)	0.020 (0.051)	0.025 (0.064)	0.020 (0.051)
NO. CHAMBER MANIFOLDS	3	3	2	2
NO. INJECTOR MANIFOLDS	2	2	3	3
FUEL TEMPERATURE, R (K)	1060 (589)	1094 (608)	1150 (639)	1272 (707)
DEVELOPMENT TESTING				
FUEL INLET PRESSURE, psia (kN/m^2)	890 (6140)	1460 (10100)	1200 (8270)	2300 (15860)
COOLANT ROUTE	INJECTOR	INJECTOR	TURBINE/INJECTOR	TURBINE/INJECTOR
FEED SYSTEM SIMULATION	ADVANTAGEOUS	ADVANTAGEOUS	NECESSARY	NECESSARY
IDLE MODE REQUIRED	—	—	X	X
POTENTIAL DEVELOPMENT PROBLEMS				
COMBUSTOR HEAT FLUX	X	XX	X	XX
NOZZLE HEAT FLUX	XX	XX	X	XX
CHANNEL CLOGGING	XX	XX	X	XX
MATERIAL PROPERTIES	X	XX	X	XX
INJECTOR HEATING	X	XX	XX	XXX
PHASE CHANGE (THROTTLED)	XX	XX	XX	XX

TABLE 52   TURBOMACHINERY DEVELOPMENT COMPARISON

DRIVE CYCLE	AUXILIARY HEAT EXCHANGER		EXPANDER	
CHAMBER PRESSURE, PSIA (k N/m^2)	500 (3450)	800 (5520)	500 (3450)	800 (5520)
FABRICATION (O/F)				
NO. OF PUMP STAGES	1/1	1/2	1/2	1/2
IMPELLER TIP WIDTH, IN (cm)	0.104 / 0.051 (0.264)/(0.13)	0.089 / 0.053 ((0.226)/(0.135))	0.104 / 0.050 (0.246)/(0.127)	0.089 / 0.053 (0.226)/(0.089)
NO. OF ENGINES	2	2	2	2
NO. OF WHEELS	2/1	2/1	1/1	1/1
TURBINE DIAMETER, IN (cm)	4.1 (10.1)/3.6 (9.15)	4.5 (11.5)/4.7 (12)	2.2 (5.6)/2.1 (5.3)	2.1 (5.3)/3.3 (8.4)
TURBINE TEMPERATURE, R (k)	1860 (1030)	1860 (1030)	1245 (690)	1326 (735)
DEVELOPMENT TESTING				
PUMP SPEED, 1000 RPM (1000 r/sec)	40 (4.2)/90 (9.4)	50 (5.2)/75 (7.8)	40 (4.2)/70 (7.3)	50 (5.2)/65 (6.8)
TURBINE FLOW, LB/SEC (kg/sec)	0.002 - 0.11 (0.0009)-(0.05)	0.005 - 0.15 (0.0023)-(0.063)	0.04 - 1.0 (0.018)-(0.454)	0.08 - 1.87 (0.036)-(0.85)
TURBINE PRESSURE, PSIA (k N/m^2)	320 (2000)	320 (2000)	1090 (7510)	2060 (14,2000)
TURBINE TEMPERATURE, R (k)	1860 (1030)	1860 (1030)	1245 (690)	1326 (735)
POTENTIAL DEVELOPMENT PROBLEMS				
EFFICIENCY CHANGE	X	X	XX	XXX
PUMP DIAMETER RATIO	XX	X	XX	X
IMPELLER TOLERANCE	X	X	X	XX
PUMP STALL	X	X	XX	XX
THERMAL GRADIENTS	XX	XX	X	X
NOZZLE HEAT FLUX	XX	XX	X	X

174

TABLE 53

ENGINE SYSTEM/CONTROLS DEVELOPMENT COMPARISON

DRIVE CYCLE	AUXILIARY HEAT EXCHANGER		EXPANDER	
CHAMBER PRESSURE psia (kN/m^2)	500 (3450)	800 (5520)	500 (3450)	800 (5520)
FABRICATION				
NO. LIQUID VALVES	2	2	2	2
NO. GAS VALVES	3	3	2	3
GAS VALVE FLOW, lb/sec (kg/sec)	0.002-0.11 (0.009-0.05)	0.005-0.15 (0.0023-0.068)	0.04-1.0 (0.018-0.454)	0.08-1.87 (0.036-0.85)
NO. PNEUMATIC VALVES	4	4	3	3
NO. DUCTS/CONNECTIONS	18/36	18/36	18/42	18/42
DEVELOPMENT TESTING				
INLET PRESSURE, psia (kN/m^2)	60 (410)	60 (410)	60 (410)	60 (410)
VACUUM TESTS	YES	YES	YES	YES
IDLE MODE TESTS	ADVANTAGEOUS	ADVANTAGEOUS	NECESSARY	NECESSARY
POTENTIAL DEVELOPMENT PROBLEMS				
ENGINE START CONTROL	X	X	XX	XX
THERMAL CONDITIONING	X	X	XX	XX
CHUGGING	XX	XX	XX	XXX
FUEL PHASE CHANGE (THROTTLING)	X	X	XX	XX
OXIDIZER PHASE CHANGE (THROTTLING)	XX	XX	XX	XXX
VALVE LEAKAGE	XX	XX	XX	XX

175

system simulation is necessary. Simulation is desirable for both drive cycles so this difference is minor. Potential thrust chamber development problems (more X's indicate more severe problem) are most likely to be encountered in the 800 psia (5520 kN/m^2) engines. The 500 psia (3450 kN/m^2) expander cycle has the least potential problems in this area.

A comparison of development ease in the turbomachinery area indicates that the low pressure engines have the easiest turbomachinery fabrication. In development testing of the turbines, the expander cycles have higher flowrates and pressures which would require a somewhat larger heat source than for the auxiliary heat exchanger cycles. For flowrates of this magnitude, heat source size differences would not be significant and may be overshadowed by the higher temperature required of the auxiliary heat exchanger cycles. In the area of potential development problems, the 800 psia (5520 kN/m^2) expander cycle has the most significant problem areas. The 800 psia (5520 kN/m^2) auxiliary heat exchanger cycle has slightly less significant potential problems than the low pressure engines.

Engine system and control development (Table 53) comparison indicates a greater number of control components associated with the auxiliary heat exchanger cycle. In addition, the gas valves must control flows approximately one-tenth the magnitude of those in the expander cycle and are consequently more difficult to fabricate. The expander cycle might need an extra liquid valve for an idle-mode but this will be avoided, if possible. Development testing requirements are similar except for the idle-mode testing which is necessary for the expander cycle. Engine system development problems are most significant for the 800 psia (5520 kN/m^2) expander cycle, since it is very sensitive to component characteristics and development problems which result in increased pressure drops. The 500 psia (3450 kN/m^2) expander will be more sensitive to engine start and thermal conditioning problems than the auxiliary heat exchanger cycles, and the system development may therefore be slightly more complex.

From an overall developmental standpoint the auxiliary heat exchanger engine at 500 psia (3450 kN/M^2) is easiest to develop, followed closely by the 500 psia (3450 kN/M^2) expander, and then by the 800 psia (5520 kN/M^2) auxiliary heat exchanger engine. The 800 psia (5520 kN/M^2) expander engine is the most difficult to develop.

DRIVE CYCLE SELECTION

The results of these investigations reaffirm the general conclusions of the investigation of the previous section summarized in Table 54. The expander cycle at 800 psia (5520 kN/M^2) chamber pressure is the highest performing engine, but because of its sensitivity and potential problems it would be the most difficult to develop. The 500 psia (3450 kN/M^2) auxiliary heat exchanger is the easiest to develop but has the lowest performance. The remaining two cycles are comparable in performance and development ease.

Engine start and throttling ease are similar for the two cycles. Engine uprating in performance and thrust is more attractive with the 500 psia (3450 kN/M^2) expander, which at equal design points will always outperform the auxiliary heat exchanger cycle (Figure 55). Form this standpoint, the expander cycle at 500 psia (3450 kN/M^2) chamber pressure was recommended for further investigation.

TABLE 54

ENGINE DRIVE CYCLE COMPARISON

| CHAMBER PRESSURE | 500 psia (3450k N/m^2) | | 800 psia (5520k N/m^2) | | |
DRIVE CYCLE / RATING AREAS	EXPANDER	AUXILIARY HEAT EXCHANGER	EXPANDER	AUXILIARY HEAT EXCHANGER	
SPECIFIC IMPULSE, sec (N-sec/kg)	398.9 (3912)	394.0 (3860)	405.6 (3980)	397.8 (3910)	
PERFORMANCE	57	52	61	55	
RELIABILITY	84	85	84	83	
DEVELOPMENT EASE	74	87	63	79	
PRODUCTION BASE	98	76	98	76	
COMMENTS		1. Single stage methane pump	1. Engine system very sensitive to component design. 2. Throttling limited.		

TASK II – ENGINE PRELIMINARY DESIGN EVALUATION

A preliminary design is provided for a flight-weight FLOX/methane engine using an expander turbine drive cycle. This engine configuration was selected in Task I on the basis of high performance, fabrication and developmental ease, and operational flexibility. For ease of control in transient operation, dual shaft turbines operating in parallel are used. Long duration operation and low fabrication cost are provided by use of a regeneratively cooled channel construction thrust chamber.

The engine is designed to reliably provide high performance for a variety of potential space missions. Capability for multiple restarts, long duration and prolonged storage in the space encironment are provided. Versatility of operation is emphasized. The nominal engine design represents a reasonable balance between these features and engine system cost. Where design alternatives exist, they are described for further consideration.

The preliminary design investigation was divided into three parts: Task IIA – Engine Control System Investigation, Task IIB – Engine System Design, and Task IIC – Engine Component and Subsystem Design. To provide a concise engine definition, the resulting engine design is described in the following sections:

        1. Engine System
        2. Engine Operation
        3. Thrust Chamber Design
        4. Injector Design
        5. Valves and Controls
        6. Turbomachinery Design

ENGINE SYSTEM DESCRIPTION

Overall engine system characteristics are described. Engine system layout, weight summary, performance description, nominal energy balances, engine ducting, engine assembly, and vehicle/engine interface requirements are described. The engine system has a nominal thrust of 5000 pounds (22200N) at 500 psia (3450 kN/M^2). Sufficient power and design margin is included to allow for development program contingencies. Should these margins not be required, engine uprating capability to 7000-8000 pounds (31100-35600N) thrust at 700-800 psia (4760-5520 kN/M^2) is available with no performance loss. A 60:1 expansion ratio nozzle has been used. Engine performance improvement capability is provided by designing for possible nozzle extensions and mixture ratio changes.

ENGINE DESIGN DESCRIPTION

System Description

The engine system design is shown in Fig. 56 and an engine schematic in Fig. 57. In the engine system, separate fuel and oxidizer turbopumps are driven in parallel by gaseous methane that has been heated in the thrust chamber coolant circuit. The cryogenic fuel enters the engine through the fuel inlet valve mounted upstream of the pump inlet. After passing through the fuel pump, all the fuel is utilized in a single up-pass coolant circuit. The fuel is heated and gasified as it passes through the coolant circuit. The hot methane is then split into three parallel flow circuits: one powers the methane turbine, one powers the FLOX turbine, and one is a bypass circuit. The bypass line and valve are used to control total turbine power. From the turbine exit, the hot gas is ducted to the injector fuel inlet manifold and into the thrust chamber.

FIGURE 56

FLOX METHANE
ENGINE CHARACTERISTICS
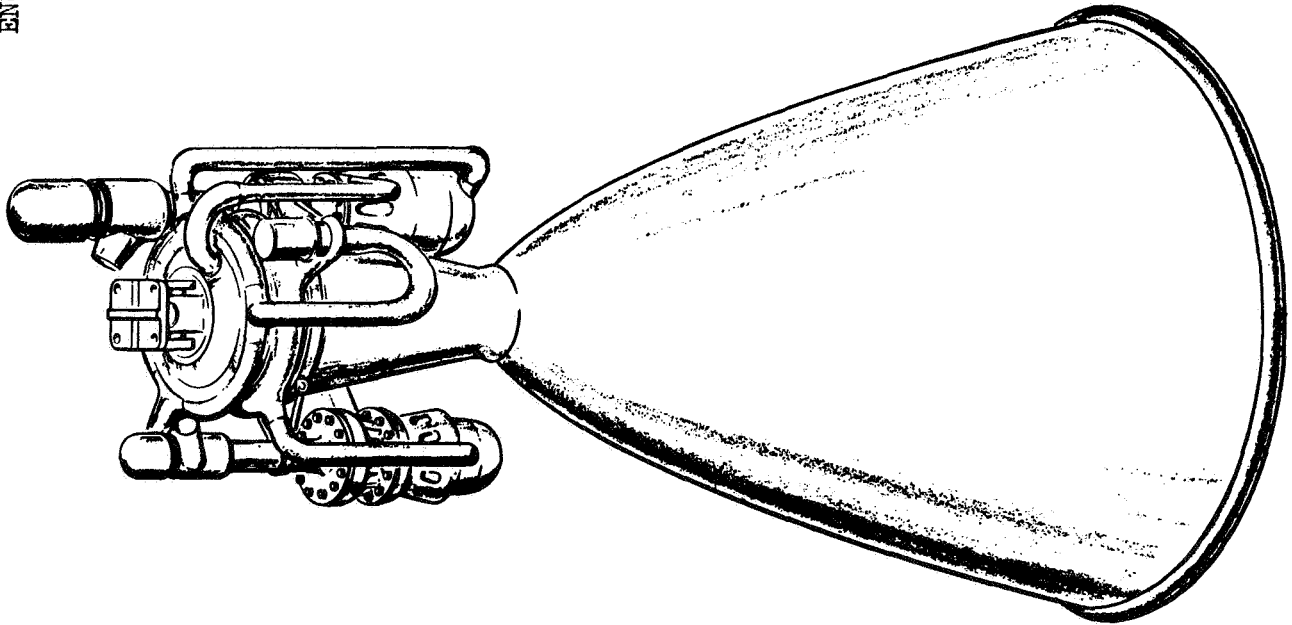
- THRUST, LB (N)   5000   (22,200)
- CHAMBER PRESSURE, PSIA (k N/m²)   500   (3450)
- MIXTURE RATIO (O/F)   5.25
- EXPANSION RATIO   60:1
- SPECIFIC IMPULSE, SEC   399   (3910)
- ENGINE WEIGHT, LB (KG)   89   (40.4)

- ALL WELDED CONSTRUCTION
- DUAL SHAFT CENTRIFUGAL TURBOPUMPS
- REGENERATIVELY COOLED
- MILLED CHANNEL THRUST CHAMBER

- GIMBALLED ± 2 DEGREES (.035 RAD)
- MULTIPLE RESTART
- REPEATABLE CUTOFF
- THROTTLED OPERATION

Fig. 57. 5K FLOX/CH$_4$ ENGINE SCHEMATIC
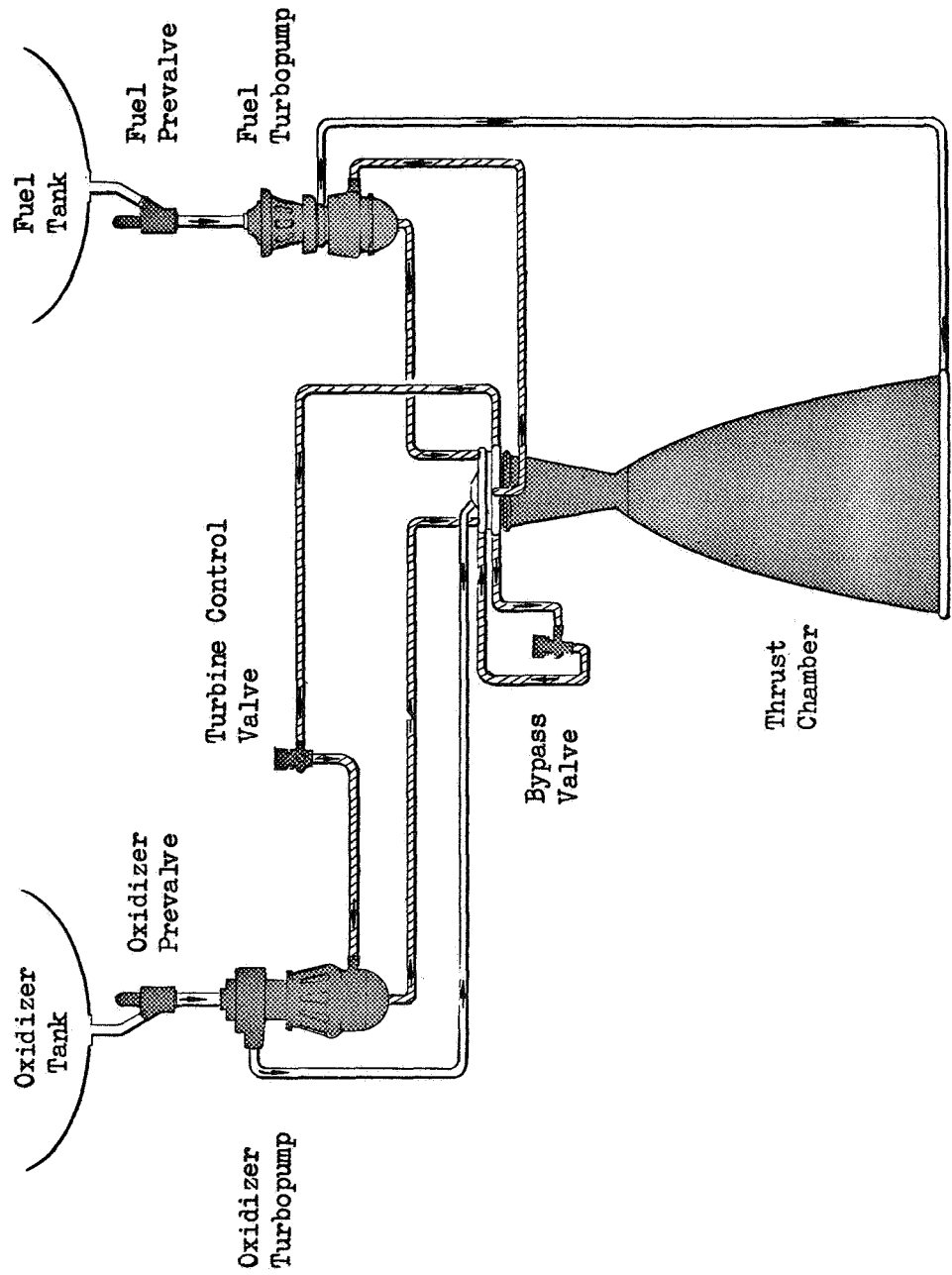
Fuel Tank

Fuel Prevalve

Fuel Turbopump

Oxidizer Tank

Oxidizer Prevalve

Oxidizer Turbopump

Turbine Control Valve

Bypass Valve

Thrust Chamber

A turbine control valve is used on the hot gas inlet line to the FLOX turbine to proportion power between the methane and FLOX pumps. Engine thrust and mixture ratio are controlled by the hot gas valves. The three parallel hot gas circuits have separate outlets on the thrust chamber and separate inlets on the injector. This system is used to minimize the size of the manifolds on the injector and thrust chamber while providing good propellant distribution and low propellant manifold volumes. By dividing the flow into three parts at its source, the ducting can be smaller, more flexible and more direct. Temperature drop across the turbines is very small ($\sim$ 40R)(22K) and **temperature drops** in the injector manifold shouldnot affect injector performance.

The FLOX enters the engine through the inlet valve mounted upstream of the pump inlet. It then passes through the pump and is ducted into the injector FLOX dome.

Design Description

An engine system layout is provided in Fig. 58.

Turbomachinery. Two separate turbopumps are used to provide control ease in transient operation and flexibility of component arrangement. Each pump operates at individually optimum speed. The FLOX pump has a single stage with a centrifugal impeller. The methane pump is a two-stage pump with centrifugal impellers. In both pumps bearings are cooled by the individual propellants. Single-row velocity compounded turbines with partial admission are used to power both pumps. These turbines use methane as the working fluid in a parallel flow arrangement. Inducers are used on both pumps to provide low NPSP requirements. To assure uniform flow to the inducers, a short section of ducting is provided between the main valves and the pump inlets.

184

40.9 in.
(103.9 cm)

1 foot

1 in.

50 cm

10 cm

21.4 in.
(54.4 cm)

40.9 in.
(103.9 cm)

1 foot

50 cm

10 cm

1 in.
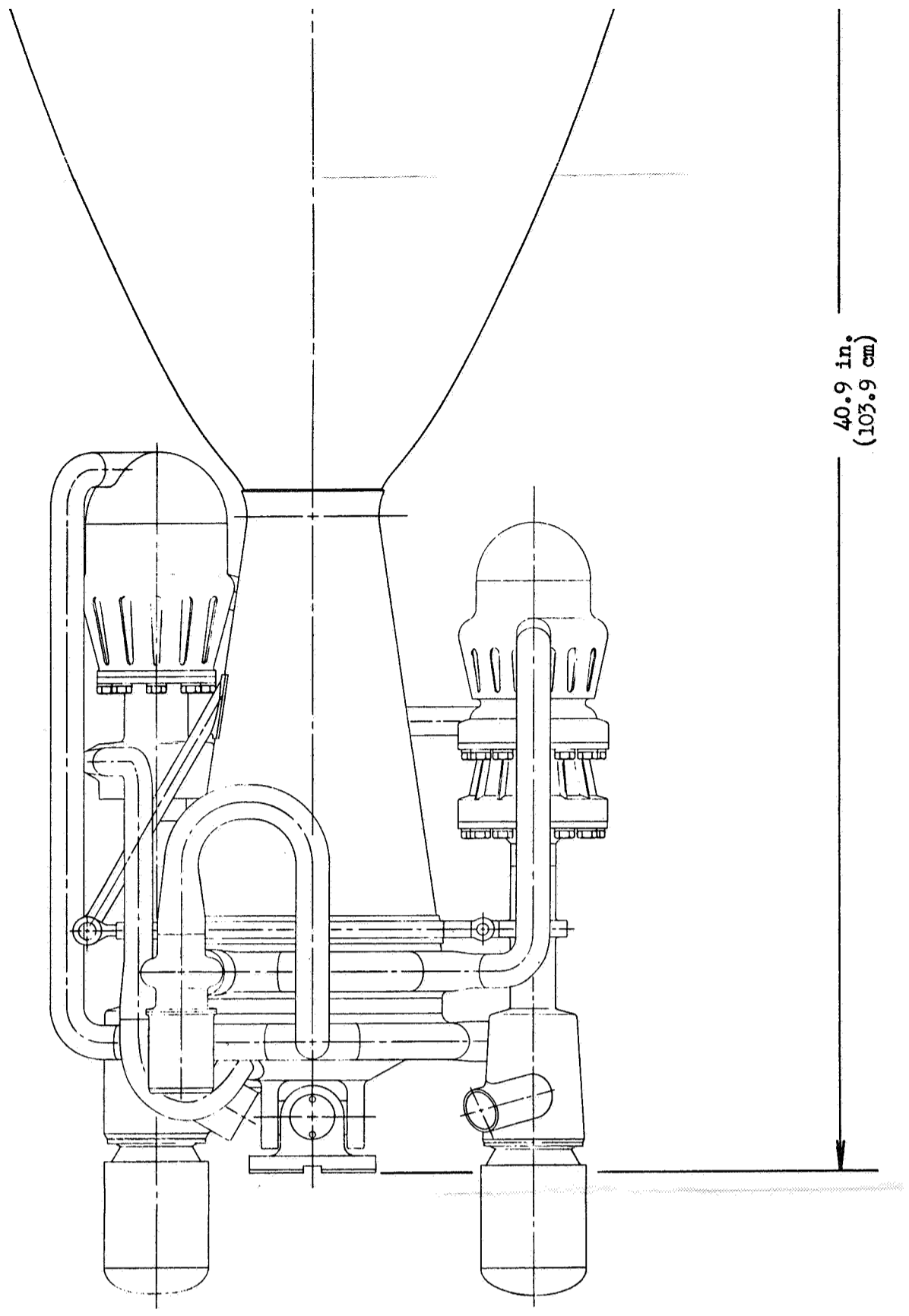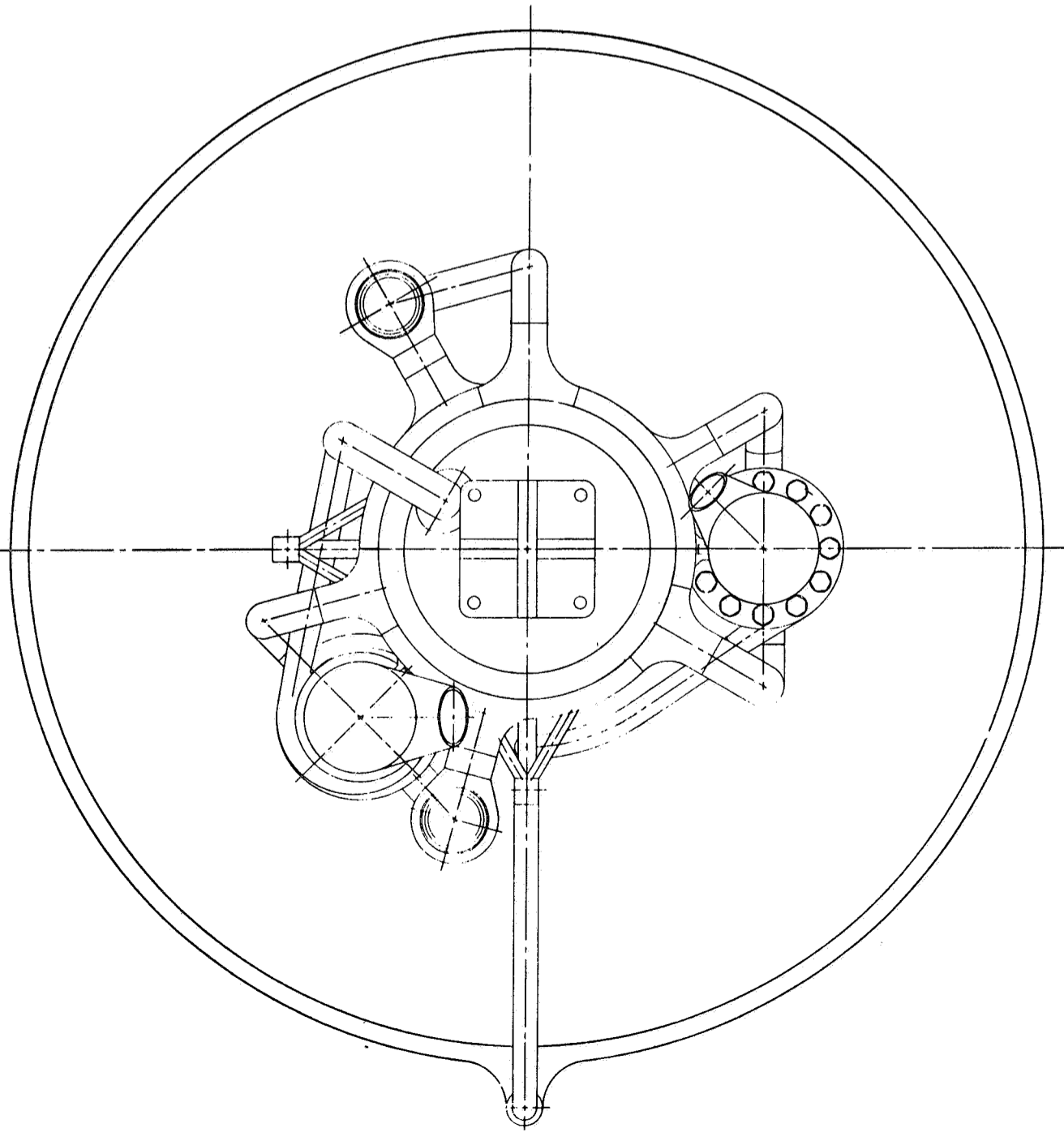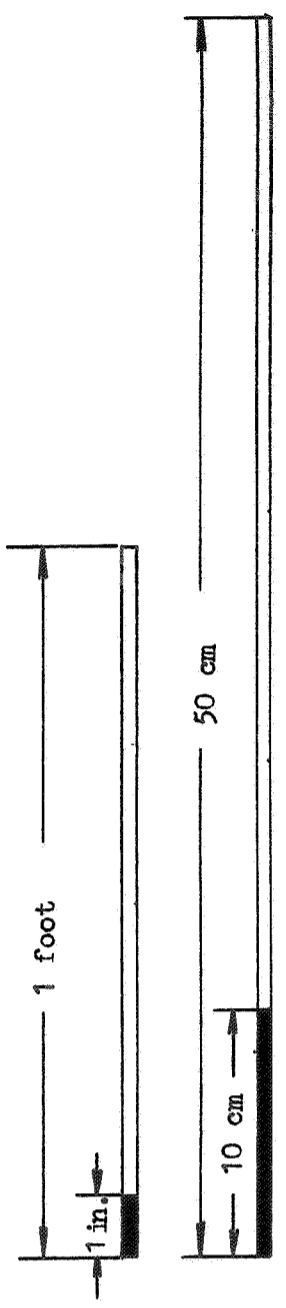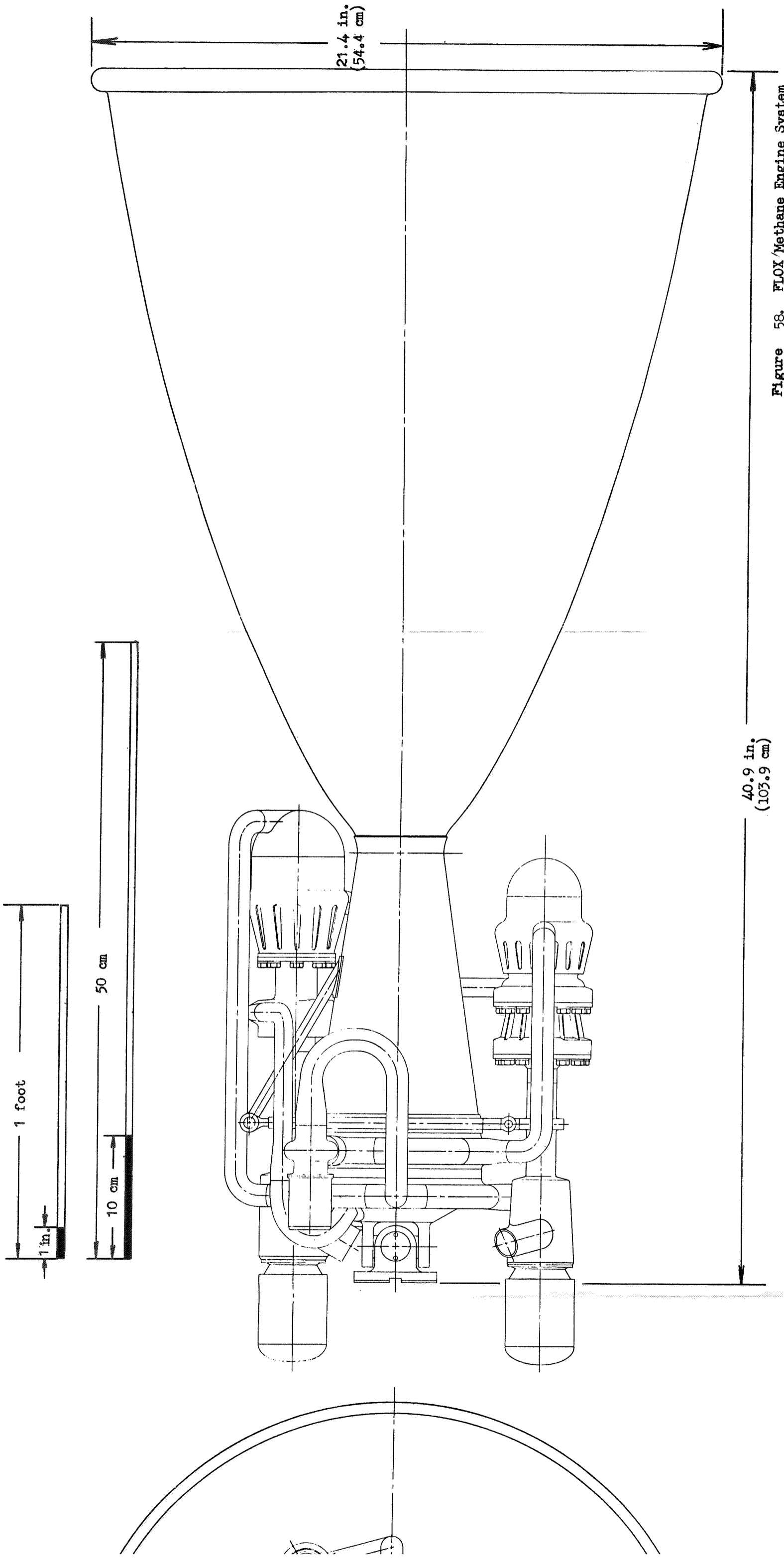
Figure 58. FLOX/Methane Engine System

185

Thrust Chamber. The regeneratively-cooled thrust chamber is made of nickel using advanced fabrication, channel construction techniques. An 80-percent bell nozzle is used with the nozzle contour designed to optimize performance within a fixed envelope. Methane enters the cooling jacket through a manifold at nozzle exit. After flowing through the jacket the hot methane is collected in a second manifold for distribution to the turbines. This up-pass cooling arrangement is used to provide good coolant properties in the high heat flux region and assure that any methane phase change will occur in the low heat flux region of the nozzle.

Injector. Hot methane from the turbine exhaust is collected in the injector fuel manifold and distributed to the injector elements. FLOX enters the oxidizer dome directly from the pump exit. The injector is of a coaxial type with a methane cooled copper face. Pressure drops during throttling are maintained by the recessed element design.

Performance is maintained by the high methane velocity which increases during throttling due to its bulk temperature increase. The injector is welded to the thrust chamber to save weight and to increase reliability. The gimbal bearing is an integral part of the injector and is a simple Hooke-type joint with Fabroid bearing surfaces. The injector oxidizer dome has a single inlet and a tapoff port for tank pressurization. The annular fuel inlet manifold has three inlets, one from each of the turbines and one from the bypass valve. A fuel tapoff port is also provided for tank pressurization.

Valves. Four valves are used in the system. The two inlet valves, located above the turbopump, are normally closed, angle-body, poppet-type designs with hard

seats. These valves are an on-off type using a pneumatic actuator with bellows seals. They are sized to the same diameter as the pump inlets. The valves are structurally attached to the turbopump inlets through a riding duct which provides sufficient length to smooth the propellant flow before it enters the pump inducer. The bypass and oxidizer turbine valves control mixture ratio and enters the pump inducer. The bypass and oxidizer turbine valves control mixture ratio and thrust level. The hot gas valves are pneumatically actuated, angle-body, poppet-type designs. The poppet is contoured to give optimum flow control characteristics over the entire throttling range.

Ducting

All ducting consists of solid lines with welded interconnects. This system eliminates the weight and complexity associated with bolted joints and bellows and provides a more reliable, lighter weight system. The routing of propellant lines was chosen to minimize line length, volume and weight while maintaining flexibility in all directions to limit duct loading on components to a reasonable value. Clearances are provided for in-place tube welding on all joints. This clearance consists of maintaining 0.375 inches (.95 cm) of straight line on both sides of the weld joint and allowing clearance for a weld head which is three inches in diameter and three quarters of an inch wide. In addition to the normal ducting being welded, the inlet valves are welded to the pump inlets and the turbine exhaust plenums are welded to the exit of the turbine housings. The number of in-place welds that have to be performed on the engine assembly will be minimized by including ducting with component sub-assemblies wherever possible. Since all lines and components are welded together, preliminary system orificing will be accomplished by calibration of each of the components before assembly. After final assembly, final calibration of the engine will be done with the hot gas control valves.

Gimbal System. A conventional gimbal system was assumed for the system layout. A simple Hooke type gimbal bearing is incorporated in the top of the injector. The gimbal angle used is $\pm$ 2 degrees (0.035 rad). Actuator attach points have been provided on the engine.

Accessories. The following items are regarded as engine accessories and are not included in the nominal engine system. Gimbal actuators of either electrical or pneumatic design can be provided for the engine. The actuator type and size will depend on gimbal requirements and the detail mission tradeoffs involved with each type. An interpropellant heat exchanger can be used to vaporize FLOX for tank pressurization. The heat exchanger can be either engine or vehicle mounted. Flow meters will be provided in the pump discharge ducts to maintain mixture ratio if it is necessary for throttling.

Component Arrangement

The component arrangement is designed to produce a compact, lightweight, low inertia system while providing maximum accessibility and vehicle compatibility. Propellant losses upstream of the pumps must remain at a minimum to provide high NPSP to the pumps. This means placement of the inlet to the propellant valves in close proximity to the gimbal plane to be compatible with the various types of flexible inlet lines that might be used. The vertical pump orientation was found to best satisfy the above requirements. The pumps are placed as close to the thrust chamber as possible to minimize the acceleration loads imposed on the pumps and the resulting mounting loads imposed on the thrust chamber. The axial location places the propellant inlets in close proximity to the gimbal plane. The circumferential location of the pumps

189

was chosen to give the most compact packaging of components while allowing maximum accessibility for installation and in-place welding.

The thrust chamber acts as the primary engine structural member. The pump mounts and actuator attach points are welded to the thrust chamber. Stress calculations indicate that the hot gas ducting is capable of providing the primary turbopump structural mounts. This mounting technique minimizes the ducting loads associated with solid lines and also eliminates the majority of the pump mount structure. Auxiliary mounts will be employed near the inlet valves to stabilize the pump-valve assembly in the radial and tangential directions.

The inlet valves are structurally mounted on the pump inlets by a short section of duct which is used to smooth the flow from the valve before it enters the pump inducer. The gimbal bearing is integral with the top of the injector which is welded to the thrust chamber. The hot gas control valves are mounted on the top thrust chamber manifold. The components and their respective structural supports are designed to withstand the ducting loads.

Assembly Sequence

The engine will be assembled from the following major components: the thrust chamber, injector, gimbal bearing, valves, turbopumps and ducting. The thrust chamber is the basic structure to which the remainder of the components are attached. The first step is to position and weld the injector to the thrust chamber. The hot gas valves are then welded to the thrust chamber outlet manifold. The turbopumps and their respective inlet valves comprise separate subassemblies. The valve exits are welded

190

to the turbopump inlets. The turbopump valve subassemblies are then attached to the thrust chamber at the pump mounts and held in position by an assembly fixture. The hot gas ducting which forms the major pump mount structure is then fitted and welded in place. The fixtures are then removed. The propellant ducts are then fitted and welded in place. The gimbal bearing is then assembled into the top of the injector.

Cost Reduction Features

In the engine system and component design engine cost was an important consideration. Some of the design features which contribute to lower engine production cost are described in Table 55. Development cost was also an important factor as described in the drive system selection of Task I.

ENGINE WEIGHT SUMMARY

The engine system weight summary is shown in Table 56. The weight reflects the nominal engine design, described in detail in the component sections. As mentioned above, a number of cost reductions involved compromises in engine weight. In the design all components are capable of operation at higher than the nominal chamber pressure for intermittent periods which occur in transient operation or slight-thrust uprating. Injector, valves, thrust chamber inner wall and turbopumps are capable of sustained operation at the 8000-pound (35,600 N) thrust level. The chamber back-up and lines can easily be modified to give the strength needed for sustained operation at uprated conditions.

DRIVE CYCLE POWER BALANCE

Engine system power balances were performed for nominal, throttled and uprated conditions. The engine characteristics at nominal thrust conditions are listed in Table 57. Pressures and temperatures at different locations on the engine are illustrated in Fig. 59.

191

TABLE 55

PRODUCTION COST REDUCTION FEATURES

Thrust Chamber

      Electroform Nickel Construction

      Milled channels

      Step Variation in Channel Width

Injector

      Cast body

      Lower half of gimbal bearing integral with dome

Gimbal Bearing

      Simplified Hooke design

Pumps

      Both impeller stages are the same geometry on the methane pump

System

      All welded construction

      Solid lines

      Line mounted turbopumps

TABLE 56

ENGINE WEIGHT SUMMARY

Description	Dry Weight (lb)	(kg)
Total System	89.8	40.7
Dome-Injector-Gimbal	(11.8)	(5.4)
Combustion Chamber	(7.4)	(3.4)
Cooling Jacket	3.7	1.7
Outer Jacket	1.9	.9
Coolant Outlet Manifold	.2	.1
Mount Ring	1.1	.5
Outriggers	.5	.2
Nozzle	(46.9)	(21.3)
Cooling Jacket	27.3	12.4
Outer Jacket	18.3	8.3
Coolant Inlet Manifold	1.3	.6
Turbopumps	(11.6)	(5.3)
Fuel	6.4	2.9
Oxidizer	4.8	2.2
Mount Provisions	0.4	.2
Valves	(5.4)	(2.4)
Fuel	1.2	.5
Oxidizer	2.4	1.1
Hot Gas, Turbine Control	0.9	.4
Hot Gas, Turbine Bypass	0.9	.4
Ducting	(1.2)	(.5)
Controls	(5.5)	(2.5)

TABLE 57

NOMINAL ENGINE BALANCES

Thrust, lb (N)	5000	(22,200)
Engine Specific Impulse, sec (N-sec/kg)	399.2	(3912)
Engine Mixture Ratio, O/F	5.25	
Thrust Chamber		
Chamber Pressure, psia (k N/m^2)	500	(3450)
Mixture Ratio, O/F	5.25	
Weight Flow, lb/sec (kg/sec)	12.52	(5.65)
Specific Impulse, sec (N-sec/kg)	399.2	(3912)
Exit Temperature, R (K)	1305	(720)
Expansion Ratio	60	
Pumps, O/F		
Flow, lb/sec (kg/sec)	10.52/2.00	(4.75/0.9)
Discharge Pressure, psia (k N/m^2)	699/1269	(4610/8700)
Number of Stages	1/2	
Speed, 1000 rpm (1000 rad/sec)	39.1/67.2	(4.08/7.0)
Horsepower (kw)	27.9/42.0	(20.8/31.3)
Efficiency, percent	71.0/61.8	
Turbine, O/F		
Flow, lb/sec (kg/sec)	0.74/0.85	(0.34/0.39)
Inlet Temperature, R (K)	1300	(720)
Pressure Ratio	1.40/1.46	
Exit Pressure, psia (k N/m^2)	673	(4610)
Number of Stages	1/1	
Efficiency, percent	49.7/58.8	
Bypass, lb/sec (kg/sec)	0.42	(0.19)

FLOX

Methane

P = 50 (340)

P = 80 (550)

(4610)   P = 669
(5)   Ẇ = 10.52

Ẇ = .74(.34)

P = 976 (6730)

Ẇ = .85(.39)

P = 1269 (8750)
Ẇ = 2.00 (0.9)

P = 939 (6470)
T = 1300 (722)

P = 976 (6730)
T = 1300 (722)

P = 673 (4640)
T = 1269 (705)

P = 673 ( )
T = 1259 (699)

P = 612 (4220)
T = 170 (94)

Ẇ = .42 (.19)

P = 647
(4460)

P = 1014 (6990)
T = 1305 (725)

P = psia (k N/m²)

T = °R (k)

Ẇ = lb/sec(kg/sec)

P = 1244 (8580)
T = 245 (136)
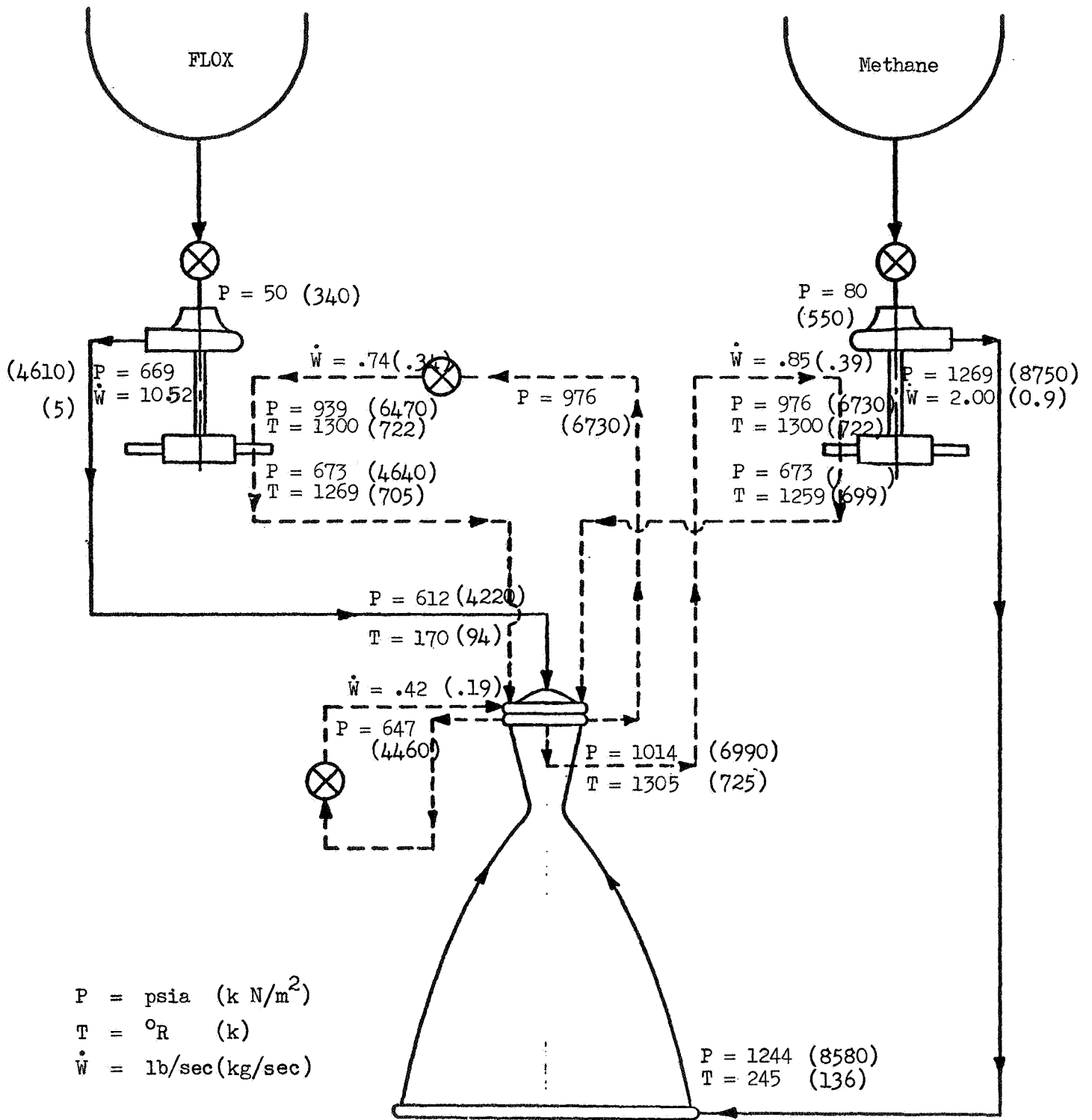
Fig. 59 . Nominal Engine Operating Conditions

195

Engine specific impulse is based upon 94-percent specific impulse efficiency at full thrust. Prediction of the performance potential of the engine based on data from NASw-1229 and NAS3-11191 indicate potential specific impulse values significantly above 400 seconds (3920N-sec/kg) at **nominal thrust.**

Engine System Perturbations

The dual turbine arrangement and the engine power margin provide considerable operational flexibility. This is further illustrated in the following examples of variations in engine inlet conditions and design values.

Engine operation over a range of mixture ratios is shown in Fig. 60. At lower mixture ratios, there is more methane to be pumped and the turbine inlet temperature is lower. A higher pump speed and discharge pressure is required as is indicated.

The nominal engine design is based upon temperatures which might be expected at the end of flight (Ref. 13). These temperatures, where propellant density is lowest, require the greatest amount of pump power. As the propellant inlet temperatures decrease, the propellant density increases and pump power requirement diminishes. With the decrease in methane temperature, turbine inlet temperature is also diminished. The net results of these temperature variations are shown in Fig. 61 to 63. Fig. 61 and 62 illustrate individual propellant temperature effects; Fig. 63 shows the combined effect.

Inlet pressures to the pumps were selected based upon studies from Ref. 13 and in Task I. A variation in these pressures has little effect on the engine power balance at full thrust.

196
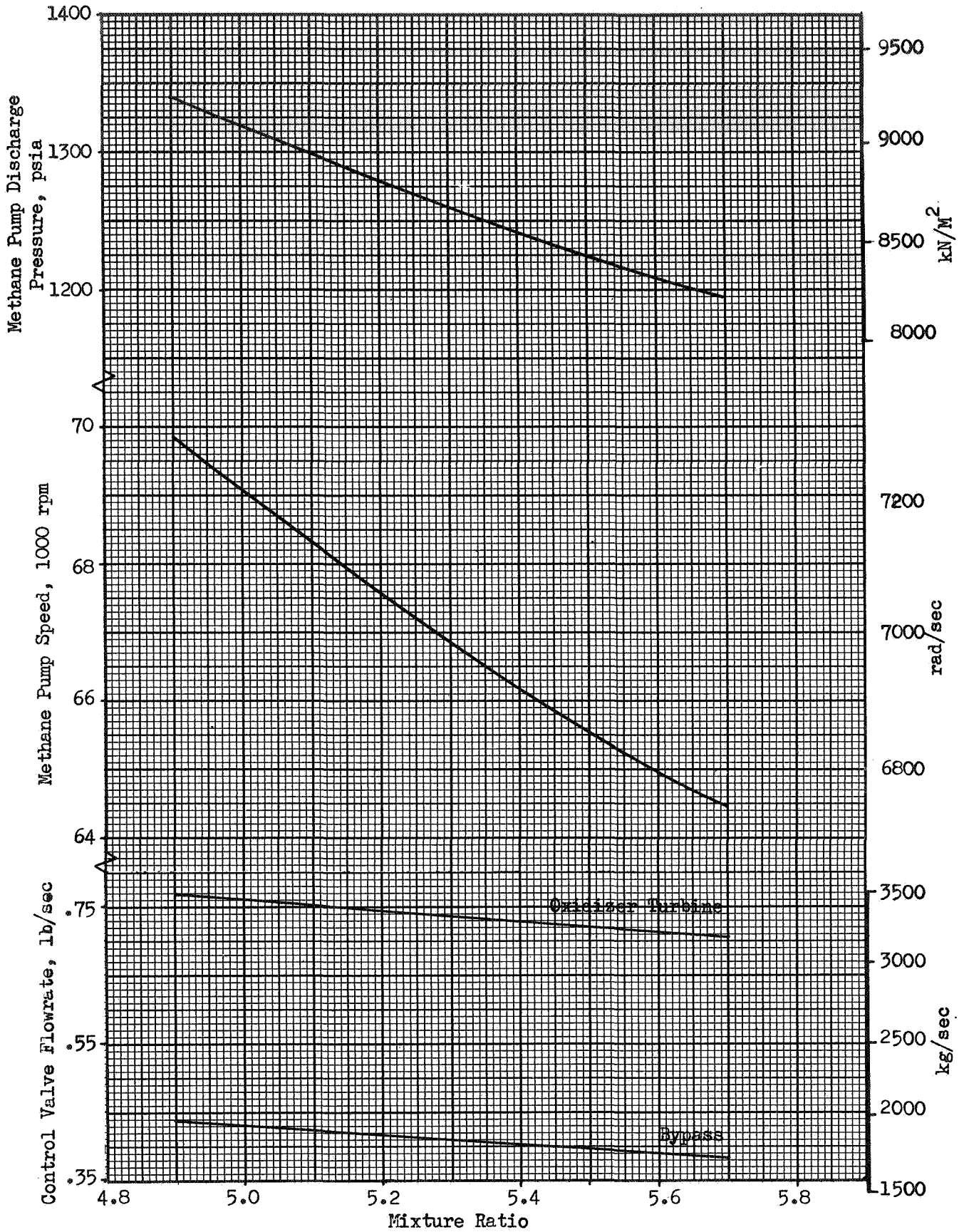
Fig. 60. Effect of Mixture Ratio Variation on Cycle Operation at
Full Thrust
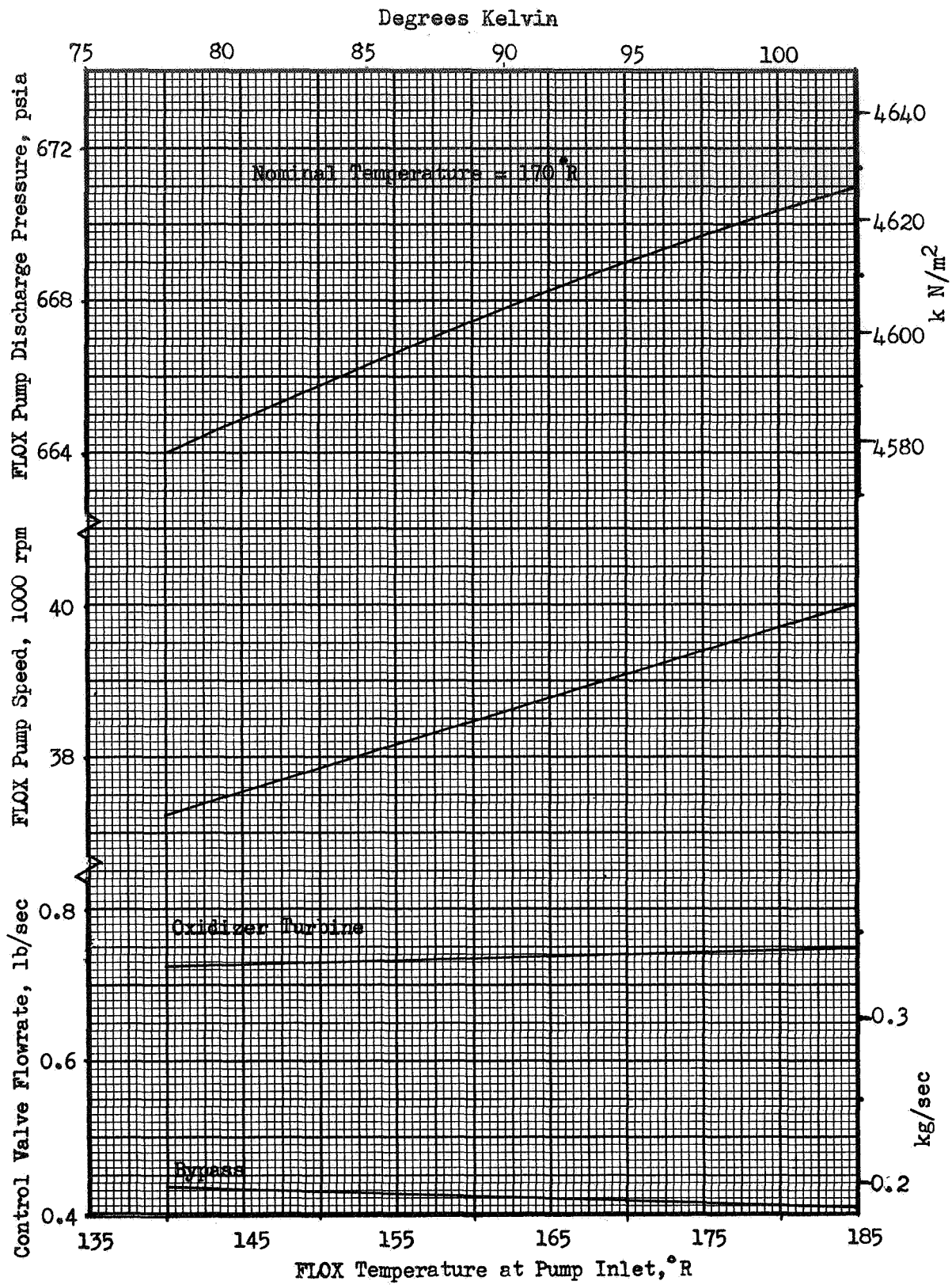
Fig. 61. Effect of FLOX Temperature on Cycle Operation at Full Thrust

198
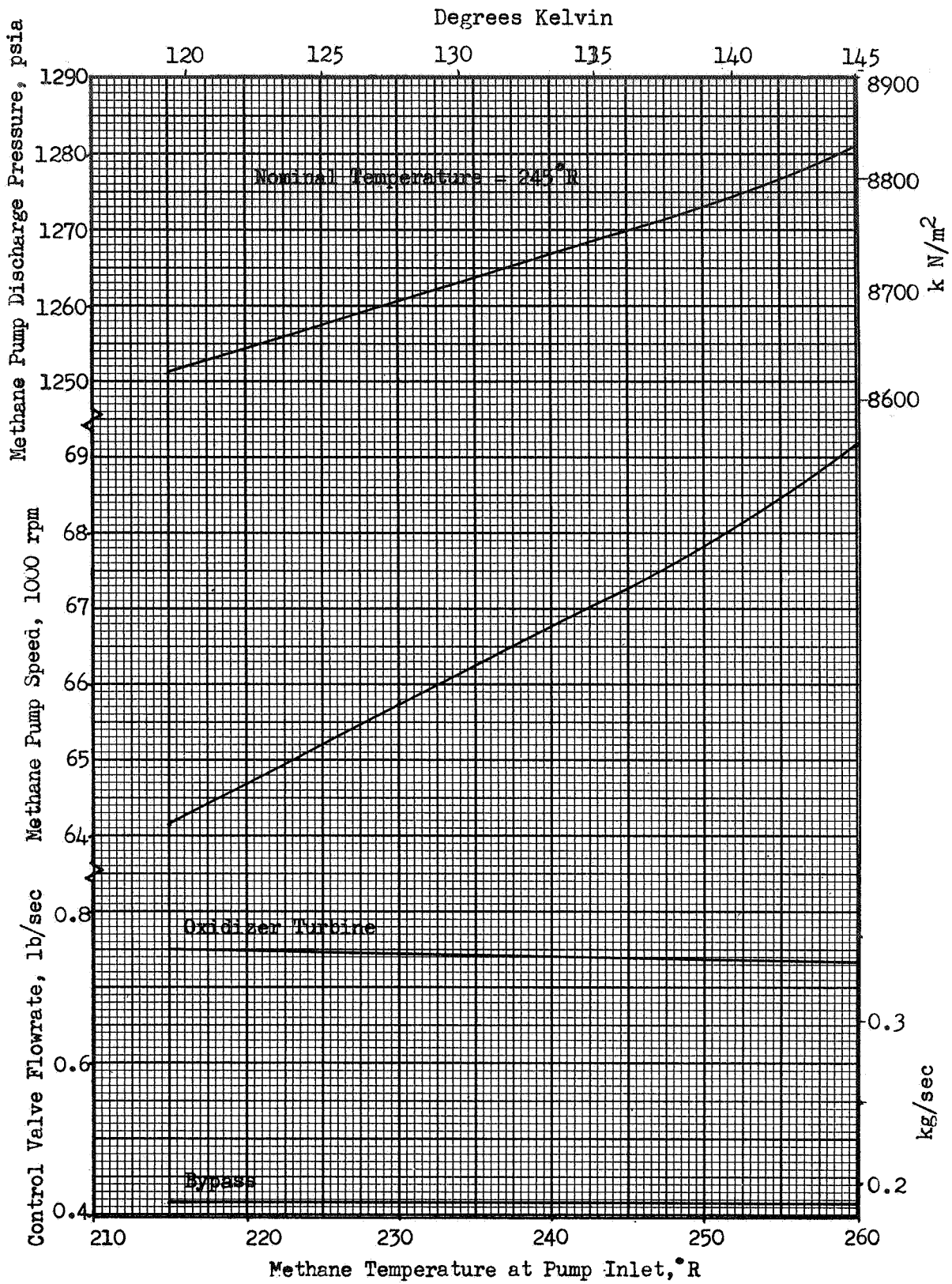
Fig. 62 . Effect of Methane Temperature on Cycle Operation at Full Thrust
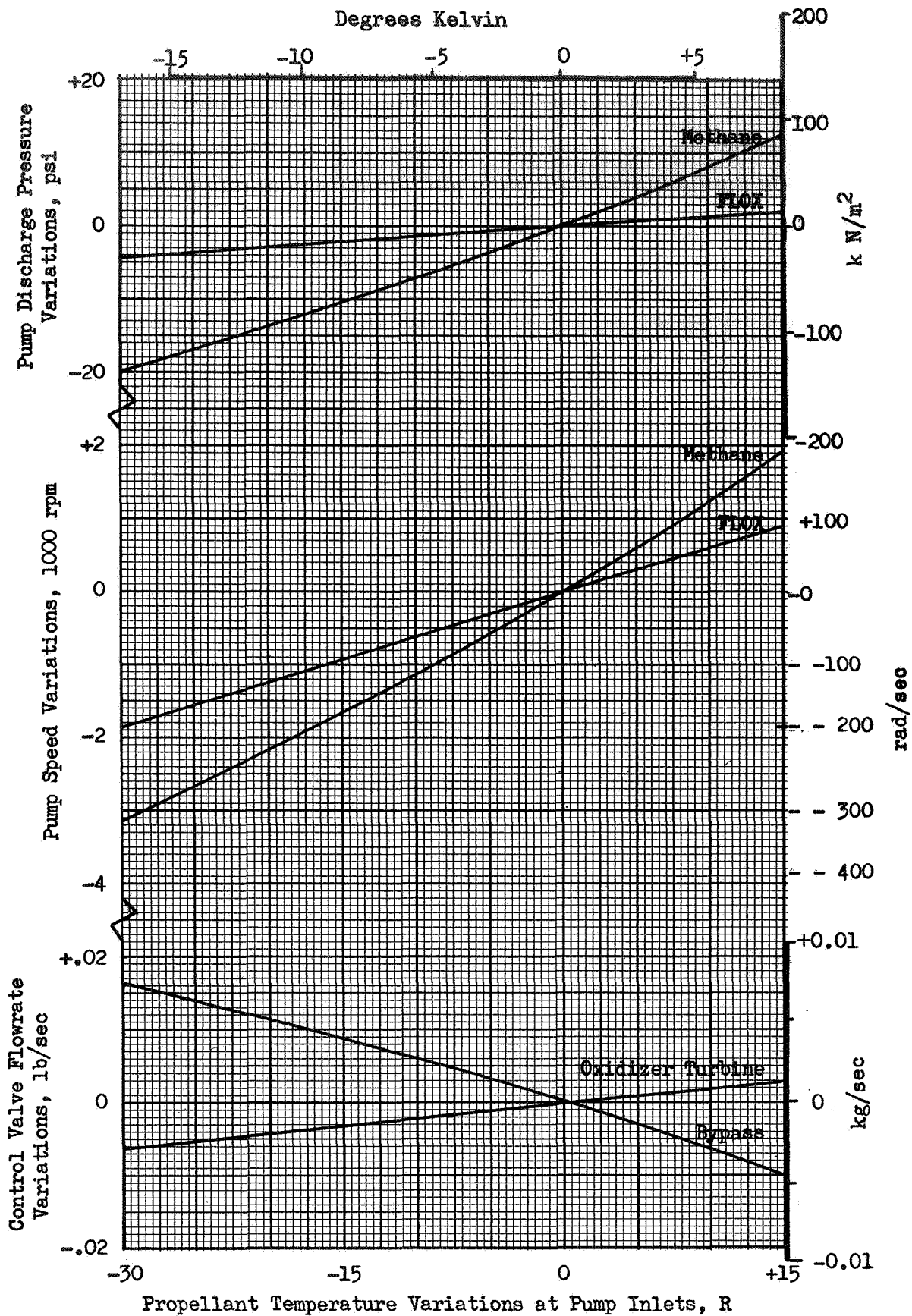
Fig. 63. Effect of Propellant Temperature Variations on Cycle Operation at Full Thrust

In the course of engine development, engine design parameters (pressure drops, temperatures, etc.) may change. The effects of some of these variations on nominal thrust operation are shown in Fig. 64 to 66. Turbine inlet temperature, system pressure drop, and turbomachinery efficiency variations are considered. As can be seen in these and the engine uprating section, the engine has sufficient power margin to assure satisfactory operation.

ENGINE PERFORMANCE UPRATING

Engine performance can be improved both through specific impulse increases and through weight reduction.

Specific Impulse Increases

The specific impulse used for the nominal thrust level performance is based on 94-percent of theoretical specific impulse for 82.6-percent F_2 - 17.4-percent O_2 with methane. Some specific impulse improvements are listed below.

(a) Test Results - Reduction of nozzle performance data of NASw-1229 and the injector performance of NAS3-11191(Ref. 3, 1) to operating conditions of the present engine indicate several seconds increase in specific impulse over the current value.

(b) Higher Expansion Ratio Nozzle - Use of a higher expansion ratio nozzle or attachment could increase specific impulse 1-1.2 percent.

201
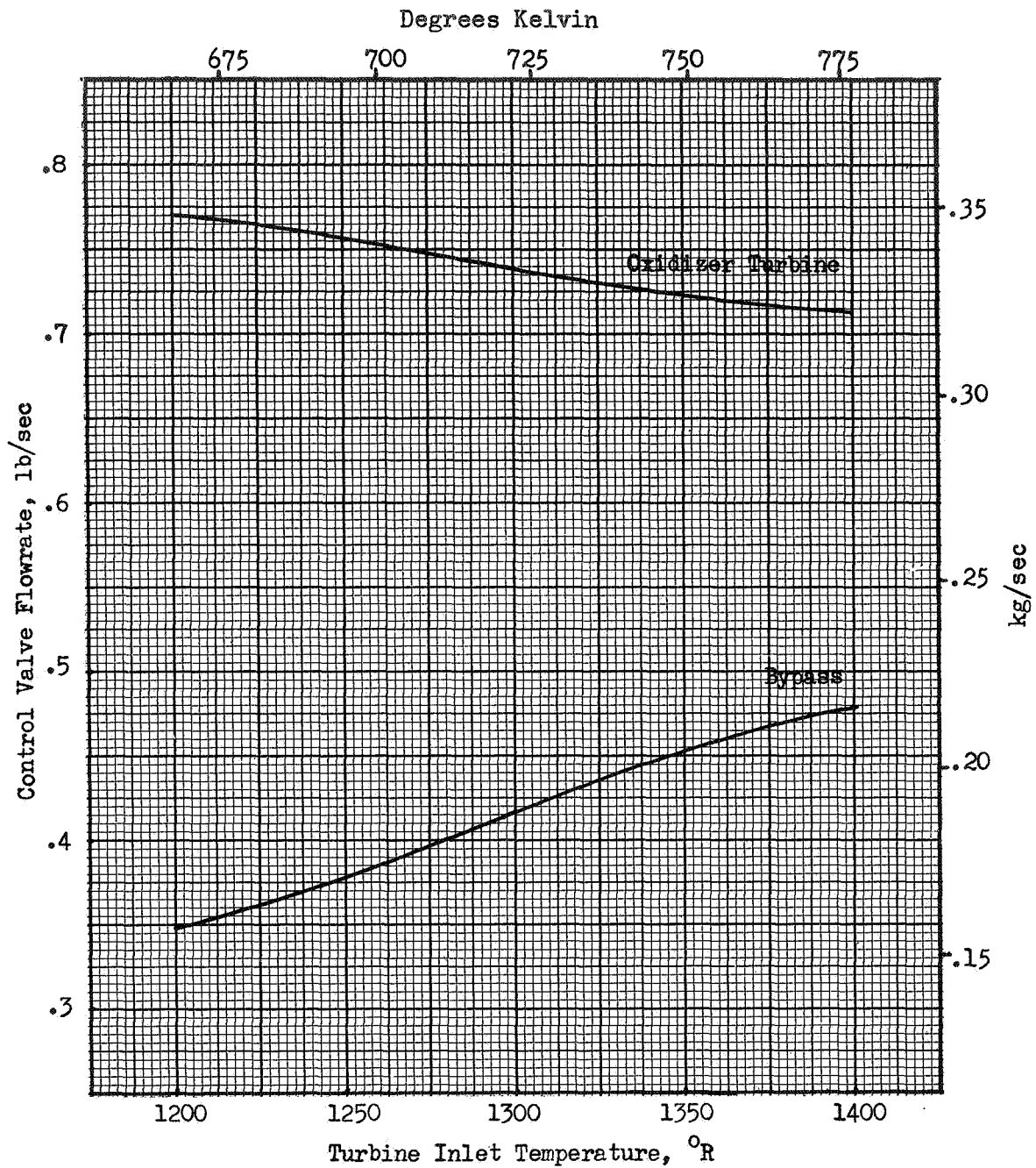
Fig. 64. Effect of Turbine Inlet Temperature on Cycle Operation at Full Thrust
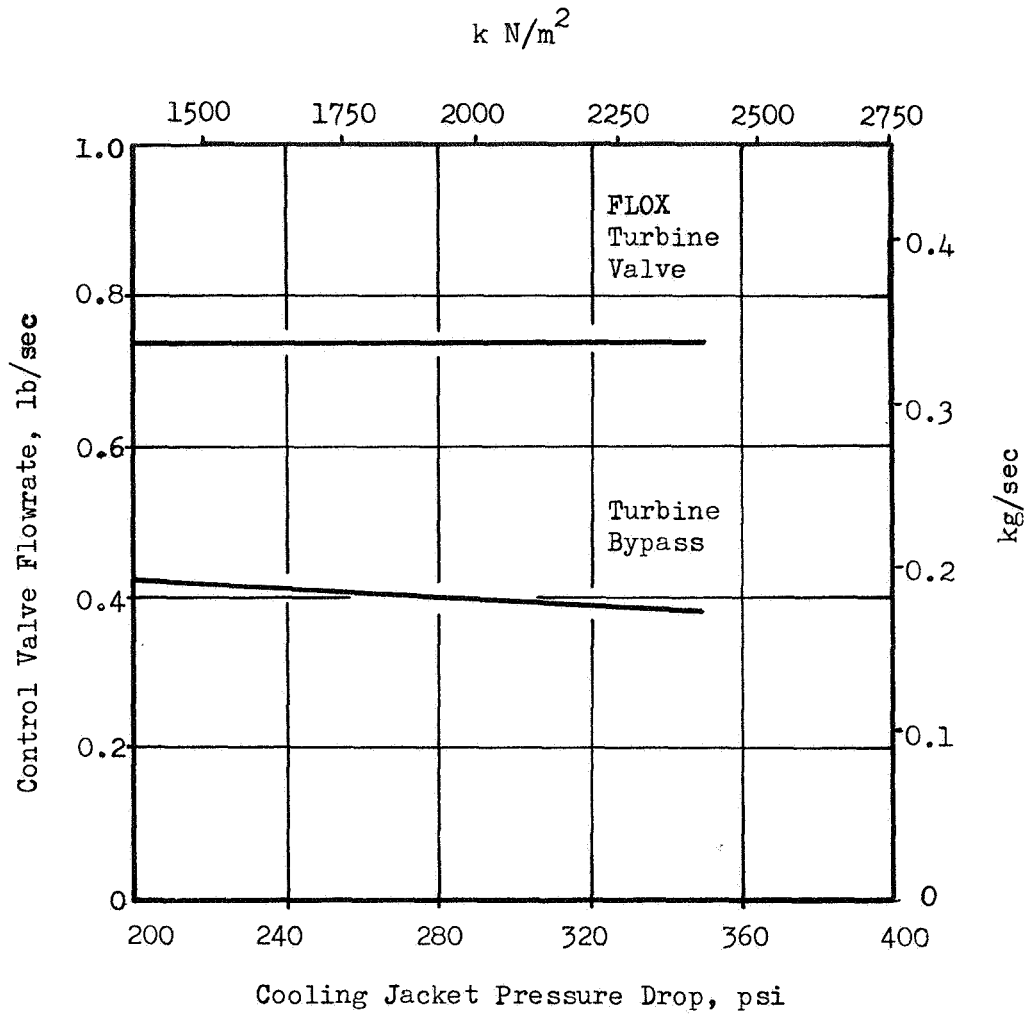
Figure   65.   Effect of Cooling Jacket Pressure Drop
on Nominal Engine Balance.
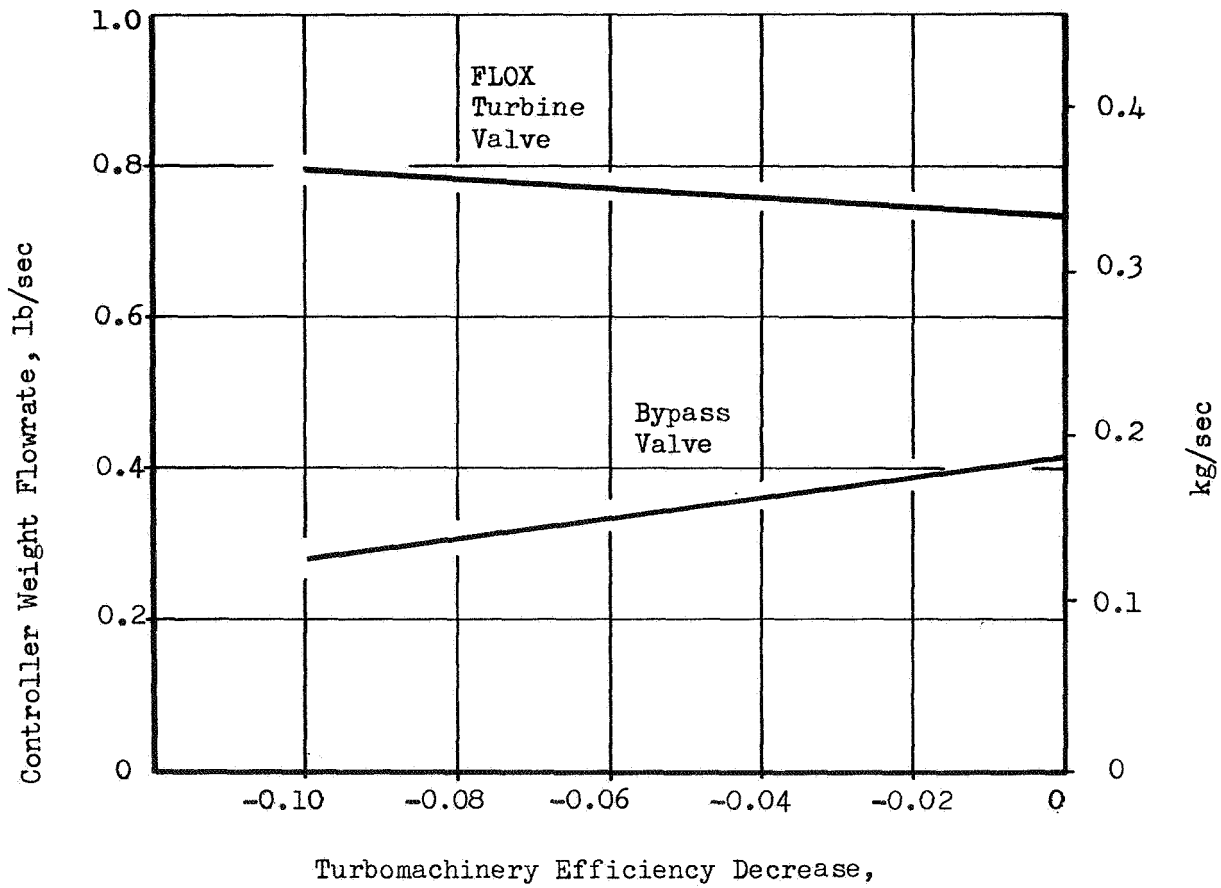
Figure 66. Effect of Turbomachinery Efficiency on Engine
Operation at Nominal Thrust.

Weight Reduction

Several areas in which engine weight reduction is possible are described below. Some of these would involve potential cost increase or operational restrictions which would necessitate more detailed evaluation.

The largest single weight item in the engine is the milled channel nozzle which accounts for over half the engine weight. Thrust chamber weight reduction can be accomplished by

(a) Channel Geometry Modification - Use of additional steps or continuous variation in channel width.

(b) Channel Number Variation - Use of blind channels or a change in channel number.

(c) Alternate Nozzle Construction - Use of tubes with electroform backup or radiation-cooled construction for the nozzle. Higher strength nozzle materials.

(d) Combustor Backup - Wire wrap and electroform to provide composite material backup.

(e) Manifold Refinement - Variable cross-section and wall thickness in the manifold.

The weight savings with any of the first three items could be 10 - 20 pounds (4.5 -9kg) With the last items weight reduction of about 1-pound (0.5kg) could be accomplished.

Other areas of weight reduction are possible but the reductions potential is not as great as in the thrust chamber. One method would be through stressing for the 5000-pound (22200N) thrust operation only. This could reduce weight by several pounds.

ENGINE/VEHICLE INTERFACE

Interface connections between the engine and the vehicle are described.
Three mechanical connections are necessary: the thrust mount and the
two gimbal actuators. Five fluid interfaces are shown, all involving
welded connections. The main propellant lines are low-pressure, low-
temperature lines which contain liquid propellant throughout the mission.
In addition to the pressure forces, they must sustain forces from thermal
expansion of engine lines during firing as well as forces from gimballing
of the engine. The pressurant lines are at higher temperatures and
pressures, the actual values being determined by the propellant tank re-
quirements. Gaseous propellant is contained only during engine operation.
A single pneumatic interface is required to provide for pump seal purge,
for FLOX line purge, and for valve actuation. This line is at high pressure
but low temperature. Isolation valves are located on the vehicle so this
line may contain gas only during engine operation.

Two electrical interfaces are required: one is for electrical power to
actuate the solenoid valves which control the pneumatics; the second elec-
trical interface is for command signals from the vehicle to the engine.

ENGINE OPERATION

Engine operational features were investigated to provide a description of engine characteristics at other than nominal conditions. Some of these engine features are listed in Table 58. From these characteristics engine control requirements were defined.

ENGINE START

Engine start operation was investigated to describe engine transient character-istics during the start phase. Two types of start, both using fuel lead were considered. In the first type, the fuel turbine is allowed to rotate during fuel side priming while the oxidizer turbine inlet valve is closed. Because the fuel turbine delivers power to the fuel pump, pump head is developed during this early phase of start and contributes to the rapid thermal conditioning of the pump. Following fuel prime, power is introduced to the oxidizer pump and pump-fed operation begins. In the second type of start, energy to both turbines may be restricted. Oxidizer is introduced following fuel priming, and the engine operates in a pressure-fed mode. This "idle mode" operation can be used for propellant settling, low-thrust maneuvers, and to provide an energy source for engine start where thrust chamber temperature is low. After a specified time of idle mode operation, power is introduced to the turbines and pump-fed operation is initiated.

Another variation exists for both the above start types; namely, powered idle mode used for low-thrust maneuvers and with an autogenous pressurization system. This mode of operation is at an intermediate thrust level with the pumps powered and is very similar to starting the engine at throttled conditions. With completely autogenous pressurization, pump operation with two-phase fluids may be necessary in the early portion of the pump-fed idle-mode when the tank pressure is building up.

TABLE 58

ENGINE FEATURES

- Engine Start

    1. Tank Head

    2. Minimum Preconditioning

    3. Minimum Controls/Sensors

    4. Range of Initial Temperatures

    5. Quick Restart

- Pressure-Fed Idle Mode

- Engine Cutoff

    1. Consistent Impulse

    2. Simple Sequence

- 10/1 Throttling

    1. Minimum Controls

- Engine Thrust Uprating

    1. No Performance Loss

    2. Small Hardware Modification

- Self-pressurization

Engine Start Conditions

Engine start investigation was directed toward determining a common start sequence for three initial hardware temperatures:

Description	Temperature, R (K)	
	Pump and Ducting	Thrust Chamber
Quick Restart	250 (140)	From Cutoff Analysis
Thermal Equilibrium		
Engine Facing Sun	530 (295)	530 (295)
Engine Away from Sun	250 (140)	250 (140)

A sequence designed to these extreme conditions would allow the engine to start under any foreseen initial engine thermal condition or vehicle orientation.

To provide maximum simplicity in the start sequence, a common sequence was devised for the entire range of initial conditions. Only pressure sensors and timers were used to control the start. The addition of temperature sensors or preflight knowledge of the vehicle orientation would allow design of the start sequence for more restrictive initial conditions with possible reduction in start times. An unrestricted start sequence was felt to be desirable at the present time.

For these start investigations, liquid or low quality propellants were defined to be available at the inlets to the main valves with the engine completely unprimed. This assumes that the propellants have either been settled or that a propellant "trap" is used in the propellant tanks. Sufficient NPSH is assumed to be available at the pump inlets to allow operation at all thrust levels. The engine start sequence is defined to allow start to any thrust level. These areas are discussed in subsequent sections.

Engine Start Analysis

Start and cutoff transient operation was analyzed with a mathematical model to simulate the low-frequency dynamic behavior of the engine. This available model was modified to represent the FLOX/methane expander cycle under investigation.

Studies were conducted by changing an independent variable (e.g., orifice diameter, valve sequencing time), computing the values of the dependent variables (e.g., pump speeds, pressures, flows), and then comparing the computed independent variables to previous solutions or to absolute requirements. In this sense, the mathematical model is used like a physical engine where optimization is achieved through a trial-and-error procedure. This modeling technique has been successfully used on F-1, J-2 and SDI programs to model start and cutoff transients, and also to model the low-frequency cooling tube oscillations which result from two-phase flow through the thrust chamber cooling tubes.

Based upon the detailed energy balances from Task I, nominal flows, pressure drops, and temperatures were defined and incorporated into the model along with the defined engine characteristics. From the initial engine system design layout, duct and manifold volumes were specified. Preliminary pump descriptions were used to estimate flow volumes, rotating hardware inertias and breakaway torque. Flow passages in both the thrust chamber and pump were defined to allow for heat transfer during the thermal conditioning and start operation.

With this specific engine description, start and cutoff operation of the engine system was investigated. Control sequences were varied until start and cutoff were achieved with no indications of potential hardware damage, and the actuation requirements reflected reasonable control design. Emphasis was placed on obtaining reasonable, safe starts rather than minimum start time.

Direct Start

For the direct engine start in which fuel turbine power is unrestricted, a common engine start sequence has been devised for the three initial engine temperatures. For the higher values of initial thrust chamber temperature, start times to

210

90-percent full thrust, were 2 to 3.5 seconds. Following introduction of power to the FLOX turbine, the thrust buildup was very rapid and proper valve sequencing was necessary to avoid pressure overshoots. For the low temperature start, very little energy is available from residual heat in the hardware. In addition, a considerable decrease in methane density occurs in the cooling jacket when combustion begins and heat is transferred to the walls. Because of this density decrease, the methane velocity in the cooling jacket is reduced and excessive wall temperatures may be encountered. A start from the low-temperature conditions was achieved without excessive wall temperature. The start time was approximately 6 seconds (90 percent of full thrust).

Start Sequence. All starts were made with the pumps and ducting unprimed. Thus the start sequence was designed to allow for thermal conditioning and priming of the pumps and ducting. Thermal conditioning of the fuel side is slow relative to the oxidizer side due to the resistance to flow of the thrust chamber channels. To avoid high mixture ratio during start, the fuel pump was given time to prime before oxidizer was admitted into the thrust chamber. To start the engine under these three conditions without knowledge at time of engine start of the actual thermal condition of the engine, the sequence described in Fig. 67 was chosen. Two pressure switches were used to signal the completion of each phase of engine start--fuel pump prime and oxidizer side prime.

At engine start, the main fuel valve is opened full and the turbine bypass valve is opened to 200 percent of mainstage position. These positions are held until the fuel pump and high pressure ducting are primed. A pressure switch monitoring fuel pump discharge pressure and set to trigger at 200 psia (1380 kN/M^2) was used to indicate fuel side prime. When the fuel pressure switch signals fuel prime, the oxidizer prevalve is opened full and the oxidizer turbine control valve is opened to 8 percent of the mainstage position. Again, all positions are held until the oxidizer side primes. This condition is signalled by a pressure switch set to trigger at oxidizer injector manifold pressure of 60 psia (415 kN/M^2)when the oxidizer side has primed, both the turbine bypass valve and the oxidizer control valve are ramped to their mainstage positions.

Start Signal

Main Fuel Valve

Turbine Bypass Valve

Fuel Pump Discharge Sensor

Oxidizer Turbine Valve

Main Oxidizer Valve

Oxidizer Injector Manifold Sensor

200 psia (1380 k N/m^2)

60 psia (415 k N/m^2)

Time
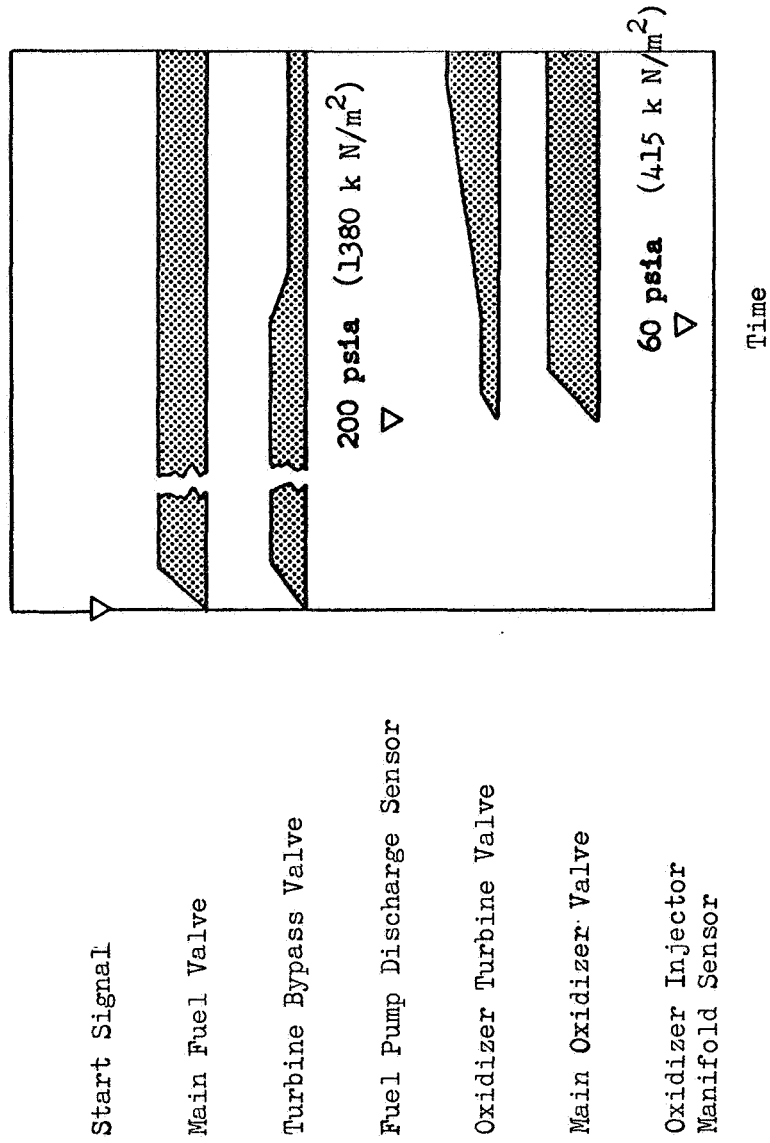
Figure 67 . Engine Start Sequence, Direct Start.

Because of the hypergolicity of the propellants an inert gas purge of the FLOX line will probably be necessary during priming of the methane side. This feature would be included in the development engine. The possibility of eliminating this purge would be determined at that time in the light of experimental data. This purge would be upstream of the FLOX turbine and is identical to the shutdown purge described in the following section.

Valve Positions. Valve positions are shown in Fig.68-70. The initial position of the oxidizer turbine control valve (8 percent of full open) was chosen to prevent excessive oxidizer pump speed before oxidizer prime (possible damage to oxidizer pump) and also to prevent a hard oxidizer prime (possible high main chamber pressure spike and mixture ratio overshoot).

The initial position of the turbine bypass valve was based upon a compromise between two of the start conditions. The immediate restart condition provides excess energy to the turbines during the start (possible turbopump overspeed), while the cold start is a very low energy start. To reduce the energy of the immediate restart and to prevent turbopump overspeeds, and yet not to reduce the energy of the cold start to such an extent that an excessive amount of time would be required, an initial bypass valve position of 200 percent of mainstage was chosen.

During the first phase of a cold start, the thrust chamber channels fill with liquid methane due to the very cold temperature of the thrust chamber. A rapid increase in heat flux to the chamber occurring when oxidizer is admitted can cause a rapid change in methane density. The resultant increase in pressure can possibly cause a local stoppage of coolant flow and damage to the chamber. To prevent this, the oxidizer turbine valve is ramped to mainstage slowly (500 ms) while the turbine bypass valve is ramped to mainstage rapidly (100 ms) to maintain power to the fuel turbine.

Transient Operation. Start transients for the three initial conditions are illustrated in Fig. 71 to 78. These starts are based upon main valve inlet pressure of 80 and 60 psia (550 and 414 kN/M^2) for the methane and FLOX, respectively.
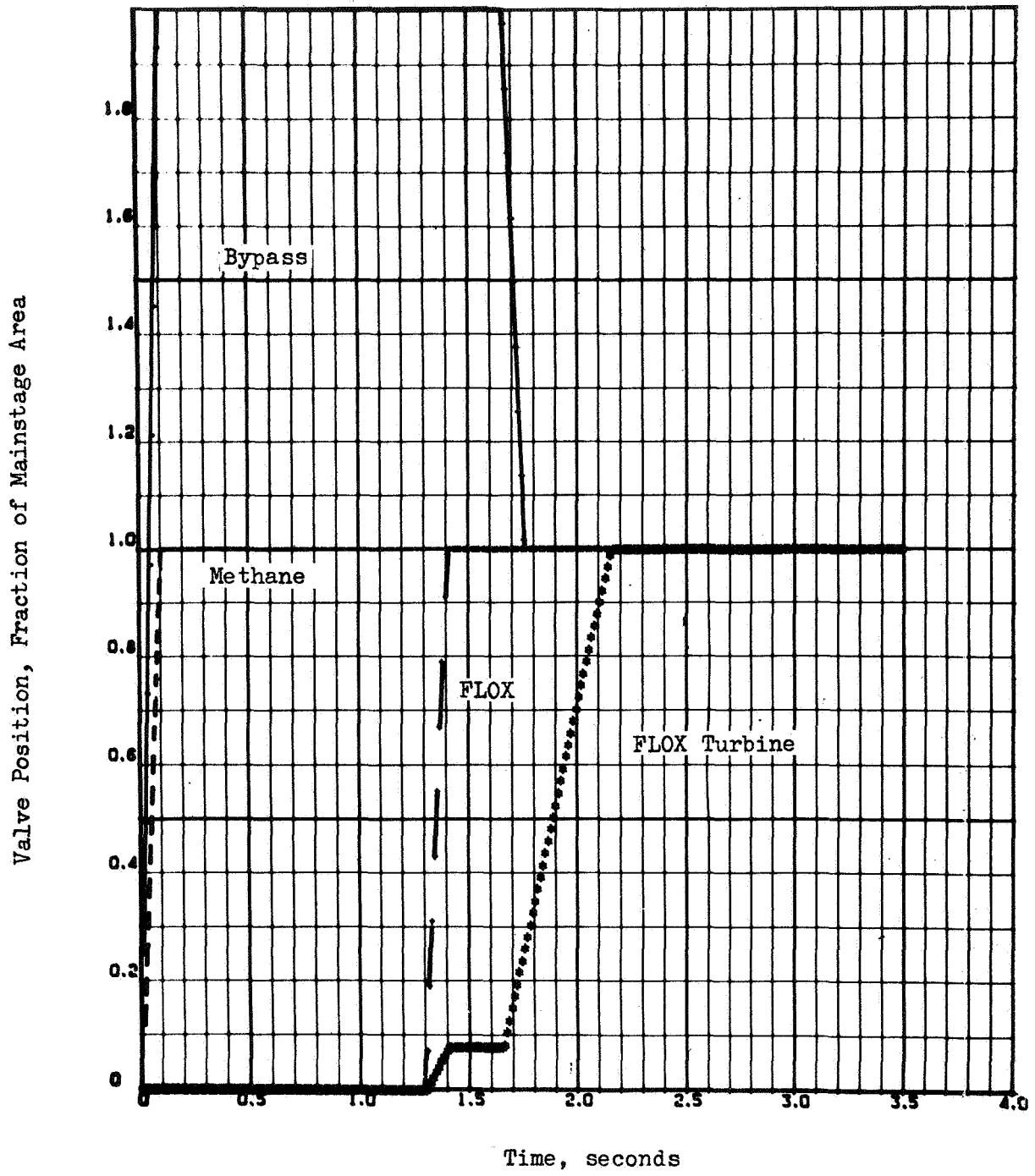
Figure 68 . Valve Positions vs Time for the Immediate Restart.
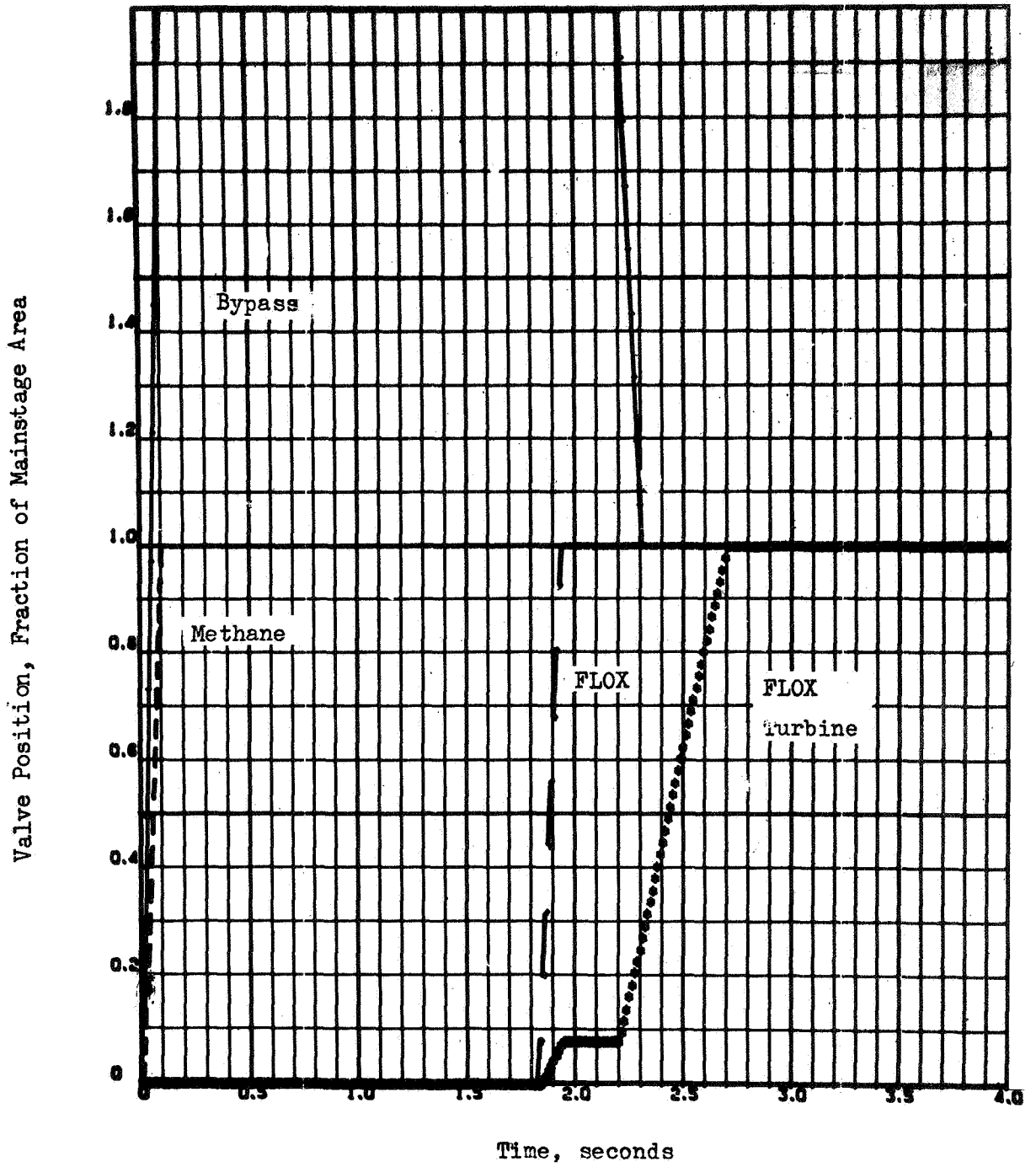
Figure 69 . Valve Positions vs Time for the Ambient Engine Start.

215
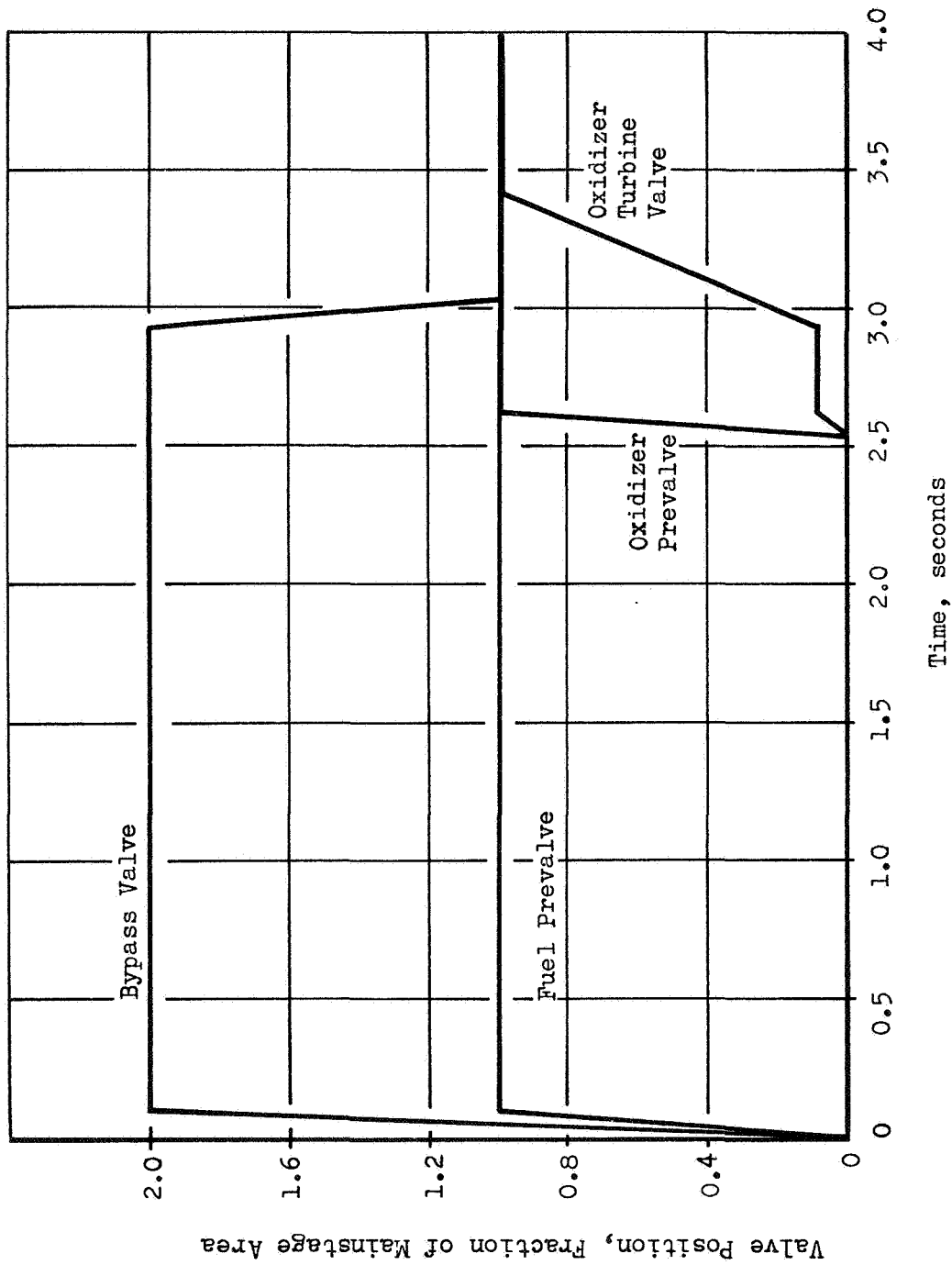
Figure 70. Valve Positions vs Time for the Cold Start (250 R, 140 k)

216
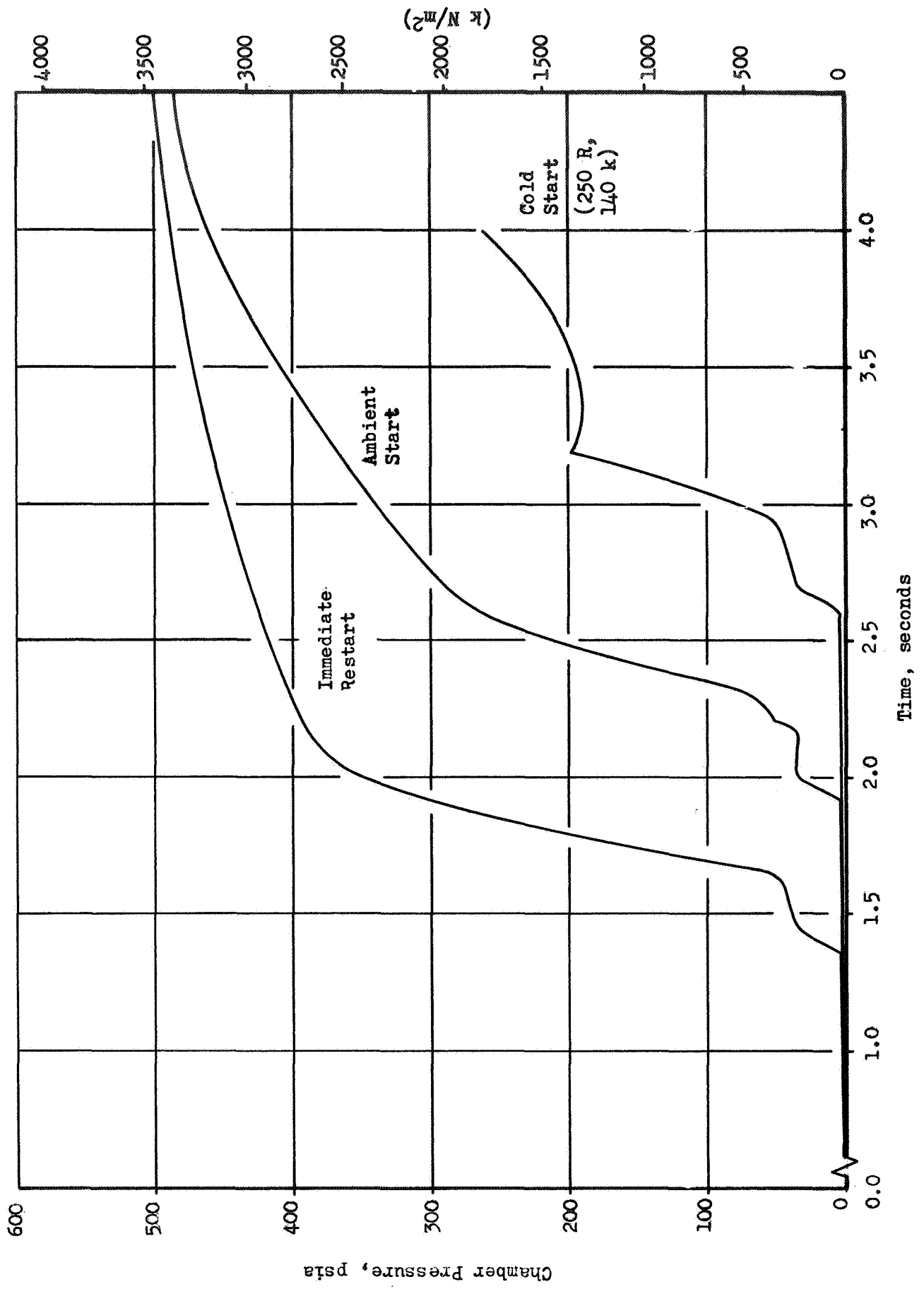
Figure 71. Chamber Pressure Transient

217
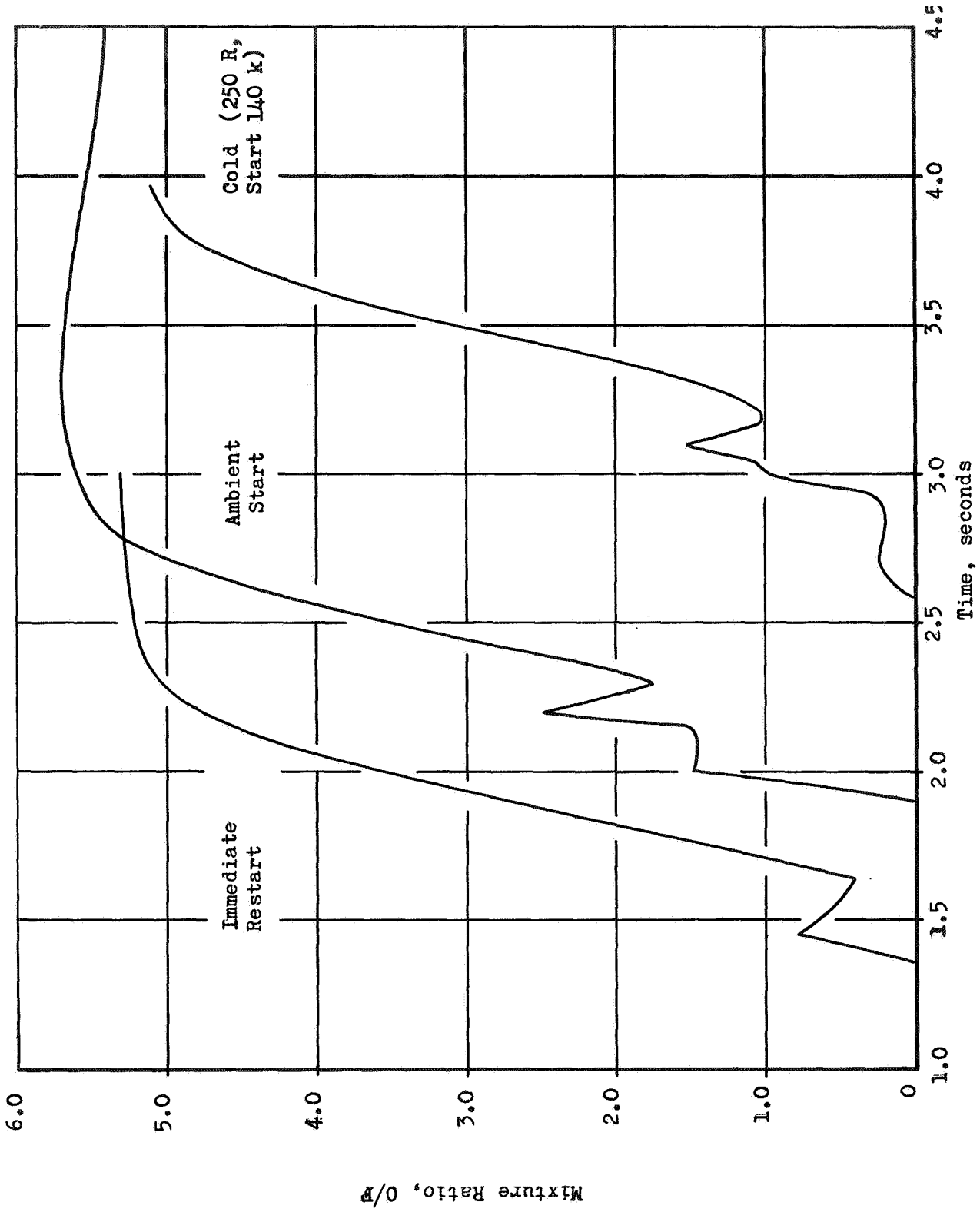
Figure 72. Thrust Chamber Mixture Ratio Transient

218
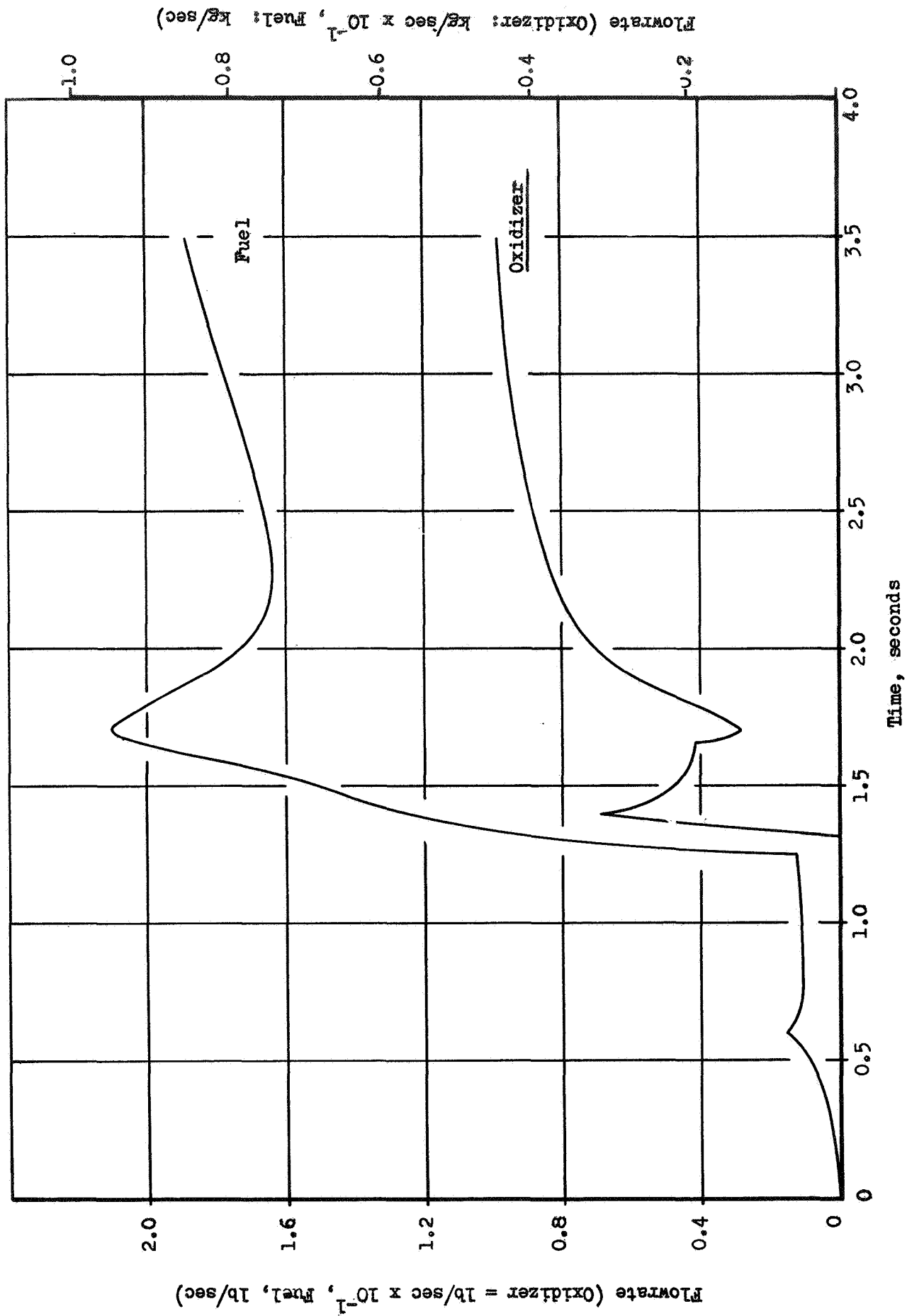
Figure 73. Main Propellant Flowrates for the Immediate Restart.
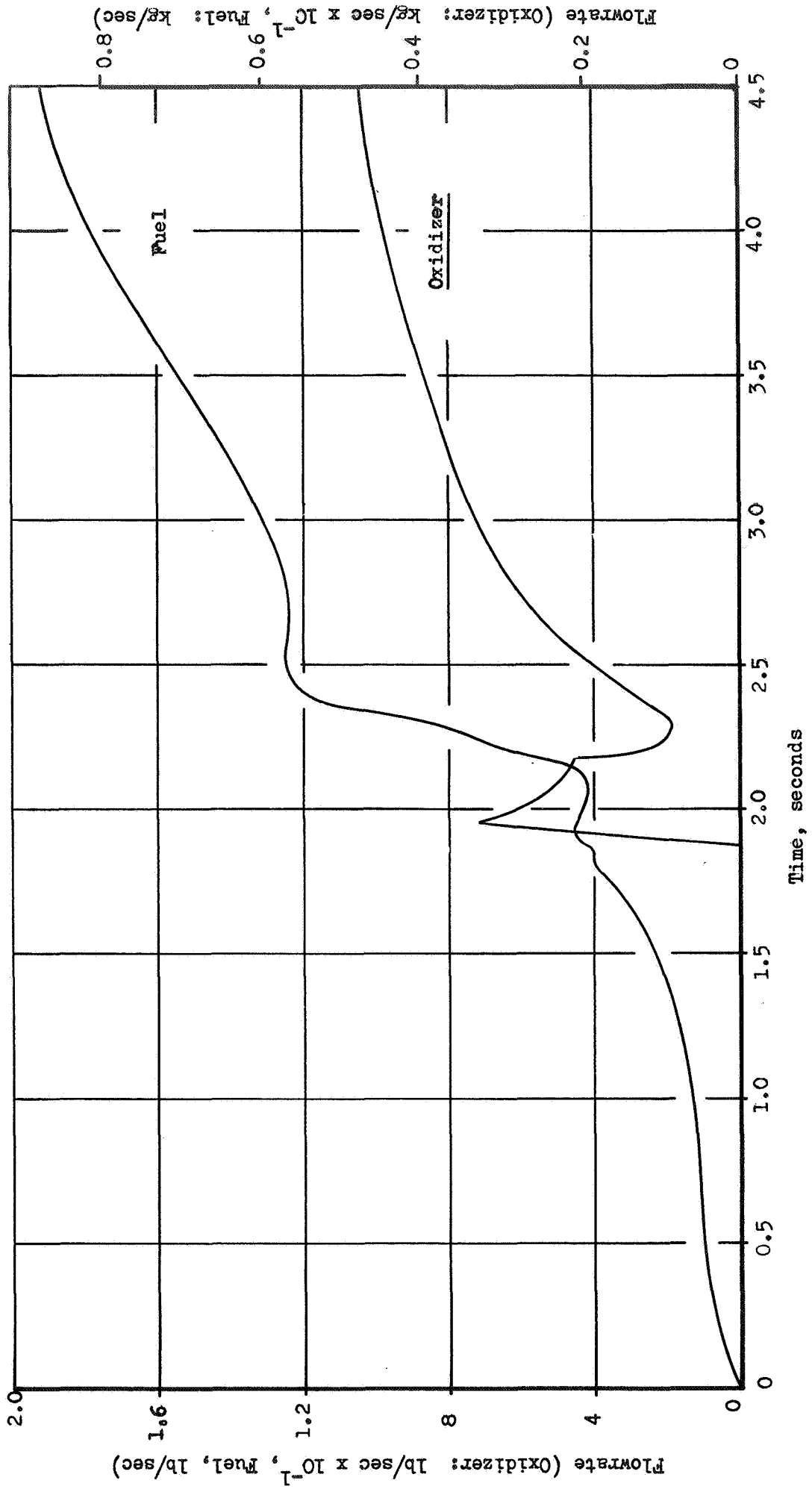
Figure 74. Main Propellant Flowrates for the Ambient Start.
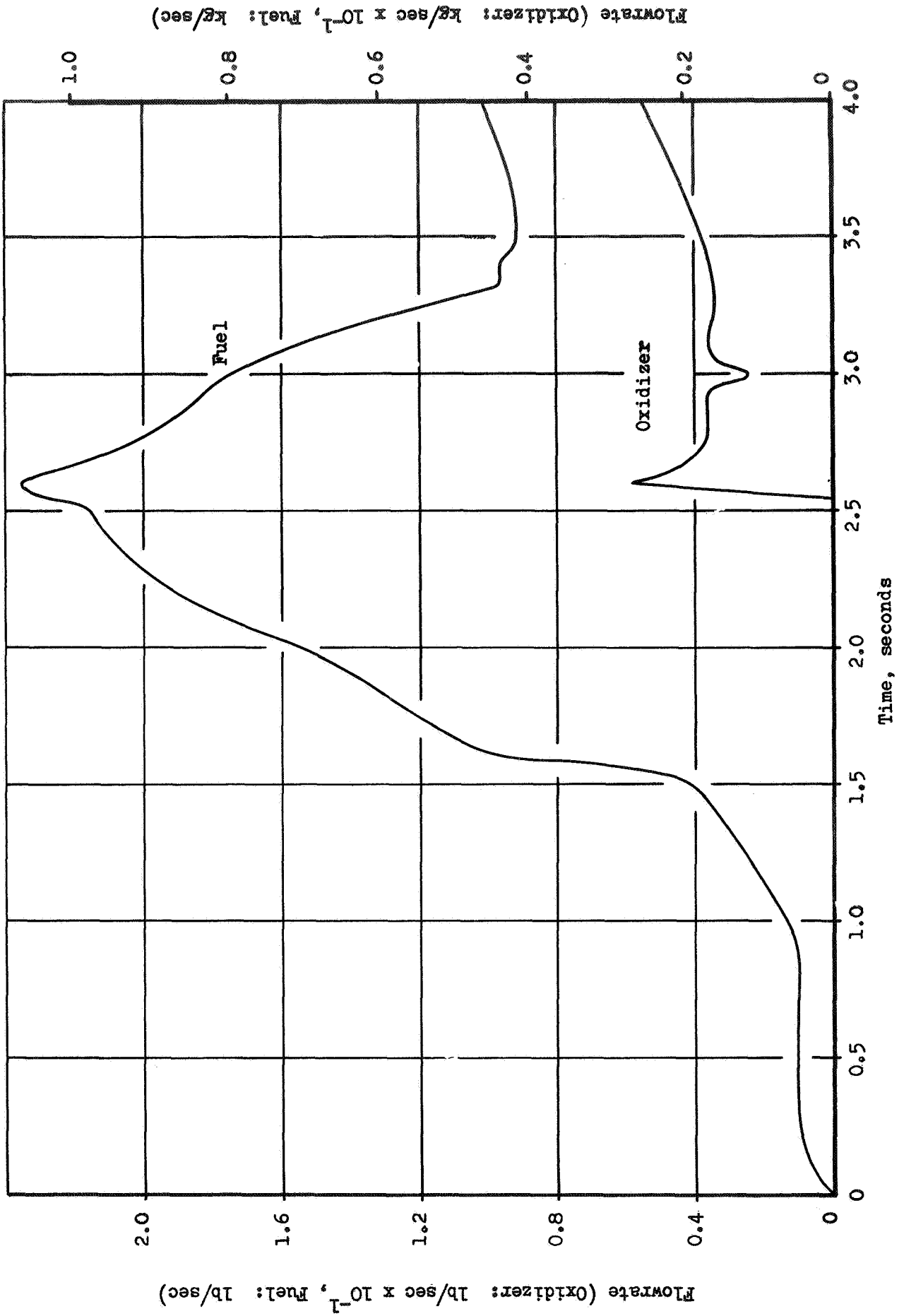
Figure 75 . Main Propellant Flowrates for the Cold Start.
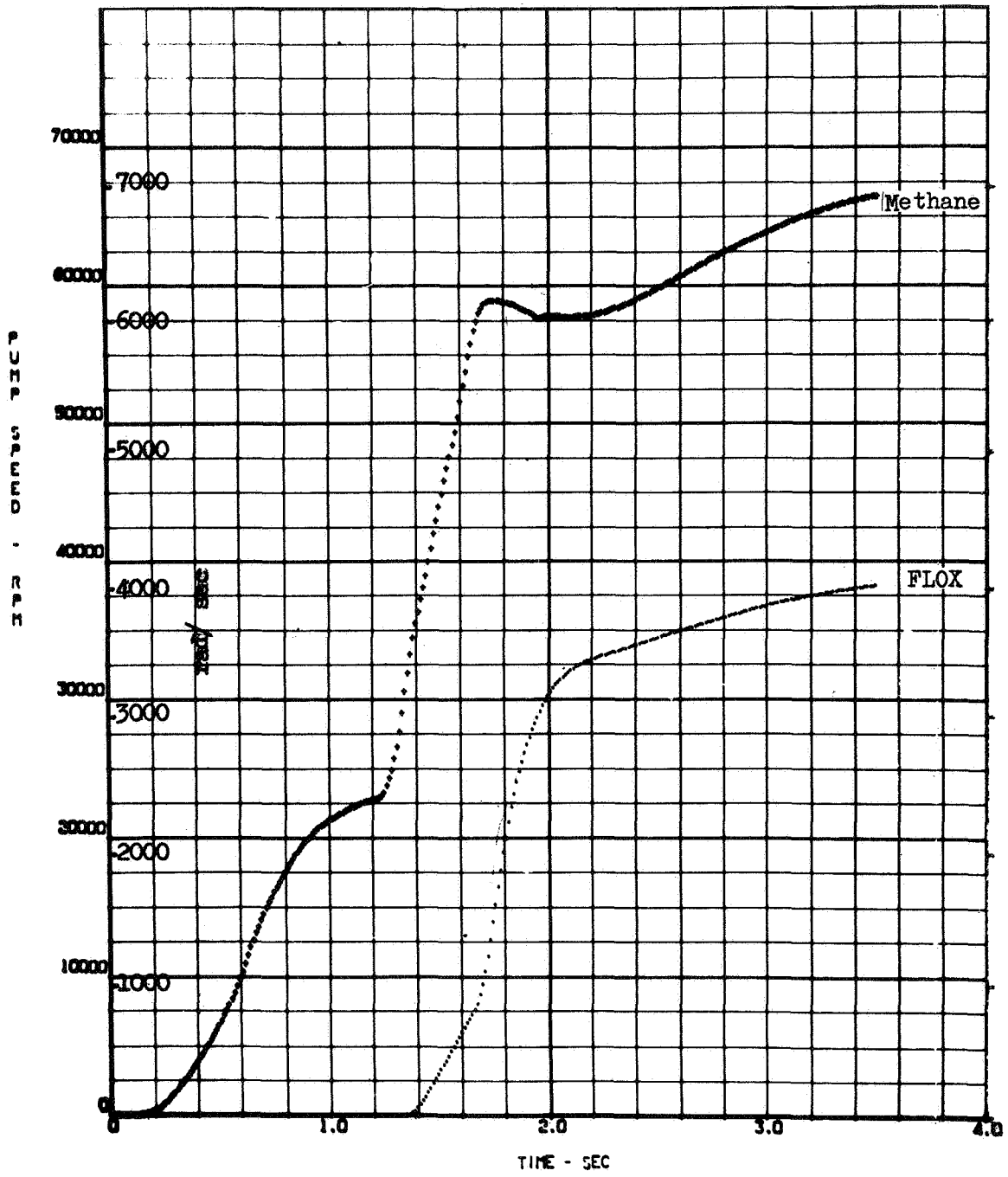
Figure 76. Turbopump Speeds for the Immediate Restart.
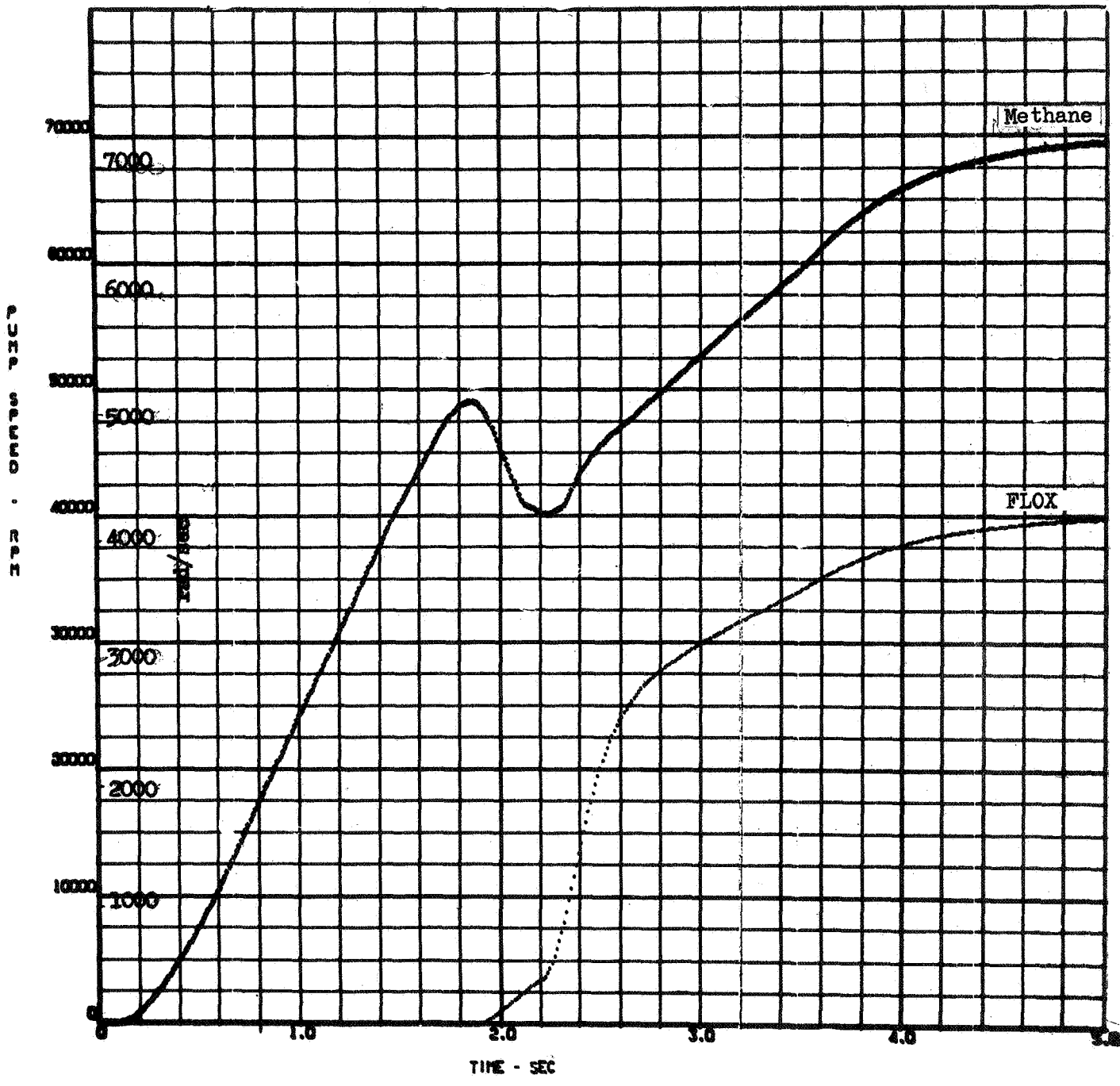
Figure   77 .   Turbopump Speeds for the Ambient Start.
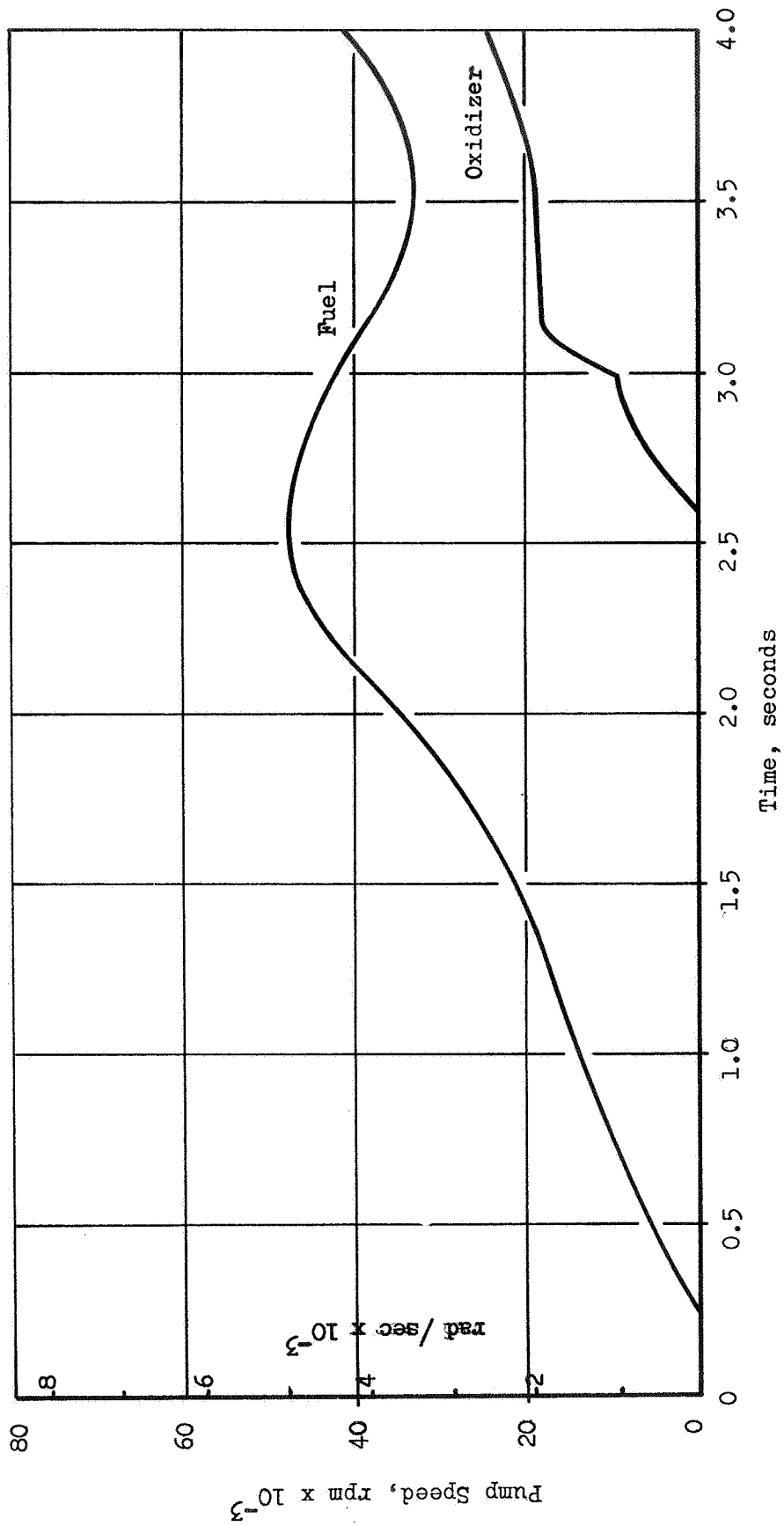
Figure 78, Turbopump Speeds for the Cold Start, 25OR (140K)

224

Chamber pressure transients are shown in Fig. 71 for the immediate restart, ambient start (530R, 295K) and cold start (250R, 140K). The start signal is given at time zero and the initial phase is occupied in methane pump, duct, manifold and chamber priming. The duct and manifold size have been significantly reduced since this initial engine model and priming time is about 50 percent of the values shown. After the priming signalled by a methane pump discharge pressure switch the main FLOX valve is opened and the oxidizer turbine valve is slightly opened. Following FLOX side priming, ignition occurs and the chamber pressure builds up as the FLOX turbine and bypass valves are adjusted.

Thrust chamber mixture ratio (oxidizer injector flow/fuel injector flow) is illustrated in Fig. 72 and propellant flowrates in Fig. 73 to 75 . Mixture ratio values are all acceptable for chamber cooling.

Turbopump speeds are illustrated in Fig. 76 to 78. Limits were placed on turbopump speed buildup to avoid damage to bearings and seals. No indication was observed of operation in regions unacceptable to the pumps.

Intermediate Thrust Levels. Starts to any thrust level would be identical for a given start condition up to the point of FLOX prime. After the pressure switch signals that the FLOX side is primed the turbine bypass valve and the FLOX turbine control valves are ramped to the positions dictated by the desired thrust level.

Idle Mode Start

Idle mode starts were investigated in which the engine is initially run in a pressure-fed mode with no power to the FLOX turbine and reduced power to the methane turbine. Engine transients were analyzed as in the direct start. After running in this mode, the engine can be accelerated to the desired thrust level. The idle mode start was investigated for the case of cold initial engine temperatures (250R, 140K). Liquid propellants were assumed at the main valve inlets.

225

For starts with the cold hardware, the main FLOX and methane valves were opened together. The oxidizer turbine valve is closed and the bypass valve position is adjusted to vary power to the methane turbine. A typical idle-mode system balance is shown in Fig. 79. Since the FLOX flow is set by the tank pressure, variation in the power to the methane turbine varies the mixture ratio. For higher initial hardware temperatures, the equilibrium conditions would be the same but valve sequencing would be different to avoid high mixture ratios during the transient phase. Typically this would involve delaying FLOX valve opening.

Valve Position. From the transient analyses the engine mixture ratio at equilibrium was determined and described as a function of bypass valve position in Fig. 80. As the bypass valve is opened the power to the methane turbine is reduced and mixture ratio increases. Tank pressures are 70 (485) and 35 psia (240 kN/m^2) for the methane and FLOX, respectively. At these pressures, the equilibrium chamber pressure is about 25 psia (170 kN/m^2). The maximum mixture ratio value, 2.5, gives thrust chamber wall temperature well below design values as discussed in the chamber design section.

Where the flow to the methane turbine is shut off with a fuel turbine valve, mixture ratio values are significantly higher, as shown in Fig. 80. Reduction of the bypass valve area would further increase mixture ratio and excessive chamber wall temperature may be encountered. Lower mixture ratios can be achieved through tank pressure variation or FLOX flow restriction.

Engine Transients. Idle mode phase transients for 250 R (140 K) initial temperatures are illustrated in Fig. 81 to 85. The time scale was compressed by reducing chamber heat capacity. Beyond ~ 1.5 sec, time values are only approximate. The time to achieve steady-state operation may be long for low initial engine temperatures and mixture ratios. Times of 20-30 seconds have been observed in low pressure FLOX/methane tests with regeneratively cooled chambers. Although these times are quite long, energy sufficient for engine powered operation is available long before steady-state operation is achieved. As shown in Fig. 84, for a case where steady-state mixture ratio is 2.8, methane exit temperatures of 500-600 R (280-335 K) are achieved in one-quarter of the period necessary to attain steady-state. Where higher mixture ratios are attained (as with a methane turbine inlet valve) these temperatures are attained earlier as illustrated by the comparison of Fig. 85.

FLOX

Methane

P = 35
(240)

P = 70
(485)

P = 87
(6000)

$\dot{W}$ = 0.033
(0.015)

T = 170 (95)

$\dot{W}$ = 0.583
(0.264)

P = 70.8 (4880)

T = 1076 (598)

$\dot{W}$ = 0.169
(0.077)

$\dot{W}$ = 0.202
(0.092)

$\dot{W}$ – lb/sec (kg)

T – R (k)

P – psia (k N/m^2)

P = 29.3
(202)

P = 86.2 (5943)

T = 242 (135)
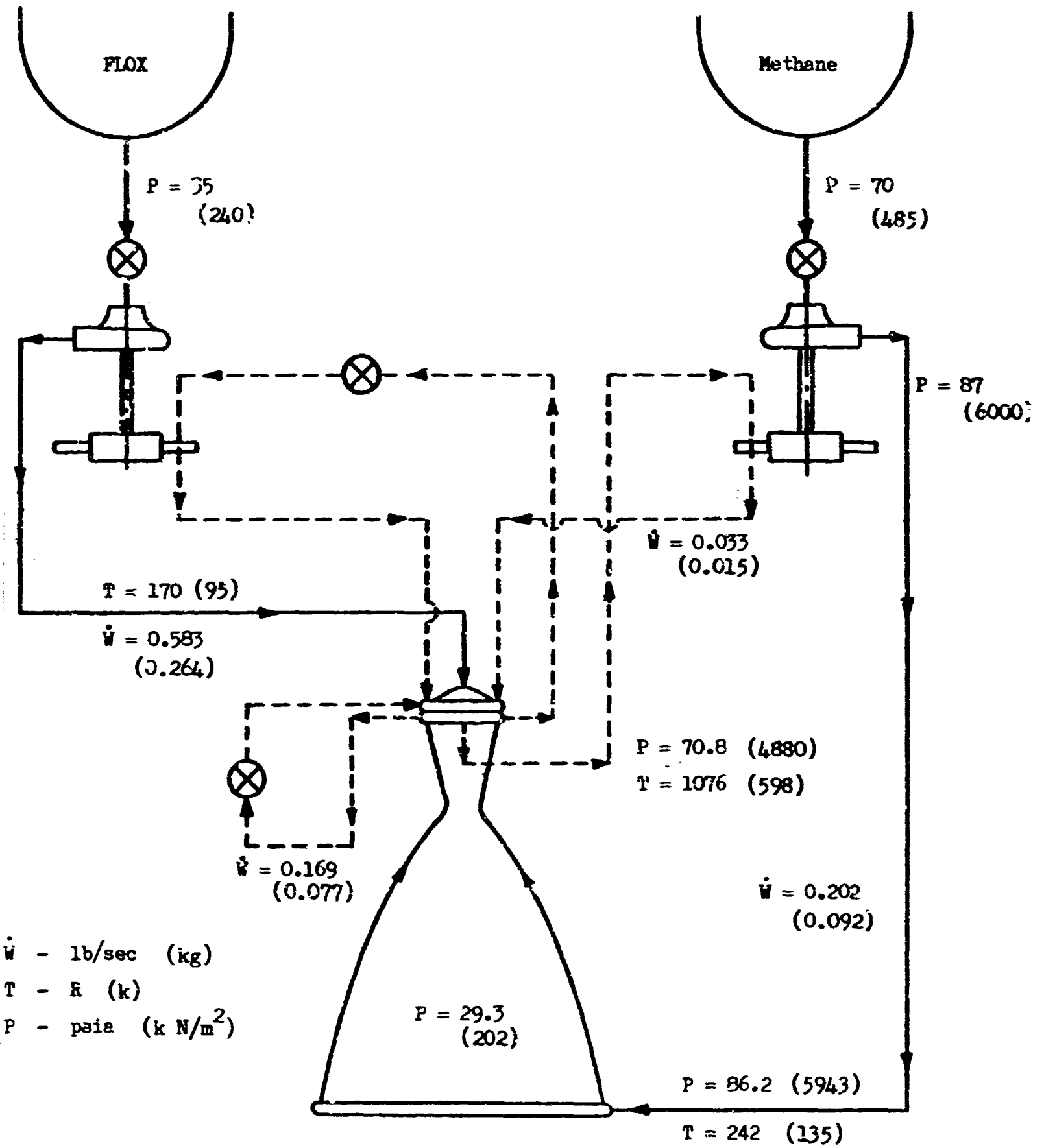
Fig. 79. Idle-Mode Balance

227
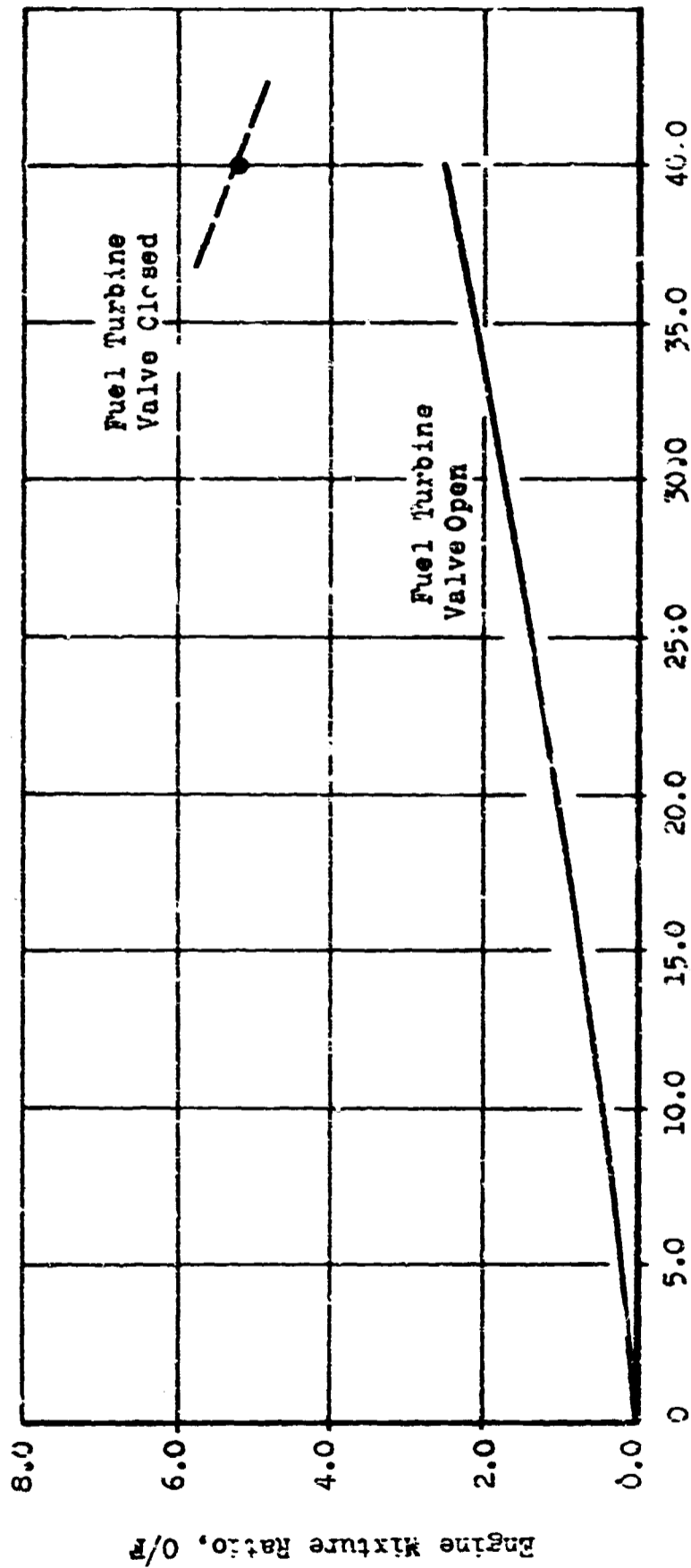
Figure 80. Pressure-Fed Idle Mode.

228

Figure 81 . Idle-Mode Operation; Pressure Transient.

Pressure-Fed Idle Mode

Inlet Pressures: Methane 70 psia $(485 \ kN/M^2)$
                   FLOX 35 psia $(240 \ kN/M^2)$

Initial Engine Temperature — 250 R (140K)

Bypass Valve Full Open
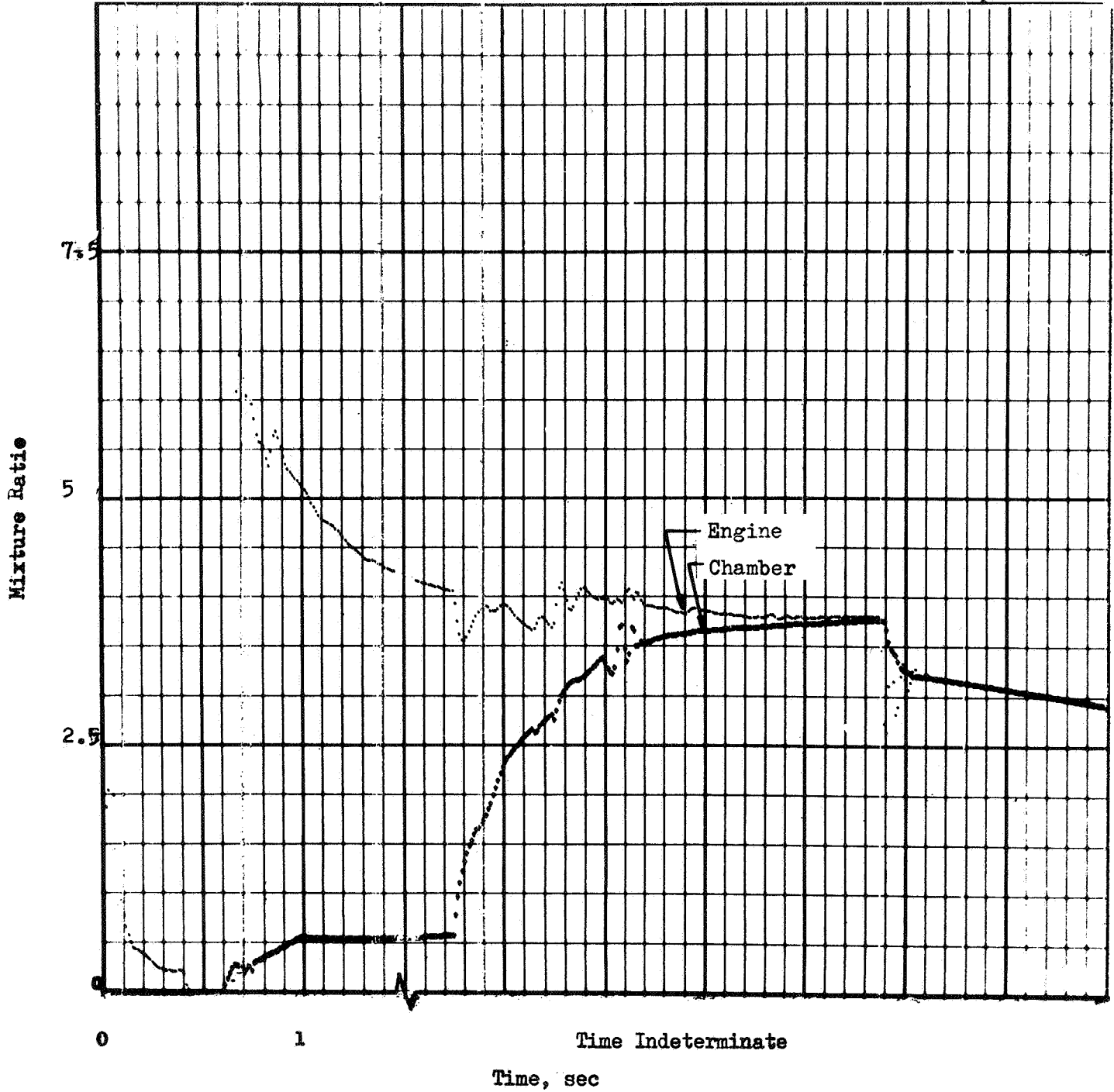
Figure   82.   Idle-Mode Operation; Mixture Ratio Transient.
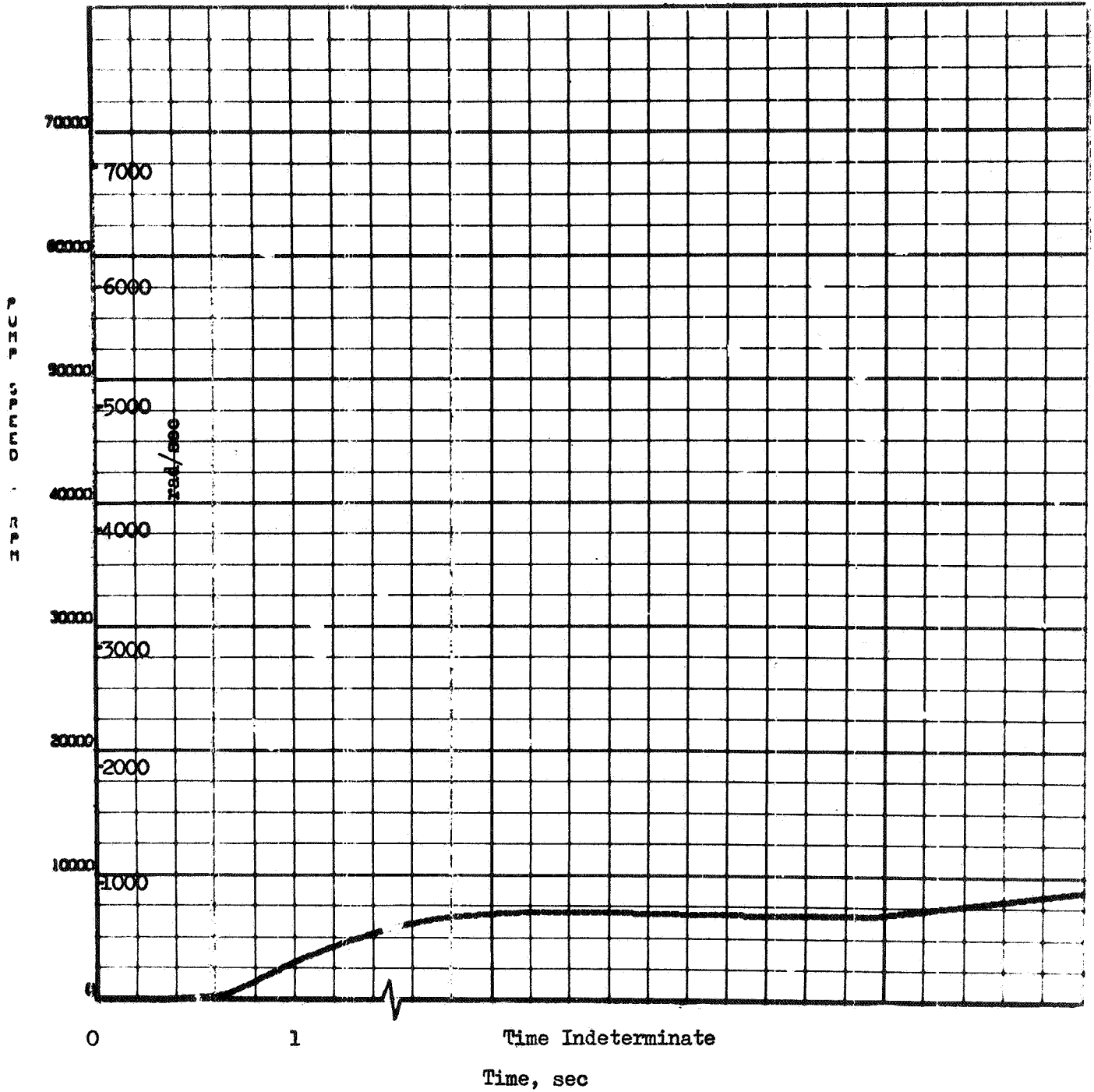
Figure   83.   Idle-Mode Operation, Methane Pump
Transient.

231
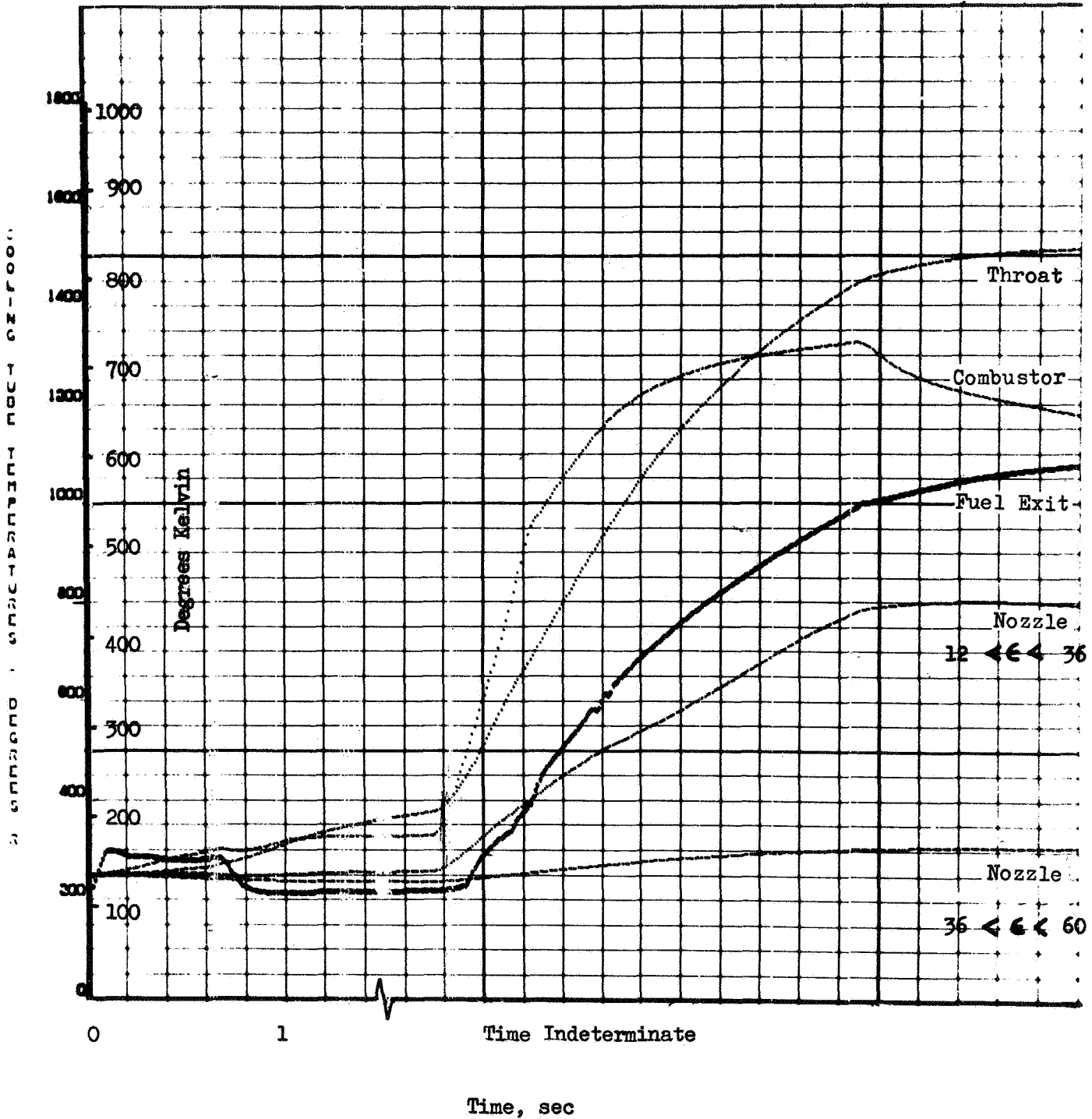
Figure 84. Idle-Mode Operation; Temperature Transients.
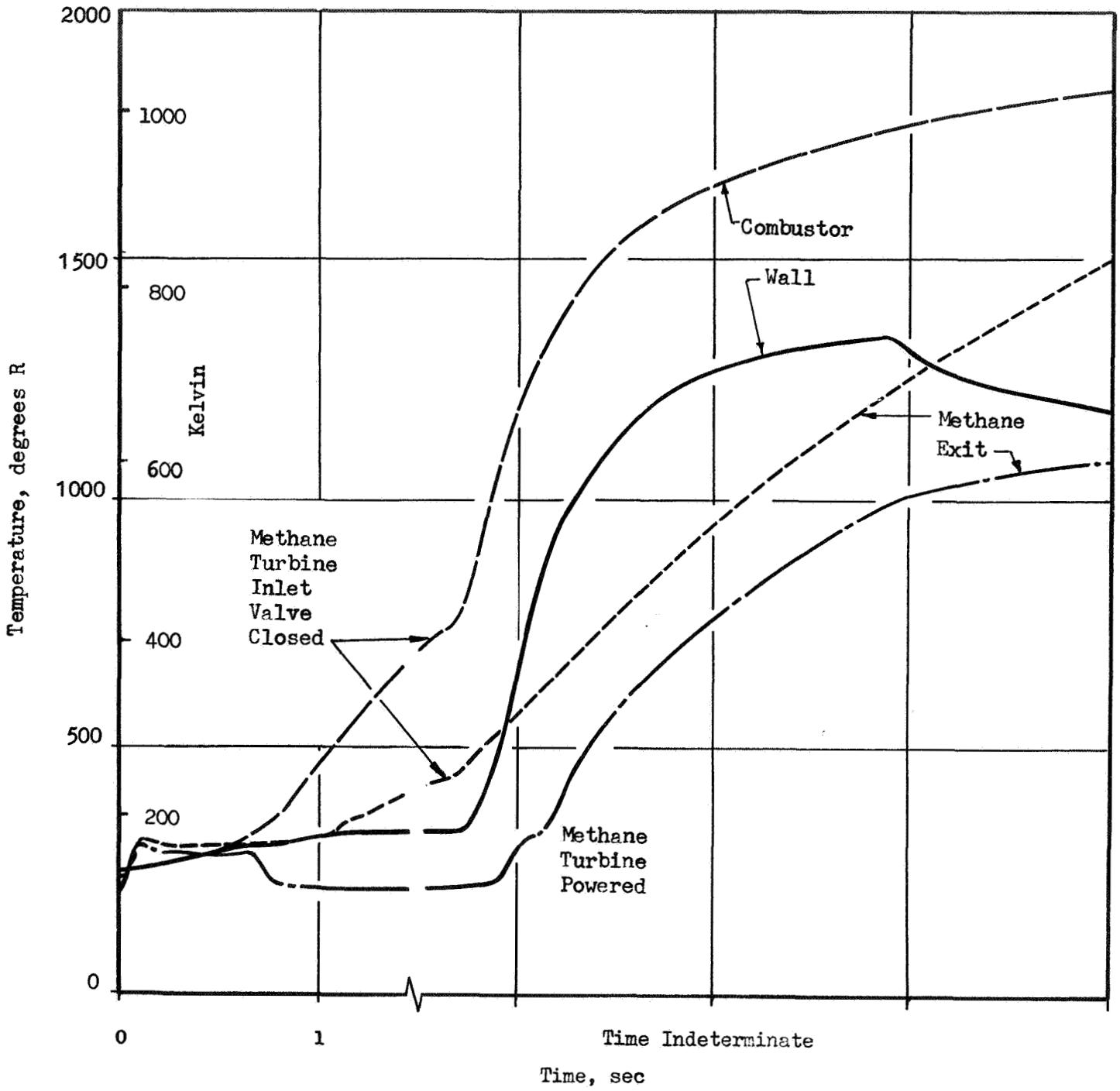
Figure 85. System Control Effect in Idle-Mode Transient

233

Inlet Pressure Effects. Variations in the inlet pressure will affect both mixture ratio and the steady-state thrust level. Lower methane pressure or restriction in the methane line will result in higher mixture ratio values. The magnitude of these effects is illustrated in Fig. 86.

Initial Hardware Temperatures. Higher hardware temperatures will generally restrict the flow of methane through the ducts and cooling jacket during transient operation. Where methane turbine power is excluded, transient operation mixture ratios would be higher than those for the cold start and would certainly require restriction of the FLOX flow. With the methane turbine powered, the higher energy of the methane due to residual hardware heat would somewhat offset the methane flow restriction. Different valve sequencing would be required. In addition, although engine steady-state conditions would be the same as for the cold start, the equilibrium conditions may be approached from a different direction. Since these low chamber pressures will involve two-phase flow in the cooling jacket, the possibility of flow oscillation should be considered. This phenomenon was not encountered in starts with cold hardware but might result with higher temperature hardware.

Powered Phase Operation. Following idle mode operation, the engine can be accelerated to a higher thrust level through opening the turbine valve and closing the bypass valve in a manner similar to the direct start. The duration of idle mode and the sensor signalling initiation of the powered phase will depend on the initial temperatures and the purpose of idle mode operation. For low thrust propulsive maneuvers or propellant settling, a timer or integrating accelerometer in the vehicle control system might be used. Operating times from 2-3 seconds for propellant settling to as much as 50-100 seconds for trajectory correction maneuvers might be encountered. Where the idle mode is used only as a start method, a timer or temperature sensor might be used to initiate the powered phase.

Engine Design Change Effects

The effect of engine design changes on the start transients are discussed in Table 59.
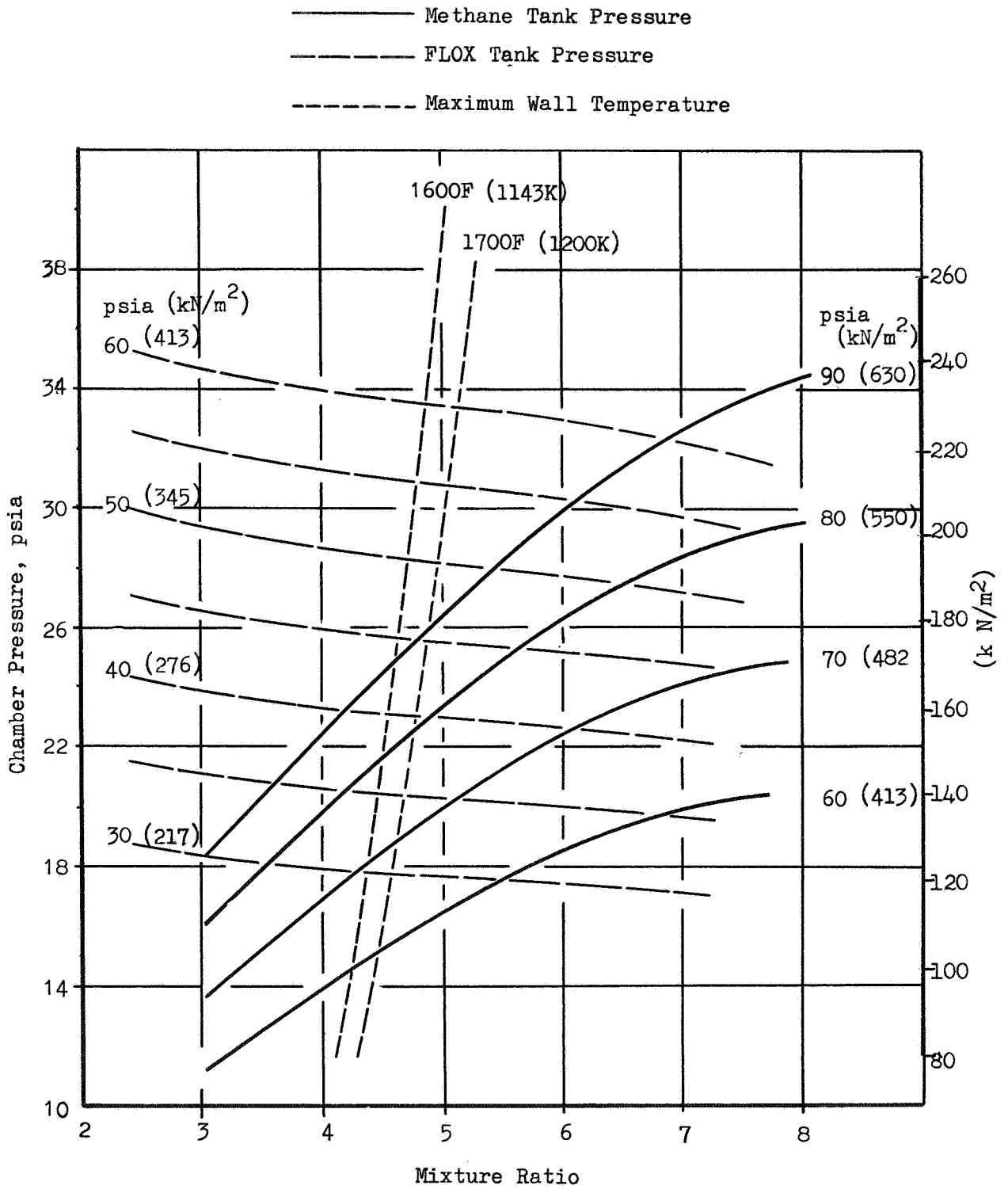
Figure   86 .   Idle Mode Operation with Liquid Propellants

TABLE 59

ENGINE DESIGN CHANGE EFFECT ON SYSTEM START

Design Change	Start Transient Effect
Eliminate Quick Restart Requirement	Bypass valve closing could be delayed slightly providing slight increase in start times for the lower energy starts
Elimination of Cold Start Requirement	This start requires the long ramp time on the FLOX turbine valve. Elimination of this requirement would reduce start times for higher energy starts
Preflight Knowledge of Specific Thermal Environment	Start sequence adjusted to specific conditions. More rapid start
Methane Tank Pressure Reduction (above vapor pressure)	Pump thermal conditioning time will increase; start time longer
FLOX Tank Pressure Reduction (above vapor pressure)	Small effect on FLOX side prime
Methane Inlet Line/Manifold Volume Reduction	Priming time reduced directly; significant start time reduction
FLOX Inlet Line/Manifold Volume Reduction	Priming time reduced directly; minor start time reduction
Close Bypass Valve During Transient	Additional Turbine Power; faster start; readjust bypass to avoid overspeed

ENGINE CUTOFF

Engine cutoff studies were conducted using dynamic simulation techniques similar
to those used in the start analysis. The engine model was identical in the
representation of each system component. Cutoff control sequences were varied to
provide shutdown operation that give no indication of potential hardware damage,
reasonable actuation times, and simple control system. Cutoff times of about
2.5 seconds were achieved.

Cutoff Investigation Ground Rules

The cutoff investigation was based upon the engine operating at design thrust.
Additional pressure sensing devices were avoided as much as possible. Emphasis
was placed on providing a consistent predictable cutoff transient. To assure that
the FLOX would not impinge on hot portions of the injector or chamber, a FLOX side
purge was used. This inlet gas purge enters just downstream of the main FLOX
valve.

Engine Cutoff Sequence

The engine cutoff sequence is shown in Fig. 87. Valve operations are de-
scribed in Fig.88, where the areas are normalized to the area for mainstage
operation at full thrust. This sequence is a reasonable compromise between low
cutoff impulse and reducing FLOX pump speed at shutdown. The turbine bypass valve
begins opening at cutoff signal and requires 100 ms to reach its maximum area of
40 times the nominal mainstage area. Opening of the bypass valve to its maximum
area is done to cause the engine operating level to decrease as rapidly as possible.
The oxidizer turbine inlet valve also begins closing at cutoff signal and requires
250 ms to reach full closed. Main oxidizer valve closing is initiated based on
oxidizer injection pressure. When the oxidizer injection pressure reaches a
predetermined level, the oxidizer valve begins closing and requires 100 ms to
reach full closed. When the oxidizer valve reaches full closed, the purge gas
downstream of the main oxidizer valve is sequenced on. About 1.5 second after the
oxidizer valve reaches full closed, the main fuel valve is signalled to close,
and requires 200 ms to reach full closed.

Cutoff Signal

Main Fuel Valve

Turbine Bypass Valve

Oxidizer Turbine Valve

Main Oxidizer Valve

Oxidizer Injector
Manifold Sensor

100 psia (690 k N/m^2)

1 sec.

Time, seconds
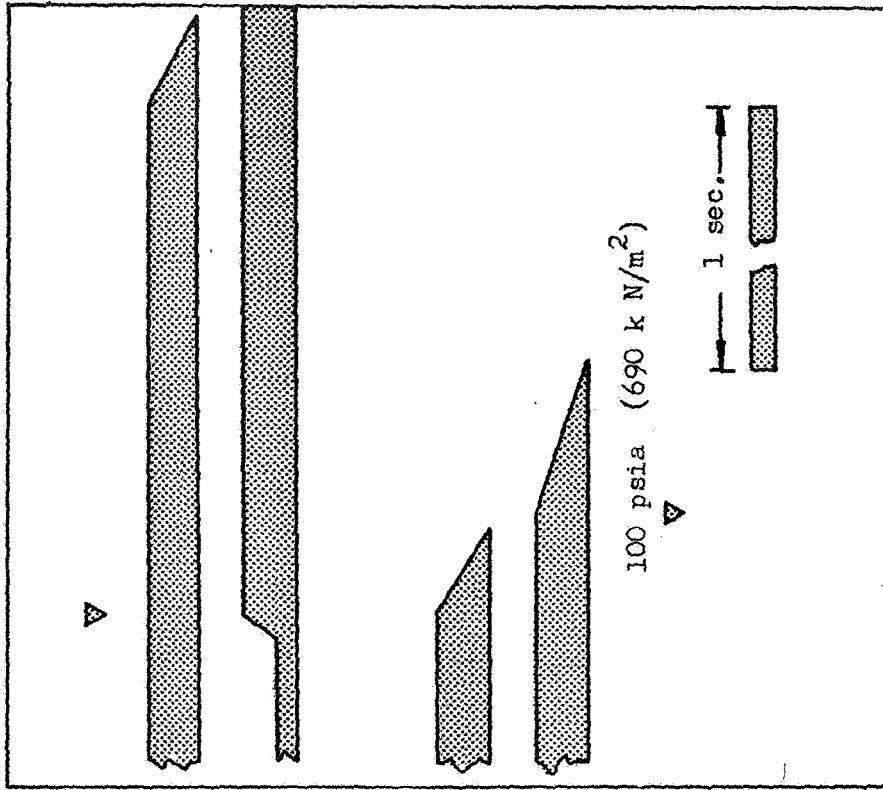
Figure 87. Engine Cutoff Sequence.

238
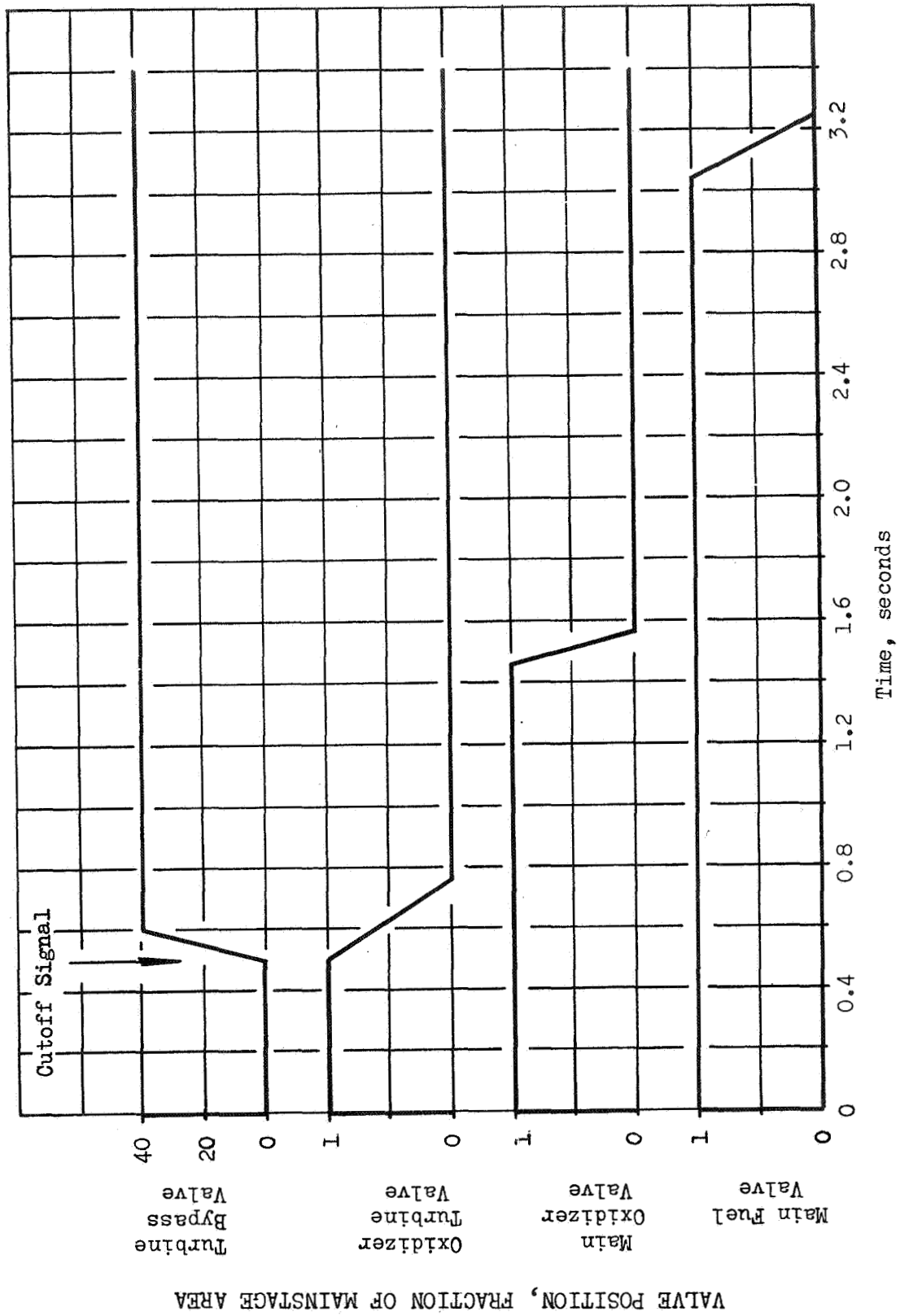
Figure 88. Engine Shutdown Valve Sequencing for Closing Main Oxidizer Valve When Oxidizer Injection Pressure = 100 psia. (690 k N/m^2)

FLOX Side Purge

The purge used is located just downstream of the main oxidizer valve. When the
main oxidizer valve was fully closed, the purge was initiated at a level of
65 psia (450 kN/m^2). This level was selected since the oxidizer pump discharge
pressure at the 10 percent throttled point is 65 psia (450 kN/cm^2). Thus, when
cutting off from minimum thrust, the purge would not cause an increase in engine
operating level which would result in high mixture ratio values. When the purge
comes on, the purge gas begins purging the FLOX out of the pump. As gas fills
the pump, the resulting loss in fluid density causes the pump head to drop to
zero. For this study, complete purging of the oxidizer through the injector was
assumed before any purge gas reached the injector. In reality, the purge will
not be this smooth and will result in a lower mixture ratio near the end of the
purge and consequently a somewhat longer time required to complete the purging.
The volume of oxidizer to be purged from the system was estimated at 31 cu in.
(508 cu cm) at a temperature of 170R (95K), 0.0026 pounds (0.0011 kg) of helium
would be required for each purge.

Cutoff Transients

The cutoff transients resulting from the sequencing shown on Fig. 88 (main FLOX
valve closure initiated at injection pressure of 100 psia (690 kN/m^2) are shown
in Fig. 80 through 92. In these transients the cutoff signal occurs at 0.5-second.
Pressure transients in the system are illustrated in Fig. 89 and 90. Figure 91
shows the mixture ratio transients. In the cutoff analysis engine mixture ratio
is given the special definition of the ratio of oxidizer injector flow to methane
pump flow. Thus, engine mixture ratio can be observed even during the purge phase
when no FLOX is flowing through the pump. Thrust chamber mixture ratio continues
to be the ratio of oxidizer injector flow to methane injector flow. Any difference
in the two curves results from change in density of the methane in the cooling
channels. Figure 92 shows the hot gas side wall temperature transients for each
of channel wall elements and the temperature of the methane in the injector.
These were the basis for the temperatures used in the quick restart analysis.
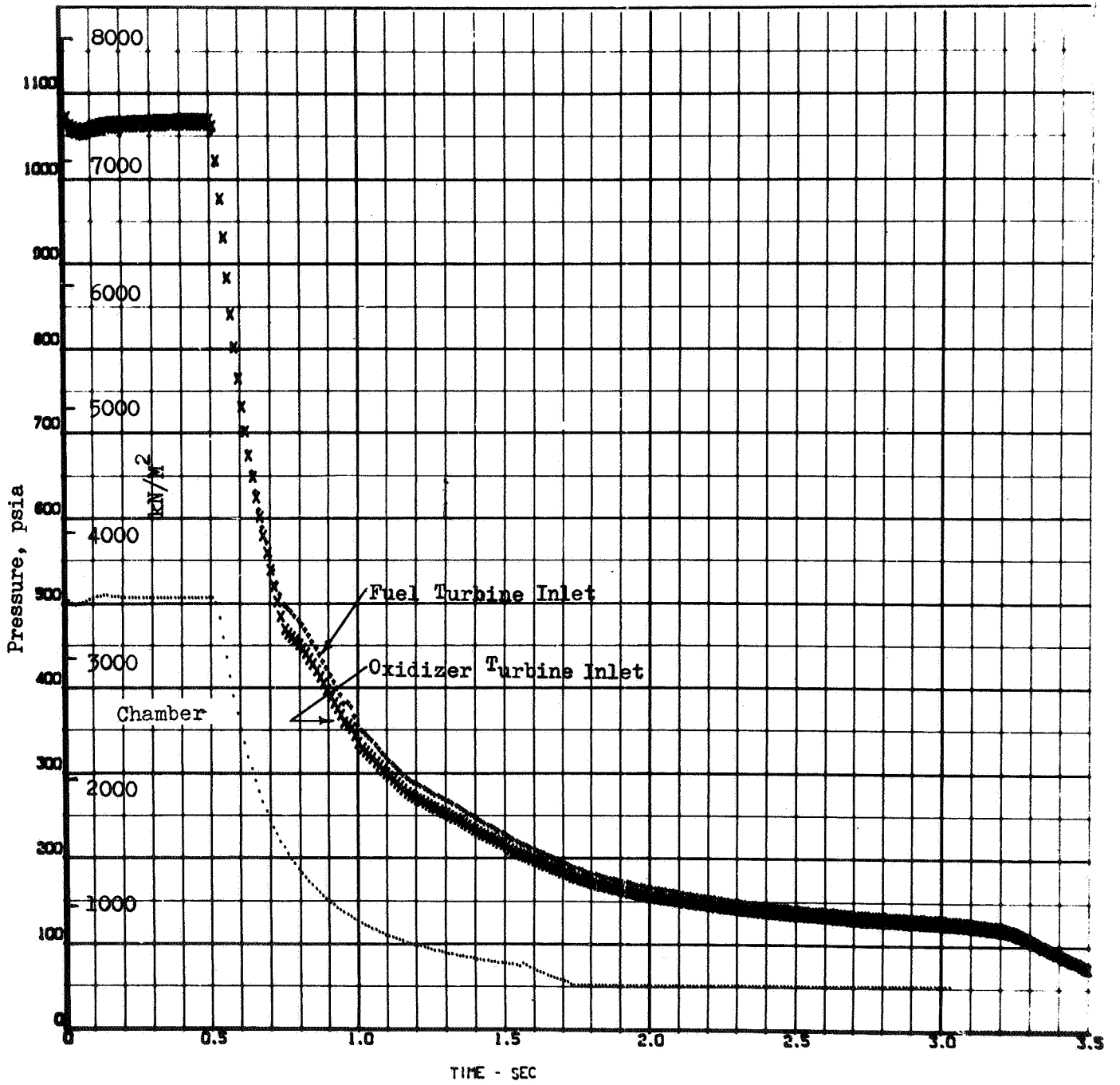
Figure 89. Engine Shutdown Pressures
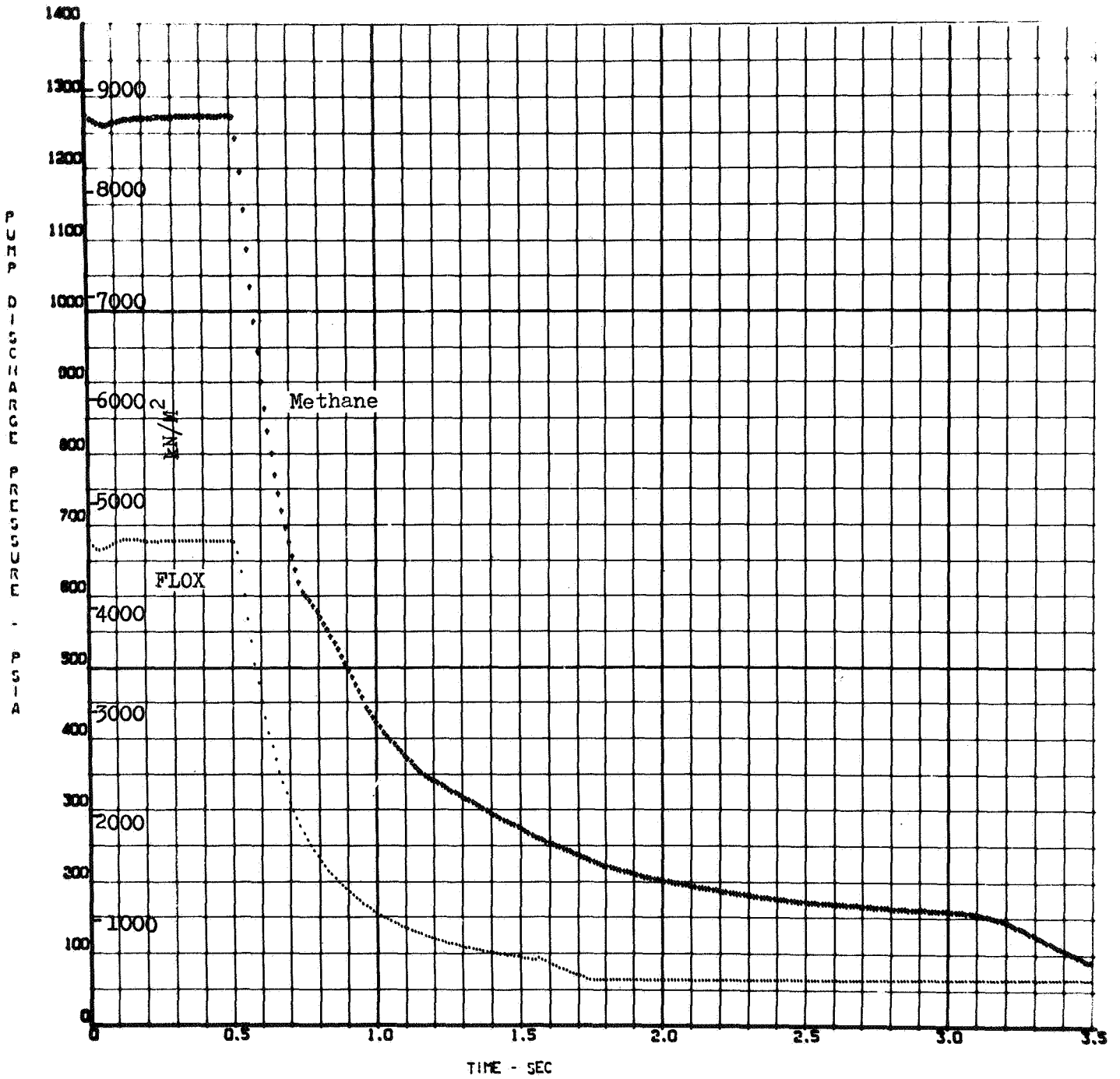
Figure 90. Engine Shutdown; Pump Discharge Transient.
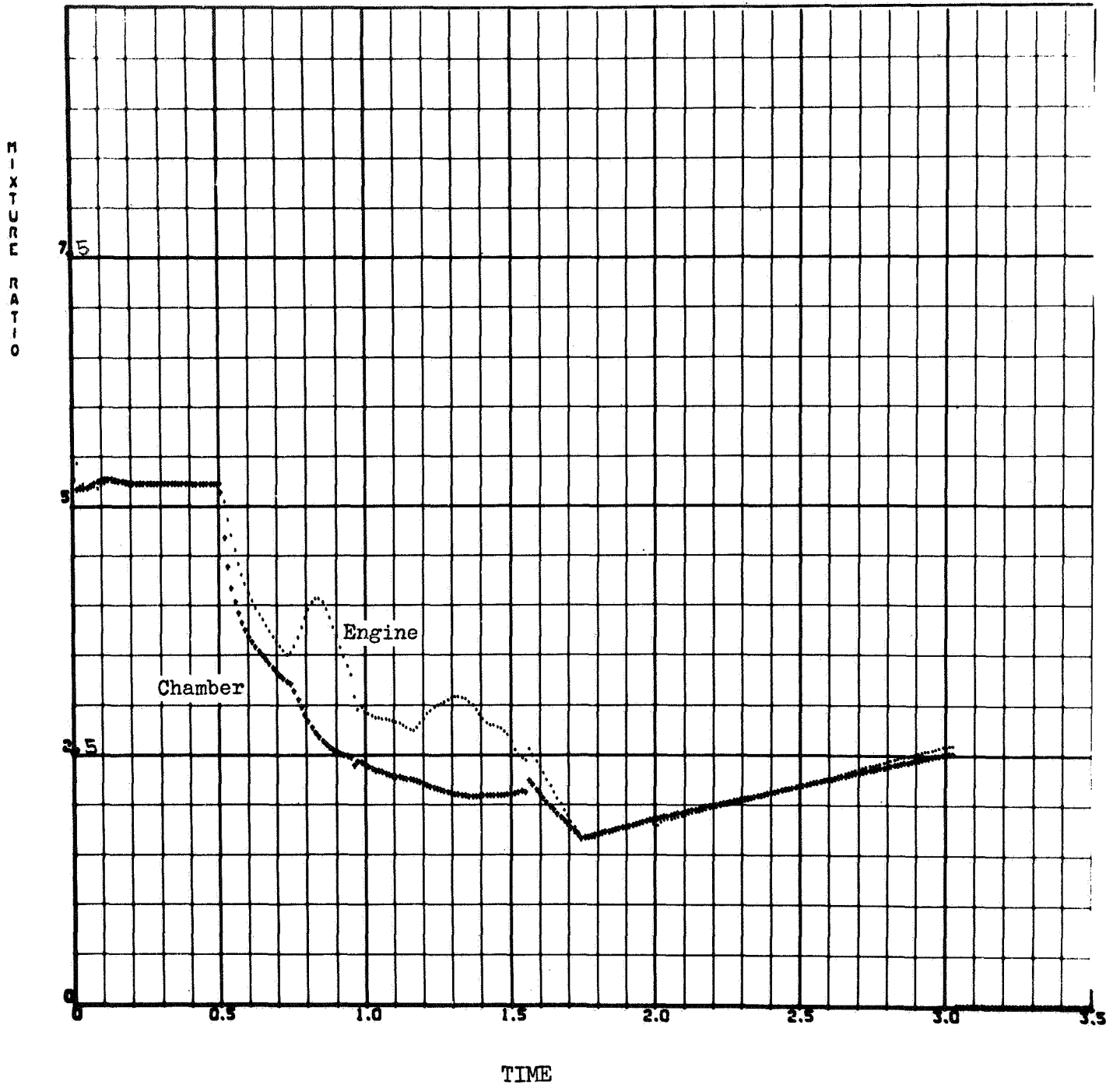
Figure 91   Engine Shutdown; Mixture Ratio Transients.
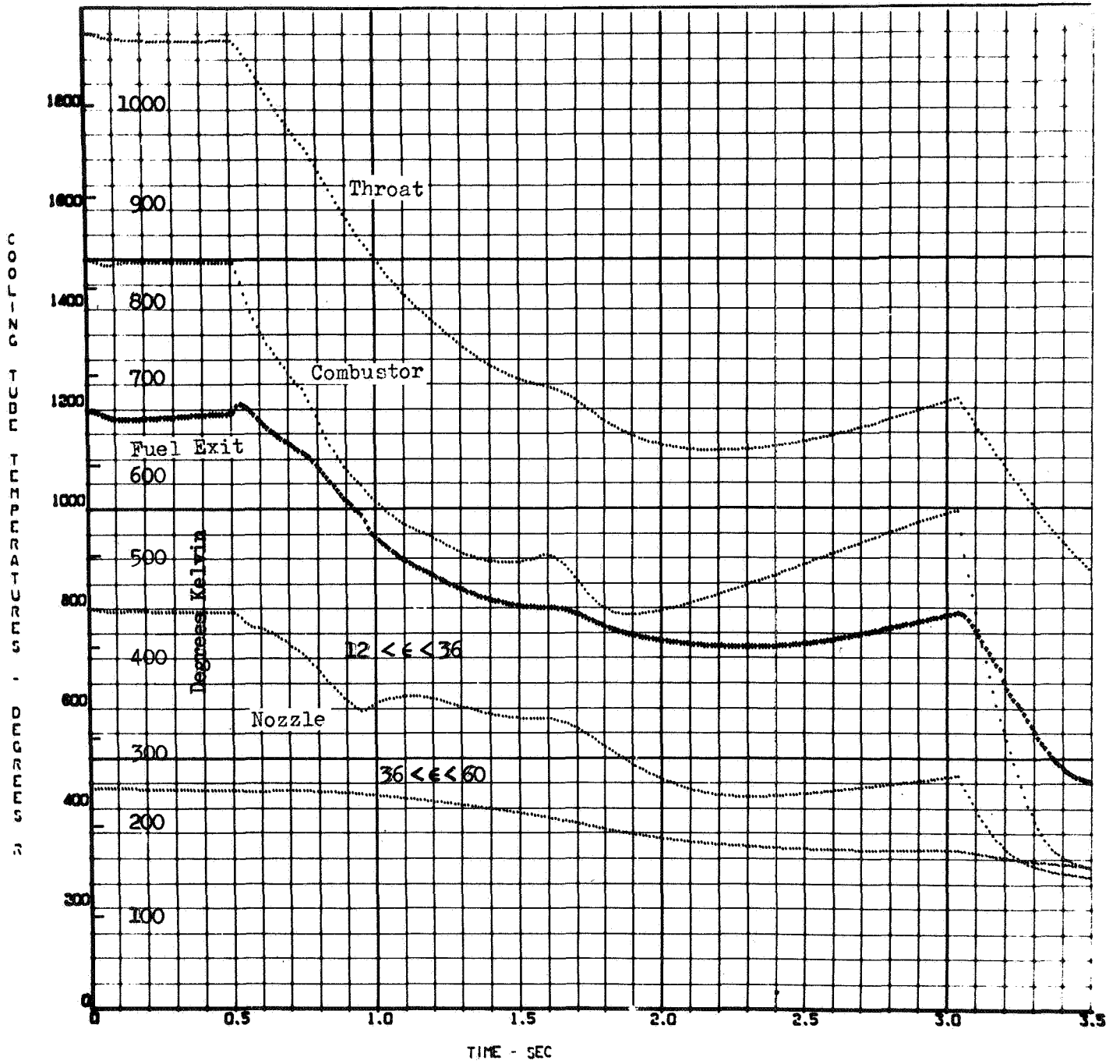
Figure 92. Engine Shutdown; Chamber Temperatures.

START AND CUTOFF IMPULSE

Impulse delivered by the engine and propellant consumption during start and cutoff operation are describ.. in Tables 60 and 67 . During transient operation there is some deviation from the nominal mixture ratio. For a multiple start mission some propellant tanking allowance may be necessary to allow for this variation as well as any deviation in idle mode operation. In addition to the previously described valve sequencing effects, reduction of manifold and line volumes downstream of the main valves will reduce both the start and cutoff impulse. In the tables both start and cutoff are for full thrust operation. The start is based upon attainment of 90-percent of design thrust; the cutoff is based upon depletion of the FLOX with main FLOX valve closure initiated at 100 psia (690 kN/M^2) injection pressure. The methane residual in the lines and chamber contributes little to the cutoff impulse.

ENGINE THROTTLED AND UPRATED OPERATION

Engine operation was evaluated at both throttled and uprated conditions.

Engine Throttling

An engine balance at the 10/1 throttled condition is presented in Table 62 and system temperatures and pressures indicated in Fig. 93 . Engine throttling is accomplished through increasing the percent methane flow through the bypass valve. As shown in Fig. 93 the bypass flow is 69 percent of the total fuel flow at 10/1 throttling in contrast to about 20 percent at nominal thrust. The FLOX turbine control valve is used to maintain constant mixture ratio. Control requirements are described in the Valve Section.

Engine specific impulse is shown as a function of chamber pressure in Fig. 94 . In determining this performance combustion efficiency decreases three percent over the 10/1 range.

245

TABLE 60

PROPELLANT CONSUMPTION DURING START/CUTOFF

Full Thrust Operation, lb (kg)

Start Conditions	Methane Consumption	FLOX Consumption	Effective Mixture Ratio
Immediate Restart	4.86 (2.22)	17.3 (7.8)	3.6
Ambient Temperature Start	4.73 (2.15)	18.0 (8.1)	3.8

TABLE 61

START AND CUTOFF IMPULSE

lb-sec (kg-sec)

Conditions	Start Impulse (90% Full Thrust)	Cutoff Impulse lb-sec (kg-sec)
Immediate Restart (Direct)	4950 (2250)	2500 (1135)
Ambient Temperature Start (Direct)	5240 (2380)	2500 (1135)
Cold Start (Direct)	8400 (3810)	2500 (1135)

TABLE 62

10/1 THROTTLED ENGINE BALANCES

Thrust, lb (N)	500	(2,200)
Engine Specific Impulse, sec (N-sec/kg)	366	(3590)
Engine Mixture Ratio, O/F	5.25	
Thrust Chamber		
Chamber Pressure, psia (k N/m^2)	52	(354)
Mixture Ratio, O/F	5.25	
Weight Flow, lb/sec (kg/sec)	1.37	(0.62)
Specific Impulse, sec (N-sec/kg)	366	(3590)
Exit Temperature, R (K)	1760	(975)
Expansion Ratio	60	
Pumps, O/F		
Flow, lb/sec (kg/sec)	1.15/.22	(0.52/.01)
Discharge Pressure, psia (k N/m^2)	79/125	(545/862)
Number of Stages	1/2	
Speed, 1000 rpm (1000 rad/sec)	8.1/12.2	(0.85/1.27)
Horsepower (kw)	.18/.20	(0.13/0.15)
Efficiency, percent	57.9/54.2	
Turbine, O/F		
Flow, lb/sec (kg/sec)	0.033/.034	(.015/.0155)
Inlet Temperature, R (K)	1750	(970)
Pressure Ratio	1.09/1.08	
Exit Pressure, psia (k N/m^2)	73	(503)
Number of Stages	1/1	
Efficiency, percent	20.8/25.8	
Bypass, lb/sec (kg/sec)	.15	(0.068

247

FLOX

Methane

P = 50
(345)

P = 80
(550)

(.015)

(545)
(0.52)

P = 79
$\dot{W}$ = 1.15

$\dot{W}$ = .033

P = 77   (530)
T = 1750 (970)

P = 78
(540)

$\dot{W}$ = .034 (.015)

P = 125 (860)
$\dot{W}$ = .22   (0.10)

P = 78   (540)
T = 1750 (970)

P = 73   (505)
T = 1746 (970)

P = 73   (530)
T = 1746 (970)

P = 78 (540)
T = 170 (95)

$\dot{W}$ = .15 (0.07)

P = 72
(495)

P = 79   (545)
T = 1760 (980)

P = psia   (k N/m^2)

T = °R   (k)

$\dot{W}$ = lb/sec (kg/sec)

P = 124 (855)
T = 245 (135)
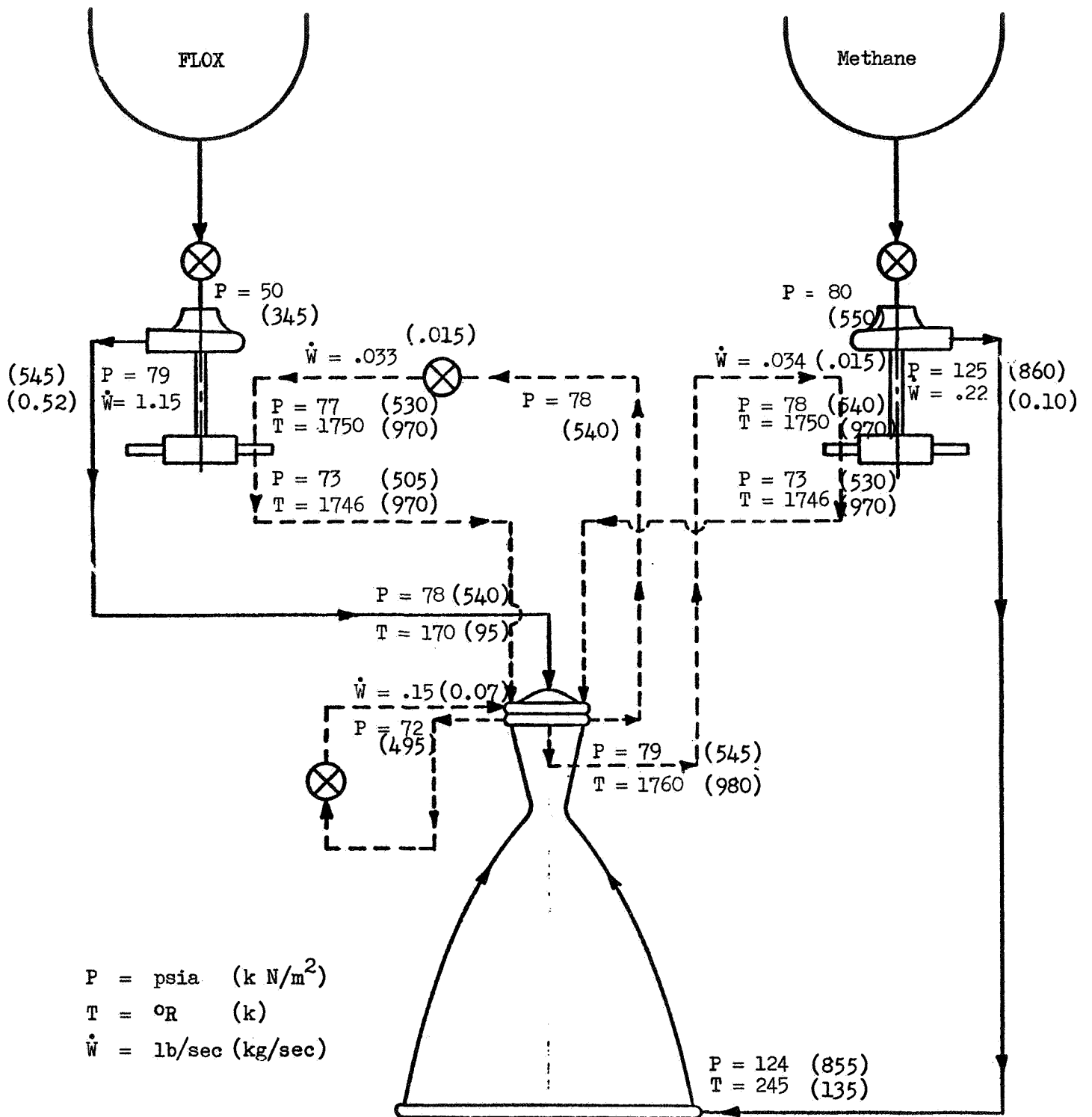
Fig. 93 10·1 Throttled Engine Operating Conditions

248
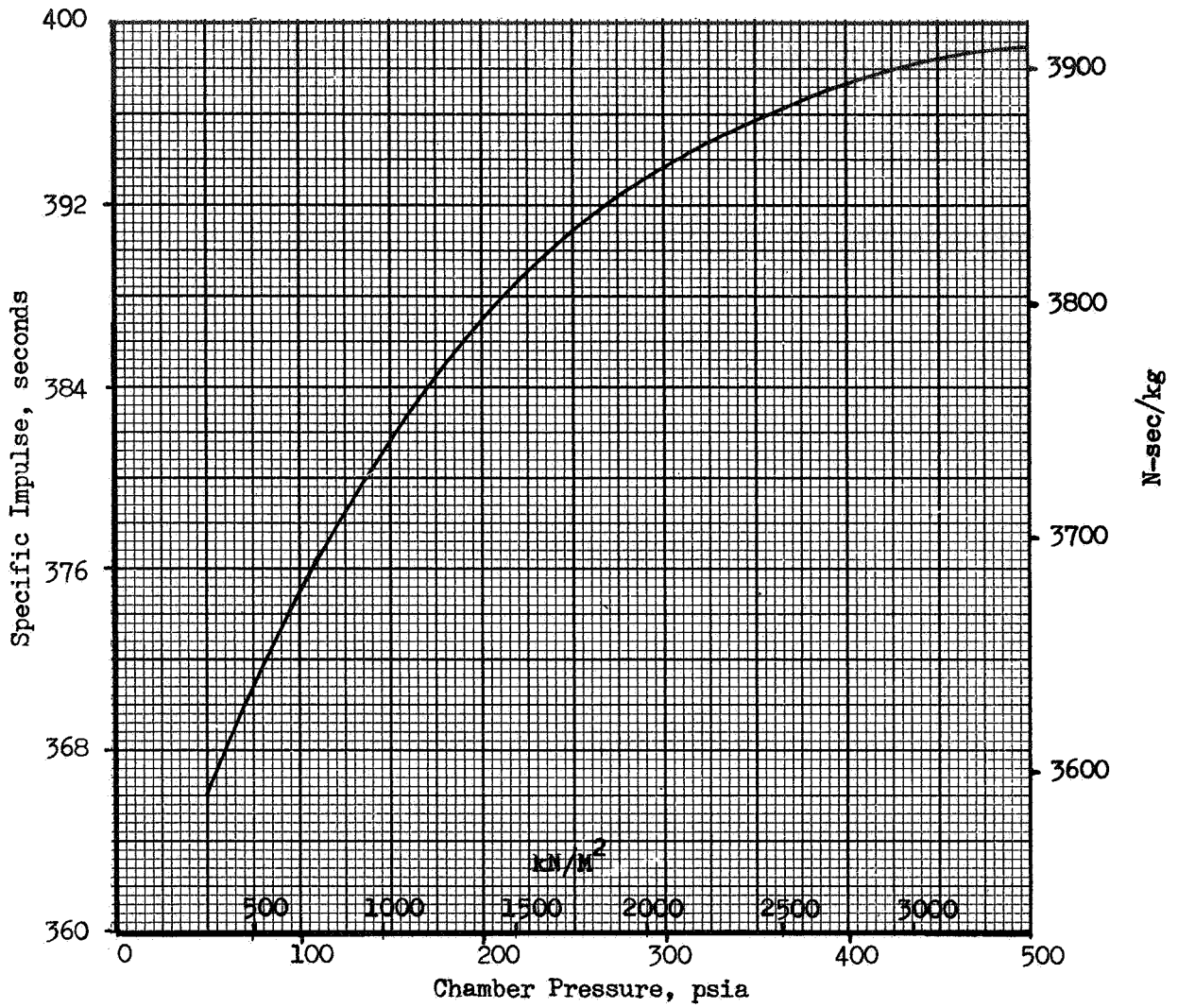
Fig. 94. Throttling Performance

Pump inlet pressures have little effect on nominal thrust operation. However, at 10/1 throttled conditions, the effect on turbopump power requirements is significant. These effects are illustrated in Fig. 95 to 96.

Engine Thrust Uprating

Engine system uprating characteristics are described in Fig. 97 and in Table 63 and illustrate the power margin of the engine system. Two approaches to uprating are illustrated. The first is essentially upthrottling of the engine with no injector or turbine modifications. In the second approach the injector orifices and turbine nozzle passages are increased in area. In both approaches the thrust chamber backup material must be strengthened and the channels redesigned. With the milled channel electroformed construction approach, this is a relatively simple modification.

As shown in Fig. 97, uprating to 7000 pound (31,100 N) thrust can be accomplished without changing injector and turbine flow areas. With flow area modifications thrust levels of 7000-8000 pound (31,100-35,600 N) thrust can be obtained. In uprating, a minimum bypass flow of 5 percent is allowed. In Table 63 an engine operating description is provided for 7000-pound (31,100 N) thrust.

AUTOGENOUS PRESSURIZATION

The engine system can supply hot methane and cold FLOX for use in propellant tank pressurization. Methane and FLOX conditions are described in Table 64 for nominal thrust operation.

TABLE 64

PROPELLANT CONDITIONS AT PRESSURANT TAPS; NOMINAL THRUST

Propellant	Location	Temperature, R (K)	Pressure, psia (k N/m^2)
Methane	Turbine Exit	1220-1260 (675-695)	673 (4640)
	Turbine Entrance	1260-1300 (695-720)	1014 (7000)
FLOX	Inlet Line	140-170 (78-94)	612 (4220)
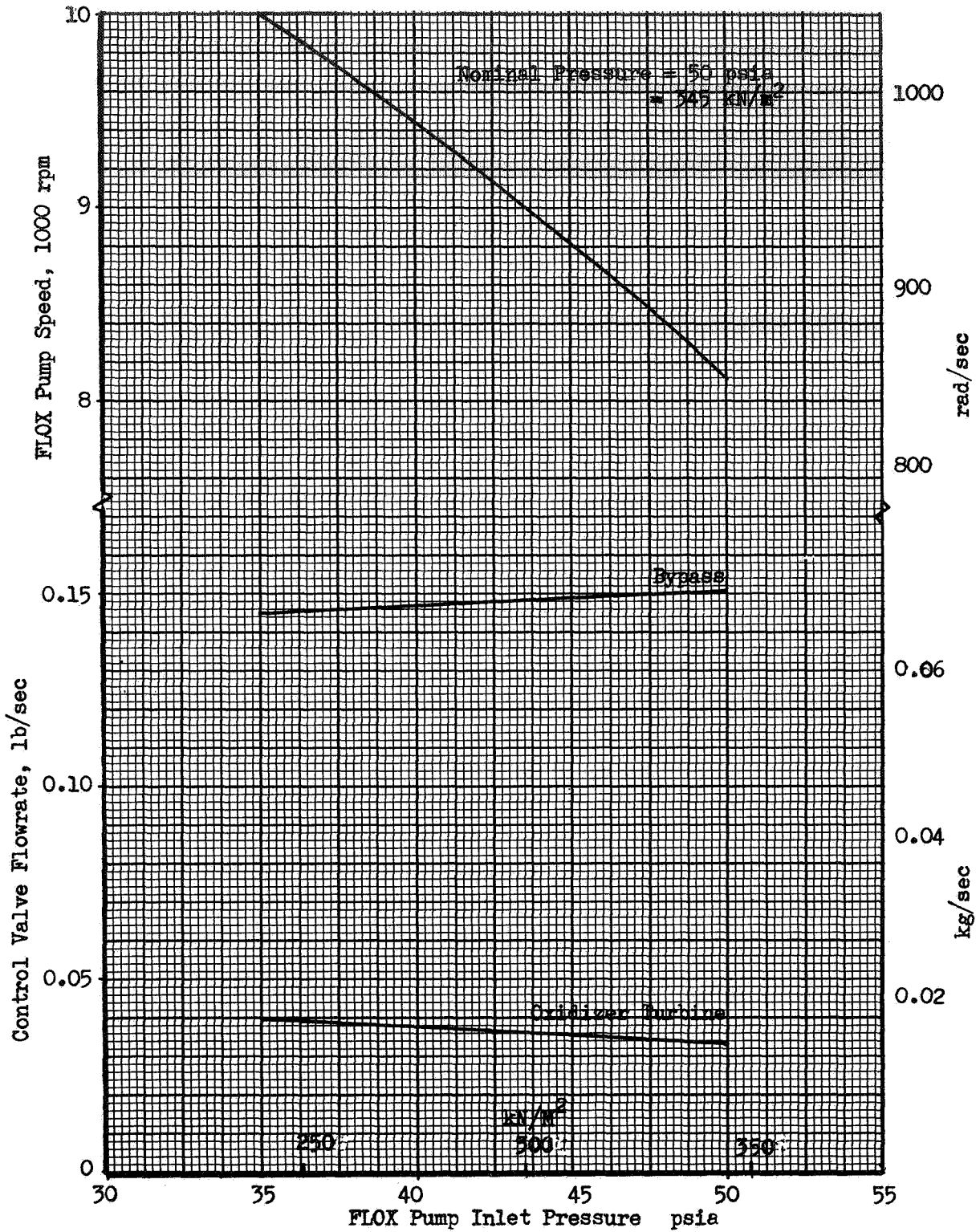
Fig. 95 . Effect of FLOX Pump Inlet Pressure on Cycle Operation at Throttle Ratio of 10:1 (Methane Inlet Pressure = 80 psia (550 kN/M²)
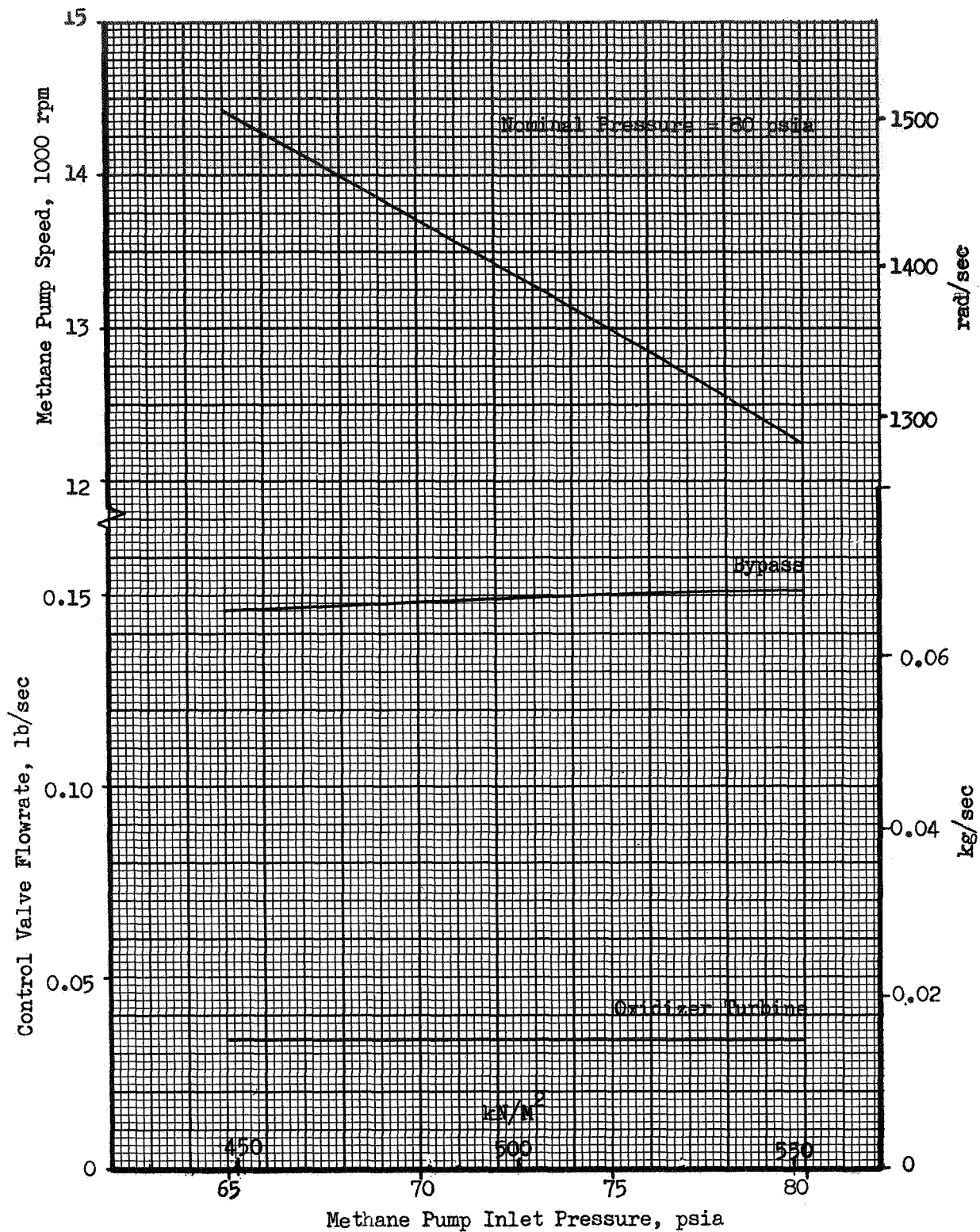
Fig. 96. Effect of Methane Pump Inlet Pressure on Cycle Operation at Throttle Ratio of 10:1 (FLOX Inlet Pressure = 50 psia) (34.5 kN/M²)
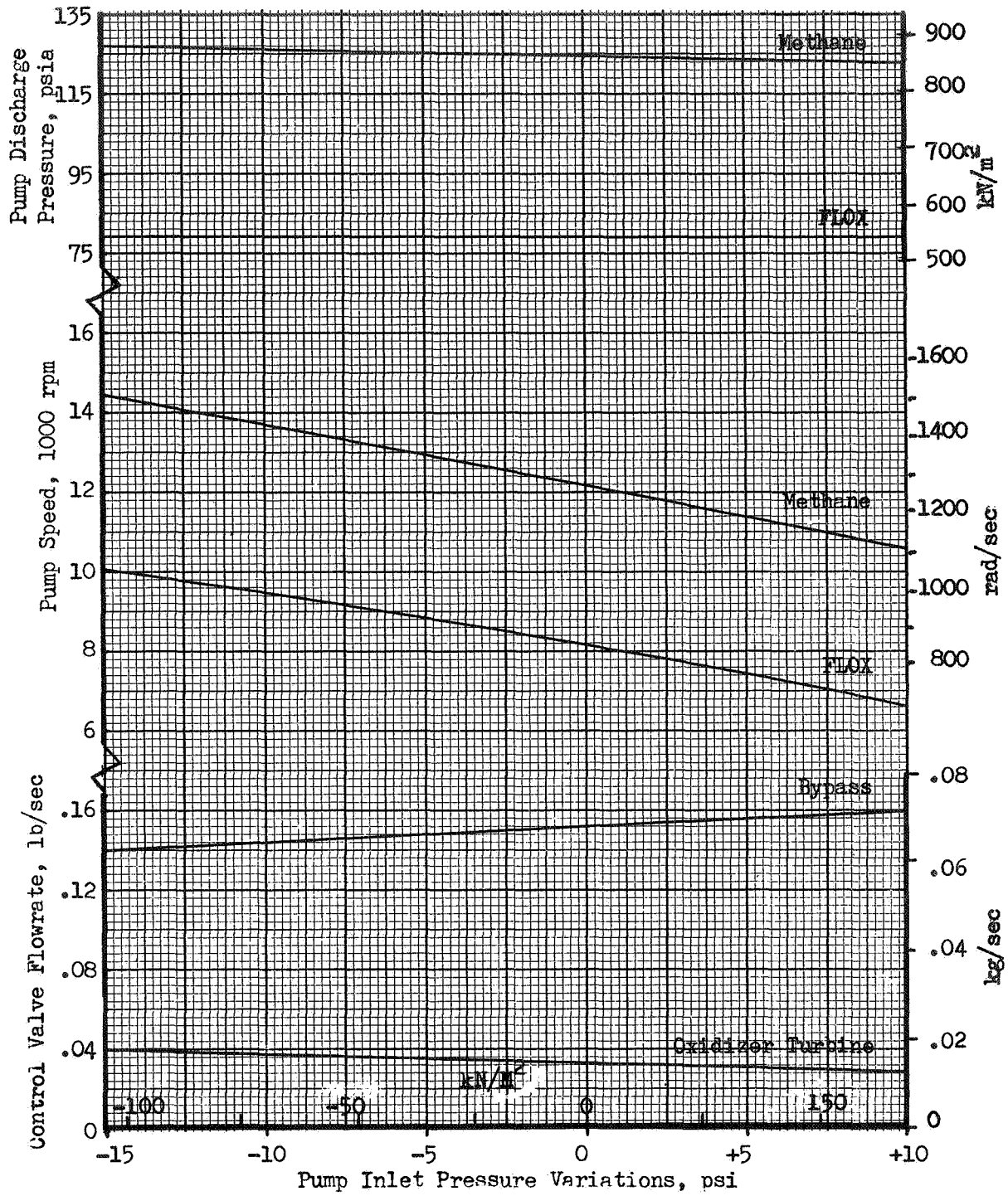
Fig. 97. Effect of Pump Inlet Pressure Variations on Cycle Operation
at Throttle Ratio of 10:1(Simultaneous Variation)
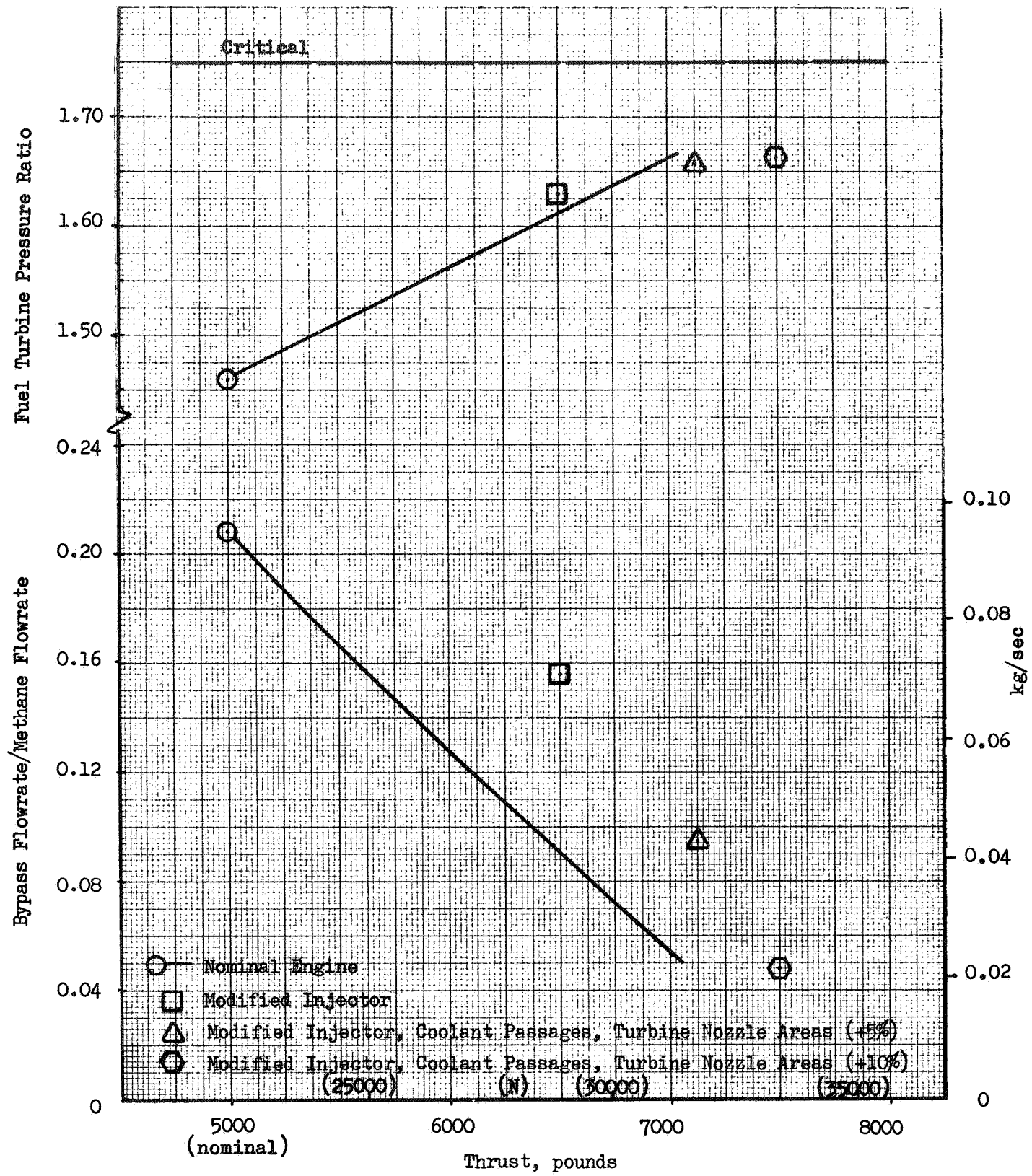
Figure 98. Uprating Capability of FLOX/Methane Engine

TABLE 63

ENGINE UPRATING BALANCES

CONFIGURATION	FIXED HARDWARE		MODIFIED HARDWARE	
Thrust, lb (N)	7000	(31,000)	7000	(31,000)
Engine Specific Impulse, sec (N-sec/kg)	399.5	(3915)	399.5	(3915)
Engine Mixture Ratio, O/F	5.25		5.25	
Thrust Chamber				
Chamber Pressure, psia (k N/m^2)	700	(4826)	700	(4826)
Mixture Ratio, O/F	5.25		5.25	
Weight Flow, lb/sec (kg/sec)	17.5	(7.9	17.5	(7.9)
Specific Impulse, sec (N-sec/kg)	399.8	(3918)	399.8	(3918)
Exit Temperature, R (K)	1243	(689)	1245	(690)
Expansion Ratio	60		60	
Pumps, O/F				
Flow, lb/sec (kg/sec)	14.7/2.8	(6.7/1.3)	14.7/2.8	(6.7/1.3)
Discharge Pressure, psia (kN/m^2)	1026/1949	(7074/13438)	926/1805	(6385/12430)
Number of Stages	1/2		1/2	
Speed, 1000 rpm (1000 rad/sec)	50.3/86.8	(5.2/9.1)	48.3/84.5	(5.1/8.8)
Horsepower (kw)	61.8/93.7	(46/70)	55.8/87.1	(41.6/65)
Efficiency, percent	70.7/61.0		70.3/60.5	
Turbine, O/F				
Flow, lb/sec (kg/sec)	1.22/1.43	(.55/.65)	1.15/1.36	(.52/.61)
Inlet Temperature, R (K)	1238	(685)	1240	(686)
Pressure Ratio	1.55/1.66		1.53/1.65	
Exit Pressure, psia (k N/m^2)	942	(6495)	863	(5950)
Number of Stages	1/1		1/1	
Efficiency, percent	54.7/61.5		54.0/61.2	
Bypass, lb/sec (kg/sec)	0.15	(0.068	0.29	(0.13)

These conditions are more than sufficient to supply pressurization for propellant expulsion. An engine mounted head exchanger could be used to exchange heat between the methane and the FLOX. Based upon a head balance for pressurant flow estimates, the methane has more than enough energy to heat the FLOX to temperatures desired for pressurization.

The thrust level at which pressurization can be initiated was examined for both transient and steady-state conditions. Assuming a minimum source pressure of 150 psia (1035 kN/M^2) for FLOX and 200 psia (1380 kN/M^2) for methane is necessary for pressurization (regulator and line P allowance), thrusts of 1000 to 1500 pound (4450 - 6670N) are necessary before pressurization can be initiated. Lower tank pressures will reduce these thrust levels somewhat. These thrust levels are attained very quickly ($\sim$1 second) after the FLOX valve is opened during the start transient.

Where the propellant tank has been prepressurized, the start can proceed directly since there is sufficient NPSH and the propellant expulsion pressurization requirements are low. For a completely autogenous system, the tank must be repressurized and some period of two-phase fluid pumping may be necessary. For this situation, powered idle-mode operation will be employed. In this operation the engine is started to a thrust level of 1000-1500 (4450-6670N) pound. During the start and the early portion of powered idle-mode operation, the pumps will pump saturated or two-phase propellants. As discussed in the turbomachinery section, operation in this thrust range with saturated propellants is possible. Two-phase operation capability appears possible but must be experimentally verified.

Once the powered idle mode thrust level has been attained, tank pressurization is initiated to raise the tank pressures to the value required for full thrust operation. Where the ullage volume is large and pressurant has collapsed, the prepressurant flow requirements may be larger than for propellant expulsion. This situation occurs in the last trajectory correction maneuver of the Mars Orbiter, for example. The flow requirements depend on the mission duty cycle may be the major factor in sizing the pressurization system. Should the flow requirements to raise the tank pressure be undesirably large, this type of maneuver could be run with the engine throttled, thereby relieving the prepressurization requirements.

IDLE MODE OPERATION

The pressure-fed idle-mode operation described for engine start also has application to low thrust maneuvers, consumption of propellant residuals, and propellant settling.

The low thrust maneuvers can be performed in idle-mode as long as engine mixture ratios are low enough to prevent thrust chamber over-heating. Chamber pressure and mixture ratio for idle-mode operation are shown as a function of tank pressures in Fig. 86. Operation to the left of the thrust chamber cooling line will assure that no chamber overheating occurs. Propellant consumption is generally small (typically 1 percent of total in 100 seconds) and the thrust should remain relatively constant even with tank pressure regulation. This idle mode operation could be used to consume propellant residuals at the end of flight and significantly extend the propulsion capability.

The engine can be used to settle propellants prior to a propulsive maneuver. This can be accomplished through use of pressure-fed idle-mode or by a combination of methane blowdown and pressure-fed idle-mode. Where liquid methane can be assumed at the engine inlet through use of a propellant screen, for example, pressure-fed idle-mode can be used for settling. In this case, there would be no possibility of having liquid FLOX and gaseous methane at engine inlet with the attendant high mixture ratio operation. Where the propellant conditions at the engine inlet are unknown, the methane alone could be used for settling. Methane gas could be blown down, creating a small thrust which would be sufficient to settle the propellants. When methane liquid was available at the engine inlet, pressure-fed idle-mode or direct engine start could be initiated.

In Ref. 9, the settling times for a Mars Orbiter system were estimated at 9-18 seconds using a 6-pound (26 N) thrust auxiliary thrustor. Thrust levels for pressure-fed idle-mode and methane blowdown are listed in Table 65. All these are based on tank pressures of 35 psia (240 kN/m^2) and 70 psia (485 kN/m^2) for FLOX and methane, estimated end of flight vapor pressures.

TABLE 65

PROPELLANT SETTLING THRUST

Method	Conditions	Thrust, lb (N)
Pressure-Fed Idle-Mode	Liquid at Pump Inlet	200-300 (890-1330)
Methane Blowdown	Liquid at Pump Inlet; Chamber Temperature	
	250 R (139K)	90 (400)
	530 R (294K)	20 (89)

With these thrusts, propellant settling times for the Mars Orbiter configuration would be very short.

THRUST CHAMBER DESIGN

A thrust chamber design utilizing advanced fabrication techniques was
established to provide low-cost chamber fabrication and design flexibil-
ity. The selected fabrication method was to use electroformed nickel
with mechanically-milled channels, as used in chambers fabricated under
Contract NAS3-11191. This technique provides a smooth inner wall and
eliminates potential problems associated with welded or brazed joints.
The thrust chamber is designed to meet the requirements for operation at
nominal, throttled and idle mode conditions. With a slight modification
to the channel contour and the use of additional backup structure, the
8000-pound thrust level can be achieved.

DESIGN GROUND RULES

The channel design is based upon the two-step variation in channel width
described in Task I. This step variation in width represents a compromise
in which slightly higher pressure drops were accepted to provide a reduction
in fabrication cost. The chamber design was based on methane coolant infor-
mation obtained from heated tube data, and the combustion side heat transfer
profile was based on data taken in a water-cooled chamber under Contract NAS3-
11191. This information is described below and in Ref. 14.

Combustion Side Heat Transfer

Recent gas side heat transfer film coefficient data from a 20-degree (0.35 rad)
convergent angle, 7.5-inch (19.1 cm) combustor (Ref. 1), using both a trip-
let and a concentric tube injector, were carefully analyzed. The data com-
pared very well with the boundary layer equation in both the convergent section
of the chamber and in the throat, assuming that the boundary layer was initiat-
ed at the start of convergence. In addition, local heat flux measurements
on the nozzle compared favorably with the analytically-predicted values.
Therefore, the boundary layer equation has been used to predict the heat
transfer film coefficients for this study.

The concentric injector tested under NAS3-11191 had very good performance and showed low combustor heat fluxes as compared to the triplet. With the up-pass coolant circuit and resultant high methane coolant temperatures and low densities in the combustor, an appreciable pressure drop savings can be achieved by designing to the concentric injector heat flux profile. Consequently, the final heat flux profile uses the experimental concentric heat flux profile, adjusted by the standard turbulent flow area ratio correction $(h_g \propto \epsilon^{-.8})$ to the start of convergence or to the point where the concentric injector heat flux profile merges with the theoretical profile, whichever occurs further downstream. Heat fluxes at other than nominal chamber pressures were extrapolated using the standard turbulent flow correlation:

$$Q/A \propto P_c^{0.8}$$

Coolant Side Heat Transfer

The correlation used for predicting coolant side heat transfer coefficients was the Dittus-Boelter equation, with properties evaluated at the bulk temperature. When compared to methane heat transfer data obtained at Rocketdyne in electrically-heated tubes, the above prediction accurately estimates the experimental values over the temperature range of 350 to 1125 R. The Dittus-Boelter bulk correlation with entrance, roughness, and curvature enhancement factors added is:

$$N_{Nu} = 0.023 \, N_{Re}^{0.8} \, N_{Pr}^{0.4} \, \overline{\frac{O}{E}} \, \overline{\frac{O}{R}} \, \overline{\frac{O}{C}}$$

Enhancement factors were selected based on a review of experimental methane data and the specific channel configuration. Curvature enhancement reaching a maximum of 1.5 was used in the throat region. Roughness enhancement of 1.18 was used based on a typical milling surface finish. Entrance region enhancement near the coolant inlet was a maximum of 1.06.

The shape of the combustion chamber is significant because it affects 1) local heat fluxes and boundary layer initiation point; 2) integrated heat load and coolant discharge temperature; 3) combustion chamber wall temperature and pressure drop; 4) performance; 5) thrust chamber size and weight; and 6) fabrication ease.

Two shapes were considered: 1) a conventional shape with a cylindrical combustor and a tapered convergence section, and 2) a uniformly tapered chamber between the injector and the throat. Both used the same injector (contraction ratio = 4), and the latter chamber is 0.5-inch (1.27 cm) longer. Comparable geometries are shown in Fig. 98, together with the geometry of the combustor tested for Contract NAS3-11191. Both chambers have about the same coolant pressure drop and coolant exit temperature (within 30 F, 17K), but the tapered chamber appeared superior.

Shape Effect on Heat Transfer

A two-dimensional heat transfer analysis was run for the throat and for critical parts of the combustor for both configurations. The critical combustor region is near the start of convergence for the conventional combustor, and about 6 inches (17.8 cm) from the throat on the tapered chamber. The tapered combustor was 150 F (83K) colder in this region due to a slightly lower heat flux (Fig. 98), and because the chamber diameter and consequently the land width is appreciably smaller (about 0.116 vs 0.138-inch (0.295 vs 0.350 cm) channels). Consequently, about 30-percent more channels, or else higher coolant velocities, would be required to maintain the same wall temperatures in the conventional manner.

A comparable difference occurs at 10:1 throttled conditions. Consequently, the tapered chamber is more attractive from a cooling standpoint. Two-dimensional wall temperatures are summarized for a 90-channel design in Table 66.
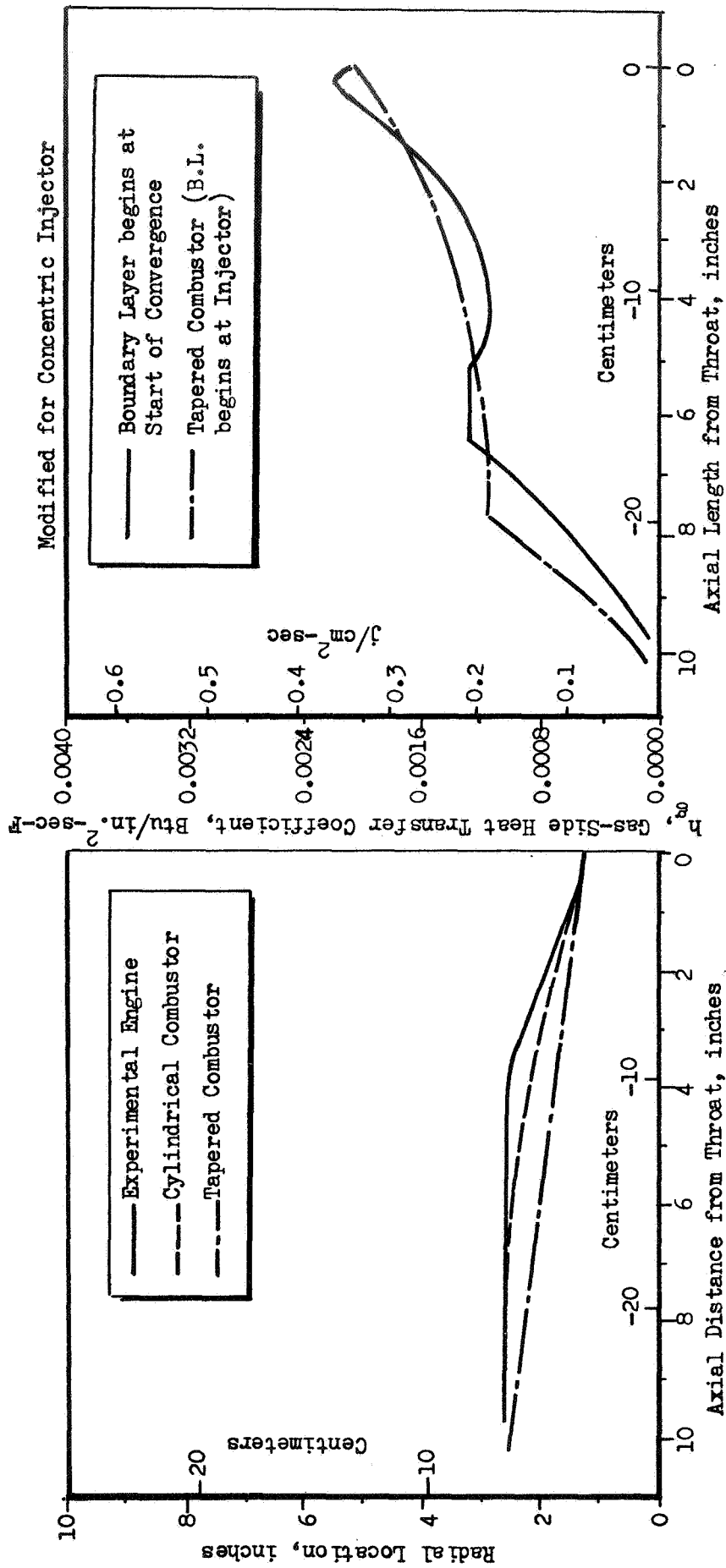
Figure 99. Combustion Chamber Configuration

TABLE 66

MAXIMUM COMBUSTION – SIDE WALL TEMPERATURES

	Full Thrust		10:1 Throttled	
	Throat	Combustor	Throat	Combustor
Conventional Contour, F (K)	1390 (1028)	1670 (1180)	1045 (835)	1750 (1220)
Tapered Contour, F (K)	1310 (985)	1525 (1095)	1050 (838)	1650 (1170)

Effect on η_c*

Tests with hydrogen (Contract NAS 8-20349, Ref. 15) indicated that for a given chamber length, higher performance was achieved with a lower contraction ratio chamber, using a concentric injector. The reason for this is two-fold: 1) the smaller cross section of the chamber confines the methane to the vicinity of the element and, thereby, promotes mixing; 2) the higher velocity of the methane and combustion gases in the chamber also promote mixing and vaporization of the FLOX. Consequently, even though the tapered chamber has a lower L^*, it is expected to have good perform- ance.

Effect of Shape on Fabrication and Weight

Fabrication and inspection of the combustion chamber is facilitated by the constant taper design. Machining of the channels and of the chamber contour which also determines the channel height profile is accomplished by following a template. The radial location of the template is generally easier to establish than the axial position. Smaller convergence angles require less accuracy in the axial location of the template for a given accuracy of the hot gas wall thickness and channel height. The tapered

263

chamber, having the smallest convergence angle, provides the easiest template setup conditions. Direct measurement of the wall thickness in the combustion chamber with calipers at all stations after machining is possible with the tapered chamber. Inspection time requirements are thereby reduced compared to requirements for the conventional shape combustor. Since the tapered combustor has a smaller surface area and a smaller average diameter the weight will be slightly less (approximately 0.5 lbs (0.027 kg) less) and the structural shell will also weigh less.

Selection

Based on projected test data the tapered combustor appears to be superior and has been chosen as the flight weight design configuration. The performance and heat transfer characteristics of the tapered combustor should be experimentally verified.

CHANNEL DESIGN SELECTION

Many design combinations for the channel configuration were examined. The ideal geometry from a weight standpoint is a constant land width channel. Stress requirements, however, fix the maximum channel width for a given wall thickness, and thus channel branching is required if the ideal geometry is to be approached in a physical design without undue wall thickness, using electroformed nickel channels. At the other extreme, the easiest and cheapest design would be a constant width channel from injector to nozzle exit, with no branching. However, this design has the highest weight and pressure drop. The compromise finally selected was a design with no branches, two step changes in nozzle width (ϵ = 4 and 16) based on wall temperature and stress considerations, and selection of a minimum

channel height in the nozzle of 0.05 inch (0.127 cm) from weight, pressure drop, and potential blockage considerations. This design is relatively low cost, and has very little weight penalty over the optimum configuration.

Channel Geometry

The following geometrical restrictions were placed on the design.

Minimum Wall Thickness = 0.025 inch (0.064 cm)

Minimum Land Width = .030 inch (0.076 cm) - (previous fabrication
experience)

Land Width   Channel Width in Throat (2-D conduction)

Other operating and design features included:

a) 10/1 throttling capability
b) Ease of manufacture
c) Minimum stress safety factor = 2.0 based on gross distortion
d) Theory at 1700 F (1200K) wall temperature in the throat and combustor
d) No branches or step changes in channel width upstream of the throat, due to the necessity of reasonably close tolerances in order to minimize pressure drop and maintain the design wall temperatures.

Stress analysis indicated the full thrust condition to be the most critical design point. Channel widths in the nozzle are based on stress requirements for electroformed nickel, using a safety factor of 2 based on gross distortion theory for rectangular channels. To permit wider channgels in the nozzle, a wall thickness of 0.040 inch (0.10 cm) was used for nozzle area ratio greater than 4.0. Channel width step changes occur at nozzle area ratios of 4 and 16. Nozzle channel widths were chosen to utilize standard cutter sizes. Channel heights in the nozzle were chosen to maintain a constant mass velocity beyond $\epsilon = 4$.

265

The throat was stressed for a safety factor of 2.0 at 1700 F (1200K) wall temperature, using a 0.025-inch (0.064 cm) wall thickness. The remainder of the combustor was stressed for a safety factor of 2 at its maximum allowable operating temperature. A minimum wall temperature margin of 150 F (83K) at full thrust was then imposed on the design. The new wall temperatures determined the required coolant mass velocities, and the corresponding channel heights. Consequently, the allowable wall temperatures in the combustor are less than in the throat, due to the lower heat fluxes and corresponding reduced wall ΔT.

Ease of fabrication was next considered, in terms of the channel height profile. Additional restrictions in the design imposed by fabrication considerations were:

1) constant height throughout throat radius of curvature
2) depth variation in combustor should be designed so that no reversal in the radial direction is required of the cutter, in order to hold closer tolerances
3) preferably design channels with constant taper angle or constant radial location.

A trade-off study was conducted to determine additional pressure drop requirements imposed by fabrication tolerances. The final selection was a channel whose height decreased linearly along two taper angles from the injector to an axial location 2.0 inches (5.08 cm) upstream of the throat, and a constant channel height section from this point through the throat. The maximum channel height at the injector end was selected as small as permitted by pressure drop considerations, in order to reduce required manifold sizes. The channel exits have been designed to diffuse the coolant flow, thereby recovering some of the dynamic pressure at the exit.

266

Otherwise, the full velocity head would be lost as the coolant entered
the exit manifold. This is expected to reduce the coolant pressure drop
by about 10 psi $(70kN/m^2)$.

Wall Temperatures

The regenerative cooling program used to design the channels and determine
pressure drops utilizes one-dimensional analysis to calculate wall temp-
eratures. Consequently, a two-dimensional thermal analysis was employed
to determine the temperature distribution at certain critical locations
in the combustor and throat for full thrust and throttled operation. For
this analysis, the channels were assumed to have a 0.030-inch (0.076 cm)
Nickel 200 closeout and a 0.090-inch (0.029 cm) Hastelloy C backup structure.
The maximum wall temperatures are summarized in Table 67.

TABLE 67

MAXIMUM WALL TEMPERATURES, TAPERED CHAMBER

No. Channels	Full Thrust			10:1 Throttled		
	72	90	120	72	90	120
Throat T_{WG}, F(K)	1350(1005)	1310(985)	1260(955)	1070(845)	1050(838)	970(790)
Combustor T_{WG}, F (X = 7.5-inch) (19.1 cm)	1630(1155)	1525(1095)	1450(1060)	1740(1220)	1650(1170)	1550(1115)

As a result of the 2-D analysis, the minimum number of channels considered
for the design was 90, because of combustor wall temperatures at 10/1
throttled conditions. While additional channels would further reduce wall
temperatures and stress levels, this must be traded off with additional
cost and with tolerance considerations.

Tolerance

The philosophy adopted with regard to tolerances is that the nominal design would represent the highest temperature operating condition. This meant that nominal channel dimensions would also be maximum dimensions. Tolerance effects, then, would result in lower wall temperatures and higher pressure drops. Typical width and height tolerances resulted in the following pressure drop values at full thrust:

TOLERANCE EFFECTS ON JACKET ΔP

Number of Channels	90	120
	psia (k N/m^2)	
Tolerance, inches (cm)		
Nominal	230 (1580)	230 (1590)
−0.004W (−0.0102W) −0.006H (−0.0152H)	325 (2240)	340 (2350)
−0.003W (−0.00762W) −0.010H (−0.0254H)	360 (2480)	380 (2620)

Above values are for a roughness of 30 μ inch (7.62 microns) and a fixed coolant jacket outlet pressure of 1090 psia (7516 k N/m^2). Pressure drops include a one velocity exit head loss. Pressure drops would increase about 30 psi (210 k N/m^2) if the roughness increased from 30 to 100 μ inch (7.62 to 25.4 microns)

In addition, the latter tolerance (−.003 width, −.010 inch height (−.008 width, −.030 cm height)) results in approximately 100 F (56K) reduction in wall temperature at the throat and 70 F (39K) reduction in the combustor [7.5 inch (19.1 cm) upstream of the throat]. This increases the stress margin even though the coolant pressures are higher. Similarly, nominal wall thicknesses were taken as minimum values. Even though larger wall thicknesses result in higher wall temperature, a net increase in the stress safety factor is obtained.

While wider tolerance limits imply potential cost savings it is desirable to hold a reasonably close tolerance for reasons of stress, pressure drop, and weight. A maximum height tolerance of $\pm$ .005 inch was found to be a satisfactory compromise.

Weight

Channel (combustion-side wall and loads) weight is a weak function of both the combustor shape and the number of channels. For the tapered combustor, the channel weight without closeout or backup structure is 32.2, 30.9, and 28.6 lbs for 72, 90, and 120 channels respectively. With the channel closeout shown in the design, the 90-channel thrust chamber would weigh approximately 54 lbs. Of this, about 75% of the weight is in the nozzle downstream of ϵ = 16.

Uprating Characteristics

When the 90 and 120 channel chambers with constant tapered combustion zones designed for 500 psia chamber pressure are operated at 800 psia the limiting factor becomes the stress induced by coolant pressure in the nozzle as shown in Table 68. The combustion zones still have acceptable safety factors at 800 psia because the channel dimensions in this region were designed to maintain a wall temperature (two dimensional) of 1500 F or less at 500 psia. The maximum wall temperatures at 800 psia are 1645 F and 1585 F for the 90 and 120 channel designs respectively.

In order to maintain a safety factor of 2.0 in the nozzle the channel width would have to be decreased to 0.094 inches in the $4 \leqq \epsilon \leqq 16$ region and to 0.156 inches in the ϵ = 16 region. These modifications would increase the jacket pressure drop by approximately 10 psi and increase the weight by 2 pounds.

TABLE 68

CHANNEL STRESS SAFETY FACTORS

TAPERED CHAMBER

500 psia (3450 k N/m^2) Design Operated at 800 psia (5520 k N/m^2)

Axial Location			Stress Safety Factor	
			No. Channels	
ϵ	X, in.	(cm)	90	120
60	26.47	(67.4)	1.5	1.5
16+	7.3	(18.6)	1.5	1.5
4+	2.22	(5.65)	1.4	1.8
1	0	(0)	2.3	2.7
	-1.5	(-3.8)	1.9	2.2
	-6.3	(-16)	2.2	2.6
	-7.5	(-19.1)	2.0	2.4

The results of these analyses indicate that only a slight modification of either the 90 channel or the 120 channel designs would be required to up-rate the thrust chambers from 500 psia (3450 kN/m^2) operation to 800 psia (5520 kN/m^2) operation.

DESIGN CHARACTERISTICS

This section covers the design characteristics of the selected 90 channel, tapered combustor configuration. Alternate designs considered in the study are included in Appendix B.

The inner nozzle contour and the corresponding gas side film coefficients at a chamber pressure of 500 psia (3450 kN/m^2) are shown in Fig. 100 and 101. Coolant channel width, height, and land width are presented in Fig. 101, 103, and 104 respectively. Channels are designed in constant width sections with step changes at area ratios of 4 and 16. The step locations were chosen to prevent the land width from dropping below the minimum value of 0.30 inches (7.62 cm). The channel widths and heights are faired in at the steps to avoid unnecessary pressure drops. Since the heat fluxes are low, and the channels are thermally over-designed in the nozzle, fairing the channel at the two step locations should not be critical. Channel height was fixed at 0.050 (0.127 cm) inch from the nozzle exit to an area ratio of 16. Between area ratios of 4 and 16, the height was tapered to maintain a constant mass velocity. Channel height is constant around the throat radius, and then increases in two linear tapers to the injector plane.

The wall temperature profile is shown in Fig. 105. The wall temperatures are very low at the exit, where the channels are over-designed to save weight. The step change in wall temperature $(X/R_T \simeq 2)$ results from a change in channel width at a nozzle area ratio of 4. One-dimensional temperatures are less than 1500F (1090K) throughout.

271
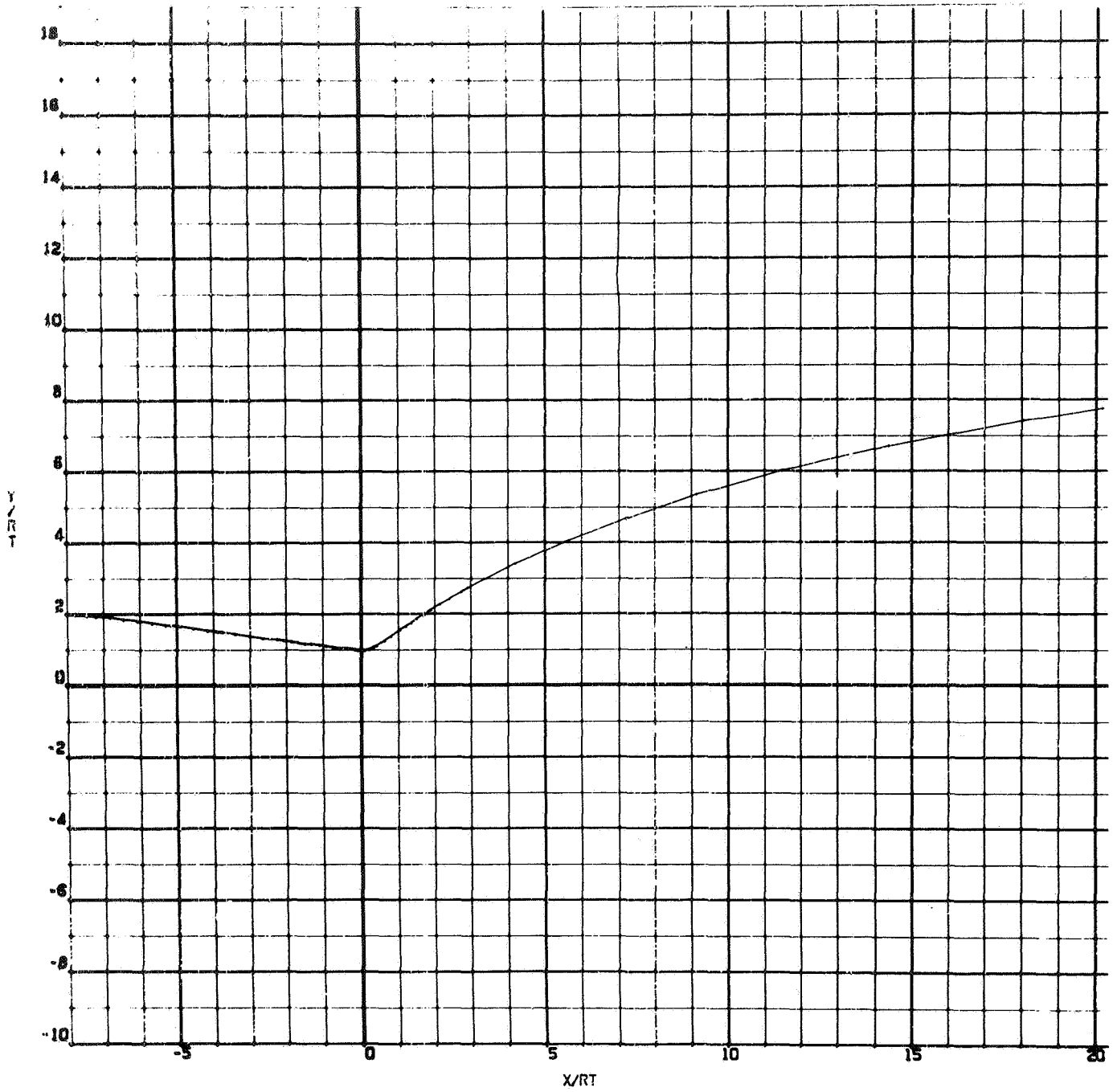
Figure 100. Thrust Chamber Contour
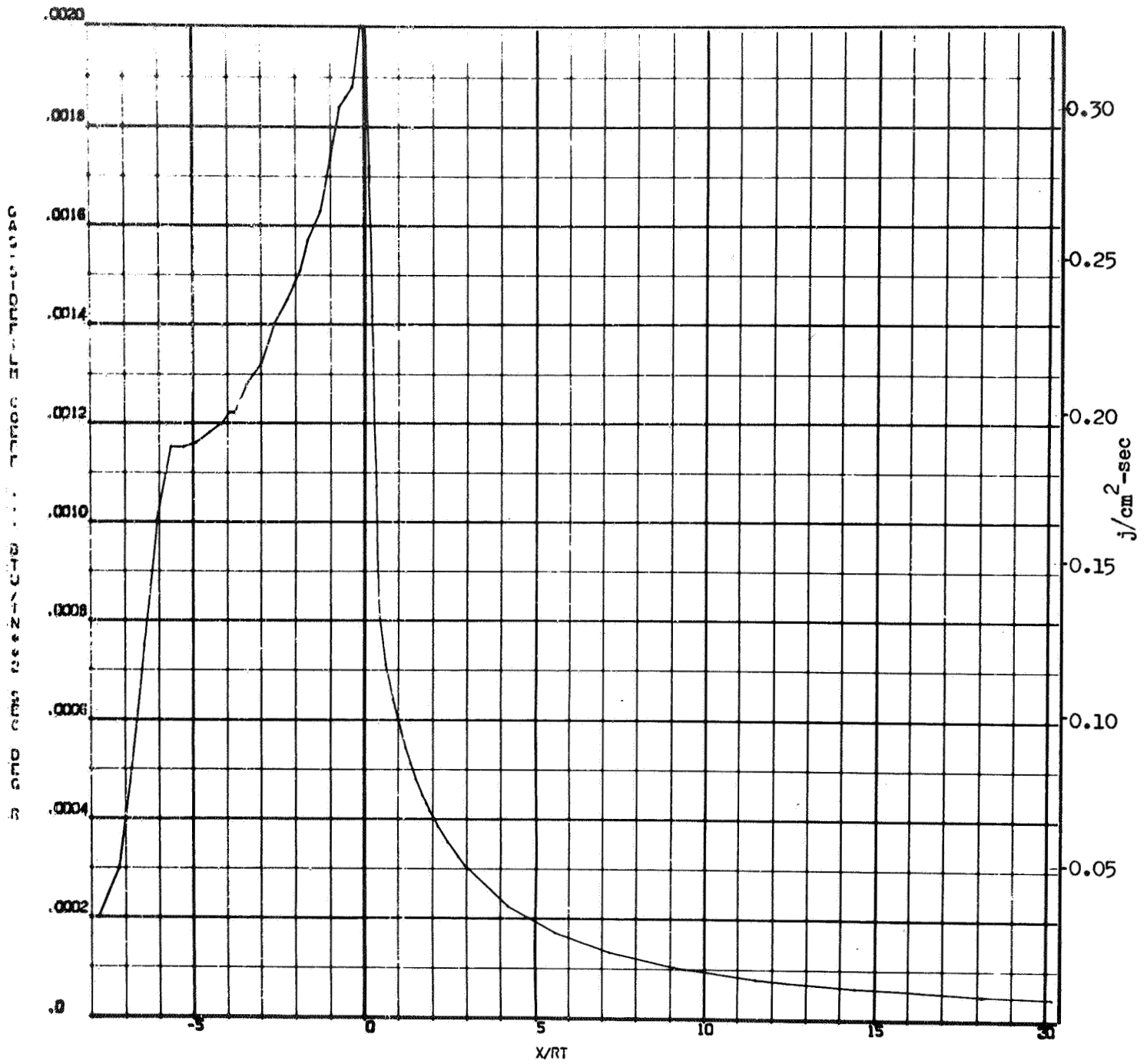
Figure 101. Gas-Side Film Coefficient Profile

273
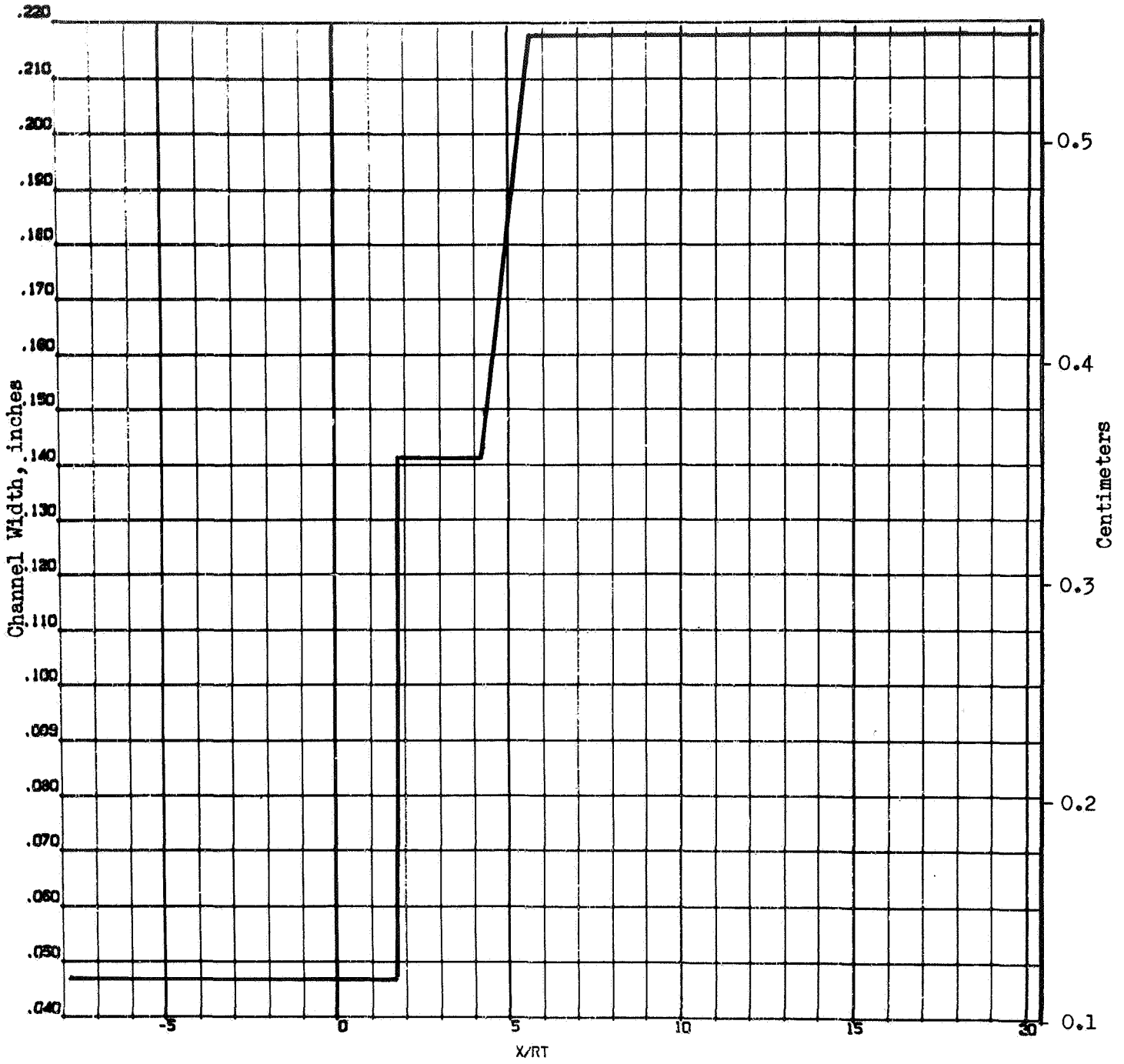
90 Channels

Figure 102. Channel Width Profile

274
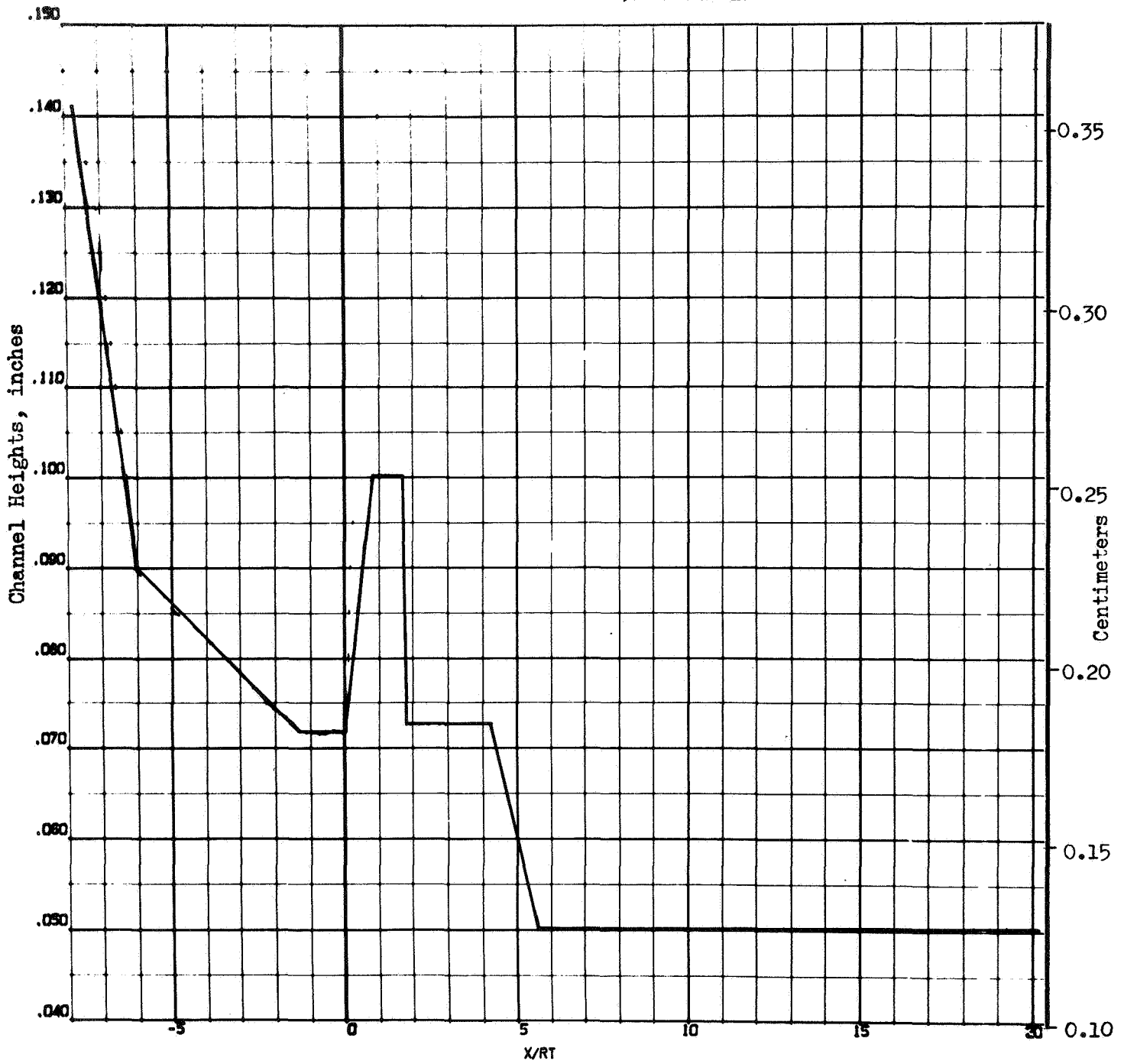
Figure 103. Channel Height Profile

275
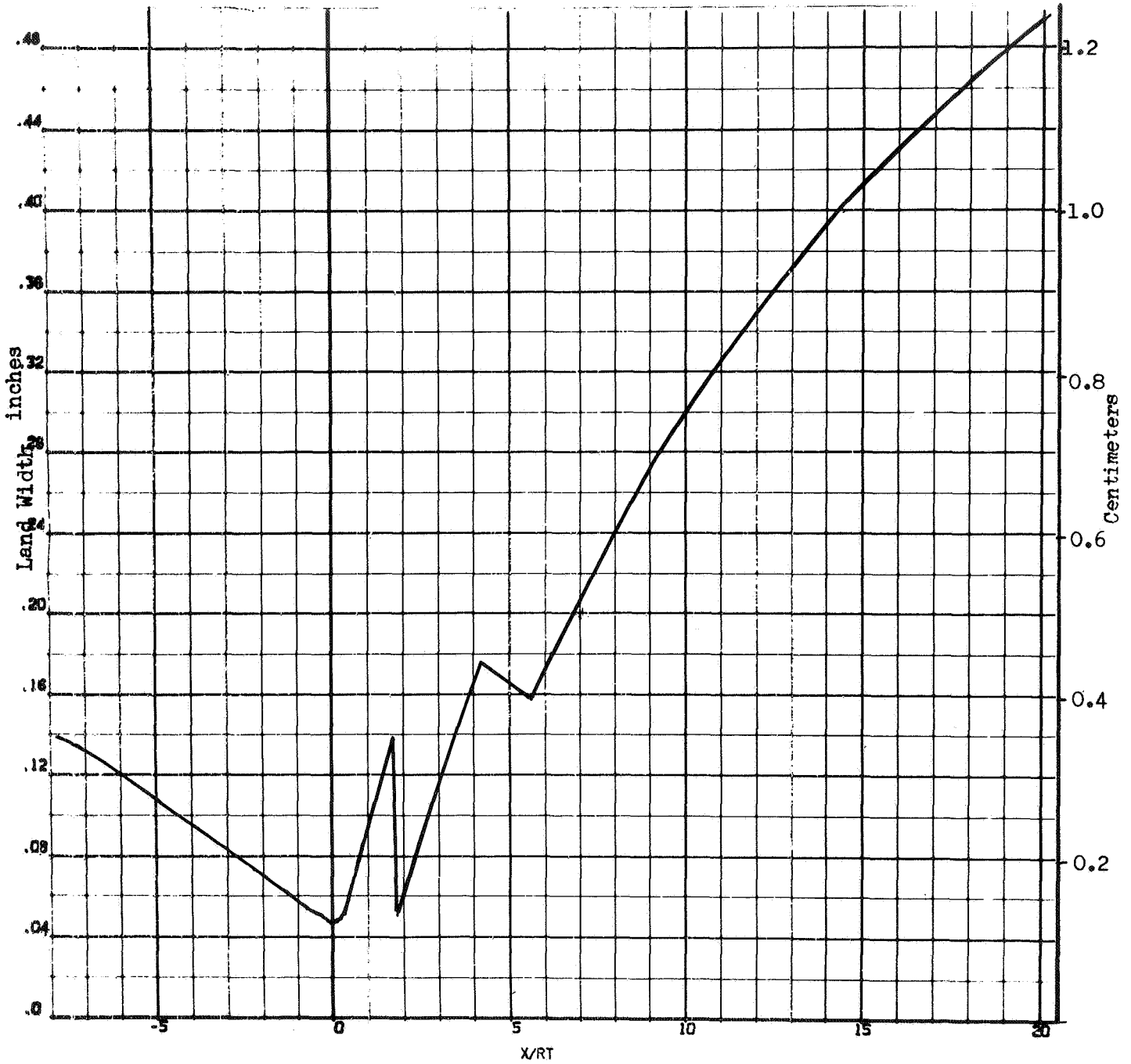
Figure 104 . Land Width Profile
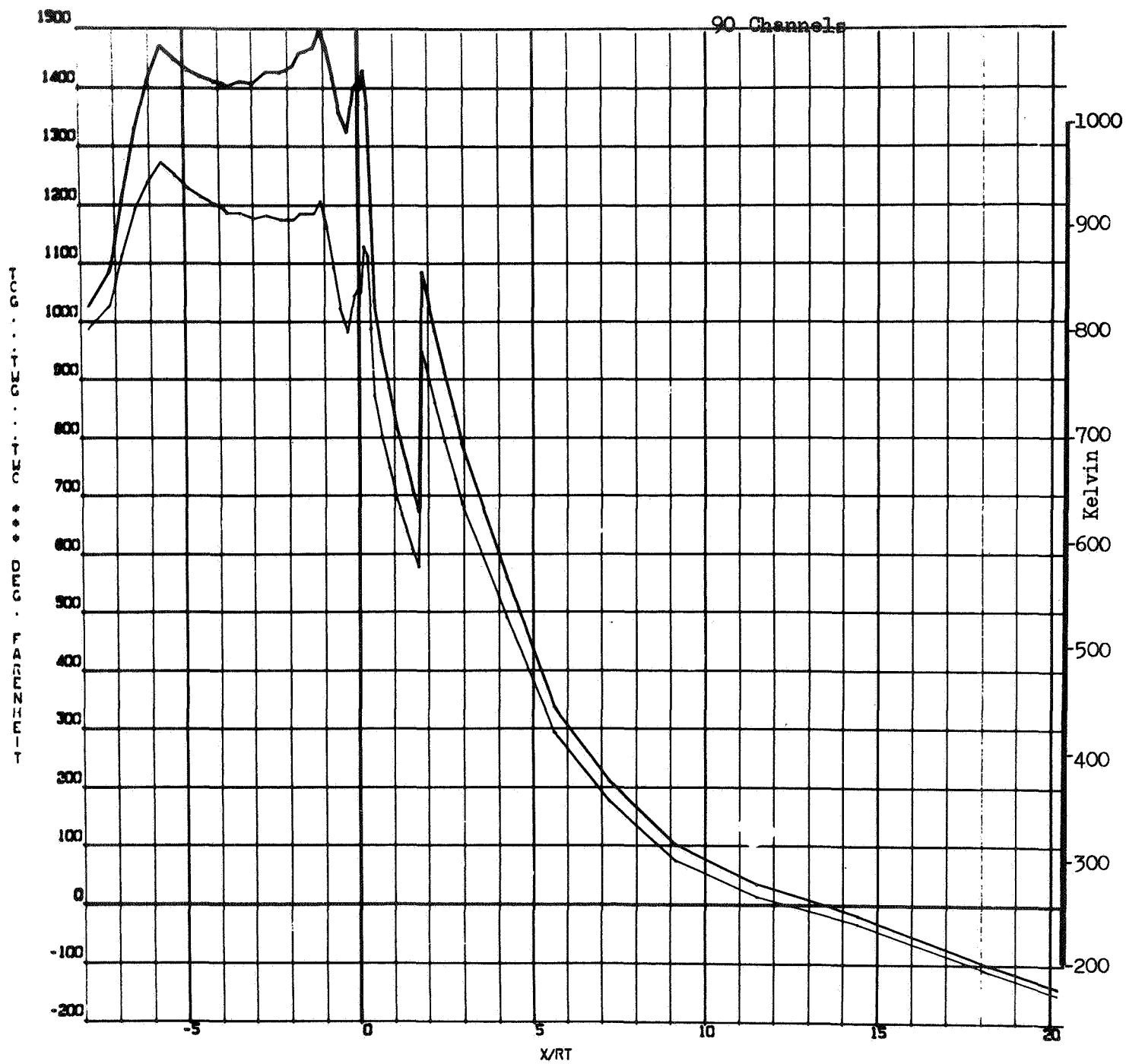
Figure 105. One-Dimensional Wall Temperature Profile

Because of the two-dimensional heat conduction characteristics of channels, the critical cooling regions near the throat and 5.5 inches (18.6 cm) upstream of the throat were examined in detail. Results for the 90 channel configuration are shown in Fig. 106. In general, the two-dimensional analysis indicates that the throat will run approximately 100 F (55K) colder than predicted on a one-dimensional basis, while the combustor would run about 70 F (39K) higher at mid-land. Mid-channel values in the combustor are close to the one-dimensional design values.

Backwall temperatures are about 100 F (55K) higher than the methane bulk temperature in the throat, and about 200 F (110K) higher in the combustor. For purposes of analysis, a 0.030 inch (0.076 cm) Nickel 200 closeout and a 0.090 inch (0.229 cm) Hastelloy C backup structure was assumed. Very little difference in the temperature distribution would be expected using only an 0.080 inch (0.203 cm) nickel backup, due to the flat temperature profile.

The coolant bulk temperatures at full thrust and at 10:1 throttled conditions are shown in Fig. 107. About half the total heat input to the cooland occurs in the nozzle. Coolant exit temperatures are 1300 R (620K) and 1750 R (970K) at full thrust and at throttled conditions, respectively. Coolant mass velocity and pressure drop profiles were determined based on a 30 μ -inch (7.62 micron) roughness. Most of the pressure drop occurs in the combustor, with only about 15-percent occurring downstream of the throat. This is partly a result of the higher combustor heat fluxes and partly due to higher coolant temperatures. The latter effect increases pressure drop through both higher mass velocity requirements and reduced density.

430	430	431
433	433	432
465	437	411
558	517	Methane
775	706	
948	914	979
1120	1121	1138
1291	1301	1310

Combustion Gas Side

Throat

970	969	968
976	970	960
1013	938	805
1089	1073	985	Methane
1241	1223	1112
1348	1315	1249 1265
1434	1406	1371
1527	1502	1466
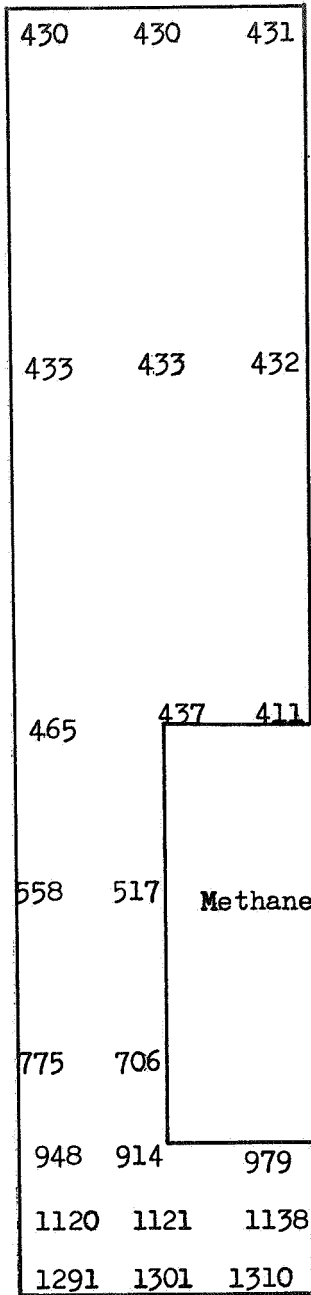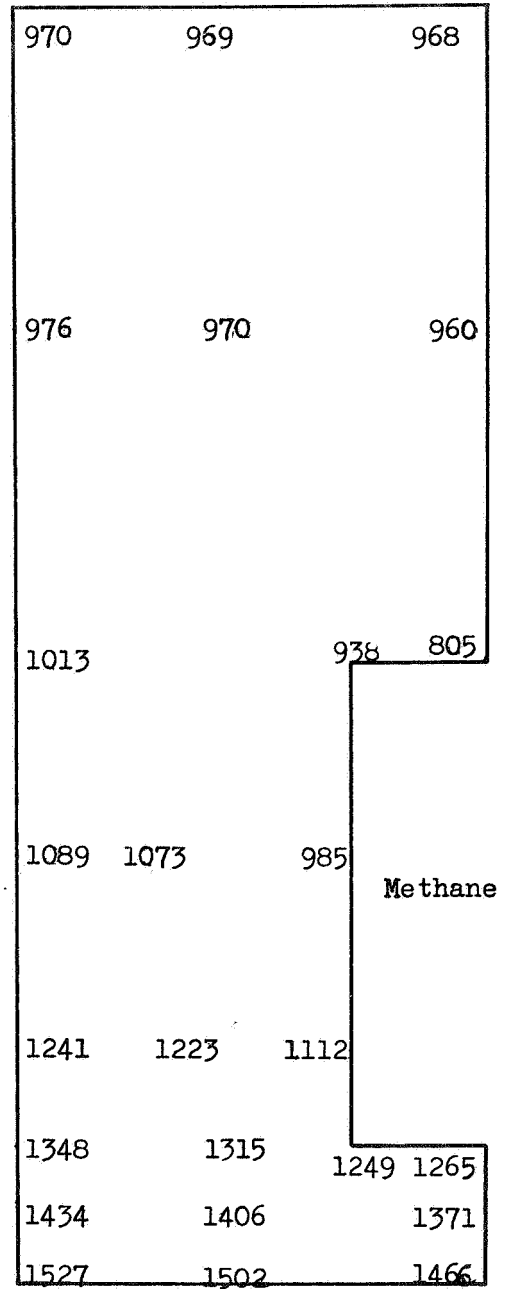
Combustion Gas Side

X = -7.5 inches   (-19.1 cm)

Figure 106   Thrust Chamber Wall Temperature, Nominal Thrust.
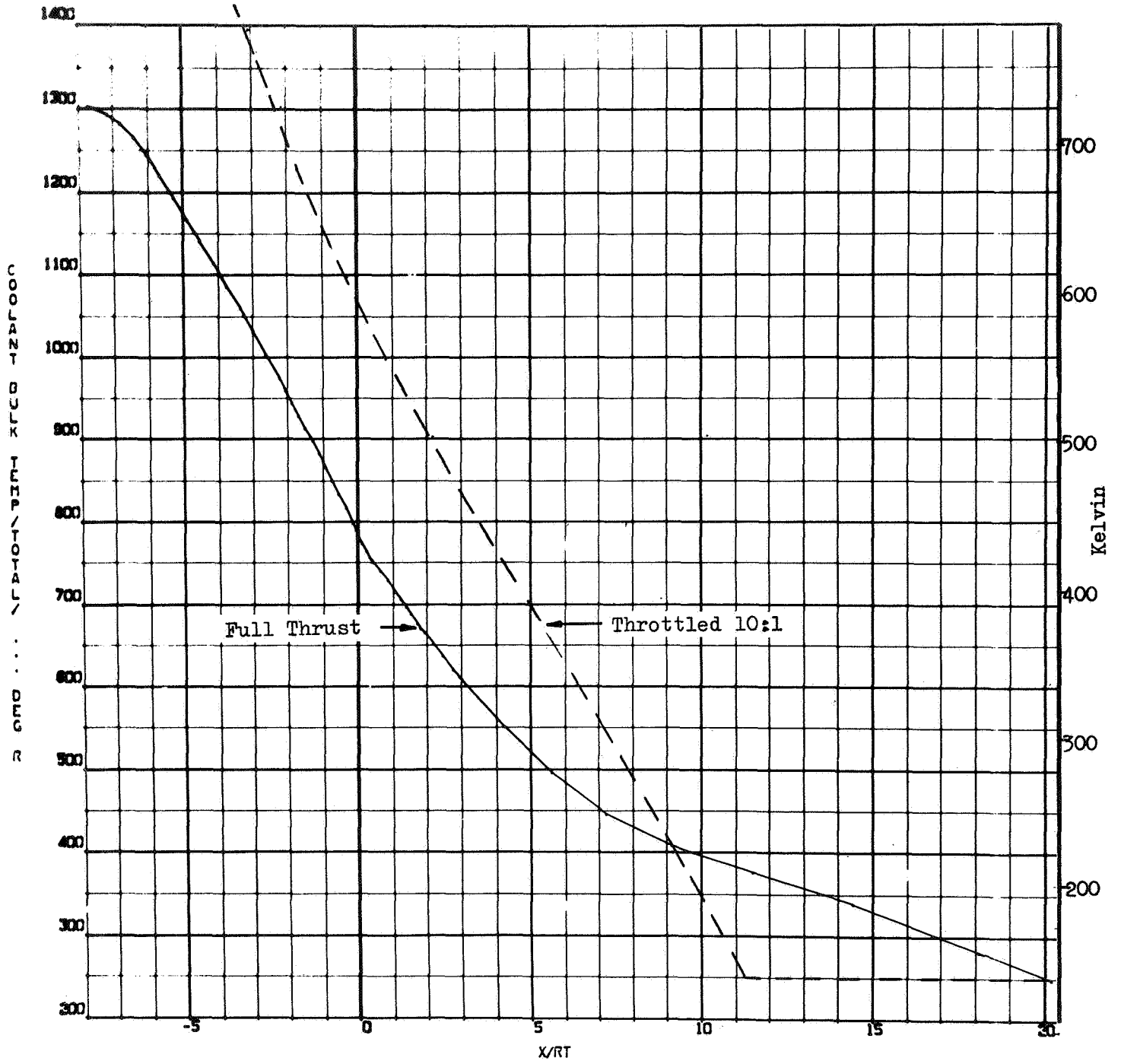
Figure 107 . Coolant Bulk Temperature Profiles.

Throttling Characteristics

Thrust chamber characteristics were analyzed over a 10/1 throttling range, holding mixture ratio constant at 5.25. The coolant bulk temperature, along with the two phase region for the 10/1 throttle case was presented in Fig. 107. A summary of the methane phase change locations is presented in Table 69. The heat fluxes are low in the phase change region. As a result, no cooling problems are anticipated with the over-designed channels. The pressure drop through the coolant jacket is 45 psi (310 kN/m^2). The chamber design is predicted to operate satisfactorily in terms of wall temperatures and stress requirements over the full throttling range profile in this region.

Two dimensional wall temperatures are shown for the throat and combustor at the 10/1 throttle condition in Fig. 108. Because of higher coolant temperatures, the backup structure temperatures increase as the engine throttles. Although the wall temperature in the combustion zone approaches 1650 F (1170K) at throttled conditions, the coolant pressures are considerably less than at full thrust and the stress safety margin is therefore satisfactory.

Idle Mode

Idle mode operation was analyzed over a range of chamber pressures and the maximum mixture ratios at which various temperatures would be acceptable were described (Fig. 109). A maximum discharge temperature for the methane was fixed at 1500 F (1030K), and this condition determined a maximum allowable mixture ratio.

In addition, maximum wall temperatures of 1600 F (1145K) and 1700F (1200K) were examined. In general, as an engine throttles, the regions with higher coolant mass velocity throttle better than regions of low mass velocity. This is

TEMPERATURES IN DEGREES FAHRENHEIT
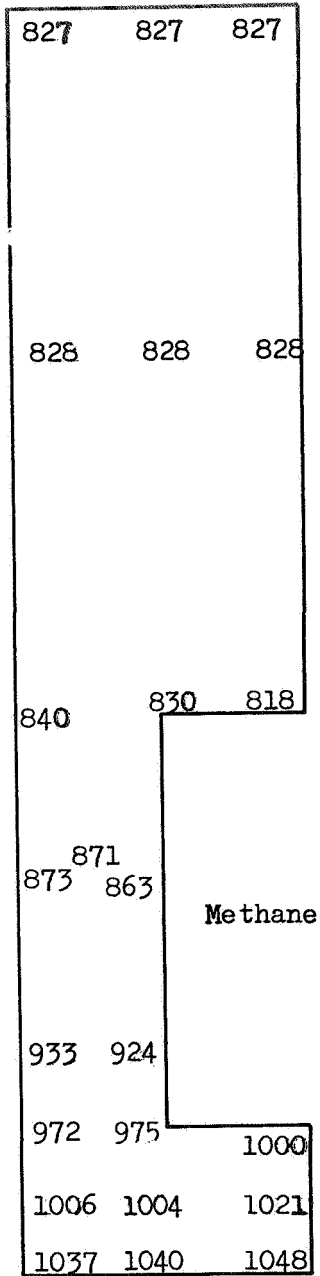
Combustion Gas Side

Throat
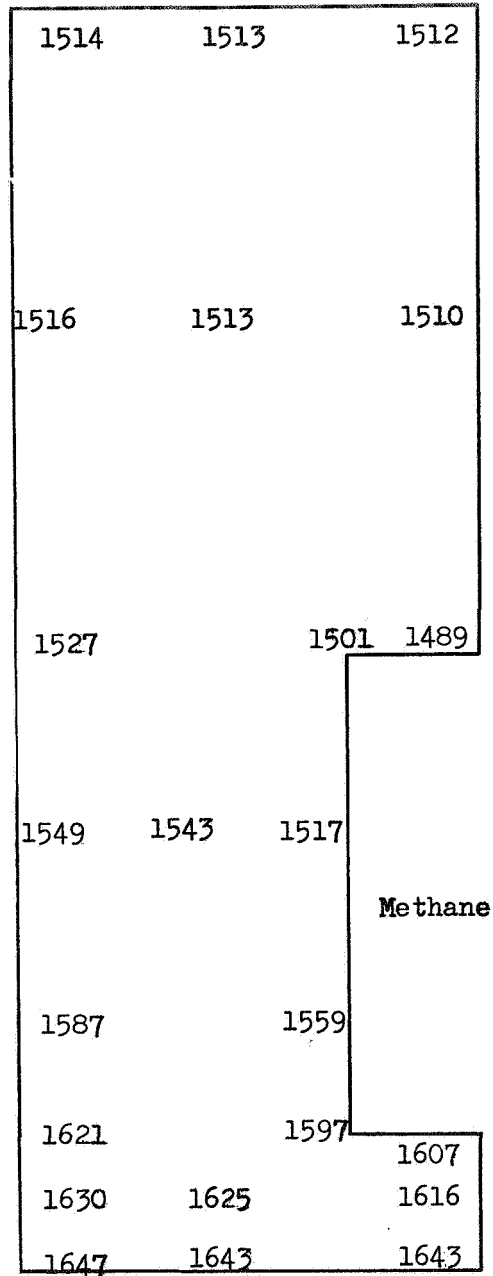
Combustion Gas Side

X = -7.5 inches   (19.1 cm)

Figure 108 . Thrust Chamber Wall Temperature, (10:1 Throttled).

TABLE 69

PHASE CHANGE LOCATIONS

$$T_{in} = 245R, \quad MR = 5.25$$
$$(135k)$$

Chamber Pressure psia, k N/m^2)		Inlet Pressure, psia, k N/m^2)		Phase Change Region, ϵ	Heat Flux	
					BTU/in^2-sec	J/cm^2-sec
500	(3450)	1310	(9050)	*	----	---
300	(2070)	790	(5450)	*	----	---
250	(1270)	660	(4550)	40	0.29	47.5
100	(690)	260	(1800)	55–29	0.10–.20	16.3–32.7
50	(345)	130	(900)	60–35	0.050–.10	8.2–16.3

*Supercritical

283

$T_{Wall} - 1600\ F\ (1145\ K)\ (I\text{-}D\ Temperatures)$

$T_{Bulk} - 1500\ F\ (1090\ K)$

0.025 Nickel Wall   Tapered Combustor
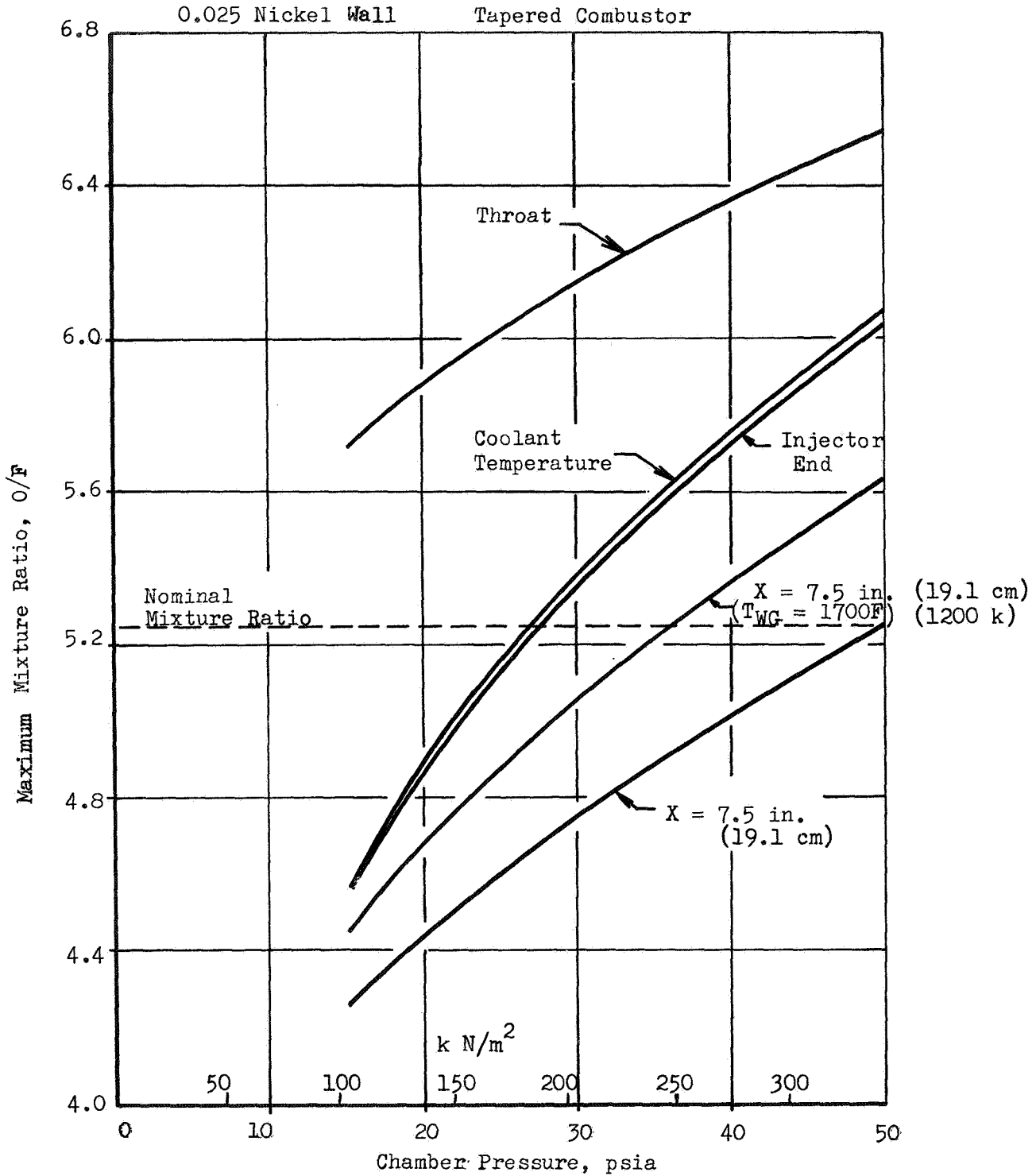
Figure 109. Heat Transfer Limits for Idle Mode Operation.

partly the reason why the throat has higher mixture ratio limits than the combustor. In addition, due to the higher coolant temperatures in the combustor, the wall temperatures are more sensitive to the coolant discharge temperature.

The combustor at the most critical cooling point located 7.5 inches (191 cm) upstream of the throat determines the maximum allowable mixture ratio based on either a 1600 F (1145K) or 1700 F (1200K) wall temperature limit. The temperature values of Fig. 109 are based on steady-state conditions. In idle-mode start, considerable time may be necessary to attain steady-state conditions. It may, therefore, be possible to operate at mixture ratio values above those shown for 10-20 seconds without achieving the indicated temperatures. In addition, higher temperatures than those shown may be encountered without exceeding the thrust chamber strength capability. Idle-mode operation should, therefore, not be restricted to mixture ratios below nominal without detailed examination of the operating requirements.

FLIGHT WEIGHT THRUST CHAMBER DESIGN AND FABRICATION

The flight weight thrust chamber consists of a one-piece slotted nickel coolant shell which is reinforced through the combustion chamber area by an Inconel 625 structural backup shell. A "J" weld joint is provided at the forward end of the combustion chamber to facilitate the attaching of the injector. The tapered straight wall chamber and the constant radius throat minimize fabrication complexity and cost.

The coolant shell will be electroformed on a two piece mandrel which is split at the throat. Although the nominal engine length is dictated by the $\epsilon = 60$ area expansion ratio, the mandrel is of a length to allow for additional axial buildup in the event a mounting surface aft of the $\epsilon = 60$ plane is required for attaching a nozzle skirt.

285

The initial electroformed nickel layer after contour machining is 0.166 inches (0.422 cm) thick at the forward end, 0.096 inches (0.244 cm) thick at the throat and 0.090 inches (0.229 cm) at the aft end. For the slot sizes considered, slot width can be held to $\pm$ 0.0015 inches (0.0033 cm) and slot depth can be held to $\pm$ 0.005 inches (0.013 cm). A smooth transition occurs in the area where the hot gas wall thickness changes (ϵ = 3). The only area where the slot contour does not follow the internal chamber contour is at the end where the slots remain on the 7.5 degree (0.131 rad) cone angle while the chamber contour becomes cylindrical for a short length to facilitate injector installation. Once the slots are machined, they are filled with wax and the entire part is activated and placed into the tank for the final electroform layer. This second electroformed layer requires additional nickel buildup at both ends of the part to provide a mounting surface for the manifolds and an attach joint for the backup structure. After electroforming, the wax is removed from the slots and the surface is contour machined. Manifold welding tabs are machined in the nickel at both ends with a 0.050 inch (0.127 cm) step machined in the forward end to accommodate the backup structure.

The coolant shell in the thrust chamber is relatively weak in the circumferentail direction as compared to the longitudinal direction because only the inner and outer walls of the channels resist circumferential loading while the webs between channels as well as inner and outer walls resist longitudinal forces. The electroformed nickel used in the cooling channel section, while being advantageous for heat transfer and fabrication requirements, has relatively low strength and is not as efficient as a material such as Inconel 625 for resisting stress. Therefore, a shell of Inconel 625 was added to provide hoop strength for the combustion chamber. Since the nickel channel section can adequately carry longitudinal loads, the Inconel 625 shell is not brazed to the nickel channel section.

286

Differential axial thermal strain between the shell and the channel section will result in longitudinal loading that may produce minor longitudinal yielding of the shell. The result depends on friction; and since the exact friction force is unpredictable, the limits of axial interaction between shell and channel section were examined. No critical condition was determined for the extreme cases of with and without friction.

The backup structure is spun from a sheet of Inconel 625 to a mandrel which has the same inner contour as the outer surface of the nickel chamber. The wall thickness of the spinning is tapered from 0.050 inch (0.127 cm) at the forward end to a 0.030 inch (0.076 cm) at the throat. Once spun, the shell is split longitudinally, placed on the chamber, and seam welded together. The shell is then welded to the chamber at the forward end.

The Inconel 625 manifolds are welded in place with the inlet and outlet ducts being welded to the manifolds after the manifolds are welded to the chamber. The cross section of the manifolds are half circles with an internal diameter of 0.700 inch (1.778 cm) and a wall thickness of 0.050 inch (0.127 cm). The wall thickness was selected to obtain an even weld joint with the nickel tabs which are structurally required to be 0.050 (0.127 cm) thick. Inconel 625 manifolds are used in order to be compatible with the inlet and outlet lines.

A box sectioned support ring is welded just below the forward coolant manifold to provide support for the gimbal actuator rigging and the turbopump mounts. Figure 110 is the thrust chamber design drawing.

SECTION ⟨B⟩ = ⟨B⟩

.080 (.203)
.025 (.064)
.046 (.117)

SECTION ⟨C⟩ = ⟨C⟩

(.076) .030 .030 (.076)
.025 (.064)
.046 (.1

SECTION ⟨D⟩ = ⟨D⟩

.030 (.076)
.025 (.064)
.046 (.117)

SECTION ⟨E⟩ = ⟨E⟩

.035 (.889)
.040 (.102)
.141 (.358)

20.38 DIA.
(51.77)

€ = 60

€ = 40

€ = 16

€ = 4

℄ THROAT

1.50 R
[3.81 cm]

7.5°

2.631 DIA. [6.683]

26.47
(67.23)

10.75
(27.31)

GIMBAL ACTUATOR
ATTACH POINT

5.262 DIA.
(13.365)

SECTION ⟨A⟩ = ⟨A⟩

UNITS — INCHES
(Centimeters)

SECTION F—F
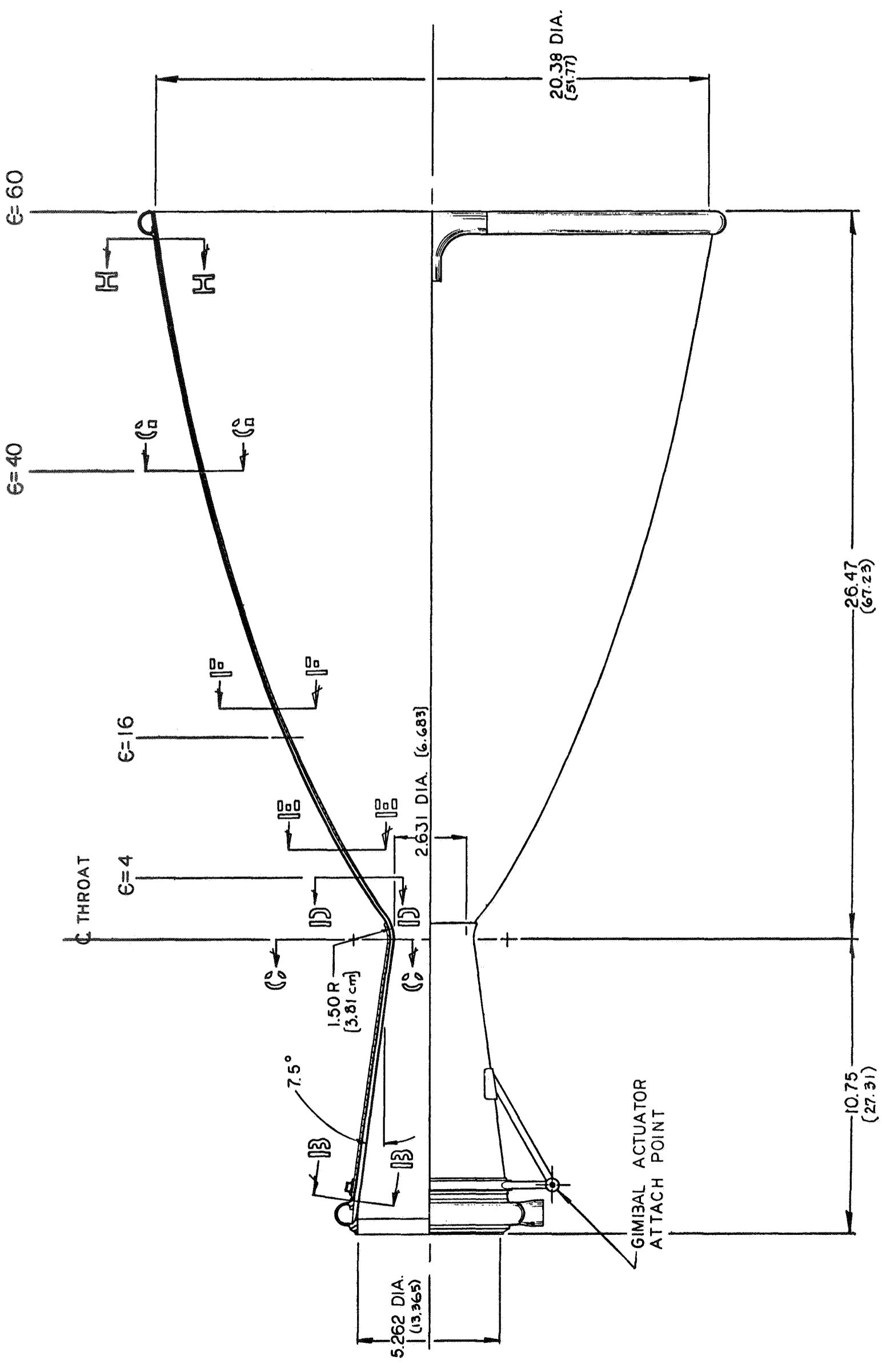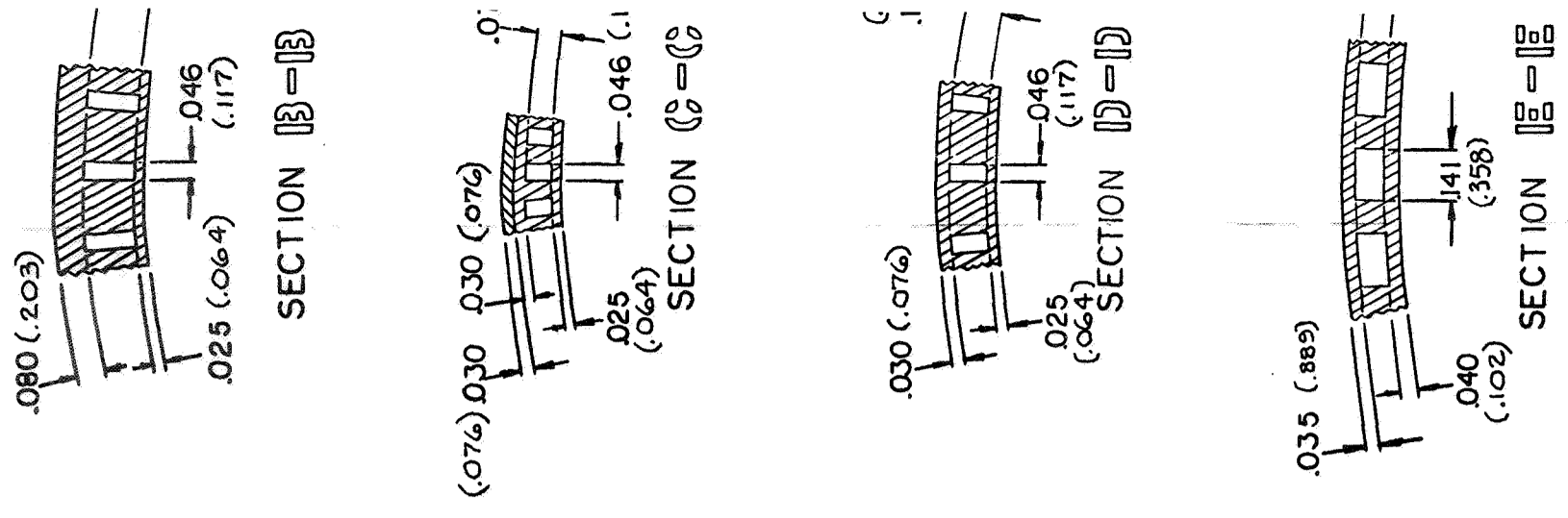
SECTION G'—G'

SECTION H—H

SECTION B—B

SECTION C—C

SECTION D—D
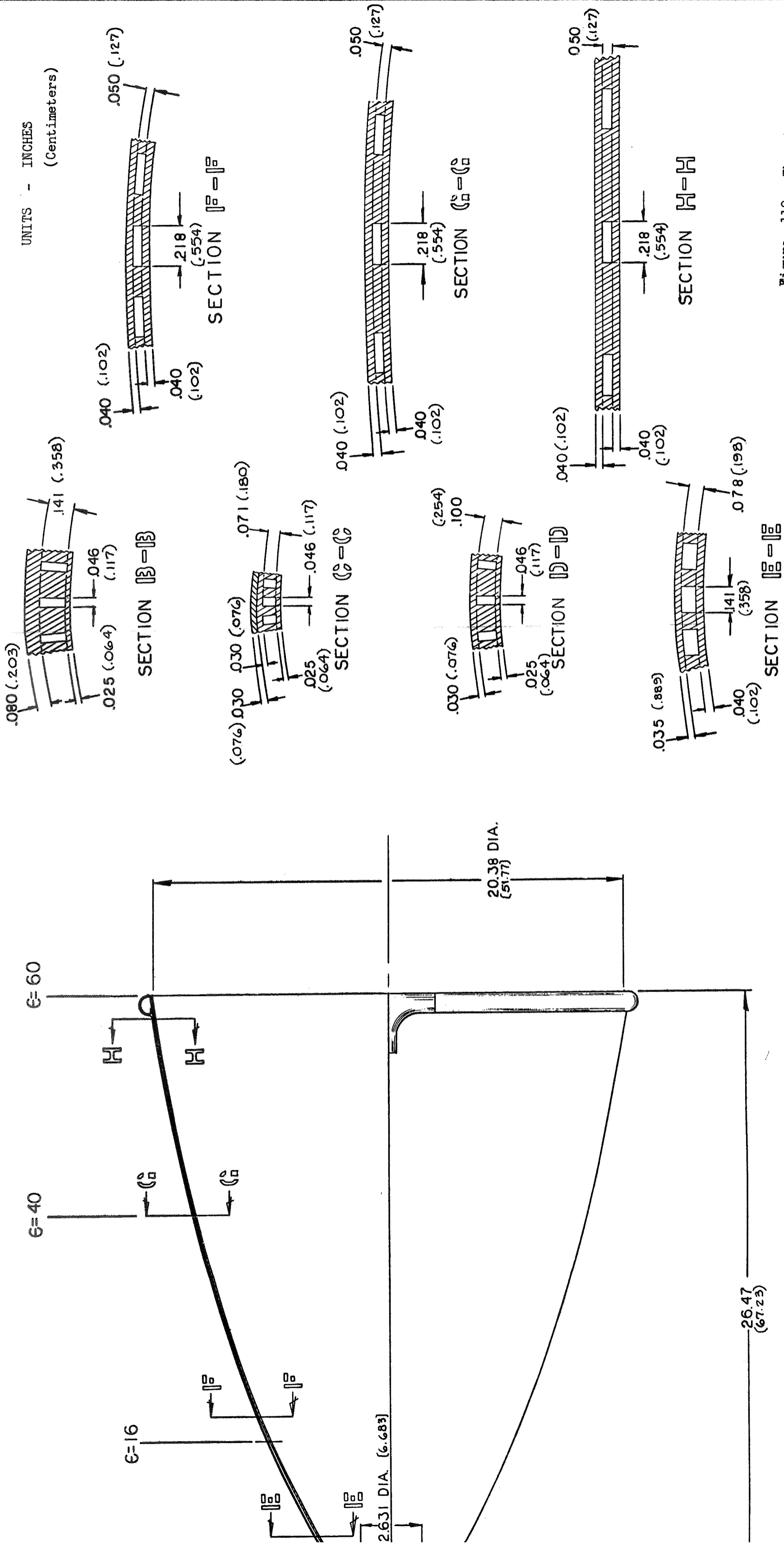
SECTION E—E

Figure 110. Thrust Chamber Design

ε=60

ε=40

ε=16

20.38 DIA.
(51.77)

26.47
(67.23)

2.631 DIA. (6.683)

SECTION A—A

The total weight of the thrust chamber is 54.3 pounds (24.7 kg). The
weight breakdown by component is as follows:

	lb	kg
Electroformed Nickel Coolant Shell	49.3	22.4
INCO 625 Structural Shell	1.9	0.86
Coolant Inlet Manifold (INCO 625)	1.3	0.59
Coolant Outlet Manifold (INCO 625)	0.2	0.09
Support Ring	1.1	0.5
Gimbal Actuator Rigging	0.5	0.23

An injector design was established to provide the high performance and operational features required by the engine system. The injector receives hot methane from the turbines at a nominal-thrust temperature of 1260 R (700K) and a temperature of 1750 R (970K) at the 10:1 throttled condition. The FLOX temperature is in the 160-170 R (90-94K) range. Design chamber pressures range from idle mode and throttled operation values of 30-50 psia (210-345 kN/m^2), up to the nominal thrust chamber pressure of 500 psia (3450 kN/m^2) and potential uprated values of 700-800 psia (4830-5520 kN/m^2). The injector design was based, to a considerable extent, upon the injector tested with FLOX/methane under NASA contract NAS 3-11191.

ELEMENT TYPE SELECTION

Various injector types were evaluated to select a candidate injector element configuration. Basic injector configurations evaluated were coaxial, impinging jet, and large thrust/element types. The impinging jet configurations included doublets, triplets, and pentad types. Data from NASA, Air Force and company-funded programs were reviewed; recent data from Contract NAS 3-11191, Space Storable Regenerative Cooling (Ref. 1), NAS 3-12011, Gas Augmented Injector (Ref. 2), the J-2S program (Ref. 24), and company-funded efforts with FLOX/CH$_4$, were most applicable. The principal evaluation criteria were performance, thrust chamber compatibility (streaking and total heat rejection), stability and fabrication cost. A comparison of the element types is provided in Table 70.

Coaxial injector elements have been successfully used with O$_2$/H$_2$ in the J-2 and J-2S engine programs at Rocketdyne, and with the PWA RL-10 engine. FLOX/methane performance and heat transfer data have been and are currently being obtained with a coaxial element injector under NAS 3-11191 testing which is directly applicable to this engine. A coaxial injector has provided good performance with FLOX/methane (97 to 98 percent) and good chamber compatibility. Chamber heating loads are 30 percent lower than comparable performing triplet injectors.

TABLE 70

INJECTOR COMPARISON

Injector Type	Performance	Heat Transfer	Fabrication Cost	Throttling	Stability
Coaxial	Good	Low	High	Good	Good
Triplet	Good	High	Moderate	Potentially Good	Good
Pentad	Good	Potentially Low	Moderate	Potentially Good.	Good
Doublet	Good	Potentially Low	Moderate	Potentially Good	Good
Large Thrust/ Element	Potentially Good	Potentially low but may streak.	Low	Potentially good.	Potentially good.

Testing of a concentric element injector with FLOX/methane in a regeneratively-cooled chamber has also been conducted under company funding. Results of these tests also show good performance over the entire throttling range. Based upon these considerations, the coaxial element was selected for the flight-weight injector design. As discussed in the following sections, two element designs should be considered as alternates because of their potentially attractive features. When additional data are obtained on these concepts, they should be evaluated for potential use in this application.

Triplet elements have been run with a variety of cryogenic propellants and provided good combustion efficiency. Under Contracts NAS 3-11191 and NASw-1229 Ref. 1,2), high combustion efficiency was obtained with FLOX/methane, but the heat transfer to the combustor was very high, particularly near the injector.

Doublet element, liquid FLOX/liquid LPG injectors have been tested at low chamber pressure (100 psia, 690 kN/m^2) under NAS 3-11199, Space Storable Propellant Performance (Ref. 16). Self-impinging doublet injectors were used extensively and design criteria have been established. This element type is moderate in cost and readily amenable to analysis. With additional test data, it could become attractive. Because of the absence of test data, this concept was regarded as having backup potential but was not selected for the current design.

Large thrust-per-element injectors (5000 to 20,000 pound thrust, 22,200 N to 89,000 N) are being evaluated in the Gas Augmented Injector Program, Ref. 2 , where they have been hot-fired with oxygen/hydrogen with combustion efficiencies of $\sim$ 97 percent. Current contract effort is being directed toward FLOX/CH$_4$ injector designs and cold-flow testing. Impinging and coaxial types are being evaluated. This program provides an interesting alternate injector design with potential high performance and low cost. In addition, considerable gas-liquid injection design data are being gathered, which will materially improve the capability to design and to predict performance for gas-liquid injectors.

INJECTOR THROTTLING TECHNIQUE SELECTION

Various methods to obtain good performance and stability over the 10:1 throttling range were evaluated. The basic techniques evaluated were: dual manifolding, gas/gas injection, and cup recess types.

Dual Manifold

Dual manifolding provides a step decrease in injection area as the propellant flowrates are reduced. The proportional reduction in area with flowrate provides reasonable injector pressure drops and injection velocities for stable and high performance operation. Study results indicated dual manifolding of the gaseous fuel side of the injector was not necessary. The injector ($\Delta P/P_c$) ratio remains essentially constant during throttling due to the density decrease of the gaseous propellant at decreased pressure during throttling. However, the dual manifold design has the disadvantage of requiring an extra FLOX valve and a step change in engine system power (FLOX pump discharge pressure) during throttling.

Two different types of dual manifolding for the liquid FLOX appear promising. Dual manifolds (feed passages) could be provided to each of the oxidizer injector elements, such that all elements would inject oxidizer during throttled operation. Dual manifolds could also be provided to shut off oxidizer flow to selected elements such that only selected elements would inject a higher flowrate of oxidizer during throttled operation. Dual manifold testing with FLOX/MMH under Contract NAS7-304 (Ref. 17) indicated good performance and that no purge of the inactive elements was necessary. Both types of dual manifolding appear to offer potential; however, the technique where each element is throttled should provide better performance and less potential for injector overheating and FLOX side contamination.

Gaseous Injection

Injection of gaseous fuel and oxidizer over the entire thrust range gives a $\Delta P/P_c$ ratio which remains relatively constant for both propellants. Therefore, high performance and stability are obtained without dual manifolding, external valve

requirements, or step changes in pump discharge pressure. Several methods of oftaining gaseous FLOX through heat exchangers with the hot methane are available: gasification in the FLOX injector tubes, gasification in the injector manifolds, and gasification in a thrust chamber heat exchanger. A heat exchanger injector with gasification in the FLOX tubes has been fabricated and tested over a 10:1 thrust range with $FLOX/CH_4$ propellants. An F_2/H_2 injector has been successfully throttled over a 10:1 range with oxidizer gasification in the injector manifold and orifices.

Gaseous propellant injection for 10:1 throttling can be provided through complete vaporization of the FLOX in a heat exchanger prior to its entering the injector oxidizer manifold. In a typical design to accomplish this, a milled channel heat exchanger is incorporated on the outside of the milled channel thrust chamber. The liquid FLOX is thus vaporized by heat transfer from the hot CH_4 in the upper thrust chamber jacket. In addition to the injector throttling capability, this design reduces back-wall temperatures, decreases jacket ΔP, and could allow higher chamber pressures. This method has been demonstrated over an 8:1 range with F_2/H_2.

Recessed Element

The third basic method of obtaining good injector performance and stability during 10:1 throttling operation was with a coaxial injector employing a recessed FLOX post. It was found in both cold-flow experiments and in engine tests that proper design of a recessed post coaxial element would result in a relatively high net pressure drop being maintained across the element over a wide range of flowrates without interpropellant heat exchange. This type of injector has demonstrated satisfactory throttled operation with oxygen/hydrogen propellants.

Figure 111 shows ΔP_{ox} vs $\dot{w}_{ox}$ for a liquid oxygen/hydrogen cup throttling element. It may be seen that the oxidizer ΔP differs significantly from a typical liquid ΔP. The initial portion of the curve follows the liquid ΔP closely, because the orifice portion of the ΔP is dropping off proportional to flowrate squared. The
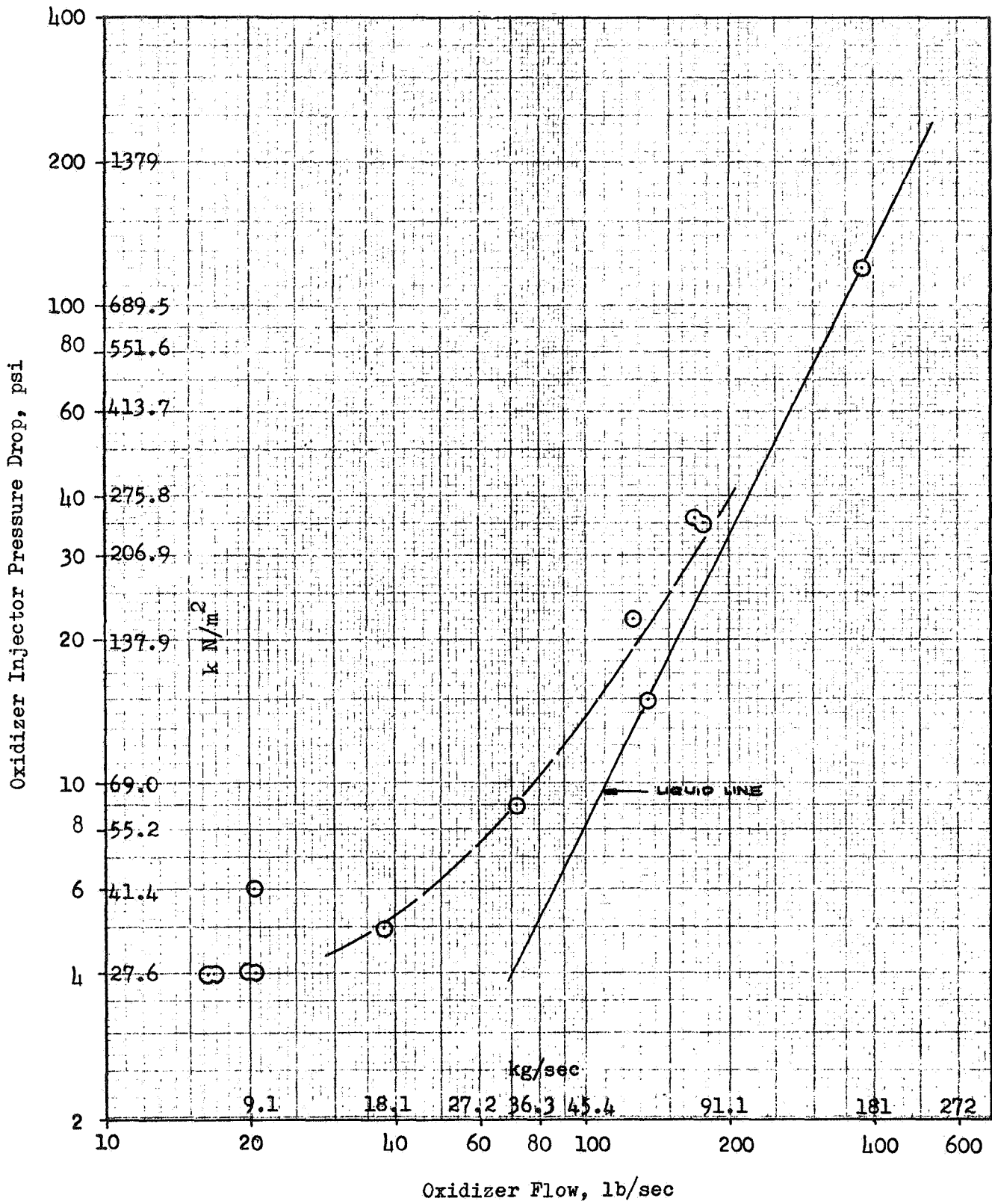
Figure 111 . Recessed Element Oxidizer Pressure Drops.

data scatter was caused by variations in fuel injection temperature (higher points indicate higher fuel temperature). The absolute values of ΔP are low at throttled conditions, basically because of the low fuel temperature which dropped during throttling due to decreasing mixture ratio. For the FLOX/CH$_4$ applications studied, fuel injection temperatures will increase during throttling and the ΔP's at the throttled conditions will be significantly higher than the data shown.

Throttling Method Selection

After careful evaluation of the throttling methods, the recessed element approach was selected based upon its similarity to the injector element being tested with FLOX/methane, upon the successful J-2S experience in throttling and upon its potential simplicity for a flight-weight engine.

Other throttling methods can provide the throttling capability with reasonable pressure drop values at nominal thrust with somewhat more system complexity. The dual manifold technique has a high level of confidence but is more complicated. The gas/gas injection with a FLOX heat exchanger is also a potentially attractive backup approach.

INJECTOR ELEMENT DESIGN

Under Contract NAS3-11191, a FLOX/methane coaxial injector has been tested at a series of mixture ratios and pressures. The injector elements are arranged in concentric rows. This injector element is shown schematically in Fig. 112. It has a tapered exit and a slight FLOX post recess to promote mixing. The methane annulus hole was broached to produce lands to center and support the FLOX post. The lands were cut back from the end of the post to provide a uniform annular hydrogen stream. Testing of the injector resulted in combustion efficiencies from 95 to 100 percent, as shown in Fig. 113.

The concentric injector element was designed based upon information from Contract NAS3-11191 and from information generated in connection with current rocket engines. Based on coaxial injector investigations in transparent chambers, in conventional chambers, and in cold-flow testing, the injection/combustion process proceeds as follows:

297

S.S. 347 Tube

OFHC Copper Face

0.262 DIA. (0.782)

0.260 (0.660)

0.245 (0.622)

0.200 (0.508)

0.150 (0.381)

0.032 DIA. (0.081 cm)

0.055 DIA. (0.140)
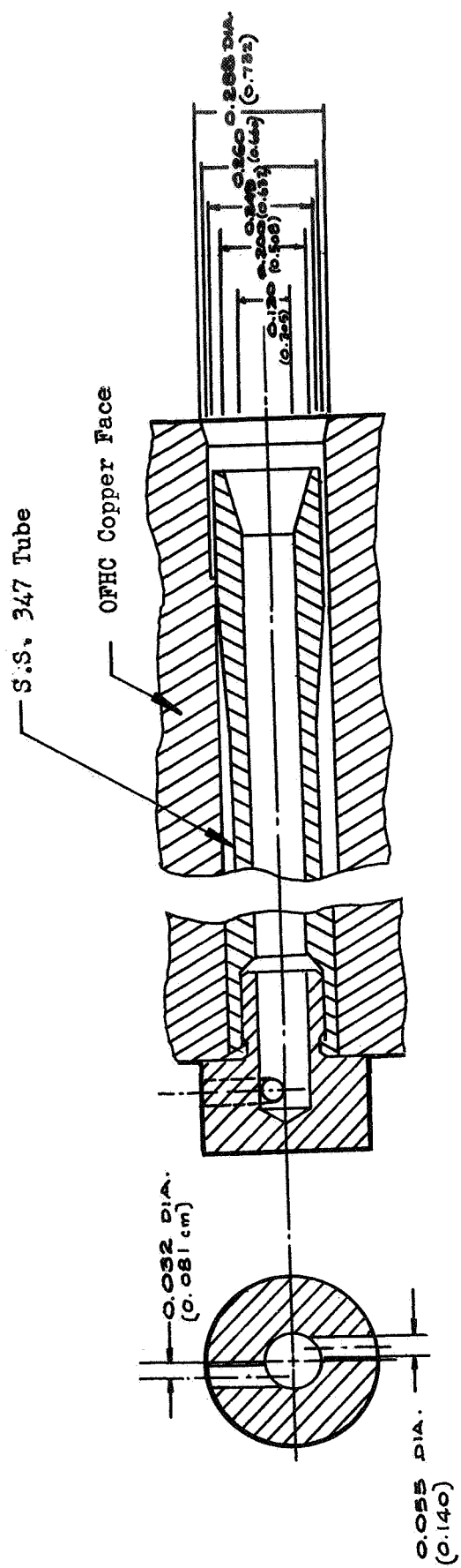
UNITS - INCHES
(Centimeters)

Figure 112. NAS3-11191 Injector Element

298
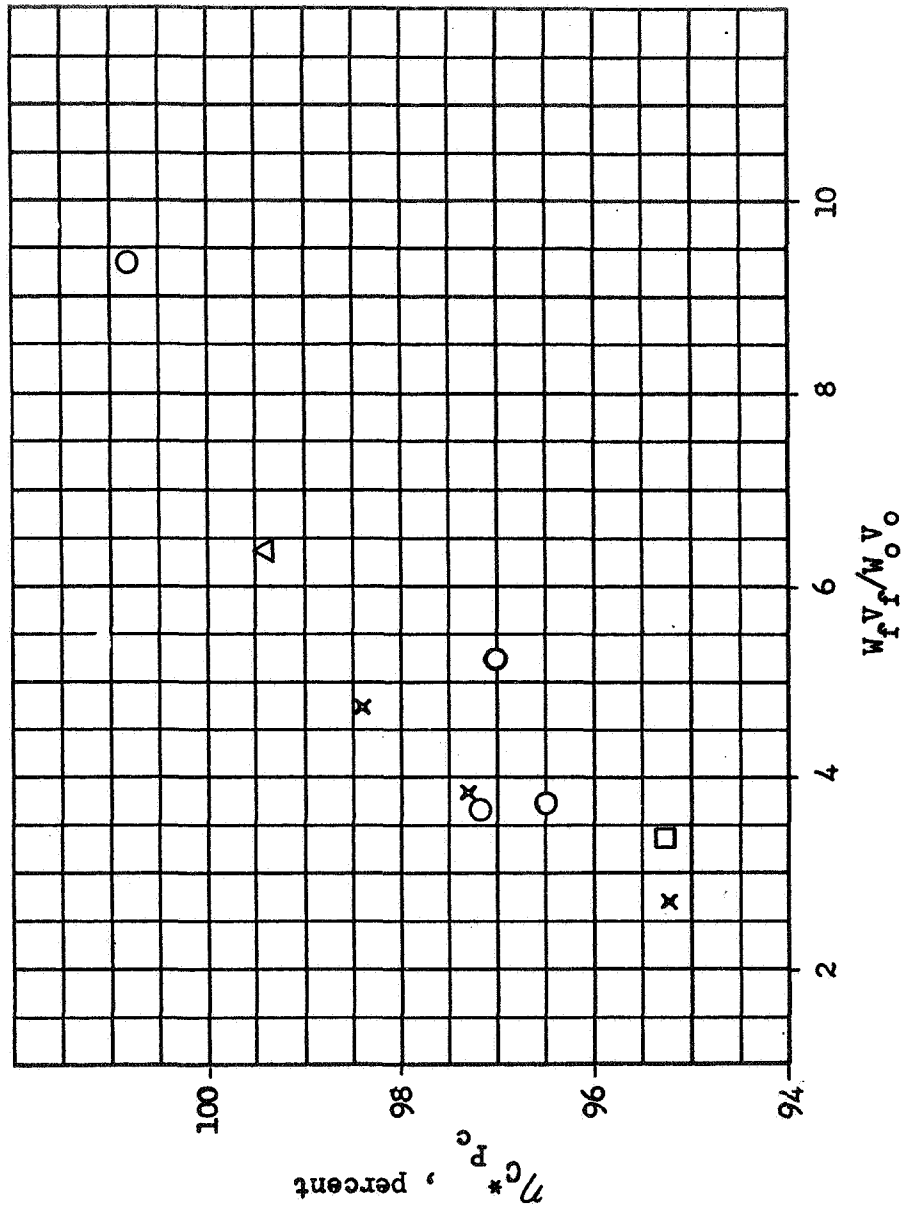
Figure 113. Propellant Injection Momentum Ratio

At the end of the oxidizer post, the annular gas stream (fuel) rapidly expands across the gap left at the end of the oxidizer post until it meets the oxidizer jet. Stripping of the oxidizer by the parallel, higher-velocity fuel proceeds, yielding oxidizer vapor and spray. The gas velocity decays relatively rapidly, due both to entrainment of the oxidizer spray and to expansion in the cup region (cylindrical portion between the end of the post and the face). Combustion proceeds in the mixing region, its extent determined by the combustion lag, the gas velocity, and the local mixture ratio. The combustion zone stripping continues until the entire oxidizer jet is consumed.

The injector pressure drop (from manifold to chamber) is composed of three parts: orifice, friction and cup. The orifice ΔP is determined by the entrance geometry. The frictional loss is determined basically by the L/D of the passage. The cup ΔP is a function of the geometry and the propellant entrance conditions. For the FLOX, which is liquid, the orifice plus frictional loss is proportional to the flowrate squared; i.e., would drop off to 1/100th its nominal value at 10:1 throttle. For the methane, which is gas, the orifice and frictional ΔP's are approximately proportional to the flowrate times the square root of the inverse of the temperature ratio. Since the methane temperature increases during throttling (1260 to 1750 R, 700 to 970K) $\Delta P/P_c$ will increase with throttling. The cup ΔP will be the same for both propellants.

It has been experimentally found that the cup ΔP is a function of $\left[\Delta P_\ell / \Delta P_g \right]$, where ΔP_ℓ is numerically equal to one velocity head of the liquid flowing full in the cup diameter, and ΔP_g is numerically equal to one velocity head of the gas flowing full in the cup at the same density as the entrance conditions. Experimentally, $\Delta P_{cup} / \Delta P_\ell$ has been correlated against $\Delta P_\ell / \Delta P_g$ as shown in Fig. 113 for a particular geometry. Testing with different geometries has established that Fig. 114 may be used as a universal curve with a geometric conversion factor (f) applied to ΔP_{cup}.

$$f = \frac{0.08}{A_{annulus}} (L/D)_{recess}$$

Since design data are empirical, element geometric parameter sizing was based on the range of parameters tested. The L/D of the cup should be maintained between
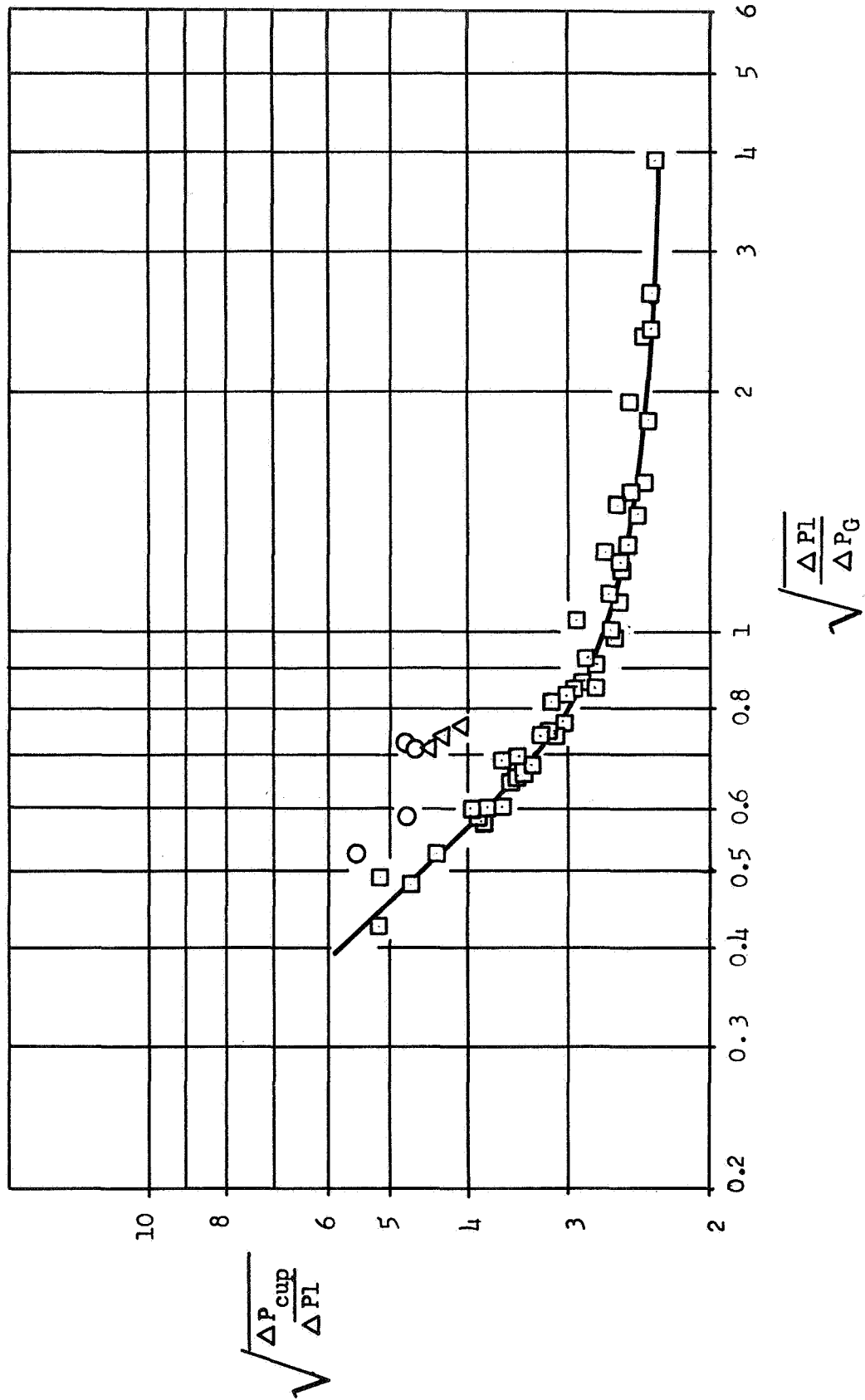
Figure 114. Recessed Element Pressure Drop Correlation.

0.4-0.5 in conjunction with a thin oxidizer post to promote rapid mixing (a short wake region). In the selected element design the entrance velocity of the gas was maintained at over 800 ft/sec (244 m/sec) for good performance; this determined the annulus area. The oxidizer post diameter was sized to give $V = 24$ ft/sec (7.3 m/sec) for a stable, full-flowing stream. It has been found experimentally that an extremely low oxidizer velocity can lead to unstable flow streams. The design recess L/D gives ΔP_{cup} at full thrust of 70 psi and 28 psia (485 and 193 kN/m^2) at throttled conditions. The total fuel ΔP is 130 psi (895 kN/m^2) at full thrust and the oxidizer is 120 psi (827 kN/m^2) [50 psi (345 kN/m^2) in the orifice and 70 psi (482 kN/m^2) in the cup]. At the 10:1 throttling flowrates, the oxidizer ΔP is approximately 28.5 psi (197 kN/m^2) [composed of 0.5 psi (3.4 kN/m^2) in the orifice and 28 psi (193 kN/m^2) in the cup].

The flight engine design injector element is shown schematically in Fig. 115. The oxidizer post is 0.128 in.(0.325 cm) I.D. and 0.180 in.(0.457 cm) O.D. The thin wall provides for a small wake region at the exit to promote mixing and to reduce the stagnation region. The O.D. of the annulus is 0.209 in.(0.531 cm) and the post recess is 0.097 in.(0.246 cm). The 0.209 in.(0.531 cm) diameter hole in the copper is to be broached, leaving lands in the upstream half of the copper and in the INCONEL sheet brazed to the back of the copper. A rounded entrance to the annulus of 0.030 in.(0.076 cm) R is provided to assure that most of the pressure drop is converted to velocity head. The exit of the cup also has a 0.030 in.(0.076 cm) radius to eliminate a sharp corner that could be exposed to burning. The oxidizer orifice at the entrance to the post is 0.0635 in.(0.1613 cm) diameter. The entrance was not rounded (which reduces cost) since the purpose of the orifice is to meter and not to produce a high velocity as in the case of the fuel.

In comparison to the NAS3-11191 injector discussed previously, the flight injector design has a thinner FLOX post and a larger recess L/D to promote mixing by shear forces. This is especially important for the throttling injector, because at the low thrust a swirler would be relatively ineffective and for this case the full thrust design must be one that maintains performance. The fuel annulus for the flight design is 0.0145 in.(0.0391 cm) compared to 0.0095 in.(0.0241 cm) for the NAS3-11191 injector; this represents a 13-percent increase in area necessitated by the higher fuel temperature and thus lower density. Experience from the NAS3-11191 injector demonstrated the suitability of the copper face design.

INCONEL 625 Body

INCONEL 625

OFHC Copper Face

0.030 R
(0.076)

0.030 R
(0.076)

0.209 Dia.
(0.531)

0.180 Dia.
(0.457)

0.128 Dia.
(0.325)

(0.1613)
0.0635 Dia.

0.097
(0.246)

0.25
(0.64)

0.070
(0.178)

0.50
(1.27)

0.21
(0.53)

0.30
(0.76)
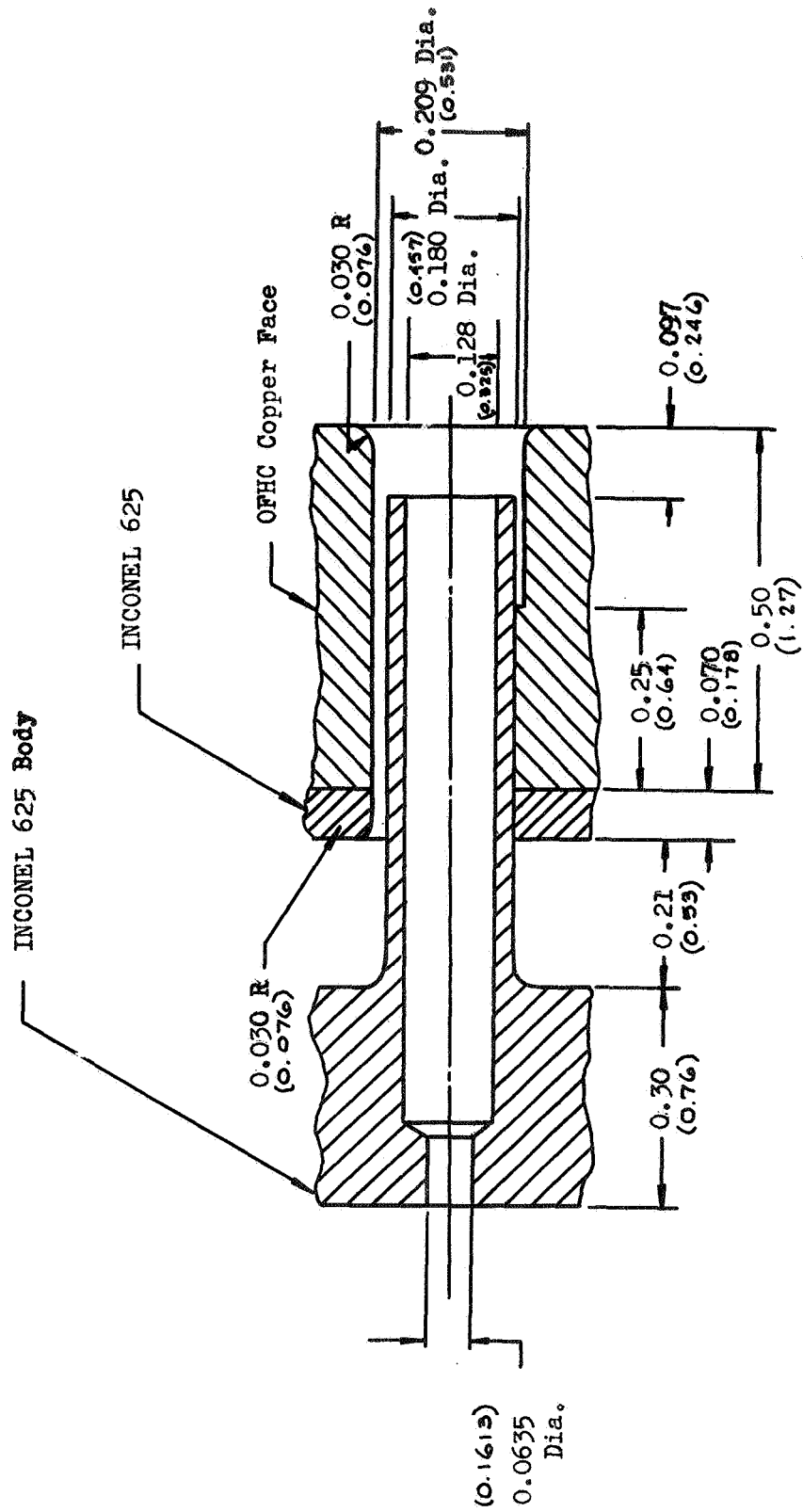
UNITS – INCHES
(Centimeters)

Figure 115 Flight Engine Injector Element.

303

The FLOX post is made of Inconel 625 to provide compatibility with the backup material and to reduce interpropellant heat transfer. A heat transfer analysis indicated that a small amount of FLOX vaporization will occur in the FLOX tube at the 10:1 throttled condition. Although not generally desirable, this small amount may not be detrimental to system operation since a number of throttling tests with vaporized fluorine or FLOX have been successfully conducted. Should reduction of the vaporization be necessary, the injector would be modified to reduce the heat input through increased material thickness, insulation or alternate materials.

The flight engine injector design may be modified to change its characteristics or performance without major injector body changes by changing only the post recess and the cup diameter. These changes can modify the pressure drop at full and throttled thrust and the shear mixing in the cup. These minor element variations could easily be built into the test hardware. The use of swirlers is optional in the basic design, however they are not currently included.

INJECTOR ASSEMBLY DESIGN

The injector controls and directs the flow of propellants to the combustion chamber, provides structural closeout and seal of the combustion chamber, and also carries load to and supports the thrust pickup or gimbal joint. The injector assembly drawing is shown in Fig. 116. The injector face is ring-type solid copper for cooling of the face by conduction of heat from the face to the fuel. It is brazed to the body in a continuous ring around the circumference and at concentric rings distributed across the face.

The annular oxidizer manifold provides closeout of the oxidizer elements and a structural member for thrust load take-out. The manifold is welded into the body. The center oxidizer manifold provides closeout of the oxidizer fuel passages under the gimbal joint. It is shaped to minimize propellant volume and material weight. The annular fuel manifold is welded to the injector body. It is sized for both pressure loads and bending loads from the solid piping connecting to it.
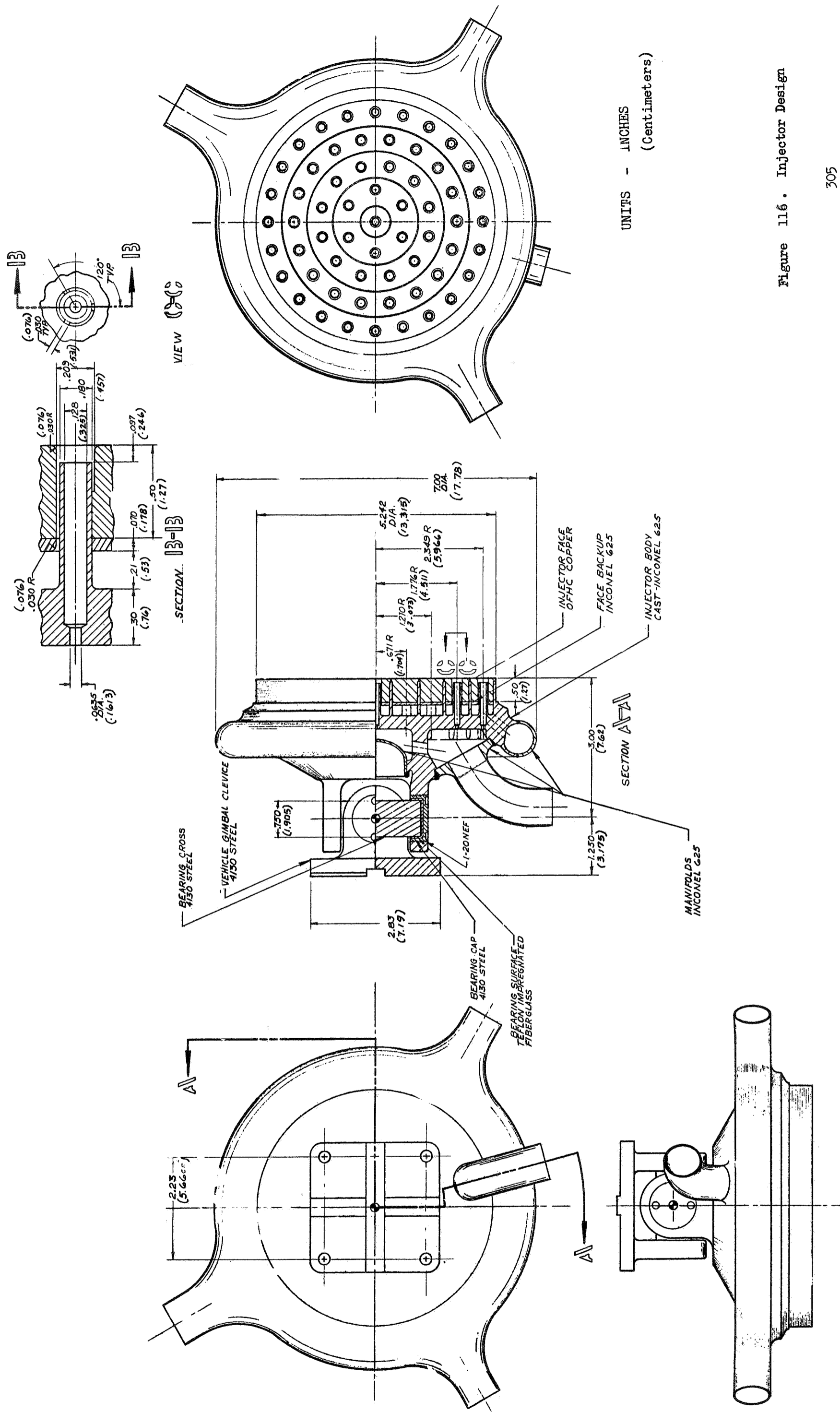
UNITS — INCHES
(Centimeters)

Figure 116. Injector Design

305

The injection pattern is made up of 61 coaxial injection elements arranged in a manner similar to the NAS3-11191 injector. The face is of solid copper rings cooled by the fuel, the face material being the outer surface of the fuel annulus. The temperature of the face will be 1150 F (895K) on the face to 1010 F (815K) at the back wall at full thrust to 1490 F (1080K) face and 1465 F (1070K) back wall at 10:1 throttled conditions. This material temperature plus a possible transient pressure differential between fuel manifold and chamber pressure of 300-400 psi (2070-2760 kN/m^2) dictate the use of distributed support for the copper face. The fuel passages are sized to keep the velocity head to 4 psi (28 kN/m^2). The oxidizer manifold is shaped and sized by its use as a structural element and results in a very low pressure drop.

The injector body is designed to be fabricated as an investment casting. The material selected is Inconel 625; selection was based upon its weldability to nickel or nickel-base alloys (for the joint to the thrust chamber), high strength and good ductility ($\sim$30%) over the -200F to +1400F (-365K to +1035K) temperature range, compatibility with FLOX, and suitability for brazing. High ductility is required to accommodate the large temperature gradients across the body and the relative thermal expansion between the face and the body. Weldability is important, since four basic parts are welded to the body: the annular oxidizer manifold cover, the center oxidizer manifold, the toroidal fuel manifold, and the thrust chamber.

The thrust chamber at the injector weld joint is electroformed nickel and thus the nickel-based alloy, Inconel 625, is desirable for the injector body to assure weldability. An alternate material would most likely be CRES 321, which has medium strength and good ductility.

The center oxidizer manifold could be cast into the body but was left open to provide accessibility for cleaning of chips, etc., after post machining. The center manifold cover is designed with a reverse curvature to minimize volume of propellant in the manifold. It is attached with a simple burn-down weld. The annular oxidizer manifold cover is designed to be made as a one-piece assembly set directly to shoulders in the body and sealed with two circular fillet welds. The toroidal fuel manifold is designed to be welded on although a portion of it, excluding the three flared inlets, could possibly be case integral with the body.

306

The gimbal joint is a simple Hooke joint (U-joint). The bearing is of Fabroid (teflon-impregnated fiberglass). The cross is put in place, then the bearing caps are screwed in from the outside; locking is provided by a pin driven in along the threads (similar to key insert points). The bearing surface was selected due to the spece environment; metal-to-metal contact such as in roller or needle bearings may result in welding at the contact points. Both side thrust and axial load are taken through the bearing cap. A standard tongue and groove cross is provided in the top half of the gimbal joint to locate on the vehicle and take torque and side loads.

The injector face is made of OFHC copper rings with a sheet of Inconel 625 brazed to the back side. The copper thickness is 1/2-inch and is sized by heat transfer area in the injection elements required to maintain face temperature at 1150 F (895K) at full thrust and 1500 F (1090K) at 10:1 throttle. The back side Inconel 625 sheet is included for a dual purpose. Lands on the back up sheet help center the ports thus taking much of the load off the lands in the copper, which is at a low strength at the operating temperature. The backup sheet operates at the same temperature as the back of the copper and thus expands approximately the same due to temperature, thus helping prevent the copper from yeilding and being distorted in the outer fuel annuli. If additional distortion relief of the copper is required, the inner face support rings, which are part of the body, may be slotted to eliminate the hoop band effect and the outer band reduced in thickness.

Fuel enters the manifold on the back side of the face from the toroidal manifold through 24 radial holes (one between each outer element). The large number of holes reduce the velocity head to about 4 psi (28 kN/m^2), thus assuring uniform distribution. The entrance to the fuel annulus is given a full rounded profile, thus converting as much as possible of the ΔP to velocity for high momentum and performance. The oxidizer orifice is sharp-edged for low cost, since its basic purpose is to meter and not to produce velocity.

Machining to be done on the body casting includes boring and tapping of gimbal bearing caps, hollow milling and drilling of posts, turning the face support rings, and turning the butt land at the thrust chamber to the injector joint to assure proper alignment.

The most critical factor in the injector structure is retention of the copper face. Ring-type construction provides adequate braze shear area for this purpose, as well as appropriate span for the copper face plate. The basic structural element in the injector is the Inconel 625 body plate, which separates the oxidizer and the fuel and provides a means of transmitting thrust and pressure forces. The injector dry weight is 11.8 pounds (5.35 kg).

Assembly operations of the injector are as follows: the injector to thrust chamber joint would be machined on the basic casting, then the face support rings, and the posts hollow milled and drilled. The face copper material would be brazed to the Inconel sheet, turned, then the orifice holes drilled and broached. The face rings would then be asembled to the body and broached. The injector manifold would be welded to the body, and finally the gimbal joint bearing holes bored and tapped.

INJECTOR HEAT TRANSFER ANALYSIS

A two-dimensional thermal analysis of the injector was made to determine material operating temperatures in the copper face. The injector face pattern has the maximum spacing between elements occurring at the center of the injector. The center element, therefore, was selected for the analysis as it represents the most severe conditions. A schematic of the center region of the injector face is shown in Fig. 117. The center region was approximated in the thermal analysis by a hollow cylinder of inner radius 0.1045-inch (0.2654 cm) and an outer radius of 0.35-inch (0.90 cm). The outer radius selected is somewhat larger than that obtained by taking the mid-point between orifices (0.33 inch, (0.84 cm). This larger effective radius was taken to account for the small triangular area that results between three tangent circles.

A cross-section of an injector element is shown in Fig. 117. The copper face thickness, H, was varied between 0.25 (0.64) and 1.50 inch (3.71 cm) in the analysis. The face is assumed to be of oxygen-free high conductivity (OFHC) copper (k = 0.00463 Btu/in.-sec F (0.756542 j/cm^2). An enlarged schematic of the geometry as used in the analysis is shown in Fig. 117. It should be note (Fig. 117) that the heat input is assumed to occur uniformly over the injector face and in the recessed
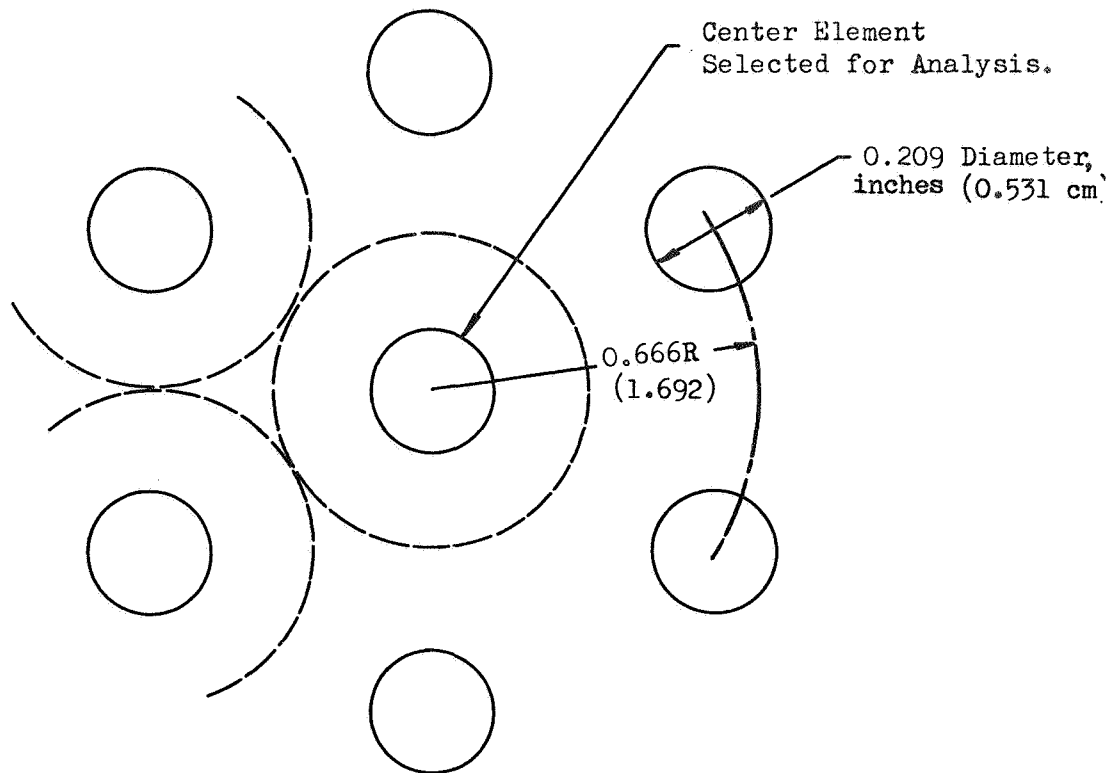
Schematic of Center of Coaxial Injector Face Pattern.
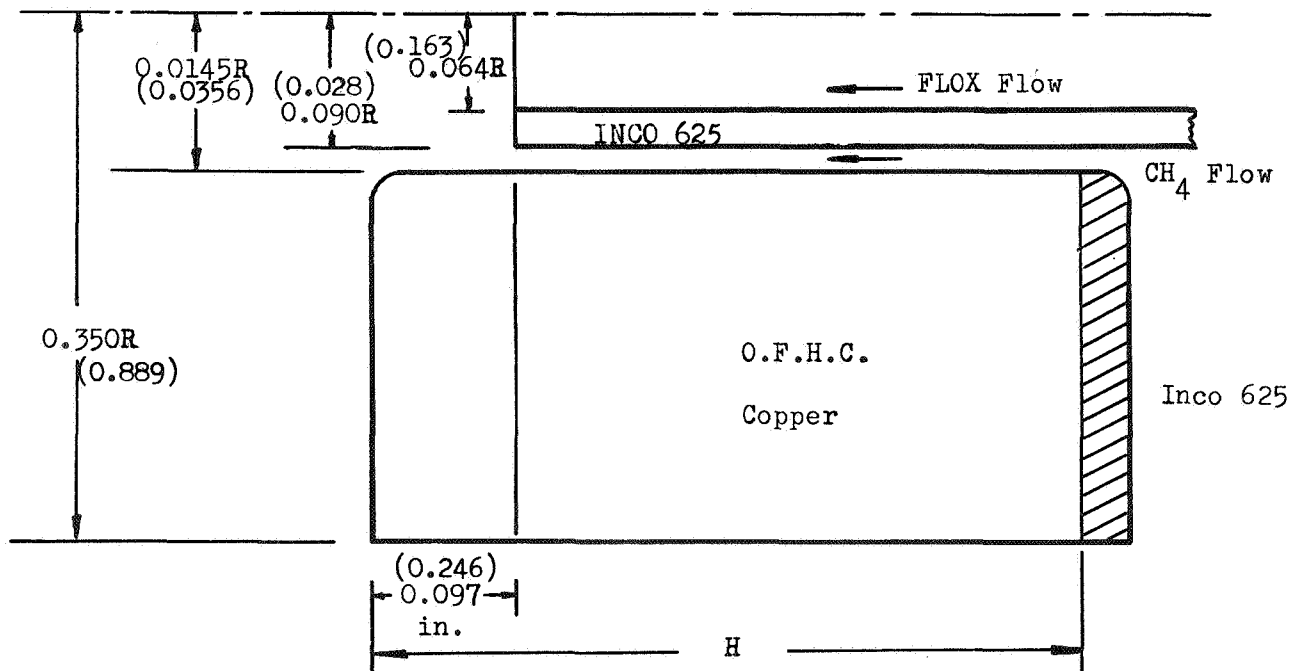
Figure 117 . Injector Face Temperature.

(cup) region. The assumption of a full heat load in the cup is probably conservative since combustion is not complete. Heat removal from the injector face is accomplished by the methane flow through the element. Due to the very low methane velocities behind the face and the Inconel 625 backup material, the back surface is taken to be effectively insulated.

The methane convective cooling coefficient was estimated from the Dittus-Boelter relation:

$$N_{NU} = 0.023 \ N_{RE}^{0.8} \ N_{PR}^{0.4} \ \overline{\phi}_E$$

where the methane properties are evaluated at the bulk temperature. The methane bulk temperature was taken to be 750 F (670K) at full thrust and 1300 F (875K) at 10:1 throttled condition. These are based on injector inlet temperatures. Heat input to the methane from the injector face increases the methane temperature about 20 degress. A hydraulic diameter (d_H) equal to twice the gap was used for the annulus. Due to the relatively low length-to-diameter ratio of the orifices, an entrance correction $\overline{\phi}_E$ was applied to the cooling correction:

$$\overline{\phi}_E = 1.8 \ (H/d_H)^{-0.15}$$

This correction amounted to about a 21-percent increase in the convective coefficient for the 0.5-inch (1.27 cm) thick face design.

The injector face heat flux is commonly assumed to be uniform and equal to that obtained at the chamber wall near the injector end. Results of testing with a coaxial injector under NAS3-11191 indicate a combustion-gas effective convective film coefficient of about 0.00030 Btu/in^2-sec (0.04902 j/cm^2) which was used in the full thrust analysis.

Temperature at various points of the injector face model are shown in Fig. 118 for a 0.5-inch (1.27 cm) thick copper face. A maximum surface temperature of 1167 F (900K) is shown for the 0.50-inch (1.27 cm) copper face thickness. The temperature distribution across the heated face of the injector is seen to be quite uniform due

Methane Flow →

979.	996.	1007.	1016.	1022.	1026.	1028.	1029.
980.	997.	1009.	1017.	1023.	1027.	1029.	1029.
982.	999.	1011.	1019.	1025.	1029.	1031.	1032.
986.	1003.	1015.	1024.	1030.	1034.	1036.	1037.
992.	1009.	1021.	1030.	1036.	1040.	1042.	1043.
999.	1017.	1029.	1038.	1044.	1048.	1050.	1051.
1009.	1027.	1039.	1048.	1054.	1058.	1060.	1060.
1020.	1039.	1052.	1060.	1066.	1069.	1071.	1072.
1036.	1055.	1067.	1074.	1079.	1082.	1084.	1084.
1058.	1075.	1085.	1091.	1095.	1097.	1098.	1099.
1095.	1102.	1106.	1109.	1111.	1113.	1114.	1114.
1129.	1124.	1123.	1124.	1125.	1126.	1126.	1127.
1151.	1142.	1139.	1138.	1139.	1139.	1139.	1140.
1167.	1157.	1153.	1152.	1152.	1152.	1153.	1153.

Face

Figure 118 . Injector Face Temperature, Nominal Thrust;
Thickness of 0.5 inches (1.27 cm)

to the excellent thermal conductivity of the copper. A plot of maximum temperatures vs face thickness is shown in Fig. 119. Decreasing the copper face thickness to 0.25-inch (0.64 cm) resulted in a maximum surface temperature of 1463 F (1067 K). The primary reason for the temperature increase is that the thinner face reduces the cooled surface area (i.e., orifice length is decreased).

Injector face temperatures were also evaluated and 10:1 throttled operation. At this throttled condition the methane bulk temperature was 1300 F (875K) and the face heat input was scaled with $P_c^{0.8}$. The high methane bulk temperature resulted in a maximum face temperature of 1490 F (1082K), as noted in Fig. 120. At 10:1 throttling the injector face is not subjected to high stress loads and this temperature is not excessive.

FLOX Vaporization in the Injector

The extent of FLOX vaporization was estimated for the 0.50-inch (1.27 cm) face thickness design. The full throttled (10:1) point represents the most severe condition, since the methane temperature is a maximum and the FLOX subcooling a minimum due to the low pressure. The forced convection correlation was used in conjunction with F_2 properties evaluated at bulk temperature to estimatea FLOX orifice convective film coefficient. The FLOX and methane film coefficients combined with the FLOX wall thermal resistance determine the total heat transferred between the methane and the FLOX.

Results at the 10:1 throttled condition indicate no FLOX vaporization in the manifold passages as a result of heat transfer from the methane. In FLOX injector tubes, the amount of vaporization depends greatly on the initial FLOX temperature and the nature of the film coefficient. Where the FLOX is initially at the normal boiling point, little or no vaporization occurs. For a FLOX temperature of 170 R (94.5K) (possible end of flight conditions) and forced-convection film at the wall, a maximum of 20-percent of the FLOX could be vaporized by the methane at 10:1 throttling. It is quite likely, however, that under throttled conditions the FLOX would undergo film boiling at the orifice wall. The thermal resistance to heat transfer increases greatly when film boiling occurs (as compared to liquid forced convection values), such that FLOX vaporization value would probably be 2- to 5-percent. Although phase-change in the manifolds is generally avoided, F_2/H_2 and FLOX/CH_4 throttling tests indicate that with proper design, phase-change in the oxidizer tubes (including complete vaporization) may not be a problem.

FLOX/Methane

Thrust = 5000 pounds (2270 kg)

Chamber Pressure = 500 psia (3450 kN/m^2)

Mixture Ratio = 5.25
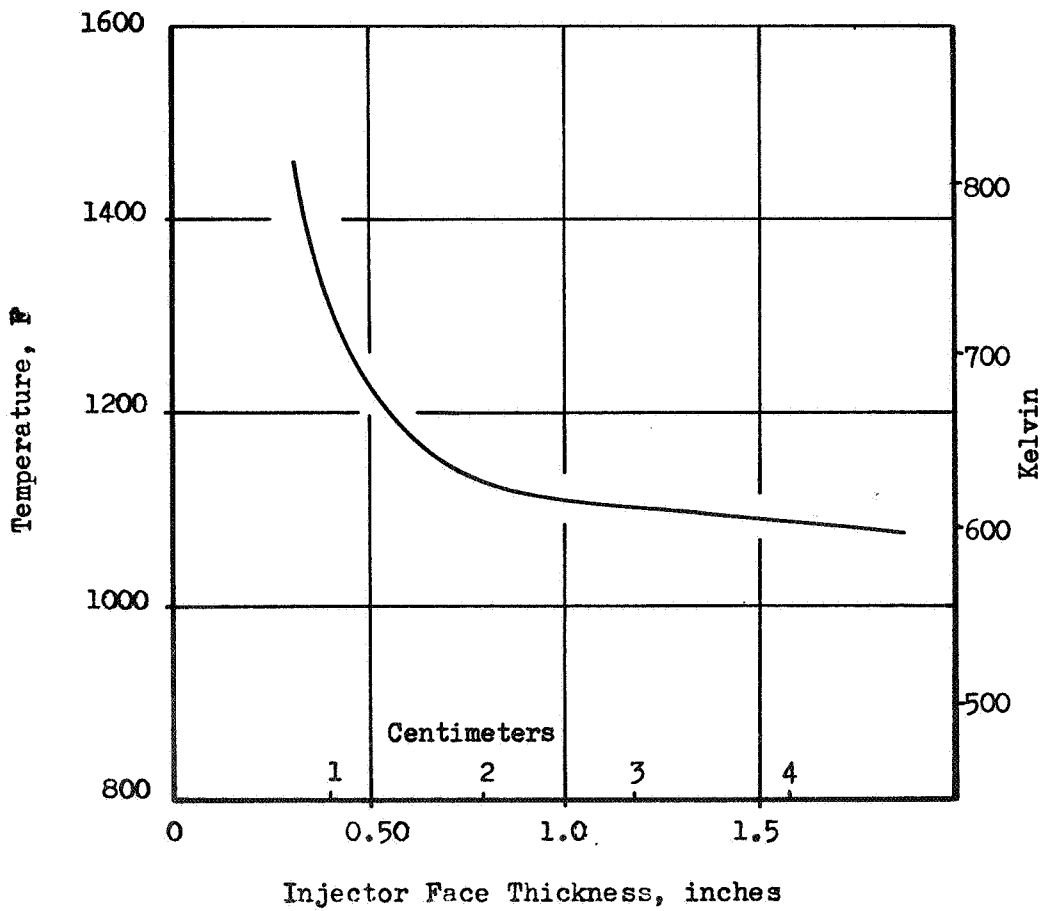
Figure 119. Injector Face Surface Temperature as a Function of Copper Face Thickness.

Methane Flow ⟶

1461.	1464.	1465.	1467.	1468.	1468.	1469.	1469.
1461.	1464.	1466.	1467.	1468.	1468.	1469.	1469.
1461.	1464.	1466.	1467.	1468.	1469.	1469.	1469.
1462.	1465.	1467.	1468.	1469.	1469.	1470.	1470.
1463.	1466.	1468.	1469.	1470.	1470.	1471.	1471.
1464.	1467.	1469.	1470.	1471.	1472.	1472.	1472.
1466.	1469.	1471.	1472.	1473.	1473.	1474.	1474.
1468.	1471.	1473.	1474.	1474.	1475.	1475.	1475.
1471.	1473.	1475.	1476.	1477.	1477.	1477.	1477.
1474.	1476.	1478.	1478.	1479.	1479.	1479.	1479.
1480.	1480.	1481.	1481.	1481.	1482.	1482.	1482.
1484.	1484.	1483.	1483.	1483.	1484.	1484.	1484.
1488.	1486.	1486.	1486.	1486.	1486.	1486.	1486.
1490.	1488.	1488.	1488.	1488.	1488.	1488.	1488.

Face

Figure 120. Injector Face Temperature, 10:1 Throttled; Thickness of 0.5 inches (1.27 cm.)

VALVES AND CONTROLS

The engine system has four control valves: two liquid valves controlling main propellant flow, one hot gas valve controlling power to the turbines and one hot gas valve regulating the power distribution between the turbines. Requirements for these valves were defined by the engine static and dynamic analysis, operating environment, and potential mission duty cycles.

PROPELLANT INLET VALVES

Inlet valves are used upstream of the turbopumps in both the FLOX and methane lines. Preliminary valve requirements are presented in Tables 71 and 72. The basic function of these valves is the on-off operation and the long term isolation of propellant from the pump. A poppet-type closure was selected for both valves because of its simplicity, ease of fabrication, low leakage and potential for short actuation times. Pneumatic actuation was selected for light weight.

Control Valve Leakage

Valve leakage is one of the more critical areas of valve design for propulsion systems which must be operable for long times in space. Excessive gas or propellant leaks could: (1) affect the performance of an onboard scientific experiment located near the leak exit; (2) require additional attitude control system compensation to create abnormal increase of operating fluid consumption; (3) create a hazardous condition resulting from accumulation in the engine; and (4) decrease the operating fluid's reserve to cause a system's decreased performance or even a malfunction.

Leakage is divided into internal and external leakage. Zero external leakage is obtained by using all welded valve bodies (and all welded flange connections). Zero leakage between propellants and the control system is obtained by using welded end fittings for internal actuator sealing bellows. Internal leakage through the valve seat and into the engine system is currently the area of greatest potential leakage. Low leakage across the valve seat can be achieved by proper material selection and the precision lapping of the valve and valve seat.

TABLE 71

FLOX INLET VALVE PRELIMINARY SPECIFICATION

1. Type of Component – Flox Inlet Valve

2. Function

   a) On-Off Operation

   b) Long Term Isolation of Flox from Turbopump

3. Operating Fluid – Flox (82.5) – 82.5% F_2/17.5% O_2

4. Fluid Characteristics at Valve Inlet

   a) Liquid of any quality condition to all gas

   b) Temperature = 159-179 R (88K to 100K)

5. Operating Environment

   a) Temperature = 159 to 600°R (88K to 333K)

   b) Atmosphere: Sea Level to Vacuum

   c) Radiation

   d) Meteor

   e) Zero g.

6. Storage Requirements

   a) Earth: Time   – TBD

             Temp.   – TBD

             Humidity – TBD

             Pressure – TBD

             Conditions – TBD

   b) Space: 2 years maximum

             250 days maximum between starts

7. Operating Life

   a) Maximum cycles – 4-10 engine restarts + all preflight tests

   b) Maximum operating time – 540 seconds + all preflight tests

8. Propellant Leakage Rates

		INITIAL	OPERATING	FINAL
a)	Internal	TBD	TBD	TBD
b)	External		10^{-7} ATM cc/sec He @ 300 psi (2070 kN/m^2)	
c)	Seat	170 SCCH @ 520°R (289K) and 50 psi H$_e$ (345 kN/m^2)	——	170 SCCH @ 520°R and 50 psi H$_e$

9. Propellant Flow Parameters

	Full Thrust	10:1 Throttled	Idle Mode	Uprated
$\dot{w}$, lb/sec (kg/sec)	10.52 (4.79)	1.15 (0.52)	0.58 (0.26)	16.84 (7.65)
$(P_{in})_{max}$, psia (kN/m^2)	55 (379)	60 (415)	35 (240)	67.5 (930)
ΔP, psia (kN/m^2)	5 (35)	0.05 (0.35)	0.013 (0.90)	12.5 (86.2)

10. Critical Sizing Criteria
   a) Maximum ΔP at nominal full thrust condition = 5 psi. (35 kN/m^2)
   b) Valve same size as pump inlet diameter

11. Actuator Type - Pneumatic

12. Actuation Time
   Full Closed to Full Open - 150 Millisec
   Full Open to Full Closed - 150 Millisec

13. Mode of Operation
   a) Goes to full open or full closed upon command.
   b) Goes to full closed upon termination of actuator power.

14. Flow Geometry
   Number of Inlets - 1
   Inlet Line I.D. - Must be compatible with inlet lines
   Number of Outlets - 1
   Outlet Line I.D. - 1.20 in. (3.05 cm)
   Line Orientation - 120° Included Angle (2.09 rad)

15. Applied Pressure, psia (kN/m^2)

	Inlet	Internal	Outlet
Initial Pressure	80 (552)	0	0
Operating Pressure	67.5 (465)	67.5 (465)	59.90 (413
Shutdown Pressure	TBD	TBD	TBD

16. Ducting Interconnect
   In-place tube welding

17. Structural Mounting Method

    Mounted from exit duct

18. Purge Provisions

    Purge port downstream of closure mechanism

19. Comments

    Must provide acceptable low flow disturbance to pump inlet.

    Valve must be designed to operate at uprated 800 psia (5520 kN/m^2) condition as well as nominal 500 psi (3450 kN/m^2).

TABLE 12

METHANE INLET VALVE PRELIMINARY SPECIFICATION

1. Type of Component - Methane Inlet Valve

2. Function
   a) On-Off Operation
   b) Long Term Isolation of Methane from Turbopump

3. Operating Fluid Methane

4. Fluid Characteristics at Valve Inlet
   a) Liquid of any quality condition to all gas
   b) Temperature = 202-248 R (112K to 138K)

5. Operating Environment
   a) Temperature = 202 to 600 R (112K to 333K)
   b) Atmosphere: Sea Level to Vacuum
   c) Radiation
   d) Meteor
   e) Zero g.

6. Storage Requirements
   a) Earth: Time   - TBD
            Temp.   - TBD
            Humidity - TBD
            Pressure - TBD
            Conditions - TBD
   b) Space: 2 years maximum
            250 days maximum between restarts

7. Operating Life
   a) Maximum cycles - 4-10 engine restarts + all preflight tests
   b) Maximum operating time - 540 seconds + all preflight tests

8. Propellant Leakage Rates

		INITIAL	OPERATING	FINAL
a)	Internal	TBD	TBD	TBD
b)	External		10^{-7} ATM cc/sec He @ 300 psi (2070 kN/m^2)	
c)	Seat	170 SCCH @ 520°R and 50 psi He (345 kN/m^2)	(289K)	170 SCCH @ 520°R and 50 psi He

319

9. Propellant Flow Parameters

	Full F	10:1 Throttled	Idle Mode	Uprated
$\overset{\bullet}{w}$, lb/sec (kg/sec)	2.004 (0.91)	0.22 (0.91)	0.2 (0.91)	3.206 (1.46)
$(P_{in})_{max}$, psia (kN/m^2)	85 (585)	89.95 (620)	70 (483)	97.5 (670)
$\triangle P$, psi (kN/m^2)	5 (35)	0.05 (0.35)	0.05 (0.35)	12.5 (85)

10. Critical Sizing Criteria

   a) Maximum $\triangle P$ at nominal full thrust condition = 5 psi (35 kN/m^2)

   b) Valve same size as pump inlet diameter

11. Actuator Type - Pneumatic

12. Actuation Time

   Full Closed to Full Open - 150 milliseconds

   Full Open to Full Closed - 150 milliseconds

13. Mode of Operation

   a) Goes to full open or full closed upon command.

   b) Goes to full closed upon termination of actuator power.

14. Flow Geometry

   Number of Inlets - 1

   Inlet Line I.D. - Must be compatible with inlet lines.

   Number of Outlets - 1

   Outlet Line I.D. - 0.87 inches (2.21 cm)

   Line Orientation - 120° Included Angle

15. Applied Pressure, psia (kN/m^2)

	INLET	INTERNAL	OUTLET	PROOF	BURST
Initial Pressure	110 3	0	0	TBD	TBD
Operating Pressure	97.5 (670)	97.5 (670)	89.9 (620)	TBD	TBD
Shutdown Pressure	TBD	TBD	TBD	TBD	TBD

16. Ducting Interconnect Method In-Place Tube Welding

17. Structural Mounting Method Mounted from Exit Duct

18. Purge Provisions Not Required

19. Comments

Must provide acceptable low flow disturbance to pump inlet.

Valve must be designed to operate at uprated condition as well as nominal 500 psi (3450 kN/m^2)

In the absence of contamination, the leakage rates that can be achieved through careful valve design are of the order 170 scch. Use of proper seat materials can provide low leakage even in the presence of some contaminants. For a 200-day storage duration, the propellant loss due to this leakage would be quite reasonable for a propulsion system of this size. However, a number of sources (for example, Ref. 16) indicate significant contamination which,if lodged in the valve seat, could increase the leakage by several orders of magnitude.

For the present system, single low-leakage poppet valves are used. These are engine-mounted upstream of the turbopumps. The successful use of these valves in a long-duration mission is based on the elimination of significant contamination from the feed system. Should this not be achieved, a set of squib-actuated isolation valves would be added upstream of the inlet valves to assure low leakage losses.

Inlet Valve Designs

The oxidizer and fuel inlet valves, as shown in Fig. 121 and 122 , are direct acting, poppet-type closures which use a high-pressure fluid for opening. The valve can easily provide actuation times of 100 to 150 milliseconds. The valves are similar in basic design and functional operation and differ only in physical size. Propellant pressure and a low-pressure fluid is required for closing. The line orientation is 120-degree included angle and the valve exit is welded to the pump inlet line. The poppet/seat surfaces are hard, flat and precision lapped to provide superior leak tightness. Poppet seat and closure are of titanium carbide. Poppet seats are flexure-mounted to isolate the impact and thermal and vibrational loads from the sealing surface. The poppet seal is made of INCO 718 which is silver plated. Flow passages are sized for minimum pressure loss through each valve.

Valve bodies are welded for zero external leakage. Valve body, housing and cover are made of 347 Stainless. Internal actuator sealing bellows are used to ensure zero leakage between propellant and control system. These bellows are formed of three-ply INCO 718. Absence of bearing surfaces within the propellant or control compartments ensure freedom from contamination or galling. A position
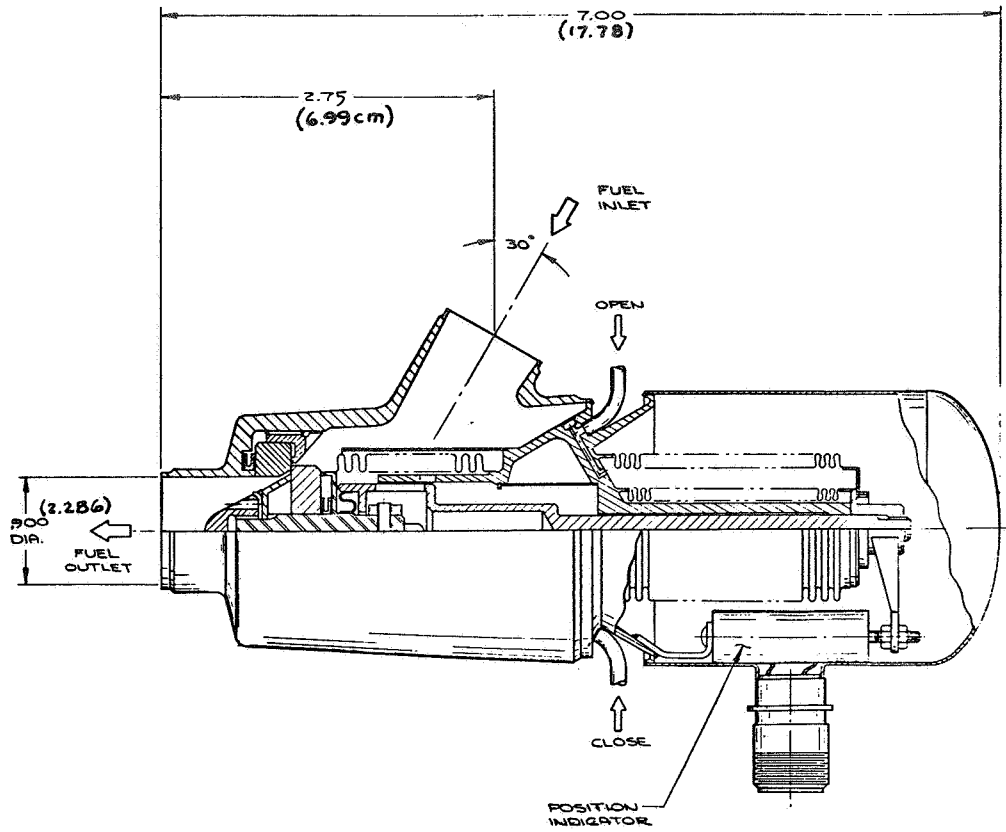
Figure 121. Methane Inlet Valve Assembly.
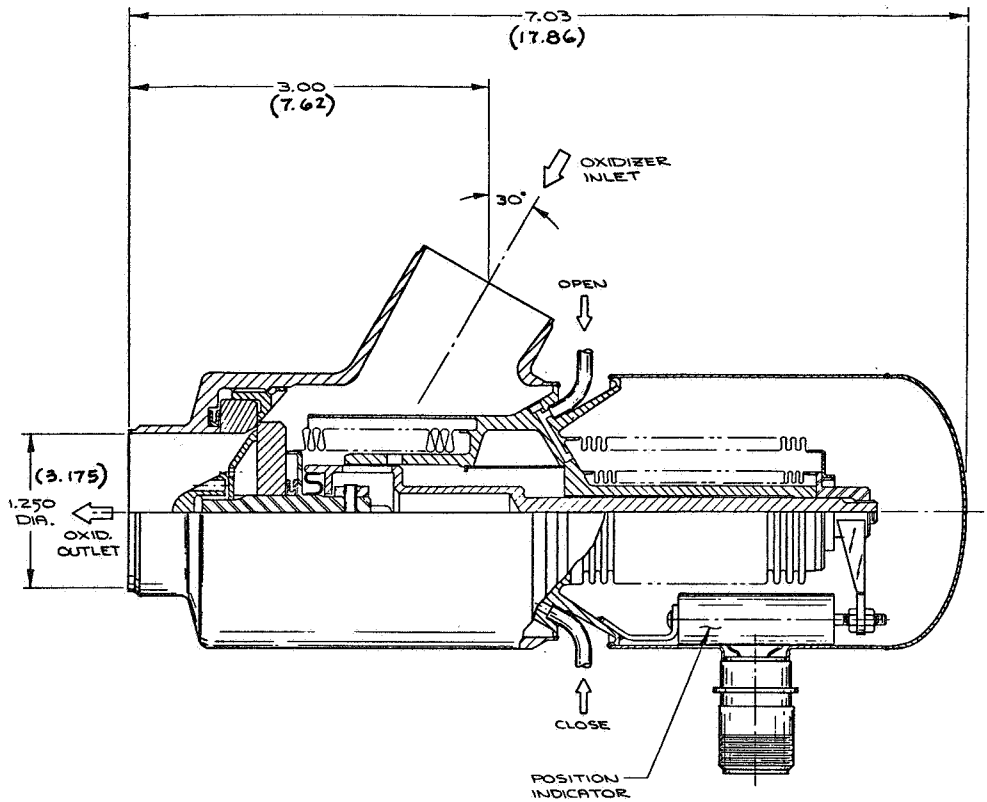
Figure 122. FLOX Inlet Valve Assembly.

323

indicator device is shown built into the valve. This device is mechanically linked to the poppet and gives a positive indication of the poppet position.

The fail-safe feature of the valve is to "close" in the event of leakage of the actuator bellows. The actuator design is such that any small amount of leakage would reduce the forces available to hold the valve open.

HOT GAS VALVES

Two hot methane control valves are used. The FLOX Turbine Control Valve is located at the entrance to the FLOX turbine and regulates the distribution of the hot methane between the two turbines. The bypass valve is located near the exit from the regenerative cooling jacket and controls the total amount of hot methane available to the turbines by regulation of the amount of gas which flows directly from the cooling jacket to the injector manifold.

FLOX Turbine Control Valve

The FLOX turbine control valve specifications are listed in Table 73. Flow characteristic requirements are illustrated in Fig. 123; start characteristics are shown in Fig. 124. The valve will encounter temperatures ranging from that of cold methane during start to values of 1300 to 1750 R (880 to 1225K) during operation. Although 4 to 10 engine starts are considered, the valve will operate a number of times during preflight tests. The valve is operating continually during an engine firing to assure maintenance of the proper engine mixture ratio. The methane flow requirements are described both in Table 73 and in Fig. 123. To cover the range of conditions from nominal thrust to 10:1 throttling, a flow area variation of five is necessary. To cover the uprated condition, the flow area variation is about eight. For the idle-mode and early start conditions, the valve is closed but is not required to maintain zero leakage. Start requirements are shown in Fig. 124 . The valve actuation time for the engine starts of Fig. 124 is 500 milliseconds. Since more rapid starts will eventually be of interest, the potential for faster actuation times should be included.

324

TABLE 73

FLOX TURBINE CONTROL VALVE PRELIMINARY SPECIFICATION

1. Type of Components - Hot Gas Turbine Control Valve

2. Function
    a) Isolate FLOX turbine during early phase of start and idle-mode
    b) Control power application to FLOX turbine
    c) Control engine mixture ratio
    d) Continual variation

3. Operating Fluid - Methane

4. Fluid Characteristics at Valve Inlet
    Start: Temperature = 200R to 500R (111K to 277K)
    Run: Temperature = 1300 R to 1750R (721K to 971K)

5. Operating Environment
    a) Temperature - 200R to 600R (111K to 333K)
    b) Atmosphere - Sea Level to Vacuum
    c) Radiation
    d) Meteor
    e) Zero g

6. Storage Requirements
    a) Earth: Time   - TBD
               Temperature - TBD
               Hunidity   - TBD
               Pressure   - TBD
               Conditions - TBD
    b) Space: 2 years maximum
               250 days maximum between restarts.

7. Operating Life
    a) Maximum Cycles - 4 to 10 engine cycles + all preflight tests
    b) Maximum Operating Time - 540 sec + all preflight tests.

8. Propellant Leakage Rates

	Initial	Operating	Final
a) Internal	TBD	TBD	TBD
b) External	10^{-7} ATM cc/sec He at 300 psi (20.7 kN/m^2)		
c) Seal	Not Required to Seal		

9. Methane Flow Parameters

	Full F	10:1 Throttled	Idle Mode	Uprated
$\dot{w}$, lb/sec (kg/sec)	0.74 (0.336)	0.033 (0.015)	0	1.30 (0.59)
T_{in}, R (K)	1300 (720)	1750 (971)	1076 (597)	1270 (705)
P_{in}, psi (kN/m^2)	976 (6780)	78 (540)	70 (480)	1690 (11650)
ΔP, psi (kN/m^2)	37 (255)	1 (7)	No Flow	120 (825)

10. Critical Sizing Criteria

Maximum allowable ΔP to balance turbine power and maintain mixture ratio during throttling, start and steady-state.

11. Actuator Type - Pneumatic

12. Actuation Time

a) 250 - 500 millisec. Stop-to-Stop

b) Proportional between any two positions

13. Mode of Operation

Valve must go to any position upon command and retain that position

14. Flow Geometry

Number of Inlets - 1

Inlet Line I.D. -0.940-inch (2.39 cm)

Number of Outlets - 1

Outlet Line I.D. -0.940-inch (2.39 cm)

Line Orientation - 180-degree opposed in line

15. Applied Pressure, psia (kN/m^2)

	Inlet	Internal	Outlet
Initial Pressure	0	0	0
Operating Pressure	1690 (11650)	1690 (11650)	1570 (10825)
Shutdown Pressure	TBD	TBD	TBD

326

16.   Ducting Interconnect Method - In-Place Tube Welding.

17.   Structural Mounting Method - Mounted from entrance duct.

18.   Purge Provision - Not required.
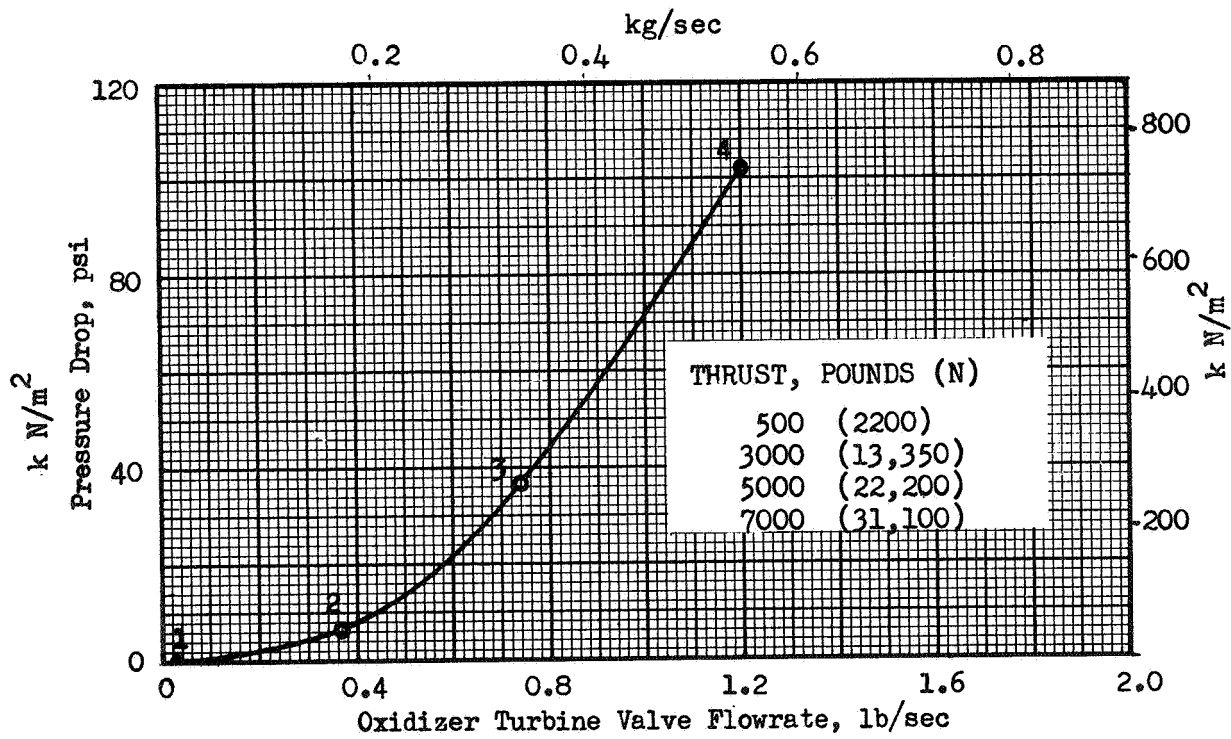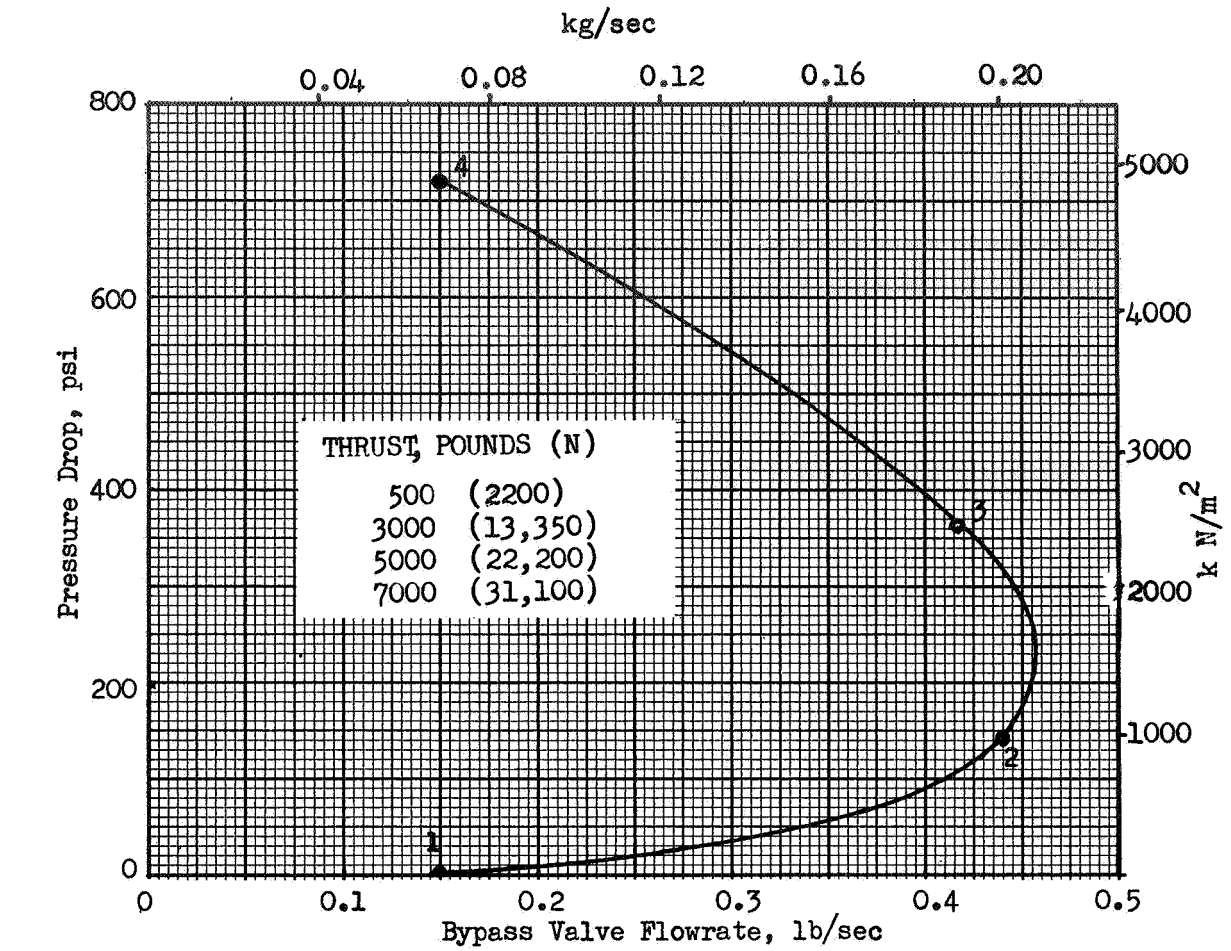
Fig. 123. Control Valve Characteristics
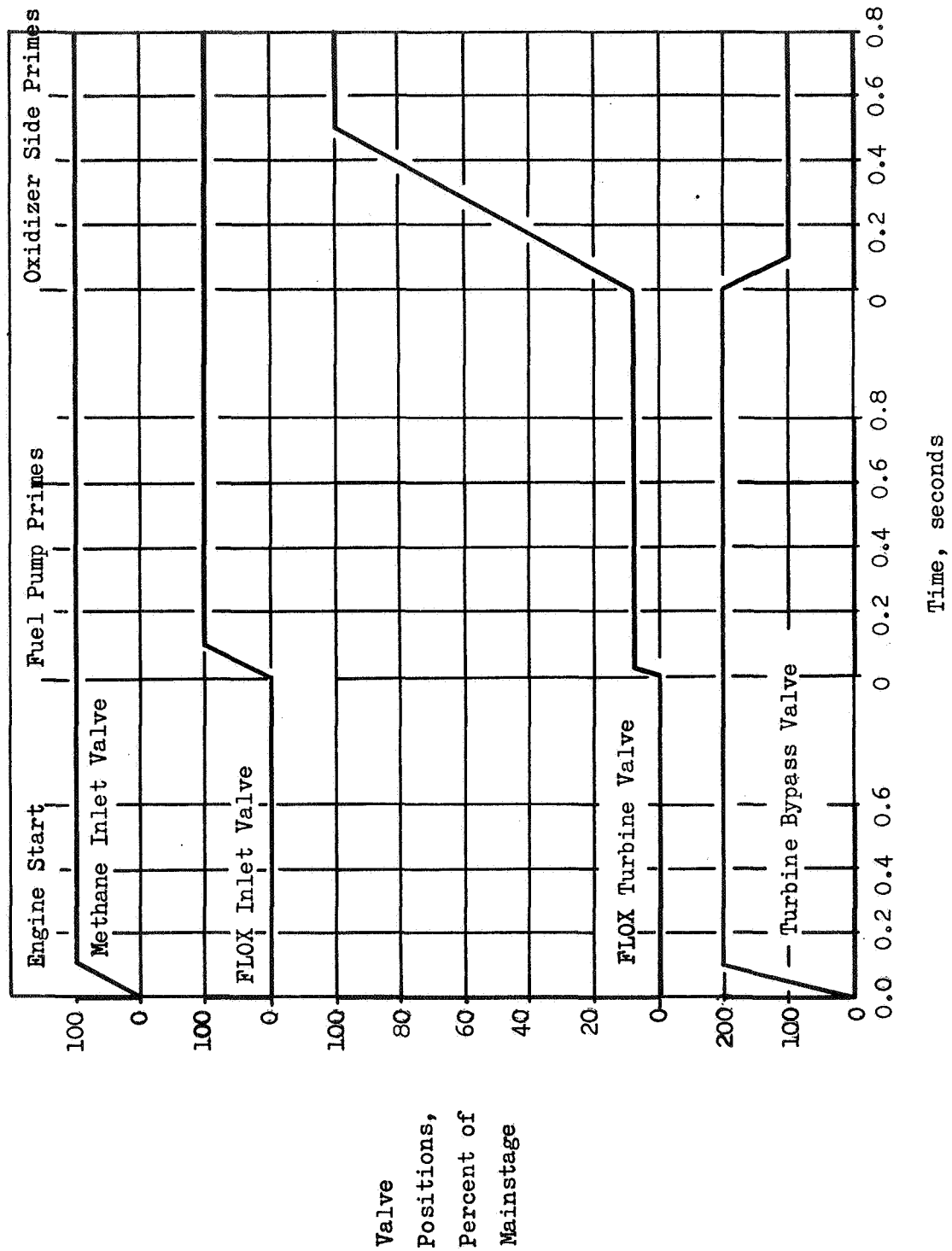
Figure 124. Valve Sequencing for FLOX-Methane, Pump-fed, Expander Cycle Engine.

329

The specification, therefore, shows a range of 250 - 500 milliseconds. An initial position of 8-percent of nominal thrust flow area is required during start.

The FLOX turbine control valve is shown in Fig. 125. The valve is a normally open poppet configuration with activation power supplied by pneumatics. A pneumatic servo control unit operating in closed loop with the linear transducer position indicator regulates valve position by varying the pressure across the piston. Pressure balance across the poppet provided by the circumferential poppet clearance minimizes the control forces necessary to actuate the valve. Some contouring of the poppet is incorporated to reduce the rate of change of area with stroke as the valve approaches the closed position. The poppet contour may be designed to achieve any desirable area/stroke relationship.

Finer control is obtainable by designing increased poppet contour length and stroke. The normal (unpressurized) valve position is midway between full-open and full-closed (1/2 stroke), which results in minimum required bellows length; approximately one-half the length required for a normally full-open or full-closed valve configuration. As shown in Fig.125, the valve flow inlet is annular, which also minimizes stroke requirements and valve length and provides a more uniform distribution of gas flow around the poppet. The flight valves employ all welded construction and bellows seals exclusively in the actuator to preclude internal and external pneumatic leakage and to minimize weight. In-place welded line connections provide structural support for the valves.

Valve material selections are dictated by the operating temperatures and pressures shown in Table 73 . The valve body is cast from INCONEL 625 selected for its good elevated temperature mechanical properties. The poppet is constructed from Stellite 21, which exhibits good resistance to erosion due to high velocity hot gas flow and good thermal shock characteristics. A Stellite 21 seat may also be welded to the cast valve body, if found necessary to prevent erosion in that area. The piston rod is Rene 41 guided by a silver impregnated carbon bearing which also serves as a partial piston rod seal.
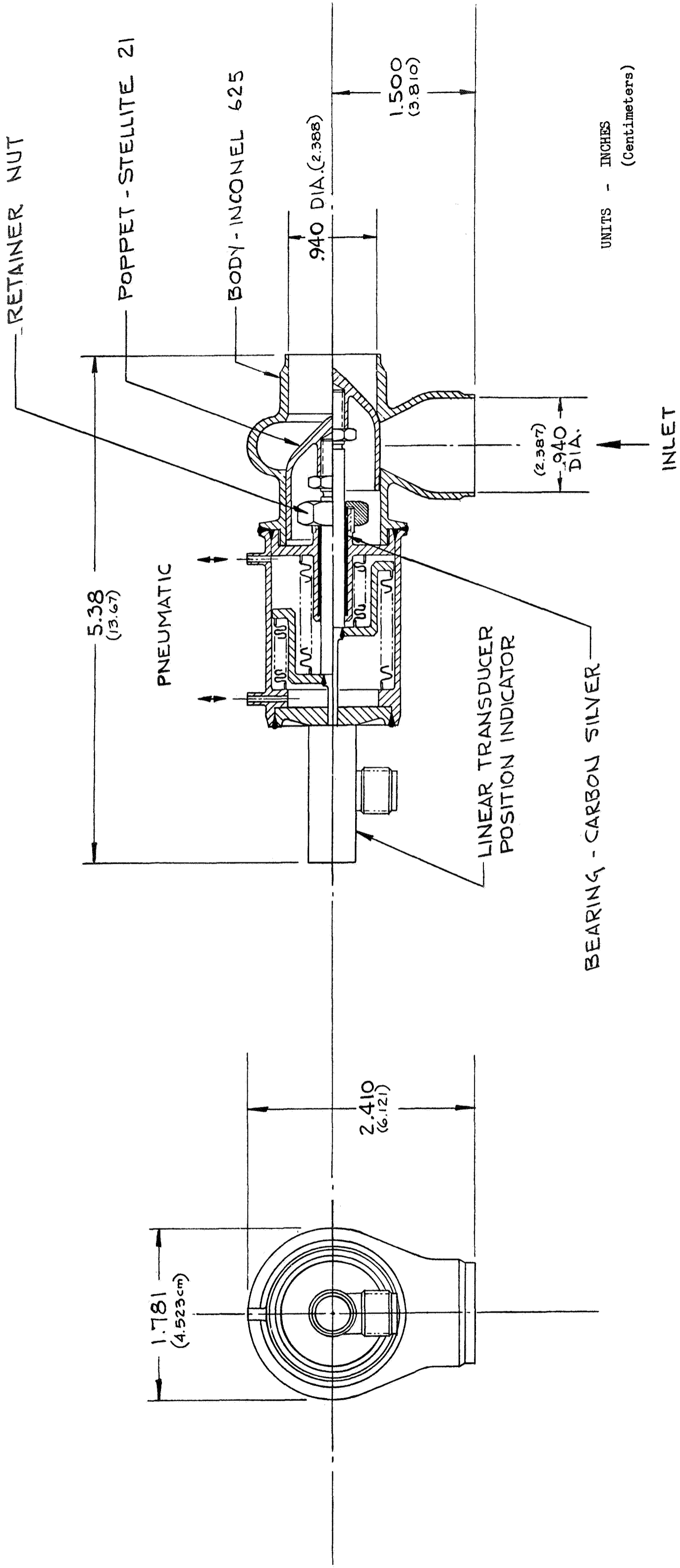
Figure 125. Hot Gas Control Valve.

RETAINER NUT

POPPET - STELLITE 21

BODY - INCONEL 625

.940 DIA. (2.388)

1.500
(3.810)

5.38
(13.67)

PNEUMATIC

(2.387)
.940
DIA.

INLET

LINEAR TRANSDUCER
POSITION INDICATOR

BEARING - CARBON SILVER

UNITS - INCHES
(Centimeters)

2.410
(6.121)

1.781
(4.523 cm)

331

Turbine Bypass Valve

Specifications for the turbine bypass valve are listed in Table 74. Flow characteristic requirements for nominal, throttled and uprated conditions are illustrated in Fig. 123. Start requirements are illustrated in Fig. 124. The bypass valve encounters the same thermal and pressure environment as the FLOX Turbine Control Valve. Also similar to the turbine control, valve operation is continual during the engine operation. Bypass flow requirements, listed in Table 74 and in Fig. 123, indicate a large area variation requirement. In throttling and uprating the flow, area requirement varies by a factor of 100. The start and idle mode flow area requirements are within this range.

The turbine bypass valve would be essentially the same in concept as the FLOX turbine control valve described in Fig. 125. A variable position pintle would control the flow area to regulate the hot methane bypassing the turbine. Materials and actuation methods would also be the same. The large area variation requirements and thrust accuracy restrictions on flow area tolerance over this range may necessitate consideration of other valve concepts.

TABLE 74

TURBINE BYPASS VALVE PRELIMINARY SPECIFICATION

1. Type of Component: Hot Gas Bypass Valve

2. Function
   a) Control of Total Turbine Hot Gas Flow
   b) Continual variation

3. Operating Fluid: Methane

4. Fluid Characteristics at Valve Inlet
   Start: Temperature = 200R to 500 R (111K to 277K)
   Run: Temperature = 1245R to 1670R (691K to 927K)

5. Operating Environment
   a) Temperature = 159 to 600 R (88K to 333K)
   b) Atmosphere: Sea Level to Vacuum
   c) Radiation
   d) Meteor
   e) Zero g

6. Storage Requirements
   a) Earth: Time   — TBD
             Temperature — TBD
             Humidity   — TBD
             Pressure   - TBD
             Conditions   — TBD
   b) Space: 2 years maximum
             250 days maximum between restarts

7. Operating Life
   a) Maximum Cycles — 4 to 10 engine cycles + all preflight tests
   b) Maximum Operating Time — 540 sec + all preflight tests.

8. Propellant Leakage Rates

	Initial	Operating	Final
a) Internal	TBD	TBD	TBD
b) External	10^{-7} ATM cc/sec He at 300 psi (2070 kN/m^2)		
c) Seat	Not Required to Seal		

9. Propellant Flow Parameters

	Full F	10:1 Throttled	Idle Mode	Uprated
$\dot{w}$, lb/sec (kg/sec)	0.42 (0.191)	0.15 (0.068)	0.169 (0.077)	0.15 (0.068)
T_{in}, R (K)	1300 (721)	1750 (971)	1079 (599)	1270 (705)
P_{in}, psia (kN/m^2)	1014 (7000)	79 (545)	71 (550)	1747 (12045)
ΔP, psi (kN/m^2)	360 (2480	7.0 (48)	---	720 (4965)

10. Maximum allowable ΔP to achieve low thrust mode (probably idle mode) with reasonable engine response time.

11. Actuator Type - Pneumatic

12. Actuation Time

 a) 100 millisecond - stop to stop

 b) Proportional between any two positions.

13. Mode of Operation

 Valve must go to any position upon command and retain that position.

14. Flow Geometry

Number of Inlets	- 1
Inlet Line I.D.	- 0.940-inch (2.39 cm)
Number of Outlets	- 1
Outlet Line I.D.	- 0.940-inch (2.39 cm)
Line Orientation	- 180-degree opposed in line (3.14 rad)

15. Applied Pressure, psia (kN/m^2)

	Inlet	Internal	Outlet
Initial Pressure	O	O	O
Operating Pressure	1747 (12045)	1747 (12045)	1020 (7032)
Shutdown Pressure	TBD	TBD	TBD

16. Ducting Interconnect Method - In-place tube welding.

17. Structural Mounting Method - Mounted from entrance duct.

18. Purge Provisions - Not required.

TURBOMACHINERY DESIGN

The turbomachinery is designed to supply the head and flow required by the engine system, as described previously . These operating conditions include the nominal thrust, 10:1 throttling, and potential thrust uprating. Low NPSH requirements are desired, particularly during pumped idle-mode operation when tank pressurization may not be available. Rapid thermal conditioning of the pumps is also considered, as well as potential variations in pump inlet pressure and temperature. In this section the pump and turbine analyses are described, inducer suction performance is evaluated, and turbopump design and fabrication are described. Use of current technology is emphasized. Where possible, existing test data are used to substantiate the analyses.

PUMP DESCRIPTION

Pump design configurations are illustrated in Fig. 126 . The pump configurations were established in Task I with the shaft speeds at nominal thrust selected from consideration of impeller tip speed and diameter ratio, bearing DN values, seal rubbing speeds, and suction performance. The values of the design limits that governed the pump designs are listed in Table 25 . The pump nominal designs are based upon propellant conditions anticipated at tne eod of an interplanetary mission which represented potentially the most severe power requirement. The pumps are mounted on separate shafts and are driven by separate turbines. The configuration allows both units to run at their most optimum speeds and provides for flexible control. Both units are equipped with a conventional inducer.

FLOX Pump

The FLOX pump is a conventional, single-stage, high specific speed centrifugal machine. At the nominal thrust level, the FLOX pump speed was limited to 40,000 rpm by the impeller eye diameter to tip diameter ratio which was set at 0.77. The limit was reached at a relatively low speed for this size pump, because of the low required head and consequent high specific speed. The FLOX pump design parameters, physical characteristics, and operating conditions at a thrust level of 5000-pounds
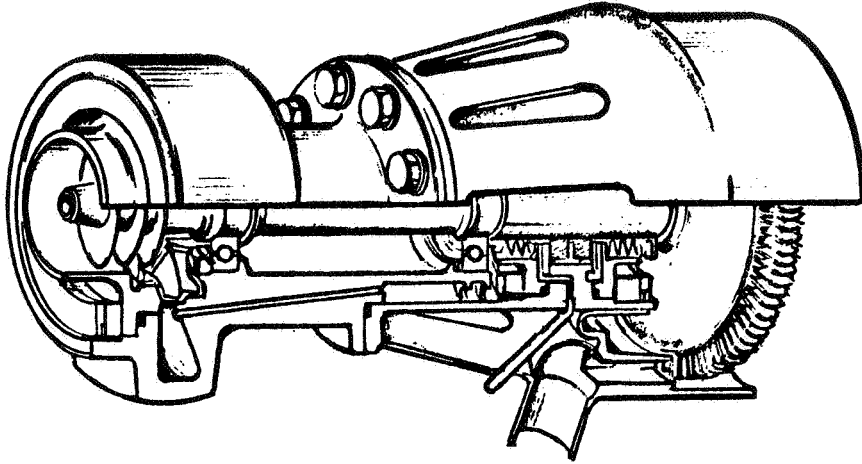
OXIDIZER PUMP
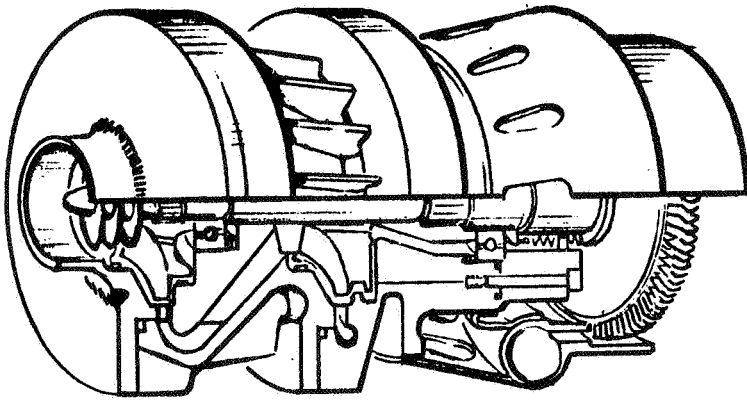
FUEL PUMP

Figure 126. Turbopump Designs.

(22200N) are presented in Table 75 . The bearings and seals operate in FLOX at DN and speed values significantly below those being demonstrated in technology programs such as NAS3-12022 (Ref. 4).

Inducer inlet flow coefficient and blade angles were selected to provide maximum suction performance. These were based upon experience with inducers in cryogenic fluids and consideration of potential blade thickness limitations. The impeller blade angle of 25 degrees was selected to provide an H-Q operating curve conducive to throttling and engine start, while at the same time being reasonable to fabricate. The impeller is shrouded to provide high efficiency with wear ring clearances reasonable for use in FLOX. The estimated head, flow and efficiency map is presented in Fig. 127 and the corresponding flow coefficient/head coefficient curves are shown in Fig. 128.

Methane Pump

The relatively low density of methane requires considerable head to produce the necessary discharge pressure. Consequently, to raise the specific speed per stage to reasonable levels for conventional centrifugal pumps, a two-stage methane pump configuration was chosen. The shrouded impellers, which are identical except for the wear ring and balance piston, are placed front-to-back to facilitate compact design, to minimize external lines, and to improve inlet conditions to the second-stage impeller. Inducer and impeller blade angles were selected from the same considerations as the FLOX pump. The two stages are equipped with radial diffusers at the impeller discharges to reduce the high discharge velocities and to equalize the circumferential static pressure distribution which, in turn, reduces radial loads. The interstage crossover is annular and is equipped with a radial inflow stator to provide proper flow to the eye of the second-stage impeller.

The rotational speed was established at 74,000 rpm by the primary seal rubbing speed. This speed is conservative and will allow higher speeds if desired for uprating. The methane pump design parameters, physical characteristics, and operating conditions at the 5000-pound (2270 kg) thrust level are presented in Table 75. The head, flow, efficiency maps, and the flow coefficient/head coefficient curve are presented in Fig. 129 and 130, respectively.

TABLE 75

DESIGN POINT PUMP DESCRIPTION

NOMINAL THRUST

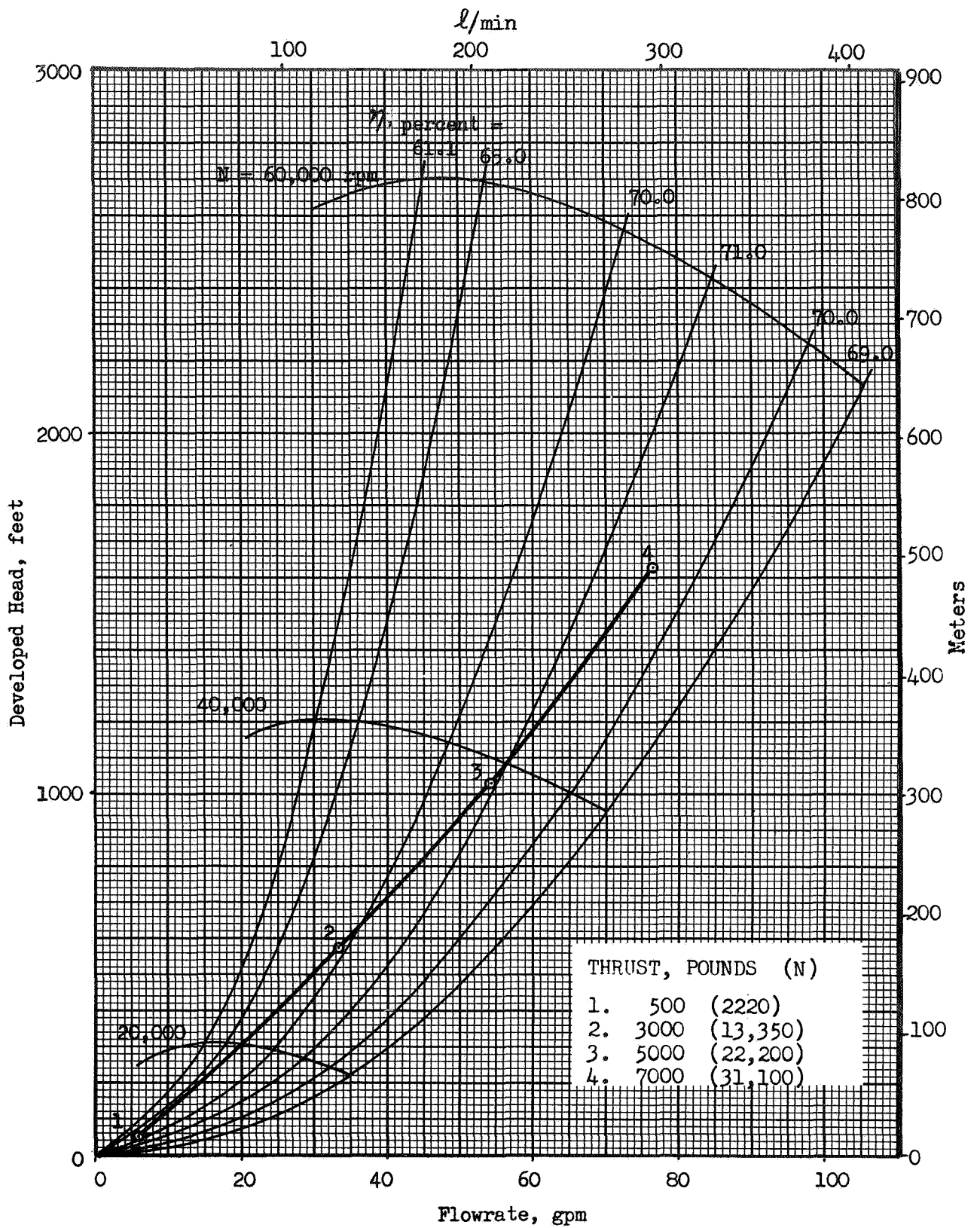|	FLOX		Methane	
Flowrate, lb/sec (kg/sec)	10.52	(4.79)	2.0	(0.91)
Flowrate, gpm (ℓ/min)	56.5	(214)	37.5	(141.8)
Inlet Pressure, psia (k N/m^2)	50	(345)	80	(550)
Inlet Temperature, R (K)	170	(94.5)	240	(133)
Discharge Pressure, psia (k N/m^2)	680	(4690)	1600	(11050)
Head Rise, ft (m)	1080	(330)	9120	(2780)
Speed, rpm (rad/sec)	40000	(4190)	74000	(7740)
Type	Centrifugal		Centrifugal	
Number of Stages	1		2	
Specific Speed Per Stage	1590		817	
Efficiency	0.71		0.62	
Horsepower (kw)	29	(21.6)	54.0	(40.3)
Discharge Flow Coefficient	0.11		0.08	
Head Coefficient Per Stage	0.469		0.542	
Inducer Inlet Diameter, inches (cm)	1.2	(3.05)	0.9	(2.29)
Inducer Inlet Flow Coefficient	0.088		0.081	
Inducer Tip Blade Angle, deg. (rad)	7.3	(0.127)	6.75	(0.118)
Inducer Tip Speed, ft/sec (m/sec)	209	(63.8)	291	(88.7)
Impeller Tip Diameter, inches (cm)	1.56	(3.96)	1.61	(4.09)
Impeller Tip Width, inches (cm)	0.170	(0.43)	0.085	(0.216)
Impeller Discharge Blade Angle, deg. (rad)	25	(0.435)	35	(0.61)
Impeller Tip Speed , ft/sec (m/sec)	272	(83)	520	(159)
Impeller Diameter Ratio	0.77		0.54	
Diffuser Inlet Blade Angle, deg. (rad)	NA		8	(0.14)
Bearing Dn x 10^{-6}, mm-rpm (mm-rad/s)	0.6	(.159)	0.89	(.236)
Seal Speed, ft/sec (m/sec)	113	(34.4)	240	(73.1)

Fig. 127. FLOX Pump Operating Line
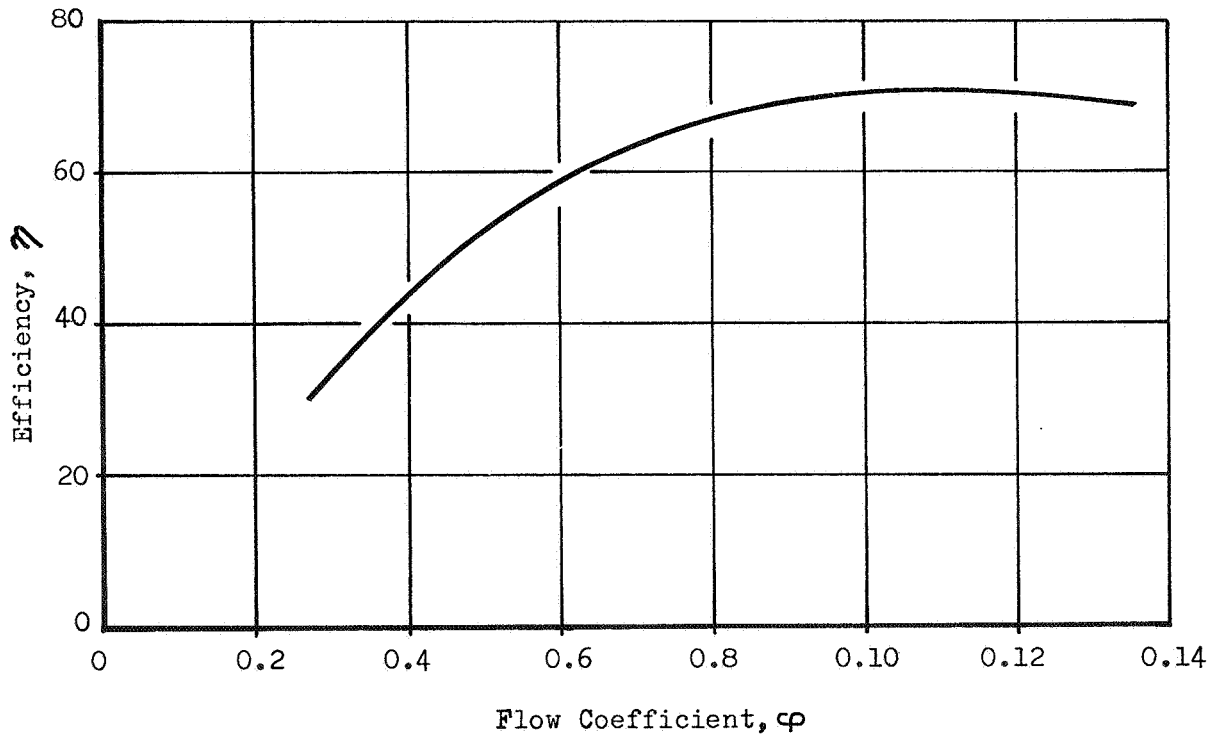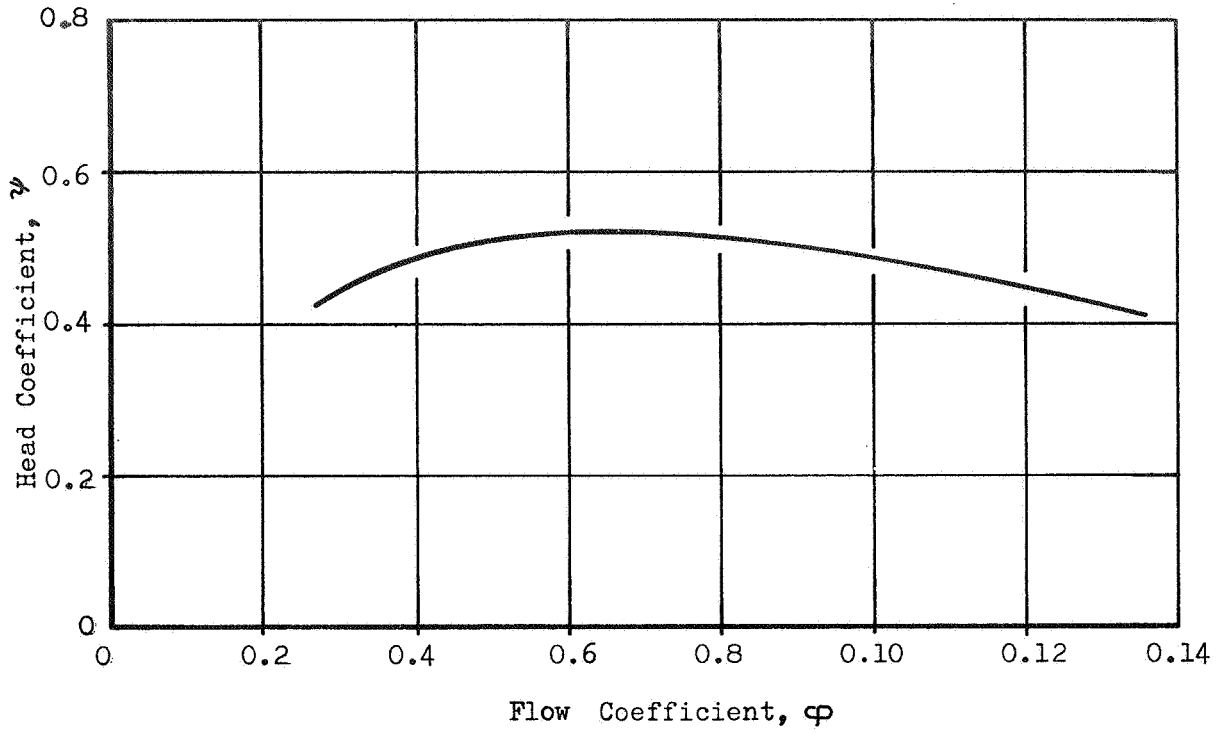
Figure 128. FLOX Turbopump Characteristics.
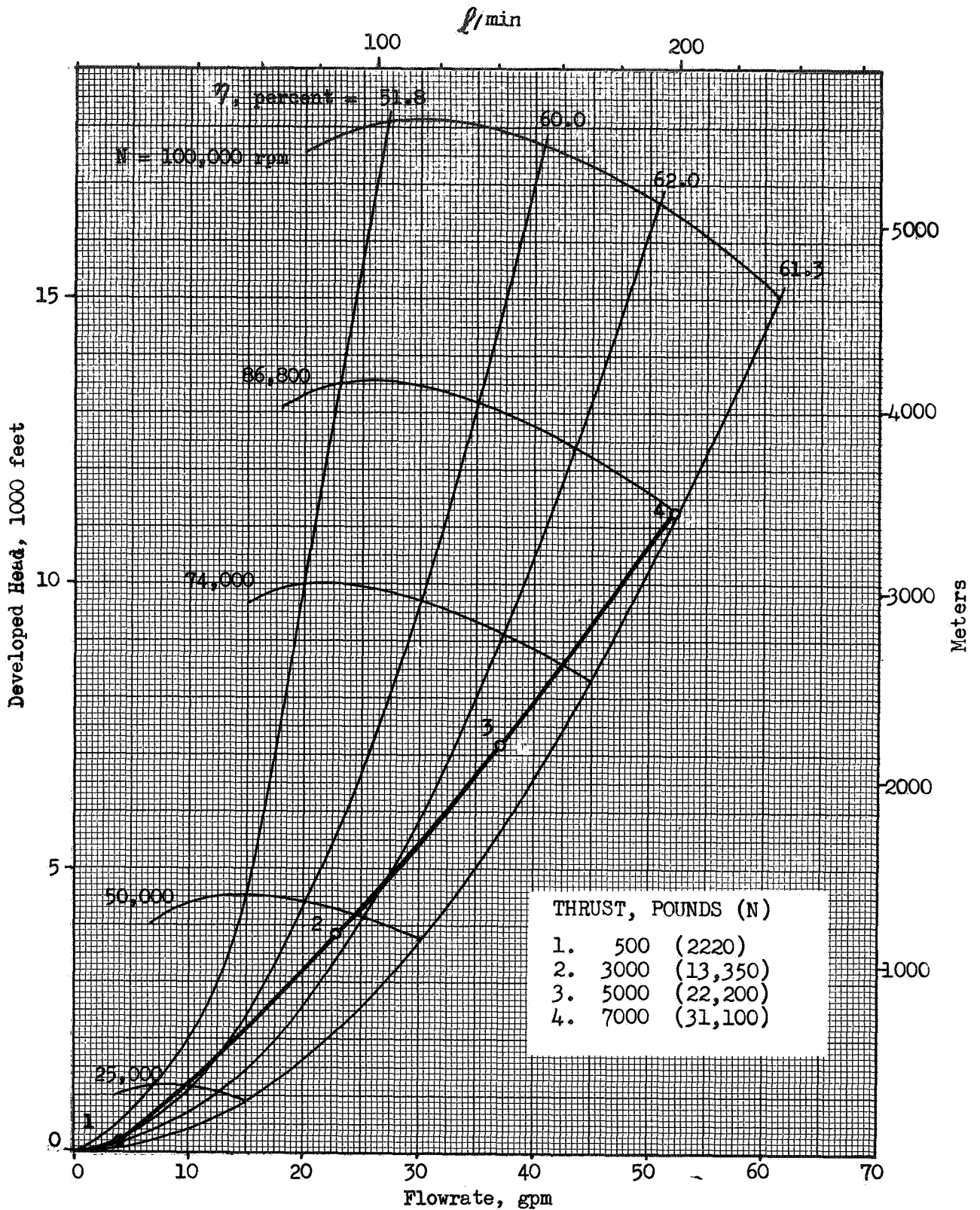
Fig. 129. Methane Pump Operating Line
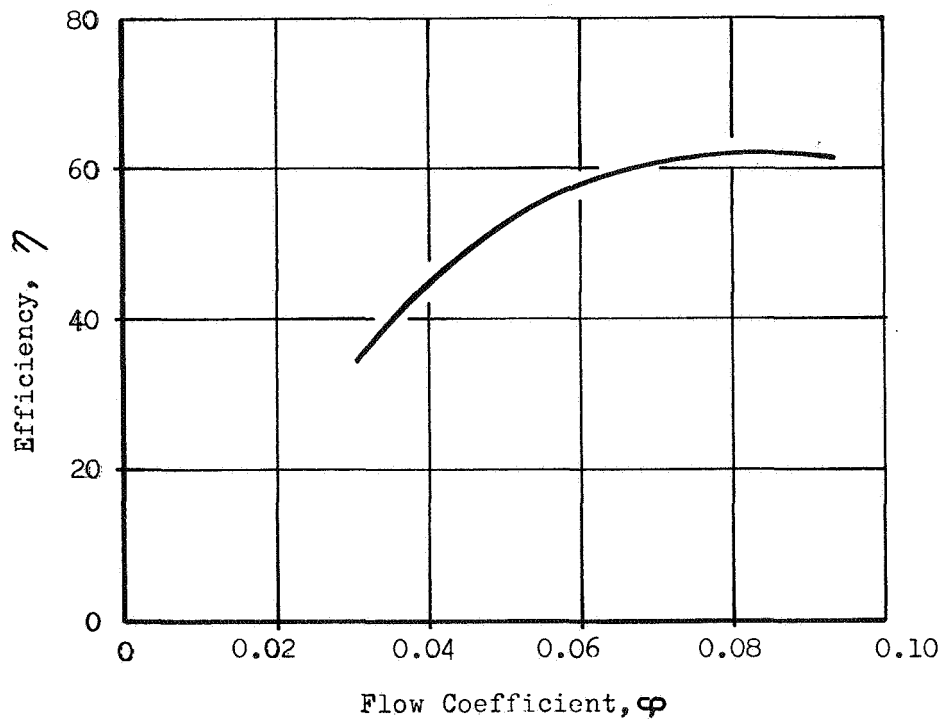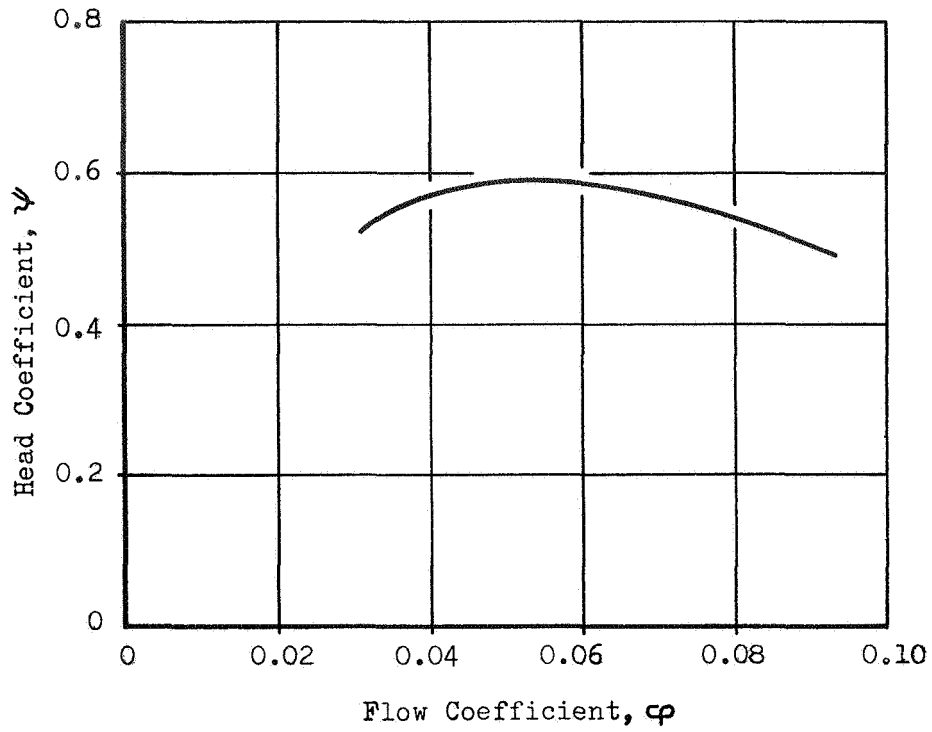
Figure   130.   Methane Turbopump Characteristics.

Pump Analysis Method

The parametric pump analysis used in **Task I** was refined to provide more exact description of pump performance and configuration. These final pump analyses and performance estimates are based upon the more detailed analytical procedure provided by Rocketdyne's Centrifugal Pump Loss Isolation Program. This program computes individual losses (e.g., incidence, diffusion, etc.) for each pump component (e.g., inducer, impeller, etc.) and subtracts them from ideal performance to get component and overall pump performance. An iterative procedure is used for calculating impeller flow and head based upon calculated wear ring leakage which is a function of, and affects, impeller head. Pure power losses, such as disk friction, are also calculated so that efficiency and required horsepower can be obtained. Design features such as blade angles, blade thicknesses, blade lengths, surface roughness and boundary layer thicknesses are estimated for the pumps based upon anticipated flow passage materials and design practice for small pumps. These are input to the program and are used in the performance calculation. Computations for larger pumps using these methods have led to reasonable agreement with test data. Tests of a 12 gpm fluorine pump under Contract NAS3-12022 (Ref.4) will provide test data for small pumps which can be used to correlate the analytical predictions.

Uprating

The 5000-pound thrust FLOX and methane pumps can be uprated to thrust levels as high as 8000 pounds merely by raising their speeds to 54,000 and 92,000 rpm, respectively. Estimated 7000-pound (31100 N) thrust operating points are shown on the H-Q maps, Fig. 127 and 129. Should the high methane pump flow coefficient become a problem, the pump could be run faster and the impellers trimmed slightly. The pump operating characteristics at 8000-pound (35600 N) thrust are presented in Table 76.

It can be seen in Table 76 that the FLOX pump seal speed of 160 ft/sec (49 m/sec) at uprated conditions is still below the state-of-the-art value of 180 ft/sec (55 m/sec). The bearing DN value of 0.81×10^6 is less than 10-percent higher than the presently accepted state-of-the-art value of 0.75×10^6. Considering the present and planned development work with fluorine lubricated bearings, no problems are anticipated in this area.

TABLE 76

PUMP DESCRIPTION: UPRATED CONDITIONS

	FLOX		Methane	
Flowrate, lb/sec (kg/sec)	16.8	(7.64)	3.2	·(1.45)
Flowrate, gpm (l/m)	90	(340)	60	(227)
Inlet Pressure, psia (k N/m^2)	67	(460)	85	(590)
Inlet Temperature, R (k)	170	(94.5)	240	(133)
Discharge Pressure, psia (k N/m^2)	1100	(7580)	2110	(14550)
Head Rise, ft (m)	1800	(550)	12200	(3720)
Speed, rpm (rad/sec)	54000	(5650)	92000	(9620)
Type	Centrifugal		Centrifugal	
Number of Stages	1		2	
Specific Speed Per Stage	1850		1020	
Efficiency	0.70		0.60	
Horsepower (kw)	79	(59)	118	(88)
Discharge Flow Coefficient	0.132		0.103	
Head Coefficient Per Stage	0.431		0.47	
Inducer Inlet Diameter, inches (cm)	1.2	(3.05)	0.9	(2.29)
Inducer Inlet Flow Coefficient	0.104		0.105	
Inducer Tip Blade Angle, deg. (rad)				
Inducer Tip Speed, ft/sec (m/sec)	282	(86)	362	(110.5)
Impeller Tip Diameter, inches (cm)	1.56	(3.96)	1.61	(4.09)
Impeller Tip Width, inches (cm)	0.170	(0.43)	0.085	(0.216)
Impeller Discharge Blade Angle, deg. (rad)	25	(0.435)	35	(0.61)
Impeller Tip Speed, ft/sec (m/sec)	367	(120)	646	(197)
Impeller Diameter Ratio	0.77		0.54	
Diffuser Inlet Blade Angle, deg. (rad)	NA		8	(0.14)
Bearing Dn x 10^{-6}, mm-rpm (mm-rad/s)	0.81	(.215)	1.08	(.287)
Seal Speed, ft/sec (m/sec)	160	(48.8)	298	(91)

The methane pump bearing DN values are well below the estimated limiting value at
both nominal and uprated thrust levels. The seal speed at uprated conditions,
however, is about 300 ft/sec (91 m/sec), which is 20-percent above the limit
presently being used for 250 ft/sec (76 m/sec). The present limit is felt to be
conservative based on RP-1 fuel seal performance, on the mild cryogenic character-
istics of methane, and on the lack of reported test problems in the literature.
It is reasonable to assume that 300 ft/sec (91 m/sec) can be obtained in methane
with little problem.

In addition to mechanical considerations listed above, the increase in speed will
also affect the amount of inlet pressure required to maintain the suction specific
speed. For constant suction specific speed, the required NPSH values approximately
double when the speeds and flows are increased to the 8000-pound (35600 N) thrust
level. Additional NPSH may be needed depending upon the inducer off-design performance.

TURBINE ANALYSIS

The two turbines operating in parallel are powered by heated methane from the thrust
chamber discharge manifold. At nominal thrust, turbine inlet temperature is 1300 R
with a small temperature drop allowed between the thrust chamber and turbine inlet.
Slightly over 20-percent of the methane flows through the bypass valve to assure
sufficient power margin and to allow for potential uprating. At higher thrust
levels the bypass is reduced to 5 percent. The remaining methane flow is split
between the turbines to minimize overall turbine pressure ratio.

Turbine operating pressures are high and reduce the available pressure ratio, and
consequently the available energy and working fluid specific volume. The low
pressure ratios coupled with a restriction on minimum pitch diameter place turbine
velocity rates in the range best served by single row turbines. The low specific
volume coupled with the low horsepower demand and the limit on minimum blade height
indicated the use of a partial admission nozzle. Turbine blades were unshrouded
to improve the ease of manufacture. A slight efficiency penalty is incurred, but
fabrication ease is significantly better. The turbine is velocity-compounded to
take the pressure drop in the nozzles, this allows larger blades and reduces
leakage across the blades.

347

Turbine efficiencies were determined through estimation of individual losses due
to gas dynamics, friction and leakage. The resulting efficiency values are very
comparable with data from Ref. 17 for a slightly larger turbine. The predicted
efficiencies are slightly lower than the data, reflecting the size difference.

Turbine characteristics were evaluated at both the nominal and uprated thrust
levels to provide a design which would give high performance at the 5000-pound
(22200 N) thrust level and yet be reasonable for operation at the 8000-pound
(35000 N) thrust level. At the 5000-pound (22200 N) thrust level, pitch diameter
had a relatively slight effect on turbine performance, and a design which was
common to both the FLOX and methane pumps was determined. This design has a 2.75-
inch (6.99 cm) pitch diameter with the same blade characteristics for both turbines.

When the nominal thrust turbine designs were evaluated for uprating, it was found
that the FLOX turbine could be uprated if the nozzle arc of admission were
increased by 3 percent and if the torus were originally made 0.050-inch (0.127 cm)
larger in diameter.

Analysis of the 5000-pound (22200 N) thrust methane turbine at 8000-pound (35600 N)
thrust revealed that the increase in turbopump speed from 74,000 to 92,000 rpm forced
operation beyond the peak efficiency point for a single-row design. Consequently,
the methane turbine was designed with a lower 2.16-inch (5.48 cm) pitch diameter
to reduce the pitch line velocity and, hence, velocity ratio. At the nominal
thrust level, the fuel turbine would have an arc of admission of 51 percent. At
uprated conditions this would have to be increased to 63 percent. Table 77 presents
the physical and operational characteristics of the selected oxidizer and fuel
turbine designs.

The turbines and pumps must be stressed for operation at the most severe conditions.
The highest operating temperatures occur at throttled conditions. However,
turbine speed and pressures are very low and the stress is not severe. The most
severe stress condition would be where the engine was operated at 10:1 throttled
conditions, and then the thrust increased rapidly while material temperatures were
still high. With the INCO-713C, -718 materials used in the turbine, strength is
maintained over the anticipated temperature range. For example, blade centrifugal

TABLE 77

TURBINE DESIGN POINT DESCRIPTION

	FLOX		Methane	
Drive Fluid	Methane			
Inlet Temperature, R (K)	1300	(723)	1300	(723)
Type	Single Row Impulse			
Inlet Pressure, psia (k N/m^2)	977	(4740)	1017	(7010)
Pressure Ratio	1.47		1.53	
Exhaust Pressure, psia (k N/m^2)	665	(4585)	665	(4585)
Speed, rpm (rad/sec)	40,000	(4190)	74,000	(7740)
Mean Blade Diameter, inches (cm)	2.75	(7.0)	2.16	(5.49)
Mean Blade Speed, ft/sec (m/sec)	480	(146.2)	697	(212.5)
Horsepower (kw)	29	(21.6)	54	(40.3)
Flowrate, lb/sec (kg/sec)	0.70	(0.318)	0.90	(0.409)
Efficiency (T-S)	0.46		0.61	
Nozzle Exit Height, inches (cm)	0.17	(0.432)	0.15	(0.381)
Nozzle Width, inches (cm)	0.30	(0.762)	0.28	(0.712)
I-R Blade Height, inches (cm)	0.20	(0.509)	0.18	(0.457)
I-R Blade Width, inches (cm)	0.26	(0.66)	0.24	(0.61)
Torus Diameter, inches (cm)	0.55	(1.40)	0.65	(1.65)
Nozzle Arc of Admission, percent	25		51	

stress is indicated by the parameter of the flow annulus area times the speed squared. For current turbines, this value is below 10^{10} for all conditions. As indicated by the maximum centrifugal blade stress of Fig. 131, material strength is more than sufficient even for the extreme condition.

TURBOPUMP SUCTION PERFORMANCE

An analytical investigation of pump suction performance was conducted to evaluate the potential for low NPSH operation, both at full thrust and during start operation where pressurization gas may be unavailable. Low NPSH and even two-phase operation have been accomplished with hydrogen and appear possible with the current propellants. In the investigation, conventional inducers are used on each pump. Use of a boost pump or preinducer could improve suction performance, however the added complexity of these devices was not felt to be desirable at this time. Available NPSH at the inducer is given by

$$(NPSH)_{avail} = \frac{144}{\rho} \left[\text{total pressure} - \text{vapor pressure} \right]_{inlet}$$

where total pressure $= P_s + \Delta P_{vel} = P_{tk} + \Delta P_{acc} - \Delta P_{fric}$

with

$$
\begin{aligned}
P_{tk} &= \text{tank pressure} \\
\Delta P_{fric} &= \text{friction loss} \\
\Delta P_{acc} &= \text{acceleration head} \\
\Delta P_{vel} &= \text{velocity head} \\
P_{vapor} &= \text{vapor pressure}
\end{aligned}
$$

For effective pump operation, the available NPSH must be equal to or greater than the NPSH required by the inducer. For the current investigation, the NPSH required is that at which less than 2-percent pump head loss occurs.

Suction Performance Prediction

The required net positive suction head (NPSH) of a pump is the difference between the basic net positive suction head, which is independent of thermodynamic
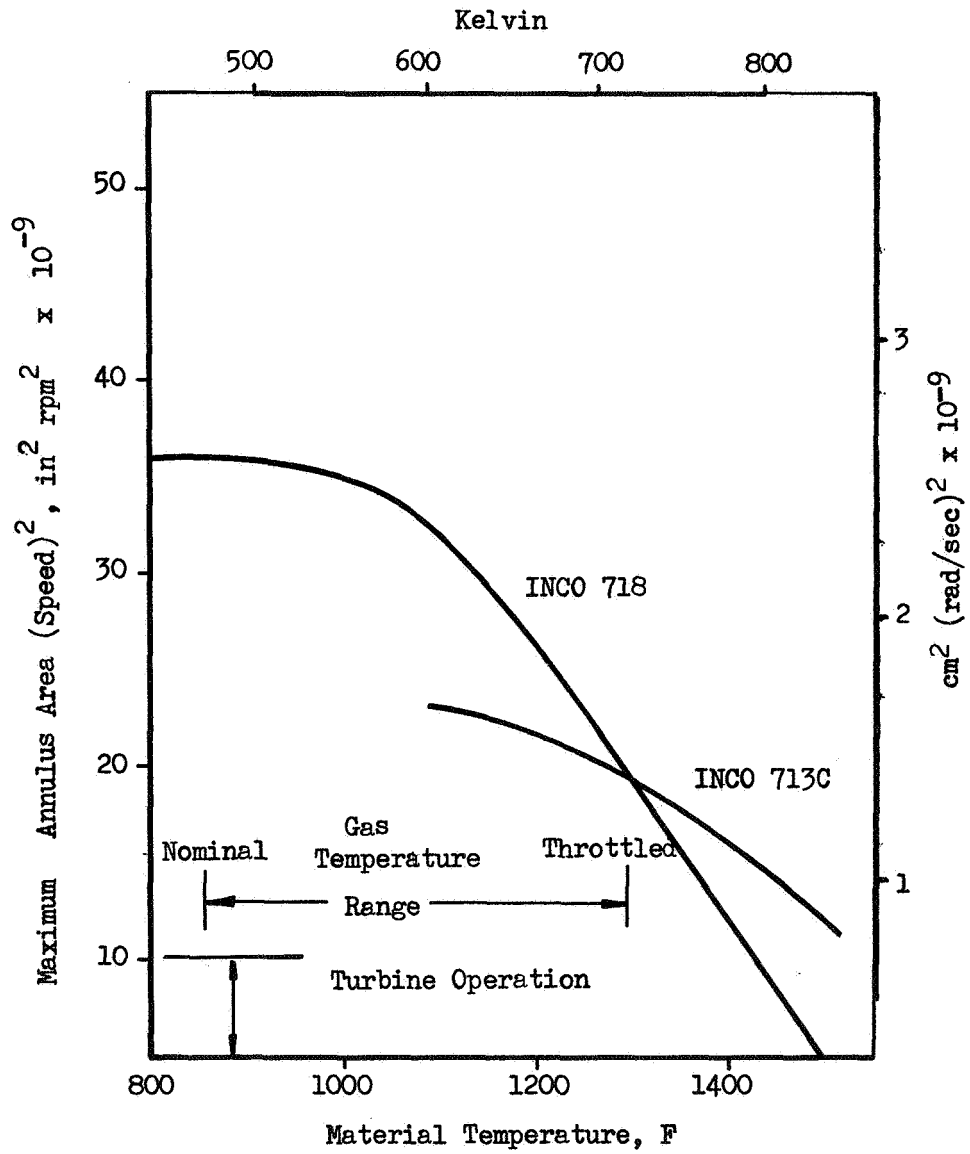
Figure 131. Turbine Blade Stress

effects, and the thermodynamic suppression head (TSH). Therefore, nondimensionalizing

$$\frac{(\text{NPSH})}{c_m^2/2g} = \frac{(\text{NPSH})_{\text{basic}}}{c_m^2/2g} - \frac{\text{TSH}}{c_m^2/2g} \qquad (1)$$

Since ambient temperature water has very little TSH, the basic NPSH is equal to the ambient water value. For moderate sized inducers, this basic NPSH of water is equal to approximately three inlet velocity heads. For smaller inducers, minimum blade thickness and leading edges may increase the basic NPSH to 4-5 inlet velocity heads.

Thermodynamic suppression head exists because vaporization within the inducer chills the liquid, thereby dropping the vapor pressure, increasing the effective NPSH, and permitting the pump to operate satisfactorily at a reduced value of inlet NPSH.

Two expressions for the thermodynamic suppression head were considered. The first expression was obtained from Ref. 12 and is referred to as the NASA-Holl expression

$$\text{TSH} = C \left(\frac{d}{12}\right)^{0.16} U^{0.85} \beta \qquad (2)$$

This equation is based upon cavitating venturi test data in both Freon 114 and liquid nitrogen, and on inducer test data in liquid hydrogen (Ref. 18, 19). The constant, C, is a function of inducer geometry and operating point and may be a function of the propellant properties. However, it was assumed to be constant in this analysis. The thermal factor, β, is the primary thermodynamic relationship in TSH (Eq. 2) and is entirely a function of propellant properties (Eq. 3).

$$\beta = \frac{g\,J\,L^2}{T\,C_{PL}\,\dfrac{\rho_L}{\rho_V}\left(\dfrac{\rho_L}{\rho_V}-1\right)\sqrt{\dfrac{K_L}{3600\,\rho_L\,C_{PL}}}}$$ (3)

Equation (2) was used to obtain the influence of fluid type and vapor pressure on the thermal factor . The factor, β, and consequently TSH, are greatest for hydrogen, followed (in order of decreasing β and TSH) by methane, oxygen, fluorine and water. For all five fluids, the β's approach simple exponential functions of vapor pressure with exponents between 1.5 and 2.0.

The reference value of TSH was obtained from the MK $15\text{-}O_2$ pump test results in which, at design values of speed and volume flowrate, $NPSH/C_M2/2g$ was approximately equal to one (Eq. 1). Consequently, based upon the MK $15\text{-}O_2$ pump design point, the nondimensional NPSH becomes:

$$\frac{(NPSH)_{REQ}}{C_m2/2g} = \frac{(NPSH)_{BASIC}}{C_m2/2g} - \left(\frac{0.109}{\phi}\right)^2 \left(\frac{258}{U}\right)^{1.15} \left(\frac{d}{6.75}\right)^{0.16} \left(\frac{\beta}{0.0841}\right)$$ (4)

The second expression for thermodynamic suppression head was developed at Rocketdyne during work on the Mark 4 pump development for the THOR engine (Ref. 20·). This expression leads to the following relation for the required NPSH:

$$\frac{(NPSH)_{req}}{C_M2/2g} = \frac{(NPSH)_{basic}}{C_M2/2g} - \frac{5.48\,(d/Z)^{0.16}}{\phi^2\,U^{1.15}} \left(\frac{\beta}{0.865}\right)$$ (5)

where

$$\beta = \frac{\rho_V}{\rho_L} \quad \frac{L}{C_{p_L}}$$

Test Data Comparison

A comparison of these equations with test data for liquid oxygen and hydrogen is presented in Fig. 132.

$$\frac{(NPSH)_{basic}}{C_M^2/2g} = 3$$

The THOR expression generally indicates higher NPSH requirements than the NASA-Holl expression. Both expressions show that the NPSH requirements decrease as the propellant vapor pressure increases. This effect is due to the increase in vapor density as the vapor pressure increases. It should be noted that the actual pressures are not decreasing as vapor pressure rises -- only the required NPSH.

At sufficiently high vapor pressures, the curves flatten and above this NPSH required is only one velocity head. In this region the pumps can function effectively with the static pressure equal to the vapor pressure or with saturated propellants. In this region , it becomes likely that two-phase pumping could be accomplished. The probability increases as vapor pressure increases. It appears that the THOR expression is a better representation of the liquid oxygen data and the NASA-Holl expression is better for liquid hydrogen. The THOR expression would, therefore, be more representative of fluorine suction performance, while the methane suction performance might be expected to be somewhere between the two expressions.

Suction Performance for Space Storable Pumps

The NPSH requirements were predicted for the FLOX and methane pumps using both prediction methods. These are shown in Fig. 133 and 134. Since these pumps are small, two values of the basic NPSH were used, 3 and 5 velocity heads; the latter value representing a conservative estimate for small pumps. The required NPSH is shown for two pump speeds, one corresponding to full thrust and the other about 50-percent of full thrust operation.

These predictions are translated into pressure requirements in Table 78 . The FLOX estimates were based upon the THOR equation, while results of both expressions are shown for methane. At full thrust and low vapor pressures, the

354
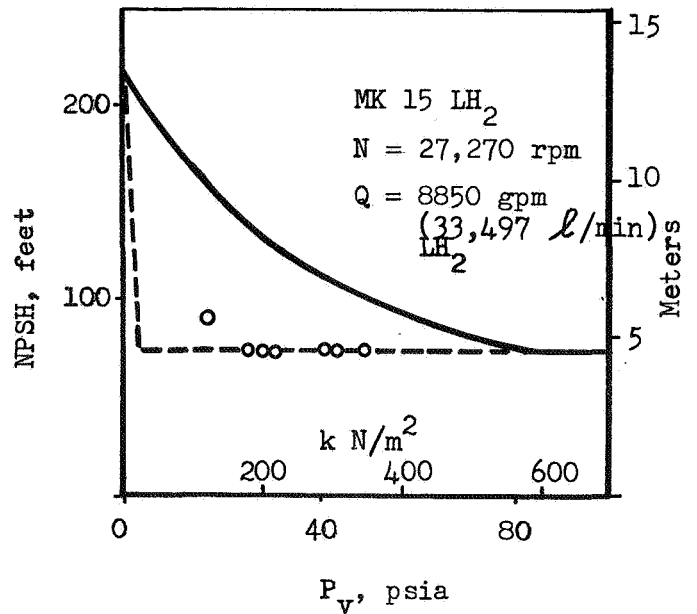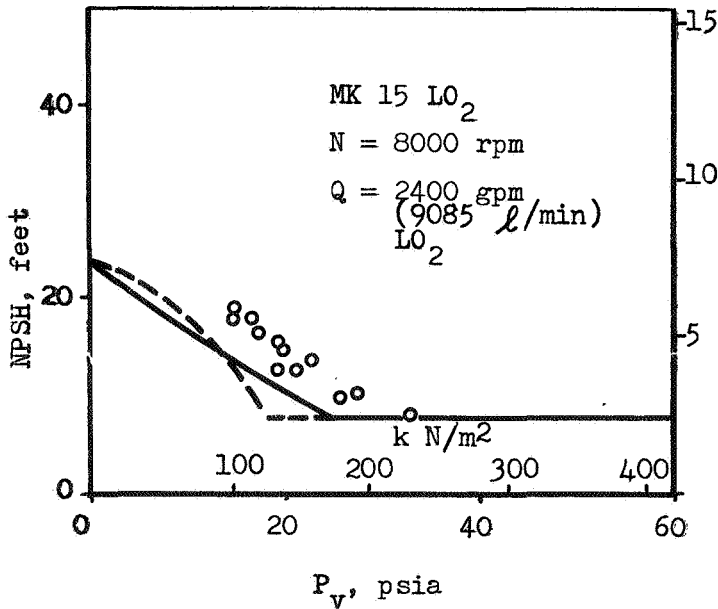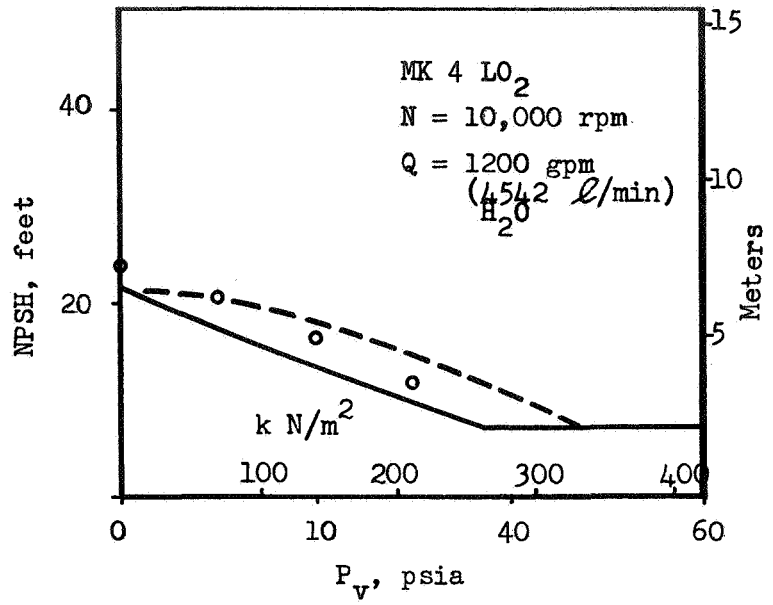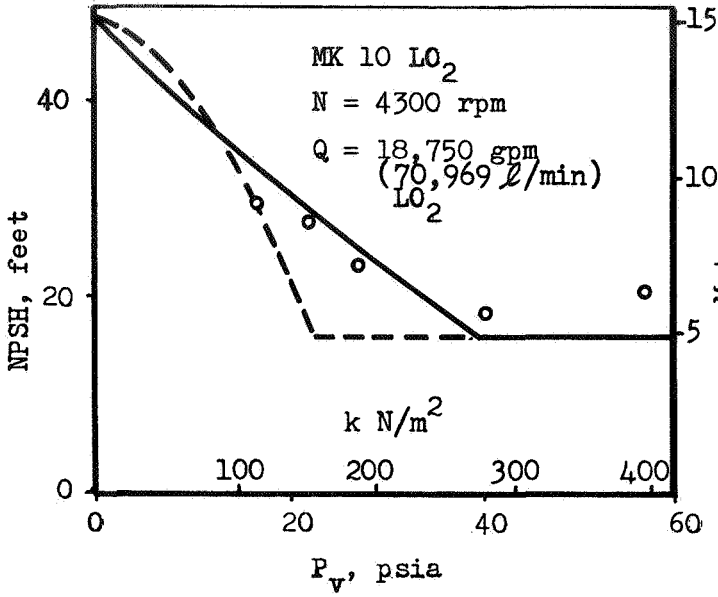
Figure 132 . Correlation of Suction Performance Test Data.
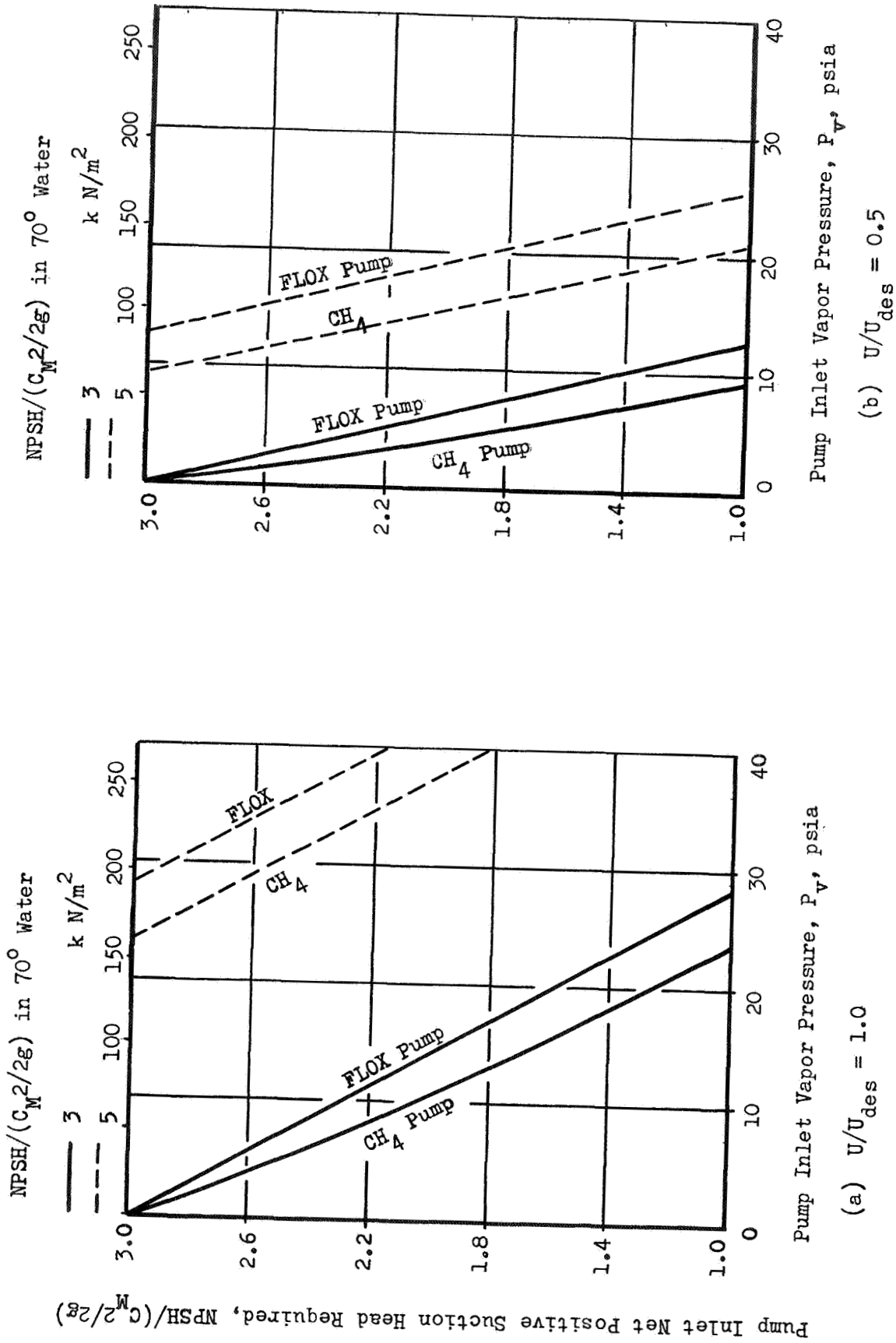
Figure 133. Pump Suction Requirements Modified Thor Relation.
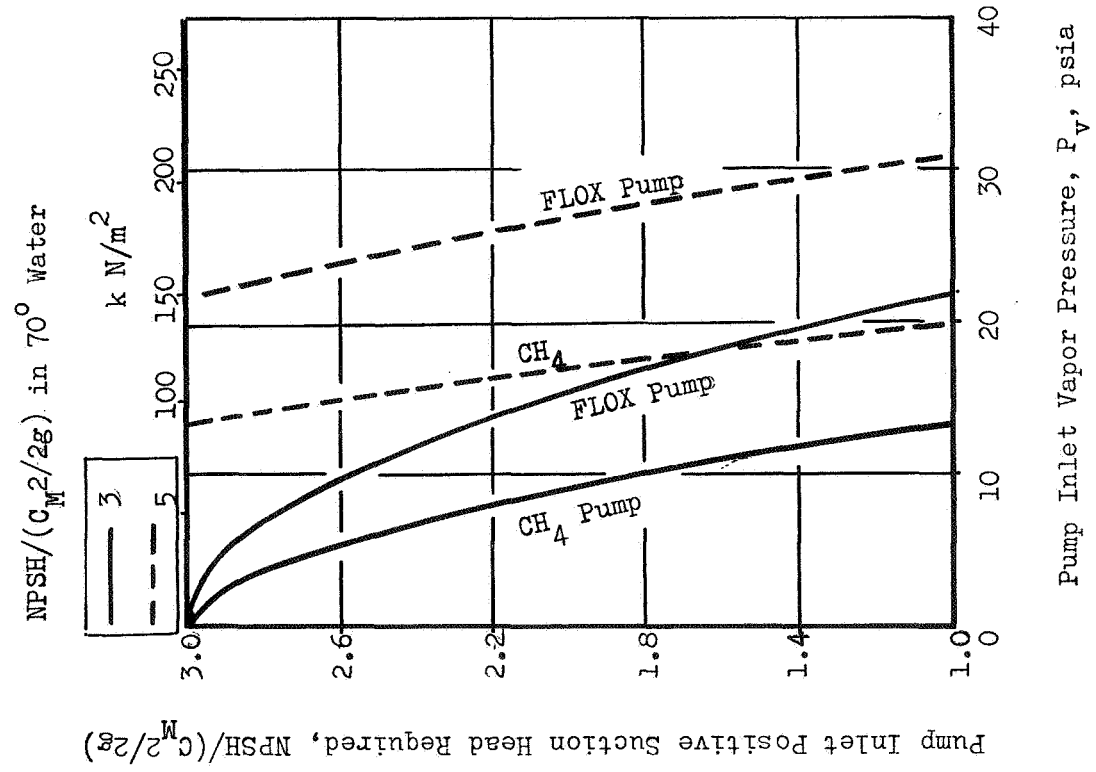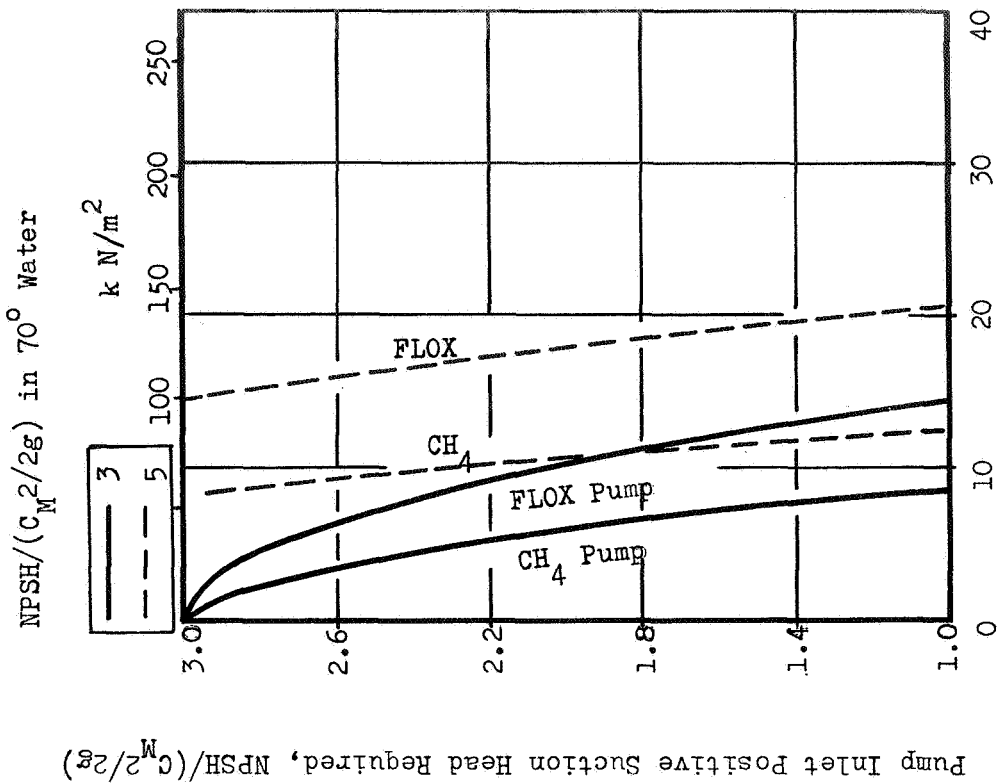
Figure 134. Pump Suction Requirements, NASA-Holl Equation.

(a) U/U_des = 1.0

(b) U/U_des = 0.5

TABLE 78

SUCTION PERFORMANCE FOR FLOX/METHANE

THRUST, POUND (N)	PROPELLANT	VAPOR PRESSURE, PSIA (k N/m^2)		REQUIRED (NPSP), PSIA (k N/m^2)	
				MAXIMUM	MINIMUM
5000 (22,200)	Methane	14.7	(100)	5.3 (36.5)	1.6 (11.0)
		30	(210	4 (27.6)	1.6 (11.0)
2500 (11,100)		14.7	(100)	0.8 (5.5)	0.4 (2.8)
		20	(140)	0.4 (2.8)	0.4 (2.8)
5000 (22,200)	FLOX	14.7	(100)	13.8 (95.2)	7 (48.3)
		30	(210)	10 (69.0)	3.5 (24.1)
2500 (11,100)		14.7	(100)	4.6 (31.7)	1.7 (12.7)
		25	(172)	1.7 (11.7	1.7 (12.7)

maximum NPSH requirements for both propellants are similar to those resulting
for a suction specific speed of 30,000, which was used in the parametric study.
As the vapor pressure increases as might occur during flight, the NPSH requirement
decreases. At the 50 percent throttled condition and lower thrust level, the NPSH
required is essentially equal to the velocity head, and the pumps could operate
with saturated propellants. For thrust levels below about 1000 pounds (450 kg),
even the most conservative prediction indicates that the pumps can perform effectively
with saturated propellants at the pump inlet for vapor pressures greater than 14.7
psia (100 kN/m^2). In this region, particularly at higher vapor pressures, the pumping
of two phase propellants appears possible.

FLOX TURBOPUMP DESIGN DESCRIPTION
AND ASSEMBLY

The FLOX turbopump is described in Fig. 135 and consists of a single-stage
centrifugal pump driven with a single-row partial admission turbine. The
pump rotor is supported with two antifriction bearings positioned between the
pump impeller and the turbine. Bearing and seal configuration is identical to
that of NAS3-12022 . The bearings are lubricated with FLOX, which is tapped from
the discharge volute and forced through an orifice, as shown in Fig. 136. The
fluid is circulated first through the bearing located closest to the turbine,
then through the bearing located behind the pump impeller, and then returned to
a low fluid pressure area through holes arranged in the hub of the impeller.
Axial rotor thrust is balanced hydraulically by the differences in diameter of the
wear rings positioned on the shroud and the back plate of the impeller. Axial
rotor thrust during transient operation is controlled by the antifriction bearing
located behind the pump impeller.

The shaft seal configuration between the pump and the turbine consists of two
primary face contact-type seals separated by an inert gas-operated purge seal.
Each primary seal has a drain cavity for removing possible primary seal leakage
aided by the purge gas pressure.

(Turbine Manifold)
with Nozzle
INCO 713-C Investm. Casting &
INCO 718 Welded Assembly

(Turbine Rotor)
INCO 718

Spacer
INCO 718

(Methane Seal)
P-5N Carbon
Mating Ring
Chrome Plated

2.75
(6.99)

(Volute)
INCO 718 Bar Stock

(Purge Seal)
Bearium B-10

(Pump Inlet)
INCO 718 Bar Stock

6.35
(16.13 cm)

(FLOX Seal)
AL-203 (Aluminum Oxide)
Mating Surface
440-C - Aluminum Oxide Coated

(Drive Shaft)
INCO 718 Bar-Stock

(Impeller)
INCO 713-C
Investm. Casting

2.95
(7.49)

1.220
(3.099)

(Inducer)
INCO 718
Bar-Stock

Figure 135. FLOX Turbopump.

360
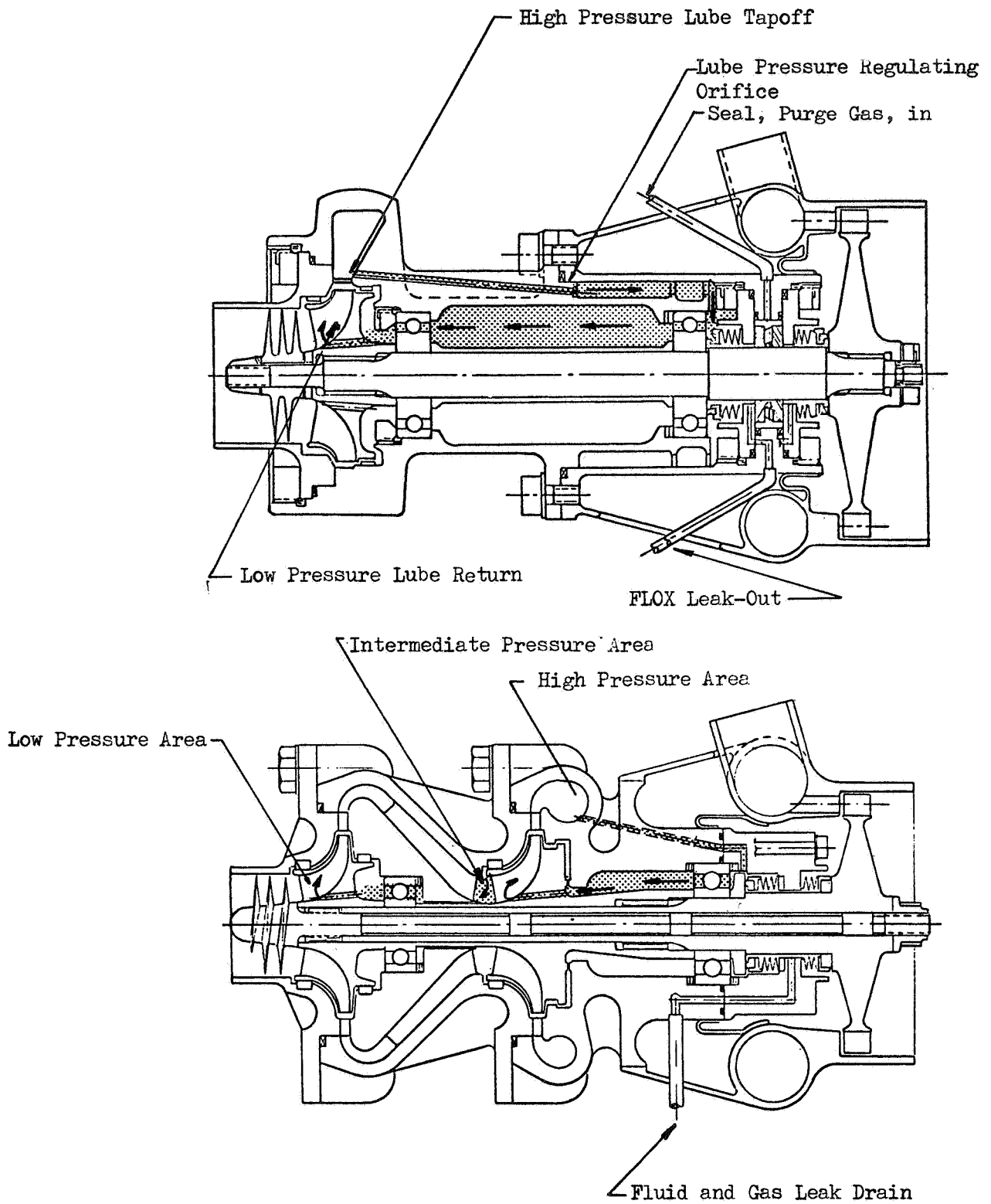
Figure 136. Turbopump Lubrication Flow

Turbopump materials are identified in Fig. 135. The primary FLOX seal rubbing face is made from Al-203 (aluminum oxide) and rides against the inner race of the modified antifriction bearing, which is made from 440-C and aluminum oxide coated.

The primary methane seal rubbing face is made from carbon riding against the turbine disk, which is made from INCO 718 and is chrome-plated on the sealing surface. The purge seal consists of two rings made from bearium B-10 (bronze-lead alloy), **separated** by a wave spring and prevented from rotation by a pin and slot arrangement. The seals are designed to be replacable with minimum complication. The rubbing speed for both primary face seals is 113 ft-sec (34 m-sec), and the rubbing speed for the purge seal rings is 83 ft/sec (25 m-sec).

The turbopump is constructed from INCO 718 bar-stock material and a combination INCO 713-C investment casting joined into a weldment, forming the turbine manifold assembly.

Turbopump Assembly

The turbopump is assembled in the following sequence. The bearing (1) is assembled onto the drive shaft (see Fig. 137) until seated against a shaft seal (2) installed between the bearing and the shaft shoulder. Next, the shaft with bearing is inserted into the volute housing (3) and the bearing is seated against the bearing preload spring (4). The bearing spacer (5) is then slipped onto the shaft until seated against bearing (1), then bearing (6) is assembled onto the shaft and into the volute and fastened with nut (7) and locked with lockwasher. The impeller is now installed onto the involute spline provided on the drive shaft followed by the inducer (8) which is locked against rotation with a slot and key arrangement (9) against the impeller. Next, the axial assembly is fastened with a nut (10) and lockwasher. The pump inlet (11) is then assembled to the volute housing (3) with seal (12) and fastened with nut (13) and lockwasher. This completes the pump subassembly.

362
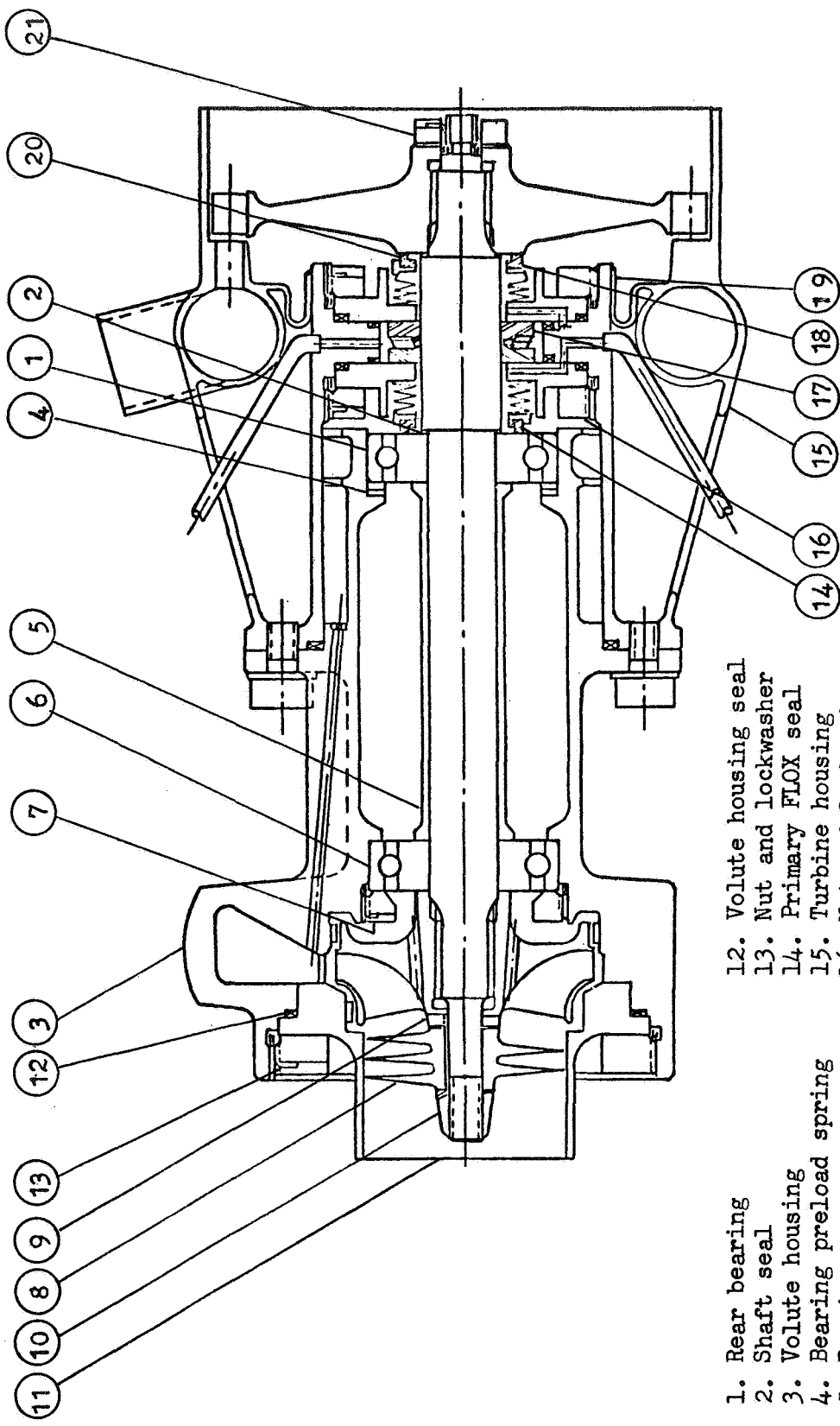
1. Rear bearing
2. Shaft seal
3. Volute housing
4. Bearing preload spring
5. Bearing spacer
6. Forward bearing
7. Nut
8. Inducer
9. Slot and key arrangement
10. Axial assembly nut
11. Pump inlet
12. Volute housing seal
13. Nut and lockwasher
14. Primary FLOX seal
15. Turbine housing
16. Nut and lockwasher
17. Purge seal components
18. Primary methane seal
19. Nut and lockwasher
20. Shaft shoulder seal
21. Turbine rotor nut

Figure 137. FLOX Turbopump Assembly Sequence

The turbine subassembly is prepared by mounting the primary FLOX seal (14) to the turbine housing (15) and is fastened with nut (16) and lockwasher. Next, insert purge seal components (17) and attach primary methane seal (18) with nut (19) and lockwasher. The turbine housing (15) with the seals mounted is then assembled onto the volute housing (3) and fastened with bolts. Next, the turbine rotor is attached to the main shaft until seated against a shaft and seal (20) between rotor and shaft shoulder. The turbine rotor is then fastened to the shaft with the nut (21) and secured with lockwasher. This completes the turbopump assembly.

METHANE TURBOPUMP DESCRIPTION AND ASSEMBLY

The liquid methane turbopump, described in Fig. 138, consists of a two-stage centrifugal pump driven with a partial admission turbine. The methane pump is a two-stage machine with an annular crossover between the front-to-back mounted impellers. The second-stage discharge flow is collected in a volute.

The pump rotor is supported with two antifriction bearings of which the upstream bearing is positioned between the first- and second-stage impellers, and the second bearing is positioned between the second-stage impeller and the turbine. The bearings are lubricated with liquid methane and operate at a DN value of 0.59×10^6 and 0.89×10^6, respectively. The lubrication flow is illustrated in Fig. 136. Axial rotor thrust is controlled with a balance piston arrangement, which is an integral part of the second-stage impeller and the volute backplate. Balance piston axial travel is restricted by limited travel of the two antifriction bearings.

The seal arrangement consists of a face contact type carbon seal operating in conjunction with a chrome-plated mating ring and a turbine seal consisting of a carbon ring riding on the shaft and simultaneously on the side of the turbine disk. A drain line arranged between the two seals removes any leakage from either seal. The face contact seal operates at a rotational contact speed of 240 ft-sec.

The turbopump is constructed from INCO 718 and INCO 713-C investment castings, as illustrated in Fig. 138. This material is used almost exclusively in this turbo-

(Pump Inlet)
INCO 713-C
Investm. Casting

(Cross-over Volute)
INCO 713-C
Investm. Casting

(Discharge Volute)
INCO 713-C
Investm. Casting

(Turbine Manifold)
with Nozzle
INCO 713-C   Investm. Casting &
INCO 718   Welded Assembly

(Turbine Disc,
Blades & Main
Shaft)
INCO 718 Forging
or Bar-Stock

(Gas Seal)
Carbon

(Seal Housing)
INCO 718

(Liquid Methane Seal)
Carbon
Mating Ring -
Chrome Plated

(First-Stage
Impeller)
INCO 713-C
Investm. Casting

(Inducer)
INCO 718
Bar-Stock

2.16
(5.49)

6.10
(15.49)

0.910
(2.31)

3.25
(8.26 cm)

Figure 138. Methane Turbopump.

365

pump assembly mainly for the purpose of strength and uniform thermal expansion and contraction. The turbine manifold assembly is welded integral with the second-stage volute.

Turbopump Assembly

The turbopump is assembled by the following sequence (Fig. 139). After the seal assembly (1) is bolted to the combined turbine and volute housing (2), the main shaft with the turbine rotor (3) is inserted through the seal mating ring (4) and the bearing (5) until seated. Next, the second-stage impeller (6) is assembled onto the drive shaft (3) and into the volute, checking also the clearance on the balance piston (7). The crossover volute (8) is then bolted to the discharge volute (9) and the upstream bearing (10) is inserted, making sure of proper spacing. Next, the first-stage impeller (11) is attached to the shaft (3) and a slot (12) in the hub aligned with a slot machined into the main shaft. The inducer (13) with its long tension rod is then inserted into the shaft (3) and two keys (14), machined onto the rod close to the inducer, are engaged together with the impeller and the main shaft slots. This makes possible proper torque transmission from the main shaft into the impeller and the inducer. Finally, the pump inlet casting (15) is bolted to the crossover volute, making the turbopump assembly complete.

Figure 139. Methane Turbopump Assembly Sequence
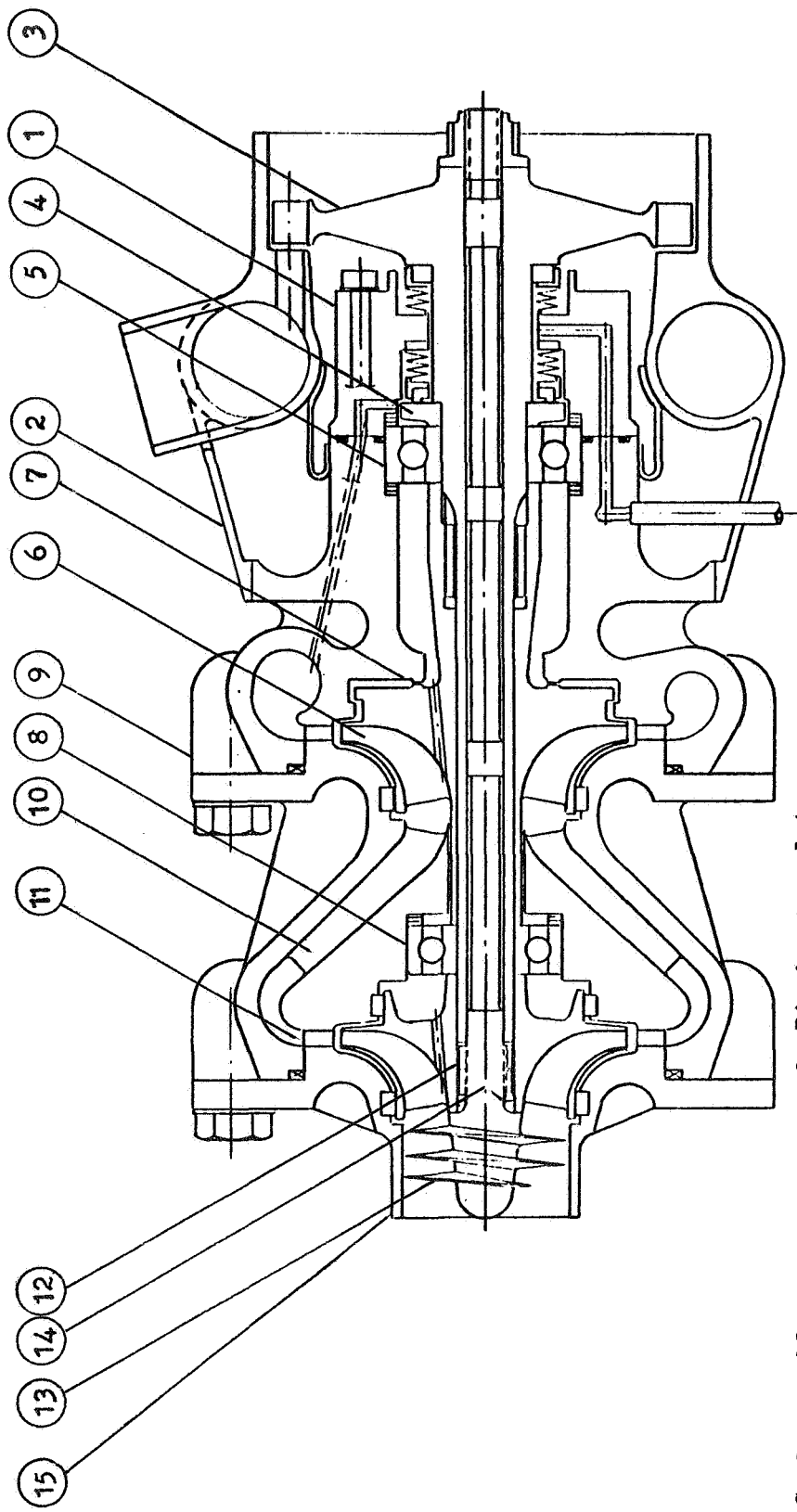
1. Seal assembly
2. Turbine and volute housing
3. Drive shaft
4. Seal mating ring
5. Rear bearing
6. Second-stage impeller
7. Balance piston
8. Crossover
9. Discharge volute
10. Upstream bearing
11. First-stage impeller
12. Shaft slot
13. Inducer
14. Keys
15. Pump inlet casting

REFERENCES

1. Space Storable Regenerative Cooling Investigation, NASA Contract NAS3-11191

2. Gas Augmented Injector Investigation, NASA Contract NAS3-12011

3. R6636-3, Fluorine/Hydrogen Performance Evaluation, Phase II: Space Storable Propellant Performance Demonstration, NASA Contract NASw-1229

4. Rotating and Positive Displacement Pumps for Low Thrust Rocket Engines, NASA Contract NAS3-12033

5. NASA CR-72360 (R7338), Interim Report, Space Storable Regenerative Cooling Investigation, Pauckert, R.P., Rocketdyne, A division of North American Rockwell Corp., 6633 Canoga Avenue, Canoga Park, California, September 1968.

6. McAdams, William H.: Heat Transmission, McGraw-Hill Book Company, Inc., New York, 1954, Third Edition

7. R-5652-4P, Final Program Progress Report for Product Engineering, Vol. 2, Rocketdyne, April 1965

8. R-6199, Investigation of Cooling Problems at High Chamber Pressures, Final Report, Rocketdyne, May 1965

9. NASA TM X-1573, Operation of a Liquid Fluorine Pump in Cavitating Flow At An Inducer Tip Speed of 188 Feet Per Second, W. M. Osborn, June 1968.

10. NASA TM X-1070, Investigation Of A Liquid Fluorine Inducer and Main-Stage Combination Design For A Suction Specific Speed of 20,000, W. M. Osborn, March 1965.

11. TR AFAPL-TR-66-12, Centrifugal Pump (High Pressure) for Power Transmissions, P. Hildebrand, et al., January 1956

12. Centrifugal and Axial Flow Pumps, A. J. Stepanoff, John Wiley & Sons, Inc., 1957

13. K-19-68-6, Final Report, Propellant Selection for Spacecraft Propulsion Systems, Lockheed Missiles and Space Company, Sunnyvale, Calif., 30 August 1968.

14. LAP 69-289, 5000 lb Thrust Flox/Methane Thrust Chamber Design Ground Rules, J. G. Gerstley, May 1969

15. Advanced Engine, Aerospike, NASA Contract NAS8-20349

REFERENCES (Con't)

16. Space Storable Propellant Performance, NASA Contract NAS3-11199

17. R-7037, Chamber Technology for Space Storable Propellants, NASA Contract NAS7-304; April 1967

18. AFRPL-TR-66-147, Poppet and Seal Design Data for Aerospace Valves, G. F. Tellier, July 1966

19. NASA TN D-4700, Cold Air Investigation of Effects of Partial Admission on Performance of 3.75-Inch-Mean-Diameter Single-Stage Axial-Flow Turbine, H. A. Klassen, August 1968

20. Ruggeri, R.S., R. D. Moore, and T. F. Gelder, Method for Predicting Pump Cavitation Performance, 9th Liquid Propulsion Symposium-Vol.2, presented October 25-27, 1967 at St. Louis, Mo., Chemical Propulsion Information Agency, pp 129-138.

21. NASA TN D-3509, Cavitation Simularity Considerations Based on Measured Pressure and Temperature Depressions in Cavitated Regions of Freon 114, T. F. Gelder, et al.

22. R-6995, Evaluation of NPSH Performance of the Model Mark-3 LOX Turbopump Used in the Thor MB-3 Propulsion System, April 1967.

23. AF RPL-TR-68-15, R-7232, Cloth Extendible Nozzle Firing Demonstration Program, Fulton, D. L. Fulton, Rocketdyne, March 1968

NOMENCLATURE

SYMBOL	NAME	UNITS ENGINEERING	SI
A	Area	in^2	cam^2
C	Constant	-	-
C*	Characteristic Velocity	ft/sec	m/sec
C_m	Inducer Inlet Axial Velocity	ft/sec	m/sec
C_p	Specific Heat	$\dfrac{Btu}{lb\ ^oR}$	
D	Diameter	in	cm
d_H	Hydraulic Diameter	in	cm
d	Inducer Inlet Tip Diameter	in	cm
DN	Bearing Characteristics		
f	Injector ΔP Factor		
F	Thrust	lb_f	N
G	Mass Flux		
g	Gravitational Constant (32.2)	ft/sec^2	
H	Enthalpy	Btu/lb	
h	Channel Height	in	cm
I_{sp}	Specific Impulse	$\dfrac{lb_f\text{-sec}}{lb_m}$	$\dfrac{N\text{-sec}}{kg}$
J	Conversion Constant (778)	$\dfrac{ft\text{-}lb}{Btu}$	
K	Thermal Conductivity	$\dfrac{Btu}{hr\ ft\ R}$	
L*	Characteristic Length	in	cm
L	Length	ft	m
l	Land Width	in	cm
MR	Mixture Ratio (O/F)	-	-
N	Rotational Speed	rpm	rad/sec
N_{PR}	Prandtl Number	-	-
N_{Nu}	Nusselt Number	-	-
N_{Re}	Reynold's Number	-	-

SYMBOL	NAME	UNITS ENGINEERING	SI
NPSH	Inducer Net Positive Suction Head	ft	m
N	Number of Channels	--	--
P	Pressure	psia	kN/m^2
P_c	Chamber Pressure	psia	kN/m^2
P_o	Outlet Pressure	psia	kN/m^2
Q	Heat Input	Btu	
Q_m	Measured Heat Input	Btu	
Q_p	Predicted Heat Input	Btu	
R	Radius	in	cm
SCCH	Standard Cubic Centimeters per Hour	--	--
T	Temperature	F, R	K
TSH	Inducer Inlet Thermodynamic Suppression Head	ft	m
t	Wall Thickness	in	cm
U	Inducer Inlet Tip Speed	fps	m/sec
V	Velocity	fps	m/sec
$\dot{W}$	Flowrate	lb/sec	kg/sec
w	Channel Width	in	cm
X	Axial Length	in	cm
Y	Radial Length	in	cm
Z			
β	Thermal Factor	$ft/sec^{3/2}$	
ϵ	Expansion Ratio	--	--
Φ	Cooling Enhancement Factor	--	--
φ	Flow Coefficient	--	--
ψ	Head Coefficient	--	--
ρ	Density	lb/ft^3	kg/m^3
η	Efficiency	--	--
λ	Heat of Vaporization	Btu/lb	

SUBSCRIPTS

L   -   Liquid

V   -   Vapor

t   -   Throat Location

WC   -   Coolant - Side Wall

WG   -   Gas - Side Wall

APPENDIX A
ENERGY BALANCE MODEL

A system balance is obtained by matching pressures throughout the system and also by matching pump and turbine horsepowers. This matching process is carried out by iterations which start with estimated values of pump speeds and turbine flowrates. Accurate estimates result in rapid convergence to a balance point. The program will fail to converge if the initial estimates are not sufficiently accurate.

Figure 5 presents a schematic of the expander cycle showing the flow paths and system resistances considered by the mathematical model. The resistances of the mixture ratio control valve (A) and the thrust control valve (B) are computed by the program. Liquid propellant line, valve, and manifold resistances are assumed to vary as the square of flowrate ($\Delta P = R \, \dot{w}^2/\rho$). For hot gas resistances, a mean fluid density is calculated from the perfect gas law. The cooling jacket pressure drop may be input for each case or computed assuming a linear variation with flowrate.

Program inputs include pump inlet pressures, pump diameters and impeller flow areas, turbine diameters, turbine effective and exit areas, resistances for all lines, valves, manifolds, and injectors, pump and turbine maps, liquid propellant densities, and estimates of pump speeds and turbine flowrates. Pump operation is described by plots of head coefficient and efficiency as a function of flow coefficient. Turbine operation is described by a plot of efficiency versus isentropic velocity ratio.
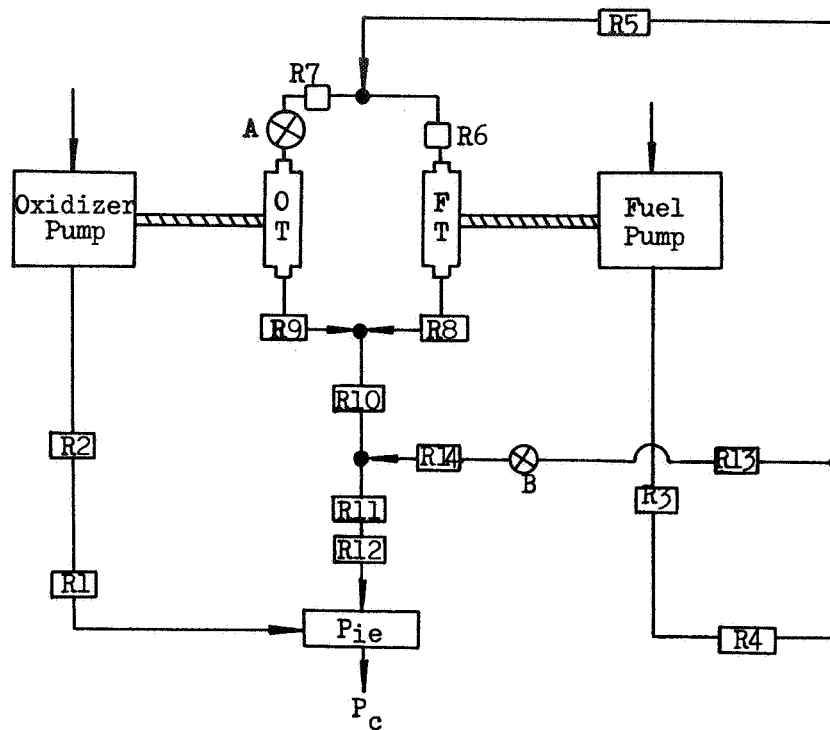
FEED SYSTEM RESISTANCES

R1 — Main Oxidizer Lines, Valves, Manifolds
R2 — Oxidizer Injector
R3 — Main Fuel Lines, Valves, Manifolds
R4 — Cooling Jacket
R5 — Turbine Inlet Line
R6 — Fuel Turbine Inlet Line, Orifice, Manifold
R7 — Oxidizer Turbine Inlet Line, Orifice
R8 — Fuel Turbine Exhaust Manifold, Line, Orifice
R9 — Oxidizer Turbine Exhaust Manifold, Line, Orifice
R10 — Turbine Exhaust Line
R11 — Turbine Exhaust Line
R12 — Fuel Injector
R13 — Bypass Line
R14 — Bypass Line
A   — Mixture Ratio Control Valve
B   — Thrust Control Valve

Figure A-1. Throttling Analysis Model — Expander Cycle, Parallel Turbines

APPENDIX B

ALTERNATIVE THRUST CHAMBER DESIGNS

Thrust chamber design alternatives are shown in Fig. B-1 and were explored
as potential weight reduction methods. In some cases the present one-piece,
milled channel, electroformed nickel design is clearly superior to the alter-
natives. In other cases, the alternative design could provide lower engine
weight where an alternate fabrication process is better reduced to practice,
or if selection criteria become very heavily weighted toward a particular goal
such as performance or cost. Although shown under five major headings in
Fig. B-1 , the design alternatives were, of course, interrelated in many in-
stances.

The combustion chamber contour and the channel configuration alternatives and
selection have already been discussed in detail. The present section compares
alternatives considered for materials, fabrication methods, and means of reduc-
ing the weight of nozzles with area ratios of 60 or greater.

MATERIALS

Several materials were considered and compared to nickel on the standpoint of
strength, thermal conductivity and fabrication characteristics. Haynes 25 and
T-D nickel initially appeared attractive but should be explored in greater de-
tail.

> Nickel   – Has good thermal conductivity but exhibits low strength at
>   elevated (1400 F (1032 K)) temperature. May be
>   electroformed, but electroformed nickel may have poor elongation
>   properties at elevated temperatures. Has high potential for
>   being fabricated by the powder metallurgy and spinning processes;
>   readily weldable to high nickel content alloys.

COMBUSTOR CONTOUR	CHANNEL CONFIGURATION	MATERIALS	FABRICATION	NOZZLE WEIGHT REDUCTION
NAS3-11191 Contour	Number of Channels	Nickel 200	Electroforming	Dummy Channels
15° Contraction Angle	Number of Passes	T. D. Nickel	Powder Metallurgy	Electroform/Tubes
Constant Taper	Channel Shape Profile	Heynes 25	Casting	Radiation-cooled Nozzles and Extensions
		Hastelloy X	Spinning	
		Inco 625		

Figure B-1. Thrust Chamber Design Alternatives

INCO 625   —   Relatively poor thermal conductivity but good strength at elevated temperatures. Has been spun. Readily weldable to nickel and high nickel content alloys.

Haynes 25   —   Thermal conductivity higher than INCO 625 but lower than T-D nickel and much lower than Nickel. Has good strength at elevated temperature. Has been spun.

T-D Nickel   —   Thermal conductivity is good but has poor elongation properties. Has good strength at elevated temperatures. Has been spun.

FABRICATION PROCESSES

Several advanced fabrication techniques are being investigated at Rocketdyne. These techniques, as well as others reported in the literature, were considered for fabrication of the thrust chamber.

Electroforming

Electroforming was selected as the method for fabricating the coolant shell (combustor and nozzle). Several nickel thrust chambers and three nickel nozzles have been electroformed and demonstrate the feasibility of the process. Being able to index directly from the electroforming mandrel ensures the best possible tolerance control of any fabrication techniques. At the present time, this fabrication method is closer to being reduced to practice with nickel than the following techniques.

Spinning

INCO 625 thrust chambers in this size range have been fabricated using a spun inner shell with electroformed nickel closeout. It is reasonable to assume that a nickel chamber could be made in a similar manner. The current configuration would be spun in two pieces, necessitating a circumferential weld joint

just aft of the throat. After spinning, the spinning tooling is removed to
allow machining of the internal surfaces and of the channels. Following
machining of the channels, a nickel closeout wall is electroformed. Channel
and wall tolerance control currently appears to be less than with the electro-
forming process.

Powder Metallurgy and Casting

Powder metal and cast nickel parts have been made for chambers in this size
range. Process parameters must be established before it can be considered a
"state-of-the-art" fabrication technique. The process, however, does show a
great deal of potential for fabrication cost reduction.

CHANNEL DESIGN

Channel design variations were considered for weight reduction potential.
Since most of the weight is in the nozzle, this area was emphasized. Nozzle
extensions to increase the area ratio and performance were also evaluated as
part of this effort.

Alternate Channel Configurations

As described in Task I channel configuration studies (Fig. 17   ), use of tapered
channels and channel branching or additional step-width variations can provide
nozzle weight reductions. Five to eight pounds reduction in nozzle weight could
potentially be achieved. Considerably more fabrication expense could be involved
in these channel configurations.

Dummy Channels

The coolant channel widths in the nozzle are limited by structural considera-
tions. As a result, the nozzle is grossly over-cooled and heavier than necessary.
Considerable weight reduction could be effected by removing material from the

center of the cold side of the lands. Machining 0.2-inch (0.5 cm) slots in the region x/R_t greater than 10 would reduce the thrust chamber weight by 4 pounds.

Combined Tube/Electroformed Nozzle

A lightweight, low-cost nozzle can be made using unspliced simply-tapered tubes with circular cross-sections throughout their full length. An electro-formed close-out would provide an integral gas-tight seal and structural member. The nozzle would extend from an area ratio of 4 to 60 and have characteristics as described in Table B-1 . The tube wall nozzle and mani-fold could provide a weight savings of 10 -12 pounds. Fabrication is illus-trated in Fig. B-2.

TABLE B-1

TUBE WALL THRUST CHAMBER EXTENSION

Attachment Point	$\epsilon = 4$
Exit	$\epsilon = 60$
Material	INCONEL 625
Tubes:	
Number	180
Wall Thickness, in. (cm)	0.025 (0.064)
Diameter	0.093-inch (0.236 cm) O.D. at $\epsilon = 4$
	0.361-inch (0.917 cm) O.D. at $\epsilon = 60$
	Cross-section remains circular
Weight	21 pounds (9.5 kg)

Radiation-Cooled Nozzle Extensions

Radiation-cooled nozzles generally weigh significantly less than regeneratively-cooled nozzles and, therefore, were investigated as alternatives to reduce chamber weight or to increase nozzle area ratio for performance improvement. Cloth and metal nozzles formed to 80-percent bell and 15-degree cone con-tours were considered.
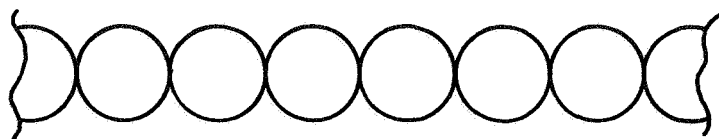
Tube ready for electroform deposit.
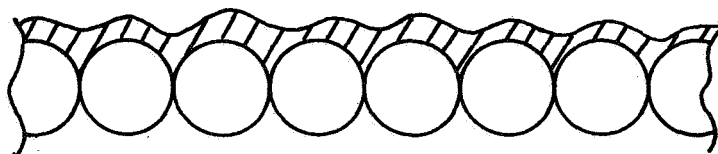
Initial electroformed nickel deposit.
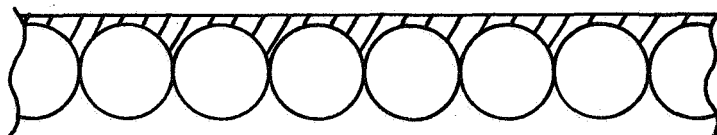
Machined smooth.
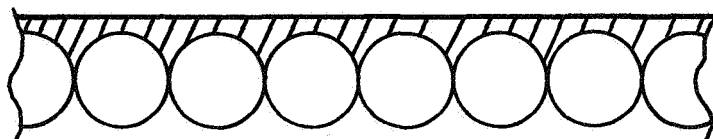
Electroformed nickel deposited to required thickness.

Figure B-2. Method Used to Form an Electroformed Nickel Shell for a Tubular Thrust Chamber.

At a chamber pressure of 500 psia (3450 kN/m^2) and with an extension attached at
ϵ = 60, the maximum wall temperature at which the extension must operate is
approximately 2100 F (1170 K) as shown in Fig. B-3. Radiation cooling is feasible
at this temperature; however, careful choice of materials will have to be made
due both to the operating temperature of 2100 F (1170 K) and to the need for
compatibility between nozzle extension material and FLOX/CH$_4$ combustion products.
Materials which could be used are nickel-based alloys (Hastelloy or INCO type)
for the metal skirts and graphite cloth for the cloth extensions. Information
on cloth nozzles was based on the results of Ref. 23.

The operating temperature of a radiation-cooled extension at area ratios significantly
lower than 60 is beyond the capability of the metals, so that graphite cloth was
selected for the radiation-cooled nozzle material to effect the most significant
weight reductions. The graphite cloth can be attached at an area ratio of 30.
Performance, weight, and dimensional data presented in Table B-2 show that very
little performance is lost by attaching a 15-degree conical extension to the
existing truncated contour at an area ratio of 30, compared to attaching an optimum
80-percent contoured extension. Fabrication ease, therefore, would suggest using
the conical extension. Reoptimization of the regeneratively-cooled portion of the
nozzle would reduce the performance difference between the nozzles. For equal
performance, however, the conical nozzle extension would be longer than a bell
nozzle extension.

The 15-degree cloth extension attached at area ratio of 30 would save 23.2 pounds
(10.5 kg) of thrust chamber weight. However, the methane would cool less nozzle
area and, therefore, would leave the jacket at a lower temperature which would
require the turbines to be driven with a higher inlet pressure. A 43 psia
(296 kN/m^2) fuel pump discharge pressure rise would result.

Extending the present contour to an area ratio of 100 or 200 would result in the
same performance, whether a bell or a conical extension were used, as shown in
Table B-2. Fabrication ease would probably supersede the slight weight penalty
for selecting a conical extension. Both metal and cloth extensions could be used
and weigh about the same; the cloth nozzle, however, is retractable.
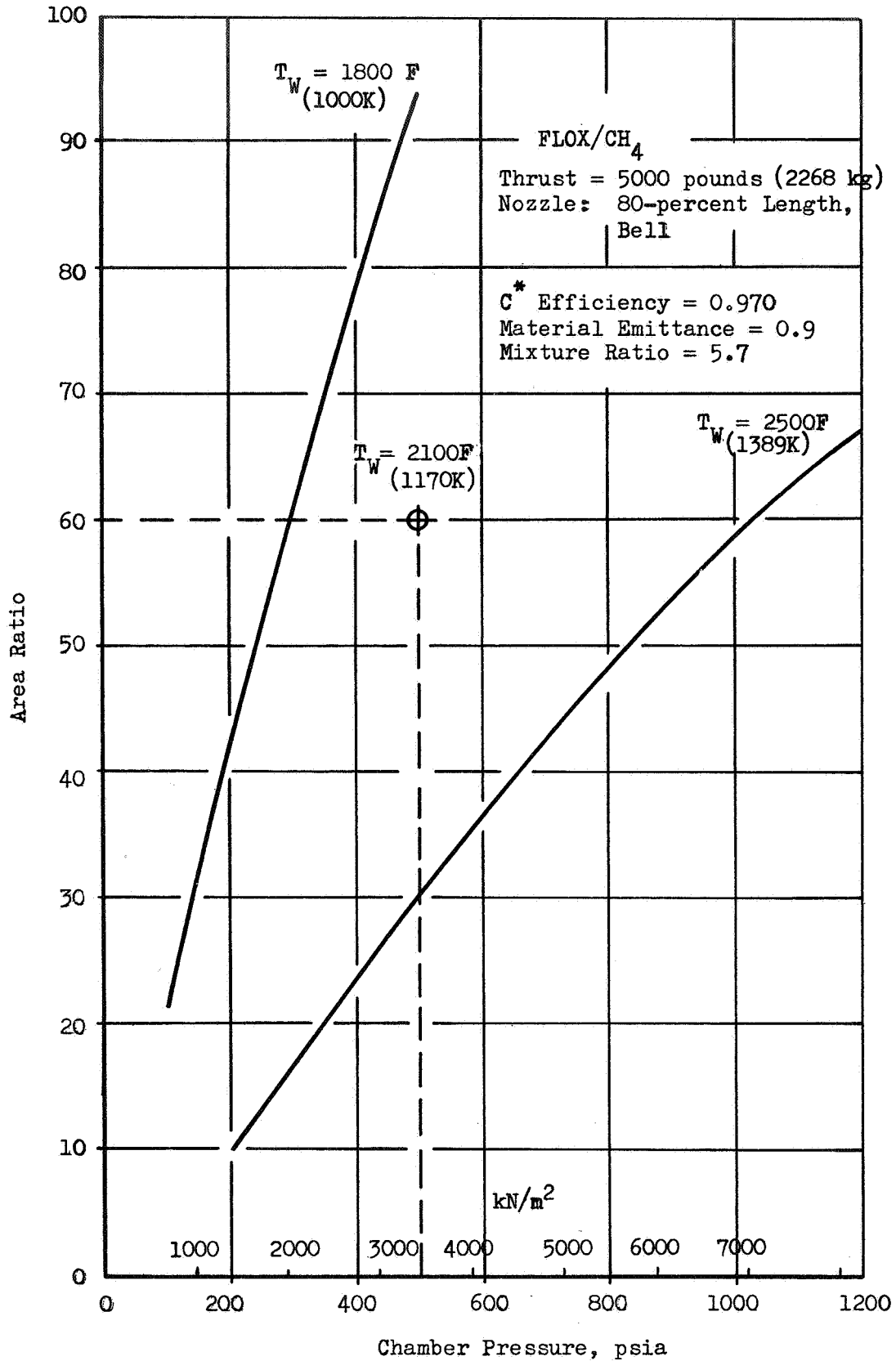
Figure B-3. Radiation Cooling Limits

B-8

TABLE B-2

GRAPHITE CLOTH EXTENDIBLE NOZZLE CONFIGURATION

AREA RATIO		I_s,	Engine Weight,	Thrust Chamber Length,	Nozzle Inside Diameter,
ATTACH	EXIT	seconds	lbm (kg)	inches (cm)	inches (cm)
15-degree Conical Extensions					
60	100	403.0	+4.25 (1.93)	47.4 (120.4)	25.88 (65.74)
60	200	405.6	+7.0 (3.18)	68.4 (173.7)	36.5 (92.71)
30	100	402.7	-23.2 (-10.52)	50.1 (127.3)	25.88 (65.74)
40	100	402.9	-16.8 (-7.62)	49.6 (126.0)	25.88 (65.74)
80-percent Bell Extensions					
60	100	403.0	+4.23 (1.92)	45.4 (115.3)	25.88 (65.74)
60	200	405.6	+6.6 (2.99)	62.1 (157.7)	36.5 (92.71)
No Extension					
		399.2	0	37.3 (94.7)	20.4 (51.82)

APPENDIX C

DISTRIBUTION LIST FOR FINAL REPORT

REPORT
COPIES
R D   RECIPIENT   DESIGNEE

National Aeronautics & Space Administration
Lewis Research Center
21000 Brookpark Road
Cleveland, Ohio   44135

R D	Recipient	Designee
1	Attn: Contracting Officer, MS 500-313	
5	Liquid Rocket Technology Branch, MS 500-209	
1	Technical Report Control Office, MS 5-5	
1	Technology Utilization Office, MS 3-16	
2	AFSC Liaison Office, MS 4-1	
2	Library	
1	Office of Reliability & Quality Assurance, MS 500-111	
1	D. L. Nored, Chief, LRTB, MS 500-209	
3	John W. Gregory Project Manager, MS 500-209	
1	E. W. Conrad, MS 500-204	
1	R. H. Kemp, MS 49-1	
1	R. H. Knoll, MS 501-2	
1	Joseph Sivo	
1	William Tomazic	
2 1	Chief, Liquid Experimental Engineering, RPX Office of Advanced Research & Technology NASA Headquarters Washington, D.C. 20546	Frank Stephenson, Jr.
2	Chief, Liquid Propulsion Technology, RPL Office of Advanced Research & Technology NASA Headquarters Washington, D.C. 20546	
1 1	Director, Launch Vehicles & Propulsion, SV Office of Space Science & Applications NASA Headquarters Washington, D.C. 20546	Robert F. Schmidt

R	D	RECIPIENT	DESIGNEE
1		Chief, Environmental Factors & Herodynamics Code RV-1 Office of Advanced Research & Technology NASA Headquarters Washington, D.C. 20546	
1		Chief, Space Vehicles Structures Office of Advanced Research & Technology Nasa Headquarters Washington, D.C. 20546	
1		Director, Advanced Manned Missions, MT Office of Manned Space Flight NASA Headquarters Washington, D.C. 20546	
6		NASA Scientific & Technical Information Facility P.O. Box 33 College Park, Maryland 20740	
1		Director, Technology Utilization Division Office of Technology Utilization NASA Headquarters Washington, D.C. 20546	
1		National Aeronautics & Space Administration Ames Research Center Moffett Field, California 94035 Attn: Library	E.R. Streed, SED Hans M. Mark Mission Analysis Division
1	1	National Aeronautics & Space Administration Goddard Space Flight Center Greenbelt, Maryland 20771	Morlund Moseson, Code 620 C.R.Gunn,Propulsion Office,Code 470
1		National Aeronautics & Space Administration John F. Kennedy Space Center Cocoa Beach, Florida 32931 Attn: Library	Dr. Kurt Debus
1		National Aeronautics & Space Administration Langley Research Center Langley Station Hampton, Virginia 23365 Attn: Library	Ed Cartwright Director
1	1	National Aeronautics & Space Administration Manned Spacecraft Center Houston, Texas 77001 X Library	J.G. Thiobodaux,Jr. Chief,Propulsion H.J. Brasseaux,PESD

R	D	RECIPIENT	DESIGNEE
1		Air Force Systems Command Andrews Air Force Base Washington, D.C. 20332 Attn: Library	Capt. S.W. Bowen SCLT
1	1	Air Force Rocket Propulsion Laboratory (RPR) Edwards, California 93523 Attn: Library	R. Wiswell
1		Air Force Rocket Propulsion Lab (RPM) Edwards, California 93523 Attn: Library	
1		Air Force FTC (FTAT*2) Edwards Air Force Base, California 93523 Attn: Library	Donald Ross
1		Air Force Office of Scientific Research Washington, D.C. 20333 Attn: Library	SREP, Dr. J.F. Masi
1		Special Missile Systems Organization Air Force Unit Post Office Los Angeles, California 90045 Attn: Technical Data Center	
1		Office of Research Analyses (OAR) Holloman Air Force Base, New Mexico 88330 Attn: Library	Maj. R.E. Bracken, Code MDGRT
1		U. S. Air Force Washington, D.C. Attn: Library	Col. C. K. Stambaugh, Code AFRST
1		Commanding Officer U. S. Army Research Office (Durham) Box CM, Duke Station Durham, North Carolina 27706 Attn: Library	
1		U. S. Army Missile Command Redstone Scientific Information Center Redstone Arsenal, Alabama 35808 Attn: Document Section	Dr. W. Wharton
1		Bureau of Naval Weapons Department of the Navy Washington, D.C. Attn: Library	J. Kay, Code RTMS-41

R D	RECIPIENT	DESIGNEE
1	Commander U. S. Naval Missile Center Point Mugu, California 93041 Attn: Technical Library	
1	Commander U. S. Naval Weapons Center China Lake, California 93557 Attn: Library	W. F. Thorm, Code 4562
1	Commanding Officer Naval Research Branch Office 1030 E. Green Street Pasadena, California 91101 Attn: Library	
1	Director (Code 0180) U. S. Naval Research Laboratory Washington, D.C. 20390 Attn: Library	H. W. Carhart J. M. Krafft
1	Picatinny Arsenal Dover, New Jersey 07801 Attn: Library	I. Forsten
1	Air Force Aero Propulsion Laboratory Research & Technology Division Air Force Systems Command United States Air Force Wright-Patterson AFB, Ohio 45433 Attn: APRP (Library)	R. Quigley C. M. Donaldson
1	Electronics Division Aerojet-General Corporation P. O. Box 296 Azusa, California 91703 Attn: Library	W. L. Rogers
1	Space Division Aerojet-General Corporation 9200 East Flair Drive El Monte, California 91734 Attn: Library	S. Machlawski
1	Ordnance Division Aerojet-General Corporation 11711 South Woodruff Avenue Downey, California 90241 Attn: Library	

REPORT COPIES R D	RECIPIENT	DESIGNEE
1	Propulsion Division Aerojet-General Corporation P. O. Box 15847 Sacramento, California 95803 Attn: Technical Library 2484-2015A	R. Stiff
1	Aeronutronic Division of Philco Ford Corp. Ford Road Newport Beach, California 92663 Attn: Technical Information Department	Dr. L. H. Linder D. A. Carrison
1	Aerospace Corporation 2400 E. El Segundo Blvd. Los Angeles, California 90045 Attn: Library-Documents	J. G. Wilder
1	Arthur D. Little, Inc. 20 Acorn Park Cambridge, Massachusetts 02140 Attn: Library	A. C. Tobey
1	Astropower Laboratory McDonnell-Douglas Aircraft Company 2121 Paularino Newport Beach, California 92163 Attn: Library	Dr. George Moc Director Research
1	Astrosystems, International 1275 Bloomfield Avenue Fairfield, New Jersey 07007 Attn: Library	A. Mendenhall
1	ARO, Incorporated Arnold Engineering Development Center Arnold AF Station, Tennessee 37389 Attn: Library	Dr. B. H. Goethert
1	Susquehanna Corporation Atlantic Research Division Shirley Highway & Edsall Road Alexandria, Virginia 22314 Attn: Library	Dr. Ray Friedman
1	Battelle Memorial Institute 505 King Avenue Columbus, Ohio 43201 Attn: Report Library, Room 6A	

REPORT COPIES R D	RECIPIENT	DESIGNEE
1	Beech Aircraft Corporation Boulder Facility Box 631 Boulder, Colorado Attn: Library	Douglas Pope
1	Bell Aerosystems, Inc. Box 1 Buffalo, New York 14205 Attn: Library	T. Reinhart W. M. Smith
1	Bendix Systems Division Bendix Corporation 3300 Plymouth Street Ann Arbor, Michigan Attn: Library	John M. Brueger
1	Bellcom 955 L'Eufant Plaza, S.W. Washington, D.C. Attn: Library	H. S. London
1	Boeing Company Space Division P. O. Box 868 Seattle, Washington 98124 Attn: Library	J. D. Alexander C. F. Tiffany
1	Boeing Company 1625 K Street N.W. Washington, D.C. 20006	
1	Boeing Company P. O. Box 1680 Huntsville, Alabama 35801	Ted Snow
1	Chemical Propulsion Information Agency Applied Physics Laboratory 8621 Georgia Avenue Silver Spring, Maryland 20910	Tom Reedy
1	Chrysler Corporation Missile Division P. O. Box 2628 Detroit, Michigan Attn: Library	John Gates

REPORT COPIES		RECIPIENT	DESIGNEE
R	D		

1	Chrysler Corporation Space Division New Orleans, Louisiana Attn: Librarian	
1	Curtiss-Wright Corporation Wright Aeronautical Division Attn: Library	G. Kelley
1	University of Denver Denver Research Institute P. O. Box 10127 Denver, Colorado 80210 Attn: Security Office	
1	Fairchild Stratos Corporation Aircraft Missiles Division Hagerstown, Maryland Attention: Library	J. S. Kerr
1	Research Center Fairchild Hiller Corporation Germantown, Maryland Attn: Library	Ralph Hall
1	Republic Aviation Fairchild Hiller Corporation Farmington, Long Island New York	
1	General Dynamics/Convair P. O. Box 1128 San Diego, California 92112 Attn: Library	Frank Dore R. Roberts
1	Missiles and Space Systems Center General Electric Company Valley Forge Space Technology Center P. O. Box 855 Philadelphia, Pa. 190101 Attn: Library	A. Cohen F. Schultz
1	General Electric Company Flight Propulsion Lab Department Cincinnati, Ohio Attn: Library	D. Suichu Leroy Smith

R	D	RECIPIENT	DESIGNEE
1	1	Grumman Aircraft Engineering Corporation Bethpage, Long Island, New York Attn: Library	Joseph Gavin Herb Siegel
1		Hercules Poweder Company Allegheny Ballistics Laboratory P. O. Box 210 Cumberland, Maryland 21501 Attn: Library	
1		Honeywell Inc. Aerospace Division 2600 Ridgeway Road Minneapolis, Minnesota Attn: Library	Gordon Harris
1		IIT Research Institute Technology Center Chicago, Illinois 60616 Attn: Library	C. K. Hersh
1		Kidde Aer-Space Division Walter Kidde & Company, Inc. 567 Main Street	R. J. Hanville
1		Ling-Temco-Vought Corporation P. O. Box 5907 Dallas, Texas 75222 Attn: Library	Warren G. Trent
1		Lockheed Missiles and Space Company P. O. Box 504 Sunnyvale, California 94087 Attn: Library	C. C. Lee J. Guill
1		Lockheed-California Company 10445 Glen Oaks Blvd. Pacoima, California Attn: Library	G. D. Brewer
1		Lockheed Propulsion Company P. O. Box 111 Redlands, California 92374 Attn: Library, Thackwell	H. L. Thackwell
1		Marquardt Corporation 16555 Saticoy Street Box 2013 - South Annex Van Nuys, California 91409	Howard McFarland L. R. Bell Jr.

R D	RECIPIENT	DESIGNEE
1	Martin-Marietta Corporation (Baltimore Div.) Baltimore, Maryland 21203 Attn: Library	John Calothes
1	Denver Division Martin-Marietta Corporation P. O. Box 179 Denver, Colorado Attn: Library	Dr. Morganthaler F. R. Schwartzberg I. W. Murphy
1	Orlando Division Martin-Marietta Corporation Box 5827 Orlando, Florida Attn: Library	J. Fern
1	Western Division McDonnell Douglas Aircraft Company, Inc. 3000 Ocean Park Blvd. Santa Monica, California 90406 Attn: Library	R. W. Hallet G. W. Burke Paul Lkevatt
1	McDonnell Douglas Aircraft P. O. Box 516 Lambert Field, Missouri 63166 Attn: Library	R. A. Herzmark
1	Space & Information Systems Division North American Rockwell 12214 Lakewood Blvd. Downey, California Attn: Library	
1	Northrop Space Laboratories 3401 West Broadway Hawthorne, California Attn: Library	Dr. Wm. Howard
1	Purdue University Lafayette, Indiana 47907 Attn: Library (Technical)	S. Fairweather
1	Radio Corporation of American Astro-Electronics Products Princeton, New Jersey Attn: Library	S. Fairweather
1	Rocket Research Corporation Willow Road at 116th Street Redmond, Washington 98052 Attn: Library	F. McCullough, Jr.

REPORT COPIES			
R	D	RECIPIENT	DESIGNEE
1		Stanford Research Institute 333 Ravenswood Avenue Menlo Park, California 94025 Attn: Library	Thor Smith Dr. Gerald Marksman
1		Thiokol Chemical Corporation Redstone Division Huntsville, Alabama Attn: Library	John Goodloe
1		TRW Systems, Inc. 1 Space Park Redondo Beach, California 90278 Attn: STL Tech. Lib. Doc. Acquisitions	D. H. Lee
1		United Aircraft Corporation Corporation Library 400 Main Street East Hartford, Connecticut 06108	Dr. David Rix Erle Martin Frank Owen Wm. E. Taylor
1	2	United Aircraft Corporation Pratt & Whitney Division Florida Research & Development Center P. O. Box 2691 West Palm Beach, Florida 33402 Attn: Library	R. J. Coar Dr. Schmitke X T. E. Bailey X A. I. Masters
1		United Aircraft Corporation United Technology Center P. O. Box 358 Sunnyvale, California 94038 Attn: Library	Dr. David Altman
1		Vickers Incorporated Box 302 Troy, Michigan	
1		Vought Astronautics Box 5907 Dallas, Texas Attn: Library	W. C. Trent
1		Jim Markowsky 221 Upson Hall Ithaca, New York 14850	
1		Propulsion Division Aerojet-General Corporation P. O. Box 15847 Sacramento, California 95803 Attention: Larry Post	